Toward particle size reduction by spray flash evaporation : the case of organic energetic crystals and cocrystals

Florent Pessina

UNIVERSITÉ DE STRASBOURG

École Doctorale de Physique et Chimie-Physique

Nanomatériaux pour les Systèmes Sous Sollicitations Extrêmes
NS3E, UMR 3208 ISL-CNRS-UNISTRA

THÈSE présentée par :

Florent PESSINA

soutenue le : **05 octobre 2016**

pour obtenir le grade de : **Docteur de l'université de Strasbourg**

Discipline/ Spécialité : Chimie Physique-Chimie

Toward Particle Size Reduction by Spray Flash Evaporation
the case of organic energetic crystals and cocrystals

THÈSE dirigée par :

M. SPITZER Denis	Dr. HDR, université de Strasbourg

RAPPORTEURS :

M. CONDORET Jean-Stéphane	Prof., Laboratoire de Génie Chimique, INP Toulouse
M. KLAPÖTKE Thomas M.	Prof., Ludwig-Maximilians Universität

AUTRES MEMBRES DU JURY :

M. JANNIN Vincent	Dr. HDR, Research Director - Pharmaceuticals GATTEFOSSÉ
M. NOUGUEZ Bruno	Head of Innovation R&D Department EURENCO
M. WELTER Richard	Prof., Institut de Biologie Moléculaire des Plantes, Unistra

«Qui a dit que la science désenchante le monde ? Assurément un ignorant, car toutes les peurs se nourrissent de l'ignorance et des ignorances entretenues.»

Pascal Pic, *Darwin et l'évolution expliqués à nos petits-enfants* (2009).

"SCIENCE: A way of finding things out and then making them work. Science explains what is happening around us the whole time. So does RELIGION, but science is better because it comes up with more understandable excuses when it is wrong."

Terry Pratchett, *Wings* (1990, 2007), 147.

since we are living in a so-called modern age where PR and economic interests seems to have won against science.

Acknowledgments

I would like to thank all the people who provided supports in any way to my PhD, at work or outside.

First and foremost, I express my gratitude to my supervisor and director of the NS3E laboratory, Dr. Denis Spitzer, for being available while having many responsibilities. His quick answers and enthusiastic support for launching new projects were a driving force. I also greatly appreciated the opportunities to participate to congresses, workshops and fairs, but also the great autonomy accorded.

I am very grateful to Dr. Thomas M. Klapötke and Dr. Jean-Stéphane Condoret to review my manuscript. A special thank goes to Dr. Vincent Jannin who has accepted to review and is now part as the committee. I am also thankful for my two others committee members, Mr. Bruno Nouguez and Prof. Richard Welter, who are very representative of the two aspects of this thesis: the industry of energetic materials and the academic research on crystallisation. I thank Prof. Chinnayya to kindly attend to my modest PhD Defence.

I would like to thank the Institute of Saint Louis staff which allowed me to improve my patience and pugnacity. I hope one day to reach the high-level of management and communication skills of the Directors. On the other hand, some sincere thanks to Mr. Stehlin, Ms. Nicollet, Mr. Urban, Dr. Han, Dr. Braun, Ms. Dietlin and many others (PEM, PCD, MC etc.) for their technical support and their kind help.

Many thanks to the whole NS3E laboratory, where each person from undergraduates to doctors made this PhD a fantastic and memorable journey. Dr. Gibot for his help in BET and XRD, Dr. Comet for his energy and knowledge on chemistry and explosives, Dr. Bonnot for her kindness and Dr. Pichot for his pragmatic analyses and very wise help in many areas. MCF. Lobry arrived lately but significantly contributed to the SFE; I'm very grateful for the ideas shared, your endorsement and support in the projects at work, and for enduring my chatty mood in our office, in the train and at Strasbourg. Dr. Klaumünzer, Dr. Doblas, Dr. Blas, Dr. Bach, Dr. Schlur and Dr. Seve, thank you all for your help in chemistry, chemical engineering and LaTeX but mostly for the good time spent together, especially the team TER. I would like to thank Ing. Schaefer and express all my gratitude to our essential multi-skilled technician Mr. Hassler for his advices and tools.

Axel –or should I say now Dr. Le Brize?– your happiness and sense of humour made this journey quite enjoyable. I wish you the best and hope we will meet again to share our common passion. Cédric, Frank and Jérémy I thank you for the great moments and wish you the best too. A special thanks to Jean Edouard who contributed to this present project and to the SFE apparatuses with enthusiasm; you were kind enough to follow the advices of a simple PhD student.

I would like to thank the SNCF and especially the wide animals for all that

great time spent on board. Crystie and the 14 wrench will miss me. I sincerely thank Mr. Canevari, Ms. Ermis and Ms. Schmitt for their crucial and hard work to provide a solid and helpful environment to PhD students.

Huge thanks to dear lovely one Dr. Nguyen Huynh, who supported me every day and endured the writing period. We shared the joy and sorrow of our PhDs and I wish to continue this mutual enrichment as long as possible. I express my deep gratitude to my family who were very understanding; I promise to be more present from now.

Extended Abstract

The development of nano-technology took off with the invention of the Scanning Tunneling Microscopy (STM) and the Atomic Force Microscopy (AFM) in the early 80's at the IBM Zurich Research Laboratory (Binnig et al. 1986, 1983, 1982). By providing accurate and advanced characterizations on nanoparticles, those two crucial microscopy techniques allowed a control of the physicochemical properties of materials down to the atomic scale. Since then, the outstanding properties of new nano-materials led the research in energetic material to embrace this trend. The nano-structuration of classical explosives, such as 2,4,6-trinitrotoluene (TNT) or 1,3,5-trinitroperhydro-1,3,5-triazine (RDX), can enhance their safety but also their reactive properties (critical diameter, tunable detonation velocity etc.).

Organic energetic materials release their intrinsic energy under an external stimulus such as a strong mechanical impulse, a great heat or an electrostatic discharge. This initiation is facilitated by the formation of hot-spots coming from the presence of impurities, open pores, entrapped gases or other inhomogeneities within the explosive matrix. Therefore, void free crystals have been an extensive research subject, but the mastering of crystallisation can be enhanced by the formation of particles smaller than the critical size of a hot spot. Moreover, achieving a controlled crystallisation enables further tailoring of the nanoparticles and thus of the physicochemical properties.

The continuous formation of nanosized energetic material is a long-standing challenge. From wet productions methods to dry crystallisation processes, Spray Flash Evaporation (SFE) is a major technique for continuously producing energetic materials at submicron or nano scale. It relies on the superheating of a solvent sprayed into vacuum and thus flashing. The versatility of the SFE internally developed (Doctoral Thesis Risse 2012; Risse et al. 2012) and patented ("Method for producing cocrystals by means of flash evaporation" 2016; "Préparation de nanoparticules par évaporation flash" 2013) allows the continuous engineering of nano-crystals and nano-cocrystals for oxides (Klaumünzer et al. 2015), medical and energetic applications (Spitzer et al. 2014).

This present research project aims to understand and control the crystallisation occurring in the SFE process, in order to reduce further the particle size of energetic crystals. 1,3,5-trinitroperhydro-1,3,5-triazine (RDX) is chosen as a reference material for its wide use for civilian and military applications. Cocrystals -two or more molecules that form a unique crystalline structure- are also relevant in energetic materials in order to decrease the sensitivity

without losing reactivity; for instance a low sensitive compound could be cocrystallised with another one having a high sensitivity and a high reactivity. Therefore, the cocrystal CL-20:HMX 2:1 was studied as proof-of-concept but also to overcome the limited *in situ* characterizations. Crystallisation depends on the supersaturation; in SFE, the supersaturation is a function of time and space as it is linked to the size distribution and velocity of droplets. Since those measurement was first out of reach, supersaturation was raised with an anti-solvent and the enhancement of the SFE with a dual nozzle system. Later, a Phase Doppler Analysis (PDA) was used to elucidate the question of supersaturation.

Another route to control the crystallisation is the addition of chemical agent. PolyVinylPyrrolidone (PVP) and PolyEthylene Glycol (PEG) were used to alter the two steps of the crystallisation, namely the nucleation and the growth. PEG 400 triggers the early nucleation of RDX with low nucleation rate leading to bigger particles up to 5 µm. PVP 40K acts as a nucleation and growth inhibitor, forming RDX spherical particles with a mean size of 160 nm. Additionally, the synthesized RDX samples were less sensitive, especially toward electrostatic discharge.

During this work, many standard analytical methods have been found to be impossible or difficult to apply on energetic material, due to their sensitivity toward heat, or toward vacuum, or their organic nature; the nano scale and so the high specific surface area worsen those phenomena. The relevancy of the sensitivity tests is also questionable when reaching the nano scale.

Bibliography

1. Binnig, Gerd, Calvin F. Quate, and Ch Gerber (1986). “Atomic force microscope”. In: *Physical review letters* 56.9, p. 930.
2. Binnig, Gerd and Heinrich Rohrer (1983). “Scanning tunneling microscopy”. In: *Surface science* 126.1, pp. 236–244.
3. Binnig, Gerd, Heinrich Rohrer, Ch Gerber, and E. Weibel (1982). “Surface studies by scanning tunneling microscopy”. In: *Physical review letters* 49.1, p. 57.

4. Klaumünzer, Martin, Laurent Schlur, Fabien Schnell, and Denis Spitzer (2015). "Continuous Crystallization of ZnO Nanoparticles by Spray Flash Evaporation versus Batch Synthesis". In: *Chemical Engineering & Technology* 38.8, pp. 1477–1484. ISSN: 1521-4125. DOI: 10.1002/ceat.201500053.

5. "Method for producing cocrystals by means of flash evaporation" (2016). WO 2016001445. B. Risse and D. Spitzer. WO Patent App. PCT/EP2015/065,335.

6. "Préparation de nanoparticules par évaporation flash" (2013). WO2013117671 A1. B. Risse, D. Hassler, and D. Spitzer.

7. Risse, Benedikt (2012). "Continuous crystallization of ultra-fine energetic particles by the Flash-Evaporation Process".

8. Risse, Benedikt, Denis Spitzer, Dominique Hassler, Fabien Schnell, Marc Comet, Vincent Pichot, and Hervé Muhr (2012). "Continuous formation of submicron energetic particles by the flash-evaporation technique". In: *Chemical Engineering Journal* 203, pp. 158–165. ISSN: 1385-8947. DOI: 10.1016/j.cej.2012.07.032.

9. Spitzer, D., B. Risse, F. Schnell, V. Pichot, M. Klaumünzer, and M. R. Schaefer (2014). "Continuous engineering of nano-cocrystals for medical and energetic applications". In: *Scientific Reports* 4. DOI: 10.1038/srep06575.

Contents

Résumé étendu français

Réduction de la taille des particules par Spray Flash Evaporation : le cas des cristaux et cocristaux organiques énergétiques.

Le développement des nanotechnologies a réellement décollé avec l'invention des microscopies par effet tunnel (STM) et à force atomique (AFM), au début des années 80 à l'Institut de Recherche IBM de Zurich (Binnig et al. 1986, 1983, 1982). Ces deux techniques permettent l'analyse directe de nanostructures jusqu'à l'échelle atomique, et sont donc devenues indispensables pour contrôler finement les propriétés physicochimiques des matériaux. Depuis quelques décennies, les nouveaux nanomatériaux ont pris leur essor dans notre société grâce à des propriétés remarquables pour de nombreuses application, et aux couts de production maîtrisés. Le développement des nanotechnologies a aussi permis la création et l'amélioration de technologies connexes. Contrairement à la révolution numérique, les secteurs scientifique et industriel des matériaux énergétiques sont restés bien longtemps en marge de cette vague technologique, et ne s'engagent que depuis peu dans l'exploration des propriétés de nanostructures énergétiques. Parmi les attentes, la nanostructuration d'explosifs classiques comme le 2,4,6-trinitrotoluene (TNT) ou le 1,3,5-trinitroperhydro-1,3,5-triazine (RDX) peut améliorer leur sensibilité et donc faciliter leur manipulation, mais aussi nombre de leurs propriétés réactives (diamètre critique, vitesse de détonation, homogénéité...).

Les explosifs étudiés ici sont les matériaux énergétiques organiques ; ils libèrent leur énergie intrinsèque suite à un stimulus tel une sollicitation mécanique importante, une forte chaleur ou une décharge électrostatique. Cette initiation est facilitée par la formation de points chauds, hot-spot, qui proviennent d'impuretés, de cavités et autres défauts dans la matrice cristalline. Ainsi, la production de cristaux à haute pureté et haute cristallinité fut un champ de recherche privilégié pendant des décennies, mais la maîtrise de la cristallisation peut être poussée encore plus loin par la formation de particules plus petites

que la taille critique d'un point chaud. De plus, atteindre une cristallisation contrôlée permet de façonner avec précision les nanoparticules et donc d'ajuster leurs propriétés physicochimiques.

L'étude des nanomatériaux énergétiques organiques commence par leur formation ; le retard pris par la communauté pyrotechnique en nanotechnologie s'explique en partie par la difficulté de produire des nanoparticules d'explosifs. Ainsi la cristallisation en continu de matériaux énergétiques à une échelle au moins submicronique est un défi de longue date. Parmi les méthodes de production de la voie humide à la voie sèche, le procédé Spray Flash Evaporation (SFE) est une technique émergente majeure pour la production continue d'explosifs nanométriques ou de compositions énergétiques nanostructurées. Cette méthode se base sur la surchauffe d'un solvant pulvérisé dans un vide primaire/moyen, provoquant alors une évaporation quasi instantanée, flash. La polyvalence du SFE, développé en interne (Thèse de Doctorat Risse 2012) et breveté ("Method for producing cocrystals by means of flash evaporation" 2016 ; "Préparation de nanoparticules par évaporation flash" 2013), permet la formation d'oxydes (Klaumünzer et al. 2015) ainsi que de nanocristaux et co-cristaux pour des applications énergétiques et médicales (Spitzer et al. 2014).

Le présent projet de recherche vise à comprendre et contrôler la cristallisation au sein du procédé SFE, afin de réduire la taille des cristaux énergétiques. Le 1,3,5-trinitroperhydro-1,3,5-triazine (RDX) a été choisi comme matériau énergétique de référence du fait de son utilisation large pour des applications civiles et militaires. La cristallisation dépend du degré de sursaturation ; dans le SFE, la sursaturation est fonction du temps et de l'espace car liée à la distribution en taille des gouttes et à leur vitesse. La caractérisation *in situ* des gouttes requiert l'utilisation de techniques avancées d'interférométrie optique acquises à la fin du projet. Pour palier cette absence, la sursaturation a été augmentée par l'ajout d'un anti-solvant et la mise en place d'un système d'injection à double buses. Finalement, un appareil d'interférométrie optique, Phase Doppler Analysis (PDA), est utilisé pour déterminer les tailles et vitesses des gouttes.

Pour déterminer la persistance des gouttes, le co-cristal CL-20:HMX 2:1 sera employé avec le système d'injection à double buses. L'utilisation de co-cristaux (deux molécules ou plus dans un même réseau cristallin unique) pour étudier la cristallisation au sein du SFE est d'autant plus pertinente que la formation de co-cristaux énergétiques est une autre stratégie actuellement explorée pour réduire la sensibilité de l'explosif sans sacrifier sa réactivité.

La cristallisation au sein du SFE peut aussi être maîtrisée par l'ajout d'agents polymériques. Le PolyVinylPyrrolidone (PVP) et le PolyEthylene Glycol (PEG) ont été employés pour modifier les conditions de cristallisation donc les étapes de nucléation et de croissance. Le PEG 400 provoque la nucléation anticipée du RDX

amenant à la formation de particules de 500 nm à 5 µm. La PVP 40k s'adsorbe en surface et agit comme agent inhibiteur de nucléation et de croissance : le RDX cristallise en nanoparticules sphériques avec une taille moyenne de 160 nm. Les échantillons de RDX synthétisés ainsi sont également moins sensibles, tout spécialement à la décharge électrostatique.

Lors de ce travail de recherche, de nombreuses méthodes de caractérisation ont été testées et bien peu se sont avérées être applicables de manière fiable sur les nanomatériaux énergétiques. En effet, ces derniers -des cristaux moléculaires- sont sensibles à la chaleur et au vide ; cette sensibilité est encore exacerbée pour les nanomatériaux du fait de leur grande surface spécifique. De plus, la pertinence des tests de sensibilité à cette échelle est critiquable.

Cristaux et cocristaux organiques énergétiques

Les matériaux énergétiques regroupent tous types de matériaux (composite, polymère, organiques…) qui peuvent libérer rapidement de l'énergie par une violente réaction d'oxydo-réduction. Un stimulus externe comme un choc, un frottement ou une décharge électrostatique peut initier localement la réaction de décomposition ; cette dernière se propage à travers le matériau via le front de réaction. La vitesse de ce front de réaction dépend du matériau et du mode de décomposition.

On distingue trois modes de décomposition : la combustion (mm/s - m/s), la déflagration (m/s - km/s) et la détonation (> km/s). La combustion requiert un apport extérieur d'oxygène alors que la déflagration est auto-entretenue. Lors d'une détonation, la réaction se propage par une onde de choc supersonique. Par la suite, on peut classer les matériaux énergétiques selon leur mode normal de décomposition et leurs autres propriétés pyrotechniques. Les poudres propulsives brûlent de manière contrôlée avec une importante génération de gaz afin de produire la poussée nécessaire aux engins autopropulsés. Les explosifs détonent et sont également classés selon leurs sensibilités et puissances : les explosifs primaires, très sensibles, servent à l'initiation par onde de choc des explosifs secondaires, tels que le RDX ou le 2,4,6-trinitrotoluene (TNT). On retrouve parfois des matériaux comme le nitrate d'ammonium et le perchlorate d'ammonium classés comme explosifs tertiaires du fait de leur grande stabilité. D'un point de vue chimique, les explosifs organiques sont des cristaux moléculaires dont la cohésion est assurée par des forces faibles (Van der Waals : π stacking, liaison hydrogène …).

Un co-cristal est un cristal comprenant plusieurs molécules électriquement neutres au sein de la même maille cristalline, avec un ratio stœchiométrique défini. La définition est toujours en débat (Sun 2013) mais les hydrates et

solvates sont généralement exclus. Bolton et al. (2012) furent les premiers à rapporter la formation et la caractérisation du co-cristal CL-20:HMX avec un ratio molaire de 2:1.

Procédés et Intérêt de la nanocristallisation

Ces matériaux hautement explosifs peuvent être accidentellement initiés, engendrant malheureusement nombre de victimes et ce bien trop souvent comme nous le rappellent les lettres de l'Inspecteur de l'armement pour les Poudres et Explosifs. Outre cet aspect, la désensibilisation du matériaux entraîne fréquemment des traitements supplémentaires (enrobage, mises en forme...) voire une perte de performances. Des inclusions, des défauts cristallins ou un habitus cristallin trop rugueux sont différents paramètres physico-chimiques pouvant fragiliser et sensibiliser le matériau ; une cristallisation contrôlée à une échelle nanométrique permet d'éviter ce type de défauts micrométriques et de réduire le nombre d'étapes aboutissant au produit fini.

De nombreux procédés de recristallisation existent et ont été appliqués aux matériaux organiques énergétiques. Les méthodes par voie liquide permettent d'atteindre des tailles nanométriques et des morphologies contrôlées, deux caractéristiques intéressantes qui sont par la suite perdues lors du séchage : les processus de séchage les plus performants tels que le séchage supercritique réduisent la dégradation des cristaux mais fonctionnent par lot et non en continu. Les méthodes en voie sèche les plus abouties actuellement sont le Spray drying (Broadhead et al. 1992 ; Stein 1973) et le Rapid Expansion of Supercritical Solutions (RESS) (Krukonis 1984 ; Matson et al. 1987a,b) : le premier fonctionne en continu mais ne permet pas d'atteindre l'échelle nano ni le submicron, alors que le second permet d'atteindre de telles tailles mais opère séquentiellement. De plus le RESS est un procédé industriel coûteux du fait de l'utilisation de fluides supercritiques (faible solubilité, pression importante) rarement utilisés dans l'industrie (Sheth et al. 2012).

Le procédé Spray Flash Evaporation (SFE) permet la production en continu et en voie sèche de particules nanométriques ou submicrométriques ou de composites nanostructurés. Il se situe entre le RESS et le Spray drying en terme de pression et de température. Inventé (Doctoral Thesis Risse 2012 ; Risse et al. 2012) et breveté ("Method for producing cocrystals by means of flash evaporation" 2016 ; "Préparation de nanoparticules par évaporation flash" 2013) au sein du laboratoire NS3E, le SFE a été précédemment optimisé grâce à la thèse de Risse (2012) ; cependant seuls cinq paramètres ont été étudiés, chacun dans une certaine mesure. Il apparaît nécessaire qu'afin de contrôler et de réduire encore la taille des particules cristallisées par SFE, une bonne compréhension

de la cristallisation au sein du SFE doit être acquise soit directement par une métrologie en ligne, soit par des variations induites dans la cristallisation.

Spray Flash Evaporation : principe et cristallisation

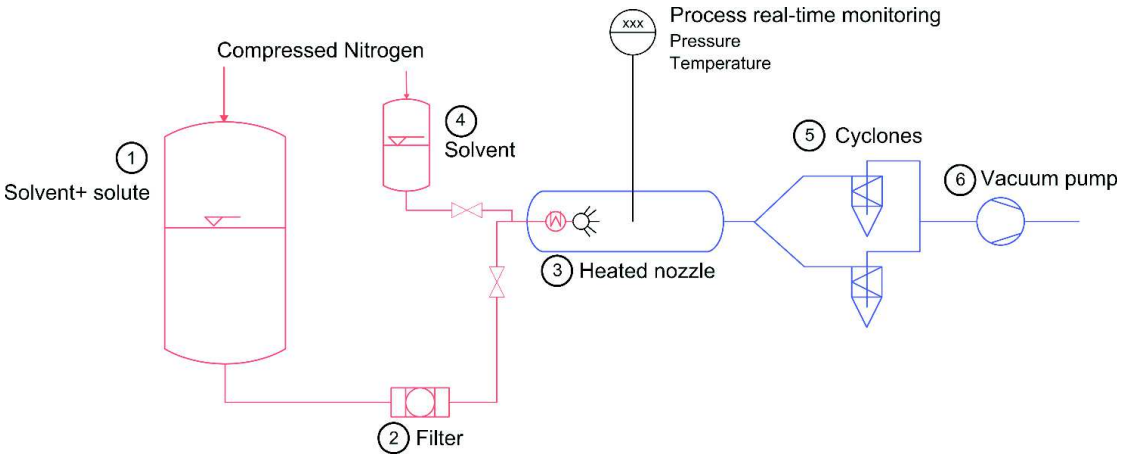

FIGURE *0.1 – Schéma du procédé de Spray Flash Evaporation (SFE)*

Le procédé SFE consiste à pressuriser et surchauffer un solvant comprenant un ou plusieurs composés organiques dissous, puis à pulvériser cette solution dans une enceinte sous vide. Le SFE repose alors sur le principe thermodynamique de flash évaporation : lorsqu'un liquide possède une énergie interne importante (ici d'origine thermique) et est soumis à un déséquilibre thermodynamique important (notamment lorsque la température du liquide est bien supérieure à sa température d'ébullition une fois sous vide), cette énergie est convertie en chaleur latente. Les gouttes se désintègrent et s'évaporent quasi instantanément.

La cristallisation est gouvernée par le degré de sursaturation dans chaque gouttelette ; la conjonction de nombreux phénomènes thermodynamiques mène à une taille nanométrique. La fission des gouttelettes diminue le volume de chaque réacteur, le niveau de surchauffe du liquide influence la solubilité du(des) composé(s) dans le solvant mais aussi la méta-stabilité des gouttes avant le flash... A cela s'ajoute une composante temporelle essentielle où on peut distinguer deux plans d'évolution en fonction du temps : le moment de l'évaporation flash avec le taux d'évaporation d'un côté, et de l'autre le début de la nucléation primaire avec le taux de nucléation (Figure 0.2).

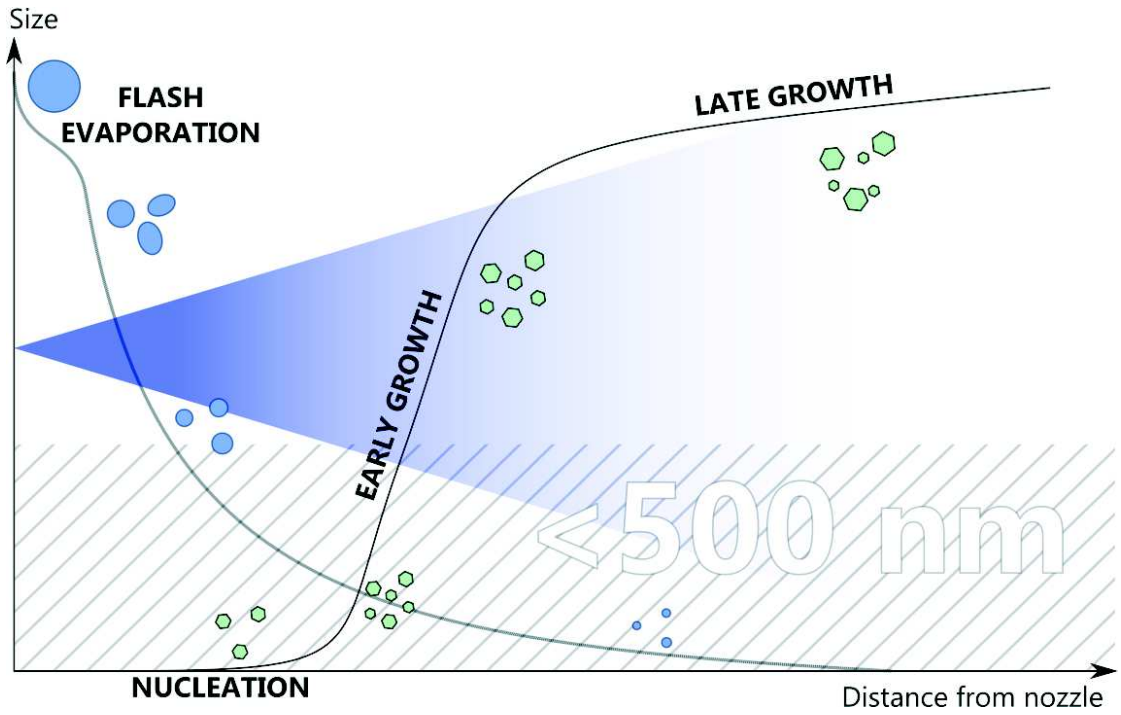

FIGURE *0.2 – Illustration schématique des phénomènes d'évaporation et cristallisation en jeu dans le SFE. La limite de 500 nm correspond à la limite actuelle de détection possible par mesure directe en ligne en anémo-granulométrie Phase Doppler*

Compréhension du SFE

Peu de techniques sont à même de mesurer des aérosols à haute vitesse et de l'ordre du micron. L'interférométrie Phase Doppler est une méthode de mesure optique avancée qui, couplée à la vélocimétrie LASER, permet la mesure *in situ*, simultanée et en temps réel de la taille et de la vitesse d'objets quasi sphériques et microniques. Elle a été pour la première fois adaptée à la technologie SFE : la mesure des tailles dans l'espace du cône de pulvérisation permettra le calcul de la sursaturation. Dans un premier lieu, il s'agit de caractériser le phénomène de flash évaporation : les Figures 0.3 et 0.4 montrent les premiers résultats obtenus avec un appareil optimisé et calibré sur l'acétone. Il est remarquable d'observer trois distributions modales centrées en 2.1, 2.8 et 3.8 µm à toutes les températures ; comme attendu, la taille moyenne chute vers la limite de détection proche du micron lorsque la température augmente. En revanche, l'étude montre alors que le phénomène de flash évaporation est transitoire et commence dès 100 °C et semble ne pas être unique à 160 °C du fait de la présence persistante de deux distributions à 2.1 et 2.8 µm.

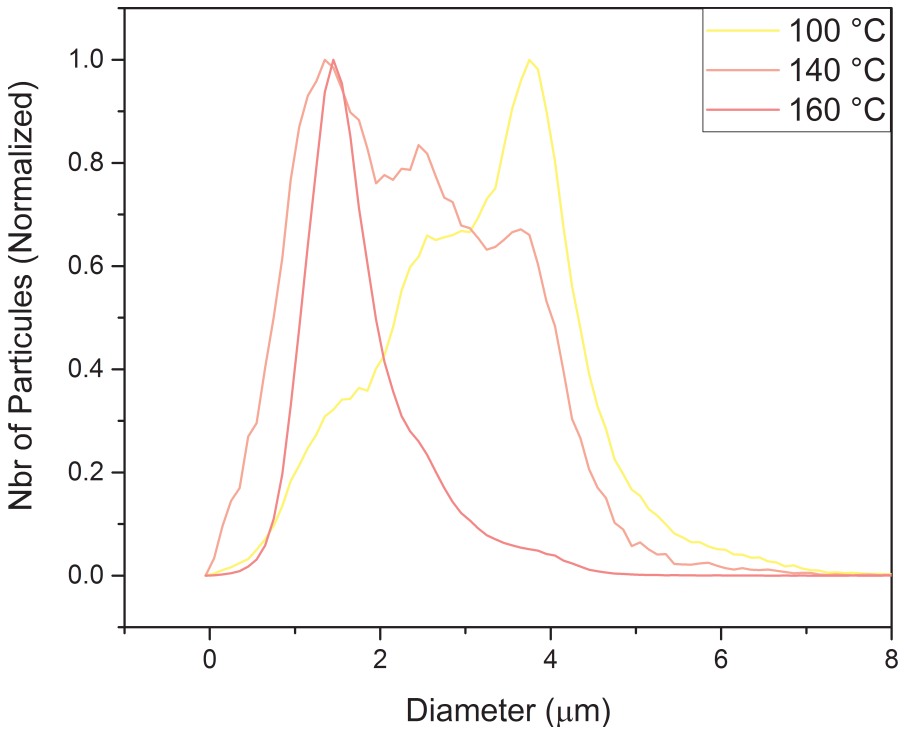

FIGURE *0.3 – Distribution en taille des gouttes pulvérisées à 100, 140 et 160°C.*

Définition d'une particule

La première année de recherche fut menée sur l'étude des paramètres du SFE influençant la taille et la morphologie des cristaux. Ces derniers ont été observés en suivant une méthode développée précédemment au sein du laboratoire : il s'agit de compresser la poudre obtenue et de lisser la surface par micro coupe pour imager par Microscopie à Force Atomique (AFM). L'AFM n'apporte aucune énergie à l'échantillon, contrairement à la Microscopie Électronique à Balayage (MEB) dont le faisceau d'électrons dégrade le matériau énergétique. La méthode par AFM souffrait en revanche d'une analyse des images longues et fastidieuses, ce qui fut tout d'abord amélioré. Une méthode semi automatique a été mise en place avec le logiciel Gwyddion et la technique Watershed. Elle est composée des étapes suivantes :

Processus de localisation des grains La surface est inversée – les particules deviennent des creux – puis de l'eau virtuelle est déposée en chaque point. Ces gouttes d'eau glissent le long des pentes et la répétition de cette pluie virtuelle forme ainsi des lacs dans les minimum locaux. Ces lacs, ces ensembles virtuels, délimitent alors la position des grains.

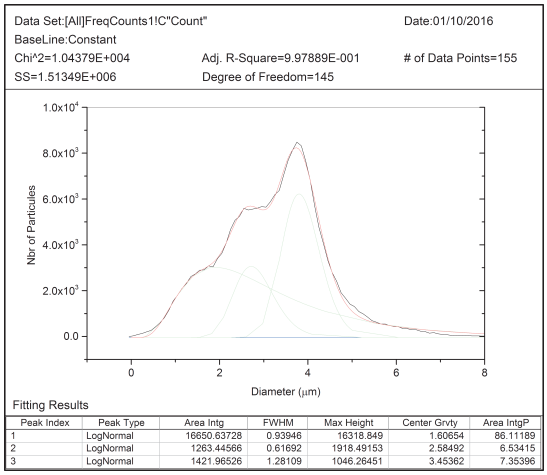

(a) 100 °C

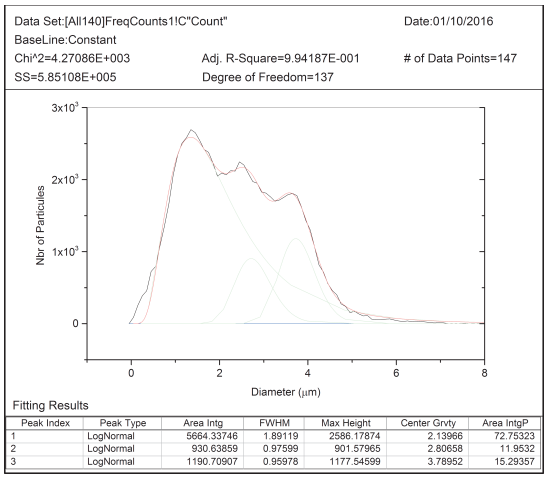

(b) 140 °C

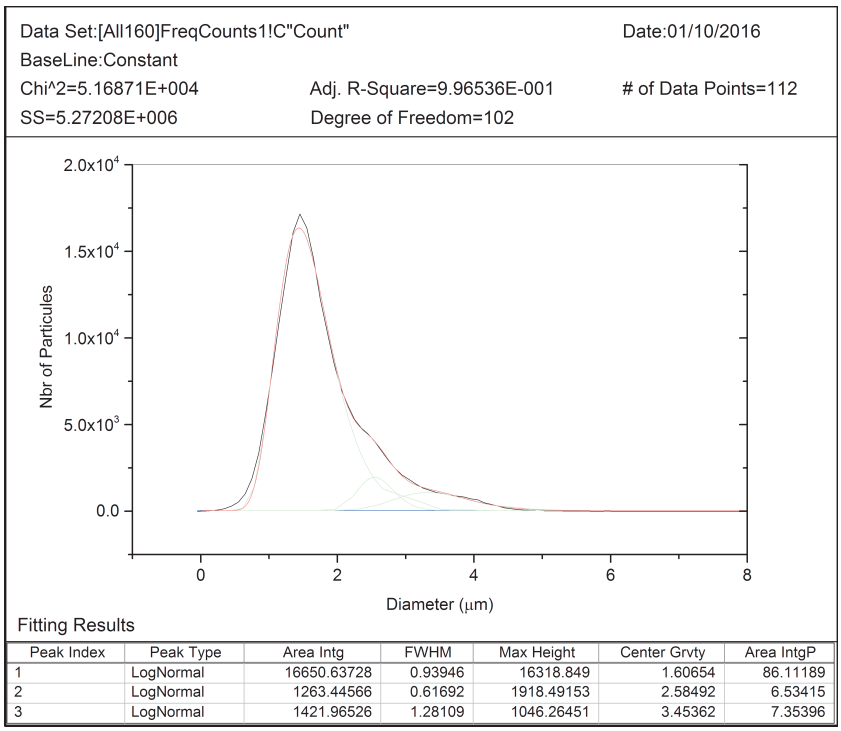

(c) 160 °C

FIGURE *0.4 – Régression des profils de distribution en taille des gouttes pulvérisées à 100, 140 et 160 °C.*

Segmentation Précédemment si deux lacs se touchaient lors d'une pluie virtuelle, ils étaient fusionnés. Dans l'étape de segmentation, deux lacs adjacents seront notés comme différents et une bordure sera définie. La qualité des frontière entre les grains s'améliore avec des gouttes plus fines, mais le temps de calcul augmente fortement avec la diminution de la taille de goutte.

Inspection visuelles et corrections mineures Le logiciel permet l'affichage en surbrillance, le marquage et l'édition manuelle des grains ainsi que plusieurs améliorations du contraste pour permettre une vérification visuelle efficace et une correction des défauts. Les autres canaux de données tels que la phase ou l'amplitude peuvent aider à déterminer la validité d'une frontière de grain.

Distribution en taille et régression Le logiciel permet l'affichage de la distribution en taille des particules mais, grâce à l'export des données, une régression des profils de distributions peut être appliquée par un logiciel tiers. Ici le diamètre est défini comme celui d'un disque d'aire équivalent à la particule mesurée. La distribution en taille semble suivre une loi log normale et non une loi Gaussienne ce qui signifie que les particules sont générées par l'effet de nombreux effets aléatoires et multiplicatifs comme le sont souvent les aérosols (Limpert et al. 2001).

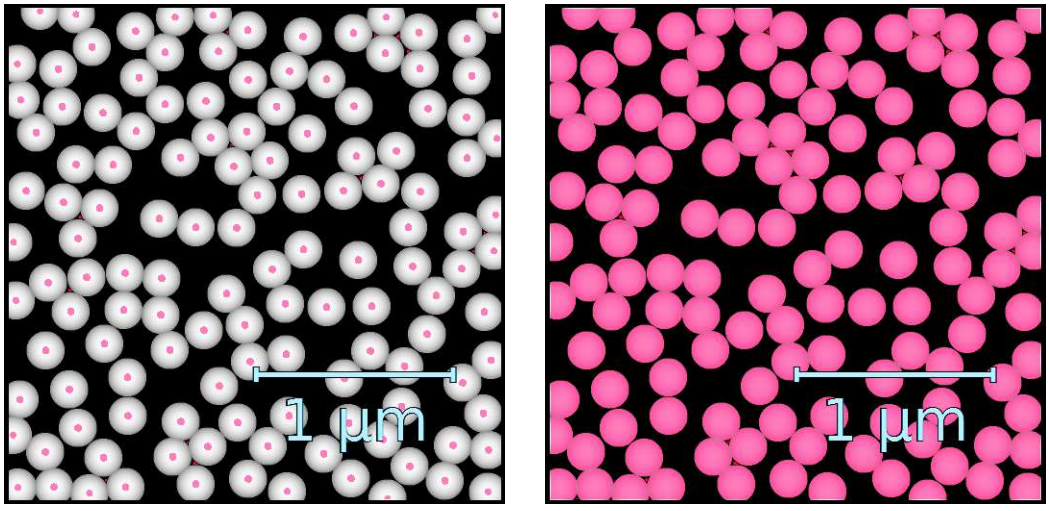

(a) Localisation des grains (b) Segmentation

Figure *0.5 – Analyse Watershed illustrée sur une simulation de sphères de 200 nm.*

Une étude de la méthode a été entreprise pour déterminer sa fiabilité et sa robustesse. Deux facteurs prépondérants sur la taille de particules ont été dégagés :

L'effet de la pression La presse utilisée pour la compression des matériaux énergétiques consiste en un levier supporté par un piston hydraulique ; à l'extrémité du levier, des masses sont accrochées, puis le piston est actionné pour descendre doucement le levier et donc former le comprimé dans des conditions adiabatiques. La pression appliquée est calculée en fonction du poids employé ; les valeurs utilisées sont affichées en Figure 0.1.

Poids (kg)	Pression (MPa)
2	12
5	26
10	50
20	97
30	140
45	210
70	330
97	460

TABLE *0.1 – Poids utilisé et pression correspondante calculée : l'effet de levier suit la loi* $P = 6 \cdot \frac{M}{A} + 31$ *où* $A = \frac{\pi}{4} \cdot \varnothing^2$ *avec M la masse du poids.*

L'effet de la pression peut s'observer en Figure 0.6, où la même face de comprimé a été analysée par AFM et aucune micro coupe n'a été réalisée. Dans la Figure 0.6a une chute brutale de la taille de particule est clairement observable dès SI140kg puis la valeur se stabilise autour de 90 nm : ce changement est aussi visible en Figure 0.6b. Dans les Figures 0.6c et 0.6d, les particules sont difficilement identifiables.

Les résultats provenant de comprimés micro coupés en Figure 0.7 montrent là encore que la pression joue un rôle crucial sur la taille de particule mesurée par AFM. La réduction de taille est progressive avec l'augmentation de la pression. Au delà de 97 MPa (20 kg), les comprimés sont bien trop cohésifs pour pouvoir être usinés par micro coupe ; leur grande dureté du fait d'un comportement quasi vitreux les rend cassants sous la lame.

Le RDX micronique (M5 Eurenco) utilisé pour la recristallisation a également été analysé selon cette méthode ; les comprimés obtenus sont friables à un tel point qu'aucune micro coupe n'a pu être effectuée. Cependant, alors que la taille moyenne reste de l'ordre du micron, à la pression maximale de 97 MPa

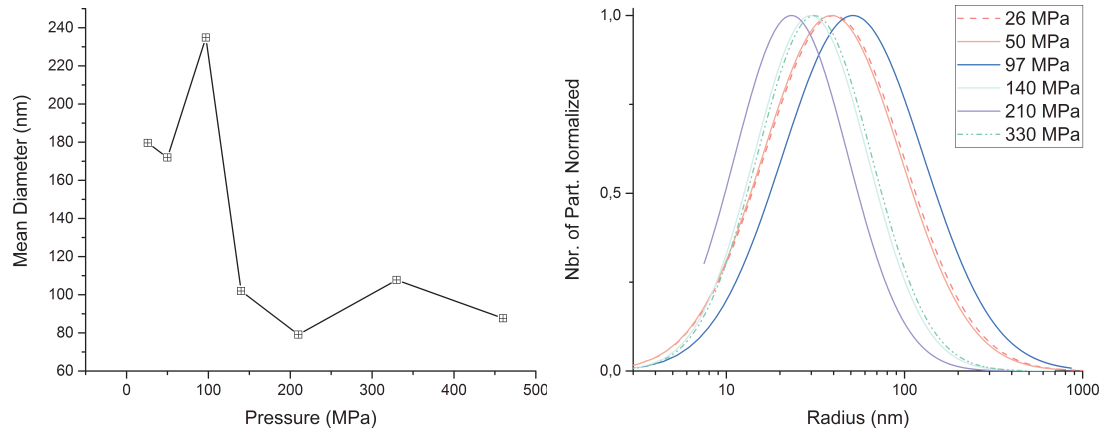

(a) Taille moyenne en fonction de la pression appliquée

(b) Influence de la pression sur la distribution en taille

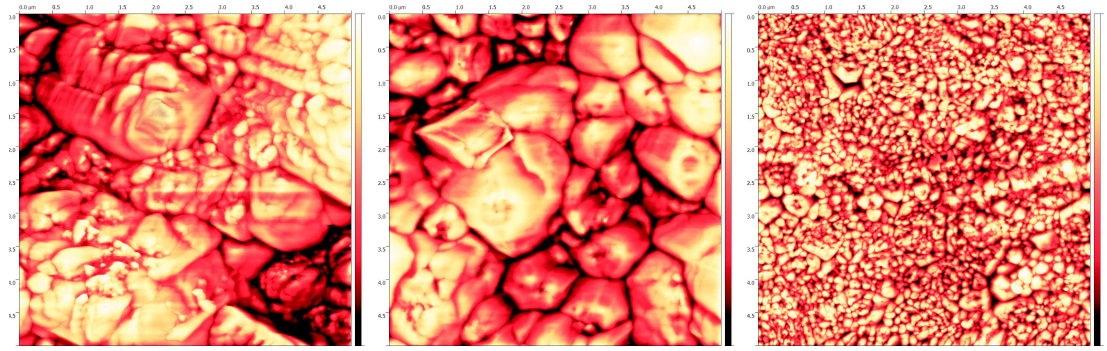

(c) 26 MPa (5 kg)

(d) 97 MPa (20 kg)

(e) 460 MPa (97 kg)

FIGURE *0.6 – Effet de la pression, sans micro coupe, 5 µm × 5 µm pour 1024 px × 1024 px, contraste amélioré.*

une chute de la taille moyenne est observée de la même manière que le RDX recristallisé par SFE. Ainsi il apparaît clairement que le nano RDX est broyé à des contraintes plus faibles et donc plus facilement : cet effet de casse ou de désagrégation doit être étudié plus en profondeur car les explosifs sont utilisés notamment en charges pressées.

Effet de la micro coupe D'après les résultats en Figures 0.7a et 0.6a, la micro coupe réduit la taille moyenne et l'effet de la pression précédemment mis en évidence est accentué. Cet effet s'explique par la dureté accrue des comprimés avec la pression : la force de micro coupe doit être plus élevée donc l'effet de broyage en surface est accru.

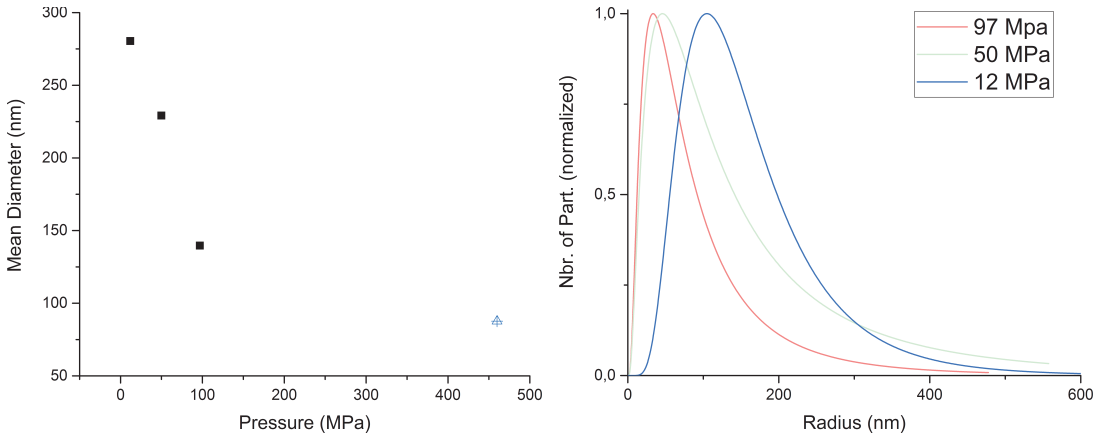

(a) Taille moyenne en fonction de la pression appliquée

(b) Influence de la pression sur la Distribution en taille

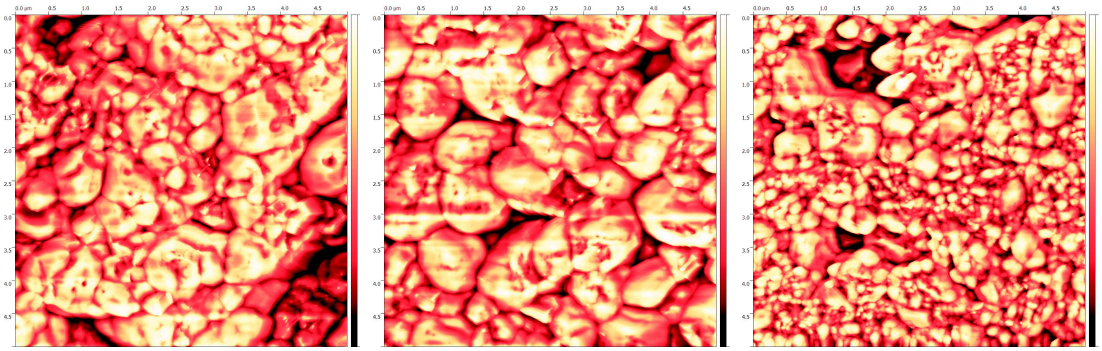

(c) 12 MPa (2 kg)

(d) 50 MPa (10 kg)

(e) 97 MPa (20 kg)

FIGURE *0.7 – Effet de la pression, avec une micro coupe, 5 µm × 5 µm pour 1024 px × 1024 px, contraste amélioré.*

Pression (MPa)	Brut	Avec micro coupe
12		280
26	180	
50	170	230
97	235	140
140	100	
210	80	
330	110	
460	90	

TABLE *0.2 – Diamètre moyen en nm selon la pression appliquée et le pré traitement par microtome ; par MEB, la taille moyenne est de 500 nm.*

Découplage des phénomènes au sein du SFE et contrôle des tailles

La cristallisation se déroule principalement en deux étapes successives : la nucléation et la croissance cristalline, qui peuvent être contrôlés par l'ajout d'additifs. La PolyVinylPyrrolidone (PVP) est un additif polymérique notamment utilisé dans l'industrie comme émulsifiant et stabilisant, et est enregistré comme l'additif alimentaire E1201. Il est également utilisé comme inhibiteur de croissance et promoteur de nucléation grâce à sa propriété d'adsorption autour de cristaux organiques (Ozaki et al. 2013 ; Patel et al. 2015 ; Posteraro et al. 2015). De même, le PolyEthylène Glycol (PEG) est un additif polymérique utilisé comme promoteur de croissance ou comme enrobant et est enregistré comme l'additif alimentaire E1521. L'effet stérique du PEG est principalement utilisé pour déclencher et permettre la croissance de cristaux de protéines (Bhat et al. 1992).

Du PVP 40k sous forme solide et du PEG 400 sous forme liquide ont été utilisés avec succès pour la cristallisation du RDX par SFE. Outre l'extension de la polyvalence du SFE en permettant la cristallisation de composés organiques avec additif polymérique sous forme solide ou liquide, la taille moyenne et la morphologie de particules ont été contrôlés. Le RDX produit avec ajout de PVP a été réduit jusqu'à 160 nm avec une morphologie sphérique ; de plus la stabilité dans le temps des tailles et morphologies ainsi que les sensibilités sont améliorées par la présence de PVP. Cette diminution de taille s'explique par la nucléation retardée par la PVP au delà du moment flash du solvant. L'ajout de PEG induit une nucléation très tôt dans des volumes de goutte plus important ainsi qu'un taux de nucléation faible. Les cristaux croissent jusqu'à des tailles micrométriques comparables à celles du RDX commercial mais avec des sensibilités grandement réduites notamment pour la décharge électrostatique.

Innovations du SFE comme outil de recherche

Au cours de ce projet, de nombreuses améliorations et changements ont été apportés au procédé SFE et ses appareils. Parmi les innovations majeures, se trouve être l'utilisation de plusieurs buses pour étudier la cristallisation par SFE.

L'hexane est un antisolvant parfait du RDX et est thermodynamiquement compatible avec le SFE. Le mélange acétone-hexane présente aussi un azéotrope permettant une température d'évaporation plus basse que les deux solvants purs : la force motrice du SFE réside dans le degré de surchauffe du fluide, ainsi une température d'ébullition plus faible permet d'atteindre plus rapidement

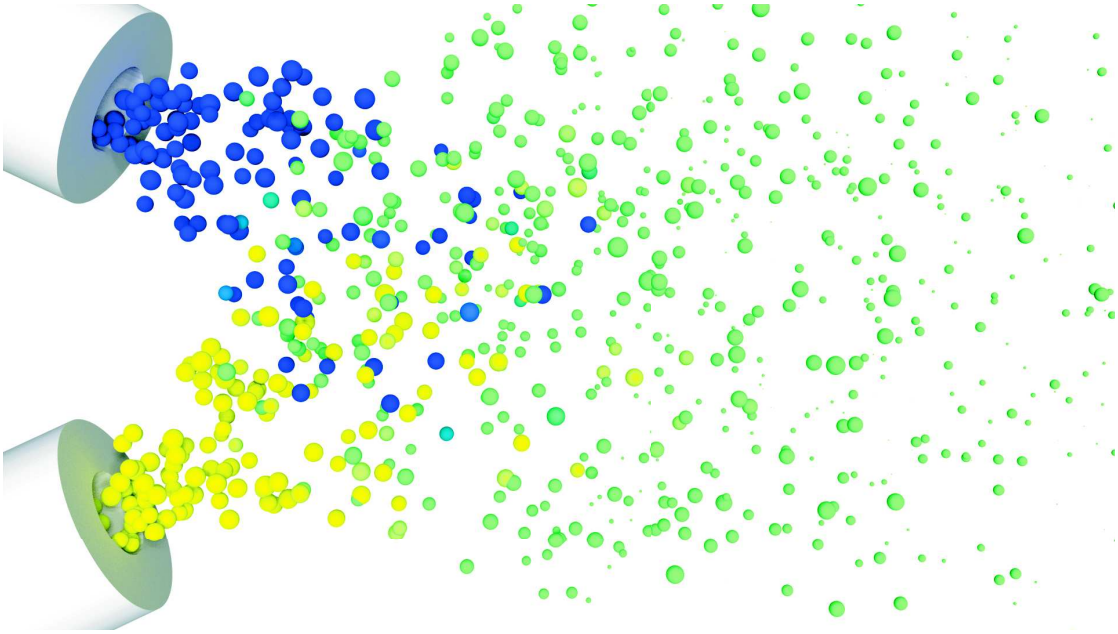

FIGURE *0.8 – Illustration du principe de cristallisation in situ via multi-buses*

un degré de surchauffe élevé. Tous ces avantages sont étudiés en mono buse selon divers ratio solvants/anti solvants ; l'abaissement du point d'ébullition et l'augmentation de la sursaturation réduisent effectivement la taille des cristaux de RDX. Dans la continuité, un système multi-buses a été mis en œuvre pour la première fois sur le SFE afin d'augmenter brutalement le degré de sursaturation, quelques instants après le début du spray alors que les gouttes sont dans un état méta-stable. Ce système a été protégé dans l'extension d'un brevet à l'internationale ("Method for producing cocrystals by means of flash evaporation" 2016). Les avantages de passer d'un système de mono buse à plusieurs buses sont nombreux. Ainsi pour des applications industrielles du SFE, l'ajout d'un anti solvent présente l'immense désavantage de réduire la solubilité du composé et donc de réduire la productivité du procédé : le multi-buse permet alors de conserver la haute solubilité du produit dans son solvant de prédilection, mais agir sur le nuage de gouttelettes permet également plus de flexibilité et autorise les réactions chimiques *in situ*.

De part la pulvérisation de l'anti solvent par une seconde buse, se pose alors la question de savoir dans quel état l'anti solvent arrive : est il gazeux ou liquide sur le nuage de gouttes de la première buse ? La cocristallisation est alors étudiée en multi-buses avec des débits contrôlés et des solvants différents. Ce système multi-buse, à débit contrôlé par débitmètres de précision à effet Coriolis avec vanne intégrée, découple alors l'éternel triptyque suivant : solubilité, débit

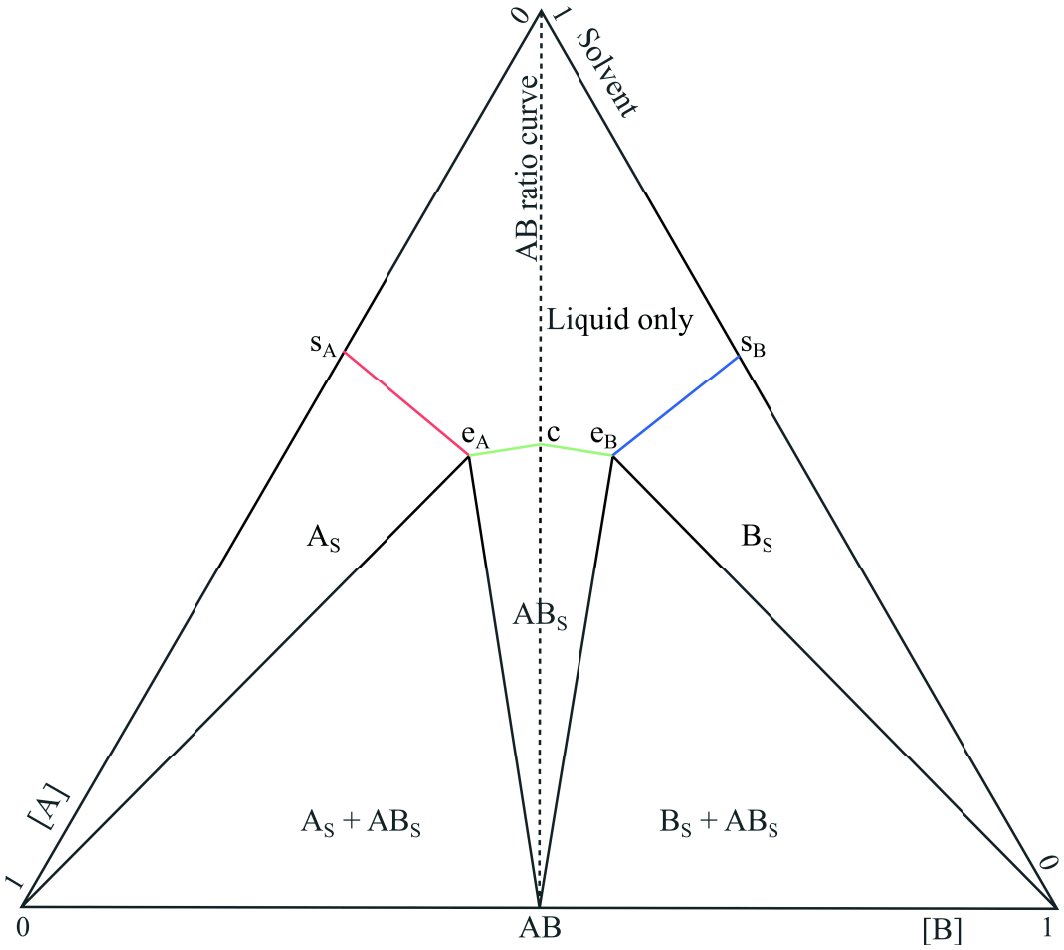

FIGURE *0.9 – Diagramme ternaire d'un cocrystal 1 :1 AB*

des buses et ratio du cocristal. La co-cristallisation à partir de deux réservoirs et buses différents a été réalisée avec succès pour la première fois au sein du SFE. En revanche, des études complémentaires sont à mener afin de déterminer les diagrammes de solubilité du cocrystal dans l'acétone-héxane.

Toutes ces études préliminaires ont posés les bases d'une étude complète et précise de la cristallisation par SFE et ont débloqué de nouvelles voies de recherche telles que les réactions *in situ*.

Liste des publications et communications

Communications

- Europyro 2015, 41e International Pyrotechnic Seminar (Toulouse).

- 4e ISL Budding Science Colloquium (Saint Louis, 2015).
- European Congress and Exhibition on Advanced Materials and Processes EUROMAT 2015, B1.3 Section Nanocrystallisation (Varsovie).
- Material Weekend Warsaw ; un atelier de travail pour doctorant alliant présentations orales et cours.
- Exposant stand DGA à l'Eurosatory 2016, Defence and Security International Exhibition (572 exposants de 56 pays, 213 délégations officielles de 94 pays)
- 5e ISL Budding Science Colloquium (Saint Louis, 2016).
- Junior EUROMAT 2016 (Lausanne).
- 6e NANOstructures and nanomaterials SElf-Assembly (NanoSEA) (Giardini Naxos (ME), Italie 2016).

- 1 poster : 3e ISL Budding Science Colloquium (2014).

Publications

- Blas, Lucia, Martin Klaumünzer, **Florent Pessina**, Silke Braun, and Denis Spitzer. "Nanostructuring of Pure and Composite-Based K6 Formulations with Low Sensitivities." Propellants, Explosives, Pyrotechnics 40, no. 6 (2015) : 938–44.
- **Florent Pessina**, Fabien Schnell, and Denis Spitzer. "Tunable Continuous Production of RDX from Microns to Nanoscale Using Polymeric Additives." Chemical Engineering Journal 291 (May 1, 2016) : 12–19. doi :10.1016/j.cej.2016.01.083.
- Martin Klaumünzer, **Florent Pessina**, and Denis Spitzer. "Indicating Inconsistency of Desensitizing High Explosives against Impact through Recrystallisation at the Nanoscale." Journal of Energetic Materials, July 1, 2016, 1–10. doi :10.1080/07370652.2016.1199610.
- Denis Spitzer, Vincent Pichot, **Florent Pessina**, Fabien Schnell, Martin Klaumünzer, and Lucia Blas. "Continuous and Reactive Nanocrystallization : New Concepts and Processes for Dual-Use Advances." Comptes Rendus Chimie, July 2016. doi :10.1016/j.crci.2016.06.009.

- **Florent Pessina** and Denis Spitzer. "The longstanding challenge of the nano crystallization of 1,3,5-trinitroperhydro-1,3,5-triazine (RDX)" Beilstein Journal of Nanotechnology *Under Review*.

Formations scientifiques suivies

- Sensibilisation à la pyrotechnie 3PSC17C, Centre de Formation de la Défense (Bourges 2013)
- Advanced Functional Materials and Characterization, CNRS-EWHA Winter School (Strasbourg 2014)
- Nano-OptoMechanics, School in Physics (Strasbourg 2014)

Bibliographie

1. Bhat, Rajiv et Serge N. Timasheff (1992). “Steric exclusion is the principal source of the preferential hydration of proteins in the presence of polyethylene glycols”. In : *Protein Science* 1.9, p. 1133–1143. issn : 1469-896X. doi : 10.1002/pro.5560010907.
2. Binnig, Gerd, Calvin F. Quate et Ch Gerber (1986). “Atomic force microscope”. In : *Physical review letters* 56.9, p. 930.
3. Binnig, Gerd et Heinrich Rohrer (1983). “Scanning tunneling microscopy”. In : *Surface science* 126.1, p. 236–244.
4. Binnig, Gerd, Heinrich Rohrer, Ch Gerber et E. Weibel (1982). “Surface studies by scanning tunneling microscopy”. In : *Physical review letters* 49.1, p. 57.
5. Bolton, Onas, Leah R. Simke, Philip F. Pagoria et Adam J. Matzger (2012). “High Power Explosive with Good Sensitivity : A 2 :1 Cocrystal of CL-20 :HMX”. In : *Crystal Growth & Design* 12.9, p. 4311–4314. issn : 1528-7483. doi : 10.1021/cg3010882.
6. Broadhead, J., S. K. Edmond Rouan et C. T. Rhodes (1992). “The spray drying of pharmaceuticals”. In : *Drug Development and Industrial Pharmacy* 18.11-12, p. 1169–1206. doi : 10.3109/03639049209046327.
7. Klaumünzer, Martin, Laurent Schlur, Fabien Schnell et Denis Spitzer (2015). “Continuous Crystallization of ZnO Nanoparticles by Spray Flash Evaporation versus Batch Synthesis”. In : *Chemical Engineering & Technology* 38.8, p. 1477–1484. issn : 1521-4125. doi : 10.1002/ceat.201500053.
8. Krukonis, Val (1984). “Supercritical Fluid Nucleation of Difficultto-Comminute Solids”. In : *Annual Meeting - American Institute of Chemical Engineers*. cited By (since 1996)0.
9. Limpert, Eckhard, Werner A. Stahel et Markus Abbt (2001). “Log-normal Distributions across the Sciences : Keys and Clues”. In : *BioScience* 51.5, p. 341–352. issn : 0006-3568. doi : 10.1641/0006-3568(2001)051[0341:LNDATS]2.0.CO;2.
10. Matson, D.W., J.L. Fulton, R.C. Petersen et R.D. Smith (1987a). “Rapid expansion of supercritical fluid solutions : solute formation of powders, thin films, and fibers”. In : *Industrial and Engineering Chemistry Research* 26.11. cited By (since 1996)248, p. 2298–2306.
11. Matson, D.W., R.C. Petersen et R.D. Smith (1987b). “Production of powders and films by the rapid expansion of supercritical solutions”. In : *Journal of Materials Science* 22.6. cited By (since 1996)56, p. 1919–1928.
12. “Method for producing cocrystals by means of flash evaporation” (2016). WO 2016001445. B. Risse et D. Spitzer. WO Patent App. PCT/EP2015/065,335.

13. Ozaki, Shunsuke, Ikuo Kushida, Taro Yamashita, Takashi Hasebe, Osamu Shirai et Kenji Kano (2013). "Inhibition of crystal nucleation and growth by water-soluble polymers and its impact on the supersaturation profiles of amorphous drugs". In : *Journal of Pharmaceutical Sciences* 102.7, p. 2273–2281. ISSN : 00223549. DOI : 10.1002/jps.23588.

14. Patel, Dhaval D. et Bradley D. Anderson (2015). "Adsorption of Polyvinylpyrrolidone and its Impact on Maintenance of Aqueous Supersaturation of Indomethacin via Crystal Growth Inhibition". In : *Journal of Pharmaceutical Sciences* 104.9, p. 2923–2933. ISSN : 1520-6017. DOI : 10.1002/jps.24493.

15. Posteraro, Dany, Jonathan Verrett, Milan Maric et Phillip Servio (2015). "New insights into the effect of polyvinylpyrrolidone (PVP) concentration on methane hydrate growth. 1. Growth rate". In : *Chemical Engineering Science* 126, p. 99–105. ISSN : 0009-2509. DOI : http://dx.doi.org/10.1016/j.ces.2014.12.009.

16. "Préparation de nanoparticules par évaporation flash" (2013). WO2013117671 A1. B. Risse, D. Hassler et D. Spitzer.

17. Risse, Benedikt (2012). "Continuous crystallization of ultra-fine energetic particles by the Flash-Evaporation Process".

18. Risse, Benedikt, Denis Spitzer, Dominique Hassler, Fabien Schnell, Marc Comet, Vincent Pichot et Hervé Muhr (2012). "Continuous formation of submicron energetic particles by the flash-evaporation technique". In : *Chemical Engineering Journal* 203, p. 158–165. ISSN : 1385-8947. DOI : 10.1016/j.cej.2012.07.032.

19. Sheth, Pratik, Harpreet Sandhu, Dharmendra Singhal, Waseem Malick, Navnit Shah et M. Serpil Kislalioglu (2012). "Nanoparticles in the Pharmaceutical Industry and the Use of Supercritical Fluid Technologies for Nanoparticle Production". In : *Current Drug Delivery* 9.3, p. 269–284. DOI : 10.2174/156720112800389052.

20. Spitzer, D., B. Risse, F. Schnell, V. Pichot, M. Klaumünzer et M. R. Schaefer (2014). "Continuous engineering of nano-cocrystals for medical and energetic applications". In : *Scientific Reports* 4. DOI : 10.1038/srep06575.

21. Stein, W. A. (1973). "Spray Drying. An Introduction to Principles, Operational Practice and Applications". In : *Chemie Ingenieur Technik* 45.13, p. 906–907. ISSN : 1522-2640. DOI : 10.1002/cite.330451311.

22. Sun, Changquan Calvin (2013). "Cocrystallization for successful drug delivery". In : *Expert Opinion on Drug Delivery* 10.2, p. 201–213. ISSN : 1742-5247. DOI : 10.1517/17425247.2013.747508. pmid : 23256822.

Chapter 1

Explosives and Characterization

1.1 Overview

The term "energetic material" encompasses any type of material (composite, polymer, organic...) which can rapidly release energy by a violent reduction-oxidation reaction. A stimulus like shock, friction, heat or electrostatic discharge triggers the local reaction; then it propagates through the material creating a reaction front. That decomposition usually produces large amount of gas and heat, and three modes of decompositions can be identified mainly from the velocity of the redox reaction front.

The **combustion** is the slowest mode of decomposition (mm/s - m/s), and is characterized by the complete oxidation of all intermediate products. The combustion requires so large amounts of oxygen, that oxygen is mainly provided by the environment. Faster than the combustion, the **deflagration** (m/s - km/s) occurs when the released heat propagates beyond the reaction front and so facilitates the redox reaction. Deflagration can be considered as a form of burning, but in contrast to pure combustion, the phenomena is self-propagating and does not require an external source of oxygen. Supersonic explosions created by high explosives are known as **detonations** which travel via supersonic shock waves (> km/s); that wave, and not the thermal front of reaction, propagates the reaction. Transition from one mode to another can happen intentionally or not; without compaction or enough ignition energy, the material may only burn (1,3,5-trinitroperhydro-1,3,5-triazine (RDX) in the C4 composition burns at 2 cm/s whereas it detonates at 8.75 km/s), or when accidentally confined, a propellant detonates.

Therefore, depending on their decomposition mode and their pyrotechnic properties, energetic materials can be sorted in three classes: propellants, primary explosives (or initiating explosives) and secondary explosives (or base

charge). Materials such as Ammonium Nitrate (AN) or Ammonium Perchlorate (AP) are sometimes classified as tertiary explosives, which are even less sensitive and energetic. From a chemical point of view, explosives are intrinsic energetic materials in which usually nitro or nitramine groups react with the closest carbon available inside the same molecule; on the contrary, thermites are a physical mix of an oxidizer (e.g.: Fe_3O_4) and a reducing agent (e.g.: Al) (Comet et al. 2016).

Used in gunpowder, solid-fuel rockets and mining industry, **propellants** are deflagrating explosives with the specificity of producing high amount of gases, usually to get a thrust. **Primary explosives** detonates through the influence of a moderate external stimulus; less sensitive detonative ones are called secondary explosives. The initiation of **secondary explosives** generally requires the shock wave energy from a primary explosive: such succession of explosive event is called explosive train involved in detonators for instance. All explosives having a higher sensitivity than pentaerythritol tetranitrate (PETN) can be considered as primary, and the less sensitive ones as secondary explosives. The sensitivity to impact and friction of PETN is 3 J–4 J and 60 N, respectively. The notion of sensitivity for energetic materials is discussed in Section 1.3.2.

1.2 Organic Secondary Explosives

This work was focused on a very few organic explosives, in order to carefully study the crystallisation parameters independently from the chemical compound. The first one, RDX, is widely used in civilian and military applications, and serves as a reference energetic material in scientific studies. Both octahydro-1,3,5,7-tetranitro-1,3,5,7-tetrazocine (HMX) and 2,4,6,8,10,12-hexanitro-2,4,6,8,10,12-hexaazaisowurtzitane (CL-20) are studied here due to their ability to cocrystallise; a cocrystal is simply a multicomponent molecular crystal, owning a unique crystalline structure with each compound included in the unit cell. The following short overview presents their structural characteristics and their physical and pyrotechnical properties.

1.2.1 1,3,5-trinitroperhydro-1,3,5-triazine (RDX)

The 1,3,5-trinitroperhydro-1,3,5-triazine is also found under the following denominations cyclo-1,3,5-trimethylene-2,4,6-trinitramine, 1,3,5-trinitrohexahydro--s-triazine, cyclotrimethylenetrinitramine, hexahydro-1,3,5-trinitro-s-triazine, trimethylenetrinitramine, T 4, cyclonite, hexogene, and RDX. The most common and widely accepted one is the acronym RDX whose origin is surprisingly not known for sure; probably from its first secret code “Research Department

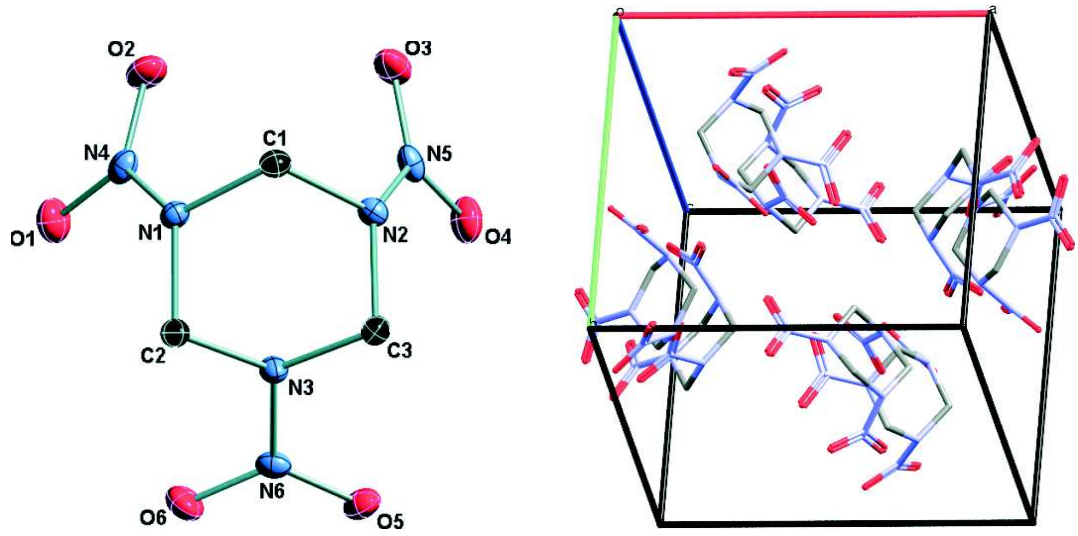

(a) Molecule of RDX with thermal ellipsoids drawn at 50 % probability level (Hakey et al. 2008)

(b) Crystallographic cell of α-RDX

Figure 1.1 – RDX visual representations. H atoms have been omitted for clarity.

Explosive". RDX is probably the most important high-brisance explosive from the Second World War to nowadays.

α-RDX is the stable form of RDX for all temperatures at 1 atm; however, at high pressures, several polymorphs of RDX exist and have been recently discovered : γ-RDX is stable above 3.8 GPa between room temperature and 225 °C, and above that temperature β-RDX lies from 2.5 GPa–7 GPa (Hakey et al. 2008). A δ form has been reported but not resolved (Ciezak et al. 2007), and the dense ε-RDX formed at 3.6 GPa can be recovered at 1 atm at 150 K–220 K (Millar et al. 2010).

RDX is soluble in acetone, dimethylsulfoxide (DMSO), DiMethylFormamide (DMF), N-Methyl-2-pyrrolidone (NMP) etc. (Sitzmann et al. 1973), sparingly soluble in ether and ethanol, almost insoluble in water (16, 35-52 and 123 mg/L at 5, 20 and 40 °C (Boyer et al. 2007)) and totally insoluble in n-hexane (PANT et al. 2013). Cyclohexanone, nitrobenzene and glycol are solvents at elevated temperatures (Sitzmann et al. 1973).

The RDX used in this work is provided by Eurenco, labelled as M5 and used as is, without further purification; the mean particle size is 6.8 µm.

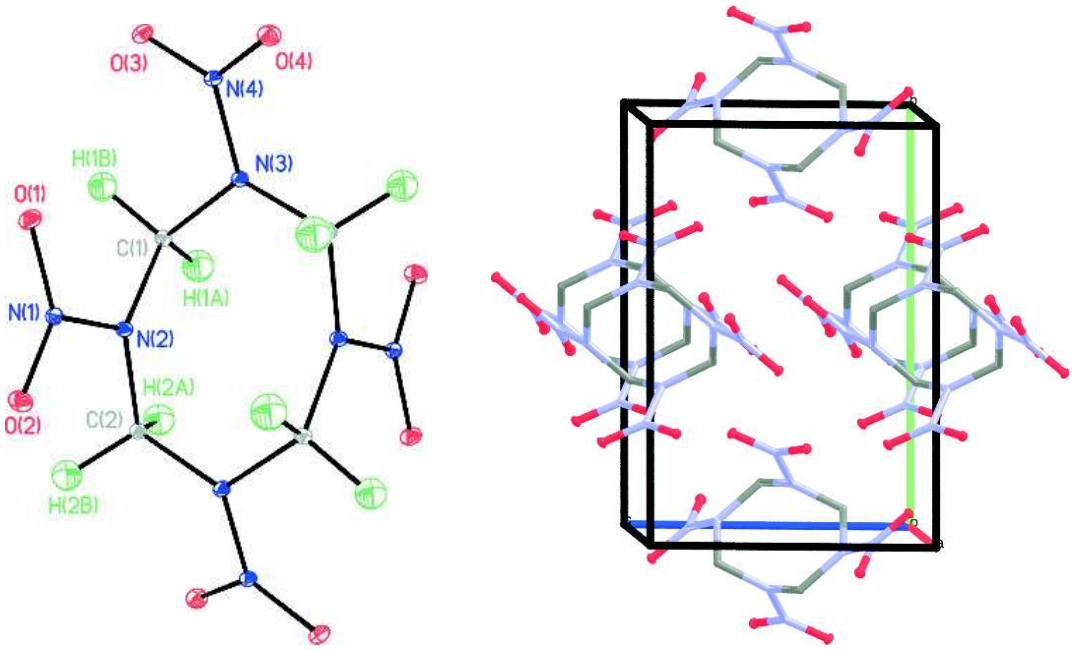

(a) Molecule of HMX with thermal ellipsoids drawn at 50 % probability level at 20 K (Zhurova et al. 2007)

(b) Crystallographic cell of β-HMX

Figure 1.2 – HMX visual representations. H atoms have been omitted for clarity.

1.2.2 Octahydro-1,3,5,7-tetranitro-1,3,5,7-tetrazocine (HMX)

The octahydro-1,3,5,7-tetranitro-1,3,5,7-tetrazocine is also found under the following denominations cyclotetramethylene tetranitramine, homocyclonit(e), octogen but is commonly named HMX. HMX was first discovered as a by-product of RDX by the Bachmann process (Bachmann et al. 1949). Therefore, like RDX, the HMX acronym may refers to High Melting eXplosive, Her Majesty's eXplosive, High-velocity Military eXplosive, or High-Molecular-weight RDX. Due the high density of its stable β phase, its high melting point and its detonation performances, the HMX is a prime secondary explosive. HMX exhibits three distinct polymorphic forms – α (105 °C–160 °C), β and δ (160 °C-m.p.) – and a γ hydrated form metastable existing at all temperatures at 1 atm.

HMX solubilities are even worst when compared to RDX; HMX is soluble in DMSO but not in DMF nor NMP, and is slightly soluble in acetone (2.8 wt% at Standard Ambient Temperature and Pressure as a temperature of 298.15 K and an absolute pressure of 100 kPa (1 bar) (SATP)).

1.2.3 2,4,6,8,10,12-hexanitro-2,4,6,8,10,12-hexaazaiso-wurtzitane (CL-20)

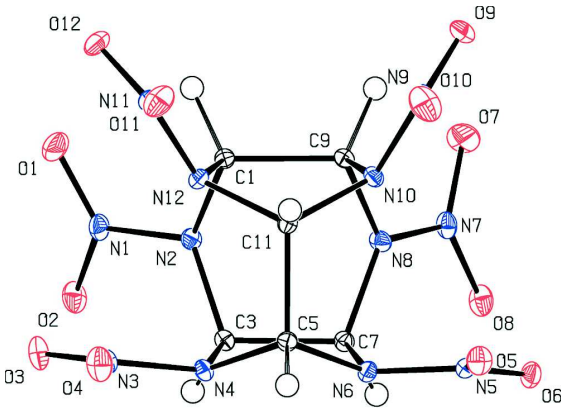

(a) Molecule of CL-20 with thermal ellipsoids drawn at 50 % probability level at 20 K (Meents et al. 2008)

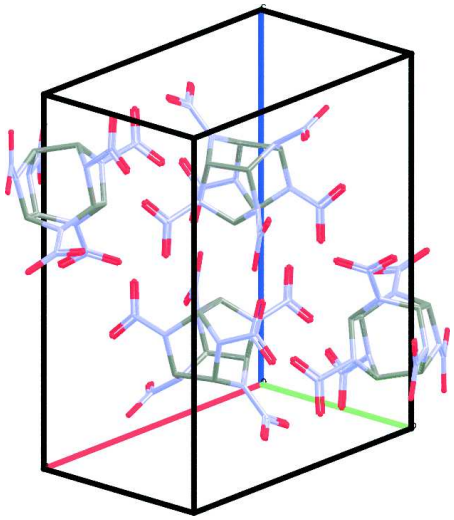

(b) Crystallographic cell of ε-CL-20

Figure 1.3 – CL-20 visual representations. H atoms have been omitted for clarity.

2,4,6,8,10,12-Hexanitro-2,4,6,8,10,12-hexaazaisowurtzitane is also found under the following denominations hexanitrohexaazaisowurtzitan(e), 2,4,6,8,10,12-(hexa-nitro-hexaaza)-tetracyclododecane, HNIW or CL-20. CL-20 is the most widely used acronym and comes from the Naval Air Weapons Station (NAWS) China Lake facility where it was first produced by Nielsen (1997). CL-20 can be considered as a potent explosive due to its high density and high detonation velocities, but the difficult detection of the decomposition gas and the high oxygen balance place the CL-20 as a remarkable propellant too.

CL-20 exhibits also a high degree of polymorphism: four forms (α, β, γ, ε) have been observed at SATP conditions (Foltz et al. 1994; Russell et al. 1993) and two (δ, ζ) under pressure. The ζ-CL-20 comes from the $\gamma \rightarrow \zeta$ transition at 0.7 GPa. The stability of different phases can be sorted as $\varepsilon > \gamma > \alpha > \beta$ and is schematically described in Figure 1.4a p. 36. However, the hydration of CL-20 plays an important role at intermediate pressures and temperatures in the stability of the α form as described in Figure 1.4b p. 36.

The solubility of ε-CL-20 is good at SATP in acetone (100 wt%), ethyl acetate (45 wt%) and tetrahydrofuran (THF) but slight in aromatic or organochloride

solvents (von Holtz et al. 1994). The ε-CL-20 is the phase of interest due the highest density (ρ_ε = 2.04 > ρ_β = 1.98 > ρ_α = 1.97 > ρ_γ = 1.92 g/cm^3) and the highest detonation velocity (v_ε = 9660 > v_β = 9380 m/s (Dumas 2003)).

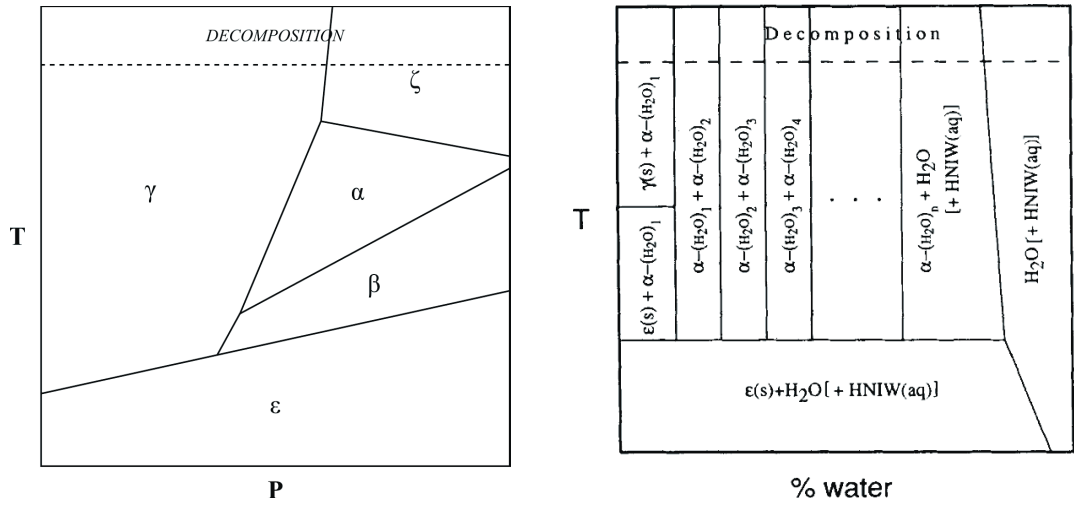

(a) Pressure-Temperature schematic diagram of CL-20 crystallographic phases.

(b) Dependancy in hydration and tempreature of CL-20 polymorphs.

Figure 1.4 – CL-20 polymorphism adapted from Foltz et al. (1994).

1.2.4 Cocrystal CL-20:HMX 2:1

Bolton et al. (2012) first reported the crystallisation and characterization of the cocrystal CL-20:HMX with a molar ratio of 2:1. An impact sensitivity as low as β-HMX was measured while a higher detonation velocity than β-HMX was predicted. Those results are representative of the advantage of crystallisation as a solid state engineering strategy for improved energetic material. This approach is well know for pharmaceutical compounds (Fleischman et al. 2003; Schultheiss et al. 2011; Vishweshwar et al. 2006) and is also emergent for optic (Sun et al. 2006; Yan et al. 2011) and semiconductors (Sato et al. 2012).

1.3 Analytical Methods

1.3.1 Classic Material Characterization Methods

X-Ray Difraction (XRD) The periodicity of a crystal can be investigated by using a X-ray beam. In X-Ray Difraction (XRD), the incident beam penetrates through the matter within several hundreds of microns; the photons interact

Characteristics	α-RDX	β-HMX	ε-CL-20
Colour	colourless	colourless	colourless
Molecular formula	$C_3H_6N_6O_6$	$C_4H_8N_8O_8$	$C_6H_6N_{12}O_{12}$
Molecular weight	222.1	296.2	438.19
Space Group	$Pbca$	$P2_1/c$	$P2_1/c$
CCDC IDs	CTMTNA, 03, 08-12	*NA*	PUBMUU 02, 05, 12-22
COD IDs	5000148, 2019354-9, 2219089	4110146	2300020-4
Stability range at 1 atm	RT to 222.1	RT to 102-150°C	RT to 56.5°C
Energy of formation	+401.8 kJ/kg	+353.6 kJ/kg	+1005.3 kJ/kg
Enthalpy of formation	+301.4 kJ/kg	+253.3 kJ/kg	+920.5 kJ/kg
Oxygen balance	–21.6%	–21.6%	–10.95%
Nitrogen content	37.84%	37.83%	38.3%
Volume of explosion gases	903 l/kg	902 l/kg	*NA*
Heat of explosion (H_2O liq.)	5647 kJ/kg	5249 kJ/kg	6314 kJ/kg
Heat of explosion (H_2O gas)	5297 kJ/kg	5599 kJ/kg	6084 kJ/kg
Heat of detonation (H_2O liq.)	6322 kJ/kg	6197 kJ/kg	*NA*
Specific energy	1375 kJ/kg	1367 kJ/kg	1323 kJ/kg
Density	1.82 g/cm3	1.91 g/cm3	2.04 g/cm3
Melting point	204 °C	280 °C	> 195 °C (decomposition)
Detonation velocity, confined	8750 m/s at 1.76 g/cm3	9100 m/s at 1.9 g/cm^3	9660 m/s (Dumas 2003)
Impact sensitivity	7.4 N.m	7.4 N.m	4 N.m
Friction sensitivity	120 N	120 N	48 N

Table 1.1 – Characteristics of the most common crystalline forms of RDX (Krause 2005; Meyer et al. 2008; Miller et al. 2001), HMX (Krause 2005; Meyer et al. 2008; Miller et al. 2001) and CL-20 (Krause 2005; Meents et al. 2008; Meyer et al. 2008; Nair et al. 2005)

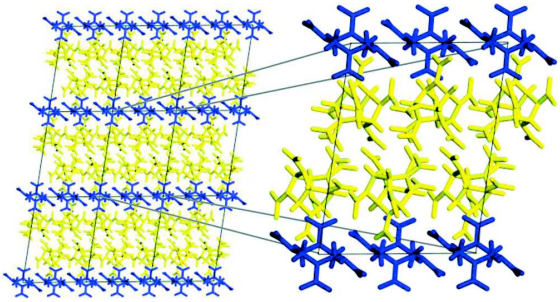

(a) Layers of CL-20 in yellow and HMX in blue in the co-crystal from CL-20 and HMX (CL-20:HMX) 2:1

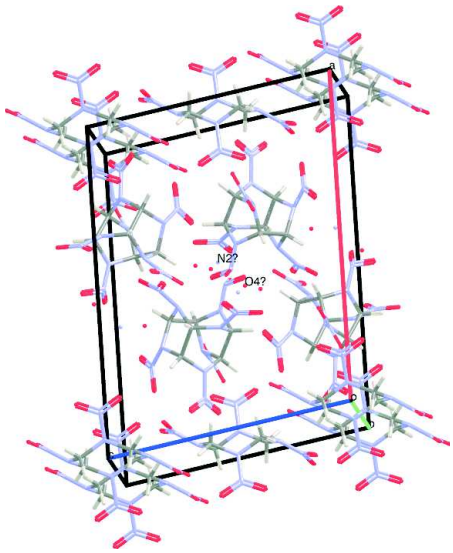

(b) Crystallographic cell of CL-20:HMX

Figure 1.5 – CL-20:HMX visual representations (Bolton et al. 2012). H atoms have been omitted for clarity.

with the electrons of the material which oscillate at the same frequency and scatter the electromagnetic waves. Waves scattered from different points in space travel different paths and consequently exhibit a phase shift, therefore causing destructive interferences. The detectable X-ray emissions in a crystalline sample come from the resonance of ordered atoms in the crystallographic cell at a specific angles. The Bragg's law determines those specific directions where the interferences are constructive: $2d \sin\theta = n\lambda$ where d is the spacing between diffracting planes, θ the incident angle, n an integer, and λ the wavelength of the incident beam. The rotation of both the emitter and detector allows the recording of the diffracted signal depending on the angle θ in a unique diffractogram. The powder diffraction pattern provides various information of the crystalline structure as summarized in Figure 1.6 p. 39.

Powder X-Ray Diffraction was obtained on a D8 Advance (Bruker), with a LynxEye detector and a copper source with no filtering of the second wavelength. Please note that hkl indexes mentioned in this work are made according to the standardization of the IUCr; so previous publications mentioning abc indices are quoted here as cab. Figure 5.7 p. 155 and crystallographic studies have been made using the open-source software VESTA (Momma et al. 2011).

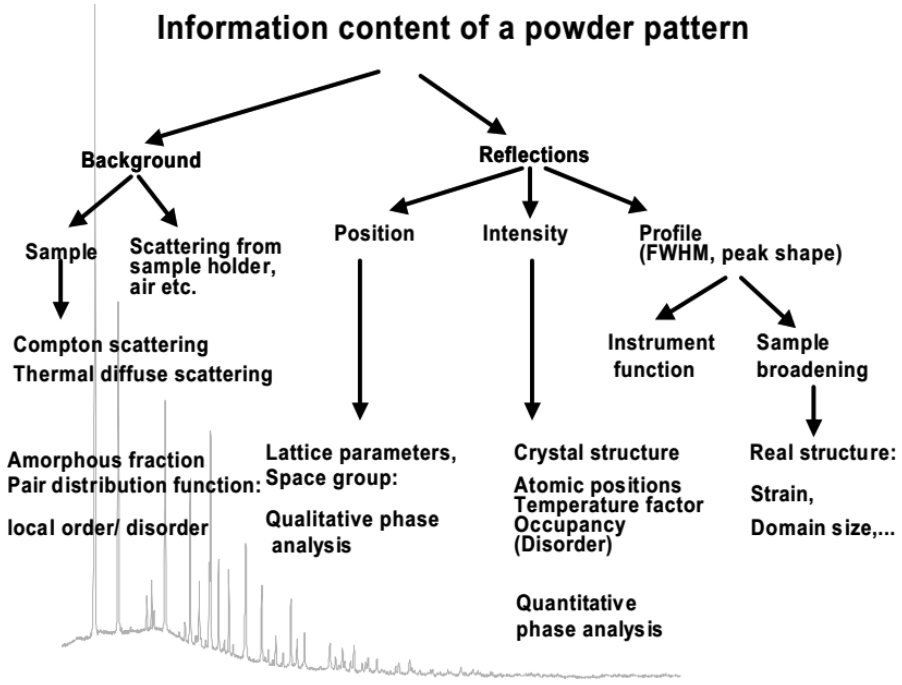

Figure 1.6 – Diagram highlighting the information available from the interpretation of an XRD pattern (Dinnebier 2001).

Scanning Electron Microscopy (SEM) allows the direct imaging of a sample at micron or nano scale with a focused beam of electrons. When interacting with the sample, both photons and electrons are emitted giving various information from the sample: X-rays for thickness and also qualitative and quantitative chemical information, secondary electrons for topology, Auger electrons for chemical information, catholuminescence for electrical information and primary backscattered electrons to determine the atomic number and the topography. Secondary electron detector and back-scattered detector are standard equipments for a Scanning Electron Microscopy (SEM). To avoid noisy interactions with gaseous molecules, the imaging occurs under vacuum. For conventional imaging in the SEM, the sample's surface must be electrically conductive and electrically grounded to prevent any accumulation of electrostatic charges.

Sizes measurements were made manually over at least one thousand particles per sample within the software Gwyddion (Nečas et al. 2012) then a log-normal fit was applied on the particles size distribution (PSD): geometrical mean and multiplicative standard deviation (dimensionless) (Limpert et al. 2001) are reported here and written as "mean(SD) unit". Gaussian fitting is in poor accordance; droplets size distributions of aerosols usually have a log-normal shape (Zender 2008) and colloids can be found also to follow a log-normal

distribution (Limpert et al. 2001).

Brunauer–Emmett–Teller theory (BET) Brunauer–Emmett–Teller theory (BET) theory explains the multilayer adsorption of gas molecules on solids. The BET apparatus measures the amount of gas adsorbed across a wide range of relative pressures at liquid nitrogen temperature (77 K) and applies the BET theory to calculate the specific surface area, the pore size distribution and the pore volume. The adsorption and desorption isotherms also return some information about the type of porosity of the sample. Decreasing the molecular size of the adsorbed gas used – for instance from nitrogen to krypton– increases the precision but limits the measurement to lower surface area ($\sim 1\,m^2/g$ for krypton).

Atomic Force Microscopy (AFM) The development of nano-technology started with the invention of the STM and quickly followed by the Atomic Force Microscopy (AFM) in the early 80's at the IBM Zurich Research Laboratory (Binnig et al. 1986, 1983, 1982). Specifically, AFM allows the visualization at the atomic scale of non-conductive samples by a vibrating cantilever with a tip at its end. When the tip is interacting with the surface of the sample (Van der Waals forces, dipole-dipole interactions, electrostatic forces, etc.), the amplitude of the cantilever oscillation decreases. Therefore, this change is used to detect the proximity of the surface: the altitude of the cantilever is regulated to keep a constant amplitude oscillation thus to give the topographic image of the sample surface. This mode of acquisition is called tapping mode and the phase of the cantilever oscillation is also recorded. Phase changes occur when heat is dissipated by the cantilever, allowing the detection of variation in hardness or adhesive properties.

Dynamic Light Scaterring (DLS) When a light source passes through a colloid, particles with a size smaller than the wavelength scatters the light in all direction. Just as in XRD, the diffraction comes from different positions in space and exhibits constructive or destructive interferences. Due to the Brownian motion, the optical path length is constantly changing in time, so the resulting noisy diffracted pattern changes in time and with the size of the particles. The intensity fluctuations from this motion, namely the computed intensity correlation function, is analysed to provide the diffusion coefficient of the particles. Then an hydrodynamic radius is calculated from the Stokes-Einstein equation

$$D = \frac{k_B T}{6\pi \eta r} \tag{1.1}$$

where η is the dynamic viscosity, r the radius of the assumed spherical particle, k_B the Boltzmann's constant, and T the absolute temperature.

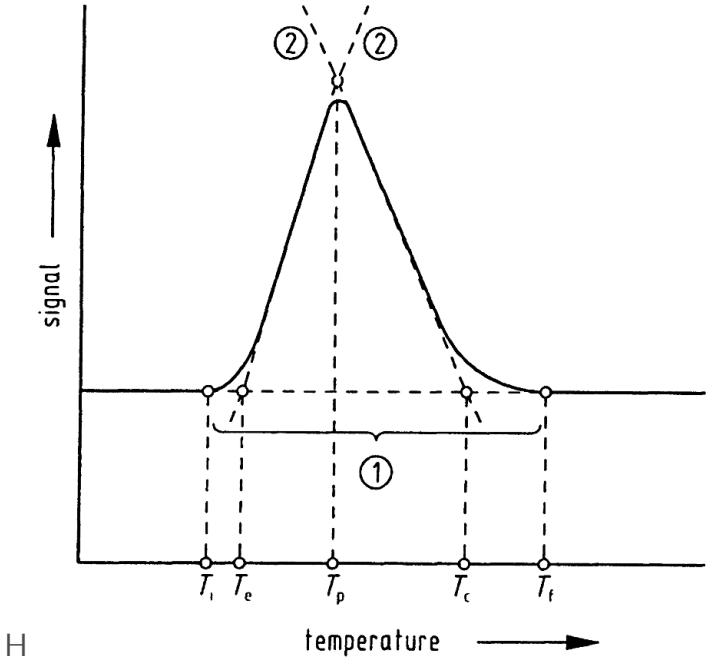

Figure 1.7 – DSC peak analysed from Höhne et al. (2003): (1) baseline (interpolated), (2) auxiliary lines, T_i initial peak temperature, T_e extrapolated peak onset temperature, T_p peak maximum temperature, T_c extrapolated peak offset temperature, T_f final peak temperature.

Differential Scanning Calorimetry (DSC) Differential Scanning Calorimeters measure the change of the differential heat flow rate between the sample and the reference while regulating the temperature. A few milligrams of the sample are placed in a hermetically closed gold crucible. An identical empty pan is used as reference. The rate of heating heavily influences the peak shapes and resolutions; keeping a small rate is of interest to separate peaks, especially for energetic materials having the melting point close to their decomposition (e.g. RDX), but too small rate will result in broad peaks of small intensities overlapping each others. So the position of the peak maximum changes with the heating rate but also with the thermal conductance and the mass of the sample. Only the extrapolated peak onset temperature is relatively independent of experimental parameters (Höhne et al. 2003).

Differential Scanning Calorimetry (DSC) was performed with a Q-1000 DSC, from TA instruments, under N_2 flow of 50 ml/min at 2 °C/min ; the low thermal ramp is a compromise between peak separation and intensity. Extrapolated temperatures were obtained using the tangent technique as described by Höhne

et al. (2003) in Figure 1.7. The exothermic energy released by the decomposition is calculated from the integration of the heat flow over the temperature range of the peak.

Infrared (IR) Spectroscopy Bonded atoms in molecules are in motion between each other; each motion is periodic with a unique frequency and different modes of molecular vibration can be distinguished such as stretching and bending. When a molecule is hit by a radiation having the same energy of the transition energy of a vibration –the resonant frequency–, that radiation is absorbed. Since the related wavelengths are in the middle-infrared, between 10 et 4000 cm^{-1}, the technique is named infrared spectroscopy (IR). The energy from the resonant frequency depends on the molecular potential energy surfaces, the masses of the atoms involved and the associated vibronic coupling, therefore allowing the identification of the chemical groups of the compounds and their interactions. However, the transition has to change the dipole moment of the molecule to be "IR active", unlike the stretching of C-C bond in ethane for instance. Furthermore, the greater the dipole is, the greater the absorbance intensity will be. The method used to measure infrared absorption and emission spectra is the Fourier Transform Infrared Spectroscopy (FTIR); the instrument uses a Michelson interferometer coupled with a Fourier transformation of the interferogram in order to obtain the final spectrum.

Nuclear Magnetic Resonance (NMR) Spectroscopy NMR occurs when the nucleus of certain atoms is placed in a static magnetic field and an additional oscillating magnetic field. Only some atoms can exhibit NMR: nuclei possessing a not null spin, more usually a spin of 1/2 such as in ^{1}H, ^{13}C, ^{19}F and ^{31}P. Schematically, the transition between the two possible energy states of such nuclei is triggered when the frequency of the oscillating magnetic field matches that transition energy: such frequencies are typically in the radio frequency range for magnetic fields or around 20 T. NMR spectroscopy detects and records that magnetic resonant absorption.

1.3.2 Explosive Specific Characterization Techniques

The determination of the sensitivity of an explosive is the prime set of characterizations. Not surprisingly, pyrotechnic scientists put safety first, especially when it comes to explore new materials based on the most devastating explosives. Various methods of evaluation exist depending on the stimuli, the mass of the studied material and the application. At the small scale of a laboratory, only

three techniques are of interest based on the three main stimuli: impact, friction and electrostatic discharge.

(a) Julius Peters Bundesanstalt für Materialprüfung (BAM) Fall-Hammer for impact test

(b) Julius Peters BAM Machine for friction test

(c) OZM Research Electrostatic Discharge (ESD) 2008 apparatus

Figure 1.8 – Apparatuses for testing the mechanical and electric sensitivity at small scale, in use at NS3E.

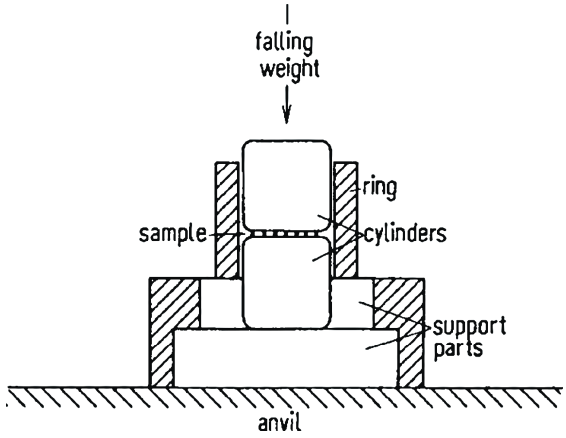

Figure 1.9 – Sample holder for BAM Fall-Hammer (Meyer et al. 2008).

Impact The small scale drop-hammer impact sensitivity test is described in the international guidelines of the UNECE (test code 3(a)(ii) (*UN Manual of*

Tests and Criteria 2016)) and in the French norm NFT 70-500. Historically the fall-hammer method was modified by the German BAM, in order to obtain better reproducible values (Meyer et al. 2008). A cylindrical spoon measures 40 mm^3 of energetic material which is placed between two cylindrical pistons maintained by a ring (Figure 1.9 on the left). Those cylinders and rings are constituting the sample holder and are made of steel with controlled hardness, dimensions, surface roughness and flatness; they are renewed for each falling test procedure. If the sample is a powder or a paste, the upper cylinder is slightly pressed into the charged confinement device. The sample holder is set below a vertical rail guiding a free movable weight (Figure 1.8a p. 43). Two masses of 1 and 5 kg are available, falling from a height of 15 cm to 100 cm, allowing the measurements over a range of energy from 1.56 J to 50 J. The energy is simply calculated from the gravitational potential energy $e = mgh$.

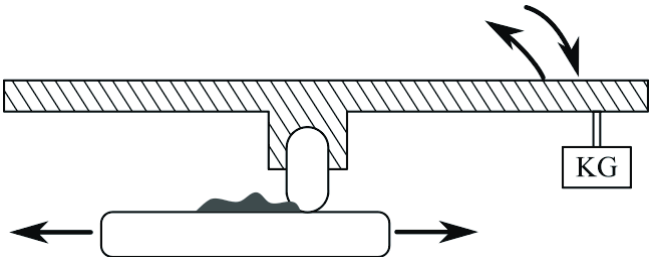

Figure 1.10 – Schematic principle of the BAM friction sensitivity test.

Friction The small scale sensitivity BAM test is described in the international guidelines of the UNECE (test code 3(b)(i) (*UN Manual of Tests and Criteria* 2016)) and in the French norm NF T70-503. Again, a cylindrical spoon measures about 10 mm^3 of energetic material which is placed on the surface of a roughened 25 mm × 25 mm × 5 mm porcelain plate. Then, on top of this plate is maintained a cylindrical porcelain peg (10 mm in diameter for a height of 15 mm), having a roughened spherical end (Figure 1.10). This peg is fasten on a rod which can be moved up and down. The pressure applied on the sample by the peg is set by a weight at the end of the lever: the nine different weights and six different mounting positions on the arm allows a measurement range from 5 N to 360 N.

Electrostatic Discharge (ESD) The sensitivity towards electrostatic discharge is a recent technique: for instance, the electrostatic stimuli are not investigated in the Manual of Tests and Criteria on the transport of dangerous goods of the UNECE (*UN Manual of Tests and Criteria* 2016). OZM Research manufactures the ESD 2008A tester used in several European laboratories. The sample is placed inside a small sacrificial plastic ring on top of the ground electrode; the volume of material is 7 mm^3. The electrostatic discharge is delivered from the top

by the main electrode; see Figure 1.11 on the left. The apparatus has several capacitors and also a potentiometer to change the tension; the energy delivered through the sample is simply $E = \frac{1}{2}CU^2$, where U is the tension in Volt and C the capacity in Farad.

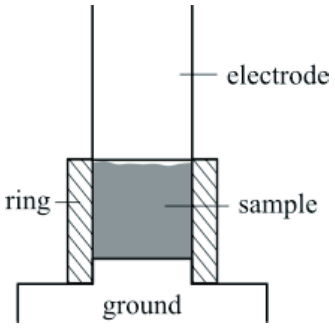

Figure 1.11 – Schematic principle of the OZM ESD 2008A tester.

Data Interpretation and Evaluation To define the reaction of a small scale sensitivity such as those mentioned above, the operator should carefully watch for any smokes, odour, sparking, popping noises, scorch marks etc. An instrumented version of the BAM fall-hammer called BIC records the overpressure and the lightening with four fibre optic detectors (Coffey et al. 1995). For instance, at the friction test, a simple odour is not significant enough to mark the event as a success full ignition, namely a Go event.

The highest stimulus level at which a predetermined number of No-Go events are observed without any Go occurring is the Threshold Initiation Level (TIL) value. For small scale (several grams) of energetic material, the predetermined number is often 6, although 10 or 20 can be used to increase the accuracy of the TIL level for hundred of grams. However, the TIL value does not refer to a zero probability of reaction. Wild and Von Collani extensively studied the statistical description of the reactivity of energetic materials; they demonstrated that the Bruceton method, which is still in use in other not-European laboratories, is lacking of accuracy and is not scientifically justified. In addition, they clearly showed that their Weibull model can discriminate and explain the sensitivity differences between coarse and fine samples (Wild et al. 2002a,b).

1.4 Submicron and nano explosives

In the past years, the outstanding properties of new nano-materials led the research in energetic materials to embrace this trend. The nano-structuring of classical explosives should enhance their properties and safety. Even if the term “nano” strictly refers to an object with at least one dimension under 100 nm, in this work on energetic material, the term “nano” will refer to nano and submicron-sized particles for the sake of readability, just like n-RDX is an abbreviation for nano or submicron particles of RDX. However, mean particle sizes are always given when available.

1.4.1 Properties and Challenges

The development of new energetic materials led to new synthesized molecules such as 1,3,3-trinitroazetidine (TNAZ), CL-20, Octanitrocubane (ONC), 1,1-diamino-2,2-dinitroethene (FOX-7), Ammonium DiNitramide (ADN) etc. Those newly available materials aim to achieve higher density, increase the processability and attain Insensitive Munitions (IM) characteristics; IM properties actually rely on the whole physic-chemistry of the system. Therefore, the development of powders with controlled particle sizes and morphologies and a well defined surface chemistry, is a whole new facet of the energetic materials largely unexplored at the submicron scale and below. Criteria that are advantageous for new energetic materials include the following:

- high decomposition temperature
- low sensitivities
- no phase transitions under compression or depression
- no autocatalytic decomposition
- no voids from solvents or gas
- mechanical behaviour independent from temperature
- good ratio availability/cost
- easy processing

Compression of gaseous inclusions, cavities and voids, deformation, frictional heating, inter-crystalline shearing and spark discharges are initiation processes which can cause areas of an energetic material to warm up to several hundred Kelvin: these areas are called hot-spots and are deflagration or detonation origins if they reach a critical temperature. Tarver (Tarver et al. 1996) calculated for HMX the critical temperature of different sized hot-spots. For a 2 µm sized hot-spot he calculated a critical temperature of 985 K, whereas the critical temperature for a 0.2 µm sized hotspot already rises to 1162 K.

Risse (Doctoral Thesis 2012) measured a noticeable desensitization towards initiation by friction and electrostatic discharge for n-RDX crystallised by Spray Flash Evaporation (SFE), compared to the raw material (Table 1.2, p. 47). The noticeably lower sensitivity towards friction can be based on the self-lubricating effect, as small particles will tend to occupy small interstices instead of breaking. Sensitivity measurements were also performed on Hexolite, which showed a clear desensitization of the nano-structured explosive (Table 1.3, p. 47).

RDX	Impact [J]	Friction [N]	ESD [mJ]
M5 (raw material)	>3.52	160	120
nano-structured	>3.52	>360	270

Table 1.2 – Sensitivity towards impact, friction and ESD of micron-sized and nano-structured RDX (Doctoral Thesis Risse 2012).

Hexolite	Impact [J]	Friction [N]	ESD [mJ]
micro	6	54	353,6
nano	25,06	72	436,6

Table 1.3 – Comparison of the sensitivity levels of micro Hexolite with those of a nano-sized Hexolite (Doctoral Thesis Risse 2012).

Using a sonocrystallisation process, Bayat and Zeynali (Bayat et al. 2011) succeeded in the preparation of n-CL-20 which was less sensitive towards friction, impact and electrostatic discharge (Table 1.4, p. 47).

Particle size [µm]	Impact [cm]	Friction [kg]	ESD [J]
15	25	6,4	45
0,095	55	No reaction	60

Table 1.4 – Comparison of the sensitivity levels of micro and nano CL-20 (Bayat et al. 2011).

Fathollahi et al. (2007) have studied the particle size effects on thermal decomposition on HMX: as the particle was getting smaller, temperature and the activation energy were decreasing.

However those trends are not always observed. Crystallised from Rapid Expansion of Supercritical Solutions (RESS), several nano RDX lots have been tested by (Stepanov et al. 2011); if both 500 nm and 200 nm RDX are less sensitive toward impact than milled 4 µm RDX, the 200 nm lot is substantially more sensitive than the 500 nm one. As it can be seen in Figure 1.12 p. 48 that minimum of sensitivity to impact is confirmed when coating the powders with a

binder; however that confirmation might reveal that the trend is more due to the intrinsic bulk properties of the particles instead of their surface.

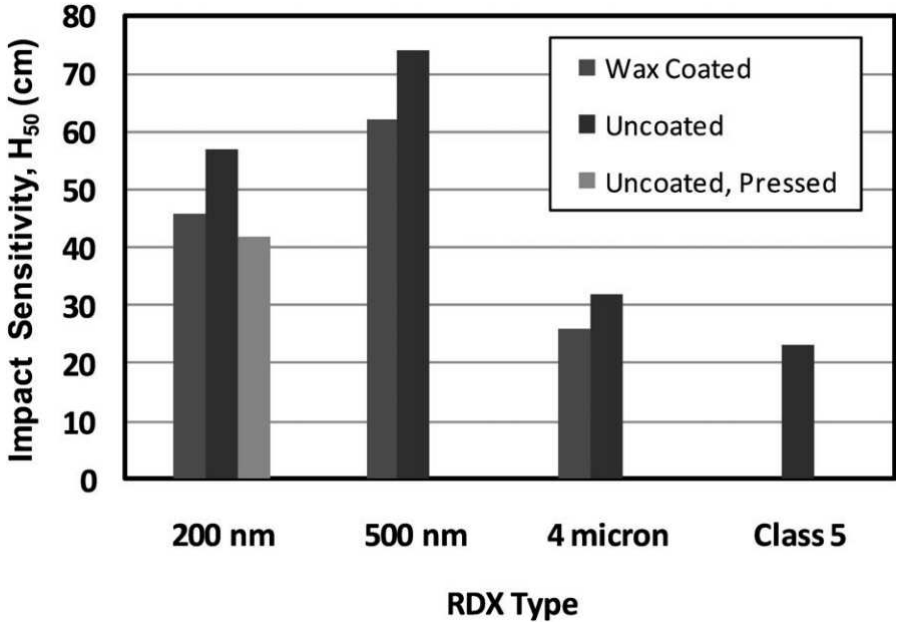

Figure 1.12 – Sensitivities of RDX with various Particle Size Distribution (PSD) (Stepanov et al. 2011).

Beside safety, other improvements can emerge from the nano scale; critical diameter, tunable detonation velocity, delay before the detonation steady state etc. may be improved by the drastic grain size reduction. Energetic nanocomposites are also promising materials improved by a more intimate mixing. Liu Jie et al. (Liu et al. 2014) show that detonation velocities of PBX composition from their milled n-RDX and n-HMX are slightly better while being significantly safer. The burning rates of nitrocellulose was also improved by Zhang et al. (2014) due to the formation of submicron spheres. Recently, Comet et al. (2015) proved that energetic nanocomposites can easily replace the hazardous primary explosives to initiate a secondary explosive: 500 nm n-RDX from SFE were mixed with a nano thermite to initiate the detonation of PETN. The Flame Propagation Velocity (FPV) of composites made of n-WO_3/n-Al/n-RDX can be tuned from 0.2 km/s to 3.5 km/s through their explosive content; in the same conditions, n-WO_3/n-Al with µ-RDX exhibit unstable regimes from 187 m/s to 733 m/s, whereas the n-WO_3/n-Al/n-RDX composite deflagrates at a constant velocity of 2529 m/s. Those results and other unpublished ones of our laboratory confirm the drastic reduction of the critical diameter with the decrease of particle size.

1.4.2 Challenges of the characterization of energetic materials

Some of the characterization techniques previously described in Section 1.3.1 p. 36 are difficult to apply on nano energetic material, due to their sensitivity toward heat, or toward vacuum, or their organic nature. Molecular solids are by their nature called soft matter, due to the type of bonds involved to create their crystalline structure: the dipole forces holding the molecules together are weaker than the covalent bonds in metals or the ionic bonds in ionic crystals.

XRD Solid organic explosives are molecular crystals: the crystallographic positions are occupied by the molecule and not just a single atom. XRD diffraction of molecular crystals produces much more reflections –up to thousands– for the very complex protein crystals. For instance in Figure 1.13, the XRD pattern of CL-20 exhibits much more diffraction lines than the magnetite Fe_2O_3. Moreover,

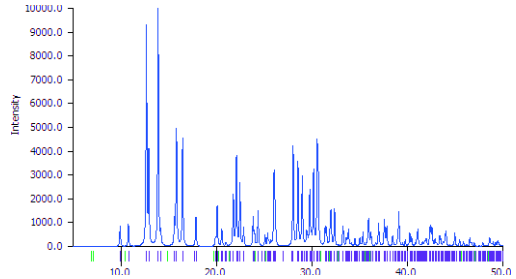

(a) CL-20 diffraction pattern from Meents et al. (Meents et al. 2008).

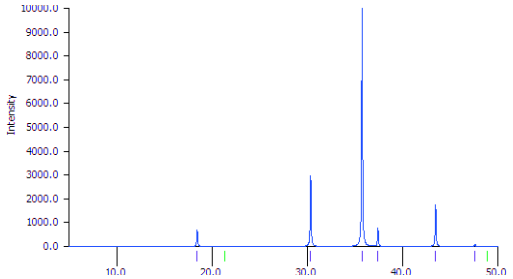

(b) magnetite diffration pattern from WH. Bragg (Bragg 1915).

Figure 1.13 – Examples of computer generated XRD patterns, both with the same broadening.

at the nano scale, the diffraction peaks are broadened. Line broadening in diffraction stems from instrumental and physical broadening; the latter is due to size effect and internal strain inside the lattice. Young and Desai (Young et al. 1989) described size broadening β_{size} as a Gaussian contribution of the Scherrer's equation:

$$\beta_{size} = \frac{\lambda K D_V}{cos(\theta)} \tag{1.2}$$

where K is the shape factor and D_V the apparent volume weighted domain size. Stokes and Wilson (Stokes et al. 1944) defined the maximum strain definition as a dependency of the broadening:

$$\varepsilon = \frac{\beta_{strain}}{4\,tan(\theta)} \tag{1.3}$$

Therefore, the broadening from the material is simply:

$$\begin{aligned} \beta_{observed} - \beta_{instrumental} &= \beta_{strain} + \beta_{size} \\ &= 4\varepsilon tan(\theta) + \frac{\lambda K D_V}{cos(\theta)} \\ \Leftrightarrow \beta_{strain} cos(\theta) &= 4\,\varepsilon\, sin(\theta) + \lambda K D_V \end{aligned} \tag{1.4}$$

Plotting $\beta cos(\theta)$ as a function of $sin(\theta)$ should give an affine function where the slope is directly related to the strain: they are known as Williamson-Hall plot. However, it requires to index and fit several reflection peak. Therefore, XRD patterns were also analysed by the Full Pattern Matching (FPM) method using the software Fullprof. The peaks shape was fitted with a Thompson-Cox-Hastings pseudo-Voigt convoluted with axial divergence asymmetry function (Finger et al. 1994). When compared to mathematical fitting features in data analysis software, the FPM technique as implemented in many XRD analysis software has the great advantage to take into account the specificity of XRD patterns, such as complex shape functions and the existence of the $K_{\alpha 2}$ radiation. Indexing many peaks by FPM gives a wider understanding of the material and increase the precision of the strain extracted of the Williamson-Hall plots. However, Williamson-Hall plot were found to be not always linear thus were not used afterwards. The assumptions leading to the Scherrer's equation and the final Equation (1.4) are not satisfied. That's why the accurate and complex Rietveld refinement method with size-broadening refinement for apparent crystallites morphology based on a spherical-harmonics representation (Balzar et al. 2005; Popa 1998; Popa et al. 2008) calibrated with LaB_6 as implemented in Fullprof was used.

SEM Organic explosives are sensitive towards heat and their submicron-sized emphasizes even more that discrepancy due to a higher surface/volume ratio; under vacuum, that heat from the electron beam can not be transferred to the surrounding of the surface. The gold coating is accordingly increased to approximatively 10 nm to increment the heat transfer from the material to the sample holder. The energy from the beam can also be tuned to reduce the degradation of the sample. However, electrons has to interact with the sample surface in order to have enough contrast and so spatial resolution. Due to the low density of organic molecular crystals, the effective tension required is usually high, around 15 kV at working distances around 5 mm. The stabilization with gold deposit improves the imaging of n-RDX allowing magnifications up to 10.000x. Further magnifications alter the material and do not allow a complete and correct data acquisition.

The damages of the electron beam on sensitive organic samples can be avoided or diminished by working at higher pressures (up to 1 Torr–50 Torr

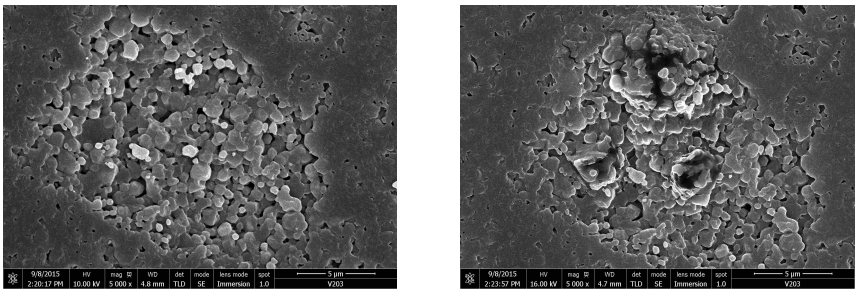

(a) before magnification (b) after

Figure 1.14 – High vacuum SEM imaging on a n-RDX pressed pellet coated with gold.

instead of 1×10^{-5} Torr to 1×10^{-7} Torr) with adjustable relative humidity up to 100 %. An Environmental Scanning Electron Microscopy (ESEM) FEG FEI XL30 was tested at the CLYM laboratory (Lyon, France) showing encouraging results about the increased stabilization at 2 Torr. As it can be seen in Figure 1.15, n-RDX without any coating exhibits at 2 Torr much more contrast compared to classical SEM with gold deposit.

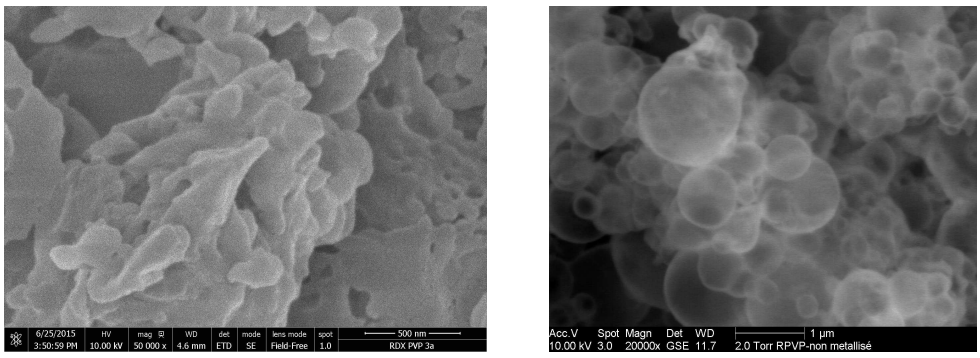

(a) high vacuum SEM picture, with gold coating (FEI Nova NanoSEM 450)

(b) ESEM image without coating (SEM-FEG FEI XL30)

Figure 1.15 – Comparison between high vacuum SEM imaging and at 2 Torr from ESEM on the same n-RDX sample

BET Prior to the measurement by gas injection, adsorbed water or organic gas have to be removed. This can be done by heating under vacuum or under a flow of dry, inert gas. The quality of the degassing influences directly the accuracy of the surface area calculated. As previously depicted, nano energetic materials are sensitive to heat and to vacuum, thus it can be expected to degrade them at the degassing step.

While using Krypton to gain in accuracy and access to smaller pores, BET results in Table 1.5 demonstrate the inaccuracy of BET measurements on n-RDX. At 100 °C the mass loss is almost one magnitude higher which may indicate a good degassing, but the specific surface area is decreasing leading us to the conclusion that the powder is starting to be affected by sintering.

degassing	mass loss	S_{BET}	extrapolated diameter
↗ 2°C/min – 50°C 10min – – ↗ 1°C/min – 80°C 1h –	0.1%	3.28 m/g	1.0 µm
↗ 2°C/min – 50°C 10min – – ↗ 1°C/min – 100°C 1h –	0.8%	3.09 m/g	1.1 µm

Table 1.5 – BET measurements on n-RDX with Kr

DLS Depending on the anisotropy and polydispersity of the system, the data interpretation may exhibit an angular dependence. For instance, small spherical particles do not have any anisotropy hence no angular dependence; the ideal case of spherical particles is usually not effective and such samples will exhibit an angular dependence. An optimum angle of detection exists for each particle size distribution and particle morphology. For a polydisperse sample and at certain angles, the scattering intensity of some particles will completely overwhelm the weak scattering signal of other particles, thus making them invisible to the data analysis at this angle. Furthermore, even if most of the organic explosives are not soluble in water, nitro and nitramine groups trend to interact strongly; energetic colloids are not stable in water and aggregates easily with quick sedimentation. Experiments have been done using the Zetasizer from Malvern. Even if the addition of PolyVinylPyrrolidone (PVP) enhances the stabilization, no reproducible measurements could have been performed as it can be seen in Figure 1.16.

DSC When gaseous species are reactive towards the decomposing substance, it leads to the autocatalytic acceleration of the reaction rate. Therefore for energetic materials, the assumed constant pressure is not satisfied for closed crucibles; consistent kinetic analysis can be acquired only by effectively removing

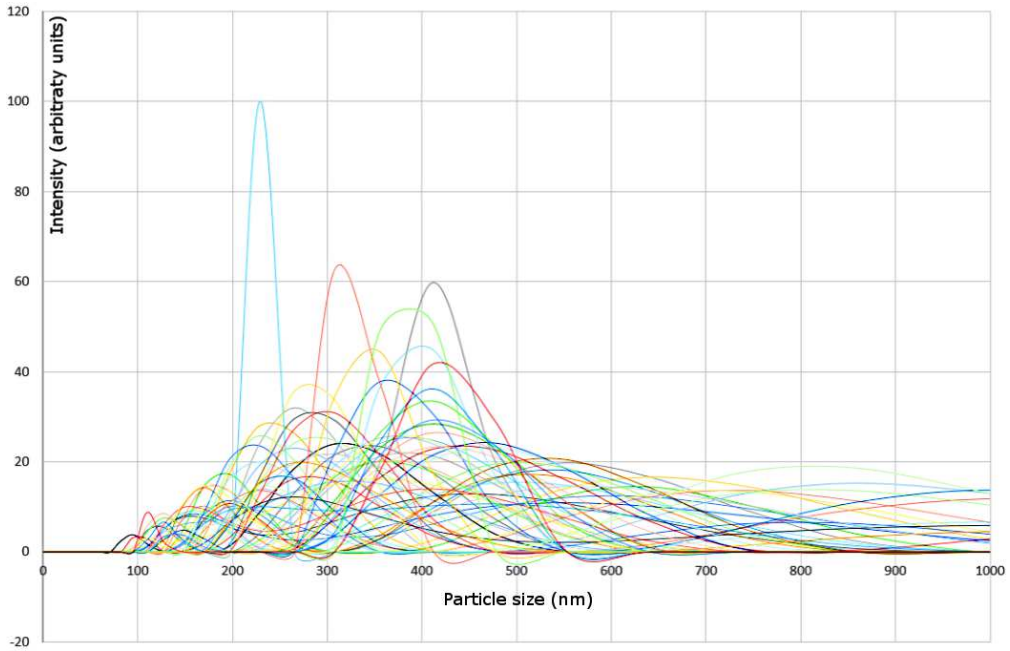

Figure 1.16 – All Dynamic Light Scaterring (DLS) results acquired from n-RDX with 5wt% of PVP: even if this figure contains data with different experimental conditions such as duration of the ultrasonic bath or the dilution, none of the PSD could have been found reliable.

reactive gaseous products. Long et al. (Long et al. 2000) clearly demonstrated that the competition between liquid and gas phase decomposition decreases over time, the activation energy in both pierced and closed pan DSC experiments from ~ 200 kJ/mol to ~ 140 kJ/mol, whereas open pan DSC and TGA experiments showed a constant value of ~ 100 kJ/mol.

1.4.3 Specific health and safety hazards

A wide variety of nano materials is now being produced, including nanoparticles as well as nanofibers, nanowires, and nanosheets, and their range and types are continually expanding. The increase of the nanomaterial uses in every day products makes the human exposure inevitable, thus asking the question of nanotoxicology. To prevent the uncontrolled penetration of foreign substances, the human body has several barriers such as epithelial cells and mucus secretion. While the protective mucus of the lung trap micron-sized particles, nanoparticles are small enough to reach the deep lung and even further the air-blood barrier (Fröhlich et al. 2014). Epidemiological studies showed that exposure of humans to ultrafine particles (<2.5 µm) in the air increased pulmonary morbidity and

mortality. Nanoparticles can also be cleared from the bronchial epithelium and then absorbed in the gastrointestinal tract. However, particles morphology, metric-related characteristics and many other physicochemical properties largely influence their toxicity. For organic particles, the solubility of the compound in its environment is a major issue since unitary molecules can directly disturb the proteins activity. The report of Boyer et al. (2007) written for the SERDP and ESTCP –US Department of Defence's environmental research programs– provides a comprehensive overview of the toxicity of RDX and CL-20. The toxicity of CL-20 for soil invertebrate population is quite high with only 0.02 mg CL-20/kg of soil to damage it significantly, whereas 44 mg RDX/kg soil–660 mg RDX/kg soil is harmless. For fish and aquatic invertebrates, CL-20 may be more toxic than RDX; but CL-20 is substantially less toxic than RDX to plants and birds: as little as 5.8 mg RDX/kg soil caused adverse effects for some plant species, while 10 mg CL-20/kg soil had no effect. Unfortunately, no studies on the toxicity of CL-20 in mammalian species –including humans– have been published. In contrast, the US Environmental Protection Agency (EPA) has established a reference dose (RfD) of 0.003 mg RDX/kg body weight/day for oral exposure based on the results of toxicity studies on rats; RDX has also been classified as possible human carcinogen, based on liver tumours in mice exposed for 2 years to 7 mg RDX/kg body weight per day.

About the pyrotechnic safety, the articles from R.4462-1 to R.4462-36 of the Code du Travail (Labour Code) regulates the practices of any work involving the creation, study, experimentation, control, packaging, storage or destruction of energetic compounds or any object containing pyrotechnic parts. In addition to the Document Unique, a legal document listing all actual potential risks, the employer has to redact a safety study for each pyrotechnic activity, with a validity of five years: the content of this pyrotechnic safety study is regulated by the decree from the 7th of November 2013 (modified in July 2014). The accidental potential modes of degradation of the energetic material has to be identified and their effects on human life determined. A probability of accident is estimated and the area of effect is identified then segmented according to the lethality; additional countermeasures are established to reduce the exposure (probability) and the consequences of an accident. At NS3E, each laboratory room has been evaluated to confine the risk inside it. The quantity of energetic material is also limited according to its stability and equivalence to TNT; in many cases only five grams (TNT equivalent) is allowed to be handled per room. The number of simultaneous workers is also limited while studying energetic material, with usually a maximum of two persons. The compounds processed for the first time by SFE are classified in the most restrictive class until the sensitivity has been determined: therefore, only one gram is recovered with a

conductive strap to avoid electrostatic discharge. In France and for the DoD activities, the Inspecteur de l'armement pour les Poudres et Explosifs (IPE) has the authority to control and delegates experts on pyrotechnic safety: the IPE frequently writes open letters (`http://www.defense.gouv.fr/dga/liens/poudres-et-explosifs/lettre-de-l-ipe/lettre-de-l-ipe`) to announce legislation changes, remind or dictate the good practices and list all recent pyrotechnic accidents from civilian or military uses.

1.5 Summary of the Chapter

The energetic material is a wide group which includes mixes of metals and oxides (thermites), amorphous materials (propellants) and organic or salt crystals (explosives). The present work focuses on a few organic secondary explosives: 1,3,5-trinitroperhydro-1,3,5-triazine (RDX), 2,4,6,8,10,12-hexanitro-2,4,6,8,10,12-hexaazaisowurtzitane (CL-20) and octahydro-1,3,5,7-tetranitro-1,3,5,7-tetrazocine (HMX). The RDX is a compound of reference still extensively used for applications but also research studies; it has only one crystalline form at ambient pressure and is soluble in acetone, sparingly soluble in ether and ethanol but almost insoluble in water. Several analysis methods where tried because the degradation of the sample is often a source of limitations when dealing with energetic organic crystals. The Dynamic Light Scaterring (DLS) needs a stable suspensions without agglomeration nor Ostwald ripening. Under the electron flow in electronic microscopy, the energetic samples heat up and are decomposed. Environmental Scanning Electron Microscopy (ESEM) is a more suitable technology to investigate the particle size and shape, due to the low vacuum able to dissipate heat.

The measurement of the Particle Size Distribution (PSD) is crucial to anticipate the properties of the material and to understand their creation. In addition to the previously mentioned issues, each characterization method measures an unique size; on DLS a hydraulic diameter is determined where the particles' agglomeration and the layers of solvating are taken into account. Electron microscopy techniques provide a direct visualization of particles and are therefore favoured. Finding a suitable and accurate method to establish the Particle Size Distribution (PSD) was the first challenge of the project and is further described in the Chapter 3.

This trend to easily agglomerate, growth, decompose etc. comes from the intrinsic nature of secondary explosive: organic crystals are also called soft matter. Their crystallisation at a nano scale has been a long-standing issue over several decades, and the result depends on the chemical nature of the compound. Therefore, RDX has been extensively studied and crystallised by

almost all the known techniques from other applications in the field of chemical engineering. The following review on processes which led to reduced size of RDX is necessary to provide a global comprehension on the specificities of RDX crystallisation.

Bibliography

1. Bachmann, W. E. and John C. Sheehan (1949). "A New Method of Preparing the High Explosive RDX". In: *Journal of the American Chemical Society* 71.5, pp. 1842–1845. ISSN: 0002-7863. DOI: 10.1021/ja01173a092.
2. Balzar, DAVOR and NICOLAE C. Popa (2005). "Analyzing microstructure by Rietveld refinement". In: *The Rigaku Journal* 22.1, p. 16.
3. Bayat, Yadollah and Vida Zeynali (2011). "Preparation and Characterization of Nano-CL-20 Explosive". In: *Journal of Energetic Materials* 29.4, pp. 281–291. ISSN: 0737-0652, 1545-8822. DOI: 10.1080/07370652.2010.527897.
4. Binnig, Gerd, Calvin F. Quate, and Ch Gerber (1986). "Atomic force microscope". In: *Physical review letters* 56.9, p. 930.
5. Binnig, Gerd and Heinrich Rohrer (1983). "Scanning tunneling microscopy". In: *Surface science* 126.1, pp. 236–244.
6. Binnig, Gerd, Heinrich Rohrer, Ch Gerber, and E. Weibel (1982). "Surface studies by scanning tunneling microscopy". In: *Physical review letters* 49.1, p. 57.
7. Bolton, Onas, Leah R. Simke, Philip F. Pagoria, and Adam J. Matzger (2012). "High Power Explosive with Good Sensitivity: A 2:1 Cocrystal of CL-20:HMX". In: *Crystal Growth & Design* 12.9, pp. 4311–4314. ISSN: 1528-7483. DOI: 10.1021/cg3010882.
8. Boyer, Ivan, John K. Miller, Rebecca E. Watson, J. DeSesso II, and C. M. Vogel (2007). *Comparison of the Relative Risks of CL-20 and RDX*. Falls Church, Virginia: Center for Science and Technology.
9. Bragg, WH (1915). "The structure of magnetite and the spinels". In: *Nature* 95, p. 561.
10. Ciezak, Jennifer A., Timothy A. Jenkins, Zhenxian Liu, and Russell J. Hemley (2007). "High-Pressure Vibrational Spectroscopy of Energetic Materials: Hexahydro-1,3,5-trinitro-1,3,5-triazine". In: *The Journal of Physical Chemistry A* 111.1, pp. 59–63. DOI: 10.1021/jp063150q. pmid: 17201388.
11. Coffey, Charles S. and V. F. De Vost (1995). "Impact testing of explosives and propellants". In: *Propellants, explosives, pyrotechnics* 20.3, pp. 105–115.
12. Comet, Marc and Eric Lafontaine (2016). *Nano-thermites*. 1 edition. Wiley-ISTE. ISBN: 978-1-84821-837-6.
13. Comet, Marc, Cédric Martin, Martin Klaumünzer, Fabien Schnell, and Denis Spitzer (2015). "Energetic nanocomposites for detonation initiation in high explosives without primary explosives". In: *Applied Physics Letters* 107.24, p. 243108. ISSN: 0003-6951, 1077-3118. DOI: 10.1063/1.4938139.

14. Dinnebier, Robert (2001). "Rietveld Refinement from Powder Diffraction Data". In: *Commission for Powder Diffraction Newsletter* 26.

15. Dumas, Séverine (2003). "Measuring of polymorphism IRTF spectrometry and chemometric. Application to the form polymorphe of CL20 (HexaazahexaNitroIsoWurtzitane / HNIW)".

16. Fathollahi, M., S. M. Pourmortazavi, and S. G. Hosseini (2007). "Particle Size Effects on Thermal Decomposition of Energetic Material". In: *Journal of Energetic Materials* 26.1, pp. 52–69. ISSN: 0737-0652, 1545-8822. DOI: 10.1080/07370650701719295.

17. Finger, L. W., D. E. Cox, and A. P. Jephcoat (1994). "A correction for powder diffraction peak asymmetry due to axial divergence". In: *Journal of Applied Crystallography* 27.6, pp. 892–900. DOI: 10.1107/S0021889894004218.

18. Fleischman, Scott G., Srinivasan S. Kuduva, Jennifer A. McMahon, Brian Moulton, Rosa D. Bailey Walsh, Naír Rodríguez-Hornedo, and Michael J. Zaworotko (2003). "Crystal Engineering of the Composition of Pharmaceutical Phases: Multiple-Component Crystalline Solids Involving Carbamazepine". In: *Crystal Growth & Design* 3.6, pp. 909–919. ISSN: 1528-7483, 1528-7505. DOI: 10.1021/cg034035x.

19. Foltz, M. Frances, Clifford L. Coon, Frank Garcia, and Albert L. Nichols (1994). "The thermal stability of the polymorphs of hexanitrohexaazaisowurtzitane, part II". In: *Propellants, Explosives, Pyrotechnics* 19.3, pp. 133–144. ISSN: 1521-4087. DOI: 10.1002/prep.19940190305.

20. Fröhlich, Eleonore and Sharareh Salar-Behzadi (2014). "Toxicological Assessment of Inhaled Nanoparticles: Role of in Vivo, ex Vivo, in Vitro, and in Silico Studies". In: *International Journal of Molecular Sciences* 15.3, pp. 4795–4822. DOI: 10.3390/ijms15034795.

21. Hakey, Patrick, Wayne Ouellette, Jon Zubieta, and Timothy Korter (2008). "Redetermination of cyclo-trimethylenetrinitramine". In: *Acta Crystallographica Section E* 64.8, o1428. DOI: 10.1107/S1600536808019727.

22. Höhne, G. W. H., W. F. Hemminger, and H.-J. Flammersheim (2003). *Differential Scanning Calorimetry*. Berlin, Heidelberg: Springer Berlin Heidelberg. ISBN: 978-3-642-05593-5 978-3-662-06710-9.

23. Krause, Horst H. (2005). "New Energetic Materials". In: *Energetic Materials*. Wiley-VCH Verlag GmbH & Co. KGaA, pp. 1–25. ISBN: 978-3-527-60392-3.

24. Limpert, Eckhard, Werner A. Stahel, and Markus Abbt (2001). "Log-normal Distributions across the Sciences: Keys and Clues". In: *BioScience* 51.5, pp. 341–352. ISSN: 0006-3568. DOI: 10.1641/0006-3568(2001)051[0341:LNDATS]2.0.CO;2.

25. Liu, Jie, Wei Jiang, Qing Yang, Jian Song, Ga-zi Hao, and Feng-sheng Li (2014). "Study of nano-nitramine explosives: preparation, sensitivity and application". In: *Defence Technology* 10.2, pp. 184–189. ISSN: 22149147. DOI: 10.1016/j.dt.2014.04.002.

26. Long, Gregory T., Sergey Vyazovkin, Brittany A. Brems, and Charles A. Wight (2000). "Competitive Vaporization and Decomposition of Liquid RDX". In: *The Journal of Physical Chemistry B* 104.11, pp. 2570–2574. ISSN: 1520-6106, 1520-5207. DOI: 10.1021/jp993334n.

27. Meents, A., B. Dittrich, S. K. J. Johnas, V. Thome, and E. F. Weckert (2008). "Charge-density studies of energetic materials: CL-20 and FOX-7". In: *Acta Crystallographica Section B Structural Science* 64.1, pp. 42–49. ISSN: 0108-7681. DOI: 10.1107/S0108768107055292.

28. Meyer, Rudolf, Josef Köhler, and Axel Homburg (2008). *Explosives*. John Wiley & Sons.

29. Millar, David I. A., Iain D. H. Oswald, Christopher Barry, Duncan J. Francis, William G. Marshall, Colin R. Pulham, and Adam S. Cumming (2010). "Pressure-cooking of explosives-the crystal structure of ε-RDX as determined by X-ray and neutron diffraction". In: *Chem. Commun.* 46.31, pp. 5662–5664. DOI: 10.1039/C0CC00368A.

30. Miller, G. R and A. N. Garroway (2001). *A Review of the Crystal Structures of Common Explosives. Part I: RDX, HMX, TNT, PETN, and Tetryl*. NAVAL RESEARCH LAB WASHINGTON DC.

31. Momma, Koichi and Fujio Izumi (2011). "VESTA3 for three-dimensional visualization of crystal, volumetric and morphology data". In: *Journal of Applied Crystallography* 44.6, pp. 1272–1276. DOI: 10.1107/S0021889811038970.

32. Nair, U. R., R. Sivabalan, G. M. Gore, M. Geetha, S. N. Asthana, and H. Singh (2005). "Hexanitrohexaazaisowurtzitane (CL-20) and CL-20-based formulations (review)". In: *Combustion, Explosion and Shock Waves* 41.2, pp. 121–132. ISSN: 0010-5082, 1573-8345. DOI: 10.1007/s10573-005-0014-2.

33. Nečas, David and Petr Klapetek (2012). "Gwyddion: an open-source software for SPM data analysis". In: *Central European Journal of Physics* 10.1, pp. 181–188. DOI: 10.2478/s11534-011-0096-2.

34. Nielsen, A.T. (1997). *Caged polynitramine compound*. US Patent 5,693,794. Google Patents.

35. PANT, Arti, Amiya Kumar NANDI, Shireeshkumar Pralhad NEWALE, Vandana Prakash GAJBHIYE, Hima PRASANTH, and Raj Kishore PANDEY (2013). "Preparation and Characterization of Ultrafine RDX". In: *Central European Journal of Energetic Materials* 10.3, pp. 393–407.

36. Popa, N. C. (1998). "The (hkl) Dependence of Diffraction-Line Broadening Caused by Strain and Size for all Laue Groups in Rietveld Refinement". In: *Journal of Applied Crystallography* 31.2, pp. 176–180. ISSN: 00218898. DOI: 10.1107/S0021889897009795.

37. Popa, N. C. and D. Balzar (2008). "Size-broadening anisotropy in whole powder pattern fitting. Application to zinc oxide and interpretation of the apparent crystallites in terms of physical models". In: *Journal of Applied Crystallography* 41.3, pp. 615–627. ISSN: 0021-8898. DOI: 10.1107/S0021889808012223.

38. Risse, Benedikt (2012). "Continuous crystallization of ultra-fine energetic particles by the Flash-Evaporation Process".

39. Russell, T. P., P. J. Miller, G. J. Piermarini, and S. Block (1993). "Pressure/temperature phase diagram of hexanitrohexaazaisowurtzitane". In: *The Journal of Physical Chemistry* 97.9, pp. 1993–1997. DOI: 10.1021/j100111a043.

40. Sato, Satoru, Hidefumi Nikawa, Shu Seki, Lu Wang, Guangfu Luo, Jing Lu, Masayuki Haranaka, Takahiro Tsuchiya, Shigeru Nagase, and Takeshi Akasaka (2012). "A Co-Crystal Composed of the Paramagnetic Endohedral Metallofullerene La@C82 and a Nickel Porphyrin with High Electron Mobility". In: *Angewandte Chemie International Edition* 51.7, pp. 1589–1591. ISSN: 1521-3773. DOI: 10.1002/anie.201106912.

41. Schultheiss, Nate, Melanie Roe, and Stephan X. M. Boerrigter (2011). "Cocrystals of nutraceutical p-coumaric acid with caffeine and theophylline: polymorphism and solid-state stability explored in detail using their crystal graphs". In: *CrystEngComm* 13.2, p. 611. ISSN: 1466-8033. DOI: 10.1039/c0ce00214c.

42. Sitzmann, Michael E., Stephen Foti, and Carroll C. Misener (1973). *Solubilities of High Explosives: Removal of High Explosive Fillers from Munitions by Chemical Dissolution*. DTIC Document.

43. Stepanov, Victor, Venant Anglade, Wendy A. Balas Hummers, Andrey V. Bezmelnitsyn, and Lev N. Krasnoperov (2011). "Production and Sensitivity Evaluation of Nanocrystalline RDX-based Explosive Compositions". In: *Propellants, Explosives, Pyrotechnics* 36.3, pp. 240–246. ISSN: 1521-4087. DOI: 10.1002/prep.201000114.

44. Stokes, AR and AJC Wilson (1944). "The diffraction of X rays by distorted crystal aggregates-I". In: *Proceedings of the Physical Society* 56.3, p. 174.

45. Sun, Aiwu, Joseph W. Lauher, and Nancy S. Goroff (2006). "Preparation of Poly(diiododiacetylene), an Ordered Conjugated Polymer of Carbon and Iodine". In: *Science* 312.5776, pp. 1030–1034. ISSN: 0036-8075, 1095-9203. DOI: 10.1126/science.1124621. pmid: 16709780.

46. Tarver, Craig M., Steven K. Chidester, and Albert L. Nichols (1996). "Critical Conditions for Impact- and Shock-Induced Hot Spots in Solid Explosives". In: *The Journal of Physical Chemistry* 100.14, pp. 5794–5799. DOI: 10.1021/jp953123s.

47. *UN Manual of Tests and Criteria* (2016). 6th. UNECE.

48. Vishweshwar, Peddy, Jennifer A. McMahon, Joanna A. Bis, and Michael J. Zaworotko (2006). "Pharmaceutical co-crystals". In: *Journal of Pharmaceutical Sciences* 95.3, pp. 499–516. ISSN: 1520-6017. DOI: 10.1002/jps.20578.

49. Von Holtz, Erica, Donald Ornellas, M. Frances Foltz, and Jack E. Clarkson (1994). "The Solubility of ε-CL-20 in Selected Materials". In: *Propellants, Explosives, Pyrotechnics* 19.4, pp. 206–212. ISSN: 1521-4087. DOI: 10.1002/prep.19940190410.

50. Wild, Roland and Elart von Collani (2002a). "Modelling of explosives sensitivity part 1: The Bruceton method". In: *Economic Quality Control* 17.1, pp. 113–122.

51. — (2002b). "Modelling of explosives sensitivity part 2: The Weibull-Model". In: *Economic Quality Control* 17.2, pp. 195–220.

52. Yan, Dongpeng, Amit Delori, Gareth O. Lloyd, Tomislav Friščić, Graeme M. Day, William Jones, Jun Lu, Min Wei, David G. Evans, and Xue Duan (2011). "A Cocrystal Strategy to Tune the Luminescent Properties of Stilbene-Type Organic Solid-State Materials". In: *Angewandte Chemie International Edition* 50.52, pp. 12483–12486. ISSN: 1521-3773. DOI: 10.1002/anie.201106391.

53. Young, RA and P Desai (1989). "Crystallite size and microstrain indicators in Rietveld refinement". In: *Archiwum Nauki o Materialach* 10, pp. 71–90.

54. Zender, Charlie (2008). "Particle size distributions: theory and application to aerosols, clouds, and soils". In: DOI: 10.1.1.210.2680.

55. Zhang, Xin and Brandon L. Weeks (2014). "Preparation of sub-micron nitrocellulose particles for improved combustion behavior". In: *Journal of Hazardous Materials* 268, pp. 224–228. ISSN: 03043894. DOI: 10.1016/j.jhazmat.2014.01.019.

56. Zhurova, Elizabeth A., Vladimir V. Zhurov, and A. Alan Pinkerton (2007). "Structure and Bonding in β-HMX-Characterization of a Trans-Annular N···N Interaction". In: *Journal of the American Chemical Society* 129.45, pp. 13887–13893. ISSN: 0002-7863. DOI: 10.1021/ja073801b.

Chapter 2

Production of Nano Explosives

The crystallisation of a compound or several ones is the phenomenon of transition between the liquid, gaseous or even solid state to the crystalline state where matter posses long range order and symmetry. Crystallisation can be used to adjust the physical properties and the morphology of a substance. Crystallisation involves the formation of nuclei and then their growth; when a solution is supersaturated, its thermodynamic equilibrium is reached through nucleation and growth. To favour smaller particle size, the trend is to increase nucleation rate, for instance through increasing supersaturation, to reduce crystal growth and avoid any aggregation. Most of the crystallisation techniques are based from solution but crystallisation processes from the melt and from the gaseous phase are also known (van der Heijden et al. 2005). Quite a few were tested on energetic materials; the following bibliography is meant to be a comprehensive review of the crystallisation of RDX and of similar energetic compounds at submicron or nano scale.

2.1 Wet production methods

2.1.1 Crystallisation from solution

The most commonly used technique is the crystallisation from solutions. Depending on the creation of supersaturation, distinctions are made between cooling, evaporation, vacuum cooling, drowning-out and reaction crystallisation. The study of the solubility of the compound is the key to determine which crystallisation process can be used: for instance if the solubility is not very temperature dependent, evaporation will be more effective than cooling (Figure 2.1 p. 62).

Fedoroff et al. (1966) indicates that the RDX solubility in acetone is divided by 4 by cooling from 60 °C to 0 °C. PANT et al. (2013) used all standard techniques

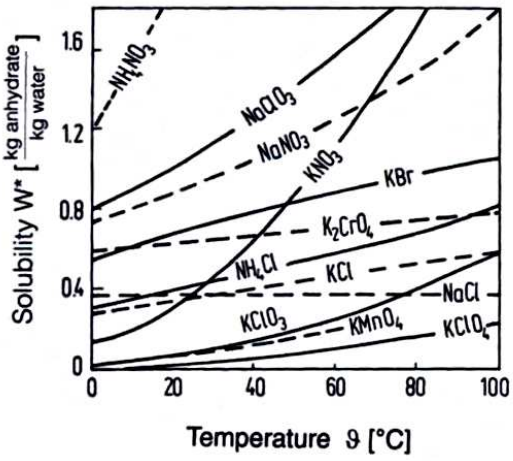

Figure 2.1 – Solubility curves for different substances (Mersmann 2001).

available to recrystallize RDX into submicrometer crystals "in a beaker": the smallest size was obtained when the anti solvent were added to a highly supersaturated solution cooled down, while applying ultrasonication and stirring. Achieving a high level of supersaturation results in a higher nucleation rate, but aggregation rises at elevated rates; for this solvent/compound system, they produced smaller particles, and reduced the agglomeration by the sonication. Particles are finally obtained by drying. This method may be suitable for industry, however, the minimal size obtained is only 850 nm under tough condition, with a yield of 60 % and rod shaped crystals.

Kumar et al. (2014) succeeded to produce finer RDX particles by quickly injecting a very small volume (100 µL) of RDX dissolved in acetone into ultra pure water: the smallest mean particle size was 38 ± 15 nm by SEM for the highest temperature (70 °C) and lowest concentration of RDX in acetone (5 mM). It is worth to mention that DLS measurements were found to be not reliable when compared to SEM analysis, which can be explained by the lack of surfactant stabilizing the colloid. This technique was also applied on HMX (Kumar et al. 2015) with a particle size around 30 nm and the same conclusions were drawn out.

Bayat et al. (2015), through an optimization of the micro-emulsion process, crystallised 80 nm plate-like β-CL-20 particles. The severe agglomeration and plate-like morphology might be due to the freeze drying, then washing of the micro-emulsion. Gao et al. (2014b) recrystallized FOX-7 in ethyl alcohol within a submicrometric range: SEM pictures show an irregular plate-like morphology and therefore highlight the inconsistency of the unique mean particle size of 340 nm claimed. Particles exhibit also a certain degree of agglomeration which

can be probably explained again by the lake of a surfactant and the air-drying.

Luo et al. (2015) reached an impressive size of 30 nm of RDX. They used a surprising technique where RDX is dispersed in bacterial cellulose. The lowest particle size was obtained with 71 %RDX/gelatine mix; however, increasing the content of RDX leads to an increment of the particle size and the maximum of RDX loading tested was 91 % for a particle size of 50 nm. The sensitivity of that composite towards impact and friction is divided by two therefore asking the legitimate question of the reactivity. Nevertheless, further efforts could be done to replace the bacterial cellulose with energetic matrix.

Crystallisation in solution allows the formation of large crystal by growth, thus allowing more parametric studies about the influence of solvents ; for instance (Li et al. 2015c) has studied the importance of temperature and supersaturation for the crystallisation for HMX in γ -butyrolactone, revealing that low temperatures and highly supersaturated solutions trend to increase the defects in HMX crystals.

2.1.2 Solvent substitution using reverse micelles

Dabin et al. (1999) have developed an ingenious method to prepare nanometre RDX using a simple technique: the crystallisation is triggered by a solvent substitution, and the nanometre scale is obtained by restricting the reactor volume to such a scale with reverse micelles. NaAOT (Sodium 1,4-bis(2-ethylhexoxy)-1,4-dioxobutane-2-sulfonate) into isooctane forms reverse micelles, then RDX in DMF is added to one solution containing these micelles, and water to another solution of micelles. Both are finally mixed together to form the nano RDX with a diameter of 70 nm to 100 nm.

2.1.3 Sol-Gel

Energetic materials processed by sol-gel method, are desensitized by embedding in a matrix, usually a silica matrix. Developed by Gash et al. (2000), Tillotson et al. (2001), and Tillotson et al. (1997), the silica-explosive gel is prepared by dissolving the energetic compound, the silica precursor and a catalyst, in a co-solvent. After the gelification, an anti-solvent of the explosive is injected to replace the solvent in the pores and precipitate the explosives in that silica matrix. By drying with heating or at low pressure, a xerogel with higher density is obtained; if supercritical CO_2 is used to extract the solvent, an aerogel with low density is formed. Therefore, the nanostructuration of the explosive comes from the porous matrix: cavities of mesoporous gels are from 2 to 50 nm large, less than 2nm for microporous gels. Macroporous materials have pore diameters of greater than 50 nm (Rouquerol et al. 1994).

RDX/Resorcinol-formaldehyde (RF) nano-composite has been synthesized (GUO Qiu-xia 2006): 38 nm large nano-RDX has crystallised in an RF aerogel matrix with a surface area of 551.5 m^2/g (measure taken without RDX). Wuillaume et al. (2014) trapped AP and RDX in a mesoporous low-density energetic organogel. At the impact test negligible decrease of sensitivity has been measured: 75 wt% RDX nano gels and macro gels have the same sensitivity and the 90 wt% nano gels are even more sensitive than the macroscopic counterparts. When compared to pure RDX, the 90 wt% nano gels are not desensitized. However, SSGT preformed on pressed gels (95% TMD) revealed an improvement of the sensitivity for the 90 wt% RDX nano-formulation. That nano gel exhibits an uncommon micro-structure of sheets, with micron-sized particles potentially formed by nano primary particles: the lack of desensitization on the loose powder may be explained with the sensitization by the sheet-like shape counteracted by the presence of the gel coating each nanoparticles.

Li et al. (2015a) used a better energetic matrix –Glycidyl Azide Polymer (GAP)– with a maximum of 40 wt% of RDX; they noticed a lower sensitivity than the physical mix. However, the claimed nano size is only deduced from porosity without RDX and from XRD patterns which only gives a mean coherence length. They also created NitroCellulose (NC)-RDX-AP nano composites by a technique similar to sol-gel (Jin et al. 2015); the matrix consist of the NC itself solidified by micron-sized AP crystals and cross-linked with Toluene Dilsocyanate (TDI) and Dibutyltin dilaurate (DBTDL), whereas RDX is dissolved in acetone inside that template. The gel and the crystallisation of RDX is triggered by supercritical CO_2 drying. Even if the sensitivity and the density were not improved, the increase of the heat of explosion measured and the originality of the approach make promising the formation of nano-composite based entirely on energetic materials through chemical binding.

2.1.4 Melting

Many high energetic materials degrade very closely to their melting point. Therefore, only a few such as TNT or TNB can be used in their molten state, since the melting temperature is at least 100 °C far from the exothermic decomposition. The melt-cast process of TNT-based composition is used for shaping charges or loading them into ammunitions since WW I. Crystallisation from an emulsified molten explosive is an innovative technique used by Anniyappan et al. (2015). 2,4,6-triazido-1,3,5-triazine or cyanuric triazide (CTA) has been processed at 95 °C to crystallise as micron-sized agglomerates. CTA is a promising primary explosive compliant with the new REACH legislation (*Regulation (EC) No 1907/2006 on the Registration, Evaluation, Authorisation and Restriction of Chemicals (REACH) and setting up a European Chemicals Agency* 2007) forbidding the use of heavy

metal based materials. Further investigation with surfactants might lead to smaller particles by counteracting the high viscosity of molten droplets.

2.1.5 Milling

Redner et al. (2006) developed a batch wet-milling process, producing submicrometer RDX. A mixture of water, isobutanol, a dispersant and RDX is filled into a unspecified mill, resulting in a minimal mean particle size of 310 nm and a crystallite size of about 65 nm. Several milling issues were mentioned such as the yield initially of around 25 % and the importance of the residence time and the drying step.

Liu et al. (2014a, 2013) studied the effect of drying nano-RDX and HMX samples under various conditions. They first obtained nano-RDX in solution from a mixture of water, ethanol, isopropanol and RDX. The suspension is put in a bi-directional rotation mill for 6h. Just as Rednere experienced, the drying is the critical point to get a nano powder. They dried the RDX under different conditions: freeze drying and supercritical drying led to quite impressive results, with medians at 160 nm and 200 nm respectively from a solution containing an average particle size of 64 nm. After RDX and HMX, CL-20 was successfully processed the same way resulting in a median size of 180 nm determined by SEM (Liu et al. 2014b). For the three compounds, nano powders are less sensitize than their micron-size counterparts.

Spray drying is a less energy intensive drying method studied by Patel et al. (2015). RDX and CL-20 have been bead milled from water with addition of isobutanol and Polyvinyl alcohol (PVOH) to stabilize the colloid by dispersion and coating, and then an unknown polymeric binder is added just before drying the slurry by spray drying. Mean particle sizes down to 400 and 200 nm respectively have been measured by DLS for RDX- and CL-20-based composites after milling. However, no PSD curve has been provided nor dispersion of the results indicated. It has been noticed that for particles of CL-20 at 200 nm, the α phase is obtained. From the same team, nanoscale cocrystal of CL-20:HMX 2:1 has been prepared by bead milling an aqueous suspension of ε-CL-20 and β-HMX in a 2:1 stoichiometric ratio (Qiu et al. 2015a). The progressive conversion of raw materials into the cocrystal is achieved after one hour, resulting in a particle size lower than 200 nm. However, not much attention has been paid to the drying effect of large scale batch; SEM and XRD were made on a drop dried at room temperature, and it is likely that the drying of several grams of such molecular crystal will behave differently. Furthermore, the accuracy of the XRD technique does not allow to conclude that a complete conversion into cocrystal has occurred, but rather indicates that the percentage of ε-CL-20 and β-HMX is

lower by 10 % approximatively. Full quantification by Rietveld or Full Pattern Matching methods would have been relevant to follow the conversion with time.

2.2 Dry production methods

2.2.1 Physical Vapor Deposition (PVD)

Frolov and Pivkina have developed together a vacuum condensation process for high energetic material first reported in 2002 (Frolov et al. 2002; Frolov et al. 2010; Pivkina et al. 2004). Vacuum deposition of ammonium nitrate (AN), RDX and a composite AN-RDX was performed on a cooled quartz-glass substrate. The mean particle size was directly measured from AFM: a size of 50 nm was obtained for the three materials, even after processing the nano-powder (removing from the quartz substrate and pressing into tablets).

Mil'chenko et al. (2015) went further in the Physical Vapor Deposition (PVD) process by the deposition of TATB, HMX, RDX, PETN and BTF as thin layers on several substrate such as Plexiglas and copper while changing operative parameters. Critical thickness of the detonating layer is an order of magnitude lower; the sensitivity toward impact and friction is barely mentioned as being similar to the raw materials but the sensitivity to Light Amplification by Stimulated Emission of Radiation (LASER) has been substantially increased.

Therefore, the PVD technique is greatly suitable for "pyrotechnic integrated circuits", whereas mass production of loose powder is not economically viable.

2.2.2 Electrospray

Radacsi et al. (2011) crystallised submicrometer RDX using an electrospray. A solution of RDX-acetone is sprayed through a nozzle electrically charged to a grounded plate: the droplet surface is charged, increasing their surface energy and so triggering their fission into smaller droplets. This Coulomb fission phenomenon and the evaporation of the solvent lead to crystallisation and the deposit of non agglomerated particles. The tweaking of the characteristics of the nozzle and the potential difference resulted in various morphology of RDX particles: for instance, micrometer hollow spheres of agglomerated RDX were produced. The minimal mean size obtained was 400 nm: that submicrometer RDX exhibited a clear insensitivity towards friction, but with the same impact sensitivity as conventional micron-sized RDX (Table 2.1, p. 67).

Reus et al. (2014) then processed bi-component systems: proteins and RDX/TNT. XRD patterns of the final products are mentioned to be different from the ones of the raw material, which seems to indicate either a strong

RDX	Impact [J]	Friction [N]
Conventional	7.5	120
submicrometer	10	>360

Table 2.1 – Comparison of the sensitivity levels of conventional and 400-nm large RDX.

degradation or a cocrystallisation. Infrared definitely demonstrates a critical partial decomposition of both RDX and TNT due to the electrospray and the same phenomenon has likely happened for Radacsi et al. too. Whatever was really obtained, Reus crystallised very small particles, estimated by me to be under or around 100 nm for any initial ratio of TNT/RDX. AFM could have been much more informative about the size and shape of such nanoparticles already well dispersed on a substrate. Sensitivity tests have been performed on those degraded materials, which were found to be as insensitive as TNT.

Electrospray can create a fine spray of micron-sized charged droplets repealing each others, ideal for crystallisation; the high voltage needed is a major handicap for processing sensitive powders such as energetic materials containing nitro groups.

2.2.3 Plasma

During his PhD project (Radacsi 2012), Radacsi used an innovative and advanced technique to crystallise submicrometer RDX: a Collison nebulizer aerosolizes a RDX-acetone solution to a Surface Dielectric Barrier Discharge (SDBD) plate where a cold plasma disrupts the droplet by the Coulomb fission. Like the electrospray, one droplet should crystallise into a unique single-crystal. The minimal mean size obtained was 500 nm, with a range from 200 nm to 900 nm and with prismatic or spherical shapes. Again like the submicrometer powder obtained from electrospray, the 500 nm-sized RDX has been desensitize to friction but not to impact (Table 2.2, p. 67).

.RDX	Impact [J]	Friction [N]
Conventional	5	144
submicrometer	5	>360

Table 2.2 – Comparison of the sensitivity levels of conventional and 500-nm large RDX (Radacsi 2012).

2.2.4 Supercritical/Gas Anti-Solvent precipitation

Supercritical Anti-Solvent precipitation (SAS) uses the same principle as liquid crystallisation, substituting the liquid anti-solvent by a supercritical fluid. The very high diffusivity of supercritical fluids leads to a rapid supersaturation and so to a sudden precipitation. Various apparatuses are used in SAS: a specific one is the Gas AntiSolvent (GAS) precipitation, where the liquid solution is first loaded into the vessel, before the addition of the supercritical anti-solvent. For RDX, CO_2 is a correct supercritical anti-solvent. Gallagher et al. (1992) first investigated GAS process of RDX in 1992. Supercritical CO_2 was injected into RDX-cyclohexanone solution at various injection times, injection quantities and temperatures: in this first use of GAS for RDX, a lot of different particle size distributions and morphologies were obtained, but none under the micrometer size. Since then, several process derived from the GAS process, and which could be referred as SAS sub-process, have been used to reach the submicrometer and nano scale for energetic materials. But from 1992, no GAS/SAS process has been reported to produce energetic materials to a size lower than the micron (Jung et al. 2001; Lee et al. 2009, 2011b; Teipel et al. 1997), excepted for 5-nitro-1,2,4-triazol-3-one (NTO) by Lim et al. (1998) (Reverchon et al. 2005).

2.2.5 Aerosol Solvent Extraction System (ASES) process

Aerosol Solvent Extraction System (ASES) process involves spraying the solution to precipitate through an atomization nozzle into supercritical CO_2. Lee et al. (2011b) used GAS and ASES apparatus to crystallise β-HMX: undesirables shapes (needle-like, irregular and aggregated) were produced by ASES at any operating conditions, whereas GAS led to regular shape and the most desired β phase. Dou et al. (2013) sprayed RDX dissolved in DMF obtaining micron-sized particles highly polydispersed. However, submicron-sized polymers and biopolymers produced by ASES have been reported since the nineties by Dixon et al. (1993) and Reverchon (1999). Nevertheless, that technique could be used on NC based composite due to its polymer-like behaviour.

2.2.6 Solution Enhanced Dispersion by Supercritical fluids (SEDS)

Solution Enhanced Dispersion by Supercritical fluids (SEDS) process was developed and patented by the Bradfort University to achieve a smaller droplet size compared to the previously described SAS methods. For SEDS process, a solution with the compound solvated is sprayed into supercritical anti-solvent gas (CO_2 for RDX) through a nozzle with two coaxial passages: this technique

can be seen as a specific implementation of the ASES process, where CO_2 is introduced through the nozzle continuously with the solution. Shang et al. (2014) produced by SEDS spherical RDX particles with a mean particle size of 770 nm, therefore finally lowering the particle size under the micron.

2.2.7 Particles from Gas-Saturated Solutions (PGSS)

Both patents "Conditioning of finely divided crude organic pigments" (1984) and "Finely dispersed carotenoid pigments prodn. - by dissolving carotenoid in a supercritical gas, pref. carbon di:oxide, and dispersing the soln. in an aq. colloidal matrix" (1981) first described a procedure that today is called Particles from Gas-Saturated Solutions (PGSS). The PGSS technique consists in dissolving a compressed gas into a solution of the substrate in a solvent, then passing it through a nozzle: the sudden decompression leads to crystallisation thus to the formation of solid particles. Although this method is widely used at large scale with a wide range of products from inorganic powder to pharmaceutical compounds (Pourmortazavi et al. 2005), nothing has been reported (Jung et al. 2001) concerning energetic materials processed by PGSS.

2.2.8 Rapid Expansion of Supercritical Solutions (RESS)

The RESS concept has been first described by Hannay and Hogart more than a century ago (Hannay et al. 1879) but studied by Krukonis (1984) and the Battelle Institute research team (Matson et al. 1987a,b). The RESS process consists in spraying in a lower pressure chamber (60-0 bar) through a nozzle a supercritical (sc) fluid containing the substrate. The sudden drop of pressure leads to rapid nucleation and so small (from micron- to nano-sized) particles which are finally collected. The use of a supercritical fluid like CO_2 allows the direct production of a dry and pure powder. Teipel et al. (1997, 2001) first reported the use of RESS for energetic materials: 10 µm large TNT particle were crystallised in those preliminary experiments. They mentioned parameters which influence strongly the crystallisation from a RESS apparatus: pressures, temperatures, geometry of the nozzle and mass flow. Stepanov in the group of Krasnoperov succeeded in the fine tuning of the RESS process to prepare dried n-RDX (Stepanov 2003, 2008; Stepanov et al. 2006, 2005). The formed RDX particles had a mean particle diameter ranging from 110 nm to 220 nm and an irregular spherical morphology. He performed an up-scaling of the RESS process in order to increase the production capacity of RDX to 6 g/h but with a CO_2 consumption of 35 kg/h. By RESS, a slight sensitization to impact and shock stimuli of the 200 nm nano-RDX occurred compared to 500 nm n-RDX (Stepanov et al. 2011).

CL-20 has also been reported to be processed by RESS from trifluoromethane (CHF_3) (Reverchon et al. 2005): sc-CHF_3 has similar thermodynamic properties and is a better solvent of CL-20 than sc-CO_2. Only micron-sized particles were produced and no article reporting the results could have been found. Changing the solvent is a line of research followed by Lee et al. (2011a) using compressed liquid DiMethyl Ether (DME) for RDX. The parametric study points out the role of inlet pressure and temperature and the nozzle diameter: increasing any of those three parameters increases the particle size. Therefore, the two minimal mean particle sizes of 370 and 360 nm were obtained for the lowest mass flow rate of 0.37 and 0.85 g/s of DME.

2.2.9 RESS-AS (or RESOLV)

After the success of the RESS process, Essel et al. developed a new method from that technique, called Rapid Expansion of Supercritical Solutions into an Aqueous Solution (RESS-AS) first reported in 2010 (Essel et al. 2010). Rapid Expansion of Supercritical Solutions into an Aqueous Solution (RESS-AS) uses the versatility of the RESS process, spraying into an aqueous solution containing a dispersant and/or growth inhibitor (Kuo et al. 2011). They reported (Essel et al. 2012) a production of 30 nm sized RDX using a pH 7-stabilized solution, although a polymer coating (PEI or PVP) was necessary to avoid any agglomeration and so stabilize the colloid from the Ostwald ripening observed when no polymer was added. No sensitivity tests have been reported about any nano-powder which could be obtained from those colloidal suspensions.

2.2.10 Light Amplification by Stimulated Emission of Radiation (LASER) Ablation

Gottfried et al. (2012) successfully produced for the first time nanoparticles of RDX using LASER ablation. Near-infrared, nanosecond pulsed LASER has been focused on military-grade RDX pellets: Scanning Mobility Particle Sizer (SMPS) and SEM analyses showed a particle size distribution around 64 nm for 200 mJ pulse and 75 mJ pulse.

2.2.11 Ultrasonic Spray Pyrolysis

Since the nineties, spray crystallisations and synthesis have been performed using several atomizers, and among them piezoelectric transducers (Messing et al. 1993; Okuyama et al. 2003). As a spray technique, the goal is to produce one particle per droplet, but here the crystallisation is controlled by the drying step, an oven just after the atomization. Kim et al. (2011a), Kim et al. (2011b),

and Spitzer et al. (2011, 2010) both developed an apparatus to produce dried submicrometer RDX from an ultrasonic transducer. After the droplet generation, the solvent is evaporated by thermal gradient applied on the flux pulled by a pump. Highly agglomerated particles 200 nm–500 nm were produced. Gao et al. (2014a,b) used the same experimental setup with the exception of the addition of a thermal gradient in the furnace, in order to produce 78 nm FOX-7 particles, and submicron-sized CL-20:HMX cocrystals.

2.2.12 Spray Drying

The development of spray drying (Broadhead et al. 1992; Stein 1973) has been expanding since many years and has recently became a suitable commercial solution at both R&D and industry scales to produce dried particles from microns to nanometres. The pyrotechnic community quickly discerned the advantages of this simple technique to process energetic compounds as pure and composite materials.

The process sprays a solution containing a dissolved compound or particles in suspension into a hot gaseous stream (air or nitrogen) thus crystallising into particles and/or drying the granules. van der Heijden et al. (2008) has proven that spray drying is able to crystallise finer RDX particles ("from 400 nm and larger") than their technique of precipitation into anti-solvent (1 µm to 10 µm). Qiu et al. studied the crystallisation of energetic compounds using the spray drying with ultrasonic (Qiu et al. 2011) or pneumatic (Qiu et al. 2012) nozzle or with both type of nozzles (Qiu et al. 2015b). All their experiments were done with the addition of Polyvinyl acetate (PVAc) and resulted in micron or submicron-sized hollow spheres made of nano primary particles; the smallest ones were estimated at 20 nm for RDX/PVAc made from a pneumatic nozzle with a mean droplet size of around 7 µm. The versatility of the process allows the production of energetic composites (coating of TATB on micron-sizedHMX, RDX or CL-20 by Ma et al. (2015)), energetic/elastomer composites (micron-sized CL-20/EPDM by Ji et al. (2015), micron-sized spheres of agglomerated HMX/Viton by Shi et al. (2015)), and even cocrystals (micron-sized spheres of agglomerated HMX/TNT by Li et al. (2015b)).

2.2.13 Spray Flash Evaporation (SFE)

Risse and Spitzer at the NS3E laboratory developed an innovative process after experimenting the limitations of the Ultrasonic Spray Pyrolysis method: beyond the inherent risk of using a high voltage electrostatic precipitators for energetic powders, the rate of evaporation of droplets is too low to avoid agglomeration and to crystallise submicrometer particles. Risse (Doctoral Thesis 2012) and Risse

et al. (2012) used the flash-evaporation behaviour of droplets to dramatically reduce the life time and the size of droplets. The compound is dissolved in a volatile solvent and that solution is heated just before being sprayed into vacuum, where the crystallisation is triggered by the sudden temperature depression and the solvent evaporation. The process is discussed in more details in Section 2.4.2.

An unconventional application of nanosized explosives used at the NS3E laboratory is the synthesis of nanostructured material by detonation. Pichot et al. (2015) and Pichot et al. (2013) demonstrated that smaller nano diamonds are generated from the detonation of n-TNT/RDX composites produced by SFE than from a physical mixing of micron-sized commercial TNT and RDX.

2.3 Discussion on production methods

The smallest size of RDX is either obtained from wet techniques, or from small-scale approaches which cannot be transferred to industry (PVD and LASER). Even if PVD has been successfully used in the semiconductor sector for our everyday electronic devices since decades, PVD for energetic material will never be able to reach a production of several hundred of grams per hour. However, PVD is perfectly suitable for the current trend to create "pyrotechnic integrated circuits". Femto second LASER ablation is used for nanoparticles synthesis of metal in solution at the laboratory scale; the colloids produced are found to be extremely stable. Used in dried conditions, a deposit of nanoparticles on a substrate could be obtained from a gas flow, or a dried powder could be collected within a cyclonic separator: this LASER technique has been used to cut high energetic material quite safely (Roeske et al. 2003) but nanoparticles production would be severely limited to high-added-value industrial applications due to low production rate and high operation cost. Besides those two aspects, neither methods would process advanced composites – with a binder for instance – or would be able to do concomitant or cocrystallisation.

The production of nanoparticles through wet techniques has became a common industrial chemical process. The Sustainable Hydrothermal Manufacturing of Nanomaterials (SHYMAN) European project aims to increase the production rate of a continuous hydrothermal process from 1-10 tons/annum to 100 tons/annum of inorganic nanomaterials (Charitidis et al. 2014). Tsuzuki (2013) statistically studied which method for inorganic nano synthesis are mostly used in industry: vapour (39 % mainly Chemical Vapor Deposition (CVD)) and liquid (45 %) phase synthesis are the main type of techniques. Patents or historic skills of the brand can restrain the choice of a technology, so such data should not be taken as indicators of the robustness or versatility of the method. Considering such wide adoption of wet techniques (Sheth et al. 2012) and the knowledge from

Process	working pressure(s)	heating (℃)	continuous	scale-up	limiting step(s)	smallest size[1]
Sol-Gel	atmo	no	no	-+	matrix, drying	100-150[2]
Anti-solvent	atmo	70	could be	-	injection, drying	38
Milling	atmo	cooling	no	+	drying	160[3]
PVD	$10^{-4} Pa$*	100-200	no	−	vacuum	50
Electrospray	atmo	no	could be	-	mass flow, electric field	400
ASES	12 MPa	yes and cooling	no	−	sCO_2	microns
SEDS	35 MPa*	yes	no	−	sCO_2	microns
RESS	35 MPa → 0.1-5 MPa	yes and cooling	could be	-+	sCO_2	200
RESS-AS	35 MPa → atmo	25	could be	-+	sCO_2, drying	30[4]
LASER	atmo	no	no	-	mass flow	64
Ultrasonic	atmo	50-150	could be	-+	transducer	200-500
Spray drying	atmo	50-100	could be	++	evaporation ratio	400
SFE	5 MPa → 5 mbar	150	yes	++	vacuum	300

*Table 2.3 – Comparison . [1] smallest pure RDX mean size reported in nm | [2] XRD measurement | [3] freeze dried from a 64 nmRDX slurry | [4] from DLS, no report about dried state | *Not available in the references, so the value is based on usual operating conditions | sCO_2 : supercritical carbon dioxide*

chemical engineering – homogenization in large reactor, processing of liquid flow, versatility, safety ... –, wet crystallisation methods are a logical choice to process organic materials. However, unlike inorganic and metal nanoparticles, organic matter is very sensitive to drying as we previously saw in Section 2.1.5; yet that delicate step is required since the reactivity of high energetic materials fully exhibits at the dried state. Freeze drying and supercritical drying seem to overcome kinetically and partially the crystal growth occurring. Only a complete growth inhibition will lead to the production of smaller nanoparticles under 100 nm from milling or anti-solvent/cooling crystallisation. From an industrial point of view, freeze or supercritical drying are batch-only processes; all current industrial drying process are not designed to tackle down the fast growth of soft-matter. Innovative techniques such as spin freezing (L. De Meyer et al. 2015) or spray drying enhance the processability and potentially the performances, but their reliability need to be tested.

The ball-milling technique raises question about the purity of the product; it is well know that after such an extensive friction process, industrial milled ceramics are not used for hight purity chemical process (Carter et al. 2013). Industry moved to other techniques such as vapour phase ones, to overcome that limitation and others like the lake of control, local heating etc. Even with soft matter, similar issues can be expected; even small quantities of metallic impurities could catalyse the degradation of the explosive and/or sensitize it.

After 25 years of research and 10 years of process engineering, the SuperCritical Fluid (SCF) technology has never convinced the industry and only marginal uses for specific commercial drug products have been reported (Sheth et al. 2012). First, the choice of the gas at industrial scale is falling back to CO_2 due to safety and affordability criteria. For instance, gases such as nitrous oxide or ethane have low critical values, but explosive mixtures can be generated. Trifluoromethane is inert, non-flammable and is usually a better solvent but is way more expensive than CO_2 and a potent greenhouse gas. Second, the main limitation –the solubility into sc-CO_2– can be overcome by the addition of organic cosolvent: such modification alters the environmentally safe nature of sc-CO_2 based SCF and complicates the process by the need to remove any residual organic solvents. The aggregation phenomenon is commonly observed in SCF processes; further investigations on the role of different particle collection environments are needed, but RESS-AS processes greatly avoid the particle aggregation. The use of a liquid anti-solvent with polymeric stabilizers has been found to be very effective. However, it compromises the recovery of a dry pure powder, going back to square one with the drying issues previously discussed.

Spray techniques are commonly used in the industry, such as micro-encapsulation massively used for food (Gibbs et al. 1999; Madene et al. 2006), spray drying in

pulmonary drug delivery for production of uniform and breathable size particles (Bhavesh B. Patel et al. 2014) or even thermal spray deposition of metallic material (Lavernia et al. 2009). Spraying is a method which allows easy implementation of an installation and easy direct control over the injection. However, because of the low technological cost of atomizing nozzles and the low control over the spray itself, details and know-how are much more important than for other processes. Direct spray drying as crystallisation technique for RDX does not produce submicron-sized particles without the help of an additive and the SCF techniques are not suitable for industry: the need for an intermediate method in terms of pressure and temperature leads to the creation of the Spray Flash Evaporation technique, especially tailored for crystallisation. SFE operates from 40 to 100 bars with an RDX solubility in acetone around 5 wt%, whereas sc-CO_2 is formed from 74 bar to 500 bars for a solubility from null to 0.025 wt%.

2.4 The Spray Flash Evaporation Technique

2.4.1 Theoretical Insights on the SFE technology

Flash Evaporation The flash evaporation is the physical phenomenon occurring when the boiling point of a liquid is lower than its actual temperature, due to a sudden drop of pressure and/or a quick increase of temperature. The excess of heat is instantly converted into latent heat of vaporization, cooling both liquid and vapour down to the saturation temperature. Multi Stage Flash (MSF) evaporators of static water have been used since the middle of the XX^{th} century ("Combined flash and vapor compression evaporator" 1956; "Flash-type distillation system" 1959; "Method of and apparatus for flash evaporation treatment" 1957) with yield of around 100 m^3 per day, receiving a growing interest mainly from the US West Coast (Resources 1969) and Japan (national research program "seawater desalting and by product recovery" launched in 1969, (Sawa et al. 1976)). Current applications are extended from solution concentration such as in wine industry (Sebastian et al. 2002) to heat dissipation of electronic chips and LASER devices (Cheng et al. 2016).

Flash Evaporation of Superheated Liquid Jet Brown and York (Brown et al. 1962) found a critical temperature above which the liquid jet was burst by rapid bubbling. They injected water up to 13 bar through simple single-hole nozzles with a minimal diameter of 500 µm into ambient pressure. The linear mean droplet sizes were found to follow a linear variation of temperature. Then in 1981, Miyatake et al. were pioneers in the field of flash evaporation and published the

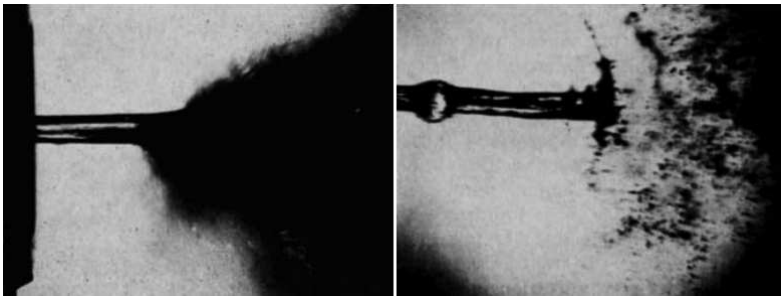

(a) Two different disruptions in flashing water jets enlarged 10X from Brown et al. (1962)

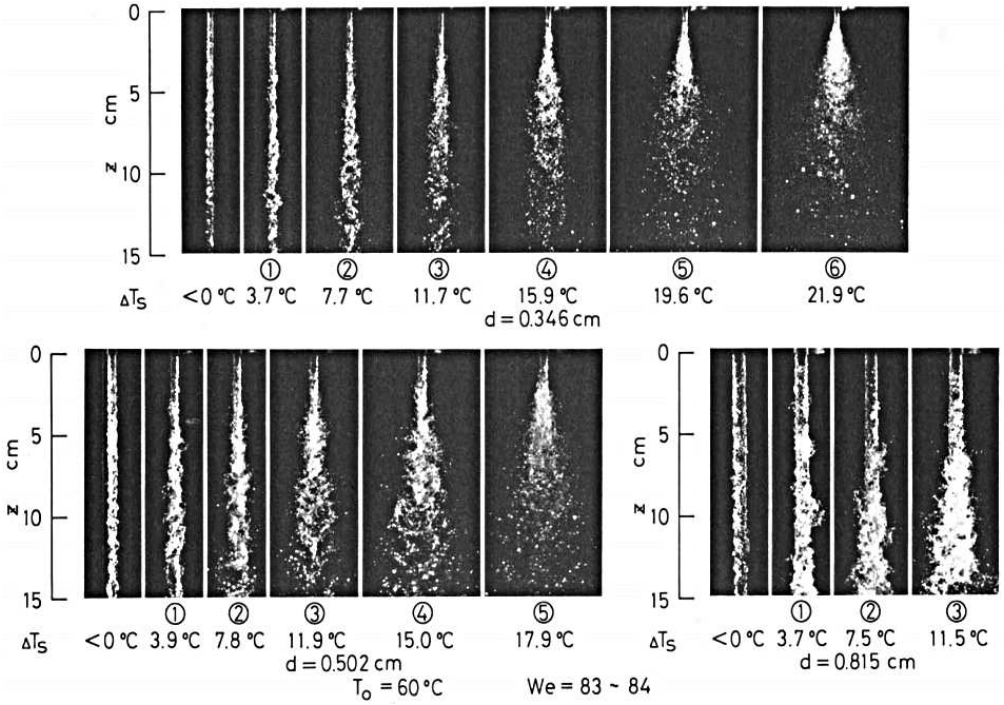

(b) Flashing water jets under various superheating from Miyatake et al. (1981a)

Figure 2.2 – Flashing in water liquid jet

first known articles about spray flash evaporation with superheating (Miyatake et al. 1981a,b), after studying flash evaporation from water pool (Miyatake et al. 1972). Many technical limitations restricted their studies for current issues: only straight-lined liquid jets were studied with basic optical techniques where the smallest drops and bubbles could not be indexed. However, Miyatake et al. (1985) interestingly used electrolysis to generate more bubbles into a flashing water jet. Nowadays, not many laboratories still investigate flashing liquid jets; Günther et al. (2013) characterized with modern techniques flashing liquid jets and noticed the formation of bubbles inside a glass nozzle for high superheating. They also demonstrated that a simple acoustic measurement can be used to monitor the atomization of superheated liquids. The current application of flashing liquid jet is the improvement of MSF desalination processes of sea water (Ikegami et al. 2006; Miyatake et al. 2001); a much higher evaporation rate is obtained in contrast to static flash evaporator where the rate is surface dependent.

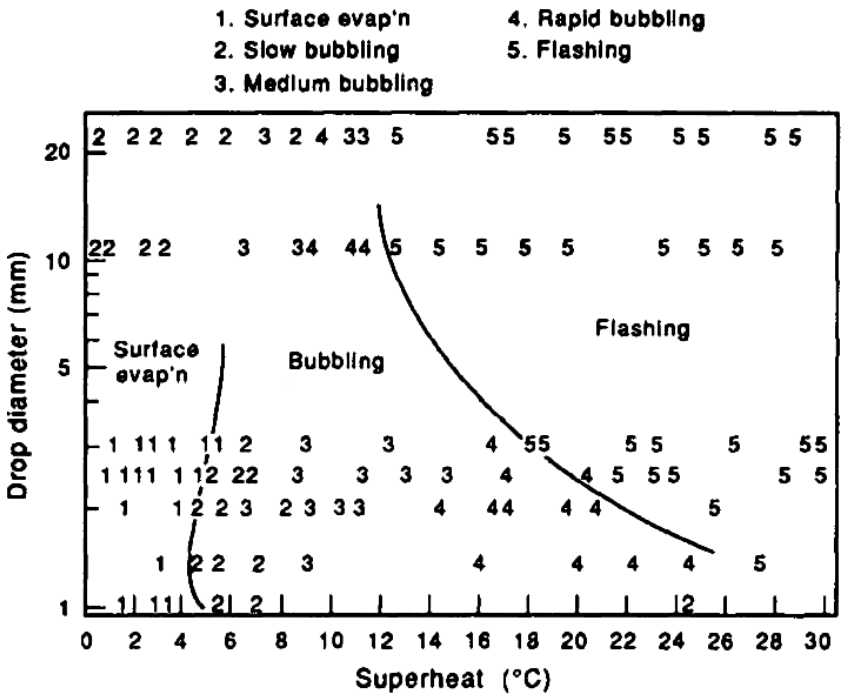

Figure 2.3 – Empirical diagram of the evaporation of a water drop (Owen et al. 1991)

Flash Evaporation of Droplets Specific studies on the flashing phenomenon are rare. Owen et al. (1991) investigated that specific form of evaporation on isolated drops. A superheat of 0 °C to 5 °C triggers only surface evaporation,

then boiling occurs at higher superheat. Flashing is triggered for superheat from 18 °C to 24 °C for drop of 1 mm–3 mm and larger drops flash more readily as illustrated in Figure 2.3. Since flash evaporation is closely related to cooling, many theoretical approaches start with a simplified model without superheating: Shin et al. (2000), Satoh et al. (2002) thoroughly described the evaporation behaviour of a water droplet in an abruptly evacuated atmosphere leading to its solidification. Sobac et al. (2015) developed a comprehensive model of the evaporation of a liquid spherical drop but not yet applicable to extremely small droplets as in flashing spray.

Interesting studies close to our SFE process came from Gebauer et al. (2012, 2015a,b, 2016). In their system, a pressurized superheated liquid is atomized through an hollow cone nozzle into a low pressure chamber and micron-size particles are recovered. However, only a partial evaporation occurs and leads to further crystal growth during the flying time and into the sump collected in the bottom of the crystalliser.

2.4.2 Comprehensive description of SFE

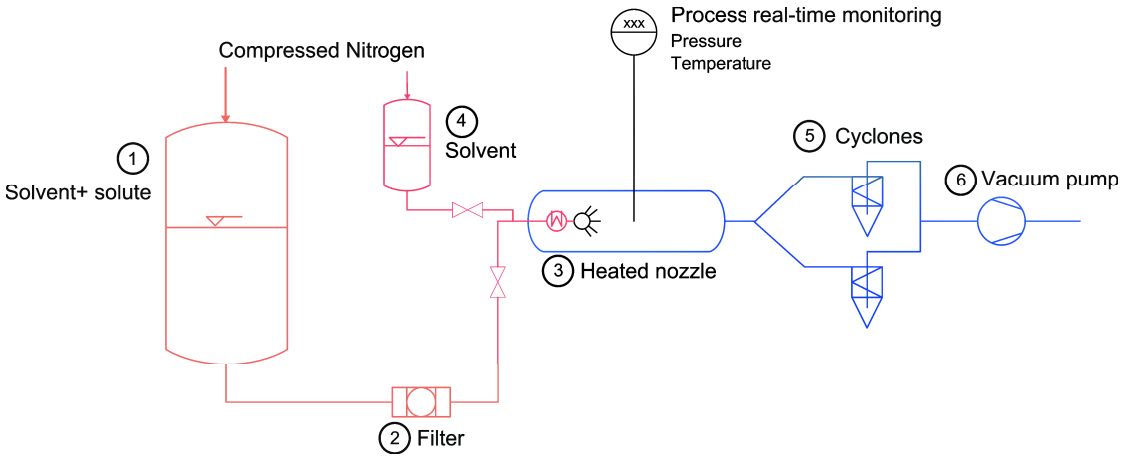

Figure 2.4 – SFE installation as patented and used in this present work

Figure 2.4 is a schematic diagram of the process, where the high pressure part is the red zone and the low pressure one in blue. One storage tank **(4)** is filled with technical grade solvent and is used for pre-heating, cooling and washing. The other tank **(1)** is filled with the solution containing the compound(s) to recrystallize. Both are closed and pressurized with compressed nitrogen at the pre-expansion pressure. Hydraulic tubes bring the fluid inside the atomization chamber; there, a heating jacket superheats the liquid, with a regulation made of thermocouple plugged to a Proportional-Integral-Derivative (PID) controller.

The superheated fluid is sprayed by a hollow cone nozzle **(3)** into the atomization chamber under a vacuum below 10 mbar. Details can be seen in Figure 2.5: the tip of the thermocouple (type K ⌀ 1.5 mm) measures the temperature after the heating jacket and just before the nozzle mounted on a full flow quick coupling.

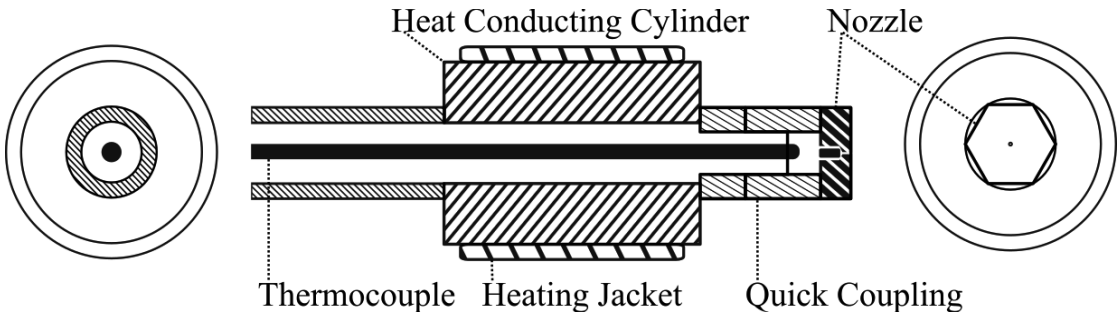

Figure 2.5 – Schematic insight of the nozzle and its heating system; from left to right, rear view, longitudinal cross-section and front view.

The gaseous flow from the evaporation and the recrystallized product is pumped to a cyclonic separator. The cyclones are made from the description of (Chen et al. 2006) who found a cut-off diameter of 21.7 nm–49.8 nm in their work. A glass flat flange reaction vessel allows to gather the powder easily as it can be seen in Figure 2.6. Each cyclone unit can be isolated from the vacuum to allow the recovery of the product from one unit and the continuous separation inside the other: the two cyclones in parallel ensure the continuous functioning of the process at any flow rate.

At the end, the flow of gaseous solvent passes through a 35 m^3/h vacuum pump; a condenser after the pump can recover the solvent for industrial installations.

The standard operating conditions are 40 bar of inlet pressure and 160 °C at the hollow cone nozzle with an orifice diameter of 60 µm.

The maintenance and constant improvements of several SFE installations took a significant part of this research project. The reliability, robustness, ergonomic and life-cycle of the process have been extended by replacing hydraulic and vacuum parts, by understanding phenomena, by developing on-line metrology and by stimulating the necessary feedback and cooperation between the various SFE users at NS3E.

2.4.3 Versatility of the SFE

Depending on the solute and the desired particle size range, the SFE can be adapted by changing the following parameters:

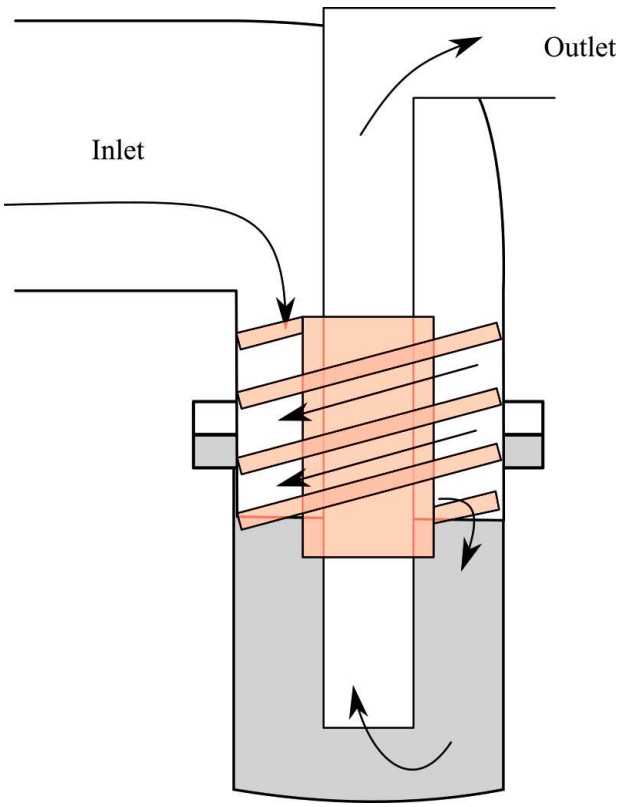

Figure 2.6 – System for the product recovery: in orange the cyclonic separator for vacuum and in gray the interchangeable vessel.

Type of solvent The most suitable solvents for SFE are low-boiling solvents with a high molar heat capacity. For easy handling and recovery, the solvents should have a boiling point in the range of 30 – 70 °C.

Superheating temperature The superheating temperature is proportional to the mass flow and the fluid properties. An increased superheating temperature enables higher evaporation rate.

Pre-expansion pressure The pre-expansion pressure has to be above the vapour pressure of the superheated solvent and compatible with nozzle diameter and type. The droplet size is also known to decrease at higher pressure.

Saturation pressure and temperature Saturation pressure and temperature of the spray cone in the atomization chamber depend mostly on the performance of the vacuum pump.

Nozzle diameter For most nozzles types like hollow cone nozzles, full cone nozzles, or flat jet nozzles, a decreasing orifice diameter decreases the

droplet size, but increases the pre-expansion pressure.

Besides the innovative applications of nano energetic materials such as the synthesis of ultra-fine nano diamonds (Pichot et al. 2015; Pichot et al. 2013) and reactivity enhancement (Comet et al. 2015), the SFE versatility allows the crystallisation at a submicron or nano scale of a wide range of organic compounds. In particular, cocrystals of medical materials are of interest for drug enhancement and were successfully processed through SFE at the nano scale (Spitzer et al. 2014). Inorganic nanoparticles were also produced at the nanoscale through SFE. ZnO was crystallised from the precursor zinc acetate dihydrate dissolved in ethanol with addition of water. From early experiments, nano primary particles of 20 nm were found to be agglomerated in sub-size structures, whereas the slightly larger nanoparticles were found much less agglomerated using the classical wet method. However, the SFE clearly demonstrated the feasibility of faster and quite efficient crystallisation of inorganic particles from precursors. Le Brize et al. (2016) processed energetic composite materials by SFE: a submicron structuration was evidenced from SEM pictures and an higher degree of chemical interaction was also found from Infrared (IR) and Raman spectra.

2.5 Scientific goals of the thesis

2.5.1 Particle Size Reduction

The first main goal of the project is to reduce further the particle size. During his PhD, Risse studied the effects of the superheating temperature, the inlet pressure, the ratio of MTBE/acetone as solvent, the nozzle diameter and the RDX-concentration. At higher superheating temperature and pressure, the droplets are likely smaller which leads to a noticeable decrease of the particle size. However, the role of solvent was not clarified; furthermore, both nozzle diameter and RDX-concentration need to be correlated with the inlet mass flow and the real superheating temperature – which is the difference between the spray and the inlet liquid – should have been monitored and kept constant. To reduce the particle size, the degree of supersaturation has to be controlled in both space and time resolution. Globally, we can distinguish two main approaches, a chemical one and a more physical one. On the chemical route, polymeric additives are studied to control the nucleation and growth steps. On the other side, different conditions of crystallisation are studied by a mixture of an anti-solvent and a solvent, and also by 'in-spray interactions' where two nozzles with overlapping spray patterns are used.

2.5.2 SFE understanding

The crystallisation by SFE results from deep and complex interactions between several physicochemical phenomena. That intricacy is illustrated by the mapping in Figure 2.7. While many parameters are involved, a few bottlenecks emerge: the volume of droplets, the degree of supersaturation and the time of the primary nucleation are keys to achieve a perfect control of the final particle size under flash-evaporation conditions. Therefore, the effort on *in situ* measurement for SFE technology is focused on those observable variables. In the meantime, other parameters has been changed such as the solvent type to influence the supersaturation and the nucleation time by additives.

2.6 Summary of the Chapter

Many crystallisation processes have been applied on RDX and similar energetic organic crystals. The smallest size of RDX is either obtained from wet techniques, or from small-scale approaches which cannot be transferred to industry (PVD and LASER). Finally, the Spray Flash Evaporation (SFE) process is a well balanced method between spray drying unable to process particles lower that the micrometer, and the expensive batch Rapid Expansion of Supercritical Solutions (RESS) process. The SFE relies on the superheating of a solvent sprayed into vacuum and thus flashing. The pressurization of the liquid before the injection provides the stability for the spray pattern and also for the overheated liquid. The flash evaporation is the physical phenomenon occurring when the boiling point of a liquid is lower than its actual temperature, due to a sudden drop of pressure and/or a quick increase of temperature. The excess of heat is instantly converted into latent heat of vaporization, thus provoking the fragmentation of the droplets called “flash”. This allows formation of smaller crystallisation reactors (droplets) with a very high rate of evaporation therefore achieving smallest particle size.

From particle size and shape many properties are resulting such as the surface related ones for catalysis but also more physical one like the apparent density and the critical diameter for explosives. However, the definition of a particle is subject to variation; a real powder may be formed of macroscopic soft agglomerates of micron-sized hard agglomerates of nano primary particles. Therefore each characterization technique measures an unique mean distance depending of the physicochemical phenomena involved and the response of the sample. The following explains the characterizations previously in use at NS3E, their scientific criticism through analytical studies and the new methods applied.

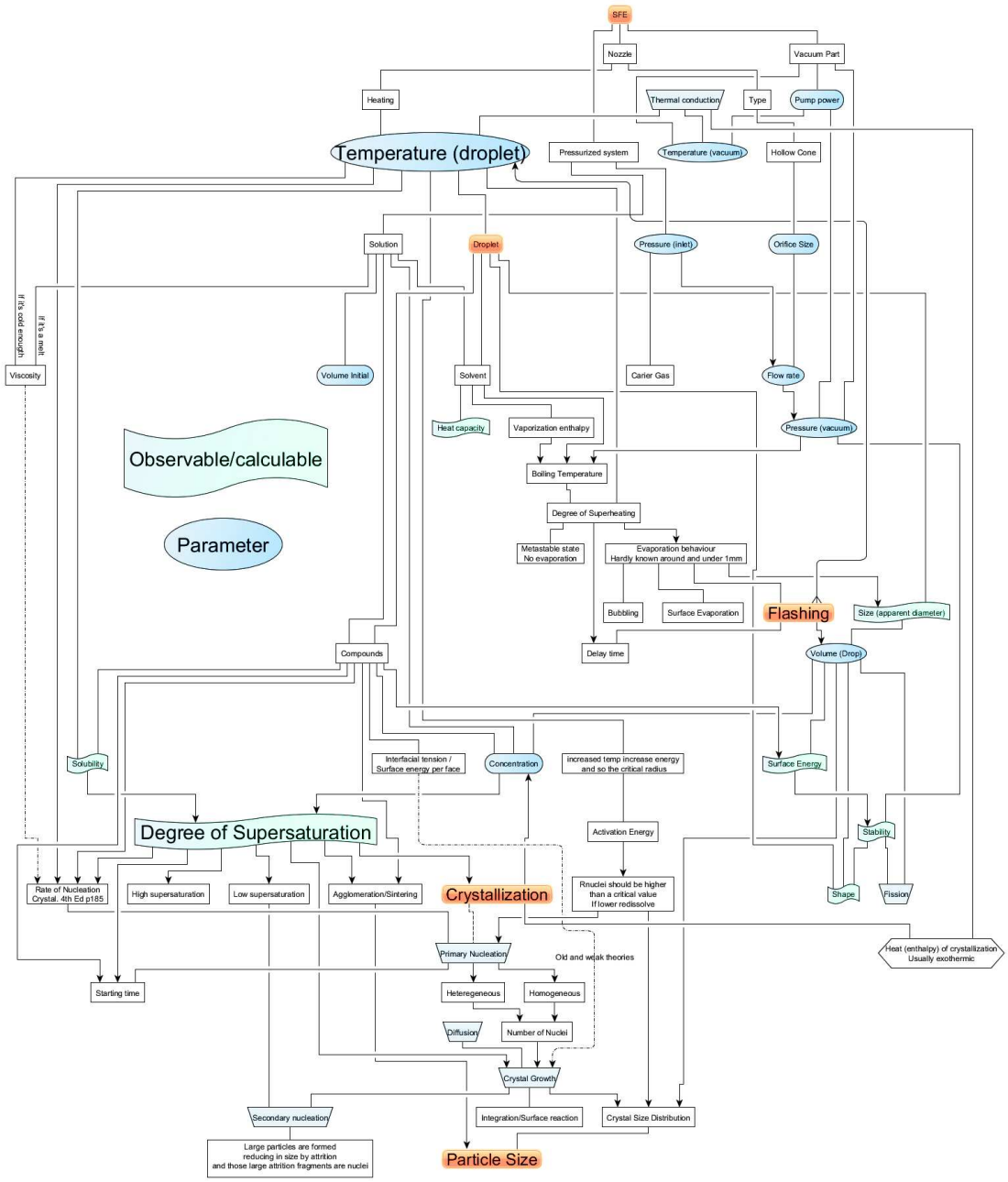

Figure 2.7 – Intricacy of the parameters and phenomena involved in the particle crystallisation by the SFE process.

Bibliography

1. Anniyappan, Marimuthu, Sanjeevani Hemanth Sonawane, Sujeet Kumar Shee, and Arun Kanti Sikder (2015). "Method of Producing Uniformly Shaped and Sized Particles of 2,4,6-Triazido-1,3,5-triazine by Emulsion Crystallization". In: *Central European Journal of Energetic Materials*.
2. Bayat, Y., M. Zarandi, P. Khadiv-Parsi, and A. Salimi Beni (2015). "Statistical optimization of the preparation of HNIW nanoparticles via oil in water microemulsions". In: *Central European Journal of Energetic Materials* 12.3, pp. 459–472. ISSN: 1733-7178.
3. Bhavesh B. Patel and Jayvadan K. Patel and Subhashis Chakraborty (2014). "Review of Patents and Application of Spray Drying in Pharmaceutical, Food and Flavor Industry". In: *Recent Patents on Drug Delivery & Formulation* 8.1, pp. 63–78. ISSN: 1872-2113/2212-4039. DOI: 10.2174/1872211308666140211122012.
4. Broadhead, J., S. K. Edmond Rouan, and C. T. Rhodes (1992). "The spray drying of pharmaceuticals". In: *Drug Development and Industrial Pharmacy* 18.11-12, pp. 1169–1206. DOI: 10.3109/03639049209046327.
5. Brown, Ralph and J. Louis York (1962). "Sprays formed by flashing liquid jets". In: *AIChE Journal* 8.2, pp. 149–153. ISSN: 1547-5905. DOI: 10.1002/aic.690080204.
6. Carter, C. Barry and M. Grant Norton (2013). *Ceramic Materials*. New York, NY: Springer New York. ISBN: 978-1-4614-3522-8 978-1-4614-3523-5.
7. Charitidis, Costas A., Pantelitsa Georgiou, Malamatenia A. Koklioti, Aikaterini-Flora Trompeta, and Vasileios Markakis (2014). "Manufacturing nanomaterials: from research to industry". In: *Manufacturing Review* 1, p. 11. ISSN: 2265-4224. DOI: 10.1051/mfreview/2014009.
8. Chen, Sheng-Chieh and Chuen-Jinn Tsai (2006). "An axial flow cyclone to remove nanoparticles at low pressure conditions". In: *Journal of Nanoparticle Research* 9.1, pp. 71–83. ISSN: 1388-0764, 1572-896X. DOI: 10.1007/s11051-006-9152-z.
9. Cheng, Wen-Long, Wei-Wei Zhang, Hua Chen, and Lei Hu (2016). "Spray cooling and flash evaporation cooling: The current development and application". In: *Renewable and Sustainable Energy Reviews* 55, pp. 614–628. ISSN: 1364-0321. DOI: 10.1016/j.rser.2015.11.014.
10. "Combined flash and vapor compression evaporator" (1956). W.E. Porter and B.F. Smith. US Patent 2,759,882.

11. Comet, Marc, Cédric Martin, Martin Klaumünzer, Fabien Schnell, and Denis Spitzer (2015). "Energetic nanocomposites for detonation initiation in high explosives without primary explosives". In: *Applied Physics Letters* 107.24, p. 243108. ISSN: 0003-6951, 1077-3118. DOI: 10.1063/1.4938139.

12. "Conditioning of finely divided crude organic pigments" (1984). US4451654 A. F. Graser and G. Wickenhaeuser.

13. Dabin, Liu, Xu Dong, and Zhao Baochang (1999). "Preparation of Nanometer RDX in Situ by Solvent Substitution Effect in Reverse Micelle". In: *26th, International pyrotechnics seminar*. PROCEEDINGS OF THE INTERNATIONAL PYROTECHNICS SEMINAR. Nanjing University of Science and Technology, pp. 269–275.

14. Dixon, David J, Keith P Johnston, and Roland A Bodmeier (1993). "Polymeric materials formed by precipitation with a compressed fluid antisolvent". In: *AIChE Journal* 39.1, pp. 127–139.

15. Dou, Haiyang, Ki-Hoon Kim, Byung-Chul Lee, Jinkyu Choe, Hyoun-Soo Kim, and Seungho Lee (2013). "Preparation and characterization of cyclo-1,3,5-trimethylene-2,4,6-trinitramine (RDX) powder: Comparison of microscopy, dynamic light scattering and field-flow fractionation for size characterization". In: *Powder Technology* 235, pp. 814–822. ISSN: 00325910. DOI: 10.1016/j.powtec.2012.11.042.

16. Essel, Jonathan T., Andrew C. Cortopassi, Kenneth K. Kuo, James H. Adair, Christopher G. Leh, and Thomas M. Klapoetke (2010). *Synthesis of Energetic Materials by Rapid Expansion of a Supercritical Solution into Aqueous Solution (RESS-AS) Process*. DTIC Document.

17. Essel, Jonathan T., Andrew C. Cortopassi, Kenneth K. Kuo, Christopher G. Leh, and James H. Adair (2012). "Formation and Characterization of Nano-sized RDX Particles Produced Using the RESS-AS Process". In: *Propellants, Explosives, Pyrotechnics* 37.6, pp. 699–706. ISSN: 07213115. DOI: 10.1002/prep.201100139.

18. Fedoroff, Basil T. and Oliver E. Sheffield (1966). *ENCYCLOPEDIA OF EXPLOSIVES AND RELATED ITEMS. VOLUME 3*. PA-TR-2700-VOL-3. PICATINNY ARSENAL DOVER NJ, PICATINNY ARSENAL DOVER NJ.

19. "Finely dispersed carotenoid pigments prodn. - by dissolving carotenoid in a supercritical gas, pref. carbon di:oxide, and dispersing the soln. in an aq. colloidal matrix" (1981). DE2943267 A1. W. D. C. D. Best, F. J. D. C. Mueller, K. D. C. D. Schmieder, R. D. C. D. Frank, and J. D. C. D. Paust.

20. "Flash-type distillation system" (1959). B.H. Edwin. US Patent 2,908,618.

21. Frolov, Yu V., A. N. Pivkina, P. A. Ul'yanova, and S. A. Zav'yalov (2002). "Synthesis of Energy-Rich Nanomaterials". In: *Combustion, Explosion and Shock Waves* 38.6, pp. 709–713. DOI: 10.1023/A:1021104714435.

22. Frolov, Yu. V., A. N. Pivkina, S. A. Zav'yalov, N. V. Murav'ev, E. A. Skryleva, and K. A. Monogarov (2010). "Physicochemical characteristics of the components of energetic condensed systems". In: *Russian Journal of Physical Chemistry B* 4.6, pp. 916–922. ISSN: 1990-7931, 1990-7923. DOI: 10.1134/S1990793110060072.

23. Gallagher, Paula M., M. P. Coffey, V. J. Krukonis, and W. W. Hillstrom (1992). "Gas antisolvent recrystallization of RDX: formation of ultra-fine particles of a difficult-to-comminute explosive". In: *The Journal of Supercritical Fluids* 5.2, pp. 130–142.

24. Gao, Bing, Dunju Wang, Juan Zhang, Yingjie Hu, Jinpeng Shen, Jun Wang, Bing Huang, Zhiqiang Qiao, Hui Huang, Fude Nie, and Guangcheng Yang (2014a). "Facile, continuous and large-scale synthesis of CL-20/HMX nano co-crystals with high-performance by ultrasonic spray-assisted electrostatic adsorption method". In: *J. Mater. Chem. A* 2.47, pp. 19969–19974. ISSN: 2050-7488, 2050-7496. DOI: 10.1039/C4TA04979A.

25. Gao, Bing, Peng Wu, Bing Huang, Jun Wang, Zhiqiang Qiao, Guangcheng Yang, and Fude Nie (2014b). "Preparation and characterization of nano-1,1-diamino-2,2-dinitroethene (FOX-7) explosive". In: *New Journal of Chemistry* 38.6, p. 2334. ISSN: 1144-0546, 1369-9261. DOI: 10.1039/c3nj01053h.

26. Gash, A E, R L Simpson, T M Tillotson, J H Satcher, and L W Hrubesh (2000). "Making nanostructured pyrotechnics in a beaker". In: Conference: International Pyrotechnics Seminars. Grand Junction, CO (US).

27. Gebauer, Jörn, Raffael Kaiser, and M. Kind (2012). "Flash-Kristallisation - Wirkungsmechanismen im Kristallisator und das Betriebsverhalten des kontinuierlichen Prozesses". In: *Chemie Ingenieur Technik* 84.11, pp. 1901–1910. ISSN: 0009286X. DOI: 10.1002/cite.201200021.

28. Gebauer, Jörn and Matthias Kind (2015a). "Experimental screening method for flash-crystallization". In: *Chemical Engineering Science* 133, pp. 75–81. ISSN: 00092509. DOI: 10.1016/j.ces.2014.12.034.

29. — (2015b). "Profiles of temperature, concentration and supersaturation within atomized droplets during flash-crystallization". In: *Chemical Engineering and Processing: Process Intensification* 91, pp. 130–140. ISSN: 02552701. DOI: 10.1016/j.cep.2015.03.012.

30. Gebauer, Jörn, Daniel Selzer, and Matthias Kind (2016). "Flash-Kristallisation". In: *Chemie Ingenieur Technik* 88.7, pp. 881–889. ISSN: 1522-2640. DOI: 10.1002/cite.201500148.

31. Gibbs, Bernard F, Selim Kermasha, Inteaz Alli, and Catherine N Mulligana (1999). "Encapsulation in the food industry: a review". In: *International Journal of Food Sciences and Nutrition* 50.3, pp. 213–224. DOI: 10.1080/096374899101256.

32. Gottfried, Jennifer L, Frank C De Lucia Jr, and Stephanie M Piraino (2012). *Characterization of the Morphology of RDX Particles Formed by Laser Ablation*.

33. Günther, A. and K.-E. Wirth (2013). "Evaporation phenomena in superheated atomization and its impact on the generated spray". In: *International Journal of Heat and Mass Transfer* 64, pp. 952–965. ISSN: 00179310. DOI: 10.1016/j.ijheatmasstransfer.2013.05.034.

34. GUO Qiu-xia (2006). "Preparation of RDX/Resorcinol-formaldehyde (RF) Nano-composite Energetic Materials by Sol-Gel Method". In:

35. Hannay, JB and James Hogarth (1879). "On the solubility of solids in gases". In: *Proceedings of the royal society of London* 30.200-205, pp. 178–188.

36. Ikegami, Yasuyuki, Hiroshi Sasaki, Tomotsugu Gouda, and Haruo Uehara (2006). "Experimental study on a spray flash desalination (influence of the direction of injection)". In: *Desalination* 194.1–3, pp. 81–89. ISSN: 0011-9164. DOI: 10.1016/j.desal.2005.10.026.

37. Ji, Wei, Xiaodong Li, and Jingyu Wang (2015). "Preparation and Characterization of CL-20/EPDM by a Crystal Refinement and Spray Drying Method". In: *Central European Journal of Energetic Materials*.

38. Jin, Miaomiao, Gang Wang, Jingke Deng, Guoping Li, Muhua Huang, and Yunjun Luo (2015). "Preparation and properties of NC/RDX/AP nano-composite energetic materials by the sol–gel method". In: *Journal of Sol-Gel Science and Technology* 76.1, pp. 58–65. ISSN: 0928-0707, 1573-4846. DOI: 10.1007/s10971-015-3750-0.

39. Jung, Jennifer and Michel Perrut (2001). "Particle design using supercritical fluids: Literature and patent survey". In: *The Journal of Supercritical Fluids* 20.3, pp. 179–219. ISSN: 0896-8446. DOI: 10.1016/S0896-8446(01)00064-X.

40. Kim, J. W., H. M. Shim, J. K. Kim, M. S. Shin, H. S. Kima, and K. K. Koo (2011a). "Effect Of Polyvinylpyrrolidone On Crystallization Of Rdx By Ultrasonic Spray". In: 18th International Symposium on Industrial Crystallization.

41. Kim, Jun-Woo, Moon-Soo Shin, Jae-Kyeong Kim, Hyoun-Soo Kim, and Kee-Kahb Koo (2011b). "Evaporation Crystallization of RDX by Ultrasonic Spray". In: *Industrial & Engineering Chemistry Research* 50.21, pp. 12186–12193. ISSN: 0888-5885, 1520-5045. DOI: 10.1021/ie201314r.

42. Krukonis, Val (1984). "Supercritical Fluid Nucleation of Difficultto-Comminute Solids". In: *Annual Meeting - American Institute of Chemical Engineers*. cited By (since 1996)0.

43. Kumar, Raj, Prem F. Siril, and Pramod Soni (2014). "Preparation of Nano-RDX by Evaporation Assisted Solvent/Antisolvent Interaction". In: *Propellants, Explosives, Pyrotechnics* 39.3, pp. 383–389. ISSN: 07213115. DOI: 10.1002/prep.201300104.

44. Kumar, Raj, Prem Felix Siril, and Pramod Soni (2015). "Optimized Synthesis of HMX Nanoparticles Using Antisolvent Precipitation Method". In: *Journal of Energetic Materials* 33.4, pp. 277–287. ISSN: 0737-0652. DOI: 10.1080/07370652.2014.988774.

45. Kuo, Kenneth K., Jonathan T. Essel, and James H. Adair (2011). "Processing Nano-Sized Energetic Materials with Supercritical Fluid Precipitation Techniques". AFOSR Nanoenergetics and Combustion Dynamics Workshop.

46. L. De Meyer, P.-J. Van Bockstal, J. Corver, C. Vervaet, J. P. Remon, and T. De Beer (2015). "Evaluation of spin freezing versus conventional freezing as part of a continuous pharmaceutical freeze-drying concept for unit doses". In: *International Journal of Pharmaceutics* 496.1. Special Issue on, pp. 75–85. ISSN: 0378-5173. DOI: http://dx.doi.org/10.1016/j.ijpharm.2015.05.025.

47. Lavernia, Enrique J. and T. S. Srivatsan (2009). "The rapid solidification processing of materials: science, principles, technology, advances, and applications". In: *Journal of Materials Science* 45.2, pp. 287–325. ISSN: 1573-4803. DOI: 10.1007/s10853-009-3995-5.

48. Le Brize, Axel and Denis Spitzer (2016). "Plasticization of Submicron-Structured LOVA Propellants by a Linear Dinitramine". In: *Central European Journal of Energetic Materials* 13.

49. Lee, Byoung-Min, Jin-Seong Jeong, Young-Ho Lee, Byung-Chul Lee, Hyoun-Soo Kim, Hwayong Kim, and Youn-Woo Lee (2009). "Supercritical Antisolvent Micronization of Cyclotrimethylenetrinitramin: Influence of the Organic Solvent". In: *Industrial & Engineering Chemistry Research* 48.24, pp. 11162–11167. ISSN: 0888-5885, 1520-5045. DOI: 10.1021/ie900448w.

50. Lee, Byoung-Min, Dae Sung Kim, Young-Ho Lee, Byung-Chul Lee, Hyoun-Soo Kim, Hwayong Kim, and Youn-Woo Lee (2011a). "Preparation of submicron-sized RDX particles by rapid expansion of solution using compressed liquid dimethyl ether". In: *The Journal of Supercritical Fluids* 57.3, pp. 251–258. ISSN: 08968446. DOI: 10.1016/j.supflu.2011.03.008.

51. Lee, Byoung-Min, Soo-Jung Kim, Byung-Chul Lee, Hyoun-Soo Kim, Hwayong Kim, and Youn-Woo Lee (2011b). "Preparation of Micronized β-HMX Using Supercritical Carbon Dioxide as Antisolvent". In: *Industrial & Engineering Chemistry Research* 50.15, pp. 9107–9115. ISSN: 0888-5885, 1520-5045. DOI: 10.1021/ie102593p.

52. Li, Guoping, Menghui Liu, Ran Zhang, Lianhua Shen, Yazhong Liu, and Yunjun Luo (2015a). "Synthesis and properties of RDX/GAP nano-composite energetic materials". In: *Colloid and Polymer Science* 293.8, pp. 2269–2279. ISSN: 0303-402X, 1435-1536. DOI: 10.1007/s00396-015-3620-x.

53. Li, Hequn, Chongwei An, Wenjian Guo, Xiaoheng Geng, Jingyu Wang, and Wenzheng Xu (2015b). "Preparation and Performance of Nano HMX/TNT Cocrystals". In: *Propellants, Explosives, Pyrotechnics*, n/a–n/a. ISSN: 1521-4087. DOI: 10.1002/prep.201400175.

54. Li, Wenpeng, Ning Liao, Xiaohui Duan, Chonghua Pei, and Xiaoqing Zhou (2015c). "Investigation of nucleation kinetics and crystal defects of HMX". In: *Crystal Research and Technology* 50.7, pp. 505–515. ISSN: 1521-4079. DOI: 10.1002/crat.201400425.

55. Lim, G. B., S. Y. Lee, K. K. Koo, B. S. Park, and H. S. Kim (1998). "Gas anti-solvent Recrystallization of Molecular Explosives under Subcritical to Supercritical Conditions". In: *Proceedings of the 5th Meeting on Supercritical Fluids*. Nice.

56. Liu, Jie, Wei Jiang, Fengsheng Li, Longxiang Wang, Jiangbao Zeng, Qing Li, Yi Wang, and Qing Yang (2014a). "Effect of Drying Conditions on the Particle Size, Dispersion State, and Mechanical Sensitivities of Nano HMX". In: *Propellants, Explosives, Pyrotechnics* 39.1, pp. 30–39. ISSN: 1521-4087. DOI: 10.1002/prep.201300050.

57. Liu, Jie, Wei Jiang, Qing Yang, Jian Song, Ga-zi Hao, and Feng-sheng Li (2014b). "Study of nano-nitramine explosives: preparation, sensitivity and application". In: *Defence Technology* 10.2, pp. 184–189. ISSN: 22149147. DOI: 10.1016/j.dt.2014.04.002.

58. Liu, Jie, Wei Jiang, Jiang-bao Zeng, Qing Yang, Yu-jiao Wang, and Feng-sheng Li (2013). "Effect of Drying on Particle Size and Sensitivities of Nano hexahydro-1,3,5-trinitro-1,3,5-triazine". In: *Defence Technology* 10.1, pp. 9–16. ISSN: 2214-9147. DOI: 10.1016/j.dt.2013.12.006.

59. Luo, Qingping, Chonghua Pei, Guixiang Liu, Yongjun Ma, and Zhaoqian Li (2015). "Insensitive High Cyclotrimethylenetrinitramine (RDX) Nanostructured Explosives Derived from Solvent/Nonsolvent Method in a Bacterial Cellulose (BC) Gelatin Matrix". In: *Nano* 10.03, p. 1550033. ISSN: 1793-2920, 1793-7094. DOI: 10.1142/S1793292015500332.

60. Ma, Zhigang, Bing Gao, Peng Wu, Jinchun Shi, Zhiqiang Qiao, Zhijian Yang, Guangcheng Yang, Bing Huang, and Fude Nie (2015). "Facile, continuous and large-scale production of core–shell HMX@TATB composites with superior mechanical properties by a spray-drying process". In: *RSC Adv.* 5.27, pp. 21042–21049. ISSN: 2046-2069. DOI: 10.1039/C4RA16527F.

61. Madene, Atmane, Muriel Jacquot, Joël Scher, and Stéphane Desobry (2006). "Flavour encapsulation and controlled release – a review". In: *International Journal of Food Science Technology* 41.1, pp. 1–21. ISSN: 1365-2621. DOI: 10.1111/j.1365-2621.2005.00980.x.

62. Matson, D.W., J.L. Fulton, R.C. Petersen, and R.D. Smith (1987a). "Rapid expansion of supercritical fluid solutions: solute formation of powders, thin films, and fibers". In: *Industrial and Engineering Chemistry Research* 26.11. cited By (since 1996)248, pp. 2298–2306.

63. Matson, D.W., R.C. Petersen, and R.D. Smith (1987b). "Production of powders and films by the rapid expansion of supercritical solutions". In: *Journal of Materials Science* 22.6. cited By (since 1996)56, pp. 1919–1928.

64. Mersmann, Alfons (2001). *Crystallization technology handbook*. CRC Press.

65. Messing, Gary L., Shi-Chang Zhang, and Gopal V. Jayanthi (1993). "Ceramic Powder Synthesis by Spray Pyrolysis". In: *Journal of the American Ceramic Society* 76.11, pp. 2707–2726. ISSN: 1551-2916. DOI: 10.1111/j.1151-2916.1993.tb04007.x.

66. "Method of and apparatus for flash evaporation treatment" (1957). E.T. Allen and K.T. Hanson. US Patent 2,803,589.

67. Mil'chenko, D. V., V. A. Gubachev, L. A. Andreevskikh, S. A. Vakhmistrov, A. L. Mikhailov, V. A. Burnashov, E. V. Khaldeev, A. I. Pyatoikina, S. S. Zhuravlev, and V. N. German (2015). "Nanostructured explosives produced by vapor deposition: Structure and explosive properties". In: *Combustion, Explosion, and Shock Waves* 51.1, pp. 80–85. ISSN: 0010-5082, 1573-8345. DOI: 10.1134/S0010508215010086.

68. Miyatake, O., T. Tomimura, and Y. Ide (1985). "Enhancement of Spray Flash Evaporation by Means of the Injection of Bubble Nuclei". In: *Journal of Solar Energy Engineering* 107.2, pp. 176–182. ISSN: 0199-6231. DOI: 10.1115/1.3267673.

69. Miyatake, O., T. Tomimura, Y. Ide, and T. Fujii (1981a). "An experimental study of spray flash evaporation". In: *Desalination* 36.2, pp. 113–128. ISSN: 0011-9164. DOI: 10.1016/S0011-9164(00)88635-X.

70. Miyatake, O., T. Tomimura, Y. Ide, M. Yuda, and T. Fujii (1981b). "Effect of liquid temperature on spray flash evaporation". In: *Desalination* 37.3, pp. 351–366. ISSN: 0011-9164. DOI: 10.1016/S0011-9164(00)88658-0.

71. Miyatake, Osamu, Yasushi Koito, Kotaro Tagawa, and Yasuhiro Maruta (2001). "Transient characteristics and performance of a novel desalination system based on heat storage and spray flashing". In: *Desalination* 137.1–3, pp. 157–166. ISSN: 0011-9164. DOI: 10.1016/S0011-9164(01)00214-4.

72. Miyatake, Osamu, Kentaro Murakami, Yoichi Kawata, and Tetsu Fujii (1972). "Fundamental Experiments of Flash Evaporation". In: *Bulletin of the Society of Sea Water Science, Japan* 26.4, pp. 189–198. DOI: 10.11457/swsj1965.26.189.

73. Okuyama, Kikuo and I. Wuled Lenggoro (2003). "Preparation of nanoparticles via spray route". In: *Chemical Engineering Science*. 17th International Symposium of Chemical Reaction Engineering (IS CRE 17) 58.3–6, pp. 537–547. ISSN: 0009-2509. DOI: 10.1016/S0009-2509(02)00578-X.

74. Owen, I. and J. M. Jalil (1991). "Heterogeneous flashing in water drops". In: *International Journal of Multiphase Flow* 17.5, pp. 653–660. ISSN: 0301-9322. DOI: 10.1016/0301-9322(91)90030-7.

75. PANT, Arti, Amiya Kumar NANDI, Shireeshkumar Pralhad NEWALE, Vandana Prakash GAJBHIYE, Hima PRASANTH, and Raj Kishore PANDEY (2013). "Preparation and Characterization of Ultrafine RDX". In: *Central European Journal of Energetic Materials* 10.3, pp. 393–407.

76. Patel, Rajen B., Victor Stepanov, Sean Swaszek, Ashok Surapaneni, and Hongwei Qiu (2015). "Investigation of CL-20 and RDX Nanocomposites". In: *Propellants, Explosives, Pyrotechnics*, n/a–n/a. ISSN: 07213115. DOI: 10.1002/prep.201500130.

77. Pichot, V., M. Comet, B. Risse, and D. Spitzer (2015). "Detonation of nanosized explosive: New mechanistic model for nanodiamond formation". In: *Diamond and Related Materials* 54, pp. 59–63. ISSN: 09259635. DOI: 10.1016/j.diamond.2014.09.013.

78. Pichot, Vincent, Benedikt Risse, Fabien Schnell, Julien Mory, and Denis Spitzer (2013). "Understanding ultrafine nanodiamond formation using nanostructured explosives". In: *Scientific Reports* 3. DOI: 10.1038/srep02159.

79. Pivkina, Alla, Polina Ulyanova, Yurii Frolov, Sergey Zavyalov, and Joop Schoonman (2004). "Nanomaterials for Heterogeneous Combustion". In: *Propellants, Explosives, Pyrotechnics* 29.1, pp. 39–48. ISSN: 0721-3115, 1521-4087. DOI: 10.1002/prep.200400025.

80. Pourmortazavi, Seied Mahdi and Seiedeh Somayyeh Hajimirsadeghi (2005). "Application of Supercritical Carbon Dioxide in Energetic Materials Processes: A Review". In: *Industrial & Engineering Chemistry Research* 44.17, pp. 6523–6533. ISSN: 0888-5885, 1520-5045. DOI: 10.1021/ie0503242.

81. Qiu, Hongwei, Rajen B. Patel, Reddy S. Damavarapu, and Victor Stepanov (2015a). "Nanoscale 2CL-20·HMX high explosive cocrystal synthesized by bead milling". In: *CrystEngComm* 17.22, pp. 4080–4083. ISSN: 1466-8033. DOI: 10.1039/C5CE00489F.

82. Qiu, Hongwei, Victor Stepanov, Tsengming Chou, Ashok Surapaneni, Anthony R. Di Stasio, and Woo Y. Lee (2012). "Single-step production and formulation of HMX nanocrystals". In: *Powder Technology* 226, pp. 235–238. ISSN: 00325910. DOI: 10.1016/j.powtec.2012.04.053.

83. Qiu, Hongwei, Victor Stepanov, Anthony R. Di Stasio, Tsengming Chou, and Woo Y. Lee (2011). "RDX-based nanocomposite microparticles for significantly reduced shock sensitivity". In: *Journal of Hazardous Materials* 185.1, pp. 489–493. ISSN: 03043894. DOI: 10.1016/j.jhazmat.2010.09.058.

84. Qiu, Hongwei, Victor Stepanov, Anthony R. Di Stasio, Ashok Surapaneni, and Woo Y. Lee (2015b). "Investigation of the crystallization of RDX during spray drying". In: *Powder Technology* 274, pp. 333–337. ISSN: 00325910. DOI: 10.1016/j.powtec.2015.01.032.

85. Radacsi, Norbert (2012). "Process Intensification in Crystallization: Submicron Particle Generation Using Alternative Energy Forms". Dissertation. Mechanical, Maritime and Materials Engineering.

86. Radacsi, Norbert, A. I. Stankiewicz, Y. L. M. Creyghton, A. E. D. M. van der Heijden, and J. H. ter Horst (2011). "Electrospray Crystallization for High-Quality Submicron-Sized Crystals". In: *Chemical Engineering & Technology* 34.4, pp. 624–630. ISSN: 09307516. DOI: 10.1002/ceat.201000538.

87. Redner, P., D. Kapoor, R. Patel, M. Chung, and D. Martin (2006). *Production and Characterization of Nano-RDX*. DTIC Document.

88. *Regulation (EC) No 1907/2006 on the Registration, Evaluation, Authorisation and Restriction of Chemicals (REACH) and setting up a European Chemicals Agency* (2007).

89. Resources, California Dept of Water (1969). *Desalting - state of the art*. Sacramento: Available from Office of Procurement, Documents Section. viii, 56.

90. Reus, M.A., G. Hoetmer, A.E.D.M. van der Heijden, and J.H. ter Horst (2014). "Concomitant crystallization for in situ encapsulation of organic materials". In: *Chemical Engineering and Processing: Process Intensification* 80, pp. 11–20. ISSN: 02552701. DOI: 10.1016/j.cep.2014.03.016.

91. Reverchon, E., H. Kröber, and U. Teipel (2005). "Crystallization with Compressed Gases". In: *Energetic Materials*. Wiley-VCH Verlag GmbH & Co. KGaA, pp. 159–182. ISBN: 978-3-527-60392-3.

92. Reverchon, Ernesto (1999). "Supercritical antisolvent precipitation of micro-and nanoparticles". In: *The journal of supercritical fluids* 15.1, pp. 1–21.

93. Risse, Benedikt (2012). "Continuous crystallization of ultra-fine energetic particles by the Flash-Evaporation Process".

94. Risse, Benedikt, Denis Spitzer, Dominique Hassler, Fabien Schnell, Marc Comet, Vincent Pichot, and Hervé Muhr (2012). "Continuous formation of submicron energetic particles by the flash-evaporation technique". In: *Chemical Engineering Journal* 203, pp. 158–165. ISSN: 1385-8947. DOI: 10.1016/j.cej.2012.07.032.

95. Roeske, Frank, Jerry Benterou, Ronald Lee, and Edward Roos (2003). "Cutting and machining energetic materials with a femtosecond laser". In: *Propellants, Explosives, Pyrotechnics* 28.2, pp. 53–57.

96. Rouquerol, J, D Avnir, CW Fairbridge, DH Everett, JM Haynes, N Pernicone, JDF Ramsay, KSW Sing, and KK Unger (1994). "Recommendations for the characterization of porous solids (Technical Report)". In: *Pure and Applied Chemistry* 66.8, pp. 1739–1758.

97. Satoh, Isao, Kazuyoshi Fushinobu, and Yu Hashimoto (2002). "Freezing of a water droplet due to evaporation—heat transfer dominating the evaporation–freezing phenomena and the effect of boiling on freezing characteristics". In: *International Journal of Refrigeration* 25.2, pp. 226–234. ISSN: 0140-7007. DOI: 10.1016/S0140-7007(01)00083-4.

98. Sawa, Toshio, Kenkichi Izumi, and Sankichi Takahashi (1976). "Decarbonation characteristics of the packed tower and its effects on scale prevention in flash evaporation plants". In: *Desalination* 19.1, pp. 369–380. ISSN: 0011-9164. DOI: 10.1016/S0011-9164(00)88045-5.

99. Sebastian, Patrick and Jean Pierre Nadeau (2002). "Experiments and modeling of falling jet flash evaporators for vintage treatment". In: *International Journal of Thermal Sciences* 41.3, pp. 269–280. ISSN: 1290-0729. DOI: 10.1016/S1290-0729(01)01315-1.

100. Shang, Feifei and Jinglin Zhang (2014). "A Successive and Scalable Process for Preparing Spherical Submicrometer-Sized RDX by the SEDS Process". In: *Journal of Energetic Materials* 32 (sup1), S71–S82. ISSN: 0737-0652. DOI: 10.1080/07370652.2013.829133.

101. Sheth, Pratik, Harpreet Sandhu, Dharmendra Singhal, Waseem Malick, Navnit Shah, and M. Serpil Kislalioglu (2012). "Nanoparticles in the Pharmaceutical Industry and the Use of Supercritical Fluid Technologies for Nanoparticle Production". In: *Current Drug Delivery* 9.3, pp. 269–284. DOI: 10.2174/156720112800389052.

102. Shi, Xiaofeng, Cailing Wang, Jingyu Wang, Xiaodong Li, Chongwei AN, Jiang WANG, and Wei JI (2015). "Process Optimization and Characterization of an HMX/Viton Nanocomposite". In: *Central European Journal of Energetic Materials* 12.3, pp. 487–495.

103. Shin, H. T., Y. P. Lee, and J. Jurng (2000). "Spherical-shaped ice particle production by spraying water in a vacuum chamber". In: *Applied Thermal Engineering* 20.5, pp. 439–454. ISSN: 1359-4311. DOI: 10.1016/S1359-4311(99)00035-6.

104. Sobac, B., P. Talbot, B. Haut, A. Rednikov, and P. Colinet (2015). "A comprehensive analysis of the evaporation of a liquid spherical drop". In: *Journal of Colloid and Interface Science* 438, pp. 306–317. ISSN: 00219797. DOI: 10.1016/j.jcis.2014.09.036.

105. Spitzer, D., B. Risse, F. Schnell, V. Pichot, M. Klaumünzer, and M. R. Schaefer (2014). "Continuous engineering of nano-cocrystals for medical and energetic applications". In: *Scientific Reports* 4. DOI: 10.1038/srep06575.

106. Spitzer, Denis, Christian Baras, Michael Richard Schäfer, Fabrice Ciszek, and Benny Siegert (2011). "Continuous Crystallization of Submicrometer Energetic Compounds". In: *Propellants, Explosives, Pyrotechnics* 36.1, pp. 65–74. ISSN: 07213115. DOI: 10.1002/prep.200900002.

107. Spitzer, Denis, Marc Comet, Christian Baras, Vincent Pichot, and Nelly Piazzon (2010). "Energetic nano-materials: Opportunities for enhanced performances". In: *Journal of Physics and Chemistry of Solids* 71.2, pp. 100–108. ISSN: 00223697. DOI: 10.1016/j.jpcs.2009.09.010.

108. Stein, W. A. (1973). "Spray Drying. An Introduction to Principles, Operational Practice and Applications". In: *Chemie Ingenieur Technik* 45.13, pp. 906–907. ISSN: 1522-2640. DOI: 10.1002/cite.330451311.

109. Stepanov, Victor (2003). "Production of nanocrystalline nitramine energetic materials by ress".

110. — (2008). "Production of nanocrystalline RDX by RESS: Process development and material characterization".

111. Stepanov, Victor, Venant Anglade, Wendy A. Balas Hummers, Andrey V. Bezmelnitsyn, and Lev N. Krasnoperov (2011). "Production and Sensitivity Evaluation of Nanocrystalline RDX-based Explosive Compositions". In: *Propellants, Explosives, Pyrotechnics* 36.3, pp. 240–246. ISSN: 1521-4087. DOI: 10.1002/prep.201000114.

112. Stepanov, Victor, Venant Anglade, Andrei Bezmelnitsyn, and Lev N. Krasnoperov (2006). "Production and characterization of nanocrystalline explosive RDX". In: *AIChE Annual Meeting, San Francisco, CA*.

113. Stepanov, Victor, Lev N. Krasnoperov, Inga B. Elkina, and Xuyean Zhang (2005). "Production of Nanocrystalline RDX by Rapid Expansion of Supercritical Solutions". In: *Propellants, Explosives, Pyrotechnics* 30.3, pp. 178–183. ISSN: 0721-3115, 1521-4087. DOI: 10.1002/prep.200500002.

114. Teipel, Ulrich, Ulrich Förter-Barth, Peter Gerber, and Horst H. Krause (1997). "Formation of particles of explosives with supercritical fluids". In: *Propellants, explosives, pyrotechnics* 22.3, pp. 165–169.

115. Teipel, Ulrich, Hartmut Kröber, and Horst H. Krause (2001). "Formation of Energetic Materials Using Supercritical Fluids". In: *Propellants, Explosives, Pyrotechnics* 26.4, pp. 168–173. ISSN: 1521-4087. DOI: 10.1002/1521-4087(200110)26:4<168::AID-PREP168>3.0.CO;2-X.

116. Tillotson, T. M., A. E. Gash, R. L. Simpson, L. W. Hrubesh, J. H. Satcher Jr, and J. F. Poco (2001). "Nanostructured energetic materials using sol–gel methodologies". In: *Journal of Non-Crystalline Solids* 285.1, pp. 338–345.

117. Tillotson, T.M., G.L. Fox, LB. Hrubesh, RL. Simpson, KW. Lee, KW. Swansiger, and LR. Simpson (1997). "Sol-Gel Processing of Energetic Materials". In: 5th International Symposium on Aerogels. Montpellier, France.

118. Tsuzuki, Takuya, ed. (2013). *Nanotechnology commercialisation*. Singapore: Pan Stanford Publ. 460 pp. ISBN: 978-981-4303-28-6 978-981-4303-29-3.

119. van der Heijden, Antoine E. D. M., Yves L. M. Creyghton, Emanuela Marino, Richard H. B. Bouma, Gert J. H. G. Scholtes, Willem Duvalois, and Marc C. P. M. Roelands (2008). "Energetic Materials: Crystallization, Characterization and Insensitive Plastic Bonded Explosives". In: *Propellants, Explosives, Pyrotechnics* 33.1, pp. 25–32. ISSN: 07213115, 15214087. DOI: 10.1002/prep.200800204.

120. Van der Heijden, A., J. ter Horst, J. Kendrick, K.-J. Kim, H. Kröber, F. Simon, and U. Teipel (2005). "Crystallization". In: *Energetic Materials*. Wiley-VCH Verlag GmbH & Co. KGaA, pp. 53–157. ISBN: 978-3-527-60392-3.

121. Wuillaume, Anne, Arnaud Beaucamp, Frank David-Quillot, and Charles Eradès (2014). "Formulation and Characterizations of Nanoenergetic Compositions with Improved Safety". In: *Propellants, Explosives, Pyrotechnics* 39.3, pp. 390–396. ISSN: 07213115. DOI: 10.1002/prep.201400021.

Chapter 3

Definition of Particle and Determination of the Particle Size Distribution of RDX processed by SFE

3.1 Size Measurement

3.1.1 Sensitivity of nano-organic energetic particles

A particle size distribution can be obtained through many methods: X-Ray Disc Centrifugation (XDC), Photon Correlation Spectroscopy (PCS), Differential Centrifugal Sedimentation (DCS), Laser Scattering (Dynamic or Static), Laser Doppler Electrophoresis, nitrogen adsorption (BET method), Differential Mobility Analysis (Scanning Mobility Particle Sizer), Phase Doppler Particle Analyzer, Electronic Microscopy, Atomic Force Microscopy etc. But only a few are suitable for organic nanoparticles. In molecular crystals, weak forces are holding the molecules together instead of covalent bonds for metals or oxide solids; therefore organic nanoparticles are much more sensitive to solvation issues. Water is commonly misused as an anti-solvent of RDX, whereas the few mg/L of solubility is enough to strengthen the growth of crystals through Ostwald ripening or to model a new crystal habit within a few hours or minutes. The liquid alkanes such as hexane are much more often used to precipitate active pharmaceutical ingredients in industry. Besides the solvation, all characterization methods from a colloid are measuring aggregates and agglomerates; some even measure a bigger diameter, a hydraulic one which includes one or several solvations or ionic layer depending of the technique.

In a dried state, measurements can be performed from an aerosol: LASER techniques such as Phase Doppler Analysis (PDA) suffer from a submicron limit of detection. The first stage of a Differential Mobility Analysis (DMA) technique is the neutralization of the aerosol from a radioactive source then particles are sorted by their mobility and so size, then counted by a Condensation Particle Counter (CPC); to overcome the size limitation, the CPS creates vapour from a working fluid (usually butanol, isopropyl alcohol, or water) which condenses onto the particles helping them grow in size and can be optically counted. It is important to notice that hard aggregates in aerosol can not be distinguished through DMA; surface area and volume can be corrected but the primary particle diameter has to be known already. However, DMA provides statistically significant and real time size distributions.

On static dried powder, particle size can also be extracted from BET theory by adsorption of a known gas. Diverse trials to investigate surface area and derive particle sizes from BET were found to be inefficient on n-RDX: no compromise between an appropriate degassing and a prevention of nanomaterial degradation and sintering could be established, due to high vacuum and heating that have to be applied on the sample (Section 1.4.2).

Direct particle observation should always be performed to verify the validity of the assumptions made from the other characterization techniques. Particle aggregation, particle morphology and degradation can be measured or at least reasonably estimated for particles under 50 nm. To reveal details at the nano scale, Atomic Force Microscopy is well suited for insulator nanoparticles. No energy is brought to the material but only a slight mechanical stress; imaging is performed at ambient temperature and pressure. Nevertheless, the tip is not a single point probe: the curvature radius and cone angle lower the heigh and also cause a “profile broadening” effect. Those side effects can be reduced by scanning in tapping mode and selecting a tip with a smaller radius to improve accuracy. However, a balance has to be found between the accuracy and the differential height that the tip can follow without being damaged. Therefore, when the particle size exceeds the hundreds nanometres, electron microscopy allows data acquisition on bigger areas in a minute.

3.1.2 AFM

3.1.2.1 Methodology

To overcome the difficulties encountered with SEM and to improve the accuracy, Atomic Force Microscopy is a good and obvious choice, especially when a laboratory has both apparatuses. For this reason, a standard procedure has been established prior to my arrival to measure particle size. To minimize the

roughness of the sample surface for an AFM tip, an original technique was introduced. The powder is pressed into pellets then its surface is flatten by the use of a rotary microtome.

A stainless steel tubular mould with an inner diameter of 4 mm is filled with the energetic material then closed with a stainless steel rod; the system is placed under a press where different weights can be hang on the extremity of a lever. The whole apparatus follows the pyrotechnic safety guidelines thanks to a mould with thick walls and a protective transparent screen. In this case, the mass of energetic materials is below 50 mg. The material is maintained under a pressure of 97 MPa for one minute, with transitions slowest as possible to avoid friction heat. Microtomy is done by a succession of cut thinner and thinner on one side of the pellet: five times 20 µm, then five times 5 µm and finally five times 1 µm to remove superficial layers and have the smoothest surface. The quality of the surface preparation can be easily seen with the naked eye, by checking its great reflectivity.

The mean apparent density is $1.406 \pm 0.035\,\mathrm{g/cm^3}$ from results reported in Table 3.1 which is in good agreement with densities from Pichot et al. (2015) and shows good reproducibility. The easy shaping of the powder into a cylindrical pellet is only possible thanks to the reduced particle size: pellets of the finer commercial available RDX with a PSD around 6.8 µm break apart (Spitzer et al. 2011). Moreover, pellet of n-RDX exhibits a glassy structure with transparency.

Height (mm)	Mass (mg)	Density ($\mathrm{g/cm^3}$)
1.09	19.69	1.395
1.61	28.42	1.377
0.92	17.33	1.462
1.56	28.04	1.395
2.08	38.89	1.451
1.50	26.23	1.357

Table 3.1 – Several apparent densities of pellets pressed at 97 MPa.

The analysis of height fields obtained by AFM is then made through a semi automatic process with the free and open source software Gwyddion (Nečas et al. 2012). Gwyddion is a modular program for SPM (Scanning Probe Microscopy) data visualization and analysis. It has been chosen thanks to its large number of data processing functions, including all the standard statistical characterization, the levelling and data correction, the filtering or grain marking functions. Among them, the watershed algorithm allows the detection of particles by local minima determination then image segmentation. The grain size analysis is made through several steps:

Grain localisation process the surface is inverted – hills become valleys – then virtual water drops are placed on each point. Then drops fall to the closest local minimum, following the steepest descent. The process is repeated and accumulated drops are forming lakes. Those small lakes filling the inverted surface depressions are the position of grains.

Segmentation While the drops are filling the surface, if a lake touches another one, they are merged in the previous step. In the segmentation step, drops are again falling but the growing lakes are not merged and their border is refined. The quality of grain boundary depends on the drop size set but computing time increases when the drop size is smaller.

Visual checking and corrections The software allows manual marking of grains and several contrast improvements to control and correct the results from the watershed method. The phase and amplitude channels can also help to determine the validity of a grain boundary.

PSD and fitting The software allows the direct display for the PSD but also can export the results. The diameter of a grain is computed from the diameter of a disc with the same surface area. A frequency count on the diameters renders the raw PSD; then the curve is fitted with a log-normal distribution function. Gaussian fitting is in poor accordance. Therefore, the PSD is generated by many small random effects that are multiplicative for the log-normal distributions (Limpert et al. 2001)

3.1.2.2 Effect of the concentration on the particle size

During his PhD in our laboratory, Risse studied the RDX concentration from 0.5 wt% to 2 wt% in acetone; as the concentration increases, the particle size decreases and so the specific surface increases. This can be linked to the increase of the degree of supersaturation with the concentration, therefore triggering a high nucleation rate. In this context, the first work of my PhD project was to start studying the crystallisation process and so the degree of supersaturation by extending that previous work.

SFE parameters were chosen from the optimized operating conditions: the nozzle temperature is set at 160 °C, the inlet pressure at 40 bar and the nozzle is an hollow cone one with a diameter of 60 µm. The walls of the vacuum chamber from the nozzle to the cyclone are heated to 80 °C to avoid any condensation and to reduce the losses of product by thermophoretic force. The solvent used for all the study is the same lot of acetone CHROMASOLV®, for HPLC, ≥99.9% , from Sigma Aldrich. The same lot of RDX provided by Eurenco, labelled as M5, is used all along this study and this PhD project.

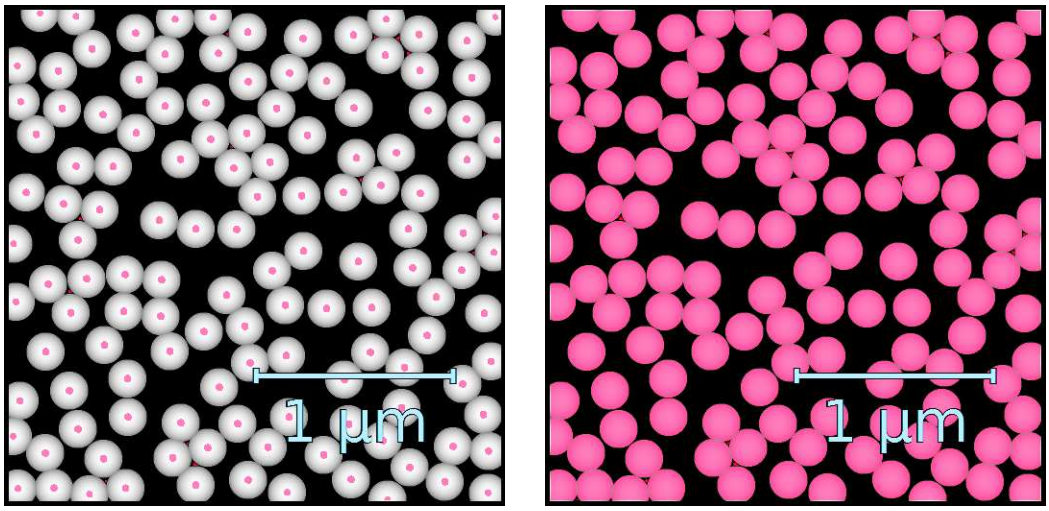

(a) Grain localisation (b) Segmentation

Figure 3.1 – Watershed analysis illustrated on simulated 200 nm spheres.

PSDs are determined by the previously mentioned method on pellets. XRD is also performed in order to calculate the apparent volume weighted domain size from the Scherrer equation as described in Section 1.4.2 p. 49. The sensitivity of the energetic powders is also quantified in order to investigate an eventual link with the mean particle size and crystallite size. Also the results are reported in Figure 3.2.

A parabolic trend could be interpreted from Figure 3.2e. However, the statistical significance of the result should be first performed. Thus, statistical analysis are made from the software GraphPad Prism 5 to compare mean particle size obtained from AFM pictures from one concentration to another. Table 3.2 shows that globally these means are not significantly different. Table 3.3 compares mean to each other and still no significance has been found.

The concentration of RDX in solution up to values close to the saturation does not influence the particle size according to the statistical analysis. Moreover, sensitivity remains constant among all samples: to up-scale the SFE process, such constant properties while increasing the RDX content is advantageous to increase the mass flow and so decrease the cost of the process.

The mean crystallite size is also always around 65 nm; RDX particles are polycrystalline and the nucleation seems to be unchanged while changing concentration.

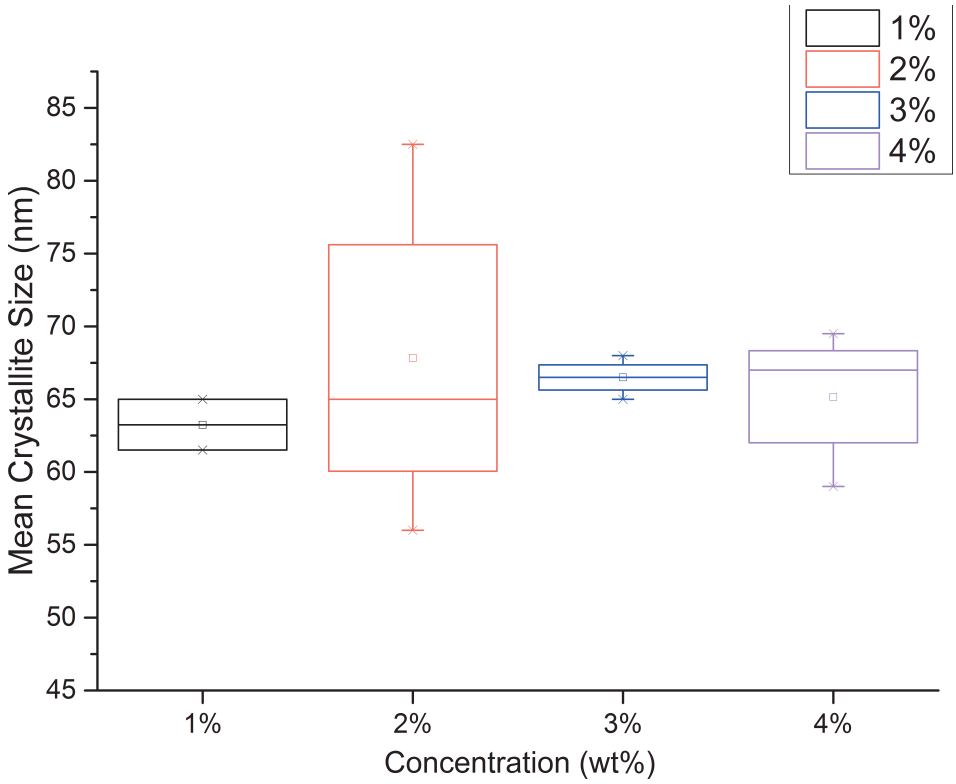

(a) Crystallite against concentration

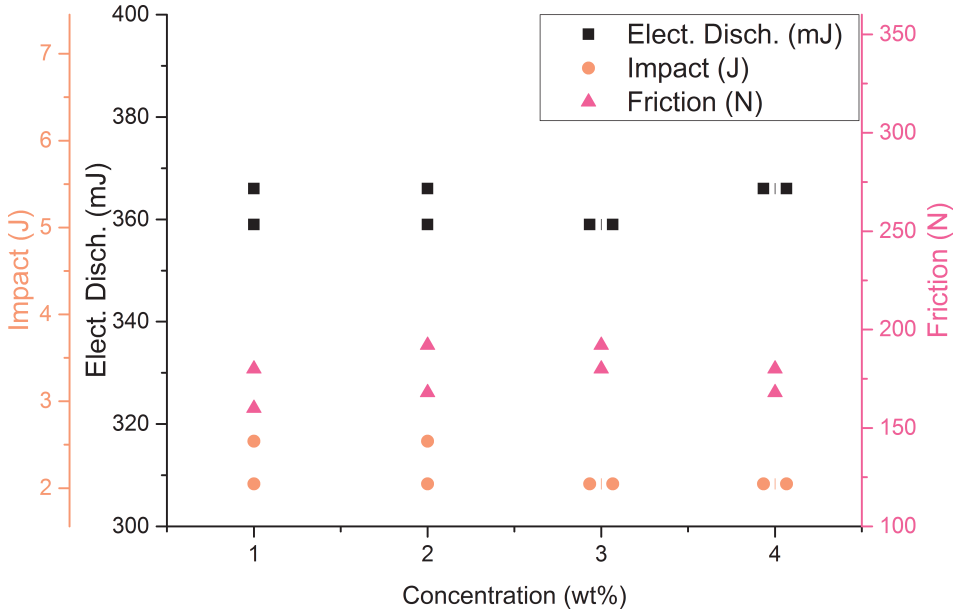

(b) Sensitivity against concentration

Figure 3.2 – Parametric study based on the variation of the concentration in solvent.

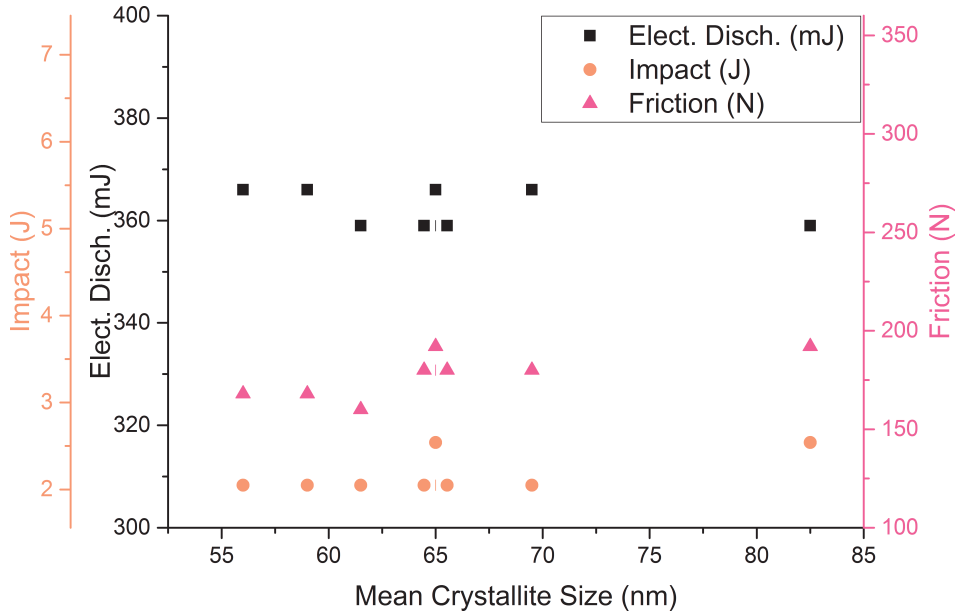

(c) Sensitivity against crystallite

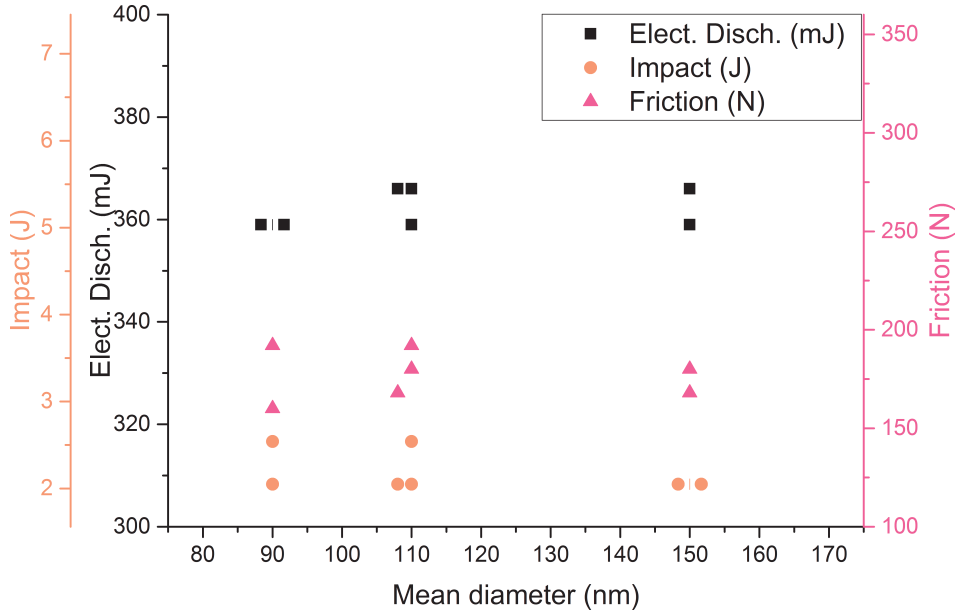

(d) Sensitivity against particle size

Figure 3.2 – Parametric study based on the variation of the concentration in solvent.

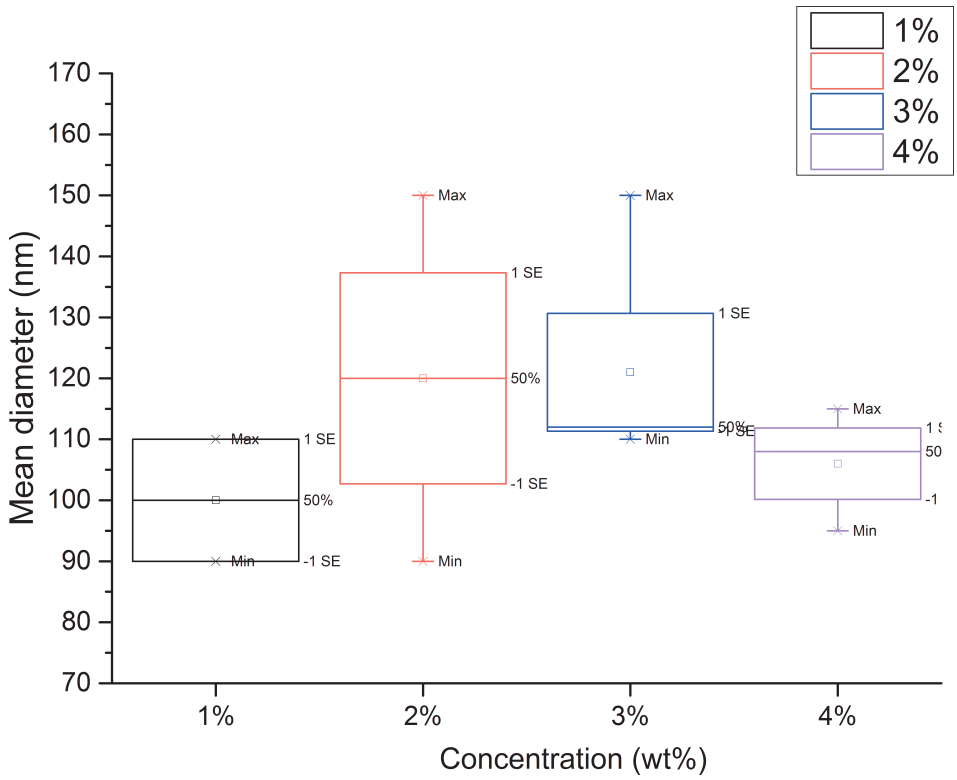

(e) Particle size against concentration

Figure 3.2 – Parametric study based on the variation of the concentration in solvent.

P value	0.5734
Are means signif. different? (P < 0.05)	No
Number of groups	4
F	0.7087
R squared	0.2100

Table 3.2 – One-way analysis of variance on the particle size from AFM pictures.

Tukey's Comparison Test	Mean Diff.	q	Significant?	95% CI of diff
1% vs 2%	-20	1.519	No	-79.64 to 39.64
1% vs 3%	21	1.681	No	-77.58 to 35.58
1% vs 4%	-6	0.4556	No	-65.64 to 53.64
2% vs 3%	-1	0.09076	No	-50.90 to 48.90
2% vs 4%	14	1.189	No	-39.35 to 67.35
3% vs 4%	15	1.361	No	-34.90 to 64.90

Table 3.3 – Tukey's multiple comparison test on the particle size from AFM pictures.

3.1.2.3 Reliability and accuracy

Risse also found that a crystallite size remained constant around 65 nm. However, the concentration had a significant influence on PSD from BET and SEM characterizations: the particle size decreased while the concentration increased. The mean particle size from SEM was 715 ± 244 nm at 0.7 wt% and 408 ± 175 nm at 2 wt%: those values were much higher than the mean particle size obtained from the AFM method.

No statistical assessment was performed previously and the repeatability of the previously work is questionable. The difference between SEM and AFM was a scientific question previously discussed. The high vacuum decreases the thermal stability of the energetic compounds which also have a very low vapour pressure (3.30×10^{-9} Torr the vapour pressure of RDX at 25 °C (Östmark et al. 2012)); it can be assumed that sublimation of the smallest particle leads to that significant difference in mean size. Sintering can also be strongly worsen by the energy brought by the electron beam.

To finally settle those long term doubts and question the reliability and accuracy of the pellet method, a parametric study was performed halfway across this PhD project thanks to the help of the ex-internship, currently PhD student, J-E Berthe. The uncertainty of the Watershed method was estimated and the following two key parameters were studied

- pressure applied
- microtomy

Uncertainty of the Watershed Method As implemented in the current version of Gwyddion (2.45), the Watershed Method suffers from a lack of optimization and synergy between the other correction tools of the software. To study the sole effect of the Watershed method, ideal AFM topographies of a virtual deposit of spherical particles were made through the build-in particle generator. In that way, all instrumental influence (AFM tip geometry, noise etc.) is totally suppressed as it can be seen from the Figure 3.1 p. 99.

Several tests were performed with different particle sizes, picture dimensions and surface sizes: values were taken from the AFM picture usually analysed. An alternative method introduced with the most recent updates was also tried: the threshold algorithm which relies on the height, slope and curvature parameters; those three options can be combined by union or intersection. The result of the algorithm is updated in real time but requires much more attempts. The Table 3.4 shows that the Watershed method is always more accurate than the threshold one due to more rigorous grain boundaries. However, the size is always minimized: this can be easily explained due to the boundary layer of

one pixel to mark grains. So the accuracy decreases with the particle size and the resolution since the missing pixels represent an higher relative area. As rule of thumb the mean particle sizes measured from AFM have to be increased by 10 % for 1024 px × 1024 px pictures and by 20 % for 512 px × 512 px pictures. The values reported in the previous study on the effect of the concentration are then corrected by 10 %.

	particle radius	resolution	simul. area	method	nbr. of analysed part.	measured radius	deviation from the initial radius
unit	nm	lines	µm			nm	
	50	512x512	5x5	threshold	1445	36.75	27%
trimmed	50	512x512	5x5	threshold	1406	36.75	27%
	50	512x512	5x5	watershed	1474	40.25	20%
	50	1024x1024	5x5	threshold	1477	40.75	19%
trimmed	50	1024x1024	5x5	threshold	1416	40.75	19%
	50	1024x1024	5x5	watershed	1539	44.25	12%
	150	512x512	5x5	threshold	215	129.75	14%
trimmed	150	512x512	5x5	threshold	177	129.75	14%
	150	512x512	5x5	watershed	248	136.75	9%
	150	1024x1024	5x5	threshold	214	133.75	11%
trimmed	150	1024x1024	5x5	threshold	176	133.75	11%
	150	1024x1024	5x5	watershed	235	137.5	8%

Table 3.4 – Watershed and threshold method tested on simulated data; the 'trimmed' results mean that the grains at the edge of the picture are removed since they are probably trimmed. The Watershed algorithm add a one pixel boundary at the edges too, so trimmed grains cannot be removed easily.

Effect of the Pressure The press used for the compression of energetic materials consists of a lever supported by an hydraulic piston; at the extremity of the lever an hook allows to put several weights on it (from 5 kg to 97 kg), then the piston is actuated to slowly lower the lever thus forming the pellet. The pressure applied on the sample is calculated according to the weights applied; values are reported in Table 3.5.

In the results reported in Figure 3.3, the same face was always inspected by AFM (the upper one here) and microtomy was not applied. The scan surface is 5 µm × 5 µm in 1024 px × 1024 px. In Figure 3.3a clear drop of the mean size begins at 140 kg and then the value fluctuates around 90 nm: that change is

Weight (kg)	Pressure (MPa)
2	12
5	26
10	50
20	97
30	140
45	210
70	330
97	460

Table 3.5 – Weights used and their calculated corresponding pressures: the leverage follows the law $P = 6 \cdot \frac{M}{A} + 31$ *where* $A = \frac{\pi}{4} \cdot \varnothing^2$ *with M the mass of the weight.*

also observed in Figure 3.3b with a shift and a major broadening of the particle distribution. On the AFM pictures in Figures 3.3c and 3.3d, particles are hardly identifiable.

The results from samples processed by microtomy in Figure 3.4 also demonstrate that the pressure has a significant influence on particle size. In that case, the particle size is reduced further and further with increasing pressure. Above 97 MPa (20 kg), the pellets start to be too glassy for microtomy; due to the the great hardness, the pellet breaks apart when the blade hits the sample.

Raw micron-sizedRDX (M5 Eurenco) were also investigated; the pellets are much less cohesive and were not flatten by microtomy. However, at the highest pressure of 97 MPa, a similar breakage appears with a much lower particle size. Therefore the milling of n-RDX processed by SFE is much easier; for industry, it would be interesting to find a balance between optimization of the SFE conditions and an additional rough milling/mixing step. Also this effect would have an huge impact on energetic pressed charges.

Effect of the Microtome From the curves in Figures 3.3a and 3.4a, the microtomy reduces the size. The surfaces from samples pressed at 97 MPa and processed by microtomy (Figure 3.4e) are quite similar to the samples pressed above the critical pressure and not processed by microtomy (Figure 3.3e).

Pressure reduces the inter-granular void which increases compactivity and hardness. Therefore, the blade of the microtome needs more energy to penetrate the pellet and a surface milling occurs reducing further the particle size.

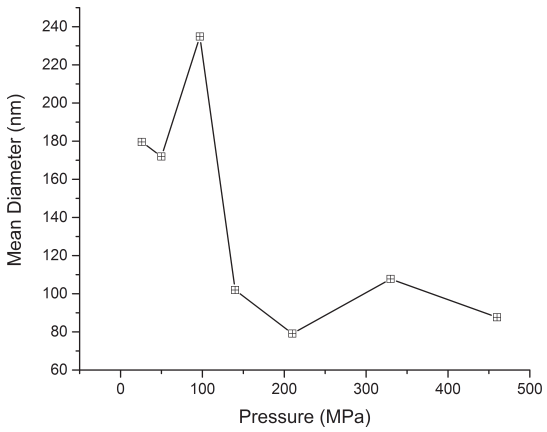

(a) Size against pressure

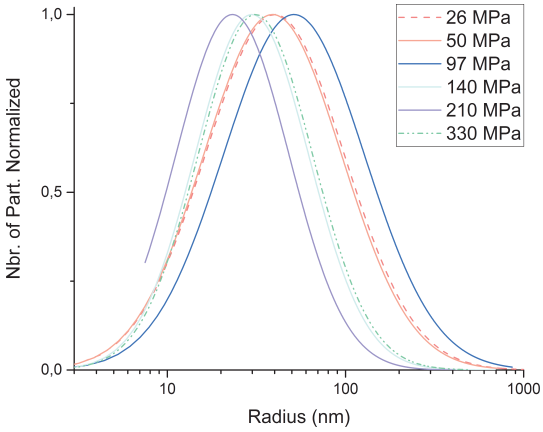

(b) Influence of the pressure on PSD

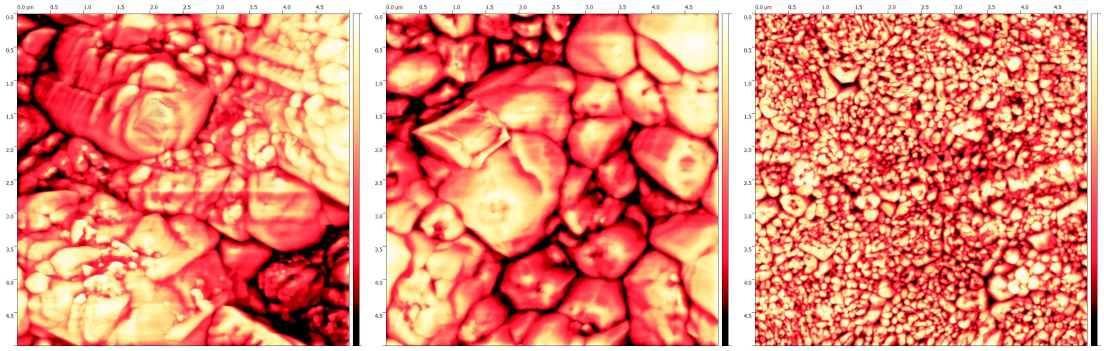

(c) 26 MPa (5 kg) (d) 97 MPa (20 kg) (e) 460 MPa (97 kg)

Figure 3.3 – Effect of the weight; same face, no microtomy, 5 µm × 5 µm for 1024 px × 1024 px, enhanced contrast.

Pressure (MPa)	Raw	With Microtomy
12		280
26	180	
50	170	230
97	235	140
140	100	
210	80	
330	110	
460	90	

Table 3.6 – Mean Diameters (nm) according to the pressure applied and the pre-treatment by microtomy; by SEM, the mean size is 500 nm.

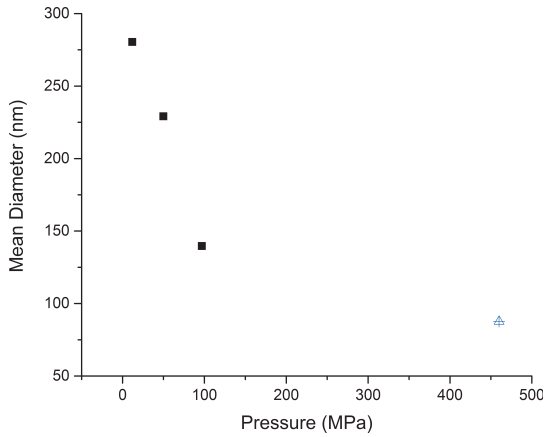

(a) Size against pressure (460 MPa sample without microtomy reported in triangle)

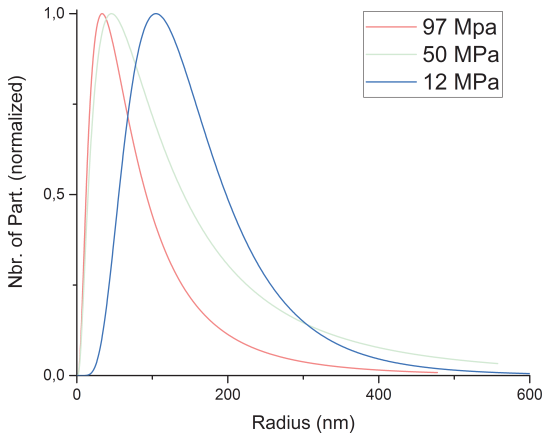

(b) Influence of the pressure on PSD

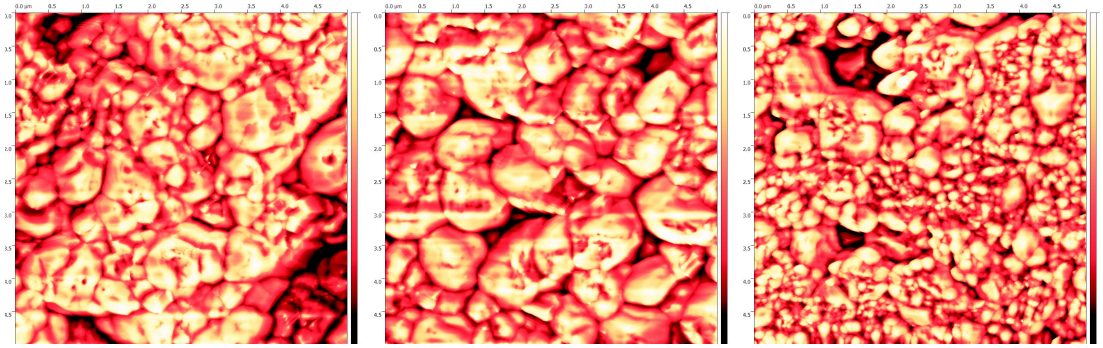

(c) 12 MPa (2 kg) (d) 50 MPa (10 kg) (e) 97 MPa (20 kg)

Figure 3.4 – Effect of the weight; same face, processed by microtomy, 5 µm × 5 µm for 1024 px × 1024 px, enhanced contrast.

3.1.2.4 Conclusion on the AFM pellet method

The particle size variation when adding PVP or PolyEthylene Glycol (PEG) studied from SEM in Chapter 5 where initially discovered from the analysis of pellets by AFM. The exact same trend from SEM was also found from AFM picture analysis whose results can be found in Table 3.7. However, instead of a particle size around 160 nm as found by direct imaging in SEM, a mean value around 70 nm is measured. The content of polymer seems to have no influence on how brittle is the energetic material since PEG samples also have an increasing size with the PEG content: those results show that not only the hardness of the material is a major parameter but also the initial size of the particles. This seems to be valid only when the pressure applied is below the critical pressure. Another interpretation would be that this critical pressure changes; for instance it could

have decreased for RDX/PVP samples, thus leading to one of the smallest PSD ever observed on RDX.

Compound(s)	Polymer content (wt%)	Mean Diameter AFM (nm)
RDX/PVP40K	1	66
RDX/PVP40K	1	73
RDX/PVP40K	1	67
RDX/PVP40K	0,5	165
RDX/PEG400	1	965
RDX/PEG400	0,1	180

Table 3.7 – Particle size from pellet imaging by AFM of some samples at 97 MPa with microtomy.

SEM pictures were taken from pellets made from n-RDX by the pressing technique mentioned above, in order to observe at larger scales their surface. After being pressed and imaged by AFM, the sample is cut in half to be analysed by SEM on one piece; the other is used as a reference.

Thanks to the results in Figure 3.5, the surface of pellets appear to have two different areas: linear grooves and holes. The holes let the inside of the pellet to appear from outside; those are rough and bumpy which is a problem for AFM. However, the particles seen from inside are very similar in size and shape to the ones observed from the loose powder. In the Figure 3.7, the particles inside have the same rounded shape as in the loose powder. On the contrary, the grooves are smooth and made from the smaller particles; those areas are perfect for landing an AFM tip and scan. The AFM method suffers so from an additional bias which is the area segregation. To land the tip, to initialize the scan and to have a correct AFM picture, the tip is moved until the scanning area is flat enough: the biggest particles inside the holes of the pellet are never investigated. Surfaces of pellets of energetic materials are not representative of the loose powder of the same material.

The comparison between AFM and SEM of the same sample clearly illustrates the reason behind the particle size difference between those two techniques. The press hardens the pellet, the microtome mills the surface and scanning by AFM selects the flattest area where the smallest particles lies.

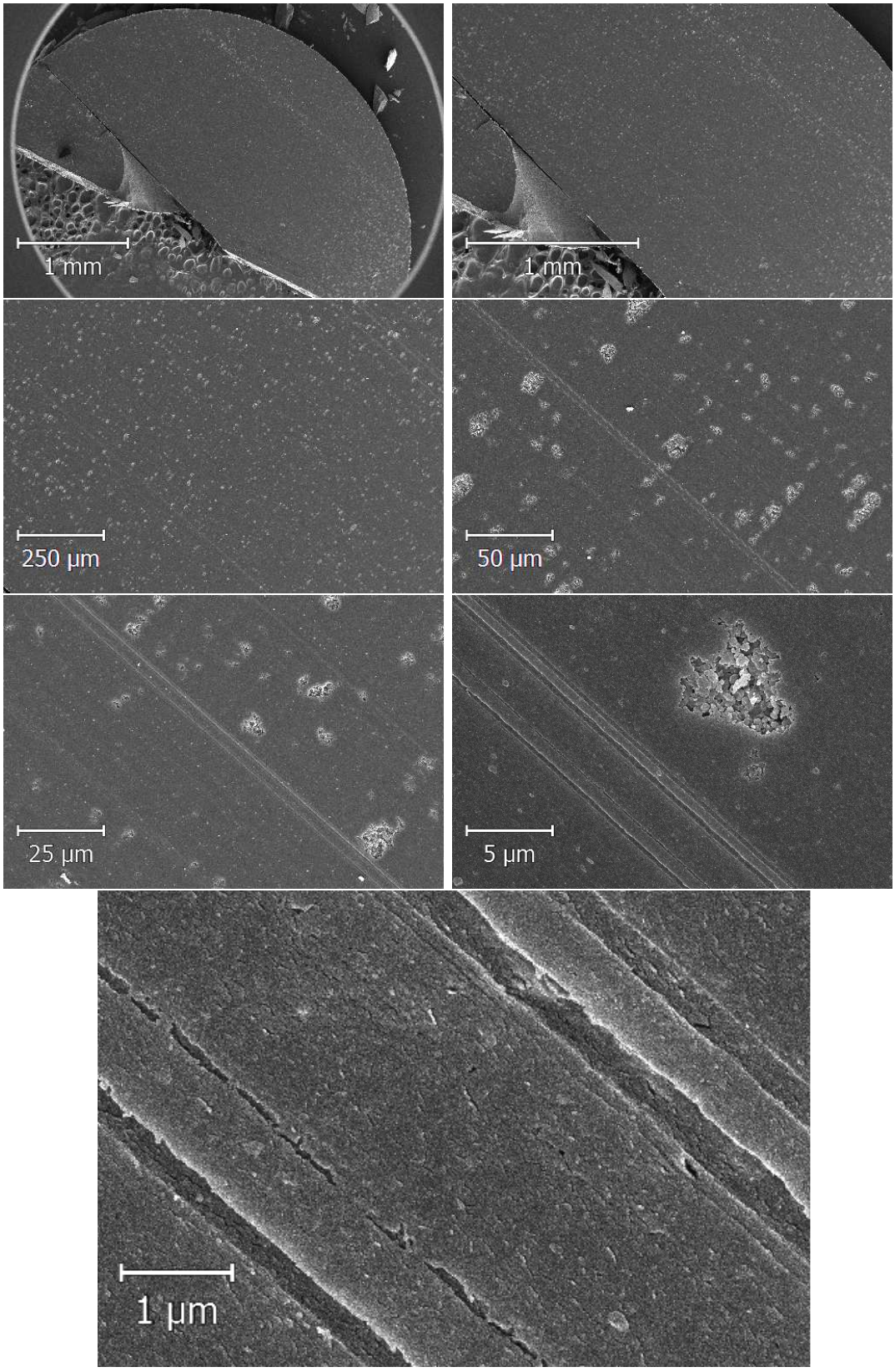

Figure 3.5 – SEM imaging of a 97 MPa pellet of RDX processed with 5 wt% of PVP 40000.

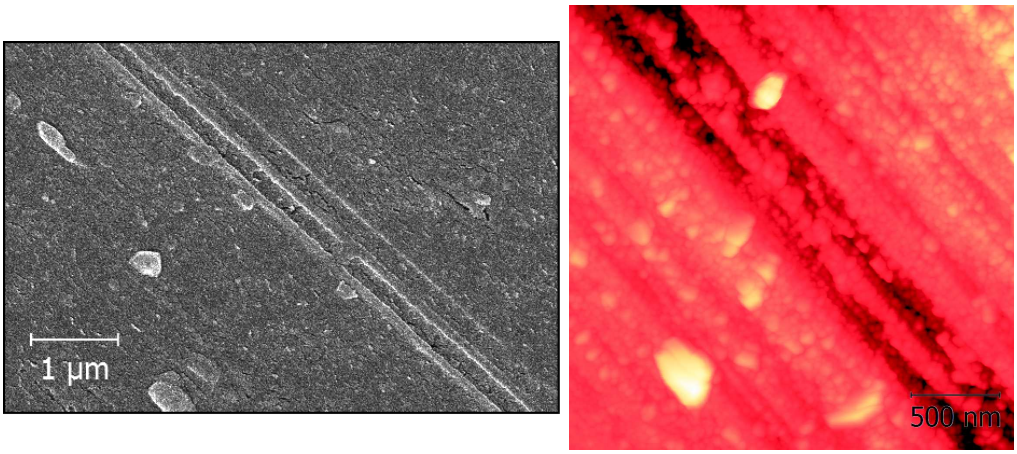

Figure 3.6 – SEM and AFM imaging of a 97 MPa pellet of RDX processed with 5 wt% of PVP 40000.

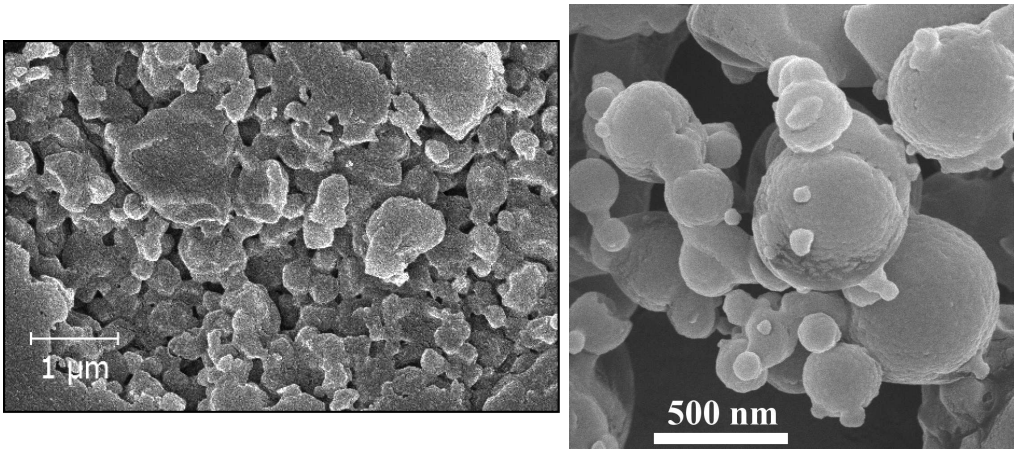

Figure 3.7 – SEM imaging of one hole of a 97 MPa pellet compared to the loose powder of the same sample of RDX processed with 5 wt% of PVP 40000.

3.2 One Technique, One Size

3.2.1 XDR

3.2.1.1 Determination of the apparent volume weighted domain size

From an XRD pattern, many information can be extracted. The mean crystallite size can easily be calculated from the Scherrer equation, the strain inside the crystal is available from more advanced analysis such as Williamson-Hall, and the morphology of the crystallite can even be 3D-modeled from a fine Rietveld refinement.

The Scherrer equation is a quick method to determine the average coherence length, so it is widely used. However, the value is calculated from the broadening which is influenced by many other physical parameters such as the lattice strain. Williamson et al. (1953) defined a alternative method taking into account the strain contribution into the broadening. Explained in the Section 1.4.2 p. 49, the analysis relies on plotting $\beta cos(\theta)$ as a function of $sin(\theta)$ and fitting it to an affine function where the slope is directly related to the strain.

Results in Figure 3.8 show the attempt to fit five n-RDX samples crystallised through SFE in the same operative conditions. The sub-figure A, on the left, illustrates different approaches in measuring the Full Width at Half Maximum (FWHM) according to the angle: due to the poor accuracy of the peak per peak measurement (peak fit from Origin or manual peak marking in EVA), data seems to be linear in the range 0.1-0.2. This also explains the large difference with the Full Pattern Matching (FPM) analysis: FPM relies on the whole pattern allowing a large number of peaks to be analysed by an algorithm. The usual mathematical functions to fit XRD peaks are implemented in the code, and the software compares the experimental data to the theoretical hkl planes calculated from the space group. The FPM is therefore more accurate, computes a large dataset and has a real meaning. Our XRD diffractometer does not filter the $K_{\alpha 2}$ ray of the Cu source: so each peak is actually a double-peak. The FPM as implemented in Fullprof can fit the pattern knowing the peak position for each radiation thus deconvoluting each peak in two. The peaks shape was fitted with a Thompson-Cox-Hastings pseudo-Voigt convoluted with axial divergence asymmetry function (Finger et al. 1994).

In Figure 3.8, only two samples could have been fitted into a linear regression. The other three evolve into parabolas. Such diverging results clearly indicates that the Williamson-Hall theory does not describe accurately the peak broadening.

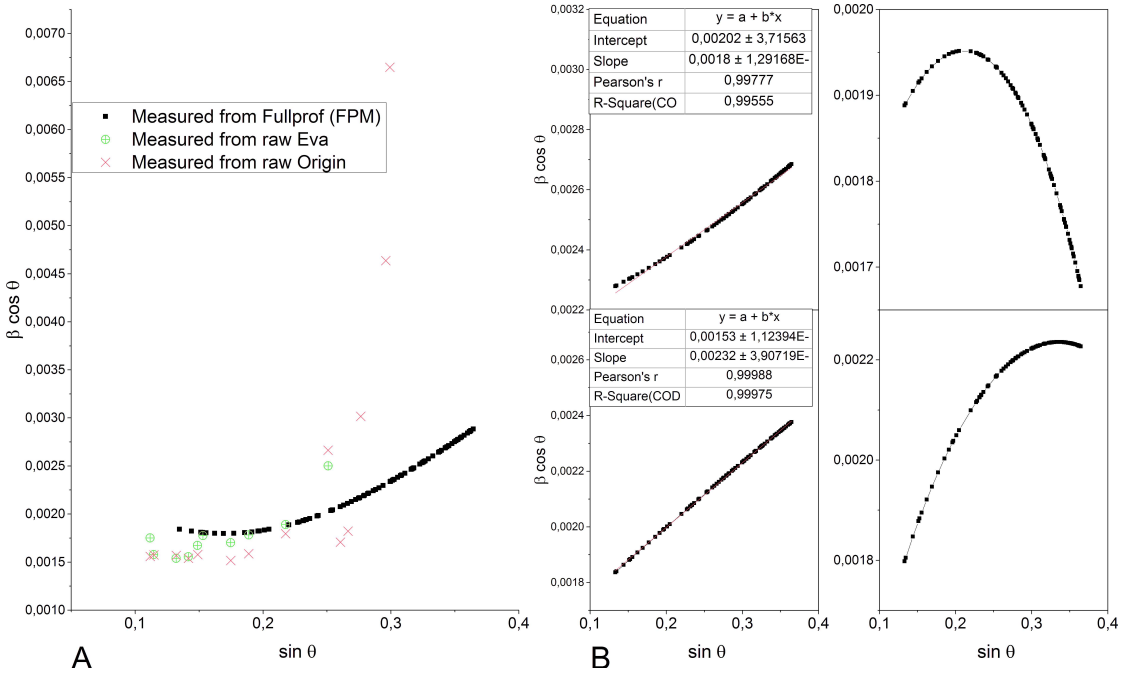

Figure 3.8 – Williamson-Hall of n-RDX processed by SFE at 2 wt% in acetone.

3.2.1.2 Rietveld refinement

The Rietveld refinement allows the fine analysis of the crystals properties (size and strain according to several models, hkl shifts, asymmetry, preferred orientation etc.) but also a complete segregation with instrumental effects on the pattern.

In most implementation of the Rietveld method, to refine crystallite structures, the microstructure (size and strain) of each lattice is modelled by considering only an average crystallite size. Although this technique gives good results, it is important to notice that the real sample has a distribution of the crystallite sizes. Usually such models for the crystallite size approximate the crystallite shape with a sphere. Some even more complicated models consider a specific morphology of the crystallites. But, the best results for the average crystallite size are obtained by modelling its shape in the reciprocal space with an expansion of symmetrized spherical harmonics; then the corresponding crystallite shape obtained in the real space would be the one obtained from direct imaging of the primary particles.

The micro-structural analysis from Rietveld refinement is implemented in several size broadening models into the free software Fullprof. We will be using the Anisotropic Lorentzian size broadening: it considers the size broadening as a linear combination of spherical harmonics (SPH). The anisotropic size is

supposed to contribute to the Lorentzian component of the total Voigt function. After refinement of the coefficients the program calculates the apparent size (in Ångströms) along each reciprocal lattice vectors if the instrumental resolution is provided.

A preliminary calibration of the peak broadening due to the apparatus is performed on LaB_6: the resulting refinement can be seen in Figure 3.9. If the peak broadening is too close to the instrumental resolution, the software will not refine the peak. The Table 3.8 contains the values used for all the following Rietveld refinement. U, V and W are parameters used to model the change of the FWHM with the angle from the instrument, by the equation $H^2 = U\tan(\theta)^2 + V\tan(\theta) + W$. The peak shape for LaB_6 is a Pseudo-Voigt; the parameters were adapted from the instrument parameter and input files of the Beamline 11-BM of Argonne National Laboratory. Then, n-RDX patterns are refined using a Thompson-Cox-Hastings pseudo-Voigt convoluted with axial divergence asymmetry function as the peak shape (Finger et al. 1994). Therefore, the FWHM of the Gaussian (H_G) and Lorentzian (H_L) components are calculated as:

$$H_G^2 = (U + D_{ST}^2)tan^2\theta + Vtan\theta + W + \frac{I_G}{cos^2\theta} \tag{3.1a}$$

$$H_L = Xtan\theta + \frac{[Y + F(S_Z)]}{cos\theta} \tag{3.1b}$$

Much more technical details can be found in the manual and help provided with FullProf.

Uins	Vins	Wins	Xins	Yins	Zins
0.001356	-0.005000	0.003910	0.063891	0.000083	0.0
0.001356	-0.005000	0.003910	0.063891	0.000083	0.0

Table 3.8 – Instrumental resolution determined from LaB_6 pattern refinement.

The Rietveld refinement requires some expertise and patience to analyse with accuracy and avoid any divergence of the parameters toward non physical meanings. The process is made step by step following this sequence:

1. Scale factor
2. Scale factor, zero point of detector, lattice constants. The background is refined if the background subtraction from EVA is not satisfactory.
3. Atomic positions

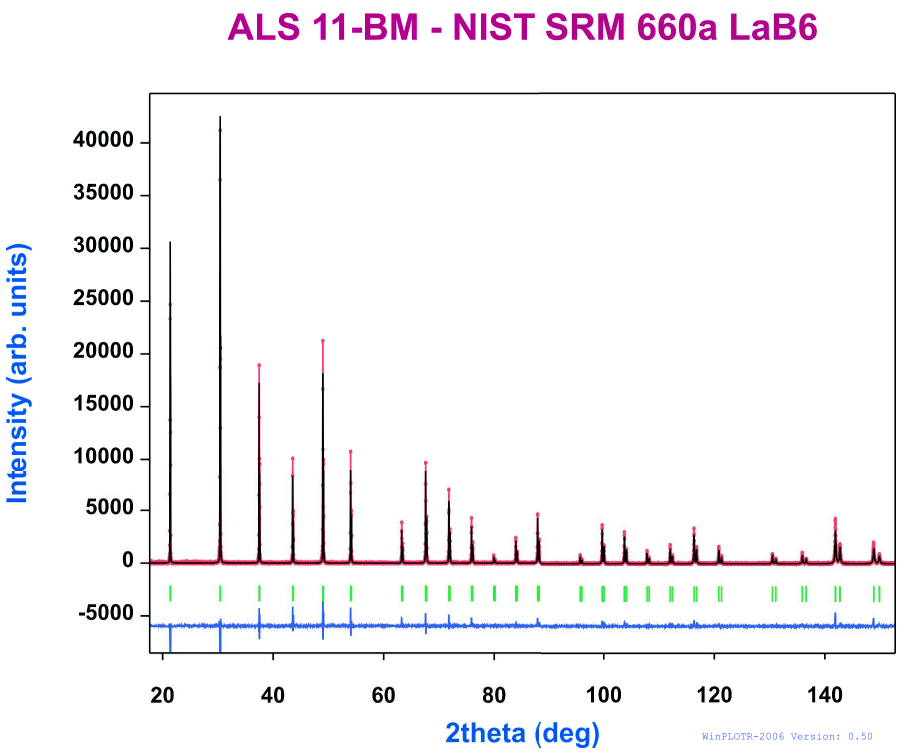

Figure 3.9 – Rietveld refinement performed on LaB_6.

4. Peak shape and asymmetry parameters
5. Atom occupancies
6. Microstructural parameters: size and strain effects. The model used is the Anisotropic Lorentzian size broadening (Spherical Harmonic) with the Laue class *mmm*, which allows the crystallite morphology determination.

The experimental pattern, refinement and residual are frequently checked during the refinement process. The final results are found in the Figures 3.10 to 3.14: the curves in black is the refined pattern, in red the experimental data and in blue below the first two is the residual. The small ticks between the residual and the curves are the hkl positions from $K_{\alpha 1}$ and $K_{\alpha 2}$ rays of the Cu source. The refinement takes a dozen minutes, with an increasing computation time when adding parameters to refine. Also the refinement diverges easily, corrupting the input file. Dozens of refinements were saved per samples with reducing χ; attempts increasing χ were not saved but are sometimes used to start from original values leading afterwards to a more accurate solution.

The refinements of the sample of n-RDX processed pure at 3 wt% acetone in Figure 3.11 and the one with a 80 µm nozzle in Figure 3.14 are acceptable but

less accurate than others, with a negative residue on the angles at small angles and a positive residue on angles above 20 °. Finding a realistic refinement was the most difficult issue to solve: having a refinement accurate enough with no bias –such as that angular dependency– and an acceptable 3D model at the same time. The results shown here are the best refinement possible with a realistic 3D model. The three other refinements are in very good agreement with the experimental data.

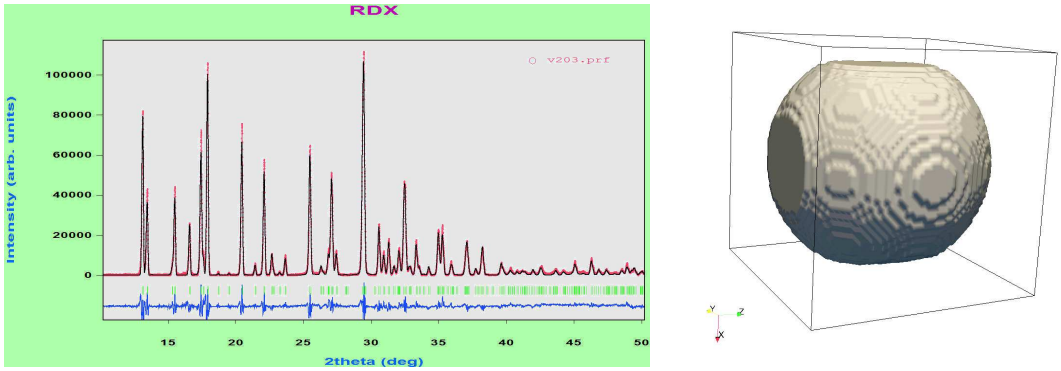

(a) Rietveld Refinement (b) Resulting crystallite morphology

Figure 3.10 – Sample of n-RDX processed pure at 2 wt% in acetone.

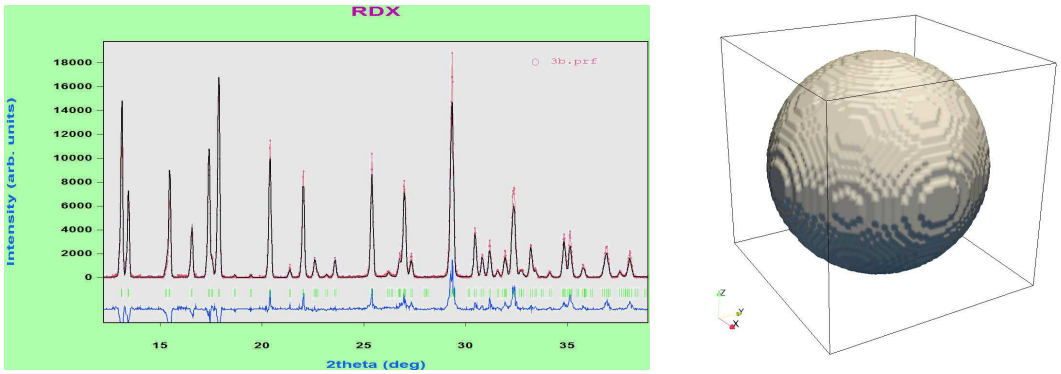

(a) Rietveld Refinement (b) Resulting crystallite morphology

Figure 3.11 – Sample of n-RDX processed pure at 3 wt% in acetone.

A global appreciation on the refinement would be a more accurate fitted solution with the smallest particles. Beyond the inherent difficulty of the micro-

structural analysis by the Rietveld theory, the organic crystals exhibit a large number of peak with many overlaps, and a natural broadening due to a lattice crystalline less ordered, which is far from the ideal condition.

Nevertheless, all the models seem to converge on spherical particles slightly flattened on two planes (4 faces/extremity). This oblate geometry is correlated to an almost homogeneous growth with no preferential direction growth. Size and morphology found with those analysis are then compared to the particle size and morphology obtained by AFM on pellets and on the smallest particles imaged on SEM.

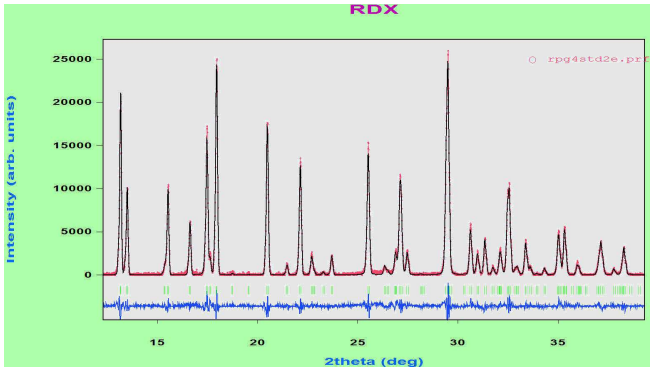

(a) Rietveld Refinement

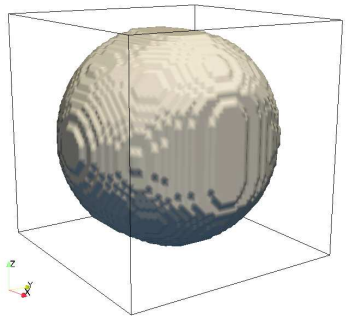

(b) Resulting crystallite morphology

Figure 3.12 – Sample of n-RDX processed with 0.1 wt% of PEG.

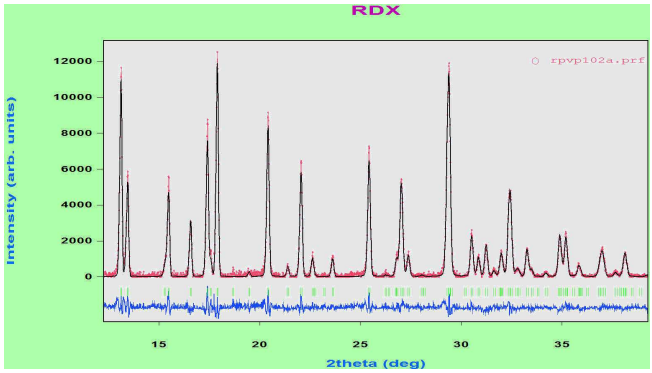

(a) Rietveld Refinement

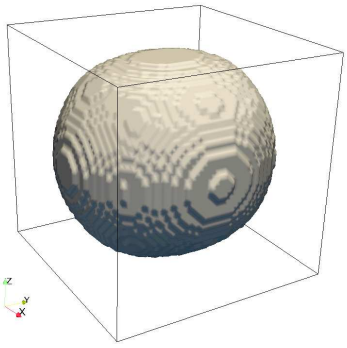

(b) Resulting crystallite morphology

Figure 3.13 – Sample of n-RDX processed with 10 wt% PVP.

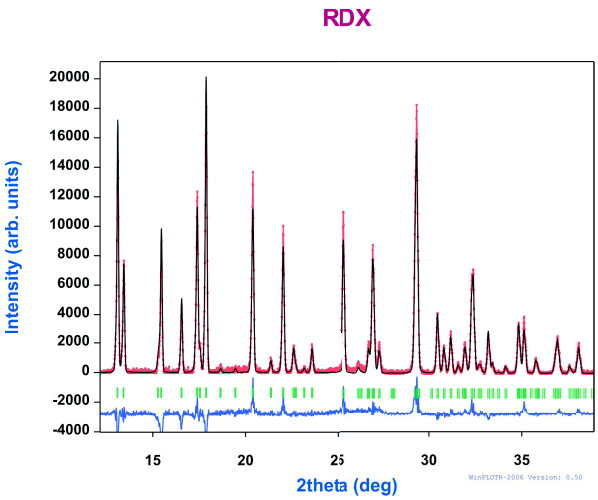

(a) Rietveld Refinement

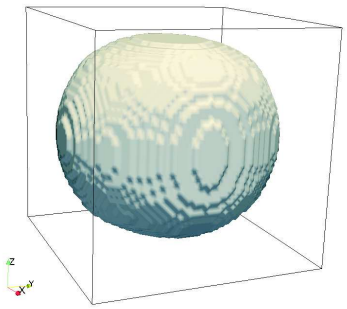

(b) Resulting crystallite morphology

Figure 3.14 – Sample of n-RDX processed with 1 wt% PVP with a 80 µm nozzle

3.2.2 Smallest observable object

In order to assess the problem of the particle size and definition of a particle, a new deposit technique for SEM was developed recently in our laboratory: it is based on the rubbing of the powder between two glass sheets. Individual and very small particles have been found to be more easily observed on a glass support. The method is still under investigation, especially to explain the influence of the support. However the spreading due to the rubbing allows the distinct imaging of the smallest particles. The particle size and morphology is studied through SEM and compared to the results from Rietveld refinement. The aim of this study is to answer to the questions of the crystallinity and aggregation of n-RDX processed by SFE.

Spray techniques may produce particles made from much smaller primary particle: Qiu et al. (2015) successfully probed the interior of their micrometer spheres (RDX) to found out a gradient of the primary particle size at the submicrometer scale. Focused ion beam (FIB) is the technique used to make the cross-sections: even if a low probe current helps to preserve the sample (Gierak 2009) no attempt has already been reported on energetic materials. An easiest solution is to use the rubbing deposition technique to image the smallest particles. Results reported in Table 3.9 show that the RDX processed with polymers actually exists as single crystals. On the contrary, the smallest pure n-RDX are still polycrystalline. The oblate shape found by Rietveld seems consistent with morphology imaged by SEM, as it can be seen in Table 3.9.

AFM on pellets of those samples were also analysed. As seen in Figure 3.16,

n-RDX	Average apparent size and standard deviation (anisotropy) (Å)	Average maximum strain and standard deviation (anisotropy) (% (x 10000))	Smallest Particle Sizes from SEM (nm)
pure at 2 wt% in acetone	716 (28)	5.53 (0.0039)	180-200
pure at 3 wt% in acetone	814 (21)	3.23 (0.0017)	125-140
with 0.1 wt% of PEG	826 (27)	5.61 (0.0046)	70-70
with 10 wt% PVP	769 (21)	8.58 (0.0068)	60-60
with 1 wt% PVP with a 80 µm nozzle	793 (29)	6.87 (0.0048)	80-95

Table 3.9 – Smallest particle imaged on SEM compared to the computed average apparent size from Rietveld refinement.

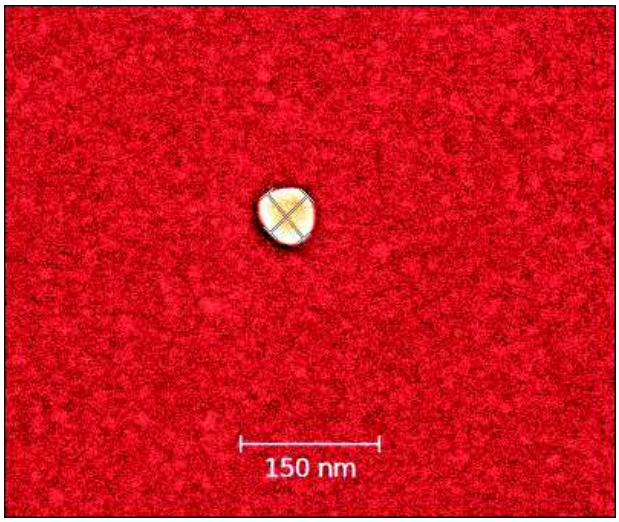

Figure 3.15 – One of the smallest particle (63x58 nm) observed by SEM on RDX processed with 10 wt% PVP.

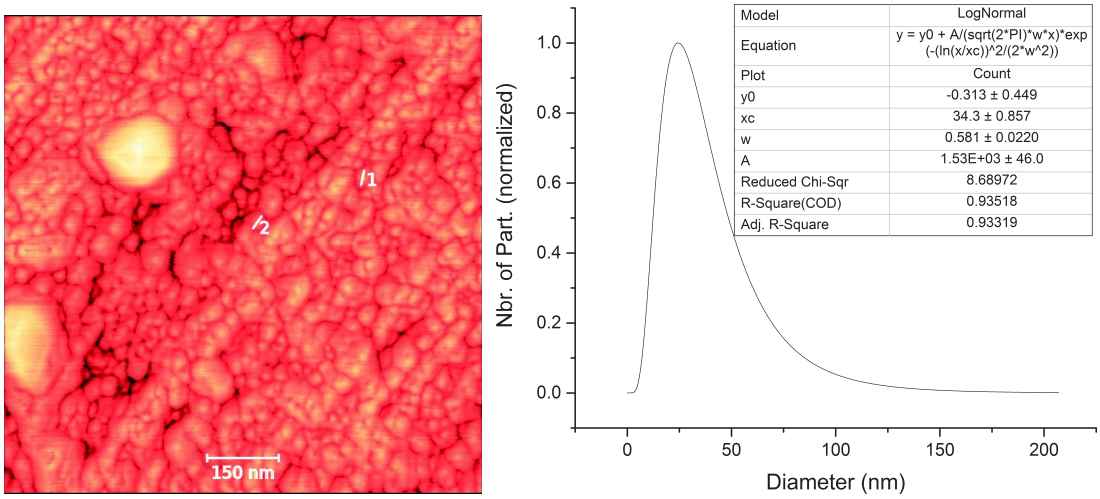

(a) AFM topography. The length of the marked particle is 30 nm

(b) Particle Size Distribution: mean at 35 nm

Figure 3.16 – n-RDX processed with 10 wt% PVP.

even much smaller particles were measured –after the surface milling– when adding more polymer and reducing the original particle size (the ones imaged by SEM). For pure n-RDX the sizes of the smallest particles stay in the same range as the particle size from AFM below the critical pressure without microtomy: this confirms that due to the segregation by AFM the smallest particles are scanned, thus implying that below the critical pressure the particles may stay unbroken. Those results raise again the question of the hardness of the nanoparticles. Since the smallest particles imaged in SEM are bigger than the one observed by AFM, the rubbing method does not bring an energy (friction work and pressure) as high as in the case of the AFM pellets: that technique seems suitable to spread the particles without breaking the brittle particles.

3.3 Summary of the Chapter

Several sizes have been measured depending on the technique and the conditions. By AFM, pellets are imaged, without or with microtomy to flatten the surface; many samples were analysed by this technique at 97 MPa plus microtomy such as the result reported by Spitzer et al. (2014) or the preliminary study with a range of RDX content. Classical SEM were made on loose powder and pellets, and a rubbing technique has been developed to spread particles on a glass substrate in order to image the smallest particles. The lattice structure and the apparent volume weighted domain size were computed from Rietveld

refinement. All that high amount of data were interpreted and correlations between techniques have been found.

n-RDX can be broken in smaller particles by compression. For pure compounds and below a critical pressure, the particles observed by AFM are about 200 nm with a irregular round shapes; that size and morphology is the same as imaged on the smallest particles, by the rubbing technique by SEM. When using a microtome on n-RDX pellets, the surface is milled and the blade imperfections imprint grooves on the surface or strip off parts which reveal the original particles inside the pellet, as seen by SEM. By AFM a segregation is made by the roughness of the surface: those holes with bigger particles are never scanned on the pellets processed by microtomy, thus only the smallest particles are counted. That bias also explains why size and shapes on AFM can be identical to the smallest particles imaged on SEM.

XRD patterns analysed by Rietveld refinement reveal an average apparent size around 80 nm with an oblate morphology for all samples, meaning that an homogeneous growth occurs in all SFE conditions. The smallest particles imaged by SEM seem to be single crystals in the case of n-RDX processed by polymers.

As the particles sizes after mechanical stress depend on purity and quantity of polymer, the hardness is probably a key property for a deeper comprehension of the phenomenon reported in this chapter. Nano indentation is used to study the mechanical properties of material: Hudson et al. (2012) found that micron-sized crystals with many internal defects have reduced modulus of elasticity, stiffness and prone to greater deformation under applied load, therefore correlate shock sensitivity and stiffness/elasticity. Nano mechanical tests can be done under the direct visualization of an SEM or Transmission Electron Microscopy (TEM). However, due to the already mentioned difficulties to image energetic organic nanoparticles, such experiments would require a dedicated scientific study.

After being able to define an absolute particle size representative of the sample, the reduction of the particle size can be studied without bias; the crystallisation has to be controlled in both space and time resolution. Two main approaches have been established, a chemical one and a more physical one. The next chapter focuses on the physical attempt by the exploration of various supersaturation conditions, just after introducing all the needed concepts for the formation of organic crystal, with a specific focus on the nucleation.

Bibliography

1. Finger, L. W., D. E. Cox, and A. P. Jephcoat (1994). "A correction for powder diffraction peak asymmetry due to axial divergence". In: *Journal of Applied Crystallography* 27.6, pp. 892–900. DOI: 10.1107/S0021889894004218.
2. Gierak, Jacques (2009). "Focused ion beam technology and ultimate applications". In: *Semiconductor Science and Technology* 24.4, p. 043001. ISSN: 0268-1242. DOI: 10.1088/0268-1242/24/4/043001.
3. Hudson, Robert J., Peter Zioupos, and Philip P. Gill (2012). "Investigating the Mechanical Properties of RDX Crystals Using Nano-Indentation". In: *Propellants, Explosives, Pyrotechnics* 37.2, pp. 191–197. ISSN: 07213115. DOI: 10.1002/prep.201100063.
4. Limpert, Eckhard, Werner A. Stahel, and Markus Abbt (2001). "Log-normal Distributions across the Sciences: Keys and Clues". In: *BioScience* 51.5, pp. 341–352. ISSN: 0006-3568. DOI: 10.1641/0006-3568(2001)051[0341:LNDATS]2.0.CO;2.
5. Nečas, David and Petr Klapetek (2012). "Gwyddion: an open-source software for SPM data analysis". In: *Central European Journal of Physics* 10.1, pp. 181–188. DOI: 10.2478/s11534-011-0096-2.
6. Östmark, Henric, Sara Wallin, and How Ghee Ang (2012). "Vapor Pressure of Explosives: A Critical Review". In: *Propellants, Explosives, Pyrotechnics* 37.1, pp. 12–23. ISSN: 07213115. DOI: 10.1002/prep.201100083.
7. Pichot, Vincent, Benedikt Risse, Julien Mory, Christelle Nicollet, Fabien Schnell, Marc Comet, and Denis Spitzer (2015). "Mechanical Behavior of Nanostructured and Microstructured Explosives". In: *Propellants, Explosives, Pyrotechnics* 40.2, pp. 203–209. ISSN: 07213115. DOI: 10.1002/prep.201400122.
8. Qiu, Hongwei, Victor Stepanov, Anthony R. Di Stasio, Ashok Surapaneni, and Woo Y. Lee (2015). "Investigation of the crystallization of RDX during spray drying". In: *Powder Technology* 274, pp. 333–337. ISSN: 00325910. DOI: 10.1016/j.powtec.2015.01.032.
9. Spitzer, D., B. Risse, F. Schnell, V. Pichot, M. Klaumünzer, and M. R. Schaefer (2014). "Continuous engineering of nano-cocrystals for medical and energetic applications". In: *Scientific Reports* 4. DOI: 10.1038/srep06575.
10. Spitzer, Denis, Christian Baras, Michael Richard Schäfer, Fabrice Ciszek, and Benny Siegert (2011). "Continuous Crystallization of Submicrometer Energetic Compounds". In: *Propellants, Explosives, Pyrotechnics* 36.1, pp. 65–74. ISSN: 07213115. DOI: 10.1002/prep.200900002.

11. Williamson, G. K and W. H Hall (1953). "X-ray line broadening from filed aluminium and wolfram". In: *Acta Metallurgica* 1.1, pp. 22–31. ISSN: 0001-6160. DOI: 10.1016/0001-6160(53)90006-6.

Chapter 4

Crystallisation study and comprehension of the SFE process

4.1 Crystallisation, Nucleation and supersaturation

Crystallisation from solution occurs when the concentration of the compound is higher than its solubility, namely in the supersaturation zone. Various strategies can be used since the solubility depends on the temperature, the solvent(s) and other compound(s): temperature change (cooling in the case of a positive gradient $\frac{dC}{dV}$ of the solubility curve or heating in the case of a negative one), solvent removing (evaporation), addition of a drowning-out agent (an anti-solvent) or reaction partners. But achieving the supersaturation may not be enough; to trigger the crystallisation in that metastable system, an external energy (stirring, mechanical shock, friction or extreme pressures) or a seed (impurity or a crystal of the compound) can be brought to the solution. Others stimuli such as electric and magnetic fields, spark discharges, UV light, X-rays and ultrasonic irradiation have also been studied since decades (Atwood et al. 1969) but no application in large-scale crystallisation has been ever reported.

Three types of nucleation can be distinguished. The secondary nucleation occurs when a crystal already exists: a seed triggers the nucleation of the metastable solution or the compound nucleates on the surface of the growing particles. Primary nucleation can be spontaneous –homogeneous nucleation– or triggered by impurities –secondary nucleation–. Since impurity free solutions are virtually impossible, cases are often reported when a system nucleates at a few degrees lower than predicted or than the previous smaller batches (Mullin 2001). The exact formation of nuclei is still not known (Sosso et al. 2016). The molecules have to coagulate, then to resist to re-dissolution but since the lattice faces are not equivalent, the molecules should have the right orientation. Even

the mechanisms are not resolved yet, a nucleus has to achieve a critical size to actually grow into a crystalline particle. From the Classical Nucleation Theory, the critical radius corresponds to the one minimizing the overall excess Gibbs energy ΔG:

$$\begin{aligned}\Delta G &= \Delta G_S + \Delta G_V \\ &= 4\pi r^2\gamma + 4/3\pi r^3 \Delta G_v\end{aligned} \tag{4.1}$$

$$\Rightarrow \frac{d\Delta G}{dr} = 8\pi r\gamma + 4\pi r^2 \Delta G_v = 0 \tag{4.2a}$$

$$\Rightarrow r_c = \frac{-2\gamma}{\delta G_c} \tag{4.2b}$$

ΔG_S is the excess Gibbs energy between the surface of the particle and the bulk, and ΔG_V is the volume excess Gibbs energy between a large (infinite) particle and the compound dissolved. $\Delta G_S > 0$ while $\Delta G_V < 0$. ΔG_S relies on the interfacial tension –also called surface energy– γ and ΔG_v is the volumetric volume excess Gibbs energy. Therefore, critical overall excess Gibbs energy can be expressed as:

$$\Delta G_c = \frac{16\pi\gamma^3}{3(\Delta G_v^2)} \tag{4.3}$$

The supersaturation S is expressed as a ratio between the concentration c and the solubility s at the given temperature: $S = c/s$. With the Gibbs-Thomson relationship, the supersaturation becomes with v the molecular volume:

$$\ln S = \frac{2\gamma V}{RTr} = \frac{2\gamma v}{k_B T r} \tag{4.4}$$

So from the Equations (4.3) and (4.4), we can finally express the critical overall excess Gibbs energy with the supersaturation:

$$\Delta G_c = \frac{16\pi\gamma^3 v^2}{3(k_B T \ln S)^2} \tag{4.5}$$

To go further, the rate of nucleation can be written as an Arrhenius velocity equation $J = A\exp(-\Delta G/kT)$, which is given from Equation (4.5)

$$J = A\exp\left(-\frac{16\pi\gamma^3 v^2}{3(k_B T)^3(\ln S)^2}\right) \tag{4.6}$$

The rate of nucleation finally relies on the temperature, surface energy and the supersaturation, and has been plotted in Figure 4.1a; after a critical value

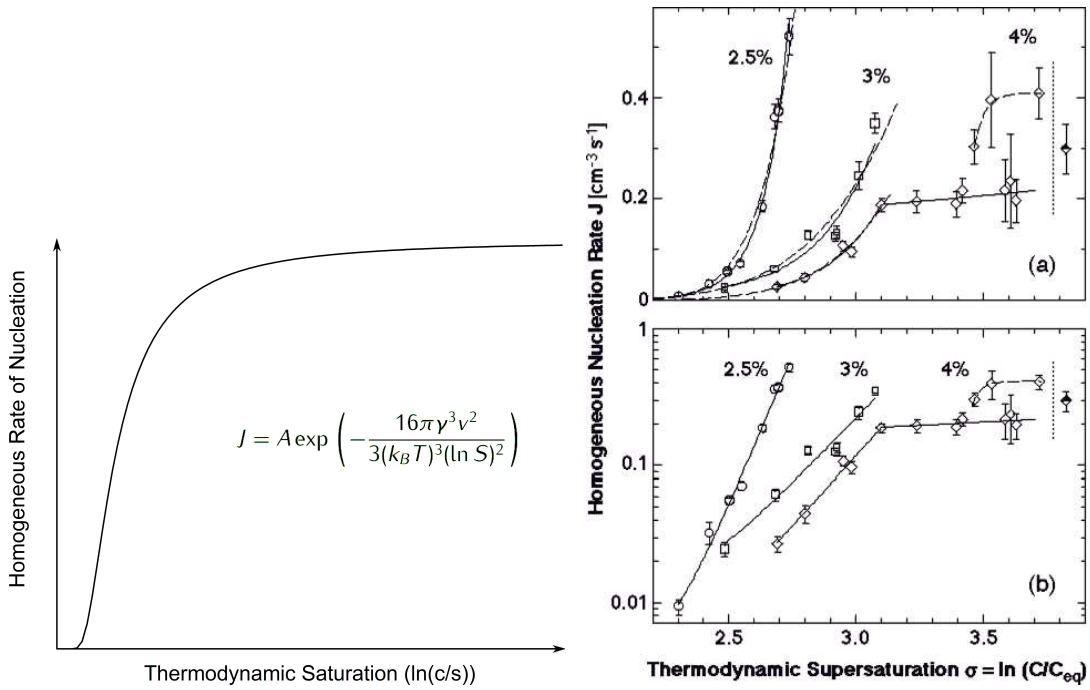

(a) Theoritical plot (b) Experimental data from Vekilov (2010a)

Figure 4.1 – Rate of nucleation against the supersaturation.

the rate increases rapidly up to an asymptotic rate. The experimental values in Figure 4.1b are in good agreement with a sudden increase followed by a plateau.

However, many efforts have been devoted since 2010 to extend and improve the Classical Nucleation Theory (CNT) (De Yoreo 2013; Gebauer et al. 2014; Vekilov 2010b; Zahn 2015). On the contrary of melts where the liquid is dense enough to neglect concentration gradients and related phenomena, the case of crystal nucleation of molecules in solution is quite different. A significant concentration fluctuation is required to bring the needed number of molecules to construct the nuclei. That's why a two-step mechanism was developed recently where two free energy barriers have to be overcome instead of an unique one expressed in Equation (4.1) from the CNT: as displayed in Figure 4.2, the first one illustrates the density variation to create a primary cluster of molecules, then the second one describes the ordering of those clusters into the crystalline nuclei. Early stages of the nucleation of organic crystals have been investigated using Molecular Dynamics (MD) backed up with experimental data from single-molecule real-time transmission electron microscopy (SMRT-TEM); Salvalaglio et al. (2015, 2012) demonstrated that different solvents can lead to different

nucleation mechanisms such as a single-step nucleation process favoured for urea molecule in methanol and ethanol and a two-step mechanism in acetonitrile and water.

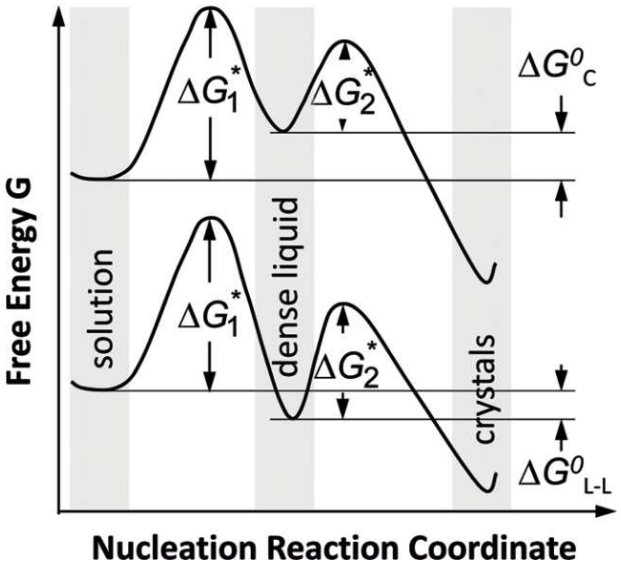

Figure 4.2 – Two possible scenarios from the two-step nucleation mechanism: the first one involves an intermediate state at a higher energy due to an unstable dense liquid existing as mesoscopic clusters, and the second lower curve applies if the dense liquid is stable ($\Delta G^0_{L-L} < 0$)

.

The link between the rate of nucleation and the crystal size is far of being established since several phenomena follow the nucleation: the firstborn nuclei are subject to growth but also aggregation. Thus an optimal value of the supersaturation exists for each system; a supersaturation too high would lead to aggregation and also to secondary nucleation on growing particles.

4.1.1 Increasing Supersaturation in SFE with an Anti-solvent

The key to control crystallisation and so particle size is to determine the supersaturation which is time dependent but also is unique in each droplet. Supersaturation, as a function of time and coordinates, was not available: since we were not able to determine *in situ* droplet size distribution, extreme variations of the supersaturation are investigated. Therefore, a suitable anti-solvent for RDX and for SFE has been searched in order to increase the supersaturation by reduced solubility. Water is commonly used as drowning out agent for RDX recrystallisation (Essel et al. 2012; Gallagher et al. 1992; Lee et al. 2014), but due

to a high temperature of evaporation and a modest heat capacity (75.28 J/mol K at 25 °C), such solvent can not be processed by SFE: a flash evaporation can be triggered but a quick condensation will occur thus wetting the particles.

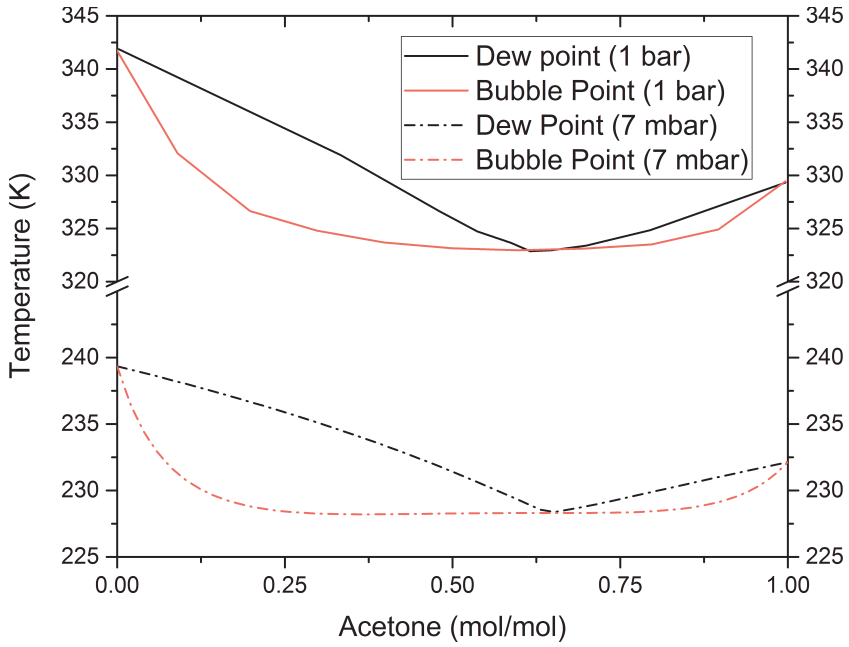

(a) Vapor-Liquid Equilibrium (VLE) diagram

pressure	temperature (K)	x (acetone)
1 bar	323	0.648
7 mbar	228.5	0.621

(b) Azeotropes

Figure 4.3 – VLE of the binary system acetone-hexane at 1 bar (solid lines) and 7 mbar (dashed lines): the data at 1 bar are obtained from the Dortmund Data Bank, and curves at 7 mbar are computed from ProSim.

n-Hexane is a perfect non-polar solvent of RDX (PANT et al. 2013). n-Hexane is miscible with acetone and has a low boiling point of 342 K at atmospheric pressure, a high vaporization enthalpy around 31 kJ/mol and a remarkably high heat capacity of 195.8 J/mol K at 298 K. All of those thermodynamic properties are better than any solvent studied by PANT et al. (2013). Moreover, n-hexane forms an azeotrope with acetone: Vapour-Liquid equilibrium data at ambient pressure are plotted in Figure 4.3a. Values at reduced pressure close to the

ones in the SFE are computed by ProSim using the Non-Random Two-Liquid (NRTL) model for the activity coefficients. The UNIFAC model was also tested, but lowered the bubble point temperatures by 0.2 K with no change on the azeotrope position. The VLE of an n-hexane/acetone system exhibits significant lower bubble points than both of the boiling temperatures: the azeotrope at atmospheric pressure is 7 ° lower than the standard boiling point of acetone and 19 ° lower than the one of n-hexane.

Beside increasing the supersaturation with a binary system solvent/anti-solvent, an original approach was developed: to understand the flash-evaporation mechanisms, especially the life-time of droplets and the time dependant crystallisation, the SFE system has been upgraded with a second nozzle. An entire second channelling for the new nozzle has been added and build on an existing system. Also the nozzles have to be oriented to effectively overlap the hollow spray cone: to achieve that the piping system has been reconsidered. The Figure 4.4 describes the new system. Due to technical limitations, a lateral distance between the inlet pipe has to be kept and the channelling has to remain parallel up to the heating elements. Therefore the distance between the end of an heater and the nozzle has been minimized and the stainless steel pipes insulated to prevent heat loss. From the experiments made in Section 4.2.2, an optimal angle around 70 ° has been found and used here. For the present study, one system is used to spray RDX dissolved at 2 wt% in acetone through a 60 µm nozzle; the other one sprays n-hexane trough a 80 µm nozzle in order to permanently have a higher flow of hexane over acetone and so to maximize the overlapping. The system was patented in the international version of the patent ("Method for producing cocrystals by means of flash evaporation" 2016).

Several molar ratio were tried: very near the azeotrope at $x_{\text{acetone}} = 0.642$ and two others flanking the azeotrope from far. But due to the specific boiling point curve of the acetone/n-hexane, the three ratio x_{acetone} 0.573, 0.642 and 0.817 correspond to the same boiling temperature at atmospheric pressure and below. Therefore the driving force of the SFE, the superheating, is kept constant and only the variation of the saturation over time varies. Then after the flash of droplets, it assumed that the nucleation already occurred and classical evaporation applies. Finally, depending on the ratio the rare remaining drops will either enrich in acetone ($x_{\text{acetone}} = 0.817$) or in hexane ($x_{\text{acetone}} = 0.573$): that phenomenon could provoke the generation of a secondary PSD. Only a single peak following a log-normal distribution is found from the frequency count of particle size determined by SEM. The classical evaporation is negligible.

The overall mean diameter of RDX particles is quite high; for instance the reference –pure RDX at 2 wt% in acetone– result in a mean diameter of 790 nm instead of the usual 500 nm (Doctoral Thesis Risse 2012). Such an increase

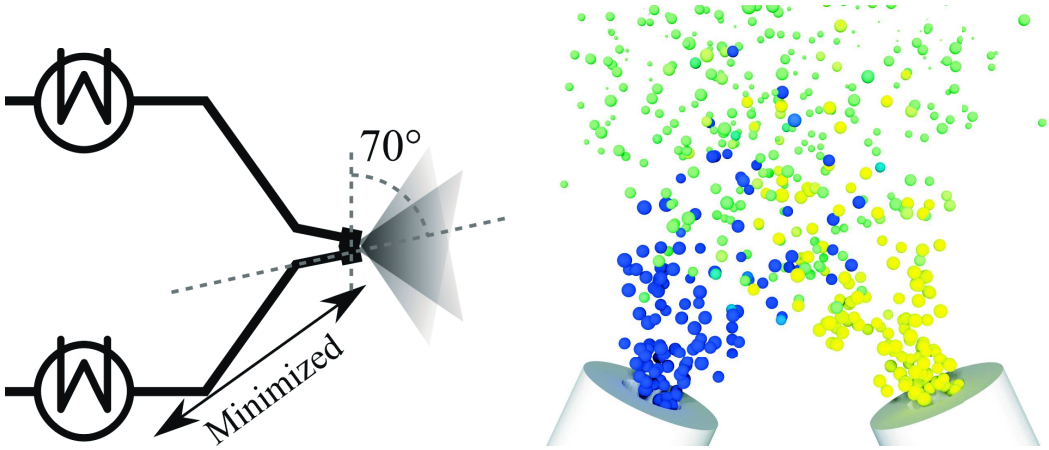

(a) Schema (b) Principle

Figure 4.4 – The dual nozzle system.

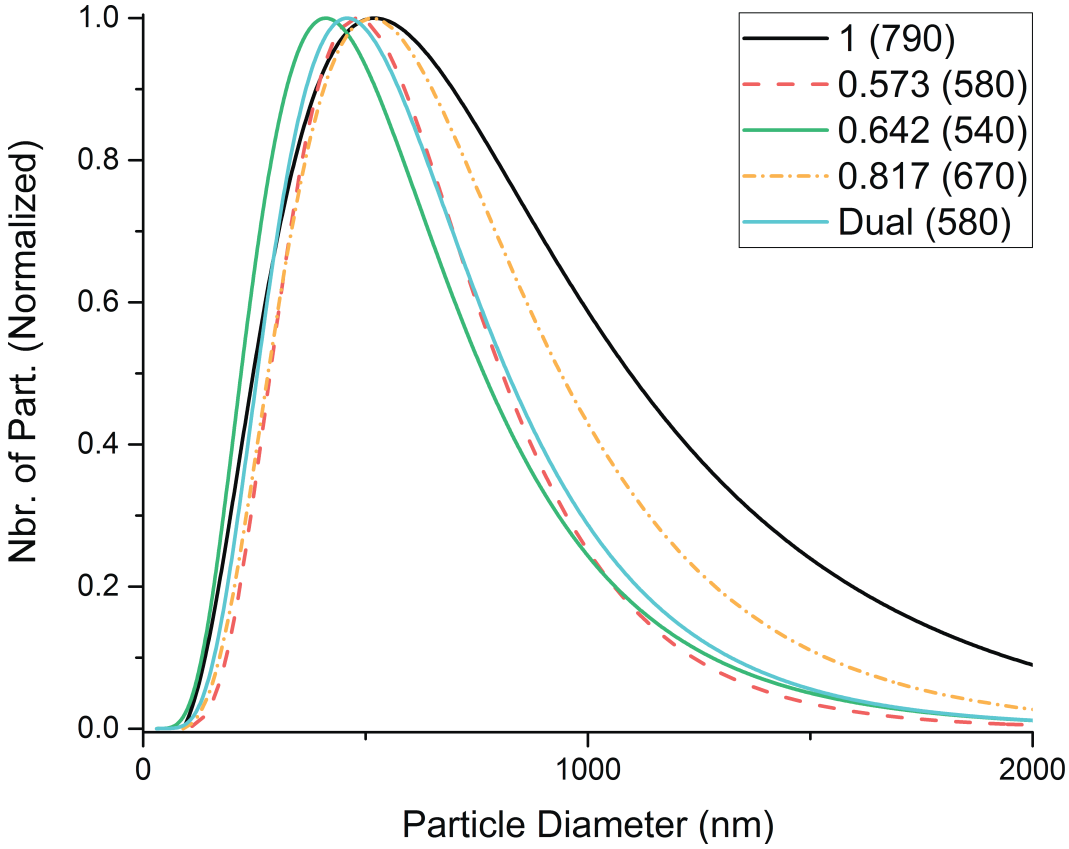

Figure 4.5 – PSD for RDX processed in the binary system acetone/n-hexane by SFE through one or two nozzles; the legend shows the molar ratio of acetone and in parenthesis the mean diameter in nm.

suggest a deterioration of the flash-evaporation due to a lower superheating: the dual nozzle is less efficient to keep the solvent superheated from the heaters to the nozzles because the distance induces higher heat losses. However, the flash-evaporation characteristics such as broadened spray and a lower vacuum pressure are still observed.

From Figure 4.5, the ratio of hexane clearly decreases the particles size from around 800 nm down to around 550 nm. That lower bound already appears for $x_{\text{acetone}} = 0.642$. Increasing the supersaturation up to a certain degree seems to improve the nucleation rate and therefore the particle size with no drawback due to aggregation. The experiment using two nozzles is very informative: droplets have enough life time for an effective overlapping. A possible interpretation would be that acetone droplets are first in a metastable state with no nucleation and no flashing thus allowing them to collide and merge with hexane droplets. The sudden saturation due to a lower solubility in the system acetone-hexane triggers the nucleation in the same conditions as for the one-nozzle at ratio 0.573 and 0.642. So the overlapping induces a ratio of acetone lower than 0.817.

The dual nozzle system has many advantages; in order to increase the mass flow rate, the percentage of the compounds in solution can be raised, then crystallisation is triggered by a second solution containing a drowning out solvent or a crystallisation partner. Advanced chemistry could also be explored when the reactive species should not be mixed until a thermal activation. Two points have to be confirmed first: the droplets interpenetrate each others from both sprays and hexane is not already gaseous thus drying acetone droplets. Therefore a reactive specie is added to the second solution: the cocrystallisation of CL-20:HMX 2:1 is chosen and explained in Section 4.2.

4.1.2 Supersaturation Determination

The supersaturation is a key element which will be unveiled by using the latest advances in LASER and phase Doppler analysers. Particle Image Velocimetry (PIV) were first tried at ambient pressure but is not suitable due to the hight density of the spray and limited spatial resolution of the technique. The LASER Doppler technique was first proposed in 1964 by Cummins et al. (1964) but was widely used only in the 70's. The phase Doppler technique exhibited a similar development about 20 years later from Bachdo et al. (1984), Bauckhage et al. (1984), and Saffman et al. (1984). The recent advances in signal filtering and analysis allows now the light-scattering interferometry to simultaneously record in real time object velocities and size distribution. The principle of Phase Doppler Analysis (PDA) is illustrated in Figure 4.6. A measurement volume is defined by the intersection of two focused LASER beams: the light is scattered by the particles passing through this volume. The second refraction order is

specifically used by the three detectors of the PDA probe. Each detector is pre-aligned and converts the optical signal into a Doppler burst with a frequency linearly proportional to the particle velocity. Then the phase shift Φ between the Doppler signals from different detectors allows the calculation of the particle diameter D:

$$\Phi = \frac{-2\pi D}{\lambda} \frac{n \sin\theta \sin\Psi}{\sqrt{2(1+\cos\theta\cos\Psi\cos\varphi)}\left(1+n^{2-n}\sqrt{2(1+\cos\theta\cos\Psi\cos\varphi)}\right)} \quad (4.7)$$

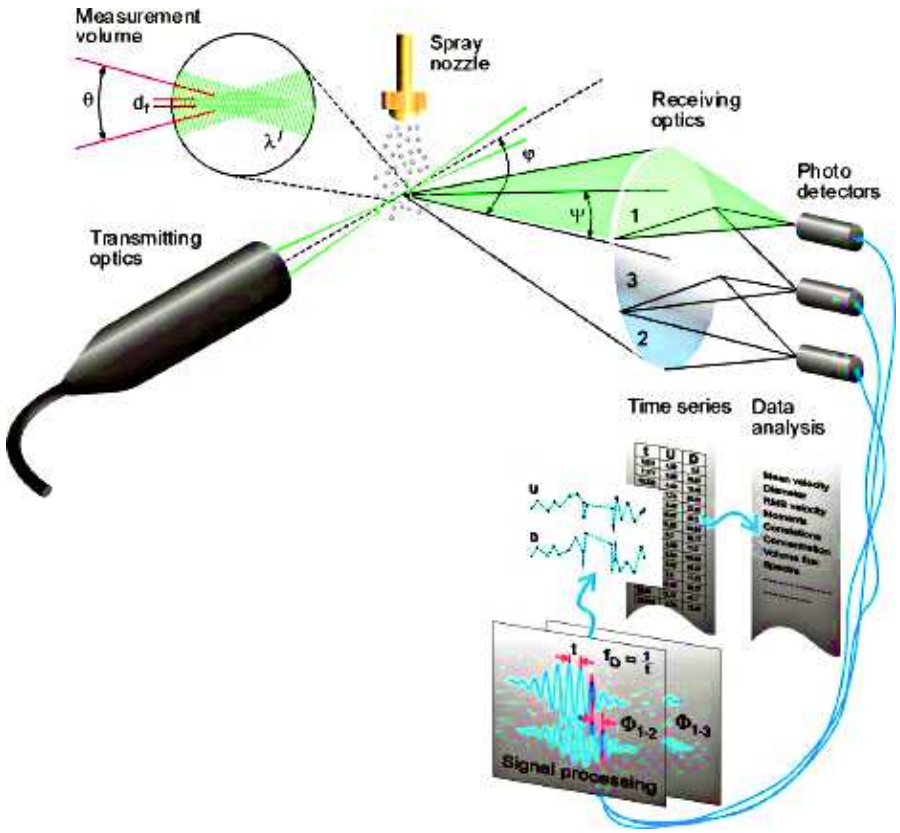

Figure 4.6 – Principle of the Phase Doppler analysis (PDA) in a glance (Dantec Documentation).

Preliminary results from a demonstration apparatus are reported in Figure 4.8. No calibration were performed to assess the accuracy of the apparatus. No optimizations nor quantification of the error were done. However, the droplets are clearly extremely small around the microns or even lower; the closer we are to flash evaporation, the smallest are the drops. The velocity is also very

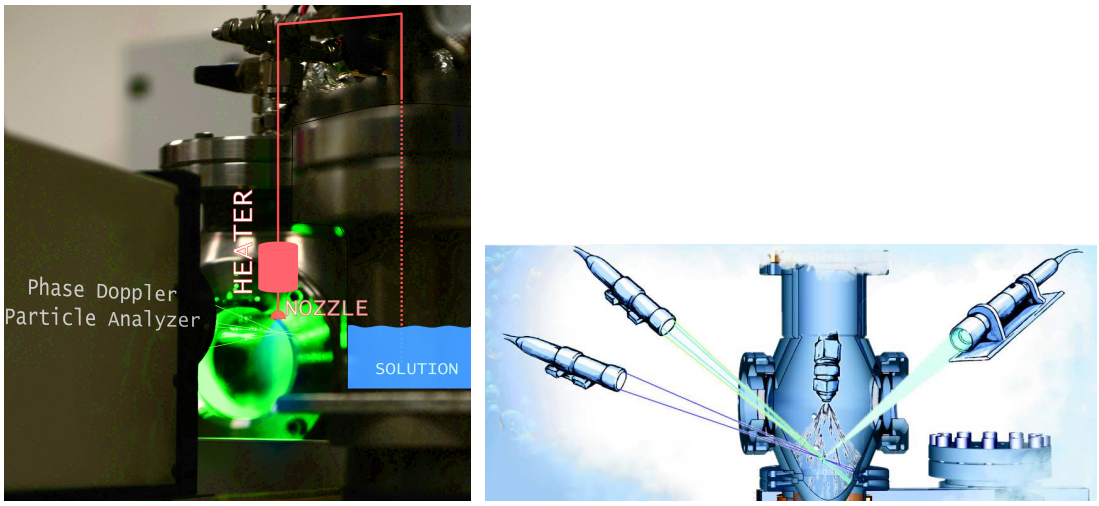

(a) Setup for PDA on SFE (b) 3D PDA on SFE, a schematic principle

Figure 4.7 – PDA in situ measurements for SFE.

high with an order of magnitude of 2 (100 m/s): it is one order above the rare velocities reported in flash-evaporation of spray by Gebauer et al. (2015) and Miyatake et al. (1981). Those preliminary data confirm that the SFE process involves high energy and fast crystallisation. It can be estimated than after 1 cm from the nozzle the spray is no more visible, which could implies that after only 0.1 µs the evaporation is complete and the crystallisation performed.

More reliable results were acquired thanks to the work of Mr Lasserre to deliver us an operational PDA apparatus quickly after the purchase. The beams were focused a few millimetre after the nozzle orifice and as closest as possible to the nozzle axe. The PDA were stabilized and operated in coincidence mode (the velocity measured by Laser velocimetry is coupled to the measurement of the diameter by Phase Doppler interferometry, resulting in the exact measure of both for each object in the measurement volume) with a sequence of 10 measurements each with 20k objects measured ; the receiving optics adjusted for the highest rate of coincidence and optimized with the Laser power. About the SFE, the temperature is stabilized for 15 min before each sequence. Each batch from the set of ten is compared to each other: no changes is the PSD has been noticed in a set of measurement for a given temperature so all the 200k objects measured per temperature are concatenated to render the Figure 4.9.

While the temperature is raised the droplet size clearly decreases close to the detection limit around one micron. Moreover the polydiversity exhibited for each PSD is reduced while increasing the temperature; multi peak fitting reveals three modes centred at 2.1, 2.8 and 3.8 µm at all temperatures. The

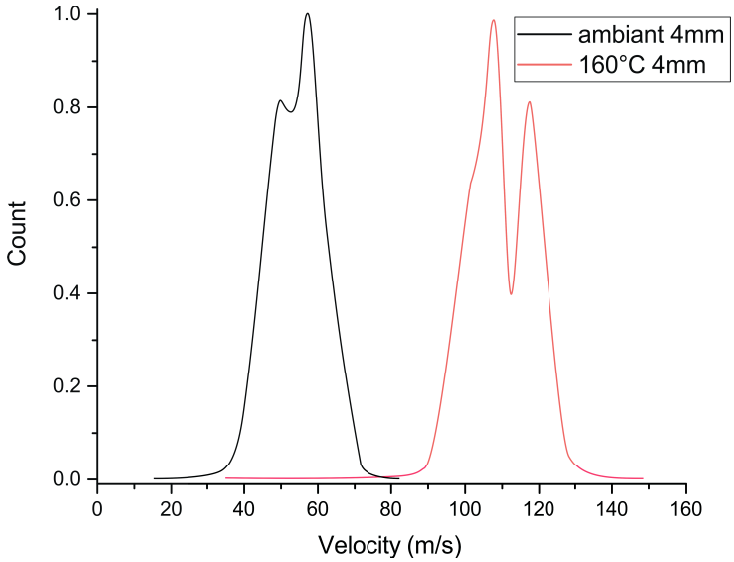

(a) Axial velocities of droplets

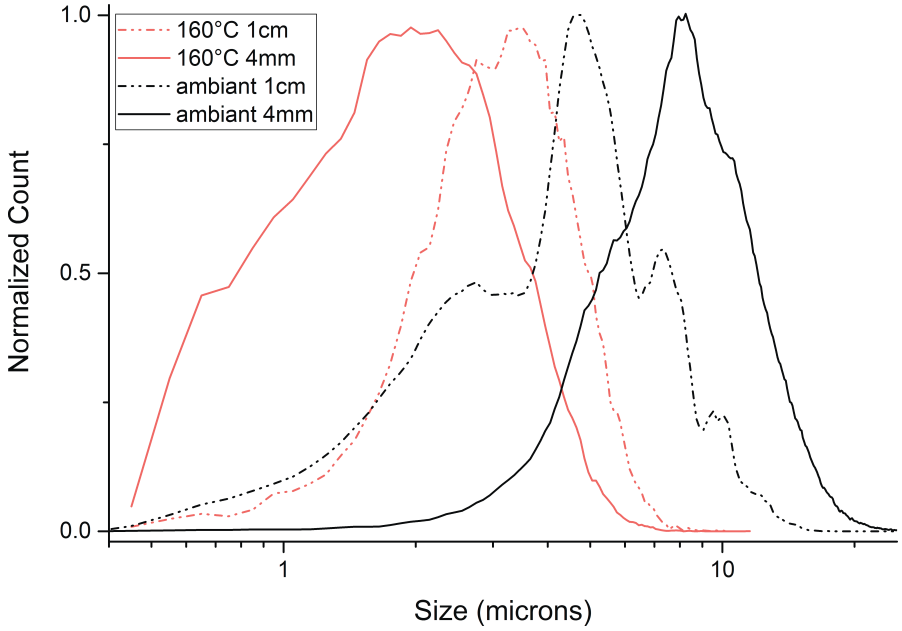

(b) PSD of droplets

Figure 4.8 – Preliminary measurements from a demonstration apparatus inside the SFE under vacuum while spraying acetone. Acquisitions were performed at two different axial distances from the nozzle orifice: at around 4 mm or quite far at around 1 cm

center of gravity doesn't change with temperature but only the area. Therefore at such temperatures the SFE is under a transition state toward flash evaporation which seems to be the dominant phenomenon at temperatures around 160 °C. To complete this study, the influence of the nozzle type should be study to evidence a potential change in the centre of gravity of the modes.

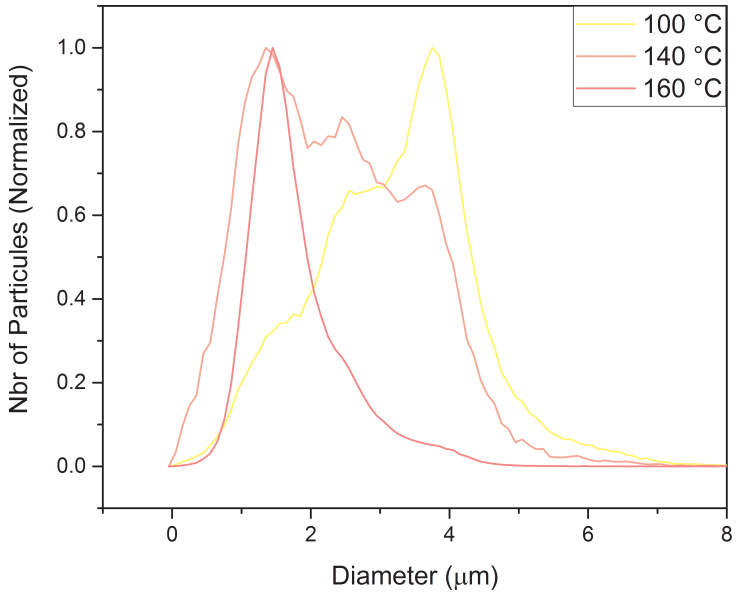

Figure 4.9 – Particle Size Distribution of droplets of acetone spayed at 100, 140 and 160°C.

4.2 CL-20:HMX 2:1 Cocrystal as a Tool for Understanding Crystallisation by SFE

4.2.1 Cocrystallisation

A cocrystal consists in the combination of two or more electrically neutral molecules within a single crystal lattice in a stoichiometric ratio. The exact definition is still under debate (Sun 2013) but hydrates and solvates are usually excluded. The constitutive compounds are often called co-formers. While cocrystals are known to potentially combine the drug effect of two Active Pharmaceutical Ingredient (API)s (Vishweshwar et al. 2006), it is interesting to notice that historically the pharmaceutical industry first avoided cocrystal, the racemic ones (Toda et al. 1997).

The formation of an existing cocrystal and the crystals of the co-formers relies on their solubility. A Phase Solubility Diagram (PhSD) shown in Figure 4.11

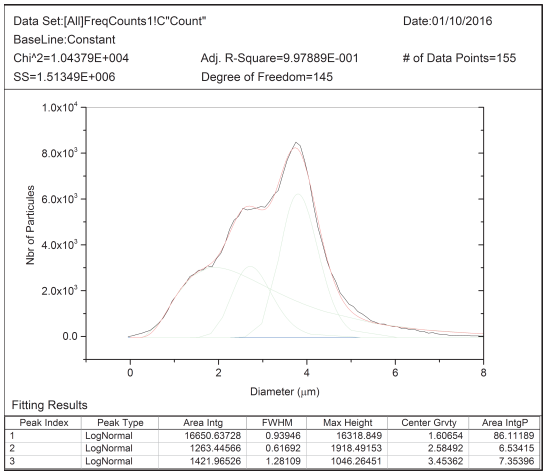

Peak Index	Peak Type	Area Intg	FWHM	Max Height	Center Grvty	Area IntgP
1	LogNormal	16650.63728	0.93946	16318.849	1.60654	86.11189
2	LogNormal	1263.44566	0.61692	1918.49153	2.58492	6.53415
3	LogNormal	1421.96526	1.28109	1046.26451	3.45362	7.35396

(a) 100 °C

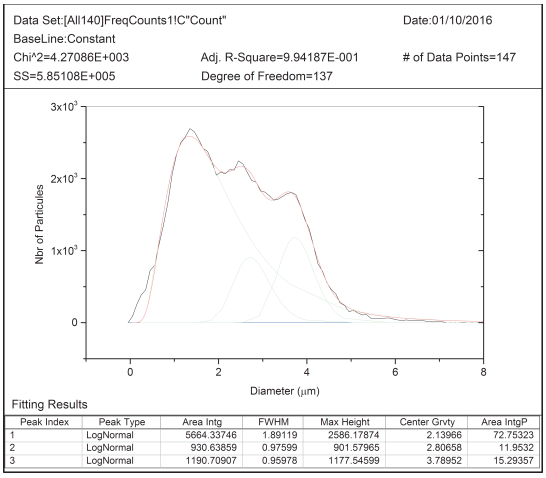

Peak Index	Peak Type	Area Intg	FWHM	Max Height	Center Grvty	Area IntgP
1	LogNormal	5664.33746	1.89119	2586.17874	2.13966	72.75323
2	LogNormal	930.63859	0.97599	901.57965	2.80658	11.9532
3	LogNormal	1190.70907	0.95978	1177.54599	3.78952	15.29357

(b) 140 °C

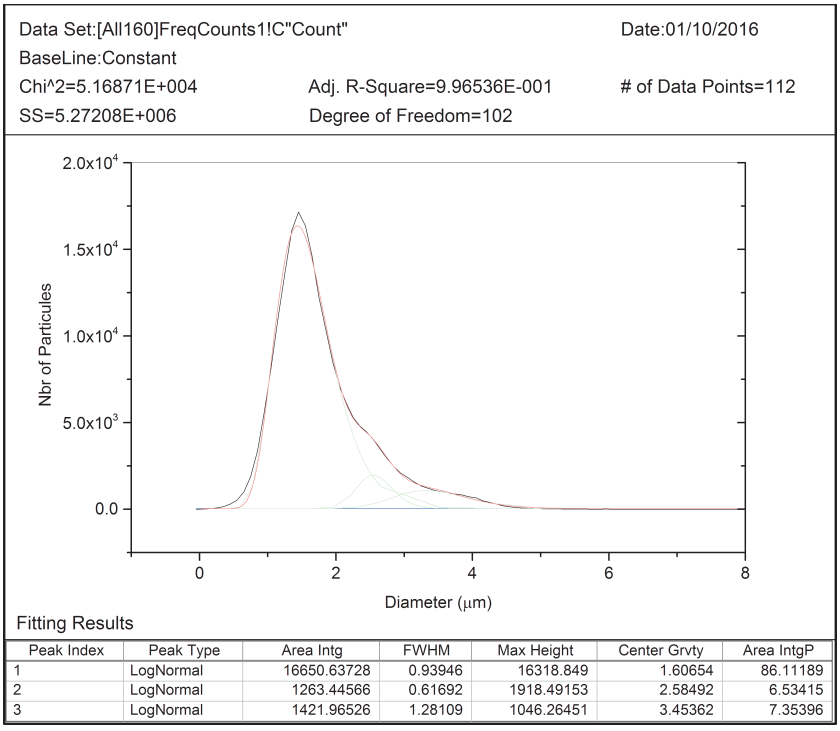

Peak Index	Peak Type	Area Intg	FWHM	Max Height	Center Grvty	Area IntgP
1	LogNormal	16650.63728	0.93946	16318.849	1.60654	86.11189
2	LogNormal	1263.44566	0.61692	1918.49153	2.58492	6.53415
3	LogNormal	1421.96526	1.28109	1046.26451	3.45362	7.35396

(c) 160 °C

Figure 4.10 – Peak fitting of the PSD of droplets of acetone spayed at 100, 140 and 160 °C.

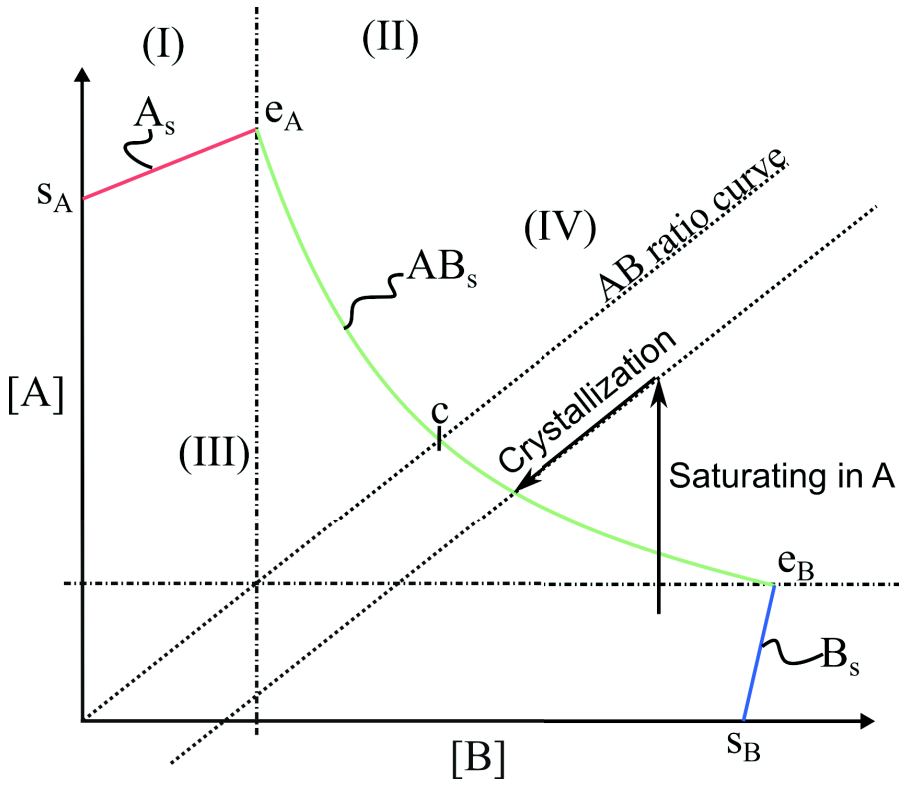

Figure 4.11 – Phase Solubility Diagram (PSD) of a 1:1 AB cocrystal from co-formers A and B; in red the solubility curve of the A crystal, in blue the one of B, and in green the cocrystal. Arrows illustrate a possible crystallisation by addition of B to the solution followed by the cocrystallisation.

depicts the co-former concentrations in a solvent at equilibrium at a given temperature with the different domain for each crystals (Nehm et al. 2006). The domain I is saturated in A and under saturated with respect of the cocrystal AB: only polymorphs from A can be crystallised. In the domain II both A_S and AB_S crystallises; the domain IV is situated above the solubility curve of the cocrystal and thus allows the crystallisation of the AB_S alone. In the domain III, the solution is under saturated for all species and no crystallisation can occur.

Unlike the PhSD, the triangular phase diagram (TPD) in Figure 4.12 shows the total composition of the system. Chiarella et al. (2007) explained why the formation of cocrystals could not occur while having the appropriate stoichiometry and underlined the need of covering a wide range of ratio when screening for cocrystals (Chadwick et al. 2009).

Beside those thermodynamic properties at equilibrium, kinetics prevail especially when crystallising from multicomponent systems. Ostwald (1897) speculated that the critical cluster to nucleate from a supercooled liquid may not be

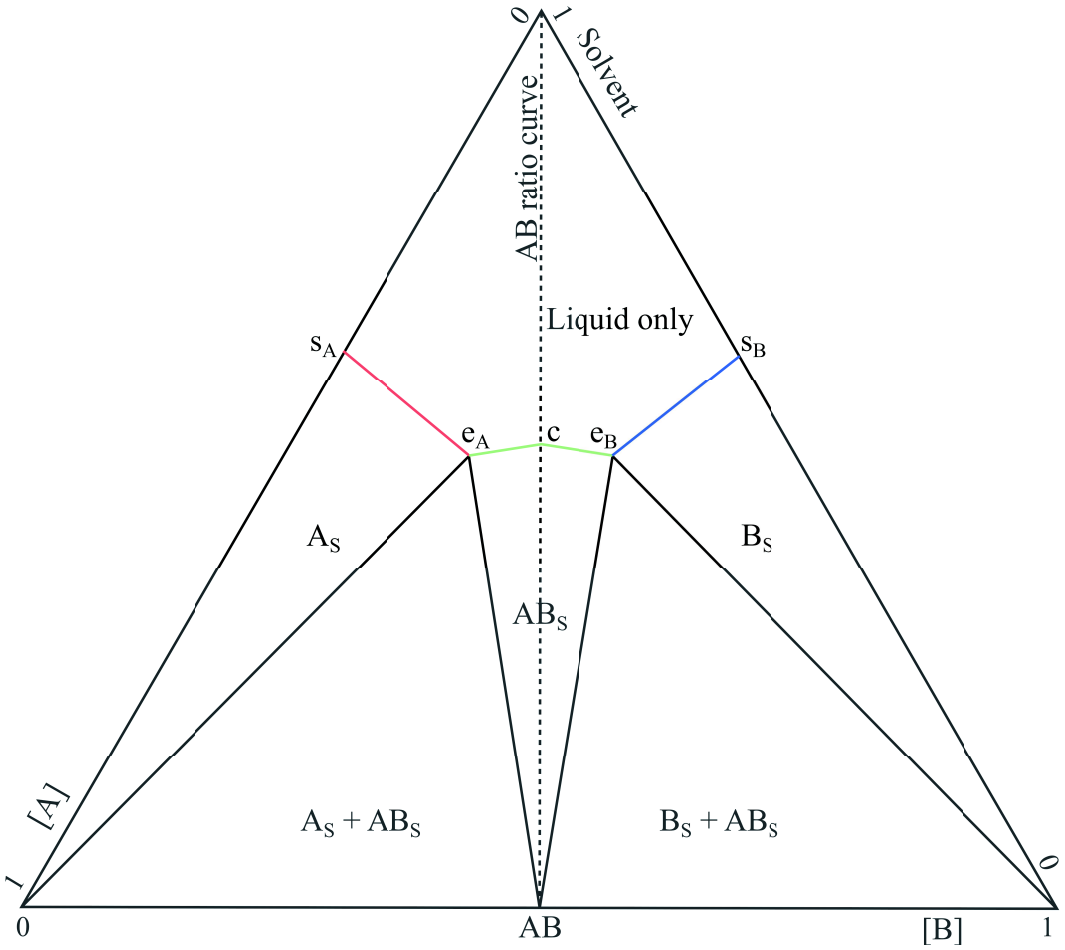

Figure 4.12 – Ternary Diagram of a 1:1 AB cocrystal from co formers A and B; coloured curves are the solubility curves from Figure 4.11.

the most stable polymorph but the polymorph closest in energy to the liquid phase. Since 1897, this behaviour has been observed a number of times (ten Wolde et al. 1999).

4.2.2 CL-20:HMX 2:1 Cocrystallisation from SFE

The SFE has already proved to be a suitable method to cocrystallise from a solution at the dried state (Spitzer et al. 2014). However to ensure a complete comprehension of the cocrystallisation by SFE, PhSD at several temperatures should be established for each compound such as the caffeine and acid glutaric from Yu et al. (2010). Unfortunately no PhSD nor ternary diagram exists for the CL-20:HMX 2:1 cocrystal.

In order to confirm the existence of metastable droplets in a state where no nucleation nor flash-evaporation occurred, an experiment with the co-formers sprayed separately was designed: the first dual-nozzle system was build for those experiments. Instead of an angle of 70 °, the nozzles were oriented at 45 ° as illustrated in Figure 4.13.

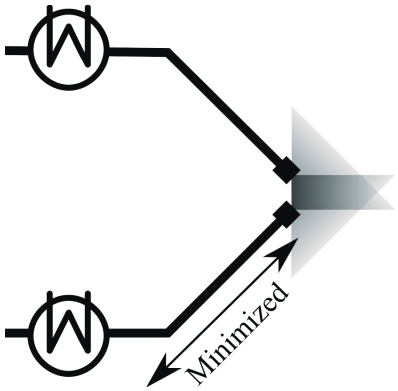

Figure 4.13 – First dual nozzle system with an orientation at 45 °.

The solutions of CL-20 and HMX were prepared in the stoichiometric ratio 2:1 of the cocrystal, using acetone (CHROMASOLV ®, for HPLC, ≥ 99.9% Sigma Aldrich). The Figure 4.14 shows mean PSD of the samples obtained through that technique; the method used is the AFM on pellets explained in the Section 3.1.2. Therefore, even if the mean size obtained here of 73 nm can not be interpreted as an absolute size, it can be compared to other samples processed by this technique: 73 nm is among the smallest mean sizes counted for n-RDX –more specifically the RDX processed with PVP– meaning that an absolute size under 300 nm can be excepted.

X-ray Diffraction was performed on samples processed from that dual nozzle setup. The XRD pattern in Figure 4.15 exhibits two crystalline structures: the main crystals present is β-CL-20 but the cocrystal is confirmed to have crystallised from the overlapped sprays. β-CL-20 is the least stable polymorph of CL-20; the crystallisation of β-CL-20 from SFE implies a kinetically controlled crystallisation and an high energy (Ostwald rule previously mentioned). The cocrystal being the minor product could be explained from a thermodynamic point of view from solubilities, but the solubility of CL-20 in acetone is much higher (100 wt%) than HMX (2.8 wt%). The explanation lies from a more practical issue.

The flow rate is not monitored in real time, but an estimation of the mean flow rate for each nozzle is calculated from the volumes left and the experiment time. It has been found that for all experiments with the dual nozzle at 45 °,

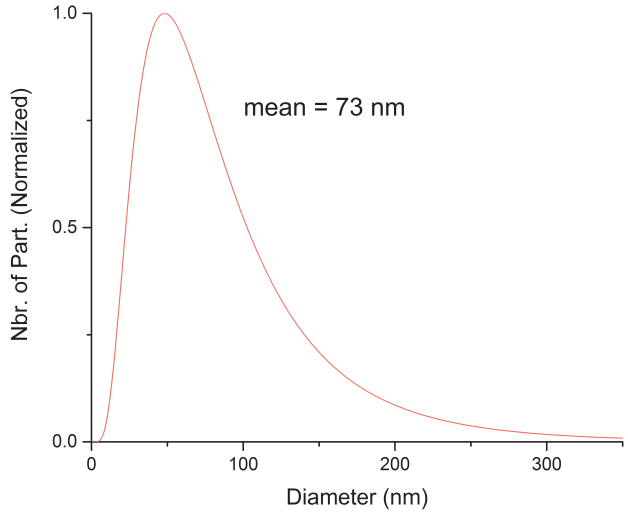

Figure 4.14 – Mean Particle Size Distribution of the cocrystal CL-20:HMX 2:1 samples processed by SFE (first batch) and counted from pellets analysed by AFM.

the nozzles have a very strong attendance to clog. Due to the angle and the spray broadening under vacuum, nozzles spray on each other; each nozzle forms a solid deposit on the opposite one and, after a while, one nozzle is clogging and blocking entirely the other one. Another system is build afterwards with an angle around 70° as previously introduced in Section 4.1.1; also to correlate the percentage of each crystal to kinetic or thermodynamic phenomena, the flow rate has to remain constant. Coriolis mass flow meters for high pressure were purchased and installed on the SFE process. To control in real time the flow rate of one inlet based on the variation of the other inlet, a master/slave system was developed: one flow meter read and transmit the flow rate of one nozzle to the second flow meter equipped with a valve and an internal PID controller. A variable resistor allows to set a ratio of flow rate between the inlets, thus allowing to have the compounds in a non stoichiometric ratio –with respect to the cocrystal– in solution but sprayed at the stoichiometric ratio. Those flow meters are currently at the testing stage before performing scientific studies.

An experiment was performed lately by spraying a solution of CL-20 in ethyl acetate and a solution of HMX in acetone at the constant stoichiometric ratio 2:1 by monitoring and controlling both mass flow rate. As it can be seen in Figure 4.16, even introduced with the right proportion with a controlled flow rate, the main product is again β-CL-20 with the cocrystal as the minor one. The amorphous content has to be calculated from the pattern; several methods

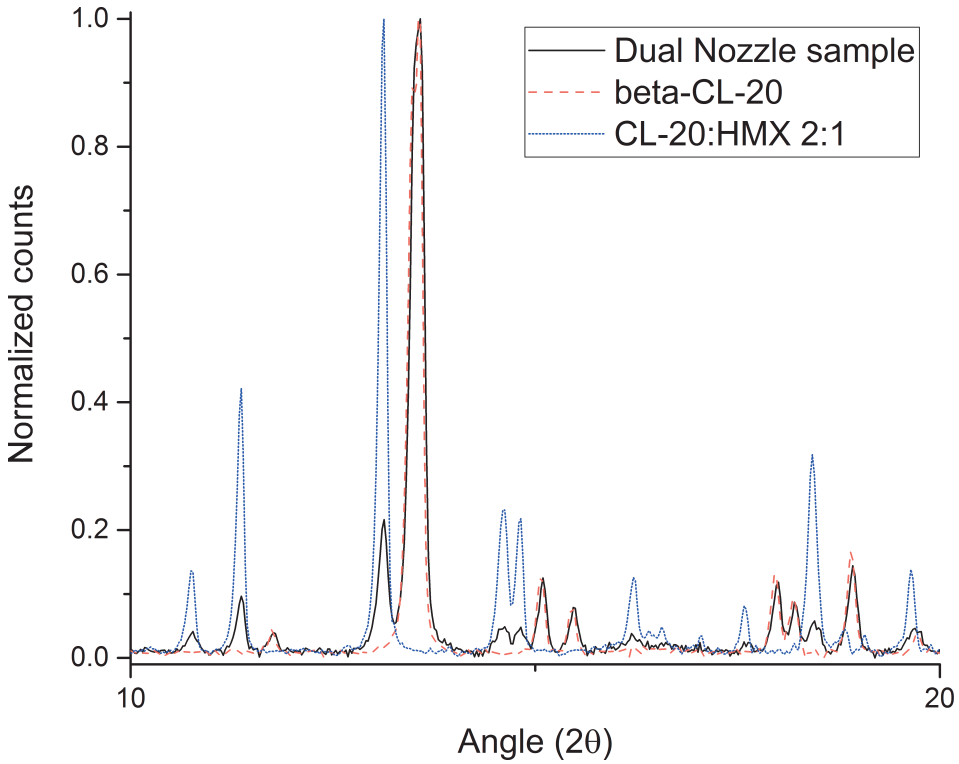

Figure 4.15 – XRD of a sample processed from dual nozzle system compared to CL-20:HMX and to β-CL-20 both from SFE via a single nozzle.

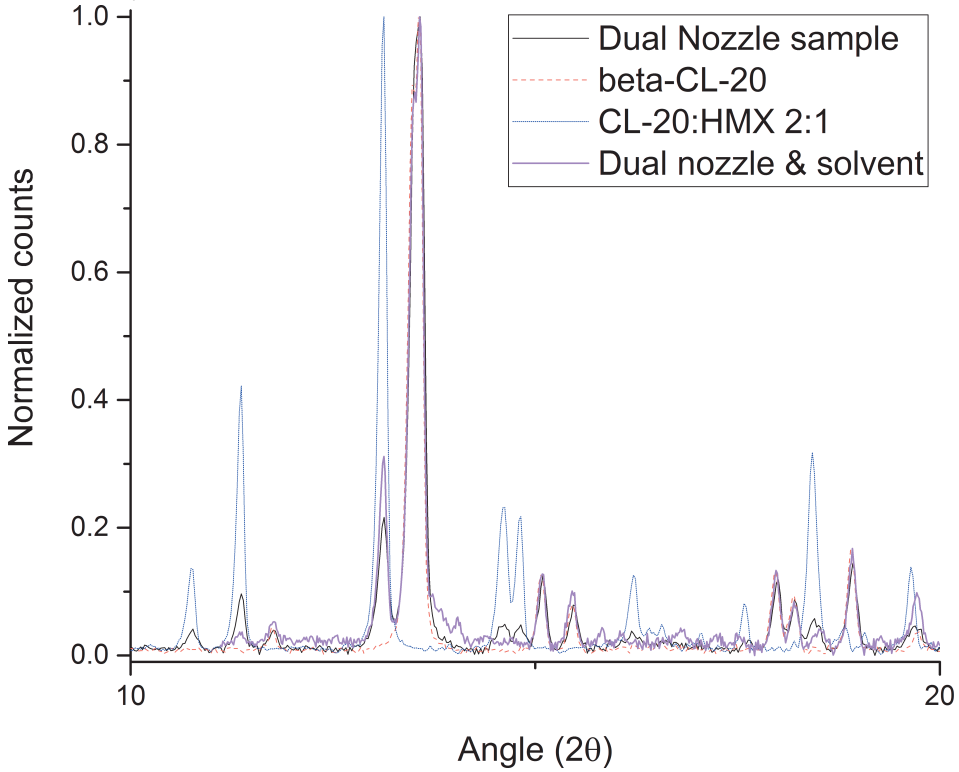

Figure 4.16 – XRD of a sample processed from a solution of CL-20 in ethyl acetate and a solution of HMX in acetone sprayed at the constant stoichiometric ratio 2:1 by monitoring and controlling mass flow rate; the pattern is compared to the sample from the Figure 4.15, CL-20:HMX and to β-CL-20 both from SFE via a single nozzle.

exists requiring calibration suite or internal/external standards. All of them would require to analyse the sample(s) with silicon or quartz zero-background sample holder: less than 20 mg are used and so the current sample holder has a strong amorphous contribution. If the HMX is found to be amorphous by chemical analysis such as IR or Raman, the system in the overlapping area is a solubility zone were the cocrystal can not be obtained pure. If no HMX is found, the crystallisation of CL-20 and HMX occurs already before the overlap and almost all crystallised HMX is lost due to a flaw in the process itself (cyclone cut-off, crust on the nozzle, affinity with walls etc.). The overlap should also been monitored to quantify the percentage of droplet interpenetration.

4.3 Summary of the Chapter

The crystallisation is a multi-step process not yet fully understood; the critical initial stage –the nucleation– is still under investigation by the crystallisation community with recent advances completing further the Classical Nucleation Theory (CNT). Nevertheless, the supersaturation still plays a major role on the rate and trigger of nucleation. Without a determination of the droplets size and evaporation rate, this present study focused on solvent exchange.

The n-hexane is used as anti-solvent to raise the supersaturation. The system acetone/n-hexane forms an azeotrope with a lower boiling point which increases the superheating. However, while using different ratios at the same boiling point, increasing amounts of n-hexane reduced the final mean particle size: from around 800 nm with pure acetone to a plateau around 550 nm. When spraying the n-hexane from a second nozzle, particle size has been improved with a mean particle size of 580 nm.

To confirm that the droplets interpenetrate each other and hexane is not already gaseous thus drying acetone droplets, the cocrystal CL-20:HMX 2:1 is studied. Two solutions of acetone are prepared and sprayed separately; one with CL-20 and another with HMX. The cocrystallisation occurs confirming the overlap. Another similar experiment where CL-20 is dissolved into ethyl acetate supports that interpretation with again a cocrystallisation.

Phase Doppler Analysis (PDA) has been used for the first time for *in situ* measurement of a superheated fluid sprayed under vacuum. The SFE technology will be studied and on-line monitored; the data acquired from both PDA and Small-Angle X-ray Scattering (SAXS) will be computed to provide evaporation rate and crystallisation kinetics, introducing a breakthrough for theSFE technology.

Size reduction can also be achieved by controlling the nucleation and growth steps by adding agents which will change the supersaturation conditions locally

or will interact with the solute favourably or not. PolyVinylPyrrolidone (PVP) and PolyEthylene Glycol (PEG) are two very common polymers identified as food additives – E1201 and E1521 respectively – but also as crystallisation agents for many organic compounds. The new chapter explores the chemical approach for controlling crystallisation by SFE, with a focus on those two polymers, resulting in a new wide range of RDX size available.

Bibliography

1. Atwood, G. R., G. W. Becker, Richard C. Bennett, George Burnet, Howard M. Dess, Vladimiro Ern, Hugh M. Hulburt, H. J. Jensen, Stanley Katz, M. A. Larson, L. M. Litz, R. A. Mercuri, M. J. Murtha, A. D. Randolph, S. A. Ring, M. B. Sherwin, Reuel Shinnar, G. J. Sloan, Denis G. Stefango, Paul D. Stone, and Maarten Van Buren (1969). *Crystallization from solutions and melts*. Ed. by J. A. Palermo and M. A. Larson. Boston, MA: Springer US. ISBN: 978-1-4899-4817-5 978-1-4899-4815-1.
2. Bachdo, WD and MJ Houser (1984). "Development of the Phase/Doppler Spray Analyzer for Liquid Drop Size and Velocity Characterizations". In: Proc. AIAA/SAE/ASME 20th Joint Propulsion Conf. Cincinnaty. Ohio.
3. Bauckhage, Klaus and Hans-Herbert Flögel (1984). "Simultaneaous Measurements of Droplets Size and Velocity in Nozzle Sprays". In: Proc. 2nd Intern. Symp. Appl. Laser Anemometry to Fluid Mechanics. Lisbon.
4. Chadwick, Keith, Roger Davey, Ghazala Sadiq, Wendy Cross, and Robin Pritchard (2009). "The utility of a ternary phase diagram in the discovery of new co-crystal forms". In: *CrystEngComm* 11.3, pp. 412–414. ISSN: 1466-8033. DOI: 10.1039/B818268J.
5. Chiarella, Renato A., Roger J. Davey, and Matthew L. Peterson (2007). "Making Co-CrystalsThe Utility of Ternary Phase Diagrams". In: *Crystal Growth & Design* 7.7, pp. 1223–1226. ISSN: 1528-7483. DOI: 10.1021/cg070218y.
6. Cummins, H. Z., N. Knable, and Y. Yeh (1964). "Observation of diffusion broadening of Rayleigh scattered light". In: *Physical Review Letters* 12.6, p. 150.
7. De Yoreo, Jim (2013). "Crystal nucleation: More than one pathway". In: *Nature Materials* 12.4, pp. 284–285. ISSN: 1476-1122. DOI: 10.1038/nmat3604.
8. Essel, Jonathan T., Andrew C. Cortopassi, Kenneth K. Kuo, Christopher G. Leh, and James H. Adair (2012). "Formation and Characterization of Nano-sized RDX Particles Produced Using the RESS-AS Process". In: *Propellants, Explosives, Pyrotechnics* 37.6, pp. 699–706. ISSN: 07213115. DOI: 10.1002/prep.201100139.
9. Gallagher, Paula M., M. P. Coffey, V. J. Krukonis, and W. W. Hillstrom (1992). "Gas anti-solvent recrystallization of RDX: formation of ultra-fine particles of a difficult-to-comminute explosive". In: *The Journal of Supercritical Fluids* 5.2, pp. 130–142.
10. Gebauer, Denis, Matthias Kellermeier, Julian D. Gale, Lennart Bergström, and Helmut Cölfen (2014). "Pre-nucleation clusters as solute precursors in crystallisation". In: *Chemical Society Reviews* 43.7, pp. 2348–2371. ISSN: 1460-4744. DOI: 10.1039/C3CS60451A.

11. Gebauer, Jörn and Matthias Kind (2015). "Profiles of temperature, concentration and supersaturation within atomized droplets during flash-crystallization". In: *Chemical Engineering and Processing: Process Intensification* 91, pp. 130–140. ISSN: 02552701. DOI: 10.1016/j.cep.2015.03.012.

12. Lee, Jae-Eun, Jun-Woo Kim, Sang-Keun Han, Joo-Seung Chae, Keun-Deuk Lee, and Kee-Kahb Koo (2014). "Production of Submicrometer-Sized Hexahydro-1,3,5-trinitro-1,3,5-triazine by Drowning-Out". In: *Industrial & Engineering Chemistry Research* 53.12, pp. 4739–4747. ISSN: 0888-5885, 1520-5045. DOI: 10.1021/ie500221c.

13. "Method for producing cocrystals by means of flash evaporation" (2016). WO 2016001445. B. Risse and D. Spitzer. WO Patent App. PCT/EP2015/065,335.

14. Miyatake, O., T. Tomimura, Y. Ide, and T. Fujii (1981). "An experimental study of spray flash evaporation". In: *Desalination* 36.2, pp. 113–128. ISSN: 0011-9164. DOI: 10.1016/S0011-9164(00)88635-X.

15. Mullin, J. W. (2001). *Crystallization*. 4th ed. Oxford ; Boston: Butterworth-Heinemann. 594 pp. ISBN: 978-0-7506-4833-2.

16. Nehm, Sarah J., Barbara Rodríguez-Spong, and Naír Rodríguez-Hornedo (2006). "Phase Solubility Diagrams of Cocrystals Are Explained by Solubility Product and Solution Complexation". In: *Crystal Growth & Design* 6.2, pp. 592–600. ISSN: 1528-7483, 1528-7505. DOI: 10.1021/cg0503346.

17. Ostwald, W (1897). "Studien über die Bildung und Umwandlung fester Körper: Übersättigung und Überkaltung". In: *Zeitschrift für Physikalische Chemie* 22, pp. 289–330.

18. PANT, Arti, Amiya Kumar NANDI, Shireeshkumar Pralhad NEWALE, Vandana Prakash GAJBHIYE, Hima PRASANTH, and Raj Kishore PANDEY (2013). "Preparation and Characterization of Ultrafine RDX". In: *Central European Journal of Energetic Materials* 10.3, pp. 393–407.

19. Risse, Benedikt (2012). "Continuous crystallization of ultra-fine energetic particles by the Flash-Evaporation Process".

20. Saffman, M., P. Buchhave, and H. Tanger (1984). "Simultaneous measurement of size, concentration and velocity of spherical particles by a laser Doppler method". In: *Proc. 2nd Int. Symp. Laser Anemometry Fluid Mech., Lisbon, Portugal*. Lisbon: LADOAN.

21. Salvalaglio, Matteo, Marco Mazzotti, and Michele Parrinello (2015). "Urea homogeneous nucleation mechanism is solvent dependent". In: *Faraday Discussions* 179, pp. 291–307. ISSN: 1364-5498. DOI: 10.1039/C4FD00235K.

22. Salvalaglio, Matteo, Thomas Vetter, Federico Giberti, Marco Mazzotti, and Michele Parrinello (2012). "Uncovering Molecular Details of Urea Crystal Growth in the Presence of Additives". In: *Journal of the American Chemical Society* 134.41, pp. 17221–17233. ISSN: 0002-7863, 1520-5126. DOI: 10.1021/ja307408x.

23. Sosso, Gabriele C., Ji Chen, Stephen J. Cox, Martin Fitzner, Philipp Pedevilla, Andrea Zen, and Angelos Michaelides (2016). "Crystal Nucleation in Liquids: Open Questions and Future Challenges in Molecular Dynamics Simulations". In: *Chemical Reviews* 116.12, pp. 7078–7116. ISSN: 0009-2665, 1520-6890. DOI: 10.1021/acs.chemrev.5b00744.

24. Spitzer, D., B. Risse, F. Schnell, V. Pichot, M. Klaumünzer, and M. R. Schaefer (2014). "Continuous engineering of nano-cocrystals for medical and energetic applications". In: *Scientific Reports* 4. DOI: 10.1038/srep06575.

25. Sun, Changquan Calvin (2013). "Cocrystallization for successful drug delivery". In: *Expert Opinion on Drug Delivery* 10.2, pp. 201–213. ISSN: 1742-5247. DOI: 10.1517/17425247.2013.747508. pmid: 23256822.

26. Ten Wolde, Pieter Rein and Daan Frenkel (1999). "Homogeneous nucleation and the Ostwald step rule". In: *Physical Chemistry Chemical Physics* 1.9, pp. 2191–2196.

27. Toda, Fumio, Koichi Tanaka, Hisakazu Miyamoto, Hideko Koshima, Ikuko Miyahara, and Ken Hirotsu (1997). "Formation of racemic compound crystals by mixing of two enantiomericcrystals in the solid state. Liquid transport of molecules from crystalto crystal". In: *Journal of the Chemical Society, Perkin Transactions 2* 9, pp. 1877–1886.

28. Vekilov, Peter G. (2010a). "Nucleation". In: *Crystal Growth & Design* 10.12, pp. 5007–5019. ISSN: 1528-7483, 1528-7505. DOI: 10.1021/cg1011633.

29. — (2010b). "The two-step mechanism of nucleation of crystals in solution". In: *Nanoscale* 2.11, pp. 2346–2357. ISSN: 2040-3372. DOI: 10.1039/C0NR00628A.

30. Vishweshwar, Peddy, Jennifer A. McMahon, Joanna A. Bis, and Michael J. Zaworotko (2006). "Pharmaceutical co-crystals". In: *Journal of Pharmaceutical Sciences* 95.3, pp. 499–516. ISSN: 1520-6017. DOI: 10.1002/jps.20578.

31. Yu, Zai Qun, Pui Shan Chow, and Reginald B. H. Tan (2010). "Operating Regions in Cooling Cocrystallization of Caffeine and Glutaric Acid in Acetonitrile". In: *Crystal Growth & Design* 10.5, pp. 2382–2387. ISSN: 1528-7483. DOI: 10.1021/cg100198u.

32. Zahn, Dirk (2015). "Thermodynamics and Kinetics of Prenucleation Clusters, Classical and Non-Classical Nucleation". In: *ChemPhysChem* 16.10, pp. 2069–2075. ISSN: 1439-7641. DOI: 10.1002/cphc.201500231.

Chapter 5

Tunable continuous production of RDX from microns to nanoscale using polymeric additives

The specificity of the SFE process arises from the intracity of many physicochemical phenomena that occur with the spray of superheated and supersaturated solutions. The whole system needs to be resolved in space and time as illustrated in Figure 5.1. Crystallisation itself happens in successive steps, namely primary nucleation, crystal growth and secondary nucleation. The complexity of the flashing behaviour is increased by the lack of both theoretical and empirical bases on flashing droplets. In order to dissociate those dynamic events, one crystallisation step over the others can be promoted by the use of additives; nucleation and growth can be inhibited or favoured selectively by polymers. PolyVinylPyrrolidone (PVP) and PolyEthylene Glycol (PEG) are two very common polymers identified as food additives – E1201 and E1521 respectively – but also as crystallisation tools. Kim et al. (2013, 2011) and Lee et al. (2014) clearly identified the PVP as a both growth and nucleation inhibitor of RDX in acetone, although only an alteration of the particles morphology was measured without any reduction of the size under electrospray. McPherson and Cudney (McPherson et al. 2006) proved the great effectiveness of PEG for triggering proteins precipitation, notably by steric exclusion as shown by Bhat and Timasheff (Bhat et al. 1992). By the addition of PVP, a delay of the crystallisation at higher supersaturation degree is expected, thus triggering an homogeneous nucleation with a higher density of nuclei. However in those conditions, aggregation or coalescence of nuclei may occur leading respectively to bigger polycrystalline particles or to bigger single crystals. The PEG would increase the supersaturation too, but with a different mechanism than PVP; PVP trends to adsorb on crystal surfaces thus inhibiting the nucleation and growth,

whereas PEG acts as nucleation promoter due to its steric effect.

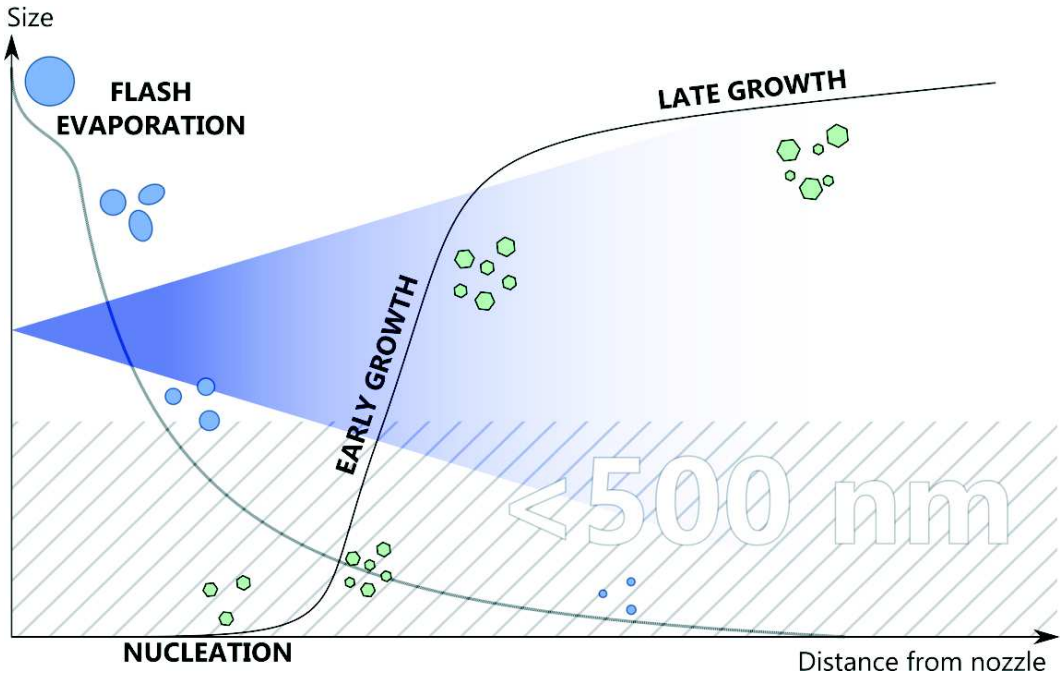

Figure 5.1 – Evaporation and crystallisation phenomena throughout the SFE process. The 500 nm limit displayed is roughly the detection limit for Phase Doppler Particle Analyzers, which allows in situ size and velocity measurements on both liquid and solid particles.

5.1 Material & Methods

As mentioned in Chapter 1, the RDX is provided by Eurenco, labelled as M5 and used as is, without further purification; the mean size is 6.8 µm. Standard PVP with an average molar weight around 40.000 mol/g and PEG 400 mol/g (liquid) are purchased from Sigma Aldrich.

RDX and the polymers when needed are dissolved in acetone by stirring one minute and then an ultrasonic bath of ten seconds achieved the dissolution. The concentration of RDX is kept constant at 2 wt% in acetone and weighted percentages of polymer are per gram of RDX.

The operating conditions of the SFE are 40 bar of inlet pressure and 160 °C at a hollow cone nozzle with an orifice diameter of 60 µm.

5.2 Results & Discussion

5.2.1 Quantification by NMR Spectroscopy

The quantification of the amount of polymer in the final RDX products is the preliminary step before further characterizations and interpretation. NRM-H were conducted in cooperation with our colleagues from the ISL specialized in analytical chemistry. The robustness and accuracy of the build-in quantification integrated in the software is first tested. A well-known lot of RDX is chosen as a standard sample, then a mass gradation is performed in two different solvents, acetonitrile and DMSO at 35 °C to ensure complete dissolution. The linear regressions shown in Figure 5.2 are acceptable . DMSO is also the most suitable solvent.

Subsequently, RDX samples processed with polymer are analysed by NRM-H and the RDX peak integrated. The value for 100 wt% of RDX is taken from a pure SFE-processed RDX sample. The final results are shown in Table 5.1. All values are close to the initial amount of RDX. However, two trends can be clearly highlighted when calculating the difference between theoretical and experimental amounts. For the samples processed with PVP, when the amount of RDX increases, the final product contains more PVP than initially; on the contrary less PEG is found when increasing the RDX content. Due to the NMR accuracy and the percentages involved, those trends should be confirmed, at least some values, by using another analytical method such as HPLC before any interpretation.Nevertheless, final and initial ratio of RDX/polymer are similar.

theoretical wt% of RDX	90.91	95.24	99.01	99.50
mean calculated value from NMR	90.9	94.5	98.0	96.8
difference	0.0	-0.7	-1.0	-2.7

(a) RDX processed with PVP.

theoretical wt% of RDX	90.91	99.01	99.90
mean calculated value from NMR	88.6	98.5	99.9
difference	-2.3	-0.5	0.0

(b) RDX processed with PEG.

Table 5.1 – Mass percentage of RDX in the final products compared to the initial loading.

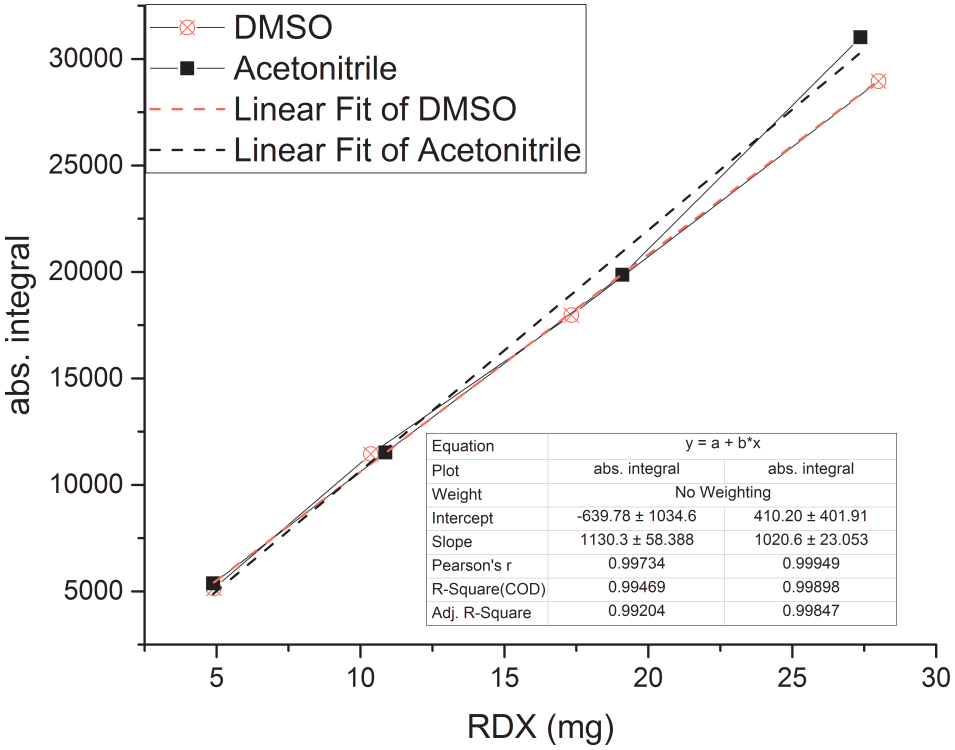

(a) Absolute integral in arbitray units plotted against the RDX mass.

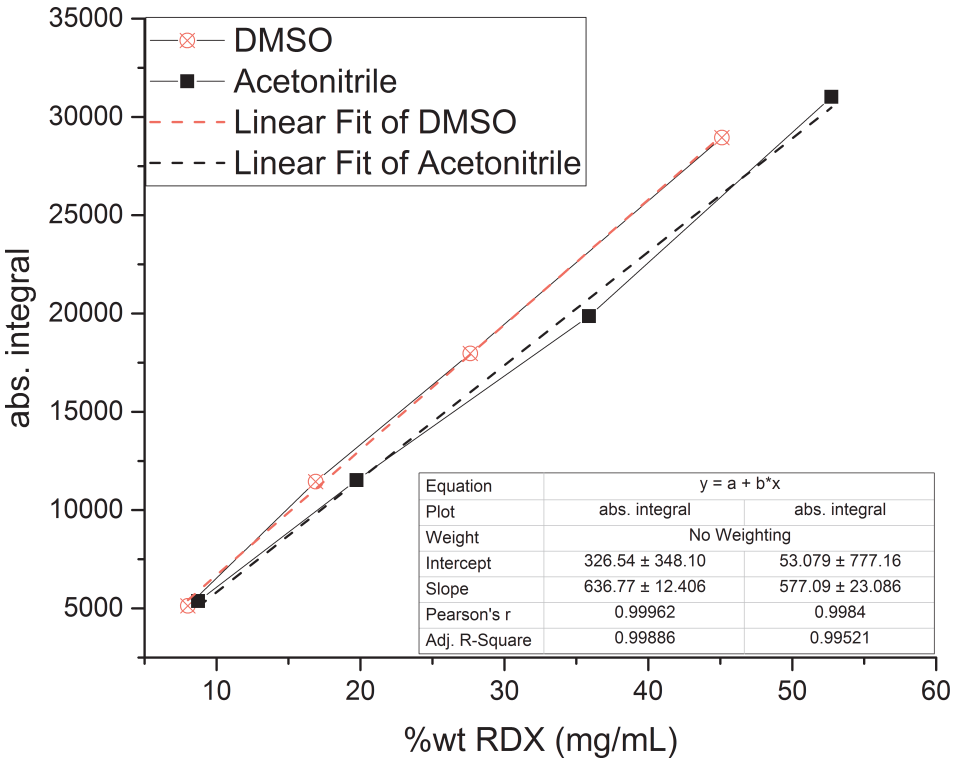

(b) Absolute integral in arbitray units plotted against the RDX concentration.

Figure 5.2 – Test of the reliability of quantification byNMR.

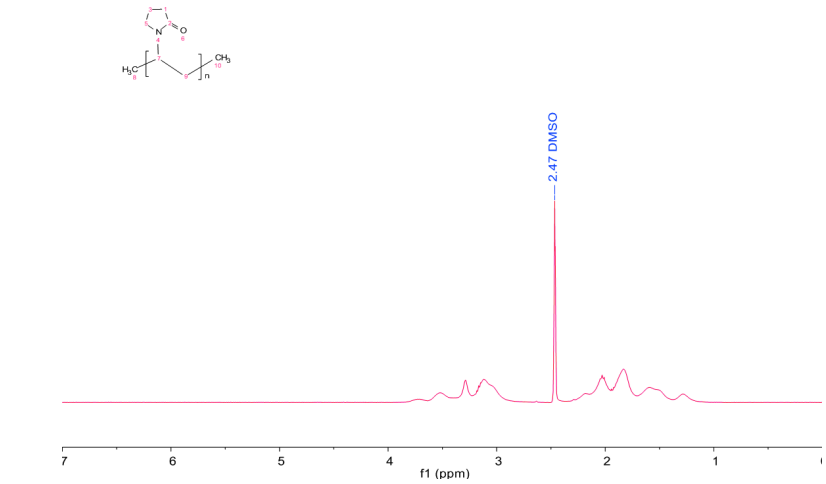

(a) PVP 40K.

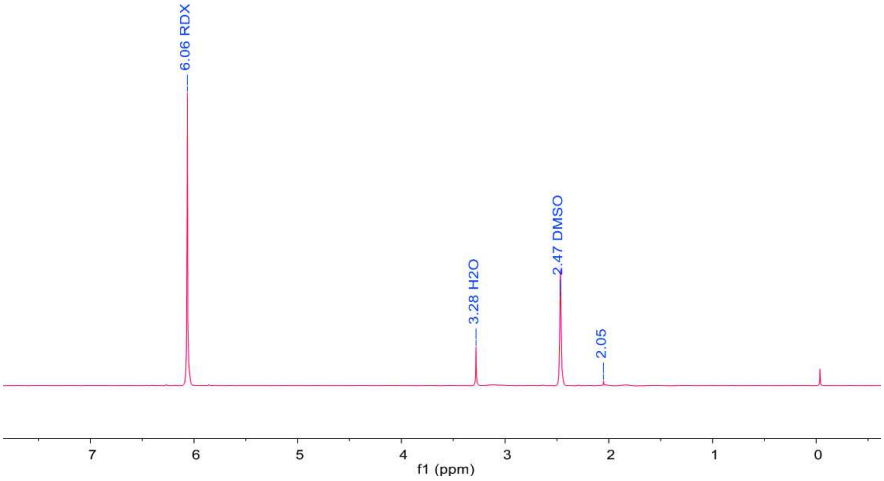

(b) RDX processed with 10 wt% PVP 40K.

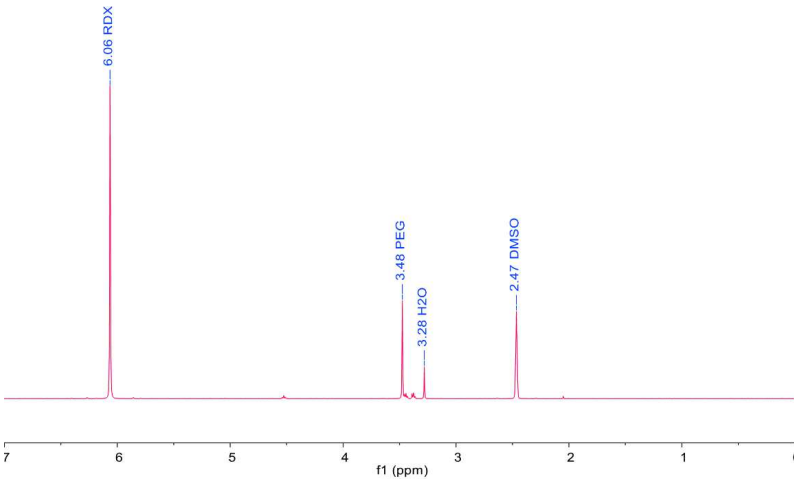

(c) RDX processed with 10 wt% PEG 400

Figure 5.3 – NMR-H spectra of various representative samples

5.2.2 RDX processed with PEG 400

5.2.2.1 Particle Size and Morphology

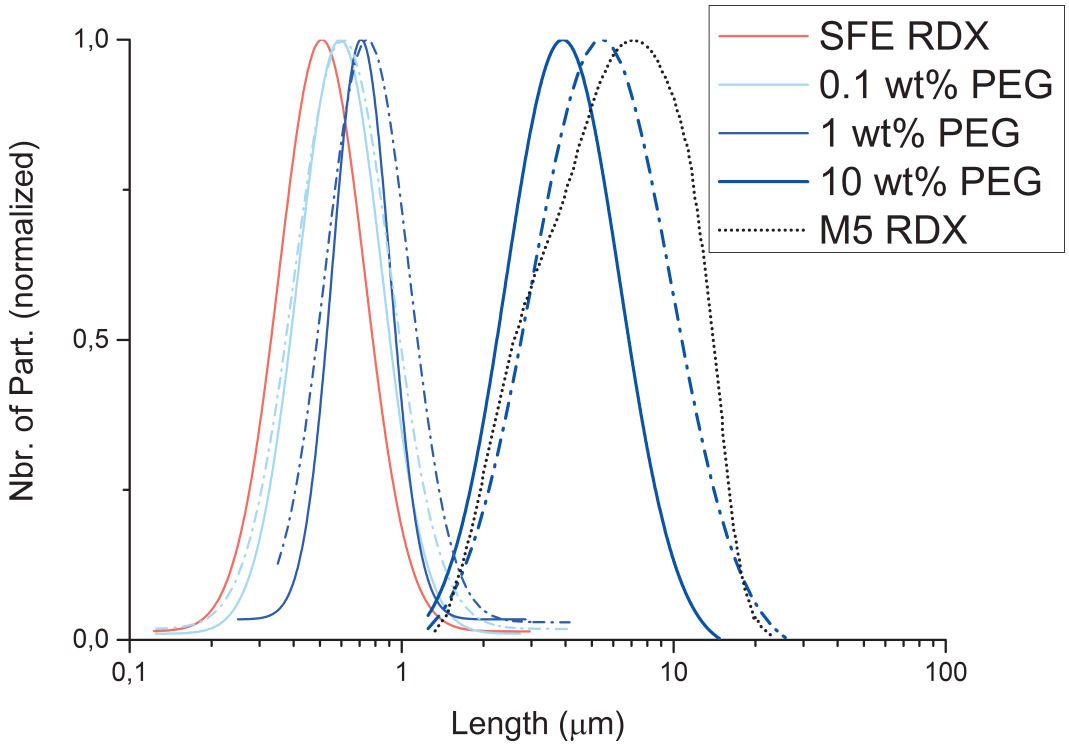

Figure 5.4 – Sizes – using a logarithmic scale – of samples processed with PEG measured from SEM micrographs; solid lines represent the smallest lengths and the dotted lines the largest. Pure RDX processed by SFE and raw M5 RDX added here for comparison.

Originally pure RDX processed by SFE can be obtained with a mean size in the range of 400 nm–900 nm depending on the conditions; with the parameters chosen for that study, the mean size would be around 500 nm (Doctoral Thesis Risse 2012). Starting with only 0.1 wt% of PEG per gram of RDX, the mean particle size increases to 670(0.356) nm. Then the mean size still increases to 750(0.244) nm with 1 wt% and reaches 4.9(0.482) µm with 10 wt%. The elongation of the particles while increasing PEG content can be clearly seen from Figure 5.4 but also when defining a roundness factor or aspect ratio by dividing the smallest length by the largest one. That width-to-length ratio is 0.94 at 0.11 wt%, 0.89 at 1 wt% and only 0.64 at 10 wt%, indicating a preferential growth in one direction.

Due to a high solubility in acetone, PEG rapidly increases supersaturation in droplets at the very beginning of the atomization and, considering its influence on particle size, the supersaturation is far from the optimal value where the

nucleation rate is maximal. Vekilov (2010) proposed an explanation of why, while the nucleation rate should be increasing exponentially with the degree of supersaturation, experiments at high supersaturations clearly show unpredictable rate of nucleation; according to the two-step mechanism, the crystalline nucleus appears inside metastable clusters of several hundred nanometres. Those clusters of dense liquid which are suspended in the solution can be favoured by the steric effect of PEG and the rapidly increasing saturation due to the flashing behaviour of droplets. Therefore, the induction time of nuclei is reduced and the nucleation rate low thus allowing the formation of bigger particles. Further characterizations involving Phase Doppler Anemometry has to be conducted to kinetically discriminate the role of PEG in the SFE process. As shown in Figure 5.1, the crystallisation of RDX with PEG would allow the particle size to exceed 500 nm; kinetic growth from the apparatus detection limit to the final particle size could be established.

Although PEG is liquid at ambient temperature, no significant change of aspect between all the final nano powders of RDX processed either pure or with an additive can be noticed. The samples processed with 10 wt% of PEG are less electrostatic and slightly yellowish.

5.2.2.2 X-Ray Difraction (XRD)

The XRD patterns in Figure 5.6 exhibit a slight different texture when micron-size RDX samples at 10 wt% of PEG are compared with others. From SEM pictures, morphology and PSD indicates a preferentially oriented growth ; the relative differences of intensity in XRD clearly shows that the face {311} is much more prominent whereas others like {111}, {002}, {102}, {020} and {021} are hindered. Those results are in contradiction with predicted and effective morphologies resulting for RDX growth in acetone; Shim and Koo (Shim et al. 2014) successfully predicted the crystal growth habit of RDX in acetone by the spiral growth model and Chen et al. (2015) went further using molecular dynamic simulations. They explained the increased growth rate of the polar faces {111}, {200}, {020} and {021} compared to the non-polar face {002} in polar solvents like acetone. From our experiment, the use of the chemical affinity of faces toward the solvent does not apply when processed by SFE with PEG ; the 311 face illustrated in Figure 5.7 exhibits both methylene and nitro group at the surface, and the non-polar {002} peak is also decreased as well as the polar faces while adding PEG, a relatively non polar molecule. A small templating effect involving a preferential organization of PEG at higher concentration could explain those differences.

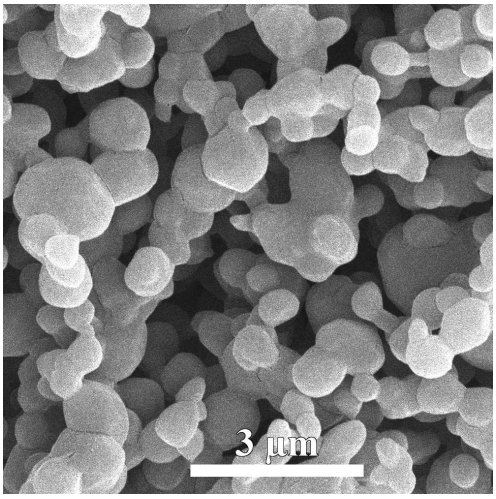

(a) SFE RDX

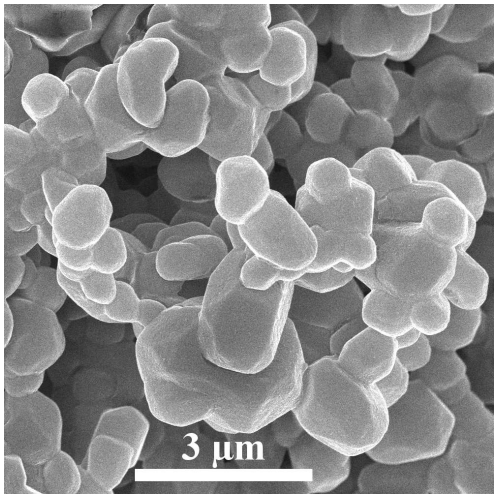

(b) RDX processed with 1 wt% PEG

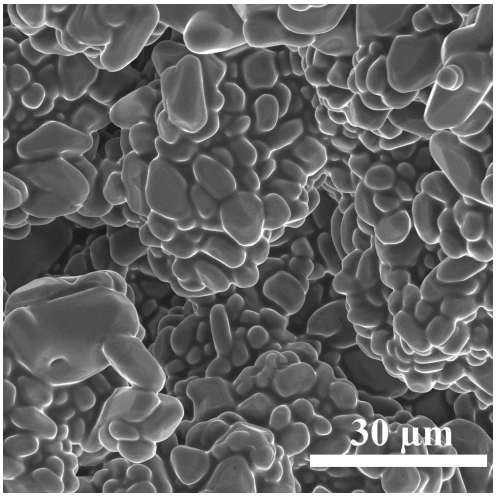

(c) RDX processed with 10 wt% PEG

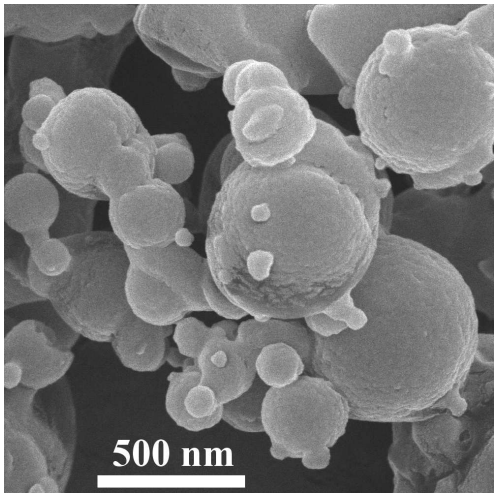

(d) RDX processed with 5 wt% PVP

Figure 5.5 – SEM micrographes of RDX samples processed by SFE in the same operating conditions.

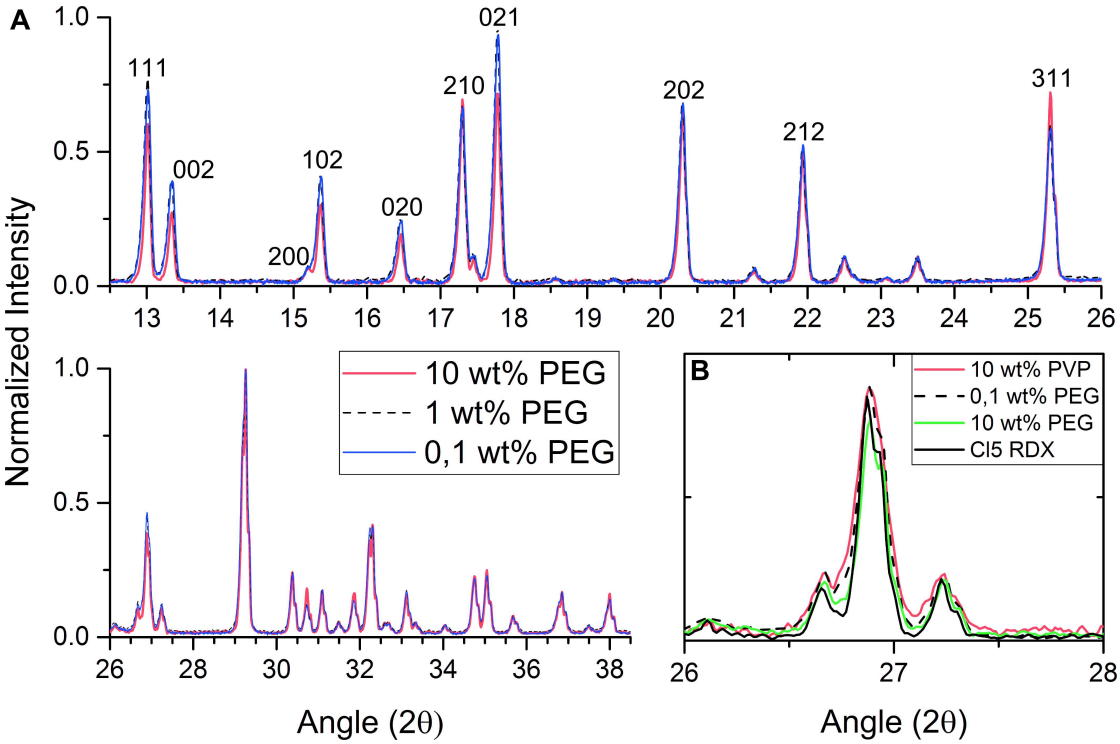

Figure 5.6 – (A) XRD patterns of RDX PEG-processed samples; only isolated peaks of major interest have been indexed for clarity. (B) inset of XRD patterns illustrating the broadening of peaks.

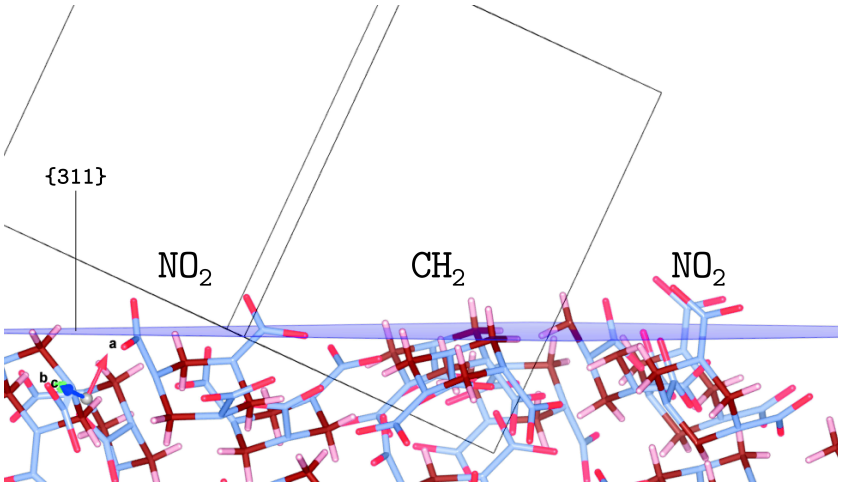

Figure 5.7 – View of the 311 plane (in violet, almost perpendicular to the plane of the drawing) and RDX molecules on the surface: both nitro and methylene group are located at the surface (on the background, the unit cell).

5.2.2.3 Thermal Analysis

The DSC results in Figure 5.8 show that the RDX processed by SFE is thermally less stable than the raw micron-size RDX, due to a higher ratio surface/volume for submicron size particles. Those results are in accordance with the work of Rosa et al. (2014) where micron size organic particles show also a similar slight melting depression. From 200 to 20 µm, they noticed a drop of 0.8 °; from 7 µm to 500 nm, the melting point of pure RDX decreases of 1.2 °. Although that ratio is decreasing while adding PEG, DSC curves in Figure 5.8 show that the content of PEG itself decreases the activation energies for melting and decomposition: the temperatures – merged in Table 5.2 – are all decreasing. The PEG 400 melts at 3 °C (peak minimum) and starts to decompose after 300 °C (data not shown). The broadening of peaks and decrease of melting temperature is a well-known trend for impure organic particles: the gain of entropy by the creation of a bi component melt drives the melting. This phenomenon appears also in PBX like formex-bonded explosives where BCHMX/Formex melts 5 °C lower (Yan et al. 2012).

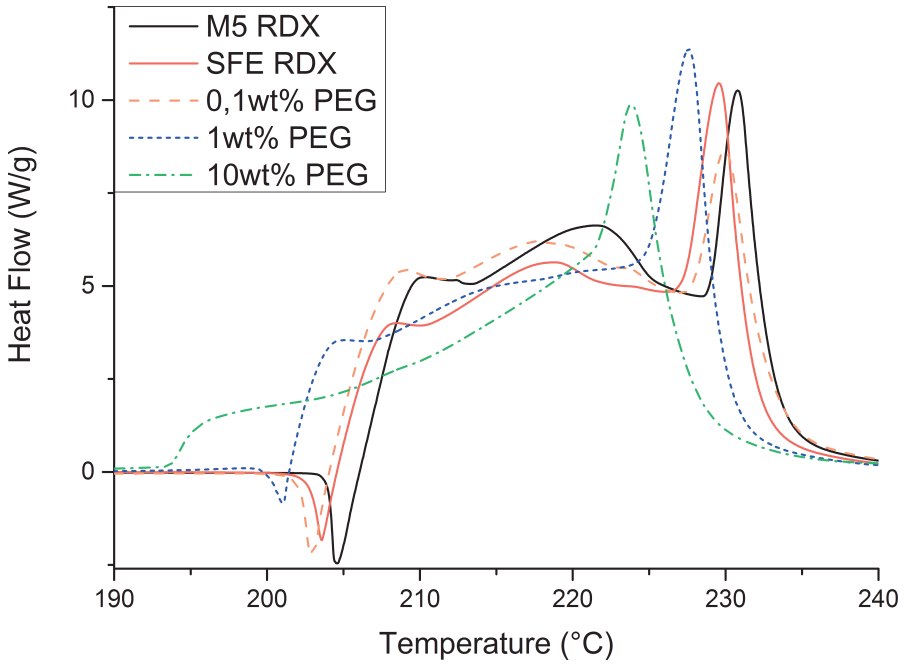

Figure 5.8 – DSC analysis of RDX samples processed with different wt% of PEG.

	$T_{e\ endo}$	$T_{e\ exo}$	$T_{p\ exo}$	$T_{c\ exo}$	$E\ (J/g)$
M5 RDX	204,0	206,1	230,8	233,6	4550
SFE RDX	202,8	204,6	229,6	232,1	4210
0.1 %PEG	202,1	204,1	230,0	233,2	4710
1 % PEG	200,0	201,4	227,6	230,0	4530
10 % PEG	n/a	193,4	223,8	227,7	4010
0.5 % PVP	202,2	204,3	229,3	231,7	4120
1 % PVP	201,7	203,6	228,9	232,4	4190
5 %PVP	197,1	199,1	226,0	229,4	2990
10 % PVP	n/a	n/a	223,5	227,4	3090

Table 5.2 – Melting (endo) and decomposition (exo) temperatures in ℃ and decomposition energy in J/g for all samples (Te extrapolated peak onset, Tp peak maximum temperature, Tc extrapolated peak offset). See Material & Methods section for more details.

5.2.2.4 Infrared (IR) Spectroscopy

In Figure 5.9, the mid-infrared spectra both 0.1 wt% and 10 wt% samples are compared to the raw PEG 400 used, and to pure RDX. The three main specific vibrations of PEG at 1000 cm^{-1}–1200 cm^{-1}, at 2800 cm^{-1}–3000 cm^{-1} and at 3200 cm^{-1}–3600 cm^{-1} are broad absorption bands which can be clearly distinguished from RDX spectra; the 10 wt% sample exhibit those bands, but samples with lower amount such as the 0.1 wt% one are almost identical to the RDX one. The RDX characteristic bands at 3065 and 3075 cm^{-1} correspond to C-H stretching aromatic vibrations while 1590 cm−1, 1570 cm−1 and 1270 cm−1 are assigned to stretching of NO_2. A slight shift of 2 cm−1 to lower wavenumber of all bands from 500 cm−1 to 1650 cm−1 can be noticed only for the sample with the higher amount of PEG; since that region regroups both nitroamines and ring vibrations it seems more appropriate to consider that shift as negligible or at least not due to a specific interaction between the polymer and RDX.

5.2.3 RDX processed with PVP 40K

5.2.3.1 Particle Size and Morphology

The processing of RDX with PVP 40K dramatically changes the particles size and morphology as it can be clearly seen when comparing side by side the Figures 5.5a and 5.5d. The PSD of samples processed with PVP in Figure 5.10

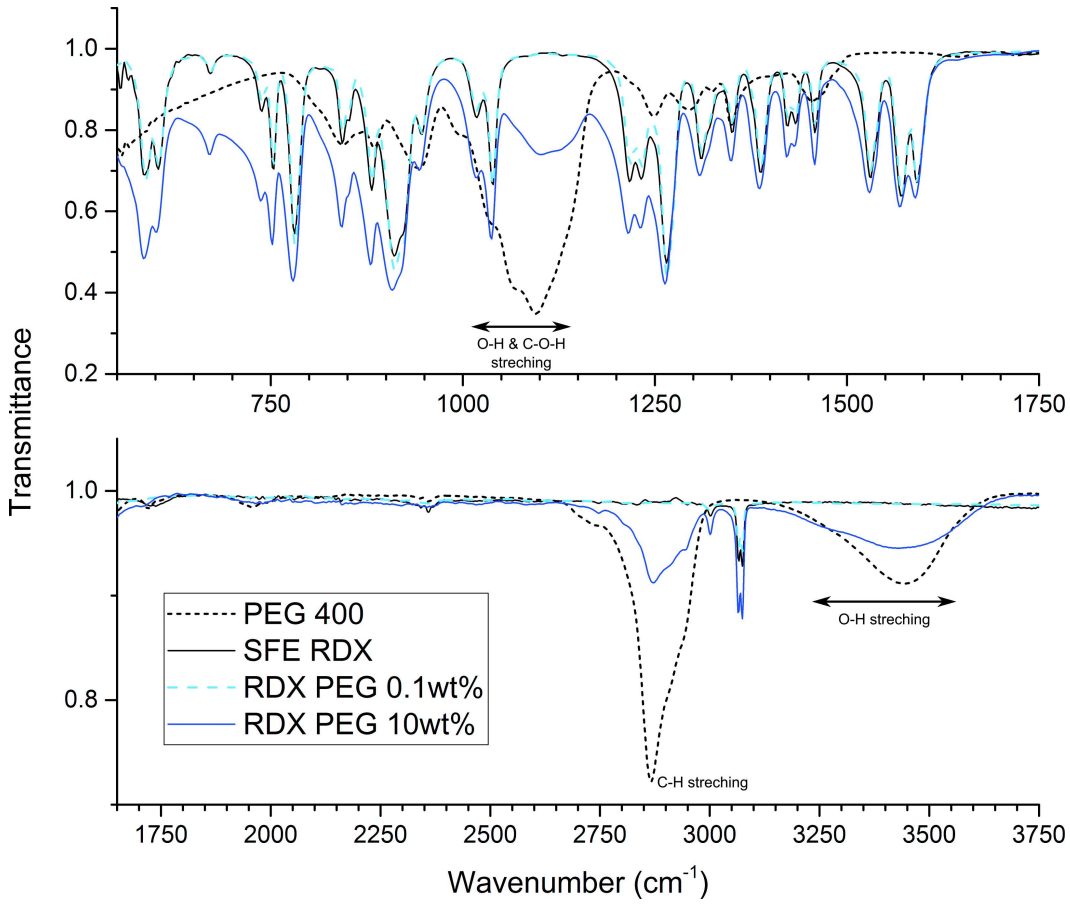

Figure 5.9 – FTIR spectra of two relevant RDX samples processed with PEG, compared to raw PEG 400 and pure RDX processed by SFE. (Socrates et al. 2001)

show a stabilized mean size around 160 nm with at least 5 wt% of PVP. At 1 wt%, the mean particle size is slightly higher at 180 nm and with a little more scattering: the multiplicative standard deviation increases from 0.843 for 5 wt% to 0.926 can be visualized from the dotted cumulative count curve in Figure 5.10.

It is very interesting to notice that only 0.05 wt% of PVP decreases the size by 34 % , from around 500 nm for pure RDX to 320 nm, and improves the spheric shape in a significant way. No preferential growth has been noticed and XRD (not shown here) confirms by identical intensity ratios within the micron-size raw RDX.

As previously mentioned Kim et al. studied the effect of additives on RDX crystallisation by electrospray and drowning-out and pointed out the role of PVP as nucleation inhibitor and growth inhibitor in acetone. The growth inhibition by PVP was only recently evidenced in their experiments of drowning-out where

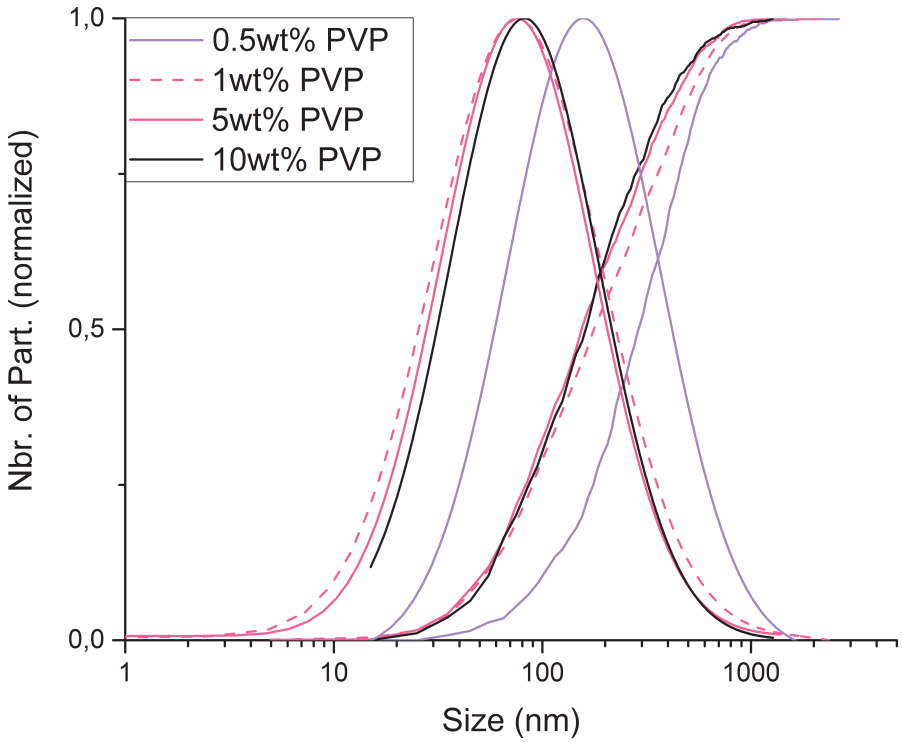

Figure 5.10 – Particle size distribution and cumulative counts – using a logarithmic scale – of samples processed with PVP measured from SEM micrographs.

RDX/acetone is sprayed into water, but not in the case of the electrospray; the difference can lye in longer times of flight in air and life in water of droplets in drowning-out and thus implies a more significant impact of the PVP on crystal growth. In contrast, the SFE process has a much higher mean evaporation rate and a two-step evaporation mechanism. Prior to the flash, the PVP inhibits the crystallisation of RDX until the flash of the droplet or delay the nucleation just before the flash. Then the sudden rise of saturation triggers the nucleation if not already, and implies a high crystal growth rate hindered again by the adsorption of PVP.

The size reaching a minimum at 1 wt% is certainly due to the mechanism of adsorption of the PVP. PVP possesses hydrophilic polar groups, that will interact preferentially on the crystal by chemical adsorption, thus slowing down crystal growth. The minima is then attained for a maximal surface coverage. Moreover, Patel et al. (2015) found out that the growth inhibition of PVP increased with the supersaturation of indomethacin in water. With the droplet fission, that trend is an additive phenomenon explaining the smaller size of RDX processed by SFE with PVP when compared to Kim's results.

In order to confirm the important role of the PVP, one small set of experiments

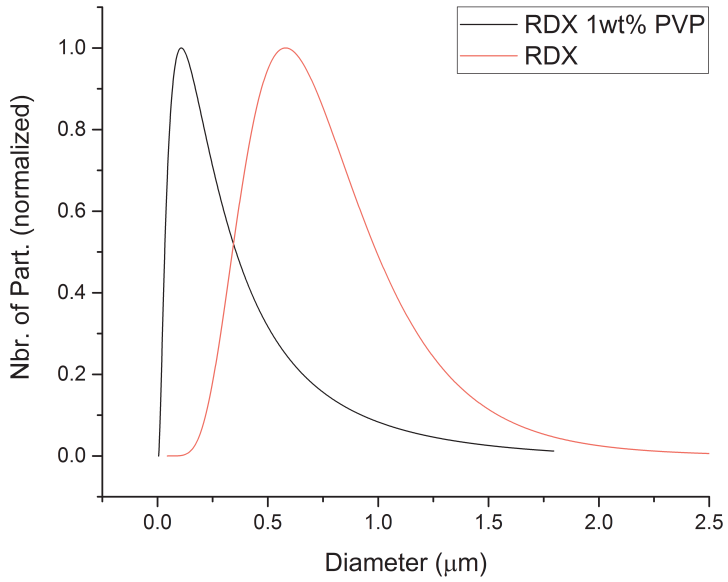

Figure 5.11 – Particle size distribution of RDX processed with a 80 µm nozzle at only 20 bar.

was conducted with a 80 µm nozzle at only 20 bar. From an industrial point of view, a higher mass flow at lowest pressure is a significant advantage; instead of a yield between 2 and 3 g/h for a 60 µm nozzle at 40 bar, RDX were recovered at a rate of 5-8g/h. However, as evidenced by Risse (Doctoral Thesis 2012), bigger particles are produced in those conditions; with only 1 wt% of PVP, the particle size decreases from 714(0.020) nm to 307(0.027) nm and again improves the sphericity. The increase of the particle size at higher flow rates can be counteracted y the addition of PVP, thus allowing both high production rate and small PSD.

5.2.3.2 Thermal Analysis

Figure 5.12 reveals that onset temperatures and temperatures at maximum decrease when adding PVP, following the same trend as the RDX samples processed with PEG. As we already discussed, a melting point depression for organic crystal can occur thanks to a decreasing particle size even above 500 nm and can be thermodynamically favoured: PVP-processed samples have a volumetric mean size well below 500 nm and the transition from a soluble solid formed by RDX and PVP to a liquid miscible solution is favourable. Moreover

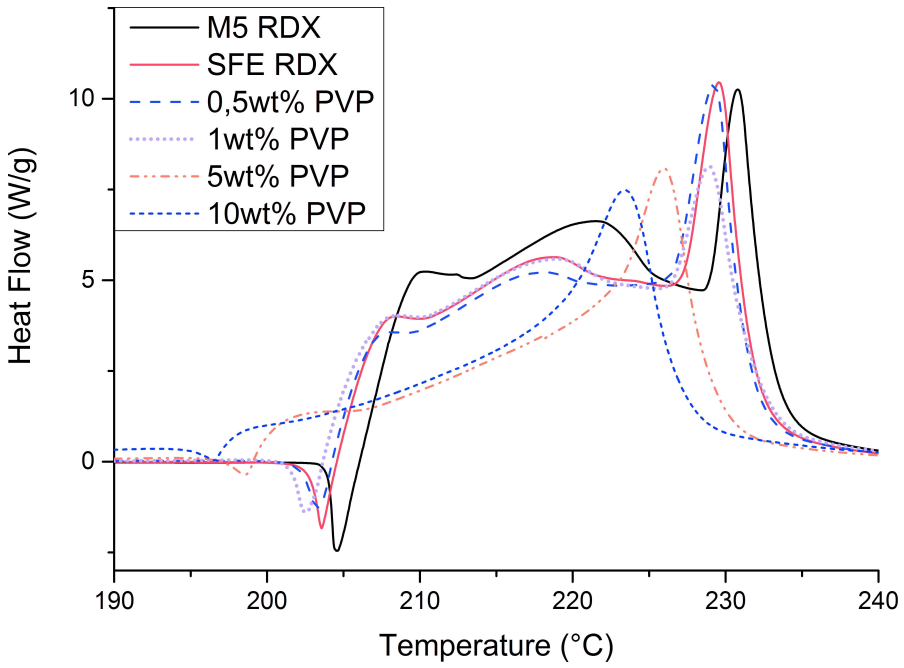

Figure 5.12 – DSC analysis of RDX samples processed with different wt% of PVP.

since PVP 40K has a glass transition temperature around 150-175 °C, solid PVP inclusion in the crystal lattice of RDX may also increase the internal energy. In case of crystal defects, micro-strain can be identified by XRD from peak broadening. Williamson Hall plotting has been found not to be a suitable model therefore a more reliable and calibrated method was required. details were given in Section 3.2.1.1; the Rietveld refinements then performed revealed an apparent volume weighted domain size always around 85±10 nm and an average maximum strain around 10±5 10^{-4} % for both pure and PVP processed samples. So it is very likely that only the effect of size and the presence of PVP are driving the melting point depression here.

5.2.3.3 IR Spectroscopy

In Figure 5.13, the mid-infrared spectrum of a 10 wt% sample is compared to the raw PVP 40K used, and to pure RDX. The two main specific vibrations of PVP around 1660 cm^{-1} and at 2850 cm^{-1}–2950 cm^{-1} (CH stretching) are broad absorption bands which can be clearly distinguished from RDX spectra. The absorption at 3200 cm^{-1}–3600 cm^{-1} is the vibration of water, the PVP being very hygroscopic. Only the 10 wt% samples exhibit a small broad peak around 1660 cm^{-1} from PVP.

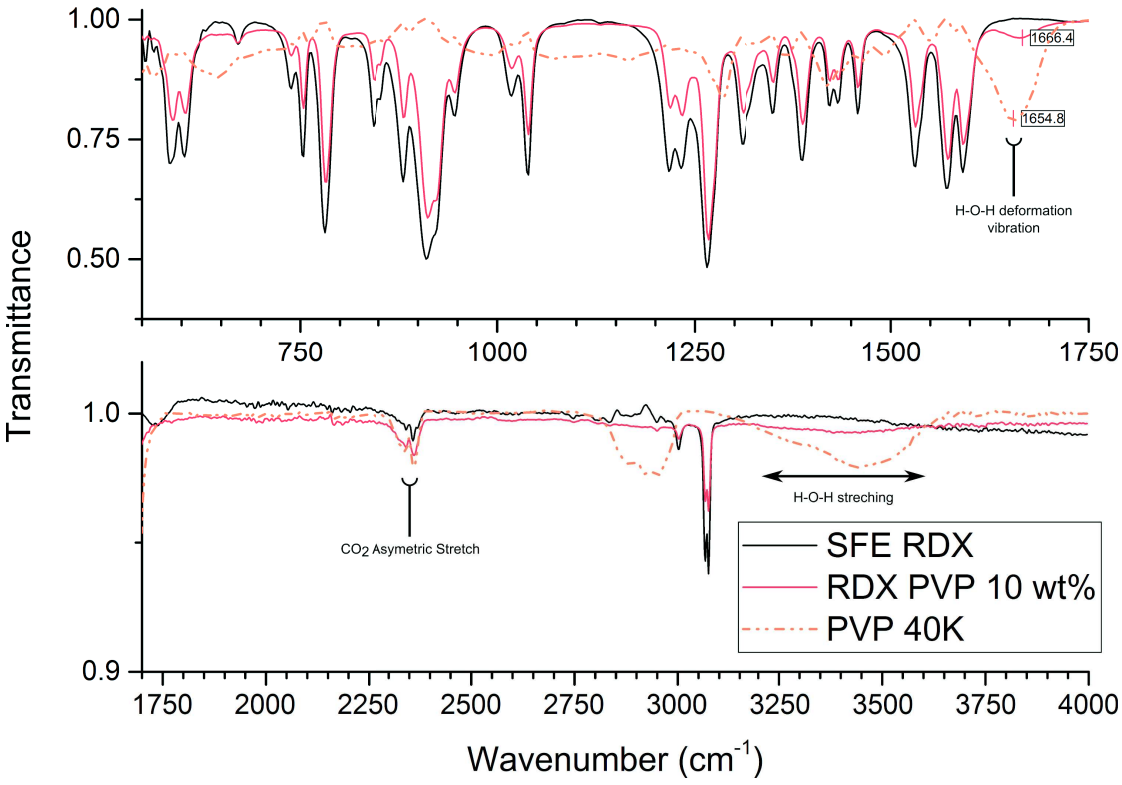

Figure 5.13 – FTIR spectra of the RDX samples processed with 10 wt% of PVP, compared to raw PVP 40K and pure RDX processed by SFE.

5.2.4 Sensitivity

In general, samples of nano-RDX have lower sensitivities with the addition of polymers as shown in the Figure 5.14. Due to the reliability issues raised by the submicrometer scale of the powders tested on macro or micron scale apparatus (Radacsi et al. 2013) and the inherent scattering of the results (Brown et al. 2015), the differences of one level higher or lower has to be moderated.

The threshold at the electrostatic discharge test is increased for all SFE processed RDX, and even further when adding at least 5 wt% of PVP (+300 % then +700 % compared to M5 RDX) or 10 wt% of PEG (+1160 % compared to M5 RDX).

The addition of at least 1 wt% of PVP or PEG desensitizes the RDX toward friction, up to +57.5 %. Taking into account the previously mentioned dispersions of sensitivity values, the slight decreased value for friction at 10 wt% for both polymers can be not significant enough, due to the inability of the apparatus to process more plasticized compositions or due to the lower thermal stability.

The micron size RDX with 10 wt% of PEG is twice insensitive at the impact

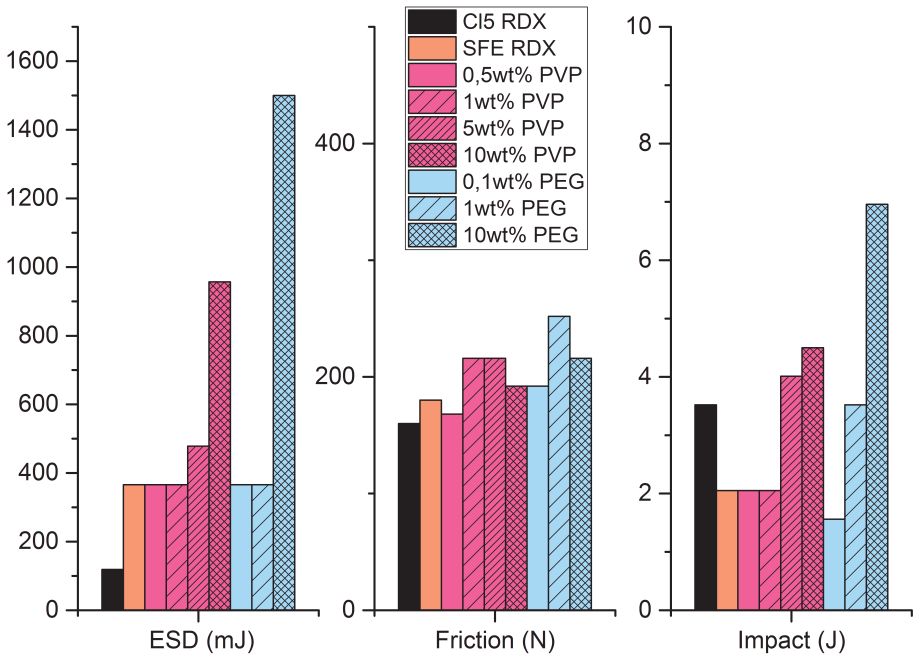

Figure 5.14 – Sensitivities of RDX processed with PVP and PEG compared with pure nano-RDX and the raw micron size RDX.

Sample	Impact test (J)	Friction (N)	ESD (mJ)
M5 RDX	3.52	160	119
SFE RDX	2.05	180	359
0.1 wt.%	1.56	192	366
1 wt.%	3.52	252	366
10 wt.%	6.96	216	1.5 J

Table 5.3 – Sensitivities of the RDX processed with PEG, compared with pure nano-RDX and the raw micron size RDX.

test than pure nano or micron size RDX; despite a morphology trending to be needle-like when adding PEG and so being more likely sensitive to impact as Chen et al. (2012) demonstrated, the sensitivity decreases due to the polymeric content and the size range.

With the exception of 10 wt% PVP samples, no loss of reactivity has been noticed during the sensitivity tests, the material has the same response as the pure nano and the raw micron size RDX. An explosion at the impact or discharge can be clearly heard with no residue left, and the friction produces an audible crackling with matter ejection; only the 10 wt% PVP samples exhibit a lower reactivity at impact with more residue left and the threshold value reported for impact corresponds to a partial ignition (at the interstice between the steel ring and the steel cylinder, therefore suggesting an ignition by friction).

5.2.5 Comparison with mechanically mixed samples

Mechanical mixes with 10 wt% of PVP or PEG and nano or the raw micron-sized M5 RDX were done: DSC results can be seen in Figure 5.15. Figure 5.15a illustrates effect of the size since the decomposition peak of the 10wt% sample (5 µm) is between the nano (500 nm) and micron (7 µm) size pure RDX, while the fusion starts at lower temperature. That's the same phenomenon for the 0.1wt% sample comparable to pure nano and micron size pure RDX. For the PVP mixes in Figure 5.15b, the comparison between the 10wt% sample, the n-mix and the µ-mix ask the question of the distribution of polymer across the sample. We will focus on the distribution of polymer in another study when theTip Enhanced Raman Spectroscopy (TERS) apparatus will be available.

Sensitivity tests were conducted with those mechanic mixes: the n-mix of 10 wt% PEG is very insensitive (it did not react at 37 J) while the impact sensitivity of the n-mix of 10 wt% PVP is higher. So in the first case the humidification and coating by the liquid PEG could totally inhibit RDX, and in the second one, the issue comes from the difficult homogenisation of a micron size solid PVP with submicron RDX. This increases the need of a TERS apparatus to have much more reliable and precise interpretation.

5.3 Summary of the Chapter

The great versatility of the Spray Flash Evaporation allows the processing of solid (PVP 40K) and liquid (PEG 400) polymers to tune the particle size distribution of the final dried nano, submicron or micron-sized powder. PEG triggers the early nucleation of RDX with low nucleation rate leading to bigger particles up to 5 µm. PVP acts as a nucleation inhibitor and a growth inhibitor:

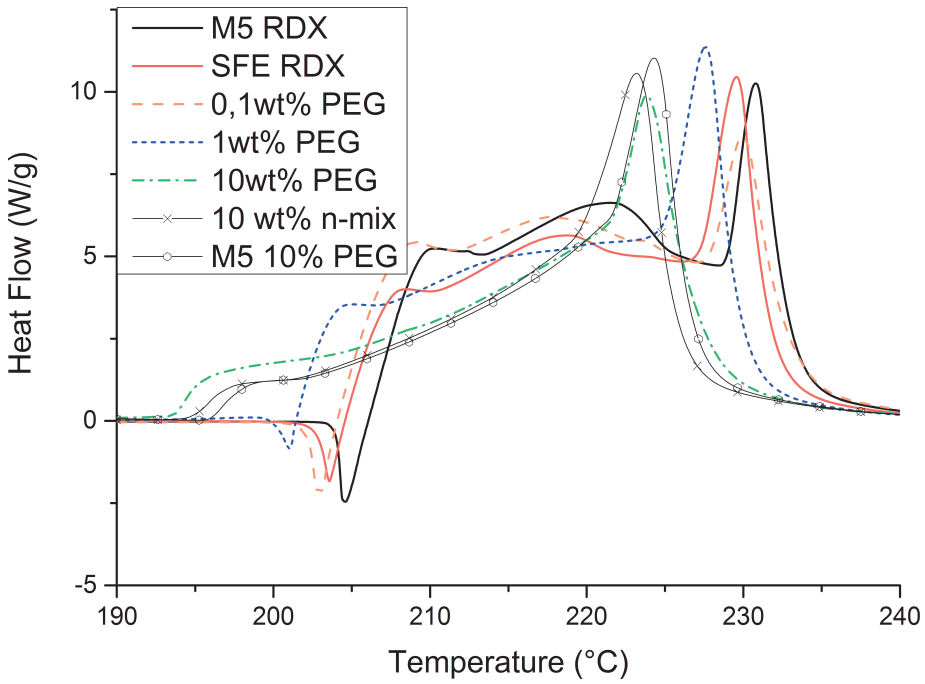

(a) RDX processed with PEG

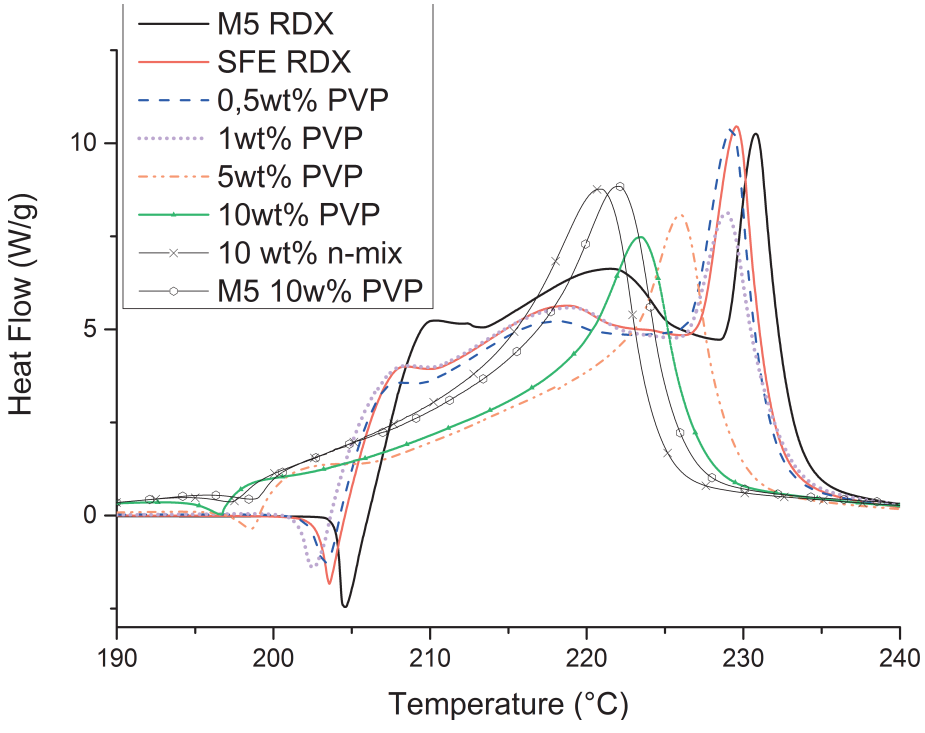

(b) RDX processed with PVP

Figure 5.15 – DSC analysis of RDX samples processed with PVP and PEG: comparison of mechanical mixes with 10 wt% of PVP or PEG.

RDX nuclei are formed in less volume available due to the fission and flashing of droplets, and then the crystal growth is slowed, thus allowing the formation of much smaller particles at 160 nm with a spherical shape. The addition of PEG could have increased supersaturation to trigger nucleation at a maximal rate but our results show that the contribution of both the evaporation behaviour and the nucleation inhibition is more effective and probably the safest choice to reduce and stabilize the particle size and morphology.

Despite a lower thermal stability, the synthesized RDX composites exhibit reduced sensitivities in electrostatic discharge, friction and impact without loss of reactivity and are less prone to Ostwald ripening. The present work is a great advance in the processability of composite and organic compounds by the SFE technology. The sample synthesized here are also promising for the control of the reactive properties of RDX. Further studies should be performed by TERS to elucidate the question of the distribution of polymer across the sample.

Linking size of droplets, and so supersaturation, to particle size and kinetics of crystallisation is still of interest. In addition to PDA, experiments under the X-Ray beam from a particle accelerator would provide more information of the crystallisation kinetics; our application for beamtime at the ESRF has been recently approved and scheduled for the end of 2016. SAXS will provide information about existing nuclei in droplets as a function of space by scanning the spray and as a function of temperature

Bibliography

1. Bhat, Rajiv and Serge N. Timasheff (1992). "Steric exclusion is the principal source of the preferential hydration of proteins in the presence of polyethylene glycols". In: *Protein Science* 1.9, pp. 1133–1143. ISSN: 1469-896X. DOI: 10.1002/pro.5560010907.

2. Brown, Geoffrey W., Mary M. Sandstrom, Daniel N. Preston, Colin J. Pollard, Kirstin F. Warner, Daniel N. Sorensen, Daniel L. Remmers, Jason J. Phillips, Timothy J. Shelley, Jose A. Reyes, Peter C. Hsu, and John G. Reynolds (2015). "Statistical Analysis of an Inter-Laboratory Comparison of Small-Scale Safety and Thermal Testing of RDX". In: *Propellants, Explosives, Pyrotechnics* 40.2, pp. 221–232. ISSN: 07213115. DOI: 10.1002/prep.201400191.

3. Chen, Gang, Chunyu Chen, Mingzhu Xia, Wu Lei, Fengyun Wang, and Xuedong Gong (2015). "A study of the solvent effect on the crystal morphology of hexogen by means of molecular dynamics simulations". In: *RSC Adv.* 5.32, pp. 25581–25589. ISSN: 2046-2069. DOI: 10.1039/C4RA07544G.

4. Chen, Huaxiong, Lijie Li, Shaohua Jin, Shusen Chen, and Qingze Jiao (2012). "Effects of Additives on ε-HNIW Crystal Morphology and Impact Sensitivity". In: *Propellants, Explosives, Pyrotechnics* 37.1, pp. 77–82. ISSN: 07213115. DOI: 10.1002/prep.201000014.

5. Kim, Jun-Woo, Ji-Hwan Park, Hong-Min Shim, and Kee-Kahb Koo (2013). "Effect of Amphiphilic Additives on Nucleation of Hexahydro-1,3,5-trinitro-1,3,5-triazine". In: *Crystal Growth & Design*, p. 130927134832004. ISSN: 1528-7483, 1528-7505. DOI: 10.1021/cg4006423.

6. Kim, Jun-Woo, Moon-Soo Shin, Jae-Kyeong Kim, Hyoun-Soo Kim, and Kee-Kahb Koo (2011). "Evaporation Crystallization of RDX by Ultrasonic Spray". In: *Industrial & Engineering Chemistry Research* 50.21, pp. 12186–12193. ISSN: 0888-5885, 1520-5045. DOI: 10.1021/ie201314r.

7. Lee, Jae-Eun, Jun-Woo Kim, Sang-Keun Han, Joo-Seung Chae, Keun-Deuk Lee, and Kee-Kahb Koo (2014). "Production of Submicrometer-Sized Hexahydro-1,3,5-trinitro-1,3,5-triazine by Drowning-Out". In: *Industrial & Engineering Chemistry Research* 53.12, pp. 4739–4747. ISSN: 0888-5885, 1520-5045. DOI: 10.1021/ie500221c.

8. McPherson, Alexander and Bob Cudney (2006). "Searching for silver bullets: An alternative strategy for crystallizing macromolecules". In: *Journal of Structural Biology* 156.3, pp. 387–406. ISSN: 1047-8477. DOI: 10.1016/j.jsb.2006.09.006.

9. Patel, Dhaval D. and Bradley D. Anderson (2015). "Adsorption of Polyvinylpyrrolidone and its Impact on Maintenance of Aqueous Supersaturation of Indomethacin via Crystal Growth Inhibition". In: *Journal of Pharmaceutical Sciences* 104.9, pp. 2923–2933. ISSN: 1520-6017. DOI: 10.1002/jps.24493.

10. Radacsi, Norbert, Richard H. B. Bouma, Ellen L. M. Krabbendam-la Haye, Joop H. ter Horst, Andrzej I. Stankiewicz, and Antoine E. D. M. van der Heijden (2013). "On the Reliability of Sensitivity Test Methods for Submicrometer-Sized RDX and HMX Particles". In: *Propellants, Explosives, Pyrotechnics* 38.6, pp. 761–769. ISSN: 1521-4087. DOI: 10.1002/prep.201200189.

11. Risse, Benedikt (2012). "Continuous crystallization of ultra-fine energetic particles by the Flash-Evaporation Process".

12. Rosa, Frédéric, Yohann Corvis, René Lai-Kuen, Christine Charrueau, and Philippe Espeau (2014). "Influence of particle size on the melting characteristics of organic compounds". In: *Journal of Thermal Analysis and Calorimetry* 120.1, pp. 783–787. ISSN: 1388-6150, 1588-2926. DOI: 10.1007/s10973-014-4210-8.

13. Shim, Hong-Min and Kee-Kahb Koo (2014). "Crystal Morphology Prediction of Hexahydro-1,3,5-trinitro-1,3,5-triazine by the Spiral Growth Model". In: *Crystal Growth & Design* 14.4, pp. 1802–1810. ISSN: 1528-7483, 1528-7505. DOI: 10.1021/cg401928m.

14. Socrates, G. and G. Socrates (2001). *Infrared and Raman characteristic group frequencies: tables and charts*. 3rd ed. Chichester ; New York: Wiley. 347 pp. ISBN: 978-0-471-85298-8.

15. Vekilov, Peter G. (2010). "Nucleation". In: *Crystal Growth & Design* 10.12, pp. 5007–5019. ISSN: 1528-7483, 1528-7505. DOI: 10.1021/cg1011633.

16. Yan, Qi-Long, Svatopluk Zeman, Roman Svoboda, and Ahmed Elbeih (2012). "Thermodynamic properties, decomposition kinetics and reaction models of BCHMX and its Formex bonded explosive". In: *Thermochimica Acta* 547, pp. 150–160. ISSN: 0040-6031. DOI: 10.1016/j.tca.2012.08.018.

Related Work

Innovations

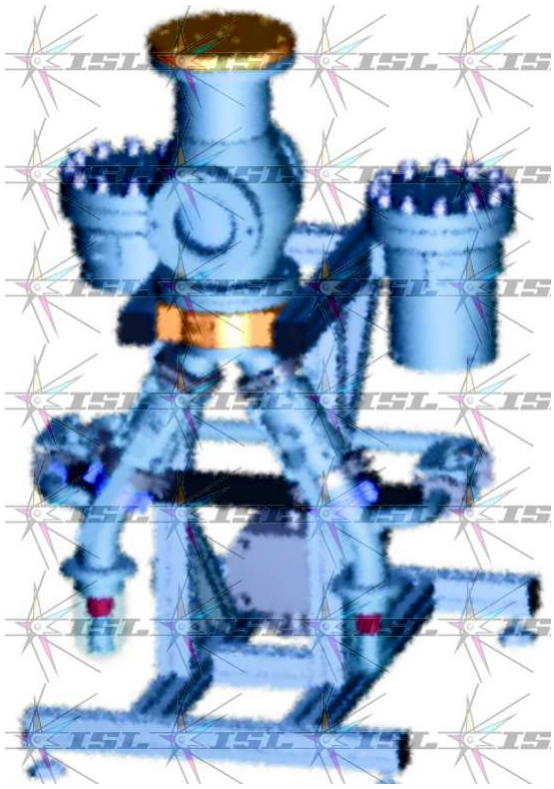

Figure 5.16 – New model of SFE with a reduced size.

SFE Apparatuses Several models of SFE were build prior to my arrival. In order to increase the number of SFE available, a new SFE model was designed with enhanced ergonomy and compactness in cooperation with Ing J. Urban from ISL. I designed and bought the hydraulic system and took care of the budget and assembly of those machines. With the PhD student Axel Le Brize, we performed the maintenance of all the SFE apparatuses and I manage the purchases and improvements on all models. To study the physico-chemical phenomena, a new vacuum chamber was designed for PDA and a whole second injection system was build on an existing apparatus. I have launched and managed the modernization of a laboratory to change the layout, to make available the use of the PDA mounted on an internally designed micrometer traverse and to enhance the whole ergonomy of the pre existing models of SFE.

SFE *in situ* measurements Additional equipments have to be purchase in order to quantify and study precisely the phenomena occurring in the SFE. The inherent risk of the use of energetic materials makes almost impossible –or at

least very limited– any scientific collaboration. I instigated this project which started by the challenging selection of an appropriate technology to measure on-line velocities and sizes. Then a sizeable budget was allocated from public funding thus delaying the effective acquisition of the PDA.

In the mean time, experiments under the X-Ray beam from a particle accelerator have been planed as part of my PhD project, in order to provide more information of the crystallisation; SAXS measurement will allows us to link existing nuclei in droplets in space by scanning the spray but also as a function of temperature.Thanks to Dr Spitzer who supported that project, our application for beamtime at the ESRF has been quite recently approved and scheduled for the end of 2016, after a long process of approval by an international committee and a Safety group.

With MCF Dr. Lobry and Dr. Bonnot, a project for *in situ* Fast Scanning Calorimetry on micro chip has also been started. The study aims to quantify the evaporation kinetics under vacuum of the metastable droplets in SFE, to analyse solid particles at different locations and so to map the crystallization and evaporation in or near an SFE spray. Dr. Bonnot conducted preliminary experiments of standard explosives dissolved in solvents, and the support system with fine controls has been designed.

Analysis Improvements The analysis of data acquired from various characterization techniques was improved. For instance, the use of the software Gwyddion increased the accuracy and the time spend on AFM images; the Rietveld method was introduced to colleagues to get more information from XRD patterns. A database of all experiments made from SFE was set to study reproducibility and perform statistical analysis

Published Work and Communication

Communications

- Europyro 2015, 41st International Pyrotechnic Seminar (Toulouse).
- 4th ISL Budding Science Colloquium (Saint Louis, 2015).
- European Congress and Exhibition on Advanced Materials and Processes EUROMAT 2015, B1.3 Section Nanocrystallisation (Warsaw).
- Material Weekend Warsaw 2015; a PhD student workshop from both E-MRS and FEMS societies.

- exhibitor at the 2016 Eurosatory, Defence and Security International Exhibition (572 exhibitors from 56 countries, 213 official delegations from 94 countries)
- 5th ISL Budding Science Colloquium (Saint Louis, 2016).
- Junior EUROMAT 2016 (Lausanne).
- 6th NANOstructures and nanomaterials SElf-Assembly (NanoSEA) (Giardini Naxos (ME), Italy 2016).
- 1 poster: 3rd ISL Budding Science Colloquium (2014)

Publications

- Blas, Lucia, Martin Klaumünzer, **Florent Pessina**, Silke Braun, and Denis Spitzer. "Nanostructuring of Pure and Composite-Based K6 Formulations with Low Sensitivities." Propellants, Explosives, Pyrotechnics 40, no. 6 (2015): 938–44.
- **Florent Pessina**, Fabien Schnell, and Denis Spitzer. "Tunable Continuous Production of RDX from Microns to Nanoscale Using Polymeric Additives." Chemical Engineering Journal 291 (May 1, 2016): 12–19. doi:10.1016/j.cej.2016.01.083.
- Martin Klaumünzer, **Florent Pessina**, and Denis Spitzer. "Indicating Inconsistency of Desensitizing High Explosives against Impact through Recrystallisation at the Nanoscale." Journal of Energetic Materials, July 1, 2016, 1–10. doi:10.1080/07370652.2016.1199610.
- Denis Spitzer, Vincent Pichot, **Florent Pessina**, Fabien Schnell, Martin Klaumünzer, and Lucia Blas. "Continuous and Reactive Nanocrystallisation: New Concepts and Processes for Dual-Use Advances." Comptes Rendus Chimie, July 2016. doi:10.1016/j.crci.2016.06.009.
- **Florent Pessina** and Denis Spitzer. "The longstanding challenge of the nano crystallization of 1,3,5-trinitroperhydro-1,3,5-triazine (RDX)" Beilstein Journal of Nanotechnology *Under Review*.

Patent

- Risse, Benedikt, Florent Pessina, and Denis Spitzer. Method for producing cocrystals by means of flash evaporation. WO 2016001445, issued January 2016.

Scientific courses

- Sensibilisation à la pyrotechnie 3PSC17C, Centre de Formation de la Défense (Bourges 2013)
- Advanced Functional Materials and Characterization, CNRS-EWHA Winter School (Strasbourg 2014)
- Nano-OptoMechanics, School in Physics (Strasbourg 2014)

Conclusion

Due to the difficult micronisation and nano crystallisation of classical organic explosives such as RDX, advances in insensitive munitions came mainly from new compounds such as NTO or optimizations of each step of the production process (Klapötke et al. 2016; Nouguez et al. 2016). The size reduction of energetic crystals is still of interest not only to produce particles under the critical hot-spot size but also to provide easier shaping and homogeneous energetic compositions. The extensive review of the crystallisation technique used on RDX performed in the Chapter 2 suggests that the Spray Flash Evaporation (SFE) is a well balanced method between spray drying unable to process particles lower that the micrometer, and the expensive batch Rapid Expansion of Supercritical Solutions (RESS) process. The crystallisation in solution is a competitive approach but limited by the drying conditions and its inability to process propellants, unlike the SFE technology (Le Brize et al. 2016).

The present research project was initially focused in the size reduction of crystals produced by this unique technique created in our laboratory. Many challenges were addressed starting by the difficult to commit characterizations of energetic materials, and of the spray itself. Then the crystallisation from SFE has been unveiled with supersaturation variations by solvent exchanges and by polymeric agents.

The nano-technology took off with the invention of the two crucial characterization methods, the Scanning Tunneling Microscopy (STM) and the Atomic Force Microscopy (AFM). The energetic materials are organic crystals where molecules are held together by weak forces; therefore energetic compounds exhibit high sensitivity towards characterization techniques providing energy to the sample. As a consequence, the pyrotechnic community experiences many limitation to assess accurately the particle morphology, their size, aggregation state etc. By trying several characterization techniques especially the microscopy ones, the Environmental Scanning Electron Microscopy (ESEM) has been found to be a suitable technique to process energetic material.

An original method where pellets are flatten then analysed by AFM was in

use previously (Spitzer et al. 2014) and also at the beginning of this present project. It was found that the size measured that way was not a function of the concentration in solution but more of the condition of preparation of the pellets. The compression breaks the brittle crystals with a critical pressure above which the particles reach an even smaller size; while using a microtome, the surface is milled and grooves appear. Sizes down to the crystallite size were found in those grooves. That phenomenon is much more pronounced for n-RDX processed by SFE than for raw micron-sized RDX, just as Spitzer et al. (2011) experienced about opacity and mechanical strength. Those properties could benefit to pressed charges to tune the apparent density and greatly improve homogeneity.

For the SFE process, particle size and shape depend on the crystallisation itself governed by the supersaturation. The degree of supersaturation is unique in each droplet and thus is a function of time and space. The restriction for *in situ* characterization of the droplets for SFE has been overcome by focusing on the chemical route to change the supersaturation and by designing a dual injection system. In that latter system, the persistence of droplet is questioned by using the cocrystal CL-20:HMX. Cocrystallisation occurs in any cases: by using a unique solution and nozzle, by using one solvent but two solutions and nozzles, and also by using two different solvents each one sprayed by one nozzle. Droplets effectively collide from both spray permitting the crystallisation; it is however not clear whether the nucleation occurs before the overlap or the Phase Solubility Diagram (PhSD) of the system does not allow the formation of the sole cocrystal. Further investigations will be performed to quantify the relative crystalline phases and the overlap.

The SFE versatility was again taken a step further within the introduction of solid and viscous polymers in solvent. Those polymers are food additives namely PolyVinylPyrrolidone (PVP) and PolyEthylene Glycol (PEG) and were successfully used to control crystallisation steps. PEG 400 triggers the early nucleation of RDX with low nucleation rate leading to bigger particles up to 5 µm. PVP 40K acts as a nucleation inhibitor and a growth inhibitor: RDX nuclei are formed in less volume available due to the fission and flashing of droplets; then the crystal growth is slowed, thus allowing the formation of much smaller particles at 160 nm with a narrow distribution and a spherical shape. The addition of PEG could have increased supersaturation to trigger nucleation at a maximal rate but results show that the contribution of both the evaporation behaviour and the nucleation inhibition is more effective and probably the surest choice to reduce and stabilize both particle size and morphology. Furthermore, those synthesized energetic composites are less sensitive.

The laboratory acquired very recently a Phase Doppler Analysis (PDA) in order to elucidate the question of supersaturation. Droplets size and velocity will be measured as a function of temperature but also in space within the spray. The dual nozzle system will also benefit from PDA analyses to define the evaporation behaviours while using two solvent or an anti-solvent. Pre-results show droplets of a few microns at high speed more than 100 m/s, suggesting the possible crystallisation from metastable systems.

To summarize, the submicron and nano scales bring to the pyrotechnic community new challenges for the characterization of nano energetic materials. Furthermore, this research project paved the way to global and deeper understanding of the crystallisation aspect of the SFE technology. New apparatuses and designs were explored and implemented as breakthrough for the SFE technology; they led to the control of particle size and shape, and to versatility and industrial-friendly enhancements of the SFE apparatuses.

Bibliography

1. Klapötke, Thomas M. and Tomasz G. Witkowski (2016). "Covalent and Ionic Insensitive High-Explosives". In: *Propellants, Explosives, Pyrotechnics*. ISSN: 07213115. DOI: 10.1002/prep.201600006.
2. Le Brize, Axel and Denis Spitzer (2016). "Plasticization of Submicron-Structured LOVA Propellants by a Linear Dinitramine". In: *Central European Journal of Energetic Materials* 13.
3. Nouguez, Bruno and Geneviève Eck (2016). "From Synthesis to Formulation and Final Application". In: *Propellants, Explosives, Pyrotechnics* 41.3, pp. 548–554. ISSN: 1521-4087. DOI: 10.1002/prep.201600031.
4. Spitzer, D., B. Risse, F. Schnell, V. Pichot, M. Klaumünzer, and M. R. Schaefer (2014). "Continuous engineering of nano-cocrystals for medical and energetic applications". In: *Scientific Reports* 4. DOI: 10.1038/srep06575.
5. Spitzer, Denis, Christian Baras, Michael Richard Schäfer, Fabrice Ciszek, and Benny Siegert (2011). "Continuous Crystallization of Submicrometer Energetic Compounds". In: *Propellants, Explosives, Pyrotechnics* 36.1, pp. 65–74. ISSN: 07213115. DOI: 10.1002/prep.200900002.

Appendix A

Rietveld refinement

A.1 Calibration

```
*******************************************************
** PROGRAM FullProf.2k (Version 5.50 - Dec2014-ILL JRC) **
*******************************************************
M U L T I -- P A T T E R N
Rietveld, Profile Matching & Integrated Intensity
Refinement of X-ray and/or Neutron Data


Date: 17/02/2015  Time: 13:47:24.271

=> PCR file code: lab6 - Copie (22) - Copie
=> DAT file code: lab6.dat             -> Relative contribution: 1.0000

==> CONDITIONS OF THIS RUN FOR PATTERN No.:  1

=> Global Refinement of X-ray powder diffraction data
=> Global Refinement of X-ray powder diffraction data
Flat plate with PSD
=> Title: ALS 11-BM - NIST SRM 660a LaB6

=> Number of phases:    1
=> Number of excluded regions:    0
=> Number of scattering factors supplied:    0
=> March-Dollase model for preferred orientation
=> Conventional weights: w=1.0/Variance(yobs)
=> Asymmetry correction as in J.Appl.Cryst. 26,128(1993)
=> Background linearly interpolated between the    7 points given
=> The    5th default profile function was selected
=> Pseudo-Voigt function (ETA variable)
X-parameter correspond to: ETA=ETA0+X*2theta
pV(x)= ETA*L(x)+(1-ETA)*G(x)

==> INPUT/OUTPUT OPTIONS:

=> Generate bacground file *.bac
=> Generate file *.PRF for plot
=> Output Integrated Intensities
=> Output Correlation Matrix
=> Generate new input file *.PCR

=> Data supplied in free format for pattern:  1
=> Plot pattern at each cycle
=> Wavelengths:  1.54059 1.54431
=> Alpha2/Alpha1 ratio:   0.5000
=> Cos(Monochromator angle)=   1.0000
=> Asymmetry correction for angles lower than   90.000 degrees
=> Absorption correction (AC), muR-eff =   0.0000  0.0000
=> Base of peaks: 2.0*HW*   20.00

=> Number of cycles:   50
=> Relaxation factors ==>    for coordinates:  1.00
=> for anisotropic temperature factors:  1.00
=> for halfwidth/strain/size parameters:  1.00
=> for lattice constants and propagation vectors:  1.00
=> EPS-value for convergence:    0.0
=> Background ==>
Position   Intensity
20.00       22.22        0.00
30.00       21.64        0.00
40.00       18.36        0.00
55.00       12.77        0.00
60.00        9.61        0.00
75.00       12.58        0.00
```

```
120.00        7.64        0.00


=> Number of Least-Squares parameters varied:    12

=>---------------------------->
=>-------->  PATTERN number:  1
=>---------------------------->
=> Global parameters and codes ==>
=> Zero-point:     -0.2111   11.0000
=> Displacement peak-shift parameter and code:     0.08   21.00
=> Transparency peak-shift parameter and code:     0.04   31.00

=> Reading Intensity data  =>>

==> Angular range, step and number of points:
2Thmin:      17.540501  2Thmax:     152.554001  Step:       0.019332  No. of points:   6985
--------------------------------------------------------------------------------
=> Phase  No. 1
NIST SRM 660a LaB6
--------------------------------------------------------------------------------
=>-------> Pattern#  1
=> Crystal Structure Refinement
=> The    7th profile function was selected for phase no.  1
=> Preferred orientation vector:   0.0000  0.0000  1.0000

=>-------> Data for PHASE: 1
=> Number of atoms:    2
=> Number of distance  constraints:    0
=> Number of angle     constraints:    0

=> Symmetry information on space group: P m 3 m
-> The multiplicity of the general position is:  48
-> The space group is Centric (-1 at origin)
-> Lattice type  P: { 000 }
-> Reduced set of symmetry operators:

No.  IT   Symmetry symbol    Rotation part     Associated Translation
1: ( 1)   1            -->     ( x, y, z) + {  0.0000  0.0000  0.0000}
2: ( 4)   2 ( x, 0, 0) -->     ( x,-y,-z) + {  0.0000  0.0000  0.0000}
3: ( 3)   2 ( 0, y, 0) -->     (-x, y,-z) + {  0.0000  0.0000  0.0000}
4: ( 2)   2 ( 0, 0, z) -->     (-x,-y, z) + {  0.0000  0.0000  0.0000}
5: ( 9)  3- ( x, x, x) -->     ( y, z, x) + {  0.0000  0.0000  0.0000}
6: (12)  3- (-x, x,-x) -->     (-y,-z, x) + {  0.0000  0.0000  0.0000}
7: (11)  3- (-x,-x, x) -->     ( y,-z,-x) + {  0.0000  0.0000  0.0000}
8: (10)  3- ( x,-x,-x) -->     (-y, z,-x) + {  0.0000  0.0000  0.0000}
9: ( 5)  3+ ( x, x, x) -->     ( z, x, y) + {  0.0000  0.0000  0.0000}
10: ( 8)  3+ (-x,-x, x) -->     (-z, x,-y) + {  0.0000  0.0000  0.0000}
11: ( 7)  3+ ( x,-x,-x) -->     (-z,-x, y) + {  0.0000  0.0000  0.0000}
12: ( 6)  3+ (-x, x,-x) -->     ( z,-x,-y) + {  0.0000  0.0000  0.0000}
13: (14)   2 ( x,-x, 0) -->     (-y,-x,-z) + {  0.0000  0.0000  0.0000}
14: (15)  4- ( 0, 0, z) -->     ( y,-x, z) + {  0.0000  0.0000  0.0000}
15: (16)  4+ ( 0, 0, z) -->     (-y, x, z) + {  0.0000  0.0000  0.0000}
16: (13)   2 ( x, x, 0) -->     ( y, x,-z) + {  0.0000  0.0000  0.0000}
17: (24)   2 (-x, 0, x) -->     (-z,-y,-x) + {  0.0000  0.0000  0.0000}
18: (21)  4+ ( 0, y, 0) -->     ( z, y,-x) + {  0.0000  0.0000  0.0000}
19: (22)   2 ( x, 0, x) -->     ( z,-y, x) + {  0.0000  0.0000  0.0000}
20: (23)  4- ( 0, y, 0) -->     (-z, y, x) + {  0.0000  0.0000  0.0000}
21: (19)   2 ( 0, y,-y) -->     (-x,-z,-y) + {  0.0000  0.0000  0.0000}
22: (18)   2 ( 0, y, y) -->     (-x, z, y) + {  0.0000  0.0000  0.0000}
23: (17)  4- ( x, 0, 0) -->     ( x, z,-y) + {  0.0000  0.0000  0.0000}
24: (20)  4+ ( x, 0, 0) -->     ( x,-z, y) + {  0.0000  0.0000  0.0000}


Information on Space Group:
---------------------------

=>  Number of Space group: 221
=> Hermann-Mauguin Symbol: P m 3 m
=>            Hall Symbol: -P 4 2 3
=>   Table Setting Choice:
=>           Setting Type: IT (Generated from Hermann-Mauguin symbol)
=>         Crystal System: Cubic
=>             Laue Class: m-3m
=>            Point Group: m-3m
=>        Bravais Lattice: P
=>         Lattice Symbol: cP
=> Reduced Number of S.O.:  24
=>   General multiplicity:  48
=>         Centrosymmetry: Centric (-1 at origin)
=> Generators (exc. -1&L):   3
=>        Asymmetric unit:  0.000 <= x <=  0.500
0.000 <= y <=  0.500
0.000 <= z <=  0.500

=> List of S.O. without inversion and lattice centring translations
=> SYMM(  1): x,y,z                                => SYMM(  2): x,-y,-z
=> SYMM(  3): -x,y,-z                              => SYMM(  4): -x,-y,z
=> SYMM(  5): y,z,x                                => SYMM(  6): -y,-z,x
=> SYMM(  7): y,-z,-x                              => SYMM(  8): -y,z,-x
```

```
=> SYMM(  9): z,x,y                              => SYMM( 10): -z,x,-y
=> SYMM( 11): -z,-x,y                            => SYMM( 12): z,-x,-y
=> SYMM( 13): y,x,z                              => SYMM( 14): -y,x,-z
=> SYMM( 15): y,-x,-z                            => SYMM( 16): -y,-x,z
=> SYMM( 17): z,y,x                              => SYMM( 18): -z,-y,x
=> SYMM( 19): -z,y,-x                            => SYMM( 20): z,-y,-x
=> SYMM( 21): x,z,y                              => SYMM( 22): x,-z,-y
=> SYMM( 23): -x,-z,y                            => SYMM( 24): -x,z,-y


=> Initial parameters ==>
Atom    Ntyp                  X         Y         Z         B         occ.         in  fin  Spc  Mult
B11       B22       B33       B12       B13       B23
La     La                0.00000   0.00000   0.00000   0.41517   0.16666          0    0    0    1
Codes:    0.00000   0.00000   0.00000   0.00000   0.00000
B      B                  0.20319   0.50000   0.50000   0.26488   1.00000          0    0    0    6
Codes:   41.00000   0.00000   0.00000   0.00000   0.00000

=> IT IS ASSUMED THAT THE FIRST GIVEN SITE IS FULLY OCCUPIED
OR THE FIRST AND SECOND ATOMS ARE IN THE SAME SITE WITH TOTAL FULL OCCUPATION
(If this is not the case, change the order of atoms to obtain correct values for the content of the unit cell)
The given occupation factors have been obtained mutiplying m/M by   7.9997
-> Atom: La   ,  Chemical element: LA  Atomic Mass:   138.9055
-> Atom: B    ,  Chemical element: B   Atomic Mass:    10.8100
=> The given value of ATZ is       1630.08 the program has calculated:       13040.11
The value of ATZ given in the input PCR file will be used for quantitative analysis
=> The chemical content of the unit cell is:
1.0000 La   +   6.0002 B
=> The normalized site occupation numbers in % are:
100.0000 La     :      100.0040 B
=> The density (volumic mass) of the compound is:    4.717 g/cm3

=>-------> PROFILE PARAMETERS FOR PATTERN:  1

=> Overall scale factor:   0.125350E-03
=> ETA (p-Voigt) OR M (Pearson VII):   0.0000
=> Overall temperature factor:      0.00000
=> Halfwidth U,V,W:      0.00136    -0.00500     0.00391
=> X and Y parameters:       0.0639      0.0001
=> Direct cell parameters:    4.1550   4.1550   4.1550  90.0000  90.0000  90.0000
=> Preferred orientation parameters:   1.0000  0.0000
=> Asymmetry parameters     :     -0.03244     0.04207     0.00000     0.00000
=> Strain parameters        :      0.00000     0.00000     0.00000
=> Size   parameters        :      0.00000     0.00000
=> Further shape parameters (S_L and D_L):   0.00000   0.00000
S_L is source width/detector distance
D_L is detector width/detector distance

==> CODEWORDS FOR PROFILE PARAMETERS of PATTERN#  1

=> Overall scale factor:   51.000
=> ETA (p-Voigt) OR M (Pearson VII):    0.000
=> Overall temperature factor:    0.000
=> Halfwidth U,V,W:   61.000  71.000  81.000
=> X and Y parameters:  101.000 110.000
=> Direct cell parameters:    0.000   0.000   0.000   0.000   0.000   0.000
=> Preferred orientation parameters:    0.000   0.000
=> Asymmetry parameters     :   91.000 121.000   0.000   0.000
=> Strain parameters        :    0.000   0.000   0.000
=> Size   parameters        :    0.000   0.000

=> Cell constraints according to Laue symmetry: m-3m

Metric information:
-------------------

=> Direct cell parameters:

a =       4.1550      b =       4.1550      c =       4.1550
alpha =       90.000   beta =       90.000  gamma =       90.000
Direct Cell Volume =      71.7313

=> Reciprocal cell parameters:

a*=     0.240675      b*=     0.240675      c*=     0.240675
alpha*=       90.000   beta*=       90.000  gamma*=       90.000
Reciprocal Cell Volume =   0.01394091

=> Direct and Reciprocal Metric Tensors:

GD                                    GR
17.2639      0.0000      0.0000          0.057924    0.000000    0.000000
0.0000     17.2639      0.0000          0.000000    0.057924    0.000000
0.0000      0.0000     17.2639          0.000000    0.000000    0.057924

=>  Cartesian frame: x // a; y is in the ab-plane; z is x ^ y

Crystal_to_Orthonormal_Matrix             Orthonormal_to_Crystal Matrix
Cr_Orth_cel                              Orth_Cr_cel
4.1550      0.0000      0.0000          0.240675    0.000000    0.000000
```

```
0.0000      4.1550      0.0000          0.000000    0.240675    0.000000
0.0000      0.0000      4.1550          0.000000    0.000000    0.240675

Busing-Levy B-matrix: Hc=B.H            Inverse of the Busing-Levy B-matrix
BL_M                                      BL_Minv
0.240675    0.000000    0.000000            4.1550      0.0000      0.0000
0.000000    0.240675    0.000000            0.0000      4.1550      0.0000
0.000000    0.000000    0.240675            0.0000      0.0000      4.1550

=> Laue symmetry m-3m  will be used to generate HKL for pattern#   1
=> Reflections generated between S(1/d)min:  0.1975 A-1 and S(1/d)max:  1.2677 A-1
=>                                  dmax:  5.0642 A   and      dmin:  0.7888 A
=> The number of reflections generated is:     30
=> The max. scatt. variable (gen.ref.) is:       155.1055
=> Scattering coefficients from internal table


=> X-ray scattering coeff. (A1, B1, A2,...C, f(0), Z, Dfp,Dfpp)

LA     20.5780   2.9482  19.5990   0.2445  11.3727  18.7726   3.2872 133.1240   2.1468  56.9837  57.0000  -1.7160  ↙
       9.0360
B       2.0545  23.2185   1.3326   1.0210   1.0979  60.3498   0.7068   0.1403  -0.1932   4.9986   5.0000   0.0080  ↙
       0.0040

-------------------------------------------------------------
SYMBOLIC NAMES AND INITIAL VALUES OF PARAMETERS TO BE VARIED:
-------------------------------------------------------------

->  Parameter number    1   -> Symbolic Name:            Zero_pat1   -0.21106000
->  Parameter number    2   -> Symbolic Name:           SyCos_pat1    0.76700002E-01
->  Parameter number    3   -> Symbolic Name:           SySin_pat1    0.38720001E-01
->  Parameter number    4   -> Symbolic Name:              X_B_ph1    0.20319000
->  Parameter number    5   -> Symbolic Name:       Scale_ph1_pat1    0.12534999E-03
->  Parameter number    6   -> Symbolic Name:      U-Cagl_ph1_pat1    0.13560000E-02
->  Parameter number    7   -> Symbolic Name:      V-Cagl_ph1_pat1   -0.49999999E-02
->  Parameter number    8   -> Symbolic Name:      W-Cagl_ph1_pat1    0.39100000E-02
->  Parameter number    9   -> Symbolic Name:       Asym1_ph1_pat1   -0.32439999E-01
->  Parameter number   10   -> Symbolic Name:       X-tan_ph1_pat1    0.63895002E-01
->  Parameter number   11   -> Symbolic Name:       Y-cos_ph1_pat1     0.0000000
->  Parameter number   12   -> Symbolic Name:       Asym2_ph1_pat1    0.42070001E-01

=> Zero counts at step no.      3 at 2theta/TOF/E(KeV):        17.5792  Intensity fixed to 1.0 and variance to 1E6
=> Zero counts at step no.      4 at 2theta/TOF/E(KeV):        17.5985  Intensity fixed to 1.0 and variance to 1E6
=> Zero counts at step no.      5 at 2theta/TOF/E(KeV):        17.6178  Intensity fixed to 1.0 and variance to 1E6
=> Zero counts at step no.      6 at 2theta/TOF/E(KeV):        17.6372  Intensity fixed to 1.0 and variance to 1E6
=> Zero counts at step no.      7 at 2theta/TOF/E(KeV):        17.6565  Intensity fixed to 1.0 and variance to 1E6
=> Zero counts at step no.      8 at 2theta/TOF/E(KeV):        17.6758  Intensity fixed to 1.0 and variance to 1E6
=> Zero counts at step no.      9 at 2theta/TOF/E(KeV):        17.6952  Intensity fixed to 1.0 and variance to 1E6
=> Zero counts at step no.     12 at 2theta/TOF/E(KeV):        17.7532  Intensity fixed to 1.0 and variance to 1E6
=> Zero counts at step no.     13 at 2theta/TOF/E(KeV):        17.7725  Intensity fixed to 1.0 and variance to 1E6
=> Zero counts at step no.     14 at 2theta/TOF/E(KeV):        17.7918  Intensity fixed to 1.0 and variance to 1E6
=> Zero counts at step no.     16 at 2theta/TOF/E(KeV):        17.8305  Intensity fixed to 1.0 and variance to 1E6
=> Zero counts at step no.     17 at 2theta/TOF/E(KeV):        17.8498  Intensity fixed to 1.0 and variance to 1E6
=> Zero counts at step no.     19 at 2theta/TOF/E(KeV):        17.8885  Intensity fixed to 1.0 and variance to 1E6
=> Zero counts at step no.     22 at 2theta/TOF/E(KeV):        17.9465  Intensity fixed to 1.0 and variance to 1E6
=> Zero counts at step no.     24 at 2theta/TOF/E(KeV):        17.9851  Intensity fixed to 1.0 and variance to 1E6
=> Zero counts at step no.     25 at 2theta/TOF/E(KeV):        18.0045  Intensity fixed to 1.0 and variance to 1E6
=> Zero counts at step no.     30 at 2theta/TOF/E(KeV):        18.1011  Intensity fixed to 1.0 and variance to 1E6
=> Zero counts at step no.     31 at 2theta/TOF/E(KeV):        18.1205  Intensity fixed to 1.0 and variance to 1E6
=> Zero counts at step no.     32 at 2theta/TOF/E(KeV):        18.1398  Intensity fixed to 1.0 and variance to 1E6
=> Zero counts at step no.     33 at 2theta/TOF/E(KeV):        18.1591  Intensity fixed to 1.0 and variance to 1E6
=> Zero counts at step no.     34 at 2theta/TOF/E(KeV):        18.1785  Intensity fixed to 1.0 and variance to 1E6
=> Zero counts at step no.     35 at 2theta/TOF/E(KeV):        18.1978  Intensity fixed to 1.0 and variance to 1E6
=> Zero counts at step no.     36 at 2theta/TOF/E(KeV):        18.2171  Intensity fixed to 1.0 and variance to 1E6
=> Zero counts at step no.     37 at 2theta/TOF/E(KeV):        18.2364  Intensity fixed to 1.0 and variance to 1E6
=> Zero counts at step no.     38 at 2theta/TOF/E(KeV):        18.2558  Intensity fixed to 1.0 and variance to 1E6
=> Zero counts at step no.     40 at 2theta/TOF/E(KeV):        18.2944  Intensity fixed to 1.0 and variance to 1E6
=> Zero counts at step no.     43 at 2theta/TOF/E(KeV):        18.3524  Intensity fixed to 1.0 and variance to 1E6
=> Zero counts at step no.     44 at 2theta/TOF/E(KeV):        18.3718  Intensity fixed to 1.0 and variance to 1E6
=> Zero counts at step no.     45 at 2theta/TOF/E(KeV):        18.3911  Intensity fixed to 1.0 and variance to 1E6
=> Zero counts at step no.     46 at 2theta/TOF/E(KeV):        18.4104  Intensity fixed to 1.0 and variance to 1E6
=> Zero counts at step no.     48 at 2theta/TOF/E(KeV):        18.4491  Intensity fixed to 1.0 and variance to 1E6
=> Zero counts at step no.     49 at 2theta/TOF/E(KeV):        18.4684  Intensity fixed to 1.0 and variance to 1E6
=> Zero counts at step no.     51 at 2theta/TOF/E(KeV):        18.5071  Intensity fixed to 1.0 and variance to 1E6
=> Zero counts at step no.     52 at 2theta/TOF/E(KeV):        18.5264  Intensity fixed to 1.0 and variance to 1E6
=> Zero counts at step no.     53 at 2theta/TOF/E(KeV):        18.5458  Intensity fixed to 1.0 and variance to 1E6
=> Zero counts at step no.     55 at 2theta/TOF/E(KeV):        18.5844  Intensity fixed to 1.0 and variance to 1E6
=> Zero counts at step no.     56 at 2theta/TOF/E(KeV):        18.6038  Intensity fixed to 1.0 and variance to 1E6
=> Zero counts at step no.     57 at 2theta/TOF/E(KeV):        18.6231  Intensity fixed to 1.0 and variance to 1E6
=> Zero counts at step no.     59 at 2theta/TOF/E(KeV):        18.6617  Intensity fixed to 1.0 and variance to 1E6
=> Zero counts at step no.     61 at 2theta/TOF/E(KeV):        18.7004  Intensity fixed to 1.0 and variance to 1E6
=> Zero counts at step no.     64 at 2theta/TOF/E(KeV):        18.7584  Intensity fixed to 1.0 and variance to 1E6
=> Zero counts at step no.     66 at 2theta/TOF/E(KeV):        18.7971  Intensity fixed to 1.0 and variance to 1E6
=> Zero counts at step no.     67 at 2theta/TOF/E(KeV):        18.8164  Intensity fixed to 1.0 and variance to 1E6
=> Zero counts at step no.     68 at 2theta/TOF/E(KeV):        18.8357  Intensity fixed to 1.0 and variance to 1E6
=> Zero counts at step no.     70 at 2theta/TOF/E(KeV):        18.8744  Intensity fixed to 1.0 and variance to 1E6
=> Zero counts at step no.     71 at 2theta/TOF/E(KeV):        18.8937  Intensity fixed to 1.0 and variance to 1E6
=> Zero counts at step no.     73 at 2theta/TOF/E(KeV):        18.9324  Intensity fixed to 1.0 and variance to 1E6
=> Zero counts at step no.     74 at 2theta/TOF/E(KeV):        18.9517  Intensity fixed to 1.0 and variance to 1E6
=> Zero counts at step no.     75 at 2theta/TOF/E(KeV):        18.9711  Intensity fixed to 1.0 and variance to 1E6
```

```
=> Zero counts at step no.     77 at 2theta/TOF/E(KeV):       19.0097  Intensity fixed to 1.0 and variance to 1E6
=> Zero counts at step no.     78 at 2theta/TOF/E(KeV):       19.0291  Intensity fixed to 1.0 and variance to 1E6
=> Zero counts at step no.     82 at 2theta/TOF/E(KeV):       19.1064  Intensity fixed to 1.0 and variance to 1E6
=> Zero counts at step no.     84 at 2theta/TOF/E(KeV):       19.1450  Intensity fixed to 1.0 and variance to 1E6
=> Zero counts at step no.     85 at 2theta/TOF/E(KeV):       19.1644  Intensity fixed to 1.0 and variance to 1E6
=> Zero counts at step no.     90 at 2theta/TOF/E(KeV):       19.2610  Intensity fixed to 1.0 and variance to 1E6
=> Zero counts at step no.     91 at 2theta/TOF/E(KeV):       19.2804  Intensity fixed to 1.0 and variance to 1E6
=> Zero counts at step no.     93 at 2theta/TOF/E(KeV):       19.3190  Intensity fixed to 1.0 and variance to 1E6
=> Zero counts at step no.     94 at 2theta/TOF/E(KeV):       19.3384  Intensity fixed to 1.0 and variance to 1E6
=> Zero counts at step no.     95 at 2theta/TOF/E(KeV):       19.3577  Intensity fixed to 1.0 and variance to 1E6
=> Zero counts at step no.     97 at 2theta/TOF/E(KeV):       19.3964  Intensity fixed to 1.0 and variance to 1E6
=> Zero counts at step no.     98 at 2theta/TOF/E(KeV):       19.4157  Intensity fixed to 1.0 and variance to 1E6
=> Zero counts at step no.     99 at 2theta/TOF/E(KeV):       19.4350  Intensity fixed to 1.0 and variance to 1E6
=> Zero counts at step no.    104 at 2theta/TOF/E(KeV):       19.5317  Intensity fixed to 1.0 and variance to 1E6
=> Zero counts at step no.    105 at 2theta/TOF/E(KeV):       19.5510  Intensity fixed to 1.0 and variance to 1E6
=> Zero counts at step no.    109 at 2theta/TOF/E(KeV):       19.6283  Intensity fixed to 1.0 and variance to 1E6
=> Zero counts at step no.    110 at 2theta/TOF/E(KeV):       19.6477  Intensity fixed to 1.0 and variance to 1E6
=> Zero counts at step no.    111 at 2theta/TOF/E(KeV):       19.6670  Intensity fixed to 1.0 and variance to 1E6
=> Zero counts at step no.    113 at 2theta/TOF/E(KeV):       19.7057  Intensity fixed to 1.0 and variance to 1E6
=> Zero counts at step no.    115 at 2theta/TOF/E(KeV):       19.7443  Intensity fixed to 1.0 and variance to 1E6
=> Zero counts at step no.    123 at 2theta/TOF/E(KeV):       19.8990  Intensity fixed to 1.0 and variance to 1E6
=> Zero counts at step no.    125 at 2theta/TOF/E(KeV):       19.9376  Intensity fixed to 1.0 and variance to 1E6
=> Zero counts at step no.    128 at 2theta/TOF/E(KeV):       19.9956  Intensity fixed to 1.0 and variance to 1E6
=> Zero counts at step no.    129 at 2theta/TOF/E(KeV):       20.0150  Intensity fixed to 1.0 and variance to 1E6
=> Zero counts at step no.    130 at 2theta/TOF/E(KeV):       20.0343  Intensity fixed to 1.0 and variance to 1E6
=> Zero counts at step no.    132 at 2theta/TOF/E(KeV):       20.0730  Intensity fixed to 1.0 and variance to 1E6
=> Zero counts at step no.    135 at 2theta/TOF/E(KeV):       20.1310  Intensity fixed to 1.0 and variance to 1E6
=> Zero counts at step no.    136 at 2theta/TOF/E(KeV):       20.1503  Intensity fixed to 1.0 and variance to 1E6
=> Zero counts at step no.    137 at 2theta/TOF/E(KeV):       20.1696  Intensity fixed to 1.0 and variance to 1E6
=> Zero counts at step no.    138 at 2theta/TOF/E(KeV):       20.1890  Intensity fixed to 1.0 and variance to 1E6
=> Zero counts at step no.    141 at 2theta/TOF/E(KeV):       20.2470  Intensity fixed to 1.0 and variance to 1E6
=> Zero counts at step no.    144 at 2theta/TOF/E(KeV):       20.3050  Intensity fixed to 1.0 and variance to 1E6
=> Zero counts at step no.    145 at 2theta/TOF/E(KeV):       20.3243  Intensity fixed to 1.0 and variance to 1E6
=> Zero counts at step no.    146 at 2theta/TOF/E(KeV):       20.3436  Intensity fixed to 1.0 and variance to 1E6
=> Zero counts at step no.    148 at 2theta/TOF/E(KeV):       20.3823  Intensity fixed to 1.0 and variance to 1E6
=> Zero counts at step no.    149 at 2theta/TOF/E(KeV):       20.4016  Intensity fixed to 1.0 and variance to 1E6
=> Zero counts at step no.    151 at 2theta/TOF/E(KeV):       20.4403  Intensity fixed to 1.0 and variance to 1E6
=> Zero counts at step no.    154 at 2theta/TOF/E(KeV):       20.4983  Intensity fixed to 1.0 and variance to 1E6
=> Zero counts at step no.    155 at 2theta/TOF/E(KeV):       20.5176  Intensity fixed to 1.0 and variance to 1E6
=> Zero counts at step no.    159 at 2theta/TOF/E(KeV):       20.5949  Intensity fixed to 1.0 and variance to 1E6
=> Zero counts at step no.    163 at 2theta/TOF/E(KeV):       20.6723  Intensity fixed to 1.0 and variance to 1E6
=> Zero counts at step no.    167 at 2theta/TOF/E(KeV):       20.7496  Intensity fixed to 1.0 and variance to 1E6
=> Zero counts at step no.    168 at 2theta/TOF/E(KeV):       20.7689  Intensity fixed to 1.0 and variance to 1E6
=> Zero counts at step no.    169 at 2theta/TOF/E(KeV):       20.7882  Intensity fixed to 1.0 and variance to 1E6
=> Zero counts at step no.    170 at 2theta/TOF/E(KeV):       20.8076  Intensity fixed to 1.0 and variance to 1E6
=> Zero counts at step no.    171 at 2theta/TOF/E(KeV):       20.8269  Intensity fixed to 1.0 and variance to 1E6
=> Zero counts at step no.    173 at 2theta/TOF/E(KeV):       20.8656  Intensity fixed to 1.0 and variance to 1E6
=> Zero counts at step no.    174 at 2theta/TOF/E(KeV):       20.8849  Intensity fixed to 1.0 and variance to 1E6
=> Zero counts at step no.    177 at 2theta/TOF/E(KeV):       20.9429  Intensity fixed to 1.0 and variance to 1E6
=> Zero counts at step no.    213 at 2theta/TOF/E(KeV):       21.6388  Intensity fixed to 1.0 and variance to 1E6
=> Zero counts at step no.    219 at 2theta/TOF/E(KeV):       21.7548  Intensity fixed to 1.0 and variance to 1E6
=> Zero counts at step no.    220 at 2theta/TOF/E(KeV):       21.7742  Intensity fixed to 1.0 and variance to 1E6
=> Zero counts at step no.    222 at 2theta/TOF/E(KeV):       21.8128  Intensity fixed to 1.0 and variance to 1E6
=> Zero counts at step no.    223 at 2theta/TOF/E(KeV):       21.8322  Intensity fixed to 1.0 and variance to 1E6
=> Zero counts at step no.    225 at 2theta/TOF/E(KeV):       21.8708  Intensity fixed to 1.0 and variance to 1E6
=> Zero counts at step no.    228 at 2theta/TOF/E(KeV):       21.9288  Intensity fixed to 1.0 and variance to 1E6
=> Zero counts at step no.    229 at 2theta/TOF/E(KeV):       21.9482  Intensity fixed to 1.0 and variance to 1E6
=> Zero counts at step no.    231 at 2theta/TOF/E(KeV):       21.9868  Intensity fixed to 1.0 and variance to 1E6
=> Zero counts at step no.    232 at 2theta/TOF/E(KeV):       22.0062  Intensity fixed to 1.0 and variance to 1E6
=> Zero counts at step no.    235 at 2theta/TOF/E(KeV):       22.0641  Intensity fixed to 1.0 and variance to 1E6
=> Zero counts at step no.    237 at 2theta/TOF/E(KeV):       22.1028  Intensity fixed to 1.0 and variance to 1E6
=> Zero counts at step no.    238 at 2theta/TOF/E(KeV):       22.1221  Intensity fixed to 1.0 and variance to 1E6
=> Zero counts at step no.    241 at 2theta/TOF/E(KeV):       22.1801  Intensity fixed to 1.0 and variance to 1E6
=> Zero counts at step no.    243 at 2theta/TOF/E(KeV):       22.2188  Intensity fixed to 1.0 and variance to 1E6
=> Zero counts at step no.    244 at 2theta/TOF/E(KeV):       22.2381  Intensity fixed to 1.0 and variance to 1E6
=> Zero counts at step no.    245 at 2theta/TOF/E(KeV):       22.2575  Intensity fixed to 1.0 and variance to 1E6
=> Zero counts at step no.    248 at 2theta/TOF/E(KeV):       22.3155  Intensity fixed to 1.0 and variance to 1E6
=> Zero counts at step no.    250 at 2theta/TOF/E(KeV):       22.3541  Intensity fixed to 1.0 and variance to 1E6
=> Zero counts at step no.    252 at 2theta/TOF/E(KeV):       22.3928  Intensity fixed to 1.0 and variance to 1E6
=> Zero counts at step no.    253 at 2theta/TOF/E(KeV):       22.4121  Intensity fixed to 1.0 and variance to 1E6
=> Zero counts at step no.    256 at 2theta/TOF/E(KeV):       22.4701  Intensity fixed to 1.0 and variance to 1E6
=> Zero counts at step no.    258 at 2theta/TOF/E(KeV):       22.5088  Intensity fixed to 1.0 and variance to 1E6
=> Zero counts at step no.    260 at 2theta/TOF/E(KeV):       22.5474  Intensity fixed to 1.0 and variance to 1E6
=> Zero counts at step no.    271 at 2theta/TOF/E(KeV):       22.7601  Intensity fixed to 1.0 and variance to 1E6
=> Zero counts at step no.    272 at 2theta/TOF/E(KeV):       22.7794  Intensity fixed to 1.0 and variance to 1E6
=> Zero counts at step no.    273 at 2theta/TOF/E(KeV):       22.7988  Intensity fixed to 1.0 and variance to 1E6
=> Zero counts at step no.    275 at 2theta/TOF/E(KeV):       22.8374  Intensity fixed to 1.0 and variance to 1E6
=> Zero counts at step no.    278 at 2theta/TOF/E(KeV):       22.8954  Intensity fixed to 1.0 and variance to 1E6
=> Zero counts at step no.    279 at 2theta/TOF/E(KeV):       22.9147  Intensity fixed to 1.0 and variance to 1E6
=> Zero counts at step no.    280 at 2theta/TOF/E(KeV):       22.9341  Intensity fixed to 1.0 and variance to 1E6
=> Zero counts at step no.    282 at 2theta/TOF/E(KeV):       22.9727  Intensity fixed to 1.0 and variance to 1E6
=> Zero counts at step no.    284 at 2theta/TOF/E(KeV):       23.0114  Intensity fixed to 1.0 and variance to 1E6
=> Zero counts at step no.    287 at 2theta/TOF/E(KeV):       23.0694  Intensity fixed to 1.0 and variance to 1E6
=> Zero counts at step no.    297 at 2theta/TOF/E(KeV):       23.2627  Intensity fixed to 1.0 and variance to 1E6
=> Zero counts at step no.    300 at 2theta/TOF/E(KeV):       23.3207  Intensity fixed to 1.0 and variance to 1E6
=> Zero counts at step no.    306 at 2theta/TOF/E(KeV):       23.4367  Intensity fixed to 1.0 and variance to 1E6
=> Zero counts at step no.    311 at 2theta/TOF/E(KeV):       23.5334  Intensity fixed to 1.0 and variance to 1E6
=> Zero counts at step no.    313 at 2theta/TOF/E(KeV):       23.5720  Intensity fixed to 1.0 and variance to 1E6
=> Zero counts at step no.    315 at 2theta/TOF/E(KeV):       23.6107  Intensity fixed to 1.0 and variance to 1E6
=> Zero counts at step no.    316 at 2theta/TOF/E(KeV):       23.6300  Intensity fixed to 1.0 and variance to 1E6
```

```
=> Zero counts at step no.    317 at 2theta/TOF/E(KeV):      23.6494  Intensity fixed to 1.0 and variance to 1E6
=> Zero counts at step no.    332 at 2theta/TOF/E(KeV):      23.9393  Intensity fixed to 1.0 and variance to 1E6
=> Zero counts at step no.    333 at 2theta/TOF/E(KeV):      23.9587  Intensity fixed to 1.0 and variance to 1E6
=> Zero counts at step no.    336 at 2theta/TOF/E(KeV):      24.0167  Intensity fixed to 1.0 and variance to 1E6
=> Zero counts at step no.    345 at 2theta/TOF/E(KeV):      24.1907  Intensity fixed to 1.0 and variance to 1E6
=> Zero counts at step no.    347 at 2theta/TOF/E(KeV):      24.2293  Intensity fixed to 1.0 and variance to 1E6
=> Zero counts at step no.    357 at 2theta/TOF/E(KeV):      24.4226  Intensity fixed to 1.0 and variance to 1E6
=> Zero counts at step no.    358 at 2theta/TOF/E(KeV):      24.4420  Intensity fixed to 1.0 and variance to 1E6
=> Zero counts at step no.    365 at 2theta/TOF/E(KeV):      24.5773  Intensity fixed to 1.0 and variance to 1E6
=> Zero counts at step no.    382 at 2theta/TOF/E(KeV):      24.9059  Intensity fixed to 1.0 and variance to 1E6
=> Zero counts at step no.    385 at 2theta/TOF/E(KeV):      24.9639  Intensity fixed to 1.0 and variance to 1E6
=> Zero counts at step no.    387 at 2theta/TOF/E(KeV):      25.0026  Intensity fixed to 1.0 and variance to 1E6
=> Zero counts at step no.    390 at 2theta/TOF/E(KeV):      25.0606  Intensity fixed to 1.0 and variance to 1E6
=> Zero counts at step no.    394 at 2theta/TOF/E(KeV):      25.1379  Intensity fixed to 1.0 and variance to 1E6
=> Zero counts at step no.    397 at 2theta/TOF/E(KeV):      25.1959  Intensity fixed to 1.0 and variance to 1E6
=> Zero counts at step no.    404 at 2theta/TOF/E(KeV):      25.3312  Intensity fixed to 1.0 and variance to 1E6
=> Zero counts at step no.    405 at 2theta/TOF/E(KeV):      25.3506  Intensity fixed to 1.0 and variance to 1E6
=> Zero counts at step no.    416 at 2theta/TOF/E(KeV):      25.5632  Intensity fixed to 1.0 and variance to 1E6
=> Zero counts at step no.    421 at 2theta/TOF/E(KeV):      25.6599  Intensity fixed to 1.0 and variance to 1E6
=> Zero counts at step no.    424 at 2theta/TOF/E(KeV):      25.7179  Intensity fixed to 1.0 and variance to 1E6
=> Zero counts at step no.    425 at 2theta/TOF/E(KeV):      25.7372  Intensity fixed to 1.0 and variance to 1E6
=> Zero counts at step no.    433 at 2theta/TOF/E(KeV):      25.8919  Intensity fixed to 1.0 and variance to 1E6
=> Zero counts at step no.    436 at 2theta/TOF/E(KeV):      25.9498  Intensity fixed to 1.0 and variance to 1E6
=> Zero counts at step no.    439 at 2theta/TOF/E(KeV):      26.0078  Intensity fixed to 1.0 and variance to 1E6
=> Zero counts at step no.    440 at 2theta/TOF/E(KeV):      26.0272  Intensity fixed to 1.0 and variance to 1E6
=> Zero counts at step no.    441 at 2theta/TOF/E(KeV):      26.0465  Intensity fixed to 1.0 and variance to 1E6
=> Zero counts at step no.    448 at 2theta/TOF/E(KeV):      26.1818  Intensity fixed to 1.0 and variance to 1E6
=> Zero counts at step no.    455 at 2theta/TOF/E(KeV):      26.3172  Intensity fixed to 1.0 and variance to 1E6
=> Zero counts at step no.    460 at 2theta/TOF/E(KeV):      26.4138  Intensity fixed to 1.0 and variance to 1E6
=> Zero counts at step no.    467 at 2theta/TOF/E(KeV):      26.5491  Intensity fixed to 1.0 and variance to 1E6
=> Zero counts at step no.    471 at 2theta/TOF/E(KeV):      26.6265  Intensity fixed to 1.0 and variance to 1E6
=> Zero counts at step no.    472 at 2theta/TOF/E(KeV):      26.6458  Intensity fixed to 1.0 and variance to 1E6
=> Zero counts at step no.    491 at 2theta/TOF/E(KeV):      27.0131  Intensity fixed to 1.0 and variance to 1E6
=> Zero counts at step no.    498 at 2theta/TOF/E(KeV):      27.1484  Intensity fixed to 1.0 and variance to 1E6
=> Zero counts at step no.    502 at 2theta/TOF/E(KeV):      27.2257  Intensity fixed to 1.0 and variance to 1E6
=> Zero counts at step no.    512 at 2theta/TOF/E(KeV):      27.4191  Intensity fixed to 1.0 and variance to 1E6
=> Zero counts at step no.    513 at 2theta/TOF/E(KeV):      27.4384  Intensity fixed to 1.0 and variance to 1E6
=> Zero counts at step no.    515 at 2theta/TOF/E(KeV):      27.4771  Intensity fixed to 1.0 and variance to 1E6
=> Zero counts at step no.    517 at 2theta/TOF/E(KeV):      27.5157  Intensity fixed to 1.0 and variance to 1E6
=> Zero counts at step no.    522 at 2theta/TOF/E(KeV):      27.6124  Intensity fixed to 1.0 and variance to 1E6
=> Zero counts at step no.    523 at 2theta/TOF/E(KeV):      27.6317  Intensity fixed to 1.0 and variance to 1E6
=> Zero counts at step no.    533 at 2theta/TOF/E(KeV):      27.8250  Intensity fixed to 1.0 and variance to 1E6
=> Zero counts at step no.    541 at 2theta/TOF/E(KeV):      27.9797  Intensity fixed to 1.0 and variance to 1E6
=> Zero counts at step no.    543 at 2theta/TOF/E(KeV):      28.0184  Intensity fixed to 1.0 and variance to 1E6
=> Zero counts at step no.    544 at 2theta/TOF/E(KeV):      28.0377  Intensity fixed to 1.0 and variance to 1E6
=> Zero counts at step no.    549 at 2theta/TOF/E(KeV):      28.1343  Intensity fixed to 1.0 and variance to 1E6
=> Zero counts at step no.    550 at 2theta/TOF/E(KeV):      28.1537  Intensity fixed to 1.0 and variance to 1E6
=> Zero counts at step no.    551 at 2theta/TOF/E(KeV):      28.1730  Intensity fixed to 1.0 and variance to 1E6
=> Zero counts at step no.    555 at 2theta/TOF/E(KeV):      28.2503  Intensity fixed to 1.0 and variance to 1E6
=> Zero counts at step no.    557 at 2theta/TOF/E(KeV):      28.2890  Intensity fixed to 1.0 and variance to 1E6
=> Zero counts at step no.    571 at 2theta/TOF/E(KeV):      28.5596  Intensity fixed to 1.0 and variance to 1E6
=> Zero counts at step no.    578 at 2theta/TOF/E(KeV):      28.6950  Intensity fixed to 1.0 and variance to 1E6
=> Zero counts at step no.    579 at 2theta/TOF/E(KeV):      28.7143  Intensity fixed to 1.0 and variance to 1E6
=> Zero counts at step no.    582 at 2theta/TOF/E(KeV):      28.7723  Intensity fixed to 1.0 and variance to 1E6
=> Zero counts at step no.    583 at 2theta/TOF/E(KeV):      28.7916  Intensity fixed to 1.0 and variance to 1E6
=> Zero counts at step no.    584 at 2theta/TOF/E(KeV):      28.8110  Intensity fixed to 1.0 and variance to 1E6
=> Zero counts at step no.    585 at 2theta/TOF/E(KeV):      28.8303  Intensity fixed to 1.0 and variance to 1E6
=> Zero counts at step no.    587 at 2theta/TOF/E(KeV):      28.8690  Intensity fixed to 1.0 and variance to 1E6
=> Zero counts at step no.    592 at 2theta/TOF/E(KeV):      28.9656  Intensity fixed to 1.0 and variance to 1E6
=> Zero counts at step no.    603 at 2theta/TOF/E(KeV):      29.1783  Intensity fixed to 1.0 and variance to 1E6
=> Zero counts at step no.    699 at 2theta/TOF/E(KeV):      31.0341  Intensity fixed to 1.0 and variance to 1E6
=> Zero counts at step no.    707 at 2theta/TOF/E(KeV):      31.1888  Intensity fixed to 1.0 and variance to 1E6
=> Zero counts at step no.    720 at 2theta/TOF/E(KeV):      31.4401  Intensity fixed to 1.0 and variance to 1E6
=> Zero counts at step no.    724 at 2theta/TOF/E(KeV):      31.5174  Intensity fixed to 1.0 and variance to 1E6
=> Zero counts at step no.    725 at 2theta/TOF/E(KeV):      31.5367  Intensity fixed to 1.0 and variance to 1E6
=> Zero counts at step no.    726 at 2theta/TOF/E(KeV):      31.5561  Intensity fixed to 1.0 and variance to 1E6
=> Zero counts at step no.    732 at 2theta/TOF/E(KeV):      31.6721  Intensity fixed to 1.0 and variance to 1E6
=> Zero counts at step no.    735 at 2theta/TOF/E(KeV):      31.7301  Intensity fixed to 1.0 and variance to 1E6
=> Zero counts at step no.    737 at 2theta/TOF/E(KeV):      31.7687  Intensity fixed to 1.0 and variance to 1E6
=> Zero counts at step no.    742 at 2theta/TOF/E(KeV):      31.8654  Intensity fixed to 1.0 and variance to 1E6
=> Zero counts at step no.    751 at 2theta/TOF/E(KeV):      32.0394  Intensity fixed to 1.0 and variance to 1E6
=> Zero counts at step no.    757 at 2theta/TOF/E(KeV):      32.1554  Intensity fixed to 1.0 and variance to 1E6
=> Zero counts at step no.    759 at 2theta/TOF/E(KeV):      32.1940  Intensity fixed to 1.0 and variance to 1E6
=> Zero counts at step no.    760 at 2theta/TOF/E(KeV):      32.2134  Intensity fixed to 1.0 and variance to 1E6
=> Zero counts at step no.    767 at 2theta/TOF/E(KeV):      32.3487  Intensity fixed to 1.0 and variance to 1E6
=> Zero counts at step no.    768 at 2theta/TOF/E(KeV):      32.3680  Intensity fixed to 1.0 and variance to 1E6
=> Zero counts at step no.    771 at 2theta/TOF/E(KeV):      32.4260  Intensity fixed to 1.0 and variance to 1E6
=> Zero counts at step no.    777 at 2theta/TOF/E(KeV):      32.5420  Intensity fixed to 1.0 and variance to 1E6
=> Zero counts at step no.    780 at 2theta/TOF/E(KeV):      32.6000  Intensity fixed to 1.0 and variance to 1E6
=> Zero counts at step no.    786 at 2theta/TOF/E(KeV):      32.7160  Intensity fixed to 1.0 and variance to 1E6
=> Zero counts at step no.    788 at 2theta/TOF/E(KeV):      32.7547  Intensity fixed to 1.0 and variance to 1E6
=> Zero counts at step no.    796 at 2theta/TOF/E(KeV):      32.9093  Intensity fixed to 1.0 and variance to 1E6
=> Zero counts at step no.    799 at 2theta/TOF/E(KeV):      32.9673  Intensity fixed to 1.0 and variance to 1E6
=> Zero counts at step no.    800 at 2theta/TOF/E(KeV):      32.9866  Intensity fixed to 1.0 and variance to 1E6
=> Zero counts at step no.    805 at 2theta/TOF/E(KeV):      33.0833  Intensity fixed to 1.0 and variance to 1E6
=> Zero counts at step no.    811 at 2theta/TOF/E(KeV):      33.1993  Intensity fixed to 1.0 and variance to 1E6
=> Zero counts at step no.    815 at 2theta/TOF/E(KeV):      33.2766  Intensity fixed to 1.0 and variance to 1E6
=> Zero counts at step no.    835 at 2theta/TOF/E(KeV):      33.6632  Intensity fixed to 1.0 and variance to 1E6
=> Zero counts at step no.    836 at 2theta/TOF/E(KeV):      33.6826  Intensity fixed to 1.0 and variance to 1E6
=> Zero counts at step no.    837 at 2theta/TOF/E(KeV):      33.7019  Intensity fixed to 1.0 and variance to 1E6
```

```
=> Zero counts at step no.    844 at 2theta/TOF/E(KeV):       33.8372  Intensity fixed to 1.0 and variance to 1E6
=> Zero counts at step no.    858 at 2theta/TOF/E(KeV):       34.1079  Intensity fixed to 1.0 and variance to 1E6
=> Zero counts at step no.    885 at 2theta/TOF/E(KeV):       34.6298  Intensity fixed to 1.0 and variance to 1E6
=> Zero counts at step no.    887 at 2theta/TOF/E(KeV):       34.6685  Intensity fixed to 1.0 and variance to 1E6
=> Zero counts at step no.    896 at 2theta/TOF/E(KeV):       34.8425  Intensity fixed to 1.0 and variance to 1E6
=> Zero counts at step no.    902 at 2theta/TOF/E(KeV):       34.9585  Intensity fixed to 1.0 and variance to 1E6
=> Zero counts at step no.    907 at 2theta/TOF/E(KeV):       35.0551  Intensity fixed to 1.0 and variance to 1E6
=> Zero counts at step no.    927 at 2theta/TOF/E(KeV):       35.4418  Intensity fixed to 1.0 and variance to 1E6
=> Zero counts at step no.    932 at 2theta/TOF/E(KeV):       35.5384  Intensity fixed to 1.0 and variance to 1E6
=> Zero counts at step no.    934 at 2theta/TOF/E(KeV):       35.5771  Intensity fixed to 1.0 and variance to 1E6
=> Zero counts at step no.    937 at 2theta/TOF/E(KeV):       35.6351  Intensity fixed to 1.0 and variance to 1E6
=> Zero counts at step no.    941 at 2theta/TOF/E(KeV):       35.7124  Intensity fixed to 1.0 and variance to 1E6
=> Zero counts at step no.    943 at 2theta/TOF/E(KeV):       35.7511  Intensity fixed to 1.0 and variance to 1E6
=> Zero counts at step no.    944 at 2theta/TOF/E(KeV):       35.7704  Intensity fixed to 1.0 and variance to 1E6
=> Zero counts at step no.    945 at 2theta/TOF/E(KeV):       35.7897  Intensity fixed to 1.0 and variance to 1E6
=> Zero counts at step no.    953 at 2theta/TOF/E(KeV):       35.9444  Intensity fixed to 1.0 and variance to 1E6
=> Zero counts at step no.    956 at 2theta/TOF/E(KeV):       36.0024  Intensity fixed to 1.0 and variance to 1E6
=> Zero counts at step no.    957 at 2theta/TOF/E(KeV):       36.0217  Intensity fixed to 1.0 and variance to 1E6
=> Zero counts at step no.    959 at 2theta/TOF/E(KeV):       36.0604  Intensity fixed to 1.0 and variance to 1E6
=> Zero counts at step no.    963 at 2theta/TOF/E(KeV):       36.1377  Intensity fixed to 1.0 and variance to 1E6
=> Zero counts at step no.    969 at 2theta/TOF/E(KeV):       36.2537  Intensity fixed to 1.0 and variance to 1E6
=> Zero counts at step no.    970 at 2theta/TOF/E(KeV):       36.2730  Intensity fixed to 1.0 and variance to 1E6
=> Zero counts at step no.    982 at 2theta/TOF/E(KeV):       36.5050  Intensity fixed to 1.0 and variance to 1E6
=> Zero counts at step no.    992 at 2theta/TOF/E(KeV):       36.6983  Intensity fixed to 1.0 and variance to 1E6
=> Zero counts at step no.    996 at 2theta/TOF/E(KeV):       36.7757  Intensity fixed to 1.0 and variance to 1E6
=> Zero counts at step no.   1005 at 2theta/TOF/E(KeV):       36.9497  Intensity fixed to 1.0 and variance to 1E6
=> Zero counts at step no.   1063 at 2theta/TOF/E(KeV):       38.0709  Intensity fixed to 1.0 and variance to 1E6
=> Zero counts at step no.   1068 at 2theta/TOF/E(KeV):       38.1676  Intensity fixed to 1.0 and variance to 1E6
=> Zero counts at step no.   1070 at 2theta/TOF/E(KeV):       38.2062  Intensity fixed to 1.0 and variance to 1E6
=> Zero counts at step no.   1071 at 2theta/TOF/E(KeV):       38.2256  Intensity fixed to 1.0 and variance to 1E6
=> Zero counts at step no.   1074 at 2theta/TOF/E(KeV):       38.2836  Intensity fixed to 1.0 and variance to 1E6
=> Zero counts at step no.   1081 at 2theta/TOF/E(KeV):       38.4189  Intensity fixed to 1.0 and variance to 1E6
=> Zero counts at step no.   1085 at 2theta/TOF/E(KeV):       38.4962  Intensity fixed to 1.0 and variance to 1E6
=> Zero counts at step no.   1090 at 2theta/TOF/E(KeV):       38.5929  Intensity fixed to 1.0 and variance to 1E6
=> Zero counts at step no.   1093 at 2theta/TOF/E(KeV):       38.6509  Intensity fixed to 1.0 and variance to 1E6
=> Zero counts at step no.   1094 at 2theta/TOF/E(KeV):       38.6702  Intensity fixed to 1.0 and variance to 1E6
=> Zero counts at step no.   1105 at 2theta/TOF/E(KeV):       38.8828  Intensity fixed to 1.0 and variance to 1E6
=> Zero counts at step no.   1107 at 2theta/TOF/E(KeV):       38.9215  Intensity fixed to 1.0 and variance to 1E6
=> Zero counts at step no.   1108 at 2theta/TOF/E(KeV):       38.9408  Intensity fixed to 1.0 and variance to 1E6
=> Zero counts at step no.   1111 at 2theta/TOF/E(KeV):       38.9988  Intensity fixed to 1.0 and variance to 1E6
=> Zero counts at step no.   1112 at 2theta/TOF/E(KeV):       39.0182  Intensity fixed to 1.0 and variance to 1E6
=> Zero counts at step no.   1125 at 2theta/TOF/E(KeV):       39.2695  Intensity fixed to 1.0 and variance to 1E6
=> Zero counts at step no.   1155 at 2theta/TOF/E(KeV):       39.8494  Intensity fixed to 1.0 and variance to 1E6
=> Zero counts at step no.   1188 at 2theta/TOF/E(KeV):       40.4874  Intensity fixed to 1.0 and variance to 1E6
=> Zero counts at step no.   1189 at 2theta/TOF/E(KeV):       40.5067  Intensity fixed to 1.0 and variance to 1E6
=> Zero counts at step no.   1192 at 2theta/TOF/E(KeV):       40.5647  Intensity fixed to 1.0 and variance to 1E6
=> Zero counts at step no.   1195 at 2theta/TOF/E(KeV):       40.6227  Intensity fixed to 1.0 and variance to 1E6
=> Zero counts at step no.   1196 at 2theta/TOF/E(KeV):       40.6420  Intensity fixed to 1.0 and variance to 1E6
=> Zero counts at step no.   1200 at 2theta/TOF/E(KeV):       40.7194  Intensity fixed to 1.0 and variance to 1E6
=> Zero counts at step no.   1212 at 2theta/TOF/E(KeV):       40.9513  Intensity fixed to 1.0 and variance to 1E6
=> Zero counts at step no.   1214 at 2theta/TOF/E(KeV):       40.9900  Intensity fixed to 1.0 and variance to 1E6
=> Zero counts at step no.   1215 at 2theta/TOF/E(KeV):       41.0093  Intensity fixed to 1.0 and variance to 1E6
=> Zero counts at step no.   1223 at 2theta/TOF/E(KeV):       41.1640  Intensity fixed to 1.0 and variance to 1E6
=> Zero counts at step no.   1226 at 2theta/TOF/E(KeV):       41.2220  Intensity fixed to 1.0 and variance to 1E6
=> Zero counts at step no.   1231 at 2theta/TOF/E(KeV):       41.3186  Intensity fixed to 1.0 and variance to 1E6
=> Zero counts at step no.   1238 at 2theta/TOF/E(KeV):       41.4540  Intensity fixed to 1.0 and variance to 1E6
=> Zero counts at step no.   1242 at 2theta/TOF/E(KeV):       41.5313  Intensity fixed to 1.0 and variance to 1E6
=> Zero counts at step no.   1249 at 2theta/TOF/E(KeV):       41.6666  Intensity fixed to 1.0 and variance to 1E6
=> Zero counts at step no.   1267 at 2theta/TOF/E(KeV):       42.0146  Intensity fixed to 1.0 and variance to 1E6
=> Zero counts at step no.   1283 at 2theta/TOF/E(KeV):       42.3239  Intensity fixed to 1.0 and variance to 1E6
=> Zero counts at step no.   1284 at 2theta/TOF/E(KeV):       42.3432  Intensity fixed to 1.0 and variance to 1E6
=> Zero counts at step no.   1292 at 2theta/TOF/E(KeV):       42.4979  Intensity fixed to 1.0 and variance to 1E6
=> Zero counts at step no.   1309 at 2theta/TOF/E(KeV):       42.8265  Intensity fixed to 1.0 and variance to 1E6
=> Zero counts at step no.   1396 at 2theta/TOF/E(KeV):       44.5084  Intensity fixed to 1.0 and variance to 1E6
=> Zero counts at step no.   1418 at 2theta/TOF/E(KeV):       44.9337  Intensity fixed to 1.0 and variance to 1E6
=> Zero counts at step no.   1419 at 2theta/TOF/E(KeV):       44.9530  Intensity fixed to 1.0 and variance to 1E6
=> Zero counts at step no.   1428 at 2theta/TOF/E(KeV):       45.1270  Intensity fixed to 1.0 and variance to 1E6
=> Zero counts at step no.   1444 at 2theta/TOF/E(KeV):       45.4363  Intensity fixed to 1.0 and variance to 1E6
=> Zero counts at step no.   1453 at 2theta/TOF/E(KeV):       45.6103  Intensity fixed to 1.0 and variance to 1E6
=> Zero counts at step no.   1457 at 2theta/TOF/E(KeV):       45.6876  Intensity fixed to 1.0 and variance to 1E6
=> Zero counts at step no.   1461 at 2theta/TOF/E(KeV):       45.7650  Intensity fixed to 1.0 and variance to 1E6
=> Zero counts at step no.   1476 at 2theta/TOF/E(KeV):       46.0549  Intensity fixed to 1.0 and variance to 1E6
=> Zero counts at step no.   1479 at 2theta/TOF/E(KeV):       46.1129  Intensity fixed to 1.0 and variance to 1E6
=> Zero counts at step no.   1491 at 2theta/TOF/E(KeV):       46.3449  Intensity fixed to 1.0 and variance to 1E6
=> Zero counts at step no.   1496 at 2theta/TOF/E(KeV):       46.4416  Intensity fixed to 1.0 and variance to 1E6
=> Zero counts at step no.   1497 at 2theta/TOF/E(KeV):       46.4609  Intensity fixed to 1.0 and variance to 1E6
=> Zero counts at step no.   1508 at 2theta/TOF/E(KeV):       46.6736  Intensity fixed to 1.0 and variance to 1E6
=> Zero counts at step no.   1515 at 2theta/TOF/E(KeV):       46.8089  Intensity fixed to 1.0 and variance to 1E6
=> Zero counts at step no.   1520 at 2theta/TOF/E(KeV):       46.9055  Intensity fixed to 1.0 and variance to 1E6
=> Zero counts at step no.   1521 at 2theta/TOF/E(KeV):       46.9249  Intensity fixed to 1.0 and variance to 1E6
=> Zero counts at step no.   1524 at 2theta/TOF/E(KeV):       46.9829  Intensity fixed to 1.0 and variance to 1E6
=> Zero counts at step no.   1538 at 2theta/TOF/E(KeV):       47.2535  Intensity fixed to 1.0 and variance to 1E6
=> Zero counts at step no.   1573 at 2theta/TOF/E(KeV):       47.9301  Intensity fixed to 1.0 and variance to 1E6
=> Zero counts at step no.   1663 at 2theta/TOF/E(KeV):       49.6700  Intensity fixed to 1.0 and variance to 1E6
=> Zero counts at step no.   1689 at 2theta/TOF/E(KeV):       50.1726  Intensity fixed to 1.0 and variance to 1E6
=> Zero counts at step no.   1691 at 2theta/TOF/E(KeV):       50.2113  Intensity fixed to 1.0 and variance to 1E6
=> Zero counts at step no.   1693 at 2theta/TOF/E(KeV):       50.2500  Intensity fixed to 1.0 and variance to 1E6
=> Zero counts at step no.   1694 at 2theta/TOF/E(KeV):       50.2693  Intensity fixed to 1.0 and variance to 1E6
=> Zero counts at step no.   1696 at 2theta/TOF/E(KeV):       50.3080  Intensity fixed to 1.0 and variance to 1E6
=> Zero counts at step no.   1708 at 2theta/TOF/E(KeV):       50.5399  Intensity fixed to 1.0 and variance to 1E6
```

```
=> Zero counts at step no.   1717 at 2theta/TOF/E(KeV):      50.7139  Intensity fixed to 1.0 and variance to 1E6
=> Zero counts at step no.   1718 at 2theta/TOF/E(KeV):      50.7333  Intensity fixed to 1.0 and variance to 1E6
=> Zero counts at step no.   1722 at 2theta/TOF/E(KeV):      50.8106  Intensity fixed to 1.0 and variance to 1E6
=> Zero counts at step no.   1723 at 2theta/TOF/E(KeV):      50.8299  Intensity fixed to 1.0 and variance to 1E6
=> Zero counts at step no.   1731 at 2theta/TOF/E(KeV):      50.9846  Intensity fixed to 1.0 and variance to 1E6
=> Zero counts at step no.   1739 at 2theta/TOF/E(KeV):      51.1392  Intensity fixed to 1.0 and variance to 1E6
=> Zero counts at step no.   1748 at 2theta/TOF/E(KeV):      51.3132  Intensity fixed to 1.0 and variance to 1E6
=> Zero counts at step no.   1752 at 2theta/TOF/E(KeV):      51.3905  Intensity fixed to 1.0 and variance to 1E6
=> Zero counts at step no.   1755 at 2theta/TOF/E(KeV):      51.4485  Intensity fixed to 1.0 and variance to 1E6
=> Zero counts at step no.   1763 at 2theta/TOF/E(KeV):      51.6032  Intensity fixed to 1.0 and variance to 1E6
=> Zero counts at step no.   1772 at 2theta/TOF/E(KeV):      51.7772  Intensity fixed to 1.0 and variance to 1E6
=> Zero counts at step no.   1775 at 2theta/TOF/E(KeV):      51.8352  Intensity fixed to 1.0 and variance to 1E6
=> Zero counts at step no.   1776 at 2theta/TOF/E(KeV):      51.8545  Intensity fixed to 1.0 and variance to 1E6
=> Zero counts at step no.   1777 at 2theta/TOF/E(KeV):      51.8738  Intensity fixed to 1.0 and variance to 1E6
=> Zero counts at step no.   1780 at 2theta/TOF/E(KeV):      51.9318  Intensity fixed to 1.0 and variance to 1E6
=> Zero counts at step no.   1781 at 2theta/TOF/E(KeV):      51.9512  Intensity fixed to 1.0 and variance to 1E6
=> Zero counts at step no.   1783 at 2theta/TOF/E(KeV):      51.9898  Intensity fixed to 1.0 and variance to 1E6
=> Zero counts at step no.   1785 at 2theta/TOF/E(KeV):      52.0285  Intensity fixed to 1.0 and variance to 1E6
=> Zero counts at step no.   1792 at 2theta/TOF/E(KeV):      52.1638  Intensity fixed to 1.0 and variance to 1E6
=> Zero counts at step no.   1796 at 2theta/TOF/E(KeV):      52.2411  Intensity fixed to 1.0 and variance to 1E6
=> Zero counts at step no.   1807 at 2theta/TOF/E(KeV):      52.4538  Intensity fixed to 1.0 and variance to 1E6
=> Zero counts at step no.   1809 at 2theta/TOF/E(KeV):      52.4924  Intensity fixed to 1.0 and variance to 1E6
=> Zero counts at step no.   1810 at 2theta/TOF/E(KeV):      52.5118  Intensity fixed to 1.0 and variance to 1E6
=> Zero counts at step no.   1824 at 2theta/TOF/E(KeV):      52.7824  Intensity fixed to 1.0 and variance to 1E6
=> Zero counts at step no.   1826 at 2theta/TOF/E(KeV):      52.8211  Intensity fixed to 1.0 and variance to 1E6
=> Zero counts at step no.   1828 at 2theta/TOF/E(KeV):      52.8598  Intensity fixed to 1.0 and variance to 1E6
=> Zero counts at step no.   1829 at 2theta/TOF/E(KeV):      52.8791  Intensity fixed to 1.0 and variance to 1E6
=> Zero counts at step no.   1834 at 2theta/TOF/E(KeV):      52.9757  Intensity fixed to 1.0 and variance to 1E6
=> Zero counts at step no.   1930 at 2theta/TOF/E(KeV):      54.8316  Intensity fixed to 1.0 and variance to 1E6
=> Zero counts at step no.   1938 at 2theta/TOF/E(KeV):      54.9863  Intensity fixed to 1.0 and variance to 1E6
=> Zero counts at step no.   1957 at 2theta/TOF/E(KeV):      55.3536  Intensity fixed to 1.0 and variance to 1E6
=> Zero counts at step no.   1958 at 2theta/TOF/E(KeV):      55.3729  Intensity fixed to 1.0 and variance to 1E6
=> Zero counts at step no.   1960 at 2theta/TOF/E(KeV):      55.4116  Intensity fixed to 1.0 and variance to 1E6
=> Zero counts at step no.   1962 at 2theta/TOF/E(KeV):      55.4502  Intensity fixed to 1.0 and variance to 1E6
=> Zero counts at step no.   1963 at 2theta/TOF/E(KeV):      55.4696  Intensity fixed to 1.0 and variance to 1E6
=> Zero counts at step no.   1969 at 2theta/TOF/E(KeV):      55.5855  Intensity fixed to 1.0 and variance to 1E6
=> Zero counts at step no.   1971 at 2theta/TOF/E(KeV):      55.6242  Intensity fixed to 1.0 and variance to 1E6
=> Zero counts at step no.   1974 at 2theta/TOF/E(KeV):      55.6822  Intensity fixed to 1.0 and variance to 1E6
=> Zero counts at step no.   1975 at 2theta/TOF/E(KeV):      55.7015  Intensity fixed to 1.0 and variance to 1E6
=> Zero counts at step no.   1980 at 2theta/TOF/E(KeV):      55.7982  Intensity fixed to 1.0 and variance to 1E6
=> Zero counts at step no.   1993 at 2theta/TOF/E(KeV):      56.0495  Intensity fixed to 1.0 and variance to 1E6
=> Zero counts at step no.   1994 at 2theta/TOF/E(KeV):      56.0688  Intensity fixed to 1.0 and variance to 1E6
=> Zero counts at step no.   1999 at 2theta/TOF/E(KeV):      56.1655  Intensity fixed to 1.0 and variance to 1E6
=> Zero counts at step no.   2000 at 2theta/TOF/E(KeV):      56.1848  Intensity fixed to 1.0 and variance to 1E6
=> Zero counts at step no.   2005 at 2theta/TOF/E(KeV):      56.2815  Intensity fixed to 1.0 and variance to 1E6
=> Zero counts at step no.   2008 at 2theta/TOF/E(KeV):      56.3395  Intensity fixed to 1.0 and variance to 1E6
=> Zero counts at step no.   2009 at 2theta/TOF/E(KeV):      56.3588  Intensity fixed to 1.0 and variance to 1E6
=> Zero counts at step no.   2011 at 2theta/TOF/E(KeV):      56.3975  Intensity fixed to 1.0 and variance to 1E6
=> Zero counts at step no.   2020 at 2theta/TOF/E(KeV):      56.5715  Intensity fixed to 1.0 and variance to 1E6
=> Zero counts at step no.   2022 at 2theta/TOF/E(KeV):      56.6101  Intensity fixed to 1.0 and variance to 1E6
=> Zero counts at step no.   2023 at 2theta/TOF/E(KeV):      56.6295  Intensity fixed to 1.0 and variance to 1E6
=> Zero counts at step no.   2026 at 2theta/TOF/E(KeV):      56.6875  Intensity fixed to 1.0 and variance to 1E6
=> Zero counts at step no.   2033 at 2theta/TOF/E(KeV):      56.8228  Intensity fixed to 1.0 and variance to 1E6
=> Zero counts at step no.   2034 at 2theta/TOF/E(KeV):      56.8421  Intensity fixed to 1.0 and variance to 1E6
=> Zero counts at step no.   2048 at 2theta/TOF/E(KeV):      57.1128  Intensity fixed to 1.0 and variance to 1E6
=> Zero counts at step no.   2049 at 2theta/TOF/E(KeV):      57.1321  Intensity fixed to 1.0 and variance to 1E6
=> Zero counts at step no.   2054 at 2theta/TOF/E(KeV):      57.2287  Intensity fixed to 1.0 and variance to 1E6
=> Zero counts at step no.   2056 at 2theta/TOF/E(KeV):      57.2674  Intensity fixed to 1.0 and variance to 1E6
=> Zero counts at step no.   2057 at 2theta/TOF/E(KeV):      57.2867  Intensity fixed to 1.0 and variance to 1E6
=> Zero counts at step no.   2062 at 2theta/TOF/E(KeV):      57.3834  Intensity fixed to 1.0 and variance to 1E6
=> Zero counts at step no.   2075 at 2theta/TOF/E(KeV):      57.6347  Intensity fixed to 1.0 and variance to 1E6
=> Zero counts at step no.   2076 at 2theta/TOF/E(KeV):      57.6540  Intensity fixed to 1.0 and variance to 1E6
=> Zero counts at step no.   2078 at 2theta/TOF/E(KeV):      57.6927  Intensity fixed to 1.0 and variance to 1E6
=> Zero counts at step no.   2087 at 2theta/TOF/E(KeV):      57.8667  Intensity fixed to 1.0 and variance to 1E6
=> Zero counts at step no.   2090 at 2theta/TOF/E(KeV):      57.9247  Intensity fixed to 1.0 and variance to 1E6
=> Zero counts at step no.   2092 at 2theta/TOF/E(KeV):      57.9634  Intensity fixed to 1.0 and variance to 1E6
=> Zero counts at step no.   2104 at 2theta/TOF/E(KeV):      58.1953  Intensity fixed to 1.0 and variance to 1E6
=> Zero counts at step no.   2107 at 2theta/TOF/E(KeV):      58.2533  Intensity fixed to 1.0 and variance to 1E6
=> Zero counts at step no.   2108 at 2theta/TOF/E(KeV):      58.2727  Intensity fixed to 1.0 and variance to 1E6
=> Zero counts at step no.   2109 at 2theta/TOF/E(KeV):      58.2920  Intensity fixed to 1.0 and variance to 1E6
=> Zero counts at step no.   2110 at 2theta/TOF/E(KeV):      58.3113  Intensity fixed to 1.0 and variance to 1E6
=> Zero counts at step no.   2126 at 2theta/TOF/E(KeV):      58.6206  Intensity fixed to 1.0 and variance to 1E6
=> Zero counts at step no.   2136 at 2theta/TOF/E(KeV):      58.8140  Intensity fixed to 1.0 and variance to 1E6
=> Zero counts at step no.   2143 at 2theta/TOF/E(KeV):      58.9493  Intensity fixed to 1.0 and variance to 1E6
=> Zero counts at step no.   2149 at 2theta/TOF/E(KeV):      59.0653  Intensity fixed to 1.0 and variance to 1E6
=> Zero counts at step no.   2152 at 2theta/TOF/E(KeV):      59.1233  Intensity fixed to 1.0 and variance to 1E6
=> Zero counts at step no.   2175 at 2theta/TOF/E(KeV):      59.5679  Intensity fixed to 1.0 and variance to 1E6
=> Zero counts at step no.   2180 at 2theta/TOF/E(KeV):      59.6646  Intensity fixed to 1.0 and variance to 1E6
=> Zero counts at step no.   2186 at 2theta/TOF/E(KeV):      59.7805  Intensity fixed to 1.0 and variance to 1E6
=> Zero counts at step no.   2191 at 2theta/TOF/E(KeV):      59.8772  Intensity fixed to 1.0 and variance to 1E6
=> Zero counts at step no.   2213 at 2theta/TOF/E(KeV):      60.3025  Intensity fixed to 1.0 and variance to 1E6
=> Zero counts at step no.   2214 at 2theta/TOF/E(KeV):      60.3218  Intensity fixed to 1.0 and variance to 1E6
=> Zero counts at step no.   2218 at 2theta/TOF/E(KeV):      60.3992  Intensity fixed to 1.0 and variance to 1E6
=> Zero counts at step no.   2221 at 2theta/TOF/E(KeV):      60.4572  Intensity fixed to 1.0 and variance to 1E6
=> Zero counts at step no.   2227 at 2theta/TOF/E(KeV):      60.5732  Intensity fixed to 1.0 and variance to 1E6
=> Zero counts at step no.   2228 at 2theta/TOF/E(KeV):      60.5925  Intensity fixed to 1.0 and variance to 1E6
=> Zero counts at step no.   2233 at 2theta/TOF/E(KeV):      60.6891  Intensity fixed to 1.0 and variance to 1E6
=> Zero counts at step no.   2236 at 2theta/TOF/E(KeV):      60.7471  Intensity fixed to 1.0 and variance to 1E6
=> Zero counts at step no.   2237 at 2theta/TOF/E(KeV):      60.7665  Intensity fixed to 1.0 and variance to 1E6
=> Zero counts at step no.   2240 at 2theta/TOF/E(KeV):      60.8245  Intensity fixed to 1.0 and variance to 1E6
```

```
=> Zero counts at step no.   2244 at 2theta/TOF/E(KeV):       60.9018  Intensity fixed to 1.0 and variance to 1E6
=> Zero counts at step no.   2246 at 2theta/TOF/E(KeV):       60.9405  Intensity fixed to 1.0 and variance to 1E6
=> Zero counts at step no.   2251 at 2theta/TOF/E(KeV):       61.0371  Intensity fixed to 1.0 and variance to 1E6
=> Zero counts at step no.   2270 at 2theta/TOF/E(KeV):       61.4044  Intensity fixed to 1.0 and variance to 1E6
=> Zero counts at step no.   2273 at 2theta/TOF/E(KeV):       61.4624  Intensity fixed to 1.0 and variance to 1E6
=> Zero counts at step no.   2274 at 2theta/TOF/E(KeV):       61.4818  Intensity fixed to 1.0 and variance to 1E6
=> Zero counts at step no.   2276 at 2theta/TOF/E(KeV):       61.5204  Intensity fixed to 1.0 and variance to 1E6
=> Zero counts at step no.   2282 at 2theta/TOF/E(KeV):       61.6364  Intensity fixed to 1.0 and variance to 1E6
=> Zero counts at step no.   2286 at 2theta/TOF/E(KeV):       61.7137  Intensity fixed to 1.0 and variance to 1E6
=> Zero counts at step no.   2287 at 2theta/TOF/E(KeV):       61.7331  Intensity fixed to 1.0 and variance to 1E6
=> Zero counts at step no.   2289 at 2theta/TOF/E(KeV):       61.7717  Intensity fixed to 1.0 and variance to 1E6
=> Zero counts at step no.   2295 at 2theta/TOF/E(KeV):       61.8877  Intensity fixed to 1.0 and variance to 1E6
=> Zero counts at step no.   2298 at 2theta/TOF/E(KeV):       61.9457  Intensity fixed to 1.0 and variance to 1E6
=> Zero counts at step no.   2309 at 2theta/TOF/E(KeV):       62.1584  Intensity fixed to 1.0 and variance to 1E6
=> Zero counts at step no.   2310 at 2theta/TOF/E(KeV):       62.1777  Intensity fixed to 1.0 and variance to 1E6
=> Zero counts at step no.   2317 at 2theta/TOF/E(KeV):       62.3130  Intensity fixed to 1.0 and variance to 1E6
=> Zero counts at step no.   2328 at 2theta/TOF/E(KeV):       62.5257  Intensity fixed to 1.0 and variance to 1E6
=> Zero counts at step no.   2331 at 2theta/TOF/E(KeV):       62.5837  Intensity fixed to 1.0 and variance to 1E6
=> Zero counts at step no.   2339 at 2theta/TOF/E(KeV):       62.7383  Intensity fixed to 1.0 and variance to 1E6
=> Zero counts at step no.   2380 at 2theta/TOF/E(KeV):       63.5309  Intensity fixed to 1.0 and variance to 1E6
=> Zero counts at step no.   2404 at 2theta/TOF/E(KeV):       63.9949  Intensity fixed to 1.0 and variance to 1E6
=> Zero counts at step no.   2419 at 2theta/TOF/E(KeV):       64.2849  Intensity fixed to 1.0 and variance to 1E6
=> Zero counts at step no.   2423 at 2theta/TOF/E(KeV):       64.3622  Intensity fixed to 1.0 and variance to 1E6
=> Zero counts at step no.   2425 at 2theta/TOF/E(KeV):       64.4009  Intensity fixed to 1.0 and variance to 1E6
=> Zero counts at step no.   2432 at 2theta/TOF/E(KeV):       64.5362  Intensity fixed to 1.0 and variance to 1E6
=> Zero counts at step no.   2436 at 2theta/TOF/E(KeV):       64.6135  Intensity fixed to 1.0 and variance to 1E6
=> Zero counts at step no.   2437 at 2theta/TOF/E(KeV):       64.6328  Intensity fixed to 1.0 and variance to 1E6
=> Zero counts at step no.   2441 at 2theta/TOF/E(KeV):       64.7102  Intensity fixed to 1.0 and variance to 1E6
=> Zero counts at step no.   2442 at 2theta/TOF/E(KeV):       64.7295  Intensity fixed to 1.0 and variance to 1E6
=> Zero counts at step no.   2444 at 2theta/TOF/E(KeV):       64.7682  Intensity fixed to 1.0 and variance to 1E6
=> Zero counts at step no.   2446 at 2theta/TOF/E(KeV):       64.8068  Intensity fixed to 1.0 and variance to 1E6
=> Zero counts at step no.   2447 at 2theta/TOF/E(KeV):       64.8262  Intensity fixed to 1.0 and variance to 1E6
=> Zero counts at step no.   2451 at 2theta/TOF/E(KeV):       64.9035  Intensity fixed to 1.0 and variance to 1E6
=> Zero counts at step no.   2456 at 2theta/TOF/E(KeV):       65.0001  Intensity fixed to 1.0 and variance to 1E6
=> Zero counts at step no.   2463 at 2theta/TOF/E(KeV):       65.1355  Intensity fixed to 1.0 and variance to 1E6
=> Zero counts at step no.   2476 at 2theta/TOF/E(KeV):       65.3868  Intensity fixed to 1.0 and variance to 1E6
=> Zero counts at step no.   2477 at 2theta/TOF/E(KeV):       65.4061  Intensity fixed to 1.0 and variance to 1E6
=> Zero counts at step no.   2479 at 2theta/TOF/E(KeV):       65.4448  Intensity fixed to 1.0 and variance to 1E6
=> Zero counts at step no.   2501 at 2theta/TOF/E(KeV):       65.8701  Intensity fixed to 1.0 and variance to 1E6
=> Zero counts at step no.   2509 at 2theta/TOF/E(KeV):       66.0247  Intensity fixed to 1.0 and variance to 1E6
=> Zero counts at step no.   2537 at 2theta/TOF/E(KeV):       66.5660  Intensity fixed to 1.0 and variance to 1E6
=> Zero counts at step no.   2628 at 2theta/TOF/E(KeV):       68.3252  Intensity fixed to 1.0 and variance to 1E6
=> Zero counts at step no.   2658 at 2theta/TOF/E(KeV):       68.9052  Intensity fixed to 1.0 and variance to 1E6
=> Zero counts at step no.   2665 at 2theta/TOF/E(KeV):       69.0405  Intensity fixed to 1.0 and variance to 1E6
=> Zero counts at step no.   2675 at 2theta/TOF/E(KeV):       69.2338  Intensity fixed to 1.0 and variance to 1E6
=> Zero counts at step no.   2683 at 2theta/TOF/E(KeV):       69.3885  Intensity fixed to 1.0 and variance to 1E6
=> Zero counts at step no.   2685 at 2theta/TOF/E(KeV):       69.4271  Intensity fixed to 1.0 and variance to 1E6
=> Zero counts at step no.   2690 at 2theta/TOF/E(KeV):       69.5238  Intensity fixed to 1.0 and variance to 1E6
=> Zero counts at step no.   2703 at 2theta/TOF/E(KeV):       69.7751  Intensity fixed to 1.0 and variance to 1E6
=> Zero counts at step no.   2709 at 2theta/TOF/E(KeV):       69.8911  Intensity fixed to 1.0 and variance to 1E6
=> Zero counts at step no.   2721 at 2theta/TOF/E(KeV):       70.1231  Intensity fixed to 1.0 and variance to 1E6
=> Zero counts at step no.   2724 at 2theta/TOF/E(KeV):       70.1811  Intensity fixed to 1.0 and variance to 1E6
=> Zero counts at step no.   2726 at 2theta/TOF/E(KeV):       70.2197  Intensity fixed to 1.0 and variance to 1E6
=> Zero counts at step no.   2742 at 2theta/TOF/E(KeV):       70.5290  Intensity fixed to 1.0 and variance to 1E6
=> Zero counts at step no.   2748 at 2theta/TOF/E(KeV):       70.6450  Intensity fixed to 1.0 and variance to 1E6
=> Zero counts at step no.   2763 at 2theta/TOF/E(KeV):       70.9350  Intensity fixed to 1.0 and variance to 1E6
=> Zero counts at step no.   2843 at 2theta/TOF/E(KeV):       72.4816  Intensity fixed to 1.0 and variance to 1E6
=> Zero counts at step no.   2875 at 2theta/TOF/E(KeV):       73.1002  Intensity fixed to 1.0 and variance to 1E6
=> Zero counts at step no.   2881 at 2theta/TOF/E(KeV):       73.2162  Intensity fixed to 1.0 and variance to 1E6
=> Zero counts at step no.   2894 at 2theta/TOF/E(KeV):       73.4675  Intensity fixed to 1.0 and variance to 1E6
=> Zero counts at step no.   2896 at 2theta/TOF/E(KeV):       73.5061  Intensity fixed to 1.0 and variance to 1E6
=> Zero counts at step no.   2897 at 2theta/TOF/E(KeV):       73.5255  Intensity fixed to 1.0 and variance to 1E6
=> Zero counts at step no.   2899 at 2theta/TOF/E(KeV):       73.5641  Intensity fixed to 1.0 and variance to 1E6
=> Zero counts at step no.   2902 at 2theta/TOF/E(KeV):       73.6221  Intensity fixed to 1.0 and variance to 1E6
=> Zero counts at step no.   2908 at 2theta/TOF/E(KeV):       73.7381  Intensity fixed to 1.0 and variance to 1E6
=> Zero counts at step no.   2941 at 2theta/TOF/E(KeV):       74.3761  Intensity fixed to 1.0 and variance to 1E6
=> Zero counts at step no.   2942 at 2theta/TOF/E(KeV):       74.3954  Intensity fixed to 1.0 and variance to 1E6
=> Zero counts at step no.   2948 at 2theta/TOF/E(KeV):       74.5114  Intensity fixed to 1.0 and variance to 1E6
=> Zero counts at step no.   2965 at 2theta/TOF/E(KeV):       74.8400  Intensity fixed to 1.0 and variance to 1E6
=> Zero counts at step no.   2980 at 2theta/TOF/E(KeV):       75.1300  Intensity fixed to 1.0 and variance to 1E6
=> Zero counts at step no.   2981 at 2theta/TOF/E(KeV):       75.1494  Intensity fixed to 1.0 and variance to 1E6
=> Zero counts at step no.   3048 at 2theta/TOF/E(KeV):       76.4446  Intensity fixed to 1.0 and variance to 1E6
=> Zero counts at step no.   3059 at 2theta/TOF/E(KeV):       76.6572  Intensity fixed to 1.0 and variance to 1E6
=> Zero counts at step no.   3063 at 2theta/TOF/E(KeV):       76.7346  Intensity fixed to 1.0 and variance to 1E6
=> Zero counts at step no.   3074 at 2theta/TOF/E(KeV):       76.9472  Intensity fixed to 1.0 and variance to 1E6
=> Zero counts at step no.   3087 at 2theta/TOF/E(KeV):       77.1985  Intensity fixed to 1.0 and variance to 1E6
=> Zero counts at step no.   3094 at 2theta/TOF/E(KeV):       77.3338  Intensity fixed to 1.0 and variance to 1E6
=> Zero counts at step no.   3096 at 2theta/TOF/E(KeV):       77.3725  Intensity fixed to 1.0 and variance to 1E6
=> Zero counts at step no.   3097 at 2theta/TOF/E(KeV):       77.3918  Intensity fixed to 1.0 and variance to 1E6
=> Zero counts at step no.   3106 at 2theta/TOF/E(KeV):       77.5658  Intensity fixed to 1.0 and variance to 1E6
=> Zero counts at step no.   3110 at 2theta/TOF/E(KeV):       77.6432  Intensity fixed to 1.0 and variance to 1E6
=> Zero counts at step no.   3116 at 2theta/TOF/E(KeV):       77.7592  Intensity fixed to 1.0 and variance to 1E6
=> Zero counts at step no.   3120 at 2theta/TOF/E(KeV):       77.8365  Intensity fixed to 1.0 and variance to 1E6
=> Zero counts at step no.   3123 at 2theta/TOF/E(KeV):       77.8945  Intensity fixed to 1.0 and variance to 1E6
=> Zero counts at step no.   3132 at 2theta/TOF/E(KeV):       78.0685  Intensity fixed to 1.0 and variance to 1E6
=> Zero counts at step no.   3137 at 2theta/TOF/E(KeV):       78.1651  Intensity fixed to 1.0 and variance to 1E6
=> Zero counts at step no.   3144 at 2theta/TOF/E(KeV):       78.3004  Intensity fixed to 1.0 and variance to 1E6
=> Zero counts at step no.   3156 at 2theta/TOF/E(KeV):       78.5324  Intensity fixed to 1.0 and variance to 1E6
=> Zero counts at step no.   3158 at 2theta/TOF/E(KeV):       78.5711  Intensity fixed to 1.0 and variance to 1E6
=> Zero counts at step no.   3159 at 2theta/TOF/E(KeV):       78.5904  Intensity fixed to 1.0 and variance to 1E6
```

```
=> Zero counts at step no.   3166 at 2theta/TOF/E(KeV):      78.7257  Intensity fixed to 1.0 and variance to 1E6
=> Zero counts at step no.   3168 at 2theta/TOF/E(KeV):      78.7644  Intensity fixed to 1.0 and variance to 1E6
=> Zero counts at step no.   3180 at 2theta/TOF/E(KeV):      78.9964  Intensity fixed to 1.0 and variance to 1E6
=> Zero counts at step no.   3181 at 2theta/TOF/E(KeV):      79.0157  Intensity fixed to 1.0 and variance to 1E6
=> Zero counts at step no.   3186 at 2theta/TOF/E(KeV):      79.1124  Intensity fixed to 1.0 and variance to 1E6
=> Zero counts at step no.   3194 at 2theta/TOF/E(KeV):      79.2670  Intensity fixed to 1.0 and variance to 1E6
=> Zero counts at step no.   3245 at 2theta/TOF/E(KeV):      80.2530  Intensity fixed to 1.0 and variance to 1E6
=> Zero counts at step no.   3253 at 2theta/TOF/E(KeV):      80.4076  Intensity fixed to 1.0 and variance to 1E6
=> Zero counts at step no.   3293 at 2theta/TOF/E(KeV):      81.1809  Intensity fixed to 1.0 and variance to 1E6
=> Zero counts at step no.   3313 at 2theta/TOF/E(KeV):      81.5675  Intensity fixed to 1.0 and variance to 1E6
=> Zero counts at step no.   3319 at 2theta/TOF/E(KeV):      81.6835  Intensity fixed to 1.0 and variance to 1E6
=> Zero counts at step no.   3337 at 2theta/TOF/E(KeV):      82.0315  Intensity fixed to 1.0 and variance to 1E6
=> Zero counts at step no.   3343 at 2theta/TOF/E(KeV):      82.1475  Intensity fixed to 1.0 and variance to 1E6
=> Zero counts at step no.   3358 at 2theta/TOF/E(KeV):      82.4375  Intensity fixed to 1.0 and variance to 1E6
=> Zero counts at step no.   3366 at 2theta/TOF/E(KeV):      82.5921  Intensity fixed to 1.0 and variance to 1E6
=> Zero counts at step no.   3379 at 2theta/TOF/E(KeV):      82.8434  Intensity fixed to 1.0 and variance to 1E6
=> Zero counts at step no.   3472 at 2theta/TOF/E(KeV):      84.6413  Intensity fixed to 1.0 and variance to 1E6
=> Zero counts at step no.   3487 at 2theta/TOF/E(KeV):      84.9313  Intensity fixed to 1.0 and variance to 1E6
=> Zero counts at step no.   3509 at 2theta/TOF/E(KeV):      85.3566  Intensity fixed to 1.0 and variance to 1E6
=> Zero counts at step no.   3516 at 2theta/TOF/E(KeV):      85.4919  Intensity fixed to 1.0 and variance to 1E6
=> Zero counts at step no.   3532 at 2theta/TOF/E(KeV):      85.8012  Intensity fixed to 1.0 and variance to 1E6
=> Zero counts at step no.   3535 at 2theta/TOF/E(KeV):      85.8592  Intensity fixed to 1.0 and variance to 1E6
=> Zero counts at step no.   3564 at 2theta/TOF/E(KeV):      86.4198  Intensity fixed to 1.0 and variance to 1E6
=> Zero counts at step no.   3565 at 2theta/TOF/E(KeV):      86.4391  Intensity fixed to 1.0 and variance to 1E6
=> Zero counts at step no.   3583 at 2theta/TOF/E(KeV):      86.7871  Intensity fixed to 1.0 and variance to 1E6
=> Zero counts at step no.   3593 at 2theta/TOF/E(KeV):      86.9804  Intensity fixed to 1.0 and variance to 1E6
=> Zero counts at step no.   3692 at 2theta/TOF/E(KeV):      88.8943  Intensity fixed to 1.0 and variance to 1E6
=> Zero counts at step no.   3700 at 2theta/TOF/E(KeV):      89.0489  Intensity fixed to 1.0 and variance to 1E6
=> Zero counts at step no.   3702 at 2theta/TOF/E(KeV):      89.0876  Intensity fixed to 1.0 and variance to 1E6
=> Zero counts at step no.   3726 at 2theta/TOF/E(KeV):      89.5516  Intensity fixed to 1.0 and variance to 1E6
=> Zero counts at step no.   3736 at 2theta/TOF/E(KeV):      89.7449  Intensity fixed to 1.0 and variance to 1E6
=> Zero counts at step no.   3737 at 2theta/TOF/E(KeV):      89.7642  Intensity fixed to 1.0 and variance to 1E6
=> Zero counts at step no.   3739 at 2theta/TOF/E(KeV):      89.8029  Intensity fixed to 1.0 and variance to 1E6
=> Zero counts at step no.   3764 at 2theta/TOF/E(KeV):      90.2862  Intensity fixed to 1.0 and variance to 1E6
=> Zero counts at step no.   3780 at 2theta/TOF/E(KeV):      90.5955  Intensity fixed to 1.0 and variance to 1E6
=> Zero counts at step no.   3784 at 2theta/TOF/E(KeV):      90.6728  Intensity fixed to 1.0 and variance to 1E6
=> Zero counts at step no.   3785 at 2theta/TOF/E(KeV):      90.6921  Intensity fixed to 1.0 and variance to 1E6
=> Zero counts at step no.   3800 at 2theta/TOF/E(KeV):      90.9821  Intensity fixed to 1.0 and variance to 1E6
=> Zero counts at step no.   3810 at 2theta/TOF/E(KeV):      91.1754  Intensity fixed to 1.0 and variance to 1E6
=> Zero counts at step no.   3814 at 2theta/TOF/E(KeV):      91.2528  Intensity fixed to 1.0 and variance to 1E6
=> Zero counts at step no.   3821 at 2theta/TOF/E(KeV):      91.3881  Intensity fixed to 1.0 and variance to 1E6
=> Zero counts at step no.   3822 at 2theta/TOF/E(KeV):      91.4074  Intensity fixed to 1.0 and variance to 1E6
=> Zero counts at step no.   3841 at 2theta/TOF/E(KeV):      91.7747  Intensity fixed to 1.0 and variance to 1E6
=> Zero counts at step no.   3845 at 2theta/TOF/E(KeV):      91.8521  Intensity fixed to 1.0 and variance to 1E6
=> Zero counts at step no.   3849 at 2theta/TOF/E(KeV):      91.9294  Intensity fixed to 1.0 and variance to 1E6
=> Zero counts at step no.   3851 at 2theta/TOF/E(KeV):      91.9680  Intensity fixed to 1.0 and variance to 1E6
=> Zero counts at step no.   3852 at 2theta/TOF/E(KeV):      91.9874  Intensity fixed to 1.0 and variance to 1E6
=> Zero counts at step no.   3858 at 2theta/TOF/E(KeV):      92.1034  Intensity fixed to 1.0 and variance to 1E6
=> Zero counts at step no.   3873 at 2theta/TOF/E(KeV):      92.3933  Intensity fixed to 1.0 and variance to 1E6
=> Zero counts at step no.   3880 at 2theta/TOF/E(KeV):      92.5287  Intensity fixed to 1.0 and variance to 1E6
=> Zero counts at step no.   3881 at 2theta/TOF/E(KeV):      92.5480  Intensity fixed to 1.0 and variance to 1E6
=> Zero counts at step no.   3886 at 2theta/TOF/E(KeV):      92.6447  Intensity fixed to 1.0 and variance to 1E6
=> Zero counts at step no.   3888 at 2theta/TOF/E(KeV):      92.6833  Intensity fixed to 1.0 and variance to 1E6
=> Zero counts at step no.   3889 at 2theta/TOF/E(KeV):      92.7027  Intensity fixed to 1.0 and variance to 1E6
=> Zero counts at step no.   3892 at 2theta/TOF/E(KeV):      92.7607  Intensity fixed to 1.0 and variance to 1E6
=> Zero counts at step no.   3899 at 2theta/TOF/E(KeV):      92.8960  Intensity fixed to 1.0 and variance to 1E6
=> Zero counts at step no.   3900 at 2theta/TOF/E(KeV):      92.9153  Intensity fixed to 1.0 and variance to 1E6
=> Zero counts at step no.   3914 at 2theta/TOF/E(KeV):      93.1859  Intensity fixed to 1.0 and variance to 1E6
=> Zero counts at step no.   3916 at 2theta/TOF/E(KeV):      93.2246  Intensity fixed to 1.0 and variance to 1E6
=> Zero counts at step no.   3929 at 2theta/TOF/E(KeV):      93.4759  Intensity fixed to 1.0 and variance to 1E6
=> Zero counts at step no.   3932 at 2theta/TOF/E(KeV):      93.5339  Intensity fixed to 1.0 and variance to 1E6
=> Zero counts at step no.   3933 at 2theta/TOF/E(KeV):      93.5533  Intensity fixed to 1.0 and variance to 1E6
=> Zero counts at step no.   3937 at 2theta/TOF/E(KeV):      93.6306  Intensity fixed to 1.0 and variance to 1E6
=> Zero counts at step no.   3944 at 2theta/TOF/E(KeV):      93.7659  Intensity fixed to 1.0 and variance to 1E6
=> Zero counts at step no.   3946 at 2theta/TOF/E(KeV):      93.8046  Intensity fixed to 1.0 and variance to 1E6
=> Zero counts at step no.   3951 at 2theta/TOF/E(KeV):      93.9012  Intensity fixed to 1.0 and variance to 1E6
=> Zero counts at step no.   3971 at 2theta/TOF/E(KeV):      94.2879  Intensity fixed to 1.0 and variance to 1E6
=> Zero counts at step no.   3975 at 2theta/TOF/E(KeV):      94.3652  Intensity fixed to 1.0 and variance to 1E6
=> Zero counts at step no.   3976 at 2theta/TOF/E(KeV):      94.3845  Intensity fixed to 1.0 and variance to 1E6
=> Zero counts at step no.   3977 at 2theta/TOF/E(KeV):      94.4039  Intensity fixed to 1.0 and variance to 1E6
=> Zero counts at step no.   3993 at 2theta/TOF/E(KeV):      94.7132  Intensity fixed to 1.0 and variance to 1E6
=> Zero counts at step no.   4001 at 2theta/TOF/E(KeV):      94.8678  Intensity fixed to 1.0 and variance to 1E6
=> Zero counts at step no.   4002 at 2theta/TOF/E(KeV):      94.8871  Intensity fixed to 1.0 and variance to 1E6
=> Zero counts at step no.   4018 at 2theta/TOF/E(KeV):      95.1965  Intensity fixed to 1.0 and variance to 1E6
=> Zero counts at step no.   4068 at 2theta/TOF/E(KeV):      96.1631  Intensity fixed to 1.0 and variance to 1E6
=> Zero counts at step no.   4080 at 2theta/TOF/E(KeV):      96.3950  Intensity fixed to 1.0 and variance to 1E6
=> Zero counts at step no.   4081 at 2theta/TOF/E(KeV):      96.4144  Intensity fixed to 1.0 and variance to 1E6
=> Zero counts at step no.   4103 at 2theta/TOF/E(KeV):      96.8397  Intensity fixed to 1.0 and variance to 1E6
=> Zero counts at step no.   4115 at 2theta/TOF/E(KeV):      97.0717  Intensity fixed to 1.0 and variance to 1E6
=> Zero counts at step no.   4143 at 2theta/TOF/E(KeV):      97.6129  Intensity fixed to 1.0 and variance to 1E6
=> Zero counts at step no.   4147 at 2theta/TOF/E(KeV):      97.6903  Intensity fixed to 1.0 and variance to 1E6
=> Zero counts at step no.   4149 at 2theta/TOF/E(KeV):      97.7289  Intensity fixed to 1.0 and variance to 1E6
=> Zero counts at step no.   4152 at 2theta/TOF/E(KeV):      97.7869  Intensity fixed to 1.0 and variance to 1E6
=> Zero counts at step no.   4159 at 2theta/TOF/E(KeV):      97.9222  Intensity fixed to 1.0 and variance to 1E6
=> Zero counts at step no.   4161 at 2theta/TOF/E(KeV):      97.9609  Intensity fixed to 1.0 and variance to 1E6
=> Zero counts at step no.   4164 at 2theta/TOF/E(KeV):      98.0189  Intensity fixed to 1.0 and variance to 1E6
=> Zero counts at step no.   4178 at 2theta/TOF/E(KeV):      98.2896  Intensity fixed to 1.0 and variance to 1E6
=> Zero counts at step no.   4191 at 2theta/TOF/E(KeV):      98.5409  Intensity fixed to 1.0 and variance to 1E6
=> Zero counts at step no.   4285 at 2theta/TOF/E(KeV):     100.3581  Intensity fixed to 1.0 and variance to 1E6
=> Zero counts at step no.   4298 at 2theta/TOF/E(KeV):     100.6094  Intensity fixed to 1.0 and variance to 1E6
```

```
=> Zero counts at step no.   4311 at 2theta/TOF/E(KeV):      100.8607  Intensity fixed to 1.0 and variance to 1E6
=> Zero counts at step no.   4333 at 2theta/TOF/E(KeV):      101.2860  Intensity fixed to 1.0 and variance to 1E6
=> Zero counts at step no.   4357 at 2theta/TOF/E(KeV):      101.7500  Intensity fixed to 1.0 and variance to 1E6
=> Zero counts at step no.   4367 at 2theta/TOF/E(KeV):      101.9433  Intensity fixed to 1.0 and variance to 1E6
=> Zero counts at step no.   4379 at 2theta/TOF/E(KeV):      102.1752  Intensity fixed to 1.0 and variance to 1E6
=> Zero counts at step no.   4387 at 2theta/TOF/E(KeV):      102.3299  Intensity fixed to 1.0 and variance to 1E6
=> Zero counts at step no.   4409 at 2theta/TOF/E(KeV):      102.7552  Intensity fixed to 1.0 and variance to 1E6
=> Zero counts at step no.   4495 at 2theta/TOF/E(KeV):      104.4177  Intensity fixed to 1.0 and variance to 1E6
=> Zero counts at step no.   4500 at 2theta/TOF/E(KeV):      104.5144  Intensity fixed to 1.0 and variance to 1E6
=> Zero counts at step no.   4511 at 2theta/TOF/E(KeV):      104.7271  Intensity fixed to 1.0 and variance to 1E6
=> Zero counts at step no.   4518 at 2theta/TOF/E(KeV):      104.8624  Intensity fixed to 1.0 and variance to 1E6
=> Zero counts at step no.   4530 at 2theta/TOF/E(KeV):      105.0944  Intensity fixed to 1.0 and variance to 1E6
=> Zero counts at step no.   4544 at 2theta/TOF/E(KeV):      105.3650  Intensity fixed to 1.0 and variance to 1E6
=> Zero counts at step no.   4545 at 2theta/TOF/E(KeV):      105.3843  Intensity fixed to 1.0 and variance to 1E6
=> Zero counts at step no.   4548 at 2theta/TOF/E(KeV):      105.4423  Intensity fixed to 1.0 and variance to 1E6
=> Zero counts at step no.   4552 at 2theta/TOF/E(KeV):      105.5197  Intensity fixed to 1.0 and variance to 1E6
=> Zero counts at step no.   4554 at 2theta/TOF/E(KeV):      105.5583  Intensity fixed to 1.0 and variance to 1E6
=> Zero counts at step no.   4555 at 2theta/TOF/E(KeV):      105.5777  Intensity fixed to 1.0 and variance to 1E6
=> Zero counts at step no.   4557 at 2theta/TOF/E(KeV):      105.6163  Intensity fixed to 1.0 and variance to 1E6
=> Zero counts at step no.   4570 at 2theta/TOF/E(KeV):      105.8676  Intensity fixed to 1.0 and variance to 1E6
=> Zero counts at step no.   4596 at 2theta/TOF/E(KeV):      106.3703  Intensity fixed to 1.0 and variance to 1E6
=> Zero counts at step no.   4601 at 2theta/TOF/E(KeV):      106.4669  Intensity fixed to 1.0 and variance to 1E6
=> Zero counts at step no.   4603 at 2theta/TOF/E(KeV):      106.5056  Intensity fixed to 1.0 and variance to 1E6
=> Zero counts at step no.   4609 at 2theta/TOF/E(KeV):      106.6216  Intensity fixed to 1.0 and variance to 1E6
=> Zero counts at step no.   4611 at 2theta/TOF/E(KeV):      106.6602  Intensity fixed to 1.0 and variance to 1E6
=> Zero counts at step no.   4625 at 2theta/TOF/E(KeV):      106.9309  Intensity fixed to 1.0 and variance to 1E6
=> Zero counts at step no.   4696 at 2theta/TOF/E(KeV):      108.3034  Intensity fixed to 1.0 and variance to 1E6
=> Zero counts at step no.   4700 at 2theta/TOF/E(KeV):      108.3808  Intensity fixed to 1.0 and variance to 1E6
=> Zero counts at step no.   4703 at 2theta/TOF/E(KeV):      108.4388  Intensity fixed to 1.0 and variance to 1E6
=> Zero counts at step no.   4711 at 2theta/TOF/E(KeV):      108.5934  Intensity fixed to 1.0 and variance to 1E6
=> Zero counts at step no.   4718 at 2theta/TOF/E(KeV):      108.7287  Intensity fixed to 1.0 and variance to 1E6
=> Zero counts at step no.   4733 at 2theta/TOF/E(KeV):      109.0187  Intensity fixed to 1.0 and variance to 1E6
=> Zero counts at step no.   4734 at 2theta/TOF/E(KeV):      109.0381  Intensity fixed to 1.0 and variance to 1E6
=> Zero counts at step no.   4735 at 2theta/TOF/E(KeV):      109.0574  Intensity fixed to 1.0 and variance to 1E6
=> Zero counts at step no.   4747 at 2theta/TOF/E(KeV):      109.2894  Intensity fixed to 1.0 and variance to 1E6
=> Zero counts at step no.   4751 at 2theta/TOF/E(KeV):      109.3667  Intensity fixed to 1.0 and variance to 1E6
=> Zero counts at step no.   4756 at 2theta/TOF/E(KeV):      109.4633  Intensity fixed to 1.0 and variance to 1E6
=> Zero counts at step no.   4757 at 2theta/TOF/E(KeV):      109.4827  Intensity fixed to 1.0 and variance to 1E6
=> Zero counts at step no.   4758 at 2theta/TOF/E(KeV):      109.5020  Intensity fixed to 1.0 and variance to 1E6
=> Zero counts at step no.   4761 at 2theta/TOF/E(KeV):      109.5600  Intensity fixed to 1.0 and variance to 1E6
=> Zero counts at step no.   4767 at 2theta/TOF/E(KeV):      109.6760  Intensity fixed to 1.0 and variance to 1E6
=> Zero counts at step no.   4772 at 2theta/TOF/E(KeV):      109.7727  Intensity fixed to 1.0 and variance to 1E6
=> Zero counts at step no.   4785 at 2theta/TOF/E(KeV):      110.0240  Intensity fixed to 1.0 and variance to 1E6
=> Zero counts at step no.   4788 at 2theta/TOF/E(KeV):      110.0820  Intensity fixed to 1.0 and variance to 1E6
=> Zero counts at step no.   4790 at 2theta/TOF/E(KeV):      110.1206  Intensity fixed to 1.0 and variance to 1E6
=> Zero counts at step no.   4791 at 2theta/TOF/E(KeV):      110.1400  Intensity fixed to 1.0 and variance to 1E6
=> Zero counts at step no.   4795 at 2theta/TOF/E(KeV):      110.2173  Intensity fixed to 1.0 and variance to 1E6
=> Zero counts at step no.   4796 at 2theta/TOF/E(KeV):      110.2366  Intensity fixed to 1.0 and variance to 1E6
=> Zero counts at step no.   4810 at 2theta/TOF/E(KeV):      110.5073  Intensity fixed to 1.0 and variance to 1E6
=> Zero counts at step no.   4817 at 2theta/TOF/E(KeV):      110.6426  Intensity fixed to 1.0 and variance to 1E6
=> Zero counts at step no.   4822 at 2theta/TOF/E(KeV):      110.7393  Intensity fixed to 1.0 and variance to 1E6
=> Zero counts at step no.   4827 at 2theta/TOF/E(KeV):      110.8359  Intensity fixed to 1.0 and variance to 1E6
=> Zero counts at step no.   4834 at 2theta/TOF/E(KeV):      110.9712  Intensity fixed to 1.0 and variance to 1E6
=> Zero counts at step no.   4856 at 2theta/TOF/E(KeV):      111.3965  Intensity fixed to 1.0 and variance to 1E6
=> Zero counts at step no.   4937 at 2theta/TOF/E(KeV):      112.9624  Intensity fixed to 1.0 and variance to 1E6
=> Zero counts at step no.   4961 at 2theta/TOF/E(KeV):      113.4264  Intensity fixed to 1.0 and variance to 1E6
=> Zero counts at step no.   4968 at 2theta/TOF/E(KeV):      113.5617  Intensity fixed to 1.0 and variance to 1E6
=> Zero counts at step no.   4976 at 2theta/TOF/E(KeV):      113.7164  Intensity fixed to 1.0 and variance to 1E6
=> Zero counts at step no.   4997 at 2theta/TOF/E(KeV):      114.1223  Intensity fixed to 1.0 and variance to 1E6
=> Zero counts at step no.   5005 at 2theta/TOF/E(KeV):      114.2770  Intensity fixed to 1.0 and variance to 1E6
=> Zero counts at step no.   5006 at 2theta/TOF/E(KeV):      114.2963  Intensity fixed to 1.0 and variance to 1E6
=> Zero counts at step no.   5010 at 2theta/TOF/E(KeV):      114.3736  Intensity fixed to 1.0 and variance to 1E6
=> Zero counts at step no.   5016 at 2theta/TOF/E(KeV):      114.4896  Intensity fixed to 1.0 and variance to 1E6
=> Zero counts at step no.   5024 at 2theta/TOF/E(KeV):      114.6443  Intensity fixed to 1.0 and variance to 1E6
=> Zero counts at step no.   5025 at 2theta/TOF/E(KeV):      114.6636  Intensity fixed to 1.0 and variance to 1E6
=> Zero counts at step no.   5034 at 2theta/TOF/E(KeV):      114.8376  Intensity fixed to 1.0 and variance to 1E6
=> Zero counts at step no.   5036 at 2theta/TOF/E(KeV):      114.8763  Intensity fixed to 1.0 and variance to 1E6
=> Zero counts at step no.   5060 at 2theta/TOF/E(KeV):      115.3402  Intensity fixed to 1.0 and variance to 1E6
=> Zero counts at step no.   5183 at 2theta/TOF/E(KeV):      117.7180  Intensity fixed to 1.0 and variance to 1E6
=> Zero counts at step no.   5195 at 2theta/TOF/E(KeV):      117.9500  Intensity fixed to 1.0 and variance to 1E6
=> Zero counts at step no.   5206 at 2theta/TOF/E(KeV):      118.1627  Intensity fixed to 1.0 and variance to 1E6
=> Zero counts at step no.   5213 at 2theta/TOF/E(KeV):      118.2980  Intensity fixed to 1.0 and variance to 1E6
=> Zero counts at step no.   5214 at 2theta/TOF/E(KeV):      118.3173  Intensity fixed to 1.0 and variance to 1E6
=> Zero counts at step no.   5230 at 2theta/TOF/E(KeV):      118.6266  Intensity fixed to 1.0 and variance to 1E6
=> Zero counts at step no.   5260 at 2theta/TOF/E(KeV):      119.2066  Intensity fixed to 1.0 and variance to 1E6
=> Zero counts at step no.   5283 at 2theta/TOF/E(KeV):      119.6512  Intensity fixed to 1.0 and variance to 1E6
=> Zero counts at step no.   5379 at 2theta/TOF/E(KeV):      121.5071  Intensity fixed to 1.0 and variance to 1E6
=> Zero counts at step no.   5407 at 2theta/TOF/E(KeV):      122.0484  Intensity fixed to 1.0 and variance to 1E6
=> Zero counts at step no.   5414 at 2theta/TOF/E(KeV):      122.1837  Intensity fixed to 1.0 and variance to 1E6
=> Zero counts at step no.   5419 at 2theta/TOF/E(KeV):      122.2803  Intensity fixed to 1.0 and variance to 1E6
=> Zero counts at step no.   5429 at 2theta/TOF/E(KeV):      122.4737  Intensity fixed to 1.0 and variance to 1E6
=> Zero counts at step no.   5435 at 2theta/TOF/E(KeV):      122.5897  Intensity fixed to 1.0 and variance to 1E6
=> Zero counts at step no.   5440 at 2theta/TOF/E(KeV):      122.6863  Intensity fixed to 1.0 and variance to 1E6
=> Zero counts at step no.   5442 at 2theta/TOF/E(KeV):      122.7250  Intensity fixed to 1.0 and variance to 1E6
=> Zero counts at step no.   5447 at 2theta/TOF/E(KeV):      122.8216  Intensity fixed to 1.0 and variance to 1E6
=> Zero counts at step no.   5455 at 2theta/TOF/E(KeV):      122.9763  Intensity fixed to 1.0 and variance to 1E6
=> Zero counts at step no.   5456 at 2theta/TOF/E(KeV):      122.9956  Intensity fixed to 1.0 and variance to 1E6
=> Zero counts at step no.   5457 at 2theta/TOF/E(KeV):      123.0150  Intensity fixed to 1.0 and variance to 1E6
=> Zero counts at step no.   5460 at 2theta/TOF/E(KeV):      123.0730  Intensity fixed to 1.0 and variance to 1E6
=> Zero counts at step no.   5464 at 2theta/TOF/E(KeV):      123.1503  Intensity fixed to 1.0 and variance to 1E6
```

```
=> Zero counts at step no.   5473 at 2theta/TOF/E(KeV):      123.3243  Intensity fixed to 1.0 and variance to 1E6
=> Zero counts at step no.   5486 at 2theta/TOF/E(KeV):      123.5756  Intensity fixed to 1.0 and variance to 1E6
=> Zero counts at step no.   5487 at 2theta/TOF/E(KeV):      123.5949  Intensity fixed to 1.0 and variance to 1E6
=> Zero counts at step no.   5489 at 2theta/TOF/E(KeV):      123.6336  Intensity fixed to 1.0 and variance to 1E6
=> Zero counts at step no.   5502 at 2theta/TOF/E(KeV):      123.8849  Intensity fixed to 1.0 and variance to 1E6
=> Zero counts at step no.   5511 at 2theta/TOF/E(KeV):      124.0589  Intensity fixed to 1.0 and variance to 1E6
=> Zero counts at step no.   5517 at 2theta/TOF/E(KeV):      124.1749  Intensity fixed to 1.0 and variance to 1E6
=> Zero counts at step no.   5519 at 2theta/TOF/E(KeV):      124.2135  Intensity fixed to 1.0 and variance to 1E6
=> Zero counts at step no.   5522 at 2theta/TOF/E(KeV):      124.2715  Intensity fixed to 1.0 and variance to 1E6
=> Zero counts at step no.   5530 at 2theta/TOF/E(KeV):      124.4262  Intensity fixed to 1.0 and variance to 1E6
=> Zero counts at step no.   5534 at 2theta/TOF/E(KeV):      124.5035  Intensity fixed to 1.0 and variance to 1E6
=> Zero counts at step no.   5554 at 2theta/TOF/E(KeV):      124.8902  Intensity fixed to 1.0 and variance to 1E6
=> Zero counts at step no.   5555 at 2theta/TOF/E(KeV):      124.9095  Intensity fixed to 1.0 and variance to 1E6
=> Zero counts at step no.   5564 at 2theta/TOF/E(KeV):      125.0835  Intensity fixed to 1.0 and variance to 1E6
=> Zero counts at step no.   5572 at 2theta/TOF/E(KeV):      125.2381  Intensity fixed to 1.0 and variance to 1E6
=> Zero counts at step no.   5573 at 2theta/TOF/E(KeV):      125.2575  Intensity fixed to 1.0 and variance to 1E6
=> Zero counts at step no.   5574 at 2theta/TOF/E(KeV):      125.2768  Intensity fixed to 1.0 and variance to 1E6
=> Zero counts at step no.   5582 at 2theta/TOF/E(KeV):      125.4314  Intensity fixed to 1.0 and variance to 1E6
=> Zero counts at step no.   5601 at 2theta/TOF/E(KeV):      125.7988  Intensity fixed to 1.0 and variance to 1E6
=> Zero counts at step no.   5604 at 2theta/TOF/E(KeV):      125.8567  Intensity fixed to 1.0 and variance to 1E6
=> Zero counts at step no.   5607 at 2theta/TOF/E(KeV):      125.9147  Intensity fixed to 1.0 and variance to 1E6
=> Zero counts at step no.   5610 at 2theta/TOF/E(KeV):      125.9727  Intensity fixed to 1.0 and variance to 1E6
=> Zero counts at step no.   5625 at 2theta/TOF/E(KeV):      126.2627  Intensity fixed to 1.0 and variance to 1E6
=> Zero counts at step no.   5627 at 2theta/TOF/E(KeV):      126.3014  Intensity fixed to 1.0 and variance to 1E6
=> Zero counts at step no.   5636 at 2theta/TOF/E(KeV):      126.4754  Intensity fixed to 1.0 and variance to 1E6
=> Zero counts at step no.   5637 at 2theta/TOF/E(KeV):      126.4947  Intensity fixed to 1.0 and variance to 1E6
=> Zero counts at step no.   5647 at 2theta/TOF/E(KeV):      126.6880  Intensity fixed to 1.0 and variance to 1E6
=> Zero counts at step no.   5648 at 2theta/TOF/E(KeV):      126.7073  Intensity fixed to 1.0 and variance to 1E6
=> Zero counts at step no.   5649 at 2theta/TOF/E(KeV):      126.7267  Intensity fixed to 1.0 and variance to 1E6
=> Zero counts at step no.   5661 at 2theta/TOF/E(KeV):      126.9586  Intensity fixed to 1.0 and variance to 1E6
=> Zero counts at step no.   5662 at 2theta/TOF/E(KeV):      126.9780  Intensity fixed to 1.0 and variance to 1E6
=> Zero counts at step no.   5663 at 2theta/TOF/E(KeV):      126.9973  Intensity fixed to 1.0 and variance to 1E6
=> Zero counts at step no.   5666 at 2theta/TOF/E(KeV):      127.0553  Intensity fixed to 1.0 and variance to 1E6
=> Zero counts at step no.   5685 at 2theta/TOF/E(KeV):      127.4226  Intensity fixed to 1.0 and variance to 1E6
=> Zero counts at step no.   5692 at 2theta/TOF/E(KeV):      127.5579  Intensity fixed to 1.0 and variance to 1E6
=> Zero counts at step no.   5704 at 2theta/TOF/E(KeV):      127.7899  Intensity fixed to 1.0 and variance to 1E6
=> Zero counts at step no.   5708 at 2theta/TOF/E(KeV):      127.8672  Intensity fixed to 1.0 and variance to 1E6
=> Zero counts at step no.   5716 at 2theta/TOF/E(KeV):      128.0219  Intensity fixed to 1.0 and variance to 1E6
=> Zero counts at step no.   5717 at 2theta/TOF/E(KeV):      128.0412  Intensity fixed to 1.0 and variance to 1E6
=> Zero counts at step no.   5723 at 2theta/TOF/E(KeV):      128.1572  Intensity fixed to 1.0 and variance to 1E6
=> Zero counts at step no.   5724 at 2theta/TOF/E(KeV):      128.1766  Intensity fixed to 1.0 and variance to 1E6
=> Zero counts at step no.   5745 at 2theta/TOF/E(KeV):      128.5825  Intensity fixed to 1.0 and variance to 1E6
=> Zero counts at step no.   5750 at 2theta/TOF/E(KeV):      128.6792  Intensity fixed to 1.0 and variance to 1E6
=> Zero counts at step no.   5753 at 2theta/TOF/E(KeV):      128.7372  Intensity fixed to 1.0 and variance to 1E6
=> Zero counts at step no.   5760 at 2theta/TOF/E(KeV):      128.8725  Intensity fixed to 1.0 and variance to 1E6
=> Zero counts at step no.   5762 at 2theta/TOF/E(KeV):      128.9112  Intensity fixed to 1.0 and variance to 1E6
=> Zero counts at step no.   5768 at 2theta/TOF/E(KeV):      129.0272  Intensity fixed to 1.0 and variance to 1E6
=> Zero counts at step no.   5774 at 2theta/TOF/E(KeV):      129.1432  Intensity fixed to 1.0 and variance to 1E6
=> Zero counts at step no.   5775 at 2theta/TOF/E(KeV):      129.1625  Intensity fixed to 1.0 and variance to 1E6
=> Zero counts at step no.   5784 at 2theta/TOF/E(KeV):      129.3365  Intensity fixed to 1.0 and variance to 1E6
=> Zero counts at step no.   5788 at 2theta/TOF/E(KeV):      129.4138  Intensity fixed to 1.0 and variance to 1E6
=> Zero counts at step no.   5891 at 2theta/TOF/E(KeV):      131.4050  Intensity fixed to 1.0 and variance to 1E6
=> Zero counts at step no.   5898 at 2theta/TOF/E(KeV):      131.5403  Intensity fixed to 1.0 and variance to 1E6
=> Zero counts at step no.   5910 at 2theta/TOF/E(KeV):      131.7723  Intensity fixed to 1.0 and variance to 1E6
=> Zero counts at step no.   5922 at 2theta/TOF/E(KeV):      132.0043  Intensity fixed to 1.0 and variance to 1E6
=> Zero counts at step no.   5926 at 2theta/TOF/E(KeV):      132.0816  Intensity fixed to 1.0 and variance to 1E6
=> Zero counts at step no.   5944 at 2theta/TOF/E(KeV):      132.4296  Intensity fixed to 1.0 and variance to 1E6
=> Zero counts at step no.   5948 at 2theta/TOF/E(KeV):      132.5069  Intensity fixed to 1.0 and variance to 1E6
=> Zero counts at step no.   5963 at 2theta/TOF/E(KeV):      132.7969  Intensity fixed to 1.0 and variance to 1E6
=> Zero counts at step no.   5976 at 2theta/TOF/E(KeV):      133.0482  Intensity fixed to 1.0 and variance to 1E6
=> Zero counts at step no.   5979 at 2theta/TOF/E(KeV):      133.1062  Intensity fixed to 1.0 and variance to 1E6
=> Zero counts at step no.   6000 at 2theta/TOF/E(KeV):      133.5121  Intensity fixed to 1.0 and variance to 1E6
=> Zero counts at step no.   6004 at 2theta/TOF/E(KeV):      133.5895  Intensity fixed to 1.0 and variance to 1E6
=> Zero counts at step no.   6016 at 2theta/TOF/E(KeV):      133.8215  Intensity fixed to 1.0 and variance to 1E6
=> Zero counts at step no.   6042 at 2theta/TOF/E(KeV):      134.3241  Intensity fixed to 1.0 and variance to 1E6
=> Zero counts at step no.   6068 at 2theta/TOF/E(KeV):      134.8267  Intensity fixed to 1.0 and variance to 1E6
=> Zero counts at step no.   6218 at 2theta/TOF/E(KeV):      137.7265  Intensity fixed to 1.0 and variance to 1E6
=> Zero counts at step no.   6240 at 2theta/TOF/E(KeV):      138.1518  Intensity fixed to 1.0 and variance to 1E6
=> Zero counts at step no.   6245 at 2theta/TOF/E(KeV):      138.2484  Intensity fixed to 1.0 and variance to 1E6
=> Zero counts at step no.   6258 at 2theta/TOF/E(KeV):      138.4998  Intensity fixed to 1.0 and variance to 1E6
=> Zero counts at step no.   6279 at 2theta/TOF/E(KeV):      138.9057  Intensity fixed to 1.0 and variance to 1E6
=> Zero counts at step no.   6281 at 2theta/TOF/E(KeV):      138.9444  Intensity fixed to 1.0 and variance to 1E6
=> Zero counts at step no.   6288 at 2theta/TOF/E(KeV):      139.0797  Intensity fixed to 1.0 and variance to 1E6
=> Zero counts at step no.   6303 at 2theta/TOF/E(KeV):      139.3697  Intensity fixed to 1.0 and variance to 1E6
=> Zero counts at step no.   6315 at 2theta/TOF/E(KeV):      139.6017  Intensity fixed to 1.0 and variance to 1E6
=> Zero counts at step no.   6318 at 2theta/TOF/E(KeV):      139.6597  Intensity fixed to 1.0 and variance to 1E6
=> Zero counts at step no.   6320 at 2theta/TOF/E(KeV):      139.6983  Intensity fixed to 1.0 and variance to 1E6
=> Zero counts at step no.   6522 at 2theta/TOF/E(KeV):      143.6034  Intensity fixed to 1.0 and variance to 1E6
=> Zero counts at step no.   6552 at 2theta/TOF/E(KeV):      144.1833  Intensity fixed to 1.0 and variance to 1E6
=> Zero counts at step no.   6599 at 2theta/TOF/E(KeV):      145.0919  Intensity fixed to 1.0 and variance to 1E6
=> Zero counts at step no.   6600 at 2theta/TOF/E(KeV):      145.1113  Intensity fixed to 1.0 and variance to 1E6
=> Zero counts at step no.   6611 at 2theta/TOF/E(KeV):      145.3239  Intensity fixed to 1.0 and variance to 1E6
=> Zero counts at step no.   6627 at 2theta/TOF/E(KeV):      145.6332  Intensity fixed to 1.0 and variance to 1E6
=> Zero counts at step no.   6632 at 2theta/TOF/E(KeV):      145.7299  Intensity fixed to 1.0 and variance to 1E6
=> Zero counts at step no.   6639 at 2theta/TOF/E(KeV):      145.8652  Intensity fixed to 1.0 and variance to 1E6
=> Zero counts at step no.   6641 at 2theta/TOF/E(KeV):      145.9038  Intensity fixed to 1.0 and variance to 1E6
=> Zero counts at step no.   6649 at 2theta/TOF/E(KeV):      146.0585  Intensity fixed to 1.0 and variance to 1E6
=> Zero counts at step no.   6656 at 2theta/TOF/E(KeV):      146.1938  Intensity fixed to 1.0 and variance to 1E6
=> Zero counts at step no.   6662 at 2theta/TOF/E(KeV):      146.3098  Intensity fixed to 1.0 and variance to 1E6
=> Zero counts at step no.   6719 at 2theta/TOF/E(KeV):      147.4117  Intensity fixed to 1.0 and variance to 1E6
```

```
=> Zero counts at step no.   6905 at 2theta/TOF/E(KeV):       151.0074  Intensity fixed to 1.0 and variance to 1E6
=> Zero counts at step no.   6910 at 2theta/TOF/E(KeV):       151.1041  Intensity fixed to 1.0 and variance to 1E6
=> Zero counts at step no.   6917 at 2theta/TOF/E(KeV):       151.2394  Intensity fixed to 1.0 and variance to 1E6
=> Zero counts at step no.   6928 at 2theta/TOF/E(KeV):       151.4521  Intensity fixed to 1.0 and variance to 1E6

=> Optimizations for routine tasks applied:
=> Calculation mode for patter#:   1  CM_PSEUDO_VOIGT

=> Square of FWHM(G) < 0 at 2theta:   99.705 for phase no.    1 -> Fixing to HG=1.0e-10
=> Square of FWHM(G) < 0 at 2theta:   99.705 for phase no.    1 -> Fixing to HG=1.0e-10
=> Square of FWHM(G) < 0 at 2theta:  100.033 for phase no.    1 -> Fixing to HG=1.0e-10
=> Square of FWHM(G) < 0 at 2theta:  100.033 for phase no.    1 -> Fixing to HG=1.0e-10
=> Square of FWHM(G) < 0 at 2theta:  103.728 for phase no.    1 -> Fixing to HG=1.0e-10
=> Square of FWHM(G) < 0 at 2theta:  103.728 for phase no.    1 -> Fixing to HG=1.0e-10
=> Square of FWHM(G) < 0 at 2theta:  104.081 for phase no.    1 -> Fixing to HG=1.0e-10
=> Square of FWHM(G) < 0 at 2theta:  104.081 for phase no.    1 -> Fixing to HG=1.0e-10
=> Square of FWHM(G) < 0 at 2theta:  107.821 for phase no.    1 -> Fixing to HG=1.0e-10
=> Square of FWHM(G) < 0 at 2theta:  108.202 for phase no.    1 -> Fixing to HG=1.0e-10
=> Square of FWHM(G) < 0 at 2theta:  112.011 for phase no.    1 -> Fixing to HG=1.0e-10
=> Square of FWHM(G) < 0 at 2theta:  112.422 for phase no.    1 -> Fixing to HG=1.0e-10
=> Square of FWHM(G) < 0 at 2theta:  116.329 for phase no.    1 -> Fixing to HG=1.0e-10
=> Square of FWHM(G) < 0 at 2theta:  116.776 for phase no.    1 -> Fixing to HG=1.0e-10
=> Square of FWHM(G) < 0 at 2theta:  120.815 for phase no.    1 -> Fixing to HG=1.0e-10
=> Square of FWHM(G) < 0 at 2theta:  121.304 for phase no.    1 -> Fixing to HG=1.0e-10
=> Square of FWHM(G) < 0 at 2theta:  130.522 for phase no.    1 -> Fixing to HG=1.0e-10
=> Square of FWHM(G) < 0 at 2theta:  131.126 for phase no.    1 -> Fixing to HG=1.0e-10
=> Square of FWHM(G) < 0 at 2theta:  135.929 for phase no.    1 -> Fixing to HG=1.0e-10
=> Square of FWHM(G) < 0 at 2theta:  135.929 for phase no.    1 -> Fixing to HG=1.0e-10
=> Square of FWHM(G) < 0 at 2theta:  136.618 for phase no.    1 -> Fixing to HG=1.0e-10
=> Square of FWHM(G) < 0 at 2theta:  136.618 for phase no.    1 -> Fixing to HG=1.0e-10
=> Square of FWHM(G) < 0 at 2theta:   99.705 for phase no.    1 -> Fixing to HG=1.0e-10
=> Square of FWHM(G) < 0 at 2theta:   99.705 for phase no.    1 -> Fixing to HG=1.0e-10
=> Square of FWHM(G) < 0 at 2theta:  100.033 for phase no.    1 -> Fixing to HG=1.0e-10
=> Square of FWHM(G) < 0 at 2theta:  100.033 for phase no.    1 -> Fixing to HG=1.0e-10
=> Square of FWHM(G) < 0 at 2theta:  103.728 for phase no.    1 -> Fixing to HG=1.0e-10
=> Square of FWHM(G) < 0 at 2theta:  103.728 for phase no.    1 -> Fixing to HG=1.0e-10
=> Square of FWHM(G) < 0 at 2theta:  104.081 for phase no.    1 -> Fixing to HG=1.0e-10
=> Square of FWHM(G) < 0 at 2theta:  104.081 for phase no.    1 -> Fixing to HG=1.0e-10
=> Square of FWHM(G) < 0 at 2theta:  107.821 for phase no.    1 -> Fixing to HG=1.0e-10
=> Square of FWHM(G) < 0 at 2theta:  108.202 for phase no.    1 -> Fixing to HG=1.0e-10
=> Square of FWHM(G) < 0 at 2theta:  112.011 for phase no.    1 -> Fixing to HG=1.0e-10
=> Square of FWHM(G) < 0 at 2theta:  112.422 for phase no.    1 -> Fixing to HG=1.0e-10
=> Square of FWHM(G) < 0 at 2theta:  116.329 for phase no.    1 -> Fixing to HG=1.0e-10
=> Square of FWHM(G) < 0 at 2theta:  116.776 for phase no.    1 -> Fixing to HG=1.0e-10
=> Square of FWHM(G) < 0 at 2theta:  120.815 for phase no.    1 -> Fixing to HG=1.0e-10
=> Square of FWHM(G) < 0 at 2theta:  121.304 for phase no.    1 -> Fixing to HG=1.0e-10
=> Square of FWHM(G) < 0 at 2theta:  130.522 for phase no.    1 -> Fixing to HG=1.0e-10
=> Square of FWHM(G) < 0 at 2theta:  131.126 for phase no.    1 -> Fixing to HG=1.0e-10
=> Square of FWHM(G) < 0 at 2theta:  135.929 for phase no.    1 -> Fixing to HG=1.0e-10
=> Square of FWHM(G) < 0 at 2theta:  135.929 for phase no.    1 -> Fixing to HG=1.0e-10
=> Square of FWHM(G) < 0 at 2theta:  136.618 for phase no.    1 -> Fixing to HG=1.0e-10
=> Square of FWHM(G) < 0 at 2theta:  136.618 for phase no.    1 -> Fixing to HG=1.0e-10
=> Square of FWHM(G) < 0 at 2theta:   99.705 for phase no.    1 -> Fixing to HG=1.0e-10
=> Square of FWHM(G) < 0 at 2theta:   99.705 for phase no.    1 -> Fixing to HG=1.0e-10
=> Square of FWHM(G) < 0 at 2theta:  100.033 for phase no.    1 -> Fixing to HG=1.0e-10
=> Square of FWHM(G) < 0 at 2theta:  100.033 for phase no.    1 -> Fixing to HG=1.0e-10
=> Square of FWHM(G) < 0 at 2theta:  103.728 for phase no.    1 -> Fixing to HG=1.0e-10
=> Square of FWHM(G) < 0 at 2theta:  103.728 for phase no.    1 -> Fixing to HG=1.0e-10
=> Square of FWHM(G) < 0 at 2theta:  104.081 for phase no.    1 -> Fixing to HG=1.0e-10
=> Square of FWHM(G) < 0 at 2theta:  104.081 for phase no.    1 -> Fixing to HG=1.0e-10
=> Square of FWHM(G) < 0 at 2theta:  107.821 for phase no.    1 -> Fixing to HG=1.0e-10
=> Square of FWHM(G) < 0 at 2theta:  108.202 for phase no.    1 -> Fixing to HG=1.0e-10
=> Square of FWHM(G) < 0 at 2theta:  112.011 for phase no.    1 -> Fixing to HG=1.0e-10
=> Square of FWHM(G) < 0 at 2theta:  112.422 for phase no.    1 -> Fixing to HG=1.0e-10
=> Square of FWHM(G) < 0 at 2theta:  116.329 for phase no.    1 -> Fixing to HG=1.0e-10
=> Square of FWHM(G) < 0 at 2theta:  116.776 for phase no.    1 -> Fixing to HG=1.0e-10
=> Square of FWHM(G) < 0 at 2theta:  120.815 for phase no.    1 -> Fixing to HG=1.0e-10
=> Square of FWHM(G) < 0 at 2theta:  121.304 for phase no.    1 -> Fixing to HG=1.0e-10
=> Square of FWHM(G) < 0 at 2theta:  130.522 for phase no.    1 -> Fixing to HG=1.0e-10
=> Square of FWHM(G) < 0 at 2theta:  131.126 for phase no.    1 -> Fixing to HG=1.0e-10
=> Square of FWHM(G) < 0 at 2theta:  135.929 for phase no.    1 -> Fixing to HG=1.0e-10
=> Square of FWHM(G) < 0 at 2theta:  135.929 for phase no.    1 -> Fixing to HG=1.0e-10
=> Square of FWHM(G) < 0 at 2theta:  136.618 for phase no.    1 -> Fixing to HG=1.0e-10
=> Square of FWHM(G) < 0 at 2theta:  136.618 for phase no.    1 -> Fixing to HG=1.0e-10
=> Square of FWHM(G) < 0 at 2theta:   99.705 for phase no.    1 -> Fixing to HG=1.0e-10
=> Square of FWHM(G) < 0 at 2theta:   99.705 for phase no.    1 -> Fixing to HG=1.0e-10
=> Square of FWHM(G) < 0 at 2theta:  100.033 for phase no.    1 -> Fixing to HG=1.0e-10
=> Square of FWHM(G) < 0 at 2theta:  100.033 for phase no.    1 -> Fixing to HG=1.0e-10
=> Square of FWHM(G) < 0 at 2theta:  103.728 for phase no.    1 -> Fixing to HG=1.0e-10
=> Square of FWHM(G) < 0 at 2theta:  103.728 for phase no.    1 -> Fixing to HG=1.0e-10
=> Square of FWHM(G) < 0 at 2theta:  104.081 for phase no.    1 -> Fixing to HG=1.0e-10
=> Square of FWHM(G) < 0 at 2theta:  104.081 for phase no.    1 -> Fixing to HG=1.0e-10
=> Square of FWHM(G) < 0 at 2theta:  107.821 for phase no.    1 -> Fixing to HG=1.0e-10
=> Square of FWHM(G) < 0 at 2theta:  108.202 for phase no.    1 -> Fixing to HG=1.0e-10
=> Square of FWHM(G) < 0 at 2theta:  112.011 for phase no.    1 -> Fixing to HG=1.0e-10
=> Square of FWHM(G) < 0 at 2theta:  112.422 for phase no.    1 -> Fixing to HG=1.0e-10
=> Square of FWHM(G) < 0 at 2theta:  116.329 for phase no.    1 -> Fixing to HG=1.0e-10
=> Square of FWHM(G) < 0 at 2theta:  116.776 for phase no.    1 -> Fixing to HG=1.0e-10
=> Square of FWHM(G) < 0 at 2theta:  120.815 for phase no.    1 -> Fixing to HG=1.0e-10
=> Square of FWHM(G) < 0 at 2theta:  121.304 for phase no.    1 -> Fixing to HG=1.0e-10
```

```
=> Square of FWHM(G) < 0 at 2theta:  130.522 for phase no.    1 -> Fixing to HG=1.0e-10
=> Square of FWHM(G) < 0 at 2theta:  131.126 for phase no.    1 -> Fixing to HG=1.0e-10
=> Square of FWHM(G) < 0 at 2theta:  135.929 for phase no.    1 -> Fixing to HG=1.0e-10
=> Square of FWHM(G) < 0 at 2theta:  135.929 for phase no.    1 -> Fixing to HG=1.0e-10
=> Square of FWHM(G) < 0 at 2theta:  136.618 for phase no.    1 -> Fixing to HG=1.0e-10
=> Square of FWHM(G) < 0 at 2theta:  136.618 for phase no.    1 -> Fixing to HG=1.0e-10
=> Square of FWHM(G) < 0 at 2theta:   99.705 for phase no.    1 -> Fixing to HG=1.0e-10
=> Square of FWHM(G) < 0 at 2theta:   99.705 for phase no.    1 -> Fixing to HG=1.0e-10
=> Square of FWHM(G) < 0 at 2theta:  100.033 for phase no.    1 -> Fixing to HG=1.0e-10
=> Square of FWHM(G) < 0 at 2theta:  100.033 for phase no.    1 -> Fixing to HG=1.0e-10
=> Square of FWHM(G) < 0 at 2theta:  103.728 for phase no.    1 -> Fixing to HG=1.0e-10
=> Square of FWHM(G) < 0 at 2theta:  103.728 for phase no.    1 -> Fixing to HG=1.0e-10
=> Square of FWHM(G) < 0 at 2theta:  104.081 for phase no.    1 -> Fixing to HG=1.0e-10
=> Square of FWHM(G) < 0 at 2theta:  104.081 for phase no.    1 -> Fixing to HG=1.0e-10
=> Square of FWHM(G) < 0 at 2theta:  107.821 for phase no.    1 -> Fixing to HG=1.0e-10
=> Square of FWHM(G) < 0 at 2theta:  108.202 for phase no.    1 -> Fixing to HG=1.0e-10
=> Square of FWHM(G) < 0 at 2theta:  112.011 for phase no.    1 -> Fixing to HG=1.0e-10
=> Square of FWHM(G) < 0 at 2theta:  112.422 for phase no.    1 -> Fixing to HG=1.0e-10
=> Square of FWHM(G) < 0 at 2theta:  116.329 for phase no.    1 -> Fixing to HG=1.0e-10
=> Square of FWHM(G) < 0 at 2theta:  116.776 for phase no.    1 -> Fixing to HG=1.0e-10
=> Square of FWHM(G) < 0 at 2theta:  120.815 for phase no.    1 -> Fixing to HG=1.0e-10
=> Square of FWHM(G) < 0 at 2theta:  121.304 for phase no.    1 -> Fixing to HG=1.0e-10
=> Square of FWHM(G) < 0 at 2theta:  130.522 for phase no.    1 -> Fixing to HG=1.0e-10
=> Square of FWHM(G) < 0 at 2theta:  131.126 for phase no.    1 -> Fixing to HG=1.0e-10
=> Square of FWHM(G) < 0 at 2theta:  135.929 for phase no.    1 -> Fixing to HG=1.0e-10
=> Square of FWHM(G) < 0 at 2theta:  135.929 for phase no.    1 -> Fixing to HG=1.0e-10
=> Square of FWHM(G) < 0 at 2theta:  136.618 for phase no.    1 -> Fixing to HG=1.0e-10
=> Square of FWHM(G) < 0 at 2theta:  136.618 for phase no.    1 -> Fixing to HG=1.0e-10
=> Square of FWHM(G) < 0 at 2theta:   99.705 for phase no.    1 -> Fixing to HG=1.0e-10
=> Square of FWHM(G) < 0 at 2theta:   99.705 for phase no.    1 -> Fixing to HG=1.0e-10
=> Square of FWHM(G) < 0 at 2theta:  100.033 for phase no.    1 -> Fixing to HG=1.0e-10
=> Square of FWHM(G) < 0 at 2theta:  100.033 for phase no.    1 -> Fixing to HG=1.0e-10
=> Square of FWHM(G) < 0 at 2theta:  103.728 for phase no.    1 -> Fixing to HG=1.0e-10
=> Square of FWHM(G) < 0 at 2theta:  103.728 for phase no.    1 -> Fixing to HG=1.0e-10
=> Square of FWHM(G) < 0 at 2theta:  104.081 for phase no.    1 -> Fixing to HG=1.0e-10
=> Square of FWHM(G) < 0 at 2theta:  104.081 for phase no.    1 -> Fixing to HG=1.0e-10
=> Square of FWHM(G) < 0 at 2theta:  107.821 for phase no.    1 -> Fixing to HG=1.0e-10
=> Square of FWHM(G) < 0 at 2theta:  108.202 for phase no.    1 -> Fixing to HG=1.0e-10
=> Square of FWHM(G) < 0 at 2theta:  112.011 for phase no.    1 -> Fixing to HG=1.0e-10
=> Square of FWHM(G) < 0 at 2theta:  112.422 for phase no.    1 -> Fixing to HG=1.0e-10
=> Square of FWHM(G) < 0 at 2theta:  116.329 for phase no.    1 -> Fixing to HG=1.0e-10
=> Square of FWHM(G) < 0 at 2theta:  116.776 for phase no.    1 -> Fixing to HG=1.0e-10
=> Square of FWHM(G) < 0 at 2theta:  120.815 for phase no.    1 -> Fixing to HG=1.0e-10
=> Square of FWHM(G) < 0 at 2theta:  121.304 for phase no.    1 -> Fixing to HG=1.0e-10
=> Square of FWHM(G) < 0 at 2theta:  130.522 for phase no.    1 -> Fixing to HG=1.0e-10
=> Square of FWHM(G) < 0 at 2theta:  131.126 for phase no.    1 -> Fixing to HG=1.0e-10
=> Square of FWHM(G) < 0 at 2theta:  135.929 for phase no.    1 -> Fixing to HG=1.0e-10
=> Square of FWHM(G) < 0 at 2theta:  135.929 for phase no.    1 -> Fixing to HG=1.0e-10
=> Square of FWHM(G) < 0 at 2theta:  136.618 for phase no.    1 -> Fixing to HG=1.0e-10
=> Square of FWHM(G) < 0 at 2theta:  136.618 for phase no.    1 -> Fixing to HG=1.0e-10
=> Square of FWHM(G) < 0 at 2theta:   99.705 for phase no.    1 -> Fixing to HG=1.0e-10
=> Square of FWHM(G) < 0 at 2theta:   99.705 for phase no.    1 -> Fixing to HG=1.0e-10
=> Square of FWHM(G) < 0 at 2theta:  100.033 for phase no.    1 -> Fixing to HG=1.0e-10
=> Square of FWHM(G) < 0 at 2theta:  100.033 for phase no.    1 -> Fixing to HG=1.0e-10
=> Square of FWHM(G) < 0 at 2theta:  103.728 for phase no.    1 -> Fixing to HG=1.0e-10
=> Square of FWHM(G) < 0 at 2theta:  103.728 for phase no.    1 -> Fixing to HG=1.0e-10
=> Square of FWHM(G) < 0 at 2theta:  104.081 for phase no.    1 -> Fixing to HG=1.0e-10
=> Square of FWHM(G) < 0 at 2theta:  104.081 for phase no.    1 -> Fixing to HG=1.0e-10
=> Square of FWHM(G) < 0 at 2theta:  107.821 for phase no.    1 -> Fixing to HG=1.0e-10
=> Square of FWHM(G) < 0 at 2theta:  108.202 for phase no.    1 -> Fixing to HG=1.0e-10
=> Square of FWHM(G) < 0 at 2theta:  112.011 for phase no.    1 -> Fixing to HG=1.0e-10
=> Square of FWHM(G) < 0 at 2theta:  112.422 for phase no.    1 -> Fixing to HG=1.0e-10
=> Square of FWHM(G) < 0 at 2theta:  116.329 for phase no.    1 -> Fixing to HG=1.0e-10
=> Square of FWHM(G) < 0 at 2theta:  116.776 for phase no.    1 -> Fixing to HG=1.0e-10
=> Square of FWHM(G) < 0 at 2theta:  120.815 for phase no.    1 -> Fixing to HG=1.0e-10
=> Square of FWHM(G) < 0 at 2theta:  121.304 for phase no.    1 -> Fixing to HG=1.0e-10
=> Square of FWHM(G) < 0 at 2theta:  130.522 for phase no.    1 -> Fixing to HG=1.0e-10
=> Square of FWHM(G) < 0 at 2theta:  131.126 for phase no.    1 -> Fixing to HG=1.0e-10
=> Square of FWHM(G) < 0 at 2theta:  135.929 for phase no.    1 -> Fixing to HG=1.0e-10
=> Square of FWHM(G) < 0 at 2theta:  135.929 for phase no.    1 -> Fixing to HG=1.0e-10
=> Square of FWHM(G) < 0 at 2theta:  136.618 for phase no.    1 -> Fixing to HG=1.0e-10
=> Square of FWHM(G) < 0 at 2theta:  136.618 for phase no.    1 -> Fixing to HG=1.0e-10
=> Square of FWHM(G) < 0 at 2theta:   99.705 for phase no.    1 -> Fixing to HG=1.0e-10
=> Square of FWHM(G) < 0 at 2theta:   99.705 for phase no.    1 -> Fixing to HG=1.0e-10
=> Square of FWHM(G) < 0 at 2theta:  100.033 for phase no.    1 -> Fixing to HG=1.0e-10
=> Square of FWHM(G) < 0 at 2theta:  100.033 for phase no.    1 -> Fixing to HG=1.0e-10
=> Square of FWHM(G) < 0 at 2theta:  103.728 for phase no.    1 -> Fixing to HG=1.0e-10
=> Square of FWHM(G) < 0 at 2theta:  103.728 for phase no.    1 -> Fixing to HG=1.0e-10
=> Square of FWHM(G) < 0 at 2theta:  104.081 for phase no.    1 -> Fixing to HG=1.0e-10
=> Square of FWHM(G) < 0 at 2theta:  104.081 for phase no.    1 -> Fixing to HG=1.0e-10
=> Square of FWHM(G) < 0 at 2theta:  107.821 for phase no.    1 -> Fixing to HG=1.0e-10
=> Square of FWHM(G) < 0 at 2theta:  108.202 for phase no.    1 -> Fixing to HG=1.0e-10
=> Square of FWHM(G) < 0 at 2theta:  112.011 for phase no.    1 -> Fixing to HG=1.0e-10
=> Square of FWHM(G) < 0 at 2theta:  112.422 for phase no.    1 -> Fixing to HG=1.0e-10
=> Square of FWHM(G) < 0 at 2theta:  116.329 for phase no.    1 -> Fixing to HG=1.0e-10
=> Square of FWHM(G) < 0 at 2theta:  116.776 for phase no.    1 -> Fixing to HG=1.0e-10
=> Square of FWHM(G) < 0 at 2theta:  120.815 for phase no.    1 -> Fixing to HG=1.0e-10
=> Square of FWHM(G) < 0 at 2theta:  121.304 for phase no.    1 -> Fixing to HG=1.0e-10
=> Square of FWHM(G) < 0 at 2theta:  130.522 for phase no.    1 -> Fixing to HG=1.0e-10
=> Square of FWHM(G) < 0 at 2theta:  131.126 for phase no.    1 -> Fixing to HG=1.0e-10
```

```
=> Square of FWHM(G) < 0 at 2theta:  135.929 for phase no.    1 -> Fixing to HG=1.0e-10
=> Square of FWHM(G) < 0 at 2theta:  135.929 for phase no.    1 -> Fixing to HG=1.0e-10
=> Square of FWHM(G) < 0 at 2theta:  136.618 for phase no.    1 -> Fixing to HG=1.0e-10
=> Square of FWHM(G) < 0 at 2theta:  136.618 for phase no.    1 -> Fixing to HG=1.0e-10
=> Square of FWHM(G) < 0 at 2theta:   99.705 for phase no.    1 -> Fixing to HG=1.0e-10
=> Square of FWHM(G) < 0 at 2theta:   99.705 for phase no.    1 -> Fixing to HG=1.0e-10
=> Square of FWHM(G) < 0 at 2theta:  100.033 for phase no.    1 -> Fixing to HG=1.0e-10
=> Square of FWHM(G) < 0 at 2theta:  100.033 for phase no.    1 -> Fixing to HG=1.0e-10
=> Square of FWHM(G) < 0 at 2theta:  103.728 for phase no.    1 -> Fixing to HG=1.0e-10
=> Square of FWHM(G) < 0 at 2theta:  103.728 for phase no.    1 -> Fixing to HG=1.0e-10
=> Square of FWHM(G) < 0 at 2theta:  104.081 for phase no.    1 -> Fixing to HG=1.0e-10
=> Square of FWHM(G) < 0 at 2theta:  104.081 for phase no.    1 -> Fixing to HG=1.0e-10
=> Square of FWHM(G) < 0 at 2theta:  107.821 for phase no.    1 -> Fixing to HG=1.0e-10
=> Square of FWHM(G) < 0 at 2theta:  108.202 for phase no.    1 -> Fixing to HG=1.0e-10
=> Square of FWHM(G) < 0 at 2theta:  112.011 for phase no.    1 -> Fixing to HG=1.0e-10
=> Square of FWHM(G) < 0 at 2theta:  112.422 for phase no.    1 -> Fixing to HG=1.0e-10
=> Square of FWHM(G) < 0 at 2theta:  116.329 for phase no.    1 -> Fixing to HG=1.0e-10
=> Square of FWHM(G) < 0 at 2theta:  116.776 for phase no.    1 -> Fixing to HG=1.0e-10
=> Square of FWHM(G) < 0 at 2theta:  120.815 for phase no.    1 -> Fixing to HG=1.0e-10
=> Square of FWHM(G) < 0 at 2theta:  121.304 for phase no.    1 -> Fixing to HG=1.0e-10
=> Square of FWHM(G) < 0 at 2theta:  130.522 for phase no.    1 -> Fixing to HG=1.0e-10
=> Square of FWHM(G) < 0 at 2theta:  131.126 for phase no.    1 -> Fixing to HG=1.0e-10
=> Square of FWHM(G) < 0 at 2theta:  135.929 for phase no.    1 -> Fixing to HG=1.0e-10
=> Square of FWHM(G) < 0 at 2theta:  135.929 for phase no.    1 -> Fixing to HG=1.0e-10
=> Square of FWHM(G) < 0 at 2theta:  136.618 for phase no.    1 -> Fixing to HG=1.0e-10
=> Square of FWHM(G) < 0 at 2theta:  136.618 for phase no.    1 -> Fixing to HG=1.0e-10
=> Square of FWHM(G) < 0 at 2theta:   99.705 for phase no.    1 -> Fixing to HG=1.0e-10
=> Square of FWHM(G) < 0 at 2theta:   99.705 for phase no.    1 -> Fixing to HG=1.0e-10
=> Square of FWHM(G) < 0 at 2theta:  100.033 for phase no.    1 -> Fixing to HG=1.0e-10
=> Square of FWHM(G) < 0 at 2theta:  100.033 for phase no.    1 -> Fixing to HG=1.0e-10
=> Square of FWHM(G) < 0 at 2theta:  103.728 for phase no.    1 -> Fixing to HG=1.0e-10
=> Square of FWHM(G) < 0 at 2theta:  103.728 for phase no.    1 -> Fixing to HG=1.0e-10
=> Square of FWHM(G) < 0 at 2theta:  104.081 for phase no.    1 -> Fixing to HG=1.0e-10
=> Square of FWHM(G) < 0 at 2theta:  104.081 for phase no.    1 -> Fixing to HG=1.0e-10
=> Square of FWHM(G) < 0 at 2theta:  107.821 for phase no.    1 -> Fixing to HG=1.0e-10
=> Square of FWHM(G) < 0 at 2theta:  108.202 for phase no.    1 -> Fixing to HG=1.0e-10
=> Square of FWHM(G) < 0 at 2theta:  112.011 for phase no.    1 -> Fixing to HG=1.0e-10
=> Square of FWHM(G) < 0 at 2theta:  112.422 for phase no.    1 -> Fixing to HG=1.0e-10
=> Square of FWHM(G) < 0 at 2theta:  116.329 for phase no.    1 -> Fixing to HG=1.0e-10
=> Square of FWHM(G) < 0 at 2theta:  116.776 for phase no.    1 -> Fixing to HG=1.0e-10
=> Square of FWHM(G) < 0 at 2theta:  120.815 for phase no.    1 -> Fixing to HG=1.0e-10
=> Square of FWHM(G) < 0 at 2theta:  121.304 for phase no.    1 -> Fixing to HG=1.0e-10
=> Square of FWHM(G) < 0 at 2theta:  130.522 for phase no.    1 -> Fixing to HG=1.0e-10
=> Square of FWHM(G) < 0 at 2theta:  131.126 for phase no.    1 -> Fixing to HG=1.0e-10
=> Square of FWHM(G) < 0 at 2theta:  135.929 for phase no.    1 -> Fixing to HG=1.0e-10
=> Square of FWHM(G) < 0 at 2theta:  135.929 for phase no.    1 -> Fixing to HG=1.0e-10
=> Square of FWHM(G) < 0 at 2theta:  136.618 for phase no.    1 -> Fixing to HG=1.0e-10
=> Square of FWHM(G) < 0 at 2theta:  136.618 for phase no.    1 -> Fixing to HG=1.0e-10
=> Square of FWHM(G) < 0 at 2theta:   99.705 for phase no.    1 -> Fixing to HG=1.0e-10
=> Square of FWHM(G) < 0 at 2theta:   99.705 for phase no.    1 -> Fixing to HG=1.0e-10
=> Square of FWHM(G) < 0 at 2theta:  100.033 for phase no.    1 -> Fixing to HG=1.0e-10
=> Square of FWHM(G) < 0 at 2theta:  100.033 for phase no.    1 -> Fixing to HG=1.0e-10
=> Square of FWHM(G) < 0 at 2theta:  103.728 for phase no.    1 -> Fixing to HG=1.0e-10
=> Square of FWHM(G) < 0 at 2theta:  103.728 for phase no.    1 -> Fixing to HG=1.0e-10
=> Square of FWHM(G) < 0 at 2theta:  104.081 for phase no.    1 -> Fixing to HG=1.0e-10
=> Square of FWHM(G) < 0 at 2theta:  104.081 for phase no.    1 -> Fixing to HG=1.0e-10
=> Square of FWHM(G) < 0 at 2theta:  107.821 for phase no.    1 -> Fixing to HG=1.0e-10
=> Square of FWHM(G) < 0 at 2theta:  108.202 for phase no.    1 -> Fixing to HG=1.0e-10
=> Square of FWHM(G) < 0 at 2theta:  112.011 for phase no.    1 -> Fixing to HG=1.0e-10
=> Square of FWHM(G) < 0 at 2theta:  112.422 for phase no.    1 -> Fixing to HG=1.0e-10
=> Square of FWHM(G) < 0 at 2theta:  116.329 for phase no.    1 -> Fixing to HG=1.0e-10
=> Square of FWHM(G) < 0 at 2theta:  116.776 for phase no.    1 -> Fixing to HG=1.0e-10
=> Square of FWHM(G) < 0 at 2theta:  120.815 for phase no.    1 -> Fixing to HG=1.0e-10
=> Square of FWHM(G) < 0 at 2theta:  121.304 for phase no.    1 -> Fixing to HG=1.0e-10
=> Square of FWHM(G) < 0 at 2theta:  130.522 for phase no.    1 -> Fixing to HG=1.0e-10
=> Square of FWHM(G) < 0 at 2theta:  131.126 for phase no.    1 -> Fixing to HG=1.0e-10
=> Square of FWHM(G) < 0 at 2theta:  135.929 for phase no.    1 -> Fixing to HG=1.0e-10
=> Square of FWHM(G) < 0 at 2theta:  135.929 for phase no.    1 -> Fixing to HG=1.0e-10
=> Square of FWHM(G) < 0 at 2theta:  136.618 for phase no.    1 -> Fixing to HG=1.0e-10
=> Square of FWHM(G) < 0 at 2theta:  136.618 for phase no.    1 -> Fixing to HG=1.0e-10
=> Square of FWHM(G) < 0 at 2theta:   99.705 for phase no.    1 -> Fixing to HG=1.0e-10
=> Square of FWHM(G) < 0 at 2theta:   99.705 for phase no.    1 -> Fixing to HG=1.0e-10
=> Square of FWHM(G) < 0 at 2theta:  100.033 for phase no.    1 -> Fixing to HG=1.0e-10
=> Square of FWHM(G) < 0 at 2theta:  100.033 for phase no.    1 -> Fixing to HG=1.0e-10
=> Square of FWHM(G) < 0 at 2theta:  103.728 for phase no.    1 -> Fixing to HG=1.0e-10
=> Square of FWHM(G) < 0 at 2theta:  103.728 for phase no.    1 -> Fixing to HG=1.0e-10
=> Square of FWHM(G) < 0 at 2theta:  104.081 for phase no.    1 -> Fixing to HG=1.0e-10
=> Square of FWHM(G) < 0 at 2theta:  104.081 for phase no.    1 -> Fixing to HG=1.0e-10
=> Square of FWHM(G) < 0 at 2theta:  107.821 for phase no.    1 -> Fixing to HG=1.0e-10
=> Square of FWHM(G) < 0 at 2theta:  108.202 for phase no.    1 -> Fixing to HG=1.0e-10
=> Square of FWHM(G) < 0 at 2theta:  112.011 for phase no.    1 -> Fixing to HG=1.0e-10
=> Square of FWHM(G) < 0 at 2theta:  112.422 for phase no.    1 -> Fixing to HG=1.0e-10
=> Square of FWHM(G) < 0 at 2theta:  116.329 for phase no.    1 -> Fixing to HG=1.0e-10
=> Square of FWHM(G) < 0 at 2theta:  116.776 for phase no.    1 -> Fixing to HG=1.0e-10
=> Square of FWHM(G) < 0 at 2theta:  120.815 for phase no.    1 -> Fixing to HG=1.0e-10
=> Square of FWHM(G) < 0 at 2theta:  121.304 for phase no.    1 -> Fixing to HG=1.0e-10
=> Square of FWHM(G) < 0 at 2theta:  130.522 for phase no.    1 -> Fixing to HG=1.0e-10
=> Square of FWHM(G) < 0 at 2theta:  131.126 for phase no.    1 -> Fixing to HG=1.0e-10
=> Square of FWHM(G) < 0 at 2theta:  135.929 for phase no.    1 -> Fixing to HG=1.0e-10
=> Square of FWHM(G) < 0 at 2theta:  135.929 for phase no.    1 -> Fixing to HG=1.0e-10
```

```
=> Square of FWHM(G) < 0 at 2theta:  136.618 for phase no.    1 -> Fixing to HG=1.0e-10
=> Square of FWHM(G) < 0 at 2theta:  136.618 for phase no.    1 -> Fixing to HG=1.0e-10
=> Square of FWHM(G) < 0 at 2theta:   99.705 for phase no.    1 -> Fixing to HG=1.0e-10
=> Square of FWHM(G) < 0 at 2theta:   99.705 for phase no.    1 -> Fixing to HG=1.0e-10
=> Square of FWHM(G) < 0 at 2theta:  100.033 for phase no.    1 -> Fixing to HG=1.0e-10
=> Square of FWHM(G) < 0 at 2theta:  100.033 for phase no.    1 -> Fixing to HG=1.0e-10
=> Square of FWHM(G) < 0 at 2theta:  103.728 for phase no.    1 -> Fixing to HG=1.0e-10
=> Square of FWHM(G) < 0 at 2theta:  103.728 for phase no.    1 -> Fixing to HG=1.0e-10
=> Square of FWHM(G) < 0 at 2theta:  104.081 for phase no.    1 -> Fixing to HG=1.0e-10
=> Square of FWHM(G) < 0 at 2theta:  104.081 for phase no.    1 -> Fixing to HG=1.0e-10
=> Square of FWHM(G) < 0 at 2theta:  107.821 for phase no.    1 -> Fixing to HG=1.0e-10
=> Square of FWHM(G) < 0 at 2theta:  108.202 for phase no.    1 -> Fixing to HG=1.0e-10
=> Square of FWHM(G) < 0 at 2theta:  112.011 for phase no.    1 -> Fixing to HG=1.0e-10
=> Square of FWHM(G) < 0 at 2theta:  112.422 for phase no.    1 -> Fixing to HG=1.0e-10
=> Square of FWHM(G) < 0 at 2theta:  116.329 for phase no.    1 -> Fixing to HG=1.0e-10
=> Square of FWHM(G) < 0 at 2theta:  116.776 for phase no.    1 -> Fixing to HG=1.0e-10
=> Square of FWHM(G) < 0 at 2theta:  120.815 for phase no.    1 -> Fixing to HG=1.0e-10
=> Square of FWHM(G) < 0 at 2theta:  121.304 for phase no.    1 -> Fixing to HG=1.0e-10
=> Square of FWHM(G) < 0 at 2theta:  130.522 for phase no.    1 -> Fixing to HG=1.0e-10
=> Square of FWHM(G) < 0 at 2theta:  131.126 for phase no.    1 -> Fixing to HG=1.0e-10
=> Square of FWHM(G) < 0 at 2theta:  135.929 for phase no.    1 -> Fixing to HG=1.0e-10
=> Square of FWHM(G) < 0 at 2theta:  135.929 for phase no.    1 -> Fixing to HG=1.0e-10
=> Square of FWHM(G) < 0 at 2theta:  136.618 for phase no.    1 -> Fixing to HG=1.0e-10
=> Square of FWHM(G) < 0 at 2theta:  136.618 for phase no.    1 -> Fixing to HG=1.0e-10
=> Square of FWHM(G) < 0 at 2theta:   99.705 for phase no.    1 -> Fixing to HG=1.0e-10
=> Square of FWHM(G) < 0 at 2theta:   99.705 for phase no.    1 -> Fixing to HG=1.0e-10
=> Square of FWHM(G) < 0 at 2theta:  100.033 for phase no.    1 -> Fixing to HG=1.0e-10
=> Square of FWHM(G) < 0 at 2theta:  100.033 for phase no.    1 -> Fixing to HG=1.0e-10
=> Square of FWHM(G) < 0 at 2theta:  103.728 for phase no.    1 -> Fixing to HG=1.0e-10
=> Square of FWHM(G) < 0 at 2theta:  103.728 for phase no.    1 -> Fixing to HG=1.0e-10
=> Square of FWHM(G) < 0 at 2theta:  104.081 for phase no.    1 -> Fixing to HG=1.0e-10
=> Square of FWHM(G) < 0 at 2theta:  104.081 for phase no.    1 -> Fixing to HG=1.0e-10
=> Square of FWHM(G) < 0 at 2theta:  107.821 for phase no.    1 -> Fixing to HG=1.0e-10
=> Square of FWHM(G) < 0 at 2theta:  108.202 for phase no.    1 -> Fixing to HG=1.0e-10
=> Square of FWHM(G) < 0 at 2theta:  112.011 for phase no.    1 -> Fixing to HG=1.0e-10
=> Square of FWHM(G) < 0 at 2theta:  112.422 for phase no.    1 -> Fixing to HG=1.0e-10
=> Square of FWHM(G) < 0 at 2theta:  116.329 for phase no.    1 -> Fixing to HG=1.0e-10
=> Square of FWHM(G) < 0 at 2theta:  116.776 for phase no.    1 -> Fixing to HG=1.0e-10
=> Square of FWHM(G) < 0 at 2theta:  120.815 for phase no.    1 -> Fixing to HG=1.0e-10
=> Square of FWHM(G) < 0 at 2theta:  121.304 for phase no.    1 -> Fixing to HG=1.0e-10
=> Square of FWHM(G) < 0 at 2theta:  130.522 for phase no.    1 -> Fixing to HG=1.0e-10
=> Square of FWHM(G) < 0 at 2theta:  131.126 for phase no.    1 -> Fixing to HG=1.0e-10
=> Square of FWHM(G) < 0 at 2theta:  135.929 for phase no.    1 -> Fixing to HG=1.0e-10
=> Square of FWHM(G) < 0 at 2theta:  135.929 for phase no.    1 -> Fixing to HG=1.0e-10
=> Square of FWHM(G) < 0 at 2theta:  136.618 for phase no.    1 -> Fixing to HG=1.0e-10
=> Square of FWHM(G) < 0 at 2theta:  136.618 for phase no.    1 -> Fixing to HG=1.0e-10
=> Square of FWHM(G) < 0 at 2theta:   99.705 for phase no.    1 -> Fixing to HG=1.0e-10
=> Square of FWHM(G) < 0 at 2theta:   99.705 for phase no.    1 -> Fixing to HG=1.0e-10
=> Square of FWHM(G) < 0 at 2theta:  100.033 for phase no.    1 -> Fixing to HG=1.0e-10
=> Square of FWHM(G) < 0 at 2theta:  100.033 for phase no.    1 -> Fixing to HG=1.0e-10
=> Square of FWHM(G) < 0 at 2theta:  103.728 for phase no.    1 -> Fixing to HG=1.0e-10
=> Square of FWHM(G) < 0 at 2theta:  103.728 for phase no.    1 -> Fixing to HG=1.0e-10
=> Square of FWHM(G) < 0 at 2theta:  104.081 for phase no.    1 -> Fixing to HG=1.0e-10
=> Square of FWHM(G) < 0 at 2theta:  104.081 for phase no.    1 -> Fixing to HG=1.0e-10
=> Square of FWHM(G) < 0 at 2theta:  107.821 for phase no.    1 -> Fixing to HG=1.0e-10
=> Square of FWHM(G) < 0 at 2theta:  108.202 for phase no.    1 -> Fixing to HG=1.0e-10
=> Square of FWHM(G) < 0 at 2theta:  112.011 for phase no.    1 -> Fixing to HG=1.0e-10
=> Square of FWHM(G) < 0 at 2theta:  112.422 for phase no.    1 -> Fixing to HG=1.0e-10
=> Square of FWHM(G) < 0 at 2theta:  116.329 for phase no.    1 -> Fixing to HG=1.0e-10
=> Square of FWHM(G) < 0 at 2theta:  116.776 for phase no.    1 -> Fixing to HG=1.0e-10
=> Square of FWHM(G) < 0 at 2theta:  120.815 for phase no.    1 -> Fixing to HG=1.0e-10
=> Square of FWHM(G) < 0 at 2theta:  121.304 for phase no.    1 -> Fixing to HG=1.0e-10
=> Square of FWHM(G) < 0 at 2theta:  130.522 for phase no.    1 -> Fixing to HG=1.0e-10
=> Square of FWHM(G) < 0 at 2theta:  131.126 for phase no.    1 -> Fixing to HG=1.0e-10
=> Square of FWHM(G) < 0 at 2theta:  135.929 for phase no.    1 -> Fixing to HG=1.0e-10
=> Square of FWHM(G) < 0 at 2theta:  135.929 for phase no.    1 -> Fixing to HG=1.0e-10
=> Square of FWHM(G) < 0 at 2theta:  136.618 for phase no.    1 -> Fixing to HG=1.0e-10
=> Square of FWHM(G) < 0 at 2theta:  136.618 for phase no.    1 -> Fixing to HG=1.0e-10
=> Square of FWHM(G) < 0 at 2theta:   99.705 for phase no.    1 -> Fixing to HG=1.0e-10
=> Square of FWHM(G) < 0 at 2theta:   99.705 for phase no.    1 -> Fixing to HG=1.0e-10
=> Square of FWHM(G) < 0 at 2theta:  100.033 for phase no.    1 -> Fixing to HG=1.0e-10
=> Square of FWHM(G) < 0 at 2theta:  100.033 for phase no.    1 -> Fixing to HG=1.0e-10
=> Square of FWHM(G) < 0 at 2theta:  103.728 for phase no.    1 -> Fixing to HG=1.0e-10
=> Square of FWHM(G) < 0 at 2theta:  103.728 for phase no.    1 -> Fixing to HG=1.0e-10
=> Square of FWHM(G) < 0 at 2theta:  104.081 for phase no.    1 -> Fixing to HG=1.0e-10
=> Square of FWHM(G) < 0 at 2theta:  104.081 for phase no.    1 -> Fixing to HG=1.0e-10
=> Square of FWHM(G) < 0 at 2theta:  107.821 for phase no.    1 -> Fixing to HG=1.0e-10
=> Square of FWHM(G) < 0 at 2theta:  108.202 for phase no.    1 -> Fixing to HG=1.0e-10
=> Square of FWHM(G) < 0 at 2theta:  112.011 for phase no.    1 -> Fixing to HG=1.0e-10
=> Square of FWHM(G) < 0 at 2theta:  112.422 for phase no.    1 -> Fixing to HG=1.0e-10
=> Square of FWHM(G) < 0 at 2theta:  116.329 for phase no.    1 -> Fixing to HG=1.0e-10
=> Square of FWHM(G) < 0 at 2theta:  116.776 for phase no.    1 -> Fixing to HG=1.0e-10
=> Square of FWHM(G) < 0 at 2theta:  120.815 for phase no.    1 -> Fixing to HG=1.0e-10
=> Square of FWHM(G) < 0 at 2theta:  121.304 for phase no.    1 -> Fixing to HG=1.0e-10
=> Square of FWHM(G) < 0 at 2theta:  130.522 for phase no.    1 -> Fixing to HG=1.0e-10
=> Square of FWHM(G) < 0 at 2theta:  131.126 for phase no.    1 -> Fixing to HG=1.0e-10
=> Square of FWHM(G) < 0 at 2theta:  135.929 for phase no.    1 -> Fixing to HG=1.0e-10
=> Square of FWHM(G) < 0 at 2theta:  135.929 for phase no.    1 -> Fixing to HG=1.0e-10
=> Square of FWHM(G) < 0 at 2theta:  136.618 for phase no.    1 -> Fixing to HG=1.0e-10
=> Square of FWHM(G) < 0 at 2theta:  136.618 for phase no.    1 -> Fixing to HG=1.0e-10
```

```
=> Square of FWHM(G) < 0 at 2theta:   99.705 for phase no.    1 -> Fixing to HG=1.0e-10
=> Square of FWHM(G) < 0 at 2theta:   99.705 for phase no.    1 -> Fixing to HG=1.0e-10
=> Square of FWHM(G) < 0 at 2theta:  100.033 for phase no.    1 -> Fixing to HG=1.0e-10
=> Square of FWHM(G) < 0 at 2theta:  100.033 for phase no.    1 -> Fixing to HG=1.0e-10
=> Square of FWHM(G) < 0 at 2theta:  103.728 for phase no.    1 -> Fixing to HG=1.0e-10
=> Square of FWHM(G) < 0 at 2theta:  103.728 for phase no.    1 -> Fixing to HG=1.0e-10
=> Square of FWHM(G) < 0 at 2theta:  104.081 for phase no.    1 -> Fixing to HG=1.0e-10
=> Square of FWHM(G) < 0 at 2theta:  104.081 for phase no.    1 -> Fixing to HG=1.0e-10
=> Square of FWHM(G) < 0 at 2theta:  107.821 for phase no.    1 -> Fixing to HG=1.0e-10
=> Square of FWHM(G) < 0 at 2theta:  108.202 for phase no.    1 -> Fixing to HG=1.0e-10
=> Square of FWHM(G) < 0 at 2theta:  112.011 for phase no.    1 -> Fixing to HG=1.0e-10
=> Square of FWHM(G) < 0 at 2theta:  112.422 for phase no.    1 -> Fixing to HG=1.0e-10
=> Square of FWHM(G) < 0 at 2theta:  116.329 for phase no.    1 -> Fixing to HG=1.0e-10
=> Square of FWHM(G) < 0 at 2theta:  116.776 for phase no.    1 -> Fixing to HG=1.0e-10
=> Square of FWHM(G) < 0 at 2theta:  120.815 for phase no.    1 -> Fixing to HG=1.0e-10
=> Square of FWHM(G) < 0 at 2theta:  121.304 for phase no.    1 -> Fixing to HG=1.0e-10
=> Square of FWHM(G) < 0 at 2theta:  130.522 for phase no.    1 -> Fixing to HG=1.0e-10
=> Square of FWHM(G) < 0 at 2theta:  131.126 for phase no.    1 -> Fixing to HG=1.0e-10
=> Square of FWHM(G) < 0 at 2theta:  135.929 for phase no.    1 -> Fixing to HG=1.0e-10
=> Square of FWHM(G) < 0 at 2theta:  135.929 for phase no.    1 -> Fixing to HG=1.0e-10
=> Square of FWHM(G) < 0 at 2theta:  136.618 for phase no.    1 -> Fixing to HG=1.0e-10
=> Square of FWHM(G) < 0 at 2theta:  136.618 for phase no.    1 -> Fixing to HG=1.0e-10
=> Square of FWHM(G) < 0 at 2theta:   99.705 for phase no.    1 -> Fixing to HG=1.0e-10
=> Square of FWHM(G) < 0 at 2theta:   99.705 for phase no.    1 -> Fixing to HG=1.0e-10
=> Square of FWHM(G) < 0 at 2theta:  100.033 for phase no.    1 -> Fixing to HG=1.0e-10
=> Square of FWHM(G) < 0 at 2theta:  100.033 for phase no.    1 -> Fixing to HG=1.0e-10
=> Square of FWHM(G) < 0 at 2theta:  103.728 for phase no.    1 -> Fixing to HG=1.0e-10
=> Square of FWHM(G) < 0 at 2theta:  103.728 for phase no.    1 -> Fixing to HG=1.0e-10
=> Square of FWHM(G) < 0 at 2theta:  104.081 for phase no.    1 -> Fixing to HG=1.0e-10
=> Square of FWHM(G) < 0 at 2theta:  104.081 for phase no.    1 -> Fixing to HG=1.0e-10
=> Square of FWHM(G) < 0 at 2theta:  107.821 for phase no.    1 -> Fixing to HG=1.0e-10
=> Square of FWHM(G) < 0 at 2theta:  108.202 for phase no.    1 -> Fixing to HG=1.0e-10
=> Square of FWHM(G) < 0 at 2theta:  112.011 for phase no.    1 -> Fixing to HG=1.0e-10
=> Square of FWHM(G) < 0 at 2theta:  112.422 for phase no.    1 -> Fixing to HG=1.0e-10
=> Square of FWHM(G) < 0 at 2theta:  116.329 for phase no.    1 -> Fixing to HG=1.0e-10
=> Square of FWHM(G) < 0 at 2theta:  116.776 for phase no.    1 -> Fixing to HG=1.0e-10
=> Square of FWHM(G) < 0 at 2theta:  120.815 for phase no.    1 -> Fixing to HG=1.0e-10
=> Square of FWHM(G) < 0 at 2theta:  121.304 for phase no.    1 -> Fixing to HG=1.0e-10
=> Square of FWHM(G) < 0 at 2theta:  130.522 for phase no.    1 -> Fixing to HG=1.0e-10
=> Square of FWHM(G) < 0 at 2theta:  131.126 for phase no.    1 -> Fixing to HG=1.0e-10
=> Square of FWHM(G) < 0 at 2theta:  135.929 for phase no.    1 -> Fixing to HG=1.0e-10
=> Square of FWHM(G) < 0 at 2theta:  135.929 for phase no.    1 -> Fixing to HG=1.0e-10
=> Square of FWHM(G) < 0 at 2theta:  136.618 for phase no.    1 -> Fixing to HG=1.0e-10
=> Square of FWHM(G) < 0 at 2theta:  136.618 for phase no.    1 -> Fixing to HG=1.0e-10
=> Square of FWHM(G) < 0 at 2theta:   99.705 for phase no.    1 -> Fixing to HG=1.0e-10
=> Square of FWHM(G) < 0 at 2theta:   99.705 for phase no.    1 -> Fixing to HG=1.0e-10
=> Square of FWHM(G) < 0 at 2theta:  100.033 for phase no.    1 -> Fixing to HG=1.0e-10
=> Square of FWHM(G) < 0 at 2theta:  100.033 for phase no.    1 -> Fixing to HG=1.0e-10
=> Square of FWHM(G) < 0 at 2theta:  103.728 for phase no.    1 -> Fixing to HG=1.0e-10
=> Square of FWHM(G) < 0 at 2theta:  103.728 for phase no.    1 -> Fixing to HG=1.0e-10
=> Square of FWHM(G) < 0 at 2theta:  104.081 for phase no.    1 -> Fixing to HG=1.0e-10
=> Square of FWHM(G) < 0 at 2theta:  104.081 for phase no.    1 -> Fixing to HG=1.0e-10
=> Square of FWHM(G) < 0 at 2theta:  107.821 for phase no.    1 -> Fixing to HG=1.0e-10
=> Square of FWHM(G) < 0 at 2theta:  108.202 for phase no.    1 -> Fixing to HG=1.0e-10
=> Square of FWHM(G) < 0 at 2theta:  112.011 for phase no.    1 -> Fixing to HG=1.0e-10
=> Square of FWHM(G) < 0 at 2theta:  112.422 for phase no.    1 -> Fixing to HG=1.0e-10
=> Square of FWHM(G) < 0 at 2theta:  116.329 for phase no.    1 -> Fixing to HG=1.0e-10
=> Square of FWHM(G) < 0 at 2theta:  116.776 for phase no.    1 -> Fixing to HG=1.0e-10
=> Square of FWHM(G) < 0 at 2theta:  120.815 for phase no.    1 -> Fixing to HG=1.0e-10
=> Square of FWHM(G) < 0 at 2theta:  121.304 for phase no.    1 -> Fixing to HG=1.0e-10
=> Square of FWHM(G) < 0 at 2theta:  130.522 for phase no.    1 -> Fixing to HG=1.0e-10
=> Square of FWHM(G) < 0 at 2theta:  131.126 for phase no.    1 -> Fixing to HG=1.0e-10
=> Square of FWHM(G) < 0 at 2theta:  135.929 for phase no.    1 -> Fixing to HG=1.0e-10
=> Square of FWHM(G) < 0 at 2theta:  135.929 for phase no.    1 -> Fixing to HG=1.0e-10
=> Square of FWHM(G) < 0 at 2theta:  136.618 for phase no.    1 -> Fixing to HG=1.0e-10
=> Square of FWHM(G) < 0 at 2theta:  136.618 for phase no.    1 -> Fixing to HG=1.0e-10
=> Square of FWHM(G) < 0 at 2theta:   99.705 for phase no.    1 -> Fixing to HG=1.0e-10
=> Square of FWHM(G) < 0 at 2theta:   99.705 for phase no.    1 -> Fixing to HG=1.0e-10
=> Square of FWHM(G) < 0 at 2theta:  100.033 for phase no.    1 -> Fixing to HG=1.0e-10
=> Square of FWHM(G) < 0 at 2theta:  100.033 for phase no.    1 -> Fixing to HG=1.0e-10
=> Square of FWHM(G) < 0 at 2theta:  103.728 for phase no.    1 -> Fixing to HG=1.0e-10
=> Square of FWHM(G) < 0 at 2theta:  103.728 for phase no.    1 -> Fixing to HG=1.0e-10
=> Square of FWHM(G) < 0 at 2theta:  104.081 for phase no.    1 -> Fixing to HG=1.0e-10
=> Square of FWHM(G) < 0 at 2theta:  104.081 for phase no.    1 -> Fixing to HG=1.0e-10
=> Square of FWHM(G) < 0 at 2theta:  107.821 for phase no.    1 -> Fixing to HG=1.0e-10
=> Square of FWHM(G) < 0 at 2theta:  108.202 for phase no.    1 -> Fixing to HG=1.0e-10
=> Square of FWHM(G) < 0 at 2theta:  112.011 for phase no.    1 -> Fixing to HG=1.0e-10
=> Square of FWHM(G) < 0 at 2theta:  112.422 for phase no.    1 -> Fixing to HG=1.0e-10
=> Square of FWHM(G) < 0 at 2theta:  116.329 for phase no.    1 -> Fixing to HG=1.0e-10
=> Square of FWHM(G) < 0 at 2theta:  116.776 for phase no.    1 -> Fixing to HG=1.0e-10
=> Square of FWHM(G) < 0 at 2theta:  120.815 for phase no.    1 -> Fixing to HG=1.0e-10
=> Square of FWHM(G) < 0 at 2theta:  121.304 for phase no.    1 -> Fixing to HG=1.0e-10
=> Square of FWHM(G) < 0 at 2theta:  130.522 for phase no.    1 -> Fixing to HG=1.0e-10
=> Square of FWHM(G) < 0 at 2theta:  131.126 for phase no.    1 -> Fixing to HG=1.0e-10
=> Square of FWHM(G) < 0 at 2theta:  135.929 for phase no.    1 -> Fixing to HG=1.0e-10
=> Square of FWHM(G) < 0 at 2theta:  135.929 for phase no.    1 -> Fixing to HG=1.0e-10
=> Square of FWHM(G) < 0 at 2theta:  136.618 for phase no.    1 -> Fixing to HG=1.0e-10
=> Square of FWHM(G) < 0 at 2theta:  136.618 for phase no.    1 -> Fixing to HG=1.0e-10
=> Square of FWHM(G) < 0 at 2theta:   99.705 for phase no.    1 -> Fixing to HG=1.0e-10
=> Square of FWHM(G) < 0 at 2theta:   99.705 for phase no.    1 -> Fixing to HG=1.0e-10
```

```
=> Square of FWHM(G) < 0 at 2theta:  100.033 for phase no.    1 -> Fixing to HG=1.0e-10
=> Square of FWHM(G) < 0 at 2theta:  100.033 for phase no.    1 -> Fixing to HG=1.0e-10
=> Square of FWHM(G) < 0 at 2theta:  103.728 for phase no.    1 -> Fixing to HG=1.0e-10
=> Square of FWHM(G) < 0 at 2theta:  103.728 for phase no.    1 -> Fixing to HG=1.0e-10
=> Square of FWHM(G) < 0 at 2theta:  104.081 for phase no.    1 -> Fixing to HG=1.0e-10
=> Square of FWHM(G) < 0 at 2theta:  104.081 for phase no.    1 -> Fixing to HG=1.0e-10
=> Square of FWHM(G) < 0 at 2theta:  107.821 for phase no.    1 -> Fixing to HG=1.0e-10
=> Square of FWHM(G) < 0 at 2theta:  108.202 for phase no.    1 -> Fixing to HG=1.0e-10
=> Square of FWHM(G) < 0 at 2theta:  112.011 for phase no.    1 -> Fixing to HG=1.0e-10
=> Square of FWHM(G) < 0 at 2theta:  112.422 for phase no.    1 -> Fixing to HG=1.0e-10
=> Square of FWHM(G) < 0 at 2theta:  116.329 for phase no.    1 -> Fixing to HG=1.0e-10
=> Square of FWHM(G) < 0 at 2theta:  116.776 for phase no.    1 -> Fixing to HG=1.0e-10
=> Square of FWHM(G) < 0 at 2theta:  120.815 for phase no.    1 -> Fixing to HG=1.0e-10
=> Square of FWHM(G) < 0 at 2theta:  121.304 for phase no.    1 -> Fixing to HG=1.0e-10
=> Square of FWHM(G) < 0 at 2theta:  130.522 for phase no.    1 -> Fixing to HG=1.0e-10
=> Square of FWHM(G) < 0 at 2theta:  131.126 for phase no.    1 -> Fixing to HG=1.0e-10
=> Square of FWHM(G) < 0 at 2theta:  135.929 for phase no.    1 -> Fixing to HG=1.0e-10
=> Square of FWHM(G) < 0 at 2theta:  135.929 for phase no.    1 -> Fixing to HG=1.0e-10
=> Square of FWHM(G) < 0 at 2theta:  136.618 for phase no.    1 -> Fixing to HG=1.0e-10
=> Square of FWHM(G) < 0 at 2theta:  136.618 for phase no.    1 -> Fixing to HG=1.0e-10
=> Square of FWHM(G) < 0 at 2theta:   99.705 for phase no.    1 -> Fixing to HG=1.0e-10
=> Square of FWHM(G) < 0 at 2theta:   99.705 for phase no.    1 -> Fixing to HG=1.0e-10
=> Square of FWHM(G) < 0 at 2theta:  100.033 for phase no.    1 -> Fixing to HG=1.0e-10
=> Square of FWHM(G) < 0 at 2theta:  100.033 for phase no.    1 -> Fixing to HG=1.0e-10
=> Square of FWHM(G) < 0 at 2theta:  103.728 for phase no.    1 -> Fixing to HG=1.0e-10
=> Square of FWHM(G) < 0 at 2theta:  103.728 for phase no.    1 -> Fixing to HG=1.0e-10
=> Square of FWHM(G) < 0 at 2theta:  104.081 for phase no.    1 -> Fixing to HG=1.0e-10
=> Square of FWHM(G) < 0 at 2theta:  104.081 for phase no.    1 -> Fixing to HG=1.0e-10
=> Square of FWHM(G) < 0 at 2theta:  107.821 for phase no.    1 -> Fixing to HG=1.0e-10
=> Square of FWHM(G) < 0 at 2theta:  108.202 for phase no.    1 -> Fixing to HG=1.0e-10
=> Square of FWHM(G) < 0 at 2theta:  112.011 for phase no.    1 -> Fixing to HG=1.0e-10
=> Square of FWHM(G) < 0 at 2theta:  112.422 for phase no.    1 -> Fixing to HG=1.0e-10
=> Square of FWHM(G) < 0 at 2theta:  116.329 for phase no.    1 -> Fixing to HG=1.0e-10
=> Square of FWHM(G) < 0 at 2theta:  116.776 for phase no.    1 -> Fixing to HG=1.0e-10
=> Square of FWHM(G) < 0 at 2theta:  120.815 for phase no.    1 -> Fixing to HG=1.0e-10
=> Square of FWHM(G) < 0 at 2theta:  121.304 for phase no.    1 -> Fixing to HG=1.0e-10
=> Square of FWHM(G) < 0 at 2theta:  130.522 for phase no.    1 -> Fixing to HG=1.0e-10
=> Square of FWHM(G) < 0 at 2theta:  131.126 for phase no.    1 -> Fixing to HG=1.0e-10
=> Square of FWHM(G) < 0 at 2theta:  135.929 for phase no.    1 -> Fixing to HG=1.0e-10
=> Square of FWHM(G) < 0 at 2theta:  135.929 for phase no.    1 -> Fixing to HG=1.0e-10
=> Square of FWHM(G) < 0 at 2theta:  136.618 for phase no.    1 -> Fixing to HG=1.0e-10
=> Square of FWHM(G) < 0 at 2theta:  136.618 for phase no.    1 -> Fixing to HG=1.0e-10
=> Square of FWHM(G) < 0 at 2theta:   99.705 for phase no.    1 -> Fixing to HG=1.0e-10
=> Square of FWHM(G) < 0 at 2theta:   99.705 for phase no.    1 -> Fixing to HG=1.0e-10
=> Square of FWHM(G) < 0 at 2theta:  100.033 for phase no.    1 -> Fixing to HG=1.0e-10
=> Square of FWHM(G) < 0 at 2theta:  100.033 for phase no.    1 -> Fixing to HG=1.0e-10
=> Square of FWHM(G) < 0 at 2theta:  103.728 for phase no.    1 -> Fixing to HG=1.0e-10
=> Square of FWHM(G) < 0 at 2theta:  103.728 for phase no.    1 -> Fixing to HG=1.0e-10
=> Square of FWHM(G) < 0 at 2theta:  104.081 for phase no.    1 -> Fixing to HG=1.0e-10
=> Square of FWHM(G) < 0 at 2theta:  104.081 for phase no.    1 -> Fixing to HG=1.0e-10
=> Square of FWHM(G) < 0 at 2theta:  107.821 for phase no.    1 -> Fixing to HG=1.0e-10
=> Square of FWHM(G) < 0 at 2theta:  108.202 for phase no.    1 -> Fixing to HG=1.0e-10
=> Square of FWHM(G) < 0 at 2theta:  112.011 for phase no.    1 -> Fixing to HG=1.0e-10
=> Square of FWHM(G) < 0 at 2theta:  112.422 for phase no.    1 -> Fixing to HG=1.0e-10
=> Square of FWHM(G) < 0 at 2theta:  116.329 for phase no.    1 -> Fixing to HG=1.0e-10
=> Square of FWHM(G) < 0 at 2theta:  116.776 for phase no.    1 -> Fixing to HG=1.0e-10
=> Square of FWHM(G) < 0 at 2theta:  120.815 for phase no.    1 -> Fixing to HG=1.0e-10
=> Square of FWHM(G) < 0 at 2theta:  121.304 for phase no.    1 -> Fixing to HG=1.0e-10
=> Square of FWHM(G) < 0 at 2theta:  130.522 for phase no.    1 -> Fixing to HG=1.0e-10
=> Square of FWHM(G) < 0 at 2theta:  131.126 for phase no.    1 -> Fixing to HG=1.0e-10
=> Square of FWHM(G) < 0 at 2theta:  135.929 for phase no.    1 -> Fixing to HG=1.0e-10
=> Square of FWHM(G) < 0 at 2theta:  135.929 for phase no.    1 -> Fixing to HG=1.0e-10
=> Square of FWHM(G) < 0 at 2theta:  136.618 for phase no.    1 -> Fixing to HG=1.0e-10
=> Square of FWHM(G) < 0 at 2theta:  136.618 for phase no.    1 -> Fixing to HG=1.0e-10
=> Square of FWHM(G) < 0 at 2theta:   99.705 for phase no.    1 -> Fixing to HG=1.0e-10
=> Square of FWHM(G) < 0 at 2theta:   99.705 for phase no.    1 -> Fixing to HG=1.0e-10
=> Square of FWHM(G) < 0 at 2theta:  100.033 for phase no.    1 -> Fixing to HG=1.0e-10
=> Square of FWHM(G) < 0 at 2theta:  100.033 for phase no.    1 -> Fixing to HG=1.0e-10
=> Square of FWHM(G) < 0 at 2theta:  103.728 for phase no.    1 -> Fixing to HG=1.0e-10
=> Square of FWHM(G) < 0 at 2theta:  103.728 for phase no.    1 -> Fixing to HG=1.0e-10
=> Square of FWHM(G) < 0 at 2theta:  104.081 for phase no.    1 -> Fixing to HG=1.0e-10
=> Square of FWHM(G) < 0 at 2theta:  104.081 for phase no.    1 -> Fixing to HG=1.0e-10
=> Square of FWHM(G) < 0 at 2theta:  107.821 for phase no.    1 -> Fixing to HG=1.0e-10
=> Square of FWHM(G) < 0 at 2theta:  108.202 for phase no.    1 -> Fixing to HG=1.0e-10
=> Square of FWHM(G) < 0 at 2theta:  112.011 for phase no.    1 -> Fixing to HG=1.0e-10
=> Square of FWHM(G) < 0 at 2theta:  112.422 for phase no.    1 -> Fixing to HG=1.0e-10
=> Square of FWHM(G) < 0 at 2theta:  116.329 for phase no.    1 -> Fixing to HG=1.0e-10
=> Square of FWHM(G) < 0 at 2theta:  116.776 for phase no.    1 -> Fixing to HG=1.0e-10
=> Square of FWHM(G) < 0 at 2theta:  120.815 for phase no.    1 -> Fixing to HG=1.0e-10
=> Square of FWHM(G) < 0 at 2theta:  121.304 for phase no.    1 -> Fixing to HG=1.0e-10
=> Square of FWHM(G) < 0 at 2theta:  130.522 for phase no.    1 -> Fixing to HG=1.0e-10
=> Square of FWHM(G) < 0 at 2theta:  131.126 for phase no.    1 -> Fixing to HG=1.0e-10
=> Square of FWHM(G) < 0 at 2theta:  135.929 for phase no.    1 -> Fixing to HG=1.0e-10
=> Square of FWHM(G) < 0 at 2theta:  135.929 for phase no.    1 -> Fixing to HG=1.0e-10
=> Square of FWHM(G) < 0 at 2theta:  136.618 for phase no.    1 -> Fixing to HG=1.0e-10
=> Square of FWHM(G) < 0 at 2theta:  136.618 for phase no.    1 -> Fixing to HG=1.0e-10
=> Square of FWHM(G) < 0 at 2theta:   99.705 for phase no.    1 -> Fixing to HG=1.0e-10
=> Square of FWHM(G) < 0 at 2theta:   99.705 for phase no.    1 -> Fixing to HG=1.0e-10
=> Square of FWHM(G) < 0 at 2theta:  100.033 for phase no.    1 -> Fixing to HG=1.0e-10
=> Square of FWHM(G) < 0 at 2theta:  100.033 for phase no.    1 -> Fixing to HG=1.0e-10
```

```
=> Square of FWHM(G) < 0 at 2theta:  103.728 for phase no.    1 -> Fixing to HG=1.0e-10
=> Square of FWHM(G) < 0 at 2theta:  103.728 for phase no.    1 -> Fixing to HG=1.0e-10
=> Square of FWHM(G) < 0 at 2theta:  104.081 for phase no.    1 -> Fixing to HG=1.0e-10
=> Square of FWHM(G) < 0 at 2theta:  104.081 for phase no.    1 -> Fixing to HG=1.0e-10
=> Square of FWHM(G) < 0 at 2theta:  107.821 for phase no.    1 -> Fixing to HG=1.0e-10
=> Square of FWHM(G) < 0 at 2theta:  108.202 for phase no.    1 -> Fixing to HG=1.0e-10
=> Square of FWHM(G) < 0 at 2theta:  112.011 for phase no.    1 -> Fixing to HG=1.0e-10
=> Square of FWHM(G) < 0 at 2theta:  112.422 for phase no.    1 -> Fixing to HG=1.0e-10
=> Square of FWHM(G) < 0 at 2theta:  116.329 for phase no.    1 -> Fixing to HG=1.0e-10
=> Square of FWHM(G) < 0 at 2theta:  116.776 for phase no.    1 -> Fixing to HG=1.0e-10
=> Square of FWHM(G) < 0 at 2theta:  120.815 for phase no.    1 -> Fixing to HG=1.0e-10
=> Square of FWHM(G) < 0 at 2theta:  121.304 for phase no.    1 -> Fixing to HG=1.0e-10
=> Square of FWHM(G) < 0 at 2theta:  130.522 for phase no.    1 -> Fixing to HG=1.0e-10
=> Square of FWHM(G) < 0 at 2theta:  131.126 for phase no.    1 -> Fixing to HG=1.0e-10
=> Square of FWHM(G) < 0 at 2theta:  135.929 for phase no.    1 -> Fixing to HG=1.0e-10
=> Square of FWHM(G) < 0 at 2theta:  135.929 for phase no.    1 -> Fixing to HG=1.0e-10
=> Square of FWHM(G) < 0 at 2theta:  136.618 for phase no.    1 -> Fixing to HG=1.0e-10
=> Square of FWHM(G) < 0 at 2theta:  136.618 for phase no.    1 -> Fixing to HG=1.0e-10
=> Square of FWHM(G) < 0 at 2theta:   99.705 for phase no.    1 -> Fixing to HG=1.0e-10
=> Square of FWHM(G) < 0 at 2theta:   99.705 for phase no.    1 -> Fixing to HG=1.0e-10
=> Square of FWHM(G) < 0 at 2theta:  100.033 for phase no.    1 -> Fixing to HG=1.0e-10
=> Square of FWHM(G) < 0 at 2theta:  100.033 for phase no.    1 -> Fixing to HG=1.0e-10
=> Square of FWHM(G) < 0 at 2theta:  103.728 for phase no.    1 -> Fixing to HG=1.0e-10
=> Square of FWHM(G) < 0 at 2theta:  103.728 for phase no.    1 -> Fixing to HG=1.0e-10
=> Square of FWHM(G) < 0 at 2theta:  104.081 for phase no.    1 -> Fixing to HG=1.0e-10
=> Square of FWHM(G) < 0 at 2theta:  104.081 for phase no.    1 -> Fixing to HG=1.0e-10
=> Square of FWHM(G) < 0 at 2theta:  107.821 for phase no.    1 -> Fixing to HG=1.0e-10
=> Square of FWHM(G) < 0 at 2theta:  108.202 for phase no.    1 -> Fixing to HG=1.0e-10
=> Square of FWHM(G) < 0 at 2theta:  112.011 for phase no.    1 -> Fixing to HG=1.0e-10
=> Square of FWHM(G) < 0 at 2theta:  112.422 for phase no.    1 -> Fixing to HG=1.0e-10
=> Square of FWHM(G) < 0 at 2theta:  116.329 for phase no.    1 -> Fixing to HG=1.0e-10
=> Square of FWHM(G) < 0 at 2theta:  116.776 for phase no.    1 -> Fixing to HG=1.0e-10
=> Square of FWHM(G) < 0 at 2theta:  120.815 for phase no.    1 -> Fixing to HG=1.0e-10
=> Square of FWHM(G) < 0 at 2theta:  121.304 for phase no.    1 -> Fixing to HG=1.0e-10
=> Square of FWHM(G) < 0 at 2theta:  130.522 for phase no.    1 -> Fixing to HG=1.0e-10
=> Square of FWHM(G) < 0 at 2theta:  131.126 for phase no.    1 -> Fixing to HG=1.0e-10
=> Square of FWHM(G) < 0 at 2theta:  135.929 for phase no.    1 -> Fixing to HG=1.0e-10
=> Square of FWHM(G) < 0 at 2theta:  135.929 for phase no.    1 -> Fixing to HG=1.0e-10
=> Square of FWHM(G) < 0 at 2theta:  136.618 for phase no.    1 -> Fixing to HG=1.0e-10
=> Square of FWHM(G) < 0 at 2theta:  136.618 for phase no.    1 -> Fixing to HG=1.0e-10
=> Square of FWHM(G) < 0 at 2theta:   99.705 for phase no.    1 -> Fixing to HG=1.0e-10
=> Square of FWHM(G) < 0 at 2theta:   99.705 for phase no.    1 -> Fixing to HG=1.0e-10
=> Square of FWHM(G) < 0 at 2theta:  100.033 for phase no.    1 -> Fixing to HG=1.0e-10
=> Square of FWHM(G) < 0 at 2theta:  100.033 for phase no.    1 -> Fixing to HG=1.0e-10
=> Square of FWHM(G) < 0 at 2theta:  103.728 for phase no.    1 -> Fixing to HG=1.0e-10
=> Square of FWHM(G) < 0 at 2theta:  103.728 for phase no.    1 -> Fixing to HG=1.0e-10
=> Square of FWHM(G) < 0 at 2theta:  104.081 for phase no.    1 -> Fixing to HG=1.0e-10
=> Square of FWHM(G) < 0 at 2theta:  104.081 for phase no.    1 -> Fixing to HG=1.0e-10
=> Square of FWHM(G) < 0 at 2theta:  107.821 for phase no.    1 -> Fixing to HG=1.0e-10
=> Square of FWHM(G) < 0 at 2theta:  108.202 for phase no.    1 -> Fixing to HG=1.0e-10
=> Square of FWHM(G) < 0 at 2theta:  112.011 for phase no.    1 -> Fixing to HG=1.0e-10
=> Square of FWHM(G) < 0 at 2theta:  112.422 for phase no.    1 -> Fixing to HG=1.0e-10
=> Square of FWHM(G) < 0 at 2theta:  116.329 for phase no.    1 -> Fixing to HG=1.0e-10
=> Square of FWHM(G) < 0 at 2theta:  116.776 for phase no.    1 -> Fixing to HG=1.0e-10
=> Square of FWHM(G) < 0 at 2theta:  120.815 for phase no.    1 -> Fixing to HG=1.0e-10
=> Square of FWHM(G) < 0 at 2theta:  121.304 for phase no.    1 -> Fixing to HG=1.0e-10
=> Square of FWHM(G) < 0 at 2theta:  130.522 for phase no.    1 -> Fixing to HG=1.0e-10
=> Square of FWHM(G) < 0 at 2theta:  131.126 for phase no.    1 -> Fixing to HG=1.0e-10
=> Square of FWHM(G) < 0 at 2theta:  135.929 for phase no.    1 -> Fixing to HG=1.0e-10
=> Square of FWHM(G) < 0 at 2theta:  135.929 for phase no.    1 -> Fixing to HG=1.0e-10
=> Square of FWHM(G) < 0 at 2theta:  136.618 for phase no.    1 -> Fixing to HG=1.0e-10
=> Square of FWHM(G) < 0 at 2theta:  136.618 for phase no.    1 -> Fixing to HG=1.0e-10
=> Square of FWHM(G) < 0 at 2theta:   99.705 for phase no.    1 -> Fixing to HG=1.0e-10
=> Square of FWHM(G) < 0 at 2theta:   99.705 for phase no.    1 -> Fixing to HG=1.0e-10
=> Square of FWHM(G) < 0 at 2theta:  100.033 for phase no.    1 -> Fixing to HG=1.0e-10
=> Square of FWHM(G) < 0 at 2theta:  100.033 for phase no.    1 -> Fixing to HG=1.0e-10
=> Square of FWHM(G) < 0 at 2theta:  103.728 for phase no.    1 -> Fixing to HG=1.0e-10
=> Square of FWHM(G) < 0 at 2theta:  103.728 for phase no.    1 -> Fixing to HG=1.0e-10
=> Square of FWHM(G) < 0 at 2theta:  104.081 for phase no.    1 -> Fixing to HG=1.0e-10
=> Square of FWHM(G) < 0 at 2theta:  104.081 for phase no.    1 -> Fixing to HG=1.0e-10
=> Square of FWHM(G) < 0 at 2theta:  107.821 for phase no.    1 -> Fixing to HG=1.0e-10
=> Square of FWHM(G) < 0 at 2theta:  108.202 for phase no.    1 -> Fixing to HG=1.0e-10
=> Square of FWHM(G) < 0 at 2theta:  112.011 for phase no.    1 -> Fixing to HG=1.0e-10
=> Square of FWHM(G) < 0 at 2theta:  112.422 for phase no.    1 -> Fixing to HG=1.0e-10
=> Square of FWHM(G) < 0 at 2theta:  116.329 for phase no.    1 -> Fixing to HG=1.0e-10
=> Square of FWHM(G) < 0 at 2theta:  116.776 for phase no.    1 -> Fixing to HG=1.0e-10
=> Square of FWHM(G) < 0 at 2theta:  120.815 for phase no.    1 -> Fixing to HG=1.0e-10
=> Square of FWHM(G) < 0 at 2theta:  121.304 for phase no.    1 -> Fixing to HG=1.0e-10
=> Square of FWHM(G) < 0 at 2theta:  130.522 for phase no.    1 -> Fixing to HG=1.0e-10
=> Square of FWHM(G) < 0 at 2theta:  131.126 for phase no.    1 -> Fixing to HG=1.0e-10
=> Square of FWHM(G) < 0 at 2theta:  135.929 for phase no.    1 -> Fixing to HG=1.0e-10
=> Square of FWHM(G) < 0 at 2theta:  135.929 for phase no.    1 -> Fixing to HG=1.0e-10
=> Square of FWHM(G) < 0 at 2theta:  136.618 for phase no.    1 -> Fixing to HG=1.0e-10
=> Square of FWHM(G) < 0 at 2theta:  136.618 for phase no.    1 -> Fixing to HG=1.0e-10
=> Square of FWHM(G) < 0 at 2theta:   99.705 for phase no.    1 -> Fixing to HG=1.0e-10
=> Square of FWHM(G) < 0 at 2theta:   99.705 for phase no.    1 -> Fixing to HG=1.0e-10
=> Square of FWHM(G) < 0 at 2theta:  100.033 for phase no.    1 -> Fixing to HG=1.0e-10
=> Square of FWHM(G) < 0 at 2theta:  100.033 for phase no.    1 -> Fixing to HG=1.0e-10
=> Square of FWHM(G) < 0 at 2theta:  103.728 for phase no.    1 -> Fixing to HG=1.0e-10
=> Square of FWHM(G) < 0 at 2theta:  103.728 for phase no.    1 -> Fixing to HG=1.0e-10
```

```
=> Square of FWHM(G) < 0 at 2theta:  104.081 for phase no.    1 -> Fixing to HG=1.0e-10
=> Square of FWHM(G) < 0 at 2theta:  104.081 for phase no.    1 -> Fixing to HG=1.0e-10
=> Square of FWHM(G) < 0 at 2theta:  107.821 for phase no.    1 -> Fixing to HG=1.0e-10
=> Square of FWHM(G) < 0 at 2theta:  108.202 for phase no.    1 -> Fixing to HG=1.0e-10
=> Square of FWHM(G) < 0 at 2theta:  112.011 for phase no.    1 -> Fixing to HG=1.0e-10
=> Square of FWHM(G) < 0 at 2theta:  112.422 for phase no.    1 -> Fixing to HG=1.0e-10
=> Square of FWHM(G) < 0 at 2theta:  116.329 for phase no.    1 -> Fixing to HG=1.0e-10
=> Square of FWHM(G) < 0 at 2theta:  116.776 for phase no.    1 -> Fixing to HG=1.0e-10
=> Square of FWHM(G) < 0 at 2theta:  120.815 for phase no.    1 -> Fixing to HG=1.0e-10
=> Square of FWHM(G) < 0 at 2theta:  121.304 for phase no.    1 -> Fixing to HG=1.0e-10
=> Square of FWHM(G) < 0 at 2theta:  130.522 for phase no.    1 -> Fixing to HG=1.0e-10
=> Square of FWHM(G) < 0 at 2theta:  131.126 for phase no.    1 -> Fixing to HG=1.0e-10
=> Square of FWHM(G) < 0 at 2theta:  135.929 for phase no.    1 -> Fixing to HG=1.0e-10
=> Square of FWHM(G) < 0 at 2theta:  135.929 for phase no.    1 -> Fixing to HG=1.0e-10
=> Square of FWHM(G) < 0 at 2theta:  136.618 for phase no.    1 -> Fixing to HG=1.0e-10
=> Square of FWHM(G) < 0 at 2theta:  136.618 for phase no.    1 -> Fixing to HG=1.0e-10
=> Square of FWHM(G) < 0 at 2theta:   99.705 for phase no.    1 -> Fixing to HG=1.0e-10
=> Square of FWHM(G) < 0 at 2theta:   99.705 for phase no.    1 -> Fixing to HG=1.0e-10
=> Square of FWHM(G) < 0 at 2theta:  100.033 for phase no.    1 -> Fixing to HG=1.0e-10
=> Square of FWHM(G) < 0 at 2theta:  100.033 for phase no.    1 -> Fixing to HG=1.0e-10
=> Square of FWHM(G) < 0 at 2theta:  103.728 for phase no.    1 -> Fixing to HG=1.0e-10
=> Square of FWHM(G) < 0 at 2theta:  103.728 for phase no.    1 -> Fixing to HG=1.0e-10
=> Square of FWHM(G) < 0 at 2theta:  104.081 for phase no.    1 -> Fixing to HG=1.0e-10
=> Square of FWHM(G) < 0 at 2theta:  104.081 for phase no.    1 -> Fixing to HG=1.0e-10
=> Square of FWHM(G) < 0 at 2theta:  107.821 for phase no.    1 -> Fixing to HG=1.0e-10
=> Square of FWHM(G) < 0 at 2theta:  108.202 for phase no.    1 -> Fixing to HG=1.0e-10
=> Square of FWHM(G) < 0 at 2theta:  112.011 for phase no.    1 -> Fixing to HG=1.0e-10
=> Square of FWHM(G) < 0 at 2theta:  112.422 for phase no.    1 -> Fixing to HG=1.0e-10
=> Square of FWHM(G) < 0 at 2theta:  116.329 for phase no.    1 -> Fixing to HG=1.0e-10
=> Square of FWHM(G) < 0 at 2theta:  116.776 for phase no.    1 -> Fixing to HG=1.0e-10
=> Square of FWHM(G) < 0 at 2theta:  120.815 for phase no.    1 -> Fixing to HG=1.0e-10
=> Square of FWHM(G) < 0 at 2theta:  121.304 for phase no.    1 -> Fixing to HG=1.0e-10
=> Square of FWHM(G) < 0 at 2theta:  130.522 for phase no.    1 -> Fixing to HG=1.0e-10
=> Square of FWHM(G) < 0 at 2theta:  131.126 for phase no.    1 -> Fixing to HG=1.0e-10
=> Square of FWHM(G) < 0 at 2theta:  135.929 for phase no.    1 -> Fixing to HG=1.0e-10
=> Square of FWHM(G) < 0 at 2theta:  135.929 for phase no.    1 -> Fixing to HG=1.0e-10
=> Square of FWHM(G) < 0 at 2theta:  136.618 for phase no.    1 -> Fixing to HG=1.0e-10
=> Square of FWHM(G) < 0 at 2theta:  136.618 for phase no.    1 -> Fixing to HG=1.0e-10
=> Square of FWHM(G) < 0 at 2theta:   99.705 for phase no.    1 -> Fixing to HG=1.0e-10
=> Square of FWHM(G) < 0 at 2theta:   99.705 for phase no.    1 -> Fixing to HG=1.0e-10
=> Square of FWHM(G) < 0 at 2theta:  100.033 for phase no.    1 -> Fixing to HG=1.0e-10
=> Square of FWHM(G) < 0 at 2theta:  100.033 for phase no.    1 -> Fixing to HG=1.0e-10
=> Square of FWHM(G) < 0 at 2theta:  103.728 for phase no.    1 -> Fixing to HG=1.0e-10
=> Square of FWHM(G) < 0 at 2theta:  103.728 for phase no.    1 -> Fixing to HG=1.0e-10
=> Square of FWHM(G) < 0 at 2theta:  104.081 for phase no.    1 -> Fixing to HG=1.0e-10
=> Square of FWHM(G) < 0 at 2theta:  104.081 for phase no.    1 -> Fixing to HG=1.0e-10
=> Square of FWHM(G) < 0 at 2theta:  107.821 for phase no.    1 -> Fixing to HG=1.0e-10
=> Square of FWHM(G) < 0 at 2theta:  108.202 for phase no.    1 -> Fixing to HG=1.0e-10
=> Square of FWHM(G) < 0 at 2theta:  112.011 for phase no.    1 -> Fixing to HG=1.0e-10
=> Square of FWHM(G) < 0 at 2theta:  112.422 for phase no.    1 -> Fixing to HG=1.0e-10
=> Square of FWHM(G) < 0 at 2theta:  116.329 for phase no.    1 -> Fixing to HG=1.0e-10
=> Square of FWHM(G) < 0 at 2theta:  116.776 for phase no.    1 -> Fixing to HG=1.0e-10
=> Square of FWHM(G) < 0 at 2theta:  120.815 for phase no.    1 -> Fixing to HG=1.0e-10
=> Square of FWHM(G) < 0 at 2theta:  121.304 for phase no.    1 -> Fixing to HG=1.0e-10
=> Square of FWHM(G) < 0 at 2theta:  130.522 for phase no.    1 -> Fixing to HG=1.0e-10
=> Square of FWHM(G) < 0 at 2theta:  131.126 for phase no.    1 -> Fixing to HG=1.0e-10
=> Square of FWHM(G) < 0 at 2theta:  135.929 for phase no.    1 -> Fixing to HG=1.0e-10
=> Square of FWHM(G) < 0 at 2theta:  135.929 for phase no.    1 -> Fixing to HG=1.0e-10
=> Square of FWHM(G) < 0 at 2theta:  136.618 for phase no.    1 -> Fixing to HG=1.0e-10
=> Square of FWHM(G) < 0 at 2theta:  136.618 for phase no.    1 -> Fixing to HG=1.0e-10
=> Square of FWHM(G) < 0 at 2theta:   99.705 for phase no.    1 -> Fixing to HG=1.0e-10
=> Square of FWHM(G) < 0 at 2theta:   99.705 for phase no.    1 -> Fixing to HG=1.0e-10
=> Square of FWHM(G) < 0 at 2theta:  100.033 for phase no.    1 -> Fixing to HG=1.0e-10
=> Square of FWHM(G) < 0 at 2theta:  100.033 for phase no.    1 -> Fixing to HG=1.0e-10
=> Square of FWHM(G) < 0 at 2theta:  103.728 for phase no.    1 -> Fixing to HG=1.0e-10
=> Square of FWHM(G) < 0 at 2theta:  103.728 for phase no.    1 -> Fixing to HG=1.0e-10
=> Square of FWHM(G) < 0 at 2theta:  104.081 for phase no.    1 -> Fixing to HG=1.0e-10
=> Square of FWHM(G) < 0 at 2theta:  104.081 for phase no.    1 -> Fixing to HG=1.0e-10
=> Square of FWHM(G) < 0 at 2theta:  107.821 for phase no.    1 -> Fixing to HG=1.0e-10
=> Square of FWHM(G) < 0 at 2theta:  108.202 for phase no.    1 -> Fixing to HG=1.0e-10
=> Square of FWHM(G) < 0 at 2theta:  112.011 for phase no.    1 -> Fixing to HG=1.0e-10
=> Square of FWHM(G) < 0 at 2theta:  112.422 for phase no.    1 -> Fixing to HG=1.0e-10
=> Square of FWHM(G) < 0 at 2theta:  116.329 for phase no.    1 -> Fixing to HG=1.0e-10
=> Square of FWHM(G) < 0 at 2theta:  116.776 for phase no.    1 -> Fixing to HG=1.0e-10
=> Square of FWHM(G) < 0 at 2theta:  120.815 for phase no.    1 -> Fixing to HG=1.0e-10
=> Square of FWHM(G) < 0 at 2theta:  121.304 for phase no.    1 -> Fixing to HG=1.0e-10
=> Square of FWHM(G) < 0 at 2theta:  130.522 for phase no.    1 -> Fixing to HG=1.0e-10
=> Square of FWHM(G) < 0 at 2theta:  131.126 for phase no.    1 -> Fixing to HG=1.0e-10
=> Square of FWHM(G) < 0 at 2theta:  135.929 for phase no.    1 -> Fixing to HG=1.0e-10
=> Square of FWHM(G) < 0 at 2theta:  135.929 for phase no.    1 -> Fixing to HG=1.0e-10
=> Square of FWHM(G) < 0 at 2theta:  136.618 for phase no.    1 -> Fixing to HG=1.0e-10
=> Square of FWHM(G) < 0 at 2theta:  136.618 for phase no.    1 -> Fixing to HG=1.0e-10
=> Square of FWHM(G) < 0 at 2theta:   99.705 for phase no.    1 -> Fixing to HG=1.0e-10
=> Square of FWHM(G) < 0 at 2theta:   99.705 for phase no.    1 -> Fixing to HG=1.0e-10
=> Square of FWHM(G) < 0 at 2theta:  100.033 for phase no.    1 -> Fixing to HG=1.0e-10
=> Square of FWHM(G) < 0 at 2theta:  100.033 for phase no.    1 -> Fixing to HG=1.0e-10
=> Square of FWHM(G) < 0 at 2theta:  103.728 for phase no.    1 -> Fixing to HG=1.0e-10
=> Square of FWHM(G) < 0 at 2theta:  103.728 for phase no.    1 -> Fixing to HG=1.0e-10
=> Square of FWHM(G) < 0 at 2theta:  104.081 for phase no.    1 -> Fixing to HG=1.0e-10
=> Square of FWHM(G) < 0 at 2theta:  104.081 for phase no.    1 -> Fixing to HG=1.0e-10
```

```
=> Square of FWHM(G) < 0 at 2theta:  107.821 for phase no.    1 -> Fixing to HG=1.0e-10
=> Square of FWHM(G) < 0 at 2theta:  108.202 for phase no.    1 -> Fixing to HG=1.0e-10
=> Square of FWHM(G) < 0 at 2theta:  112.011 for phase no.    1 -> Fixing to HG=1.0e-10
=> Square of FWHM(G) < 0 at 2theta:  112.422 for phase no.    1 -> Fixing to HG=1.0e-10
=> Square of FWHM(G) < 0 at 2theta:  116.329 for phase no.    1 -> Fixing to HG=1.0e-10
=> Square of FWHM(G) < 0 at 2theta:  116.776 for phase no.    1 -> Fixing to HG=1.0e-10
=> Square of FWHM(G) < 0 at 2theta:  120.815 for phase no.    1 -> Fixing to HG=1.0e-10
=> Square of FWHM(G) < 0 at 2theta:  121.304 for phase no.    1 -> Fixing to HG=1.0e-10
=> Square of FWHM(G) < 0 at 2theta:  130.522 for phase no.    1 -> Fixing to HG=1.0e-10
=> Square of FWHM(G) < 0 at 2theta:  131.126 for phase no.    1 -> Fixing to HG=1.0e-10
=> Square of FWHM(G) < 0 at 2theta:  135.929 for phase no.    1 -> Fixing to HG=1.0e-10
=> Square of FWHM(G) < 0 at 2theta:  135.929 for phase no.    1 -> Fixing to HG=1.0e-10
=> Square of FWHM(G) < 0 at 2theta:  136.618 for phase no.    1 -> Fixing to HG=1.0e-10
=> Square of FWHM(G) < 0 at 2theta:  136.618 for phase no.    1 -> Fixing to HG=1.0e-10
=> Square of FWHM(G) < 0 at 2theta:   99.705 for phase no.    1 -> Fixing to HG=1.0e-10
=> Square of FWHM(G) < 0 at 2theta:   99.705 for phase no.    1 -> Fixing to HG=1.0e-10
=> Square of FWHM(G) < 0 at 2theta:  100.033 for phase no.    1 -> Fixing to HG=1.0e-10
=> Square of FWHM(G) < 0 at 2theta:  100.033 for phase no.    1 -> Fixing to HG=1.0e-10
=> Square of FWHM(G) < 0 at 2theta:  103.728 for phase no.    1 -> Fixing to HG=1.0e-10
=> Square of FWHM(G) < 0 at 2theta:  103.728 for phase no.    1 -> Fixing to HG=1.0e-10
=> Square of FWHM(G) < 0 at 2theta:  104.081 for phase no.    1 -> Fixing to HG=1.0e-10
=> Square of FWHM(G) < 0 at 2theta:  104.081 for phase no.    1 -> Fixing to HG=1.0e-10
=> Square of FWHM(G) < 0 at 2theta:  107.821 for phase no.    1 -> Fixing to HG=1.0e-10
=> Square of FWHM(G) < 0 at 2theta:  108.202 for phase no.    1 -> Fixing to HG=1.0e-10
=> Square of FWHM(G) < 0 at 2theta:  112.011 for phase no.    1 -> Fixing to HG=1.0e-10
=> Square of FWHM(G) < 0 at 2theta:  112.422 for phase no.    1 -> Fixing to HG=1.0e-10
=> Square of FWHM(G) < 0 at 2theta:  116.329 for phase no.    1 -> Fixing to HG=1.0e-10
=> Square of FWHM(G) < 0 at 2theta:  116.776 for phase no.    1 -> Fixing to HG=1.0e-10
=> Square of FWHM(G) < 0 at 2theta:  120.815 for phase no.    1 -> Fixing to HG=1.0e-10
=> Square of FWHM(G) < 0 at 2theta:  121.304 for phase no.    1 -> Fixing to HG=1.0e-10
=> Square of FWHM(G) < 0 at 2theta:  130.522 for phase no.    1 -> Fixing to HG=1.0e-10
=> Square of FWHM(G) < 0 at 2theta:  131.126 for phase no.    1 -> Fixing to HG=1.0e-10
=> Square of FWHM(G) < 0 at 2theta:  135.929 for phase no.    1 -> Fixing to HG=1.0e-10
=> Square of FWHM(G) < 0 at 2theta:  135.929 for phase no.    1 -> Fixing to HG=1.0e-10
=> Square of FWHM(G) < 0 at 2theta:  136.618 for phase no.    1 -> Fixing to HG=1.0e-10
=> Square of FWHM(G) < 0 at 2theta:  136.618 for phase no.    1 -> Fixing to HG=1.0e-10
=> Square of FWHM(G) < 0 at 2theta:   99.705 for phase no.    1 -> Fixing to HG=1.0e-10
=> Square of FWHM(G) < 0 at 2theta:   99.705 for phase no.    1 -> Fixing to HG=1.0e-10
=> Square of FWHM(G) < 0 at 2theta:  100.033 for phase no.    1 -> Fixing to HG=1.0e-10
=> Square of FWHM(G) < 0 at 2theta:  100.033 for phase no.    1 -> Fixing to HG=1.0e-10
=> Square of FWHM(G) < 0 at 2theta:  103.728 for phase no.    1 -> Fixing to HG=1.0e-10
=> Square of FWHM(G) < 0 at 2theta:  103.728 for phase no.    1 -> Fixing to HG=1.0e-10
=> Square of FWHM(G) < 0 at 2theta:  104.081 for phase no.    1 -> Fixing to HG=1.0e-10
=> Square of FWHM(G) < 0 at 2theta:  104.081 for phase no.    1 -> Fixing to HG=1.0e-10
=> Square of FWHM(G) < 0 at 2theta:  107.821 for phase no.    1 -> Fixing to HG=1.0e-10
=> Square of FWHM(G) < 0 at 2theta:  108.202 for phase no.    1 -> Fixing to HG=1.0e-10
=> Square of FWHM(G) < 0 at 2theta:  112.011 for phase no.    1 -> Fixing to HG=1.0e-10
=> Square of FWHM(G) < 0 at 2theta:  112.422 for phase no.    1 -> Fixing to HG=1.0e-10
=> Square of FWHM(G) < 0 at 2theta:  116.329 for phase no.    1 -> Fixing to HG=1.0e-10
=> Square of FWHM(G) < 0 at 2theta:  116.776 for phase no.    1 -> Fixing to HG=1.0e-10
=> Square of FWHM(G) < 0 at 2theta:  120.815 for phase no.    1 -> Fixing to HG=1.0e-10
=> Square of FWHM(G) < 0 at 2theta:  121.304 for phase no.    1 -> Fixing to HG=1.0e-10
=> Square of FWHM(G) < 0 at 2theta:  130.522 for phase no.    1 -> Fixing to HG=1.0e-10
=> Square of FWHM(G) < 0 at 2theta:  131.126 for phase no.    1 -> Fixing to HG=1.0e-10
=> Square of FWHM(G) < 0 at 2theta:  135.929 for phase no.    1 -> Fixing to HG=1.0e-10
=> Square of FWHM(G) < 0 at 2theta:  135.929 for phase no.    1 -> Fixing to HG=1.0e-10
=> Square of FWHM(G) < 0 at 2theta:  136.618 for phase no.    1 -> Fixing to HG=1.0e-10
=> Square of FWHM(G) < 0 at 2theta:  136.618 for phase no.    1 -> Fixing to HG=1.0e-10
=> Square of FWHM(G) < 0 at 2theta:   99.705 for phase no.    1 -> Fixing to HG=1.0e-10
=> Square of FWHM(G) < 0 at 2theta:   99.705 for phase no.    1 -> Fixing to HG=1.0e-10
=> Square of FWHM(G) < 0 at 2theta:  100.033 for phase no.    1 -> Fixing to HG=1.0e-10
=> Square of FWHM(G) < 0 at 2theta:  100.033 for phase no.    1 -> Fixing to HG=1.0e-10
=> Square of FWHM(G) < 0 at 2theta:  103.728 for phase no.    1 -> Fixing to HG=1.0e-10
=> Square of FWHM(G) < 0 at 2theta:  103.728 for phase no.    1 -> Fixing to HG=1.0e-10
=> Square of FWHM(G) < 0 at 2theta:  104.081 for phase no.    1 -> Fixing to HG=1.0e-10
=> Square of FWHM(G) < 0 at 2theta:  104.081 for phase no.    1 -> Fixing to HG=1.0e-10
=> Square of FWHM(G) < 0 at 2theta:  107.821 for phase no.    1 -> Fixing to HG=1.0e-10
=> Square of FWHM(G) < 0 at 2theta:  108.202 for phase no.    1 -> Fixing to HG=1.0e-10
=> Square of FWHM(G) < 0 at 2theta:  112.011 for phase no.    1 -> Fixing to HG=1.0e-10
=> Square of FWHM(G) < 0 at 2theta:  112.422 for phase no.    1 -> Fixing to HG=1.0e-10
=> Square of FWHM(G) < 0 at 2theta:  116.329 for phase no.    1 -> Fixing to HG=1.0e-10
=> Square of FWHM(G) < 0 at 2theta:  116.776 for phase no.    1 -> Fixing to HG=1.0e-10
=> Square of FWHM(G) < 0 at 2theta:  120.815 for phase no.    1 -> Fixing to HG=1.0e-10
=> Square of FWHM(G) < 0 at 2theta:  121.304 for phase no.    1 -> Fixing to HG=1.0e-10
=> Square of FWHM(G) < 0 at 2theta:  130.522 for phase no.    1 -> Fixing to HG=1.0e-10
=> Square of FWHM(G) < 0 at 2theta:  131.126 for phase no.    1 -> Fixing to HG=1.0e-10
=> Square of FWHM(G) < 0 at 2theta:  135.929 for phase no.    1 -> Fixing to HG=1.0e-10
=> Square of FWHM(G) < 0 at 2theta:  135.929 for phase no.    1 -> Fixing to HG=1.0e-10
=> Square of FWHM(G) < 0 at 2theta:  136.618 for phase no.    1 -> Fixing to HG=1.0e-10
=> Square of FWHM(G) < 0 at 2theta:  136.618 for phase no.    1 -> Fixing to HG=1.0e-10
=> Square of FWHM(G) < 0 at 2theta:   99.705 for phase no.    1 -> Fixing to HG=1.0e-10
=> Square of FWHM(G) < 0 at 2theta:   99.705 for phase no.    1 -> Fixing to HG=1.0e-10
=> Square of FWHM(G) < 0 at 2theta:  100.033 for phase no.    1 -> Fixing to HG=1.0e-10
=> Square of FWHM(G) < 0 at 2theta:  100.033 for phase no.    1 -> Fixing to HG=1.0e-10
=> Square of FWHM(G) < 0 at 2theta:  103.728 for phase no.    1 -> Fixing to HG=1.0e-10
=> Square of FWHM(G) < 0 at 2theta:  103.728 for phase no.    1 -> Fixing to HG=1.0e-10
=> Square of FWHM(G) < 0 at 2theta:  104.081 for phase no.    1 -> Fixing to HG=1.0e-10
=> Square of FWHM(G) < 0 at 2theta:  104.081 for phase no.    1 -> Fixing to HG=1.0e-10
=> Square of FWHM(G) < 0 at 2theta:  107.821 for phase no.    1 -> Fixing to HG=1.0e-10
=> Square of FWHM(G) < 0 at 2theta:  108.202 for phase no.    1 -> Fixing to HG=1.0e-10
```

```
=> Square of FWHM(G) < 0 at 2theta:  112.011 for phase no.    1 -> Fixing to HG=1.0e-10
=> Square of FWHM(G) < 0 at 2theta:  112.422 for phase no.    1 -> Fixing to HG=1.0e-10
=> Square of FWHM(G) < 0 at 2theta:  116.329 for phase no.    1 -> Fixing to HG=1.0e-10
=> Square of FWHM(G) < 0 at 2theta:  116.776 for phase no.    1 -> Fixing to HG=1.0e-10
=> Square of FWHM(G) < 0 at 2theta:  120.815 for phase no.    1 -> Fixing to HG=1.0e-10
=> Square of FWHM(G) < 0 at 2theta:  121.304 for phase no.    1 -> Fixing to HG=1.0e-10
=> Square of FWHM(G) < 0 at 2theta:  130.522 for phase no.    1 -> Fixing to HG=1.0e-10
=> Square of FWHM(G) < 0 at 2theta:  131.126 for phase no.    1 -> Fixing to HG=1.0e-10
=> Square of FWHM(G) < 0 at 2theta:  135.929 for phase no.    1 -> Fixing to HG=1.0e-10
=> Square of FWHM(G) < 0 at 2theta:  135.929 for phase no.    1 -> Fixing to HG=1.0e-10
=> Square of FWHM(G) < 0 at 2theta:  136.618 for phase no.    1 -> Fixing to HG=1.0e-10
=> Square of FWHM(G) < 0 at 2theta:  136.618 for phase no.    1 -> Fixing to HG=1.0e-10
=> Square of FWHM(G) < 0 at 2theta:   99.705 for phase no.    1 -> Fixing to HG=1.0e-10
=> Square of FWHM(G) < 0 at 2theta:   99.705 for phase no.    1 -> Fixing to HG=1.0e-10
=> Square of FWHM(G) < 0 at 2theta:  100.033 for phase no.    1 -> Fixing to HG=1.0e-10
=> Square of FWHM(G) < 0 at 2theta:  100.033 for phase no.    1 -> Fixing to HG=1.0e-10
=> Square of FWHM(G) < 0 at 2theta:  103.728 for phase no.    1 -> Fixing to HG=1.0e-10
=> Square of FWHM(G) < 0 at 2theta:  103.728 for phase no.    1 -> Fixing to HG=1.0e-10
=> Square of FWHM(G) < 0 at 2theta:  104.081 for phase no.    1 -> Fixing to HG=1.0e-10
=> Square of FWHM(G) < 0 at 2theta:  104.081 for phase no.    1 -> Fixing to HG=1.0e-10
=> Square of FWHM(G) < 0 at 2theta:  107.821 for phase no.    1 -> Fixing to HG=1.0e-10
=> Square of FWHM(G) < 0 at 2theta:  108.202 for phase no.    1 -> Fixing to HG=1.0e-10
=> Square of FWHM(G) < 0 at 2theta:  112.011 for phase no.    1 -> Fixing to HG=1.0e-10
=> Square of FWHM(G) < 0 at 2theta:  112.422 for phase no.    1 -> Fixing to HG=1.0e-10
=> Square of FWHM(G) < 0 at 2theta:  116.329 for phase no.    1 -> Fixing to HG=1.0e-10
=> Square of FWHM(G) < 0 at 2theta:  116.776 for phase no.    1 -> Fixing to HG=1.0e-10
=> Square of FWHM(G) < 0 at 2theta:  120.815 for phase no.    1 -> Fixing to HG=1.0e-10
=> Square of FWHM(G) < 0 at 2theta:  121.304 for phase no.    1 -> Fixing to HG=1.0e-10
=> Square of FWHM(G) < 0 at 2theta:  130.522 for phase no.    1 -> Fixing to HG=1.0e-10
=> Square of FWHM(G) < 0 at 2theta:  131.126 for phase no.    1 -> Fixing to HG=1.0e-10
=> Square of FWHM(G) < 0 at 2theta:  135.929 for phase no.    1 -> Fixing to HG=1.0e-10
=> Square of FWHM(G) < 0 at 2theta:  135.929 for phase no.    1 -> Fixing to HG=1.0e-10
=> Square of FWHM(G) < 0 at 2theta:  136.618 for phase no.    1 -> Fixing to HG=1.0e-10
=> Square of FWHM(G) < 0 at 2theta:  136.618 for phase no.    1 -> Fixing to HG=1.0e-10
=> Square of FWHM(G) < 0 at 2theta:   99.705 for phase no.    1 -> Fixing to HG=1.0e-10
=> Square of FWHM(G) < 0 at 2theta:   99.705 for phase no.    1 -> Fixing to HG=1.0e-10
=> Square of FWHM(G) < 0 at 2theta:  100.033 for phase no.    1 -> Fixing to HG=1.0e-10
=> Square of FWHM(G) < 0 at 2theta:  100.033 for phase no.    1 -> Fixing to HG=1.0e-10
=> Square of FWHM(G) < 0 at 2theta:  103.728 for phase no.    1 -> Fixing to HG=1.0e-10
=> Square of FWHM(G) < 0 at 2theta:  103.728 for phase no.    1 -> Fixing to HG=1.0e-10
=> Square of FWHM(G) < 0 at 2theta:  104.081 for phase no.    1 -> Fixing to HG=1.0e-10
=> Square of FWHM(G) < 0 at 2theta:  104.081 for phase no.    1 -> Fixing to HG=1.0e-10
=> Square of FWHM(G) < 0 at 2theta:  107.821 for phase no.    1 -> Fixing to HG=1.0e-10
=> Square of FWHM(G) < 0 at 2theta:  108.202 for phase no.    1 -> Fixing to HG=1.0e-10
=> Square of FWHM(G) < 0 at 2theta:  112.011 for phase no.    1 -> Fixing to HG=1.0e-10
=> Square of FWHM(G) < 0 at 2theta:  112.422 for phase no.    1 -> Fixing to HG=1.0e-10
=> Square of FWHM(G) < 0 at 2theta:  116.329 for phase no.    1 -> Fixing to HG=1.0e-10
=> Square of FWHM(G) < 0 at 2theta:  116.776 for phase no.    1 -> Fixing to HG=1.0e-10
=> Square of FWHM(G) < 0 at 2theta:  120.815 for phase no.    1 -> Fixing to HG=1.0e-10
=> Square of FWHM(G) < 0 at 2theta:  121.304 for phase no.    1 -> Fixing to HG=1.0e-10
=> Square of FWHM(G) < 0 at 2theta:  130.522 for phase no.    1 -> Fixing to HG=1.0e-10
=> Square of FWHM(G) < 0 at 2theta:  131.126 for phase no.    1 -> Fixing to HG=1.0e-10
=> Square of FWHM(G) < 0 at 2theta:  135.929 for phase no.    1 -> Fixing to HG=1.0e-10
=> Square of FWHM(G) < 0 at 2theta:  135.929 for phase no.    1 -> Fixing to HG=1.0e-10
=> Square of FWHM(G) < 0 at 2theta:  136.618 for phase no.    1 -> Fixing to HG=1.0e-10
=> Square of FWHM(G) < 0 at 2theta:  136.618 for phase no.    1 -> Fixing to HG=1.0e-10
=> Square of FWHM(G) < 0 at 2theta:   99.705 for phase no.    1 -> Fixing to HG=1.0e-10
=> Square of FWHM(G) < 0 at 2theta:   99.705 for phase no.    1 -> Fixing to HG=1.0e-10
=> Square of FWHM(G) < 0 at 2theta:  100.033 for phase no.    1 -> Fixing to HG=1.0e-10
=> Square of FWHM(G) < 0 at 2theta:  100.033 for phase no.    1 -> Fixing to HG=1.0e-10
=> Square of FWHM(G) < 0 at 2theta:  103.728 for phase no.    1 -> Fixing to HG=1.0e-10
=> Square of FWHM(G) < 0 at 2theta:  103.728 for phase no.    1 -> Fixing to HG=1.0e-10
=> Square of FWHM(G) < 0 at 2theta:  104.081 for phase no.    1 -> Fixing to HG=1.0e-10
=> Square of FWHM(G) < 0 at 2theta:  104.081 for phase no.    1 -> Fixing to HG=1.0e-10
=> Square of FWHM(G) < 0 at 2theta:  107.821 for phase no.    1 -> Fixing to HG=1.0e-10
=> Square of FWHM(G) < 0 at 2theta:  108.202 for phase no.    1 -> Fixing to HG=1.0e-10
=> Square of FWHM(G) < 0 at 2theta:  112.011 for phase no.    1 -> Fixing to HG=1.0e-10
=> Square of FWHM(G) < 0 at 2theta:  112.422 for phase no.    1 -> Fixing to HG=1.0e-10
=> Square of FWHM(G) < 0 at 2theta:  116.329 for phase no.    1 -> Fixing to HG=1.0e-10
=> Square of FWHM(G) < 0 at 2theta:  116.776 for phase no.    1 -> Fixing to HG=1.0e-10
=> Square of FWHM(G) < 0 at 2theta:  120.815 for phase no.    1 -> Fixing to HG=1.0e-10
=> Square of FWHM(G) < 0 at 2theta:  121.304 for phase no.    1 -> Fixing to HG=1.0e-10
=> Square of FWHM(G) < 0 at 2theta:  130.522 for phase no.    1 -> Fixing to HG=1.0e-10
=> Square of FWHM(G) < 0 at 2theta:  131.126 for phase no.    1 -> Fixing to HG=1.0e-10
=> Square of FWHM(G) < 0 at 2theta:  135.929 for phase no.    1 -> Fixing to HG=1.0e-10
=> Square of FWHM(G) < 0 at 2theta:  135.929 for phase no.    1 -> Fixing to HG=1.0e-10
=> Square of FWHM(G) < 0 at 2theta:  136.618 for phase no.    1 -> Fixing to HG=1.0e-10
=> Square of FWHM(G) < 0 at 2theta:  136.618 for phase no.    1 -> Fixing to HG=1.0e-10
=> Square of FWHM(G) < 0 at 2theta:   99.705 for phase no.    1 -> Fixing to HG=1.0e-10
=> Square of FWHM(G) < 0 at 2theta:   99.705 for phase no.    1 -> Fixing to HG=1.0e-10
=> Square of FWHM(G) < 0 at 2theta:  100.033 for phase no.    1 -> Fixing to HG=1.0e-10
=> Square of FWHM(G) < 0 at 2theta:  100.033 for phase no.    1 -> Fixing to HG=1.0e-10
=> Square of FWHM(G) < 0 at 2theta:  103.728 for phase no.    1 -> Fixing to HG=1.0e-10
=> Square of FWHM(G) < 0 at 2theta:  103.728 for phase no.    1 -> Fixing to HG=1.0e-10
=> Square of FWHM(G) < 0 at 2theta:  104.081 for phase no.    1 -> Fixing to HG=1.0e-10
=> Square of FWHM(G) < 0 at 2theta:  104.081 for phase no.    1 -> Fixing to HG=1.0e-10
=> Square of FWHM(G) < 0 at 2theta:  107.821 for phase no.    1 -> Fixing to HG=1.0e-10
=> Square of FWHM(G) < 0 at 2theta:  108.202 for phase no.    1 -> Fixing to HG=1.0e-10
=> Square of FWHM(G) < 0 at 2theta:  112.011 for phase no.    1 -> Fixing to HG=1.0e-10
=> Square of FWHM(G) < 0 at 2theta:  112.422 for phase no.    1 -> Fixing to HG=1.0e-10
```

```
=> Square of FWHM(G) < 0 at 2theta:  116.329 for phase no.    1 -> Fixing to HG=1.0e-10
=> Square of FWHM(G) < 0 at 2theta:  116.776 for phase no.    1 -> Fixing to HG=1.0e-10
=> Square of FWHM(G) < 0 at 2theta:  120.815 for phase no.    1 -> Fixing to HG=1.0e-10
=> Square of FWHM(G) < 0 at 2theta:  121.304 for phase no.    1 -> Fixing to HG=1.0e-10
=> Square of FWHM(G) < 0 at 2theta:  130.522 for phase no.    1 -> Fixing to HG=1.0e-10
=> Square of FWHM(G) < 0 at 2theta:  131.126 for phase no.    1 -> Fixing to HG=1.0e-10
=> Square of FWHM(G) < 0 at 2theta:  135.929 for phase no.    1 -> Fixing to HG=1.0e-10
=> Square of FWHM(G) < 0 at 2theta:  135.929 for phase no.    1 -> Fixing to HG=1.0e-10
=> Square of FWHM(G) < 0 at 2theta:  136.618 for phase no.    1 -> Fixing to HG=1.0e-10
=> Square of FWHM(G) < 0 at 2theta:  136.618 for phase no.    1 -> Fixing to HG=1.0e-10
=> Square of FWHM(G) < 0 at 2theta:   99.705 for phase no.    1 -> Fixing to HG=1.0e-10
=> Square of FWHM(G) < 0 at 2theta:   99.705 for phase no.    1 -> Fixing to HG=1.0e-10
=> Square of FWHM(G) < 0 at 2theta:  100.033 for phase no.    1 -> Fixing to HG=1.0e-10
=> Square of FWHM(G) < 0 at 2theta:  100.033 for phase no.    1 -> Fixing to HG=1.0e-10
=> Square of FWHM(G) < 0 at 2theta:  103.728 for phase no.    1 -> Fixing to HG=1.0e-10
=> Square of FWHM(G) < 0 at 2theta:  103.728 for phase no.    1 -> Fixing to HG=1.0e-10
=> Square of FWHM(G) < 0 at 2theta:  104.081 for phase no.    1 -> Fixing to HG=1.0e-10
=> Square of FWHM(G) < 0 at 2theta:  104.081 for phase no.    1 -> Fixing to HG=1.0e-10
=> Square of FWHM(G) < 0 at 2theta:  107.821 for phase no.    1 -> Fixing to HG=1.0e-10
=> Square of FWHM(G) < 0 at 2theta:  108.202 for phase no.    1 -> Fixing to HG=1.0e-10
=> Square of FWHM(G) < 0 at 2theta:  112.011 for phase no.    1 -> Fixing to HG=1.0e-10
=> Square of FWHM(G) < 0 at 2theta:  112.422 for phase no.    1 -> Fixing to HG=1.0e-10
=> Square of FWHM(G) < 0 at 2theta:  116.329 for phase no.    1 -> Fixing to HG=1.0e-10
=> Square of FWHM(G) < 0 at 2theta:  116.776 for phase no.    1 -> Fixing to HG=1.0e-10
=> Square of FWHM(G) < 0 at 2theta:  120.815 for phase no.    1 -> Fixing to HG=1.0e-10
=> Square of FWHM(G) < 0 at 2theta:  121.304 for phase no.    1 -> Fixing to HG=1.0e-10
=> Square of FWHM(G) < 0 at 2theta:  130.522 for phase no.    1 -> Fixing to HG=1.0e-10
=> Square of FWHM(G) < 0 at 2theta:  131.126 for phase no.    1 -> Fixing to HG=1.0e-10
=> Square of FWHM(G) < 0 at 2theta:  135.929 for phase no.    1 -> Fixing to HG=1.0e-10
=> Square of FWHM(G) < 0 at 2theta:  135.929 for phase no.    1 -> Fixing to HG=1.0e-10
=> Square of FWHM(G) < 0 at 2theta:  136.618 for phase no.    1 -> Fixing to HG=1.0e-10
=> Square of FWHM(G) < 0 at 2theta:  136.618 for phase no.    1 -> Fixing to HG=1.0e-10
=> Square of FWHM(G) < 0 at 2theta:   99.705 for phase no.    1 -> Fixing to HG=1.0e-10
=> Square of FWHM(G) < 0 at 2theta:   99.705 for phase no.    1 -> Fixing to HG=1.0e-10
=> Square of FWHM(G) < 0 at 2theta:  100.033 for phase no.    1 -> Fixing to HG=1.0e-10
=> Square of FWHM(G) < 0 at 2theta:  100.033 for phase no.    1 -> Fixing to HG=1.0e-10
=> Square of FWHM(G) < 0 at 2theta:  103.728 for phase no.    1 -> Fixing to HG=1.0e-10
=> Square of FWHM(G) < 0 at 2theta:  103.728 for phase no.    1 -> Fixing to HG=1.0e-10
=> Square of FWHM(G) < 0 at 2theta:  104.081 for phase no.    1 -> Fixing to HG=1.0e-10
=> Square of FWHM(G) < 0 at 2theta:  104.081 for phase no.    1 -> Fixing to HG=1.0e-10
=> Square of FWHM(G) < 0 at 2theta:  107.821 for phase no.    1 -> Fixing to HG=1.0e-10
=> Square of FWHM(G) < 0 at 2theta:  108.202 for phase no.    1 -> Fixing to HG=1.0e-10
=> Square of FWHM(G) < 0 at 2theta:  112.011 for phase no.    1 -> Fixing to HG=1.0e-10
=> Square of FWHM(G) < 0 at 2theta:  112.422 for phase no.    1 -> Fixing to HG=1.0e-10
=> Square of FWHM(G) < 0 at 2theta:  116.329 for phase no.    1 -> Fixing to HG=1.0e-10
=> Square of FWHM(G) < 0 at 2theta:  116.776 for phase no.    1 -> Fixing to HG=1.0e-10
=> Square of FWHM(G) < 0 at 2theta:  120.815 for phase no.    1 -> Fixing to HG=1.0e-10
=> Square of FWHM(G) < 0 at 2theta:  121.304 for phase no.    1 -> Fixing to HG=1.0e-10
=> Square of FWHM(G) < 0 at 2theta:  130.522 for phase no.    1 -> Fixing to HG=1.0e-10
=> Square of FWHM(G) < 0 at 2theta:  131.126 for phase no.    1 -> Fixing to HG=1.0e-10
=> Square of FWHM(G) < 0 at 2theta:  135.929 for phase no.    1 -> Fixing to HG=1.0e-10
=> Square of FWHM(G) < 0 at 2theta:  135.929 for phase no.    1 -> Fixing to HG=1.0e-10
=> Square of FWHM(G) < 0 at 2theta:  136.618 for phase no.    1 -> Fixing to HG=1.0e-10
=> Square of FWHM(G) < 0 at 2theta:  136.618 for phase no.    1 -> Fixing to HG=1.0e-10
=> Square of FWHM(G) < 0 at 2theta:   99.705 for phase no.    1 -> Fixing to HG=1.0e-10
=> Square of FWHM(G) < 0 at 2theta:   99.705 for phase no.    1 -> Fixing to HG=1.0e-10
=> Square of FWHM(G) < 0 at 2theta:  100.033 for phase no.    1 -> Fixing to HG=1.0e-10
=> Square of FWHM(G) < 0 at 2theta:  100.033 for phase no.    1 -> Fixing to HG=1.0e-10
=> Square of FWHM(G) < 0 at 2theta:  103.728 for phase no.    1 -> Fixing to HG=1.0e-10
=> Square of FWHM(G) < 0 at 2theta:  103.728 for phase no.    1 -> Fixing to HG=1.0e-10
=> Square of FWHM(G) < 0 at 2theta:  104.081 for phase no.    1 -> Fixing to HG=1.0e-10
=> Square of FWHM(G) < 0 at 2theta:  104.081 for phase no.    1 -> Fixing to HG=1.0e-10
=> Square of FWHM(G) < 0 at 2theta:  107.821 for phase no.    1 -> Fixing to HG=1.0e-10
=> Square of FWHM(G) < 0 at 2theta:  108.202 for phase no.    1 -> Fixing to HG=1.0e-10
=> Square of FWHM(G) < 0 at 2theta:  112.011 for phase no.    1 -> Fixing to HG=1.0e-10
=> Square of FWHM(G) < 0 at 2theta:  112.422 for phase no.    1 -> Fixing to HG=1.0e-10
=> Square of FWHM(G) < 0 at 2theta:  116.329 for phase no.    1 -> Fixing to HG=1.0e-10
=> Square of FWHM(G) < 0 at 2theta:  116.776 for phase no.    1 -> Fixing to HG=1.0e-10
=> Square of FWHM(G) < 0 at 2theta:  120.815 for phase no.    1 -> Fixing to HG=1.0e-10
=> Square of FWHM(G) < 0 at 2theta:  121.304 for phase no.    1 -> Fixing to HG=1.0e-10
=> Square of FWHM(G) < 0 at 2theta:  130.522 for phase no.    1 -> Fixing to HG=1.0e-10
=> Square of FWHM(G) < 0 at 2theta:  131.126 for phase no.    1 -> Fixing to HG=1.0e-10
=> Square of FWHM(G) < 0 at 2theta:  135.929 for phase no.    1 -> Fixing to HG=1.0e-10
=> Square of FWHM(G) < 0 at 2theta:  135.929 for phase no.    1 -> Fixing to HG=1.0e-10
=> Square of FWHM(G) < 0 at 2theta:  136.618 for phase no.    1 -> Fixing to HG=1.0e-10
=> Square of FWHM(G) < 0 at 2theta:  136.618 for phase no.    1 -> Fixing to HG=1.0e-10
=> Square of FWHM(G) < 0 at 2theta:   99.705 for phase no.    1 -> Fixing to HG=1.0e-10
=> Square of FWHM(G) < 0 at 2theta:   99.705 for phase no.    1 -> Fixing to HG=1.0e-10
=> Square of FWHM(G) < 0 at 2theta:  100.033 for phase no.    1 -> Fixing to HG=1.0e-10
=> Square of FWHM(G) < 0 at 2theta:  100.033 for phase no.    1 -> Fixing to HG=1.0e-10
=> Square of FWHM(G) < 0 at 2theta:  103.728 for phase no.    1 -> Fixing to HG=1.0e-10
=> Square of FWHM(G) < 0 at 2theta:  103.728 for phase no.    1 -> Fixing to HG=1.0e-10
=> Square of FWHM(G) < 0 at 2theta:  104.081 for phase no.    1 -> Fixing to HG=1.0e-10
=> Square of FWHM(G) < 0 at 2theta:  104.081 for phase no.    1 -> Fixing to HG=1.0e-10
=> Square of FWHM(G) < 0 at 2theta:  107.821 for phase no.    1 -> Fixing to HG=1.0e-10
=> Square of FWHM(G) < 0 at 2theta:  108.202 for phase no.    1 -> Fixing to HG=1.0e-10
=> Square of FWHM(G) < 0 at 2theta:  112.011 for phase no.    1 -> Fixing to HG=1.0e-10
=> Square of FWHM(G) < 0 at 2theta:  112.422 for phase no.    1 -> Fixing to HG=1.0e-10
=> Square of FWHM(G) < 0 at 2theta:  116.329 for phase no.    1 -> Fixing to HG=1.0e-10
=> Square of FWHM(G) < 0 at 2theta:  116.776 for phase no.    1 -> Fixing to HG=1.0e-10
```

```
=> Square of FWHM(G) < 0 at 2theta:  120.815 for phase no.    1 -> Fixing to HG=1.0e-10
=> Square of FWHM(G) < 0 at 2theta:  121.304 for phase no.    1 -> Fixing to HG=1.0e-10
=> Square of FWHM(G) < 0 at 2theta:  130.522 for phase no.    1 -> Fixing to HG=1.0e-10
=> Square of FWHM(G) < 0 at 2theta:  131.126 for phase no.    1 -> Fixing to HG=1.0e-10
=> Square of FWHM(G) < 0 at 2theta:  135.929 for phase no.    1 -> Fixing to HG=1.0e-10
=> Square of FWHM(G) < 0 at 2theta:  135.929 for phase no.    1 -> Fixing to HG=1.0e-10
=> Square of FWHM(G) < 0 at 2theta:  136.618 for phase no.    1 -> Fixing to HG=1.0e-10
=> Square of FWHM(G) < 0 at 2theta:  136.618 for phase no.    1 -> Fixing to HG=1.0e-10
=> Square of FWHM(G) < 0 at 2theta:   99.705 for phase no.    1 -> Fixing to HG=1.0e-10
=> Square of FWHM(G) < 0 at 2theta:   99.705 for phase no.    1 -> Fixing to HG=1.0e-10
=> Square of FWHM(G) < 0 at 2theta:  100.033 for phase no.    1 -> Fixing to HG=1.0e-10
=> Square of FWHM(G) < 0 at 2theta:  100.033 for phase no.    1 -> Fixing to HG=1.0e-10
=> Square of FWHM(G) < 0 at 2theta:  103.728 for phase no.    1 -> Fixing to HG=1.0e-10
=> Square of FWHM(G) < 0 at 2theta:  103.728 for phase no.    1 -> Fixing to HG=1.0e-10
=> Square of FWHM(G) < 0 at 2theta:  104.081 for phase no.    1 -> Fixing to HG=1.0e-10
=> Square of FWHM(G) < 0 at 2theta:  104.081 for phase no.    1 -> Fixing to HG=1.0e-10
=> Square of FWHM(G) < 0 at 2theta:  107.821 for phase no.    1 -> Fixing to HG=1.0e-10
=> Square of FWHM(G) < 0 at 2theta:  108.202 for phase no.    1 -> Fixing to HG=1.0e-10
=> Square of FWHM(G) < 0 at 2theta:  112.011 for phase no.    1 -> Fixing to HG=1.0e-10
=> Square of FWHM(G) < 0 at 2theta:  112.422 for phase no.    1 -> Fixing to HG=1.0e-10
=> Square of FWHM(G) < 0 at 2theta:  116.329 for phase no.    1 -> Fixing to HG=1.0e-10
=> Square of FWHM(G) < 0 at 2theta:  116.776 for phase no.    1 -> Fixing to HG=1.0e-10
=> Square of FWHM(G) < 0 at 2theta:  120.815 for phase no.    1 -> Fixing to HG=1.0e-10
=> Square of FWHM(G) < 0 at 2theta:  121.304 for phase no.    1 -> Fixing to HG=1.0e-10
=> Square of FWHM(G) < 0 at 2theta:  130.522 for phase no.    1 -> Fixing to HG=1.0e-10
=> Square of FWHM(G) < 0 at 2theta:  131.126 for phase no.    1 -> Fixing to HG=1.0e-10
=> Square of FWHM(G) < 0 at 2theta:  135.929 for phase no.    1 -> Fixing to HG=1.0e-10
=> Square of FWHM(G) < 0 at 2theta:  135.929 for phase no.    1 -> Fixing to HG=1.0e-10
=> Square of FWHM(G) < 0 at 2theta:  136.618 for phase no.    1 -> Fixing to HG=1.0e-10
=> Square of FWHM(G) < 0 at 2theta:  136.618 for phase no.    1 -> Fixing to HG=1.0e-10
=> Square of FWHM(G) < 0 at 2theta:   99.705 for phase no.    1 -> Fixing to HG=1.0e-10
=> Square of FWHM(G) < 0 at 2theta:   99.705 for phase no.    1 -> Fixing to HG=1.0e-10
=> Square of FWHM(G) < 0 at 2theta:  100.033 for phase no.    1 -> Fixing to HG=1.0e-10
=> Square of FWHM(G) < 0 at 2theta:  100.033 for phase no.    1 -> Fixing to HG=1.0e-10
=> Square of FWHM(G) < 0 at 2theta:  103.728 for phase no.    1 -> Fixing to HG=1.0e-10
=> Square of FWHM(G) < 0 at 2theta:  103.728 for phase no.    1 -> Fixing to HG=1.0e-10
=> Square of FWHM(G) < 0 at 2theta:  104.081 for phase no.    1 -> Fixing to HG=1.0e-10
=> Square of FWHM(G) < 0 at 2theta:  104.081 for phase no.    1 -> Fixing to HG=1.0e-10
=> Square of FWHM(G) < 0 at 2theta:  107.821 for phase no.    1 -> Fixing to HG=1.0e-10
=> Square of FWHM(G) < 0 at 2theta:  108.202 for phase no.    1 -> Fixing to HG=1.0e-10
=> Square of FWHM(G) < 0 at 2theta:  112.011 for phase no.    1 -> Fixing to HG=1.0e-10
=> Square of FWHM(G) < 0 at 2theta:  112.422 for phase no.    1 -> Fixing to HG=1.0e-10
=> Square of FWHM(G) < 0 at 2theta:  116.329 for phase no.    1 -> Fixing to HG=1.0e-10
=> Square of FWHM(G) < 0 at 2theta:  116.776 for phase no.    1 -> Fixing to HG=1.0e-10
=> Square of FWHM(G) < 0 at 2theta:  120.815 for phase no.    1 -> Fixing to HG=1.0e-10
=> Square of FWHM(G) < 0 at 2theta:  121.304 for phase no.    1 -> Fixing to HG=1.0e-10
=> Square of FWHM(G) < 0 at 2theta:  130.522 for phase no.    1 -> Fixing to HG=1.0e-10
=> Square of FWHM(G) < 0 at 2theta:  131.126 for phase no.    1 -> Fixing to HG=1.0e-10
=> Square of FWHM(G) < 0 at 2theta:  135.929 for phase no.    1 -> Fixing to HG=1.0e-10
=> Square of FWHM(G) < 0 at 2theta:  135.929 for phase no.    1 -> Fixing to HG=1.0e-10
=> Square of FWHM(G) < 0 at 2theta:  136.618 for phase no.    1 -> Fixing to HG=1.0e-10
=> Square of FWHM(G) < 0 at 2theta:  136.618 for phase no.    1 -> Fixing to HG=1.0e-10
=> Square of FWHM(G) < 0 at 2theta:   99.705 for phase no.    1 -> Fixing to HG=1.0e-10
=> Square of FWHM(G) < 0 at 2theta:   99.705 for phase no.    1 -> Fixing to HG=1.0e-10
=> Square of FWHM(G) < 0 at 2theta:  100.033 for phase no.    1 -> Fixing to HG=1.0e-10
=> Square of FWHM(G) < 0 at 2theta:  100.033 for phase no.    1 -> Fixing to HG=1.0e-10
=> Square of FWHM(G) < 0 at 2theta:  103.728 for phase no.    1 -> Fixing to HG=1.0e-10
=> Square of FWHM(G) < 0 at 2theta:  103.728 for phase no.    1 -> Fixing to HG=1.0e-10
=> Square of FWHM(G) < 0 at 2theta:  104.081 for phase no.    1 -> Fixing to HG=1.0e-10
=> Square of FWHM(G) < 0 at 2theta:  104.081 for phase no.    1 -> Fixing to HG=1.0e-10
=> Square of FWHM(G) < 0 at 2theta:  107.821 for phase no.    1 -> Fixing to HG=1.0e-10
=> Square of FWHM(G) < 0 at 2theta:  108.202 for phase no.    1 -> Fixing to HG=1.0e-10
=> Square of FWHM(G) < 0 at 2theta:  112.011 for phase no.    1 -> Fixing to HG=1.0e-10
=> Square of FWHM(G) < 0 at 2theta:  112.422 for phase no.    1 -> Fixing to HG=1.0e-10
=> Square of FWHM(G) < 0 at 2theta:  116.329 for phase no.    1 -> Fixing to HG=1.0e-10
=> Square of FWHM(G) < 0 at 2theta:  116.776 for phase no.    1 -> Fixing to HG=1.0e-10
=> Square of FWHM(G) < 0 at 2theta:  120.815 for phase no.    1 -> Fixing to HG=1.0e-10
=> Square of FWHM(G) < 0 at 2theta:  121.304 for phase no.    1 -> Fixing to HG=1.0e-10
=> Square of FWHM(G) < 0 at 2theta:  130.522 for phase no.    1 -> Fixing to HG=1.0e-10
=> Square of FWHM(G) < 0 at 2theta:  131.126 for phase no.    1 -> Fixing to HG=1.0e-10
=> Square of FWHM(G) < 0 at 2theta:  135.929 for phase no.    1 -> Fixing to HG=1.0e-10
=> Square of FWHM(G) < 0 at 2theta:  135.929 for phase no.    1 -> Fixing to HG=1.0e-10
=> Square of FWHM(G) < 0 at 2theta:  136.618 for phase no.    1 -> Fixing to HG=1.0e-10
=> Square of FWHM(G) < 0 at 2theta:  136.618 for phase no.    1 -> Fixing to HG=1.0e-10
=> Square of FWHM(G) < 0 at 2theta:   99.705 for phase no.    1 -> Fixing to HG=1.0e-10
=> Square of FWHM(G) < 0 at 2theta:   99.705 for phase no.    1 -> Fixing to HG=1.0e-10
=> Square of FWHM(G) < 0 at 2theta:  100.033 for phase no.    1 -> Fixing to HG=1.0e-10
=> Square of FWHM(G) < 0 at 2theta:  100.033 for phase no.    1 -> Fixing to HG=1.0e-10
=> Square of FWHM(G) < 0 at 2theta:  103.728 for phase no.    1 -> Fixing to HG=1.0e-10
=> Square of FWHM(G) < 0 at 2theta:  103.728 for phase no.    1 -> Fixing to HG=1.0e-10
=> Square of FWHM(G) < 0 at 2theta:  104.081 for phase no.    1 -> Fixing to HG=1.0e-10
=> Square of FWHM(G) < 0 at 2theta:  104.081 for phase no.    1 -> Fixing to HG=1.0e-10
=> Square of FWHM(G) < 0 at 2theta:  107.821 for phase no.    1 -> Fixing to HG=1.0e-10
=> Square of FWHM(G) < 0 at 2theta:  108.202 for phase no.    1 -> Fixing to HG=1.0e-10
=> Square of FWHM(G) < 0 at 2theta:  112.011 for phase no.    1 -> Fixing to HG=1.0e-10
=> Square of FWHM(G) < 0 at 2theta:  112.422 for phase no.    1 -> Fixing to HG=1.0e-10
=> Square of FWHM(G) < 0 at 2theta:  116.329 for phase no.    1 -> Fixing to HG=1.0e-10
=> Square of FWHM(G) < 0 at 2theta:  116.776 for phase no.    1 -> Fixing to HG=1.0e-10
=> Square of FWHM(G) < 0 at 2theta:  120.815 for phase no.    1 -> Fixing to HG=1.0e-10
=> Square of FWHM(G) < 0 at 2theta:  121.304 for phase no.    1 -> Fixing to HG=1.0e-10
```

```
=> Square of FWHM(G) < 0 at 2theta:  130.522 for phase no.    1 -> Fixing to HG=1.0e-10
=> Square of FWHM(G) < 0 at 2theta:  131.126 for phase no.    1 -> Fixing to HG=1.0e-10
=> Square of FWHM(G) < 0 at 2theta:  135.929 for phase no.    1 -> Fixing to HG=1.0e-10
=> Square of FWHM(G) < 0 at 2theta:  135.929 for phase no.    1 -> Fixing to HG=1.0e-10
=> Square of FWHM(G) < 0 at 2theta:  136.618 for phase no.    1 -> Fixing to HG=1.0e-10
=> Square of FWHM(G) < 0 at 2theta:  136.618 for phase no.    1 -> Fixing to HG=1.0e-10
=> Square of FWHM(G) < 0 at 2theta:   99.705 for phase no.    1 -> Fixing to HG=1.0e-10
=> Square of FWHM(G) < 0 at 2theta:   99.705 for phase no.    1 -> Fixing to HG=1.0e-10
=> Square of FWHM(G) < 0 at 2theta:  100.033 for phase no.    1 -> Fixing to HG=1.0e-10
=> Square of FWHM(G) < 0 at 2theta:  100.033 for phase no.    1 -> Fixing to HG=1.0e-10
=> Square of FWHM(G) < 0 at 2theta:  103.728 for phase no.    1 -> Fixing to HG=1.0e-10
=> Square of FWHM(G) < 0 at 2theta:  103.728 for phase no.    1 -> Fixing to HG=1.0e-10
=> Square of FWHM(G) < 0 at 2theta:  104.081 for phase no.    1 -> Fixing to HG=1.0e-10
=> Square of FWHM(G) < 0 at 2theta:  104.081 for phase no.    1 -> Fixing to HG=1.0e-10
=> Square of FWHM(G) < 0 at 2theta:  107.821 for phase no.    1 -> Fixing to HG=1.0e-10
=> Square of FWHM(G) < 0 at 2theta:  108.202 for phase no.    1 -> Fixing to HG=1.0e-10
=> Square of FWHM(G) < 0 at 2theta:  112.011 for phase no.    1 -> Fixing to HG=1.0e-10
=> Square of FWHM(G) < 0 at 2theta:  112.422 for phase no.    1 -> Fixing to HG=1.0e-10
=> Square of FWHM(G) < 0 at 2theta:  116.329 for phase no.    1 -> Fixing to HG=1.0e-10
=> Square of FWHM(G) < 0 at 2theta:  116.776 for phase no.    1 -> Fixing to HG=1.0e-10
=> Square of FWHM(G) < 0 at 2theta:  120.815 for phase no.    1 -> Fixing to HG=1.0e-10
=> Square of FWHM(G) < 0 at 2theta:  121.304 for phase no.    1 -> Fixing to HG=1.0e-10
=> Square of FWHM(G) < 0 at 2theta:  130.522 for phase no.    1 -> Fixing to HG=1.0e-10
=> Square of FWHM(G) < 0 at 2theta:  131.126 for phase no.    1 -> Fixing to HG=1.0e-10
=> Square of FWHM(G) < 0 at 2theta:  135.929 for phase no.    1 -> Fixing to HG=1.0e-10
=> Square of FWHM(G) < 0 at 2theta:  135.929 for phase no.    1 -> Fixing to HG=1.0e-10
=> Square of FWHM(G) < 0 at 2theta:  136.618 for phase no.    1 -> Fixing to HG=1.0e-10
=> Square of FWHM(G) < 0 at 2theta:  136.618 for phase no.    1 -> Fixing to HG=1.0e-10


Standard deviations have to be multiplied by: 2.1538
(correlated residuals) See references:
-J.F.Berar & P.Lelann, J. Appl. Cryst. 24, 1-5 (1991)
-J.F.Berar, Acc. in Pow. Diff. II,NIST Sp.Pub. 846, 63(1992)

++++++++++++++++++++++++++++++++++++++++++++++++++++++++++++++++++++++++++++++++++++++++++++++++++++++++++++++++++++++++++++++++++++++ ↙


=> CYCLE No.:   50
-------------------------------------------------------------------------------
=> Phase  1 Name: NIST SRM 660a LaB6
-------------------------------------------------------------------------------
=> New parameters, shifts, and standard deviations

Atom        x       dx      sx       y       dy      sy       z       dz      sz       B       dB      sB      occ.  ↙
         docc.   socc.

La       0.00000 0.00000 0.00000  0.00000 0.00000 0.00000  0.00000 0.00000 0.00000  0.41517 0.00000 0.00000    ↙
     0.16666 0.00000 0.00000
B        0.20319 0.00001 0.00193  0.50000 0.00000 0.00000  0.50000 0.00000 0.00000  0.26488 0.00000 0.00000    ↙
     1.00000 0.00000 0.00000

==> PROFILE PARAMETERS FOR PATTERN#  1

=> Overall scale factor:      0.000125355     0.000000003     0.000000635
=> Eta(p-Voigt) or m(Pearson VII):   0.000000  0.000000  0.000000
=> Overall tem. factor:   0.000000  0.000000  0.000000
=> Halfwidth parameters:
0.001356  0.000000  0.000000
-0.005000  0.000000  0.000000
0.003910  0.000000  0.000000
=> Cell parameters:
4.154987   0.000000   0.000000
4.154987   0.000000   0.000000
4.154987   0.000000   0.000000
90.000000   0.000000   0.000000
90.000000   0.000000   0.000000
90.000000   0.000000   0.000000
=> Preferred orientation:
1.000000  0.000000  0.000000
0.000000  0.000000  0.000000
=> Asymmetry parameters:
-0.032396  0.000130  0.031169
0.042064  0.000018  0.004032
0.000000  0.000000  0.000000
0.000000  0.000000  0.000000
=> X and Y parameters:
0.063891 -0.000003  0.001582
0.000083  0.000000  0.000000
=> Strain parameters:
0.000000  0.000000  0.000000
0.000000  0.000000  0.000000
0.000000  0.000000  0.000000
=> Size   parameters (G,L):
0.000000  0.000000  0.000000
0.000000  0.000000  0.000000
=> Further shape parameters (S_L and D_L):
0.000000  0.000000  0.000000
0.000000  0.000000  0.000000
```

```
==> GLOBAL PARAMETERS FOR PATTERN#  1


=> Zero-point:    -0.2111    0.0000    0.0033

=> Cos( theta)-shift parameter :   0.0767  0.0000  0.0034
=> Sin(2theta)-shift parameter :   0.0387  0.0000  0.0025

==> RELIABILITY FACTORS WITH ALL NON-EXCLUDED POINTS FOR PATTERN:  1

=> R-Factors:   20.8      31.0     Chi2:  18.6     DW-Stat.:  1.2720   Patt#:  1
=> Expected :            7.20                                1.9292
=> Deviance : 0.187E+06     Dev*:   26.62
=> GoF-index:  4.3         Sqrt(Residual/N)
=> N-P+C:  6973

=>    SumYdif       SumYobs      SumYcal      SumwYobsSQ     Residual    Condition
0.2802E+06    0.1347E+07    0.1232E+07    0.1347E+07    0.1296E+06    0.5539E+19


=> Conventional Rietveld Rp,Rwp,Re and Chi2:   22.2      32.2      7.47      18.59
=> (Values obtained using Ynet, but true sigma(y))
=>  SumYnet, Sum(w Ynet**2):     0.1263E+07    0.1250E+07

=> N-sigma of the GoF: 1038.716

==> RELIABILITY FACTORS FOR POINTS WITH BRAGG CONTRIBUTIONS FOR PATTERN:  1

=> R-Factors:   18.1      27.0     Chi2:  20.7     DW-Stat.:  1.7601   Patt#:
=> Expected :            5.94                                1.9131
=> Deviance : 0.115E+06     Dev*:   25.16
=> GoF-index:  4.5         Sqrt(Residual/N)
=> N-P+C:  4520

=>    SumYdif       SumYobs      SumYcal      SumwYobsSQ     Residual    Condition
0.2316E+06    0.1282E+07    0.1196E+07    0.1282E+07    0.9369E+05    0.5539E+19


=> Conventional Rietveld Rp,Rwp,Re and Chi2:   18.8      27.8      6.10      20.73
=> (Values obtained using Ynet, but true sigma(y))
=>  SumYnet, Sum(w Ynet**2):     0.1234E+07    0.1214E+07

=> N-sigma of the GoF:      937.871

=> Global user-weigthed Chi2 (Bragg contrib.):   28.7


=> Parameters with Correlation greater that 50% ==>
-> Correlation of parameter:           SyCos_pat1      with:       Asym1_ph1_pat1  ->   59%
-> Correlation of parameter:      U-Cagl_ph1_pat1      with:      W-Cagl_ph1_pat1  ->   97%
-> Correlation of parameter:       Asym1_ph1_pat1      with:       Asym2_ph1_pat1  ->   78%

-------------------------------------------------------------------------------------------------------------
Pattern#  1 Phase No:   1 Phase name: NIST SRM 660a LaB6
-------------------------------------------------------------------------------------------------------------

No.  Code     H   K   L  Mult     Hw         2theta       Icalc       Iobs      Sigma      HwG     HwL       ETA   ↙
          d-hkl         CORR

1   1      1   0   0     6  0.061502      21.368     1797.6     1521.0    249.828  0.054909  0.012139  0.251880    ↙
    4.154987     165.860336
2   1      1   1   0    12  0.061195      30.399     2934.7     2710.7    207.324  0.051494  0.017445  0.353212    ↙
    2.938020     157.740463
3   1      1   1   1     8  0.061081      37.460     1202.4     1216.5     52.185  0.048689  0.021752  0.430965    ↙
    2.398883      66.773720
4   1      2   0   0     6  0.061089      43.528      608.9      699.3    107.291  0.046151  0.025598  0.496798    ↙
    2.077493      35.848160
5   1      2   1   0    24  0.061194      48.981     1366.4     1486.0    130.218  0.043746  0.029197  0.555200    ↙
    1.858167     109.784355
6   1      2   1   1    24  0.061383      54.016      718.7      764.6     61.204  0.041398  0.032660  0.608466    ↙
    1.696266      87.862114
7   1      2   2   0    12  0.062005      63.251      258.8      307.7     73.329  0.036676  0.039444  0.704498    ↙
    1.469010      30.818932
8   1      2   2   1    24  0.062452      67.583      685.8      728.3     47.546  0.034222  0.042859  0.748658    ↙
    1.384996      53.468040
9   1      3   0   0     6  0.062452      67.583       64.2       68.2      4.452  0.034222  0.042859  0.748658    ↙
    1.384996      13.367010
10   1      3   1   0    24  0.063010      71.784      526.5      579.4     64.701  0.031651  0.046340  0.790745    ↙
    1.313922      47.309349
11   1      3   1   1    24  0.063710      75.885      328.0      394.7     87.832  0.028913  0.049921  0.830880    ↙
    1.252776      42.641338
12   1      2   2   2     8  0.064590      79.914       56.5       80.4     61.407  0.025937  0.053640  0.868999    ↙
    1.199441      13.040545
13   1      3   2   0    24  0.065710      83.893      215.7      254.5     53.076  0.022620  0.057534  0.904843    ↙
    1.152386      36.518417
14   1      3   2   1    48  0.067145      87.842      440.7      517.2     95.924  0.018773  0.061647  0.937958    ↙
    1.110467      69.344658
15   1      4   0   0     6  0.071370      95.729       78.4      107.3     64.667  0.006325  0.070749  0.993505    ↙
    1.038747       8.212687
16   1      3   2   2    24  0.075877      99.705      230.5      275.6     55.802  0.000000  0.075877  1.000000    ↙
```

```
     1.007732      32.758747
17   1      4   1   0    24  0.075877      99.705      153.8      183.9      37.232  0.000000  0.075877  1.000000    ↙
     1.007732      32.758747
18   1      3   3   0    12  0.081515     103.728      149.2      177.3      36.422  0.000000  0.081515  1.000000    ↙
     0.979340      16.589645
19   1      4   1   1    24  0.081515     103.728      180.6      214.6      44.076  0.000000  0.081515  1.000000    ↙
     0.979340      33.179291
20   1      3   3   1    24  0.087795     107.821      141.2      182.3      68.989  0.000000  0.087795  1.000000    ↙
     0.953219      34.118217
21   1      4   2   0    24  0.094895     112.011      206.7      261.2      92.342  0.000000  0.094895  1.000000    ↙
     0.929083      35.608879
22   1      4   2   1    48  0.103065     116.329      435.8      522.1     114.945  0.000000  0.103065  1.000000    ↙
     0.906693      75.439613
23   1      3   3   2    24  0.112675     120.815      224.1      291.6      93.741  0.000000  0.112675  1.000000    ↙
     0.885846      40.570278
24   1      4   2   2    24  0.138865     130.522      165.4      232.8     116.853  0.000000  0.138865  1.000000    ↙
     0.848133      49.438599
25   1      4   3   0    24  0.158083     135.929      146.5      214.0     100.787  0.000000  0.158083  1.000000    ↙
     0.830997      56.440228
26   1      5   0   0     6  0.158083     135.929       48.4       70.7      33.271  0.000000  0.158083  1.000000    ↙
     0.830997      14.110057
27   1      4   3   1    48  0.189935     141.927      652.1      799.8     181.250  0.028438  0.185430  0.982242    ↙
     0.814860     133.368210
28   1      5   1   0    24  0.189935     141.927      258.1      316.6      71.748  0.028438  0.185430  0.982242    ↙
     0.814860      66.684105
29   1      3   3   3     8  0.244371     148.866       64.1       82.6      23.763  0.058602  0.229661  0.954600    ↙
     0.799628      27.829784
30   1      5   1   1    24  0.244371     148.866      448.9      577.8     166.343  0.058602  0.229661  0.954600    ↙
     0.799628      83.489349

-------------------------------------------------------
BRAGG R-Factors and weight fractions for Pattern #  1
-------------------------------------------------------

=> Phase:  1     NIST SRM 660a LaB6
=> Bragg R-factor:   13.0       Vol:   71.731( 0.000)  Fract(%):  100.00( 0.72)
=> Rf-factor=  8.65             ATZ:        1630.079   Brindley:  1.0000

---------------------------------------------------------------------
SYMBOLIC NAMES AND FINAL VALUES AND SIGMA OF REFINED PARAMETERS:
---------------------------------------------------------------------

->  Parameter number    1 :            Zero_pat1    -0.21106540    ( +/-    0.32565552E-02 )
->  Parameter number    2 :           SyCos_pat1     0.76720364E-01( +/-    0.33641579E-02 )
->  Parameter number    3 :           SySin_pat1     0.38725469E-01( +/-    0.24757127E-02 )
->  Parameter number    4 :              X_B_ph1     0.20319004    ( +/-    0.19287585E-02 )
->  Parameter number    5 :       Scale_ph1_pat1     0.12535467E-03( +/-    0.63530314E-06 )
->  Parameter number    6 :      U-Cagl_ph1_pat1     0.13559998E-02( +/-    0.38470202E-09 )
->  Parameter number    7 :      V-Cagl_ph1_pat1    -0.49999999E-02( +/-    0.13145328E-08 )
->  Parameter number    8 :      W-Cagl_ph1_pat1     0.39100000E-02( +/-    0.10740180E-08 )
->  Parameter number    9 :       Asym1_ph1_pat1    -0.32395910E-01( +/-    0.31169372E-01 )
->  Parameter number   10 :       X-tan_ph1_pat1     0.63890785E-01( +/-    0.15823194E-02 )
->  Parameter number   11 :       Y-cos_ph1_pat1      0.0000000    ( +/-     0.0000000     )
->  Parameter number   12 :       Asym2_ph1_pat1     0.42063739E-01( +/-    0.40319548E-02 )

---------------------------------------------------------------------
=> Number of bytes for floating point variables: 4
=> Dimensions of dynamic allocated arrays in this run of FullProf:
---------------------------------------------------------------------

=> Total approximate array memory (dynamic + static): 107719993 bytes

MaxPOINT=    60000 Max.num. of points(+int. Inten.)/diffraction pattern
MaxREFLT=    20000 Max.num. of reflections/diffraction pattern
MaxPARAM=      300 Max.num. of refinable parameters
MaxOVERL=     2096 Max.num. of overlapping reflections

-----------------------------------------------------------
=> Number of bytes for floating point arrays: 4
=> Dimensions of fixed arrays in this release of FullProf:
-----------------------------------------------------------

NPATT   =       80 Max.num. of powder diffraction patterns
NATS    =      830 Max.num. of atoms (all kind) in asymmetric unit
MPAR    =     1800 Max.num. of non atomic parameters/phase
IEXCL   =       30 Max.num. of excluded regions
IBACP   =      277 Max.num. of background points for interpolation
NPHT    =       16 Max.num. of phases
NMAGM   =        8 Max.num. of rotation-matrices sets for magnetic structure
NBASIS  =       12 Max.num. of basis functions associated to a single atom
NIREPS  =        9 Max.num. of irreducible representations to be combined
N_EQ    =      384 Max.num. of user-supplied symmetry operators/propagation vectors
NGL     =      300 Max.num. of global parameters/diffraction pattern
N_LINC  =       30 Max.num. of global linear restraints
NAT_P   =       64 Max.num. of atomic parameters per atom
NCONST  =      500 Max.num. of slack constraints per phase
N_SPE   =       16 Max.num. of different chemical species
N_FORM  =       60 Max.num. of scattering factor values in a table
NPR     =      150 Max.num. of points defining a numerical profile
INPR    =       25 Max.num. of different numerical peak shapes
```

```
NPRC    =      150 Max.num. of terms in the table for correcting intensities
NSOL    =       10 Max.num. of solutions to be stored in Montecarlo searchs


CPU Time:     5.328 seconds
0.089 minutes

=> Run finished at:     Date: 17/02/2015  Time: 13:47:29.606
%\end{Verbatim}
```

A.2 Sample of n-RDX processed pure at 2 wt% in acetone

```
*******************************************************
** PROGRAM FullProf.2k (Version 5.60 - Jan2015-ILL JRC) **
*******************************************************
M U L T I -- P A T T E R N
Rietveld, Profile Matching & Integrated Intensity
Refinement of X-ray and/or Neutron Data


Date: 15/06/2015  Time: 11:00:34.452

=> PCR file code: v203
=> DAT file code: v203.dat             -> Relative contribution: 1.0000

==> CONDITIONS OF THIS RUN FOR PATTERN No.:  1

=> Global Refinement of X-ray powder diffraction data
=> Global Refinement of X-ray powder diffraction data
Flat plate with PSD
=> Title:RDX

=> Number of phases:    1
=> Number of excluded regions:    0
=> Number of scattering factors supplied:    0
=> March-Dollase model for preferred orientation
=> Conventional weights: w=1.0/Variance(yobs)
=> Asymmetry correction as in J.Appl.Cryst. 26,128(1993)
=> Background refined by polynomial function
=> The    5th default profile function was selected
=> Pseudo-Voigt function (ETA variable)
X-parameter correspond to: ETA=ETA0+X*2theta
pV(x)= ETA*L(x)+(1-ETA)*G(x)

==> INPUT/OUTPUT OPTIONS:

=> Generate file *.PRF for plot
=> Output Integrated Intensities
=> Generate new input file *.PCR

=> Data supplied in free format for pattern:  1
=> Plot pattern at each cycle
=> Wavelengths:  1.54056 1.54439
=> Alpha2/Alpha1 ratio:   0.5000
=> Cos(Monochromator angle)=   1.0000
=> Asymmetry correction for angles lower than   90.000 degrees
=> Absorption correction (AC), muR-eff =   0.0000  0.0000
=> Base of peaks: 2.0*HW*   20.00

=> Number of cycles:   50
=> Relaxation factors ==>    for coordinates:  1.00
=> for anisotropic temperature factors:  1.00
=> for halfwidth/strain/size parameters:  1.00
=> for lattice constants and propagation vectors:  1.00
=> EPS-value for convergence:    0.0
=> Instrumental Resolution read from file: xray-res.irf
=> Title of data: Approximate resolution function of a conventional X-ray diffractometer CuKalpha1,2

=> The resolution function is IRESOL:   1 for profile function #   5
Input resolution parameters:

U-inst     V-inst     W-inst     X-inst     Y-inst     Z-inst
0.00136   -0.00500    0.00391    0.06389    0.00008    0.00000
0.00136   -0.00500    0.00391    0.06389    0.00008    0.00000

=> Number of Least-Squares parameters varied:    60

=>--------------------------->
=>-------->  PATTERN number:  1
=>--------------------------->
=> Global parameters and codes ==>
=> Zero-point:    -0.2016   21.0000
=> Background parameters and codes ==>
=> Origin of polynomial at 2theta/TOF/E(KeV):   70.000
0.11847E+06 0.72376E+06 -47087.    -0.18536E+07-0.14029E+07 -35943.
0.00        0.00        0.00        0.00        0.00        0.00
=> Displacement peak-shift parameter and code:     0.00    0.00
=> Transparency peak-shift parameter and code:     0.00    0.00
```

```
=> Reading Intensity data  =>>

==> Angular range, step and number of points:
2Thmin:      10.000000  2Thmax:      49.998600  Step:       0.003700  No. of points:  10811
--------------------------------------------------------------------------------
=> Phase  No. 1
rdx
--------------------------------------------------------------------------------
=>-------> Pattern#  1
=> Crystal Structure Refinement
=> The    7th profile function was selected for phase no.  1
=> Preferred orientation vector:   0.0000  0.0000  1.0000

=>-------> Data for PHASE: 1
=> Number of atoms:   21
=> Number of distance  constraints:    0
=> Number of angle     constraints:    0

=> Symmetry information on space group: P b c a
-> The multiplicity of the general position is:   8
-> The space group is Centric (-1 at origin)
-> Lattice type  P: { 000 }
-> Reduced set of symmetry operators:

No.  IT   Symmetry symbol    Rotation part     Associated Translation
1: ( 1)   1             -->     ( x, y, z) + {  0.0000  0.0000  0.0000}
2: ( 4)   2 ( x, 0, 0) -->     ( x,-y,-z) + {  0.5000  0.5000  0.0000}
3: ( 3)   2 ( 0, y, 0) -->     (-x, y,-z) + {  0.0000  0.5000  0.5000}
4: ( 2)   2 ( 0, 0, z) -->     (-x,-y, z) + {  0.5000  0.0000  0.5000}


Information on Space Group:
---------------------------

=>  Number of Space group:  61
=> Hermann-Mauguin Symbol: P b c a
=>            Hall Symbol: -P 2ac 2ab
=>   Table Setting Choice:
=>           Setting Type: IT (Generated from Hermann-Mauguin symbol)
=>         Crystal System: Orthorhombic
=>             Laue Class: mmm
=>            Point Group: mmm
=>        Bravais Lattice: P
=>         Lattice Symbol: oP
=> Reduced Number of S.O.:   4
=>   General multiplicity:   8
=>         Centrosymmetry: Centric (-1 at origin)
=> Generators (exc. -1&L):   2
=>        Asymmetric unit:  0.000 <= x <=  0.500
0.000 <= y <=  0.500
0.000 <= z <=  0.500

=> List of S.O. without inversion and lattice centring translations
=> SYMM(  1): x,y,z                              => SYMM(  2): x+1/2,-y+1/2,-z
=> SYMM(  3): -x,y+1/2,-z+1/2                    => SYMM(  4): -x+1/2,-y,z+1/2


=> Initial parameters ==>
Atom    Ntyp                X         Y         Z         B         occ.         in  fin  Spc  Mult
B11       B22       B33       B12       B13       B23
O(1)   O                 0.56985   0.44154   0.26709   3.70830   1.00000           0    0    0    8
Codes:   81.00000  91.00000 101.00000   0.00000   0.00000
O(2)   O                 0.59912   0.23245   0.22393   4.41110   1.00000           0    0    0    8
Codes:  111.00000 121.00000 131.00000   0.00000   0.00000
O(3)   O                 0.47739   0.13249  -0.01670   4.98480   1.00000           0    0    0    8
Codes:  141.00000 151.00000 161.00000   0.00000   0.00000
O(4)   O                 0.34915   0.25989  -0.10972   4.76640   1.00000           0    0    0    8
Codes:  171.00000 181.00000 191.00000   0.00000   0.00000
O(5)   O                 0.30776   0.51770  -0.07890   5.32170   1.00000           0    0    0    8
Codes:  201.00000 211.00000 221.00000   0.00000   0.00000
O(6)   O                 0.42684   0.60012   0.05358   5.10850   1.00000           0    0    0    8
Codes:  231.00000 241.00000 251.00000   0.00000   0.00000
N(1)   N                 0.44586   0.33585   0.17311   2.73980   1.00000           0    0    0    8
Codes:  261.00000 271.00000 281.00000   0.00000   0.00000
N(2)   N                 0.32972   0.23290   0.05472   2.40240   1.00000           0    0    0    8
Codes:  291.00000 301.00000 311.00000   0.00000   0.00000
N(3)   N                 0.30485   0.45556   0.08268   2.59240   1.00000           0    0    0    8
Codes:  321.00000 331.00000 341.00000   0.00000   0.00000
N(4)   N                 0.53974   0.33264   0.23717   2.76530   1.00000           0    0    0    8
Codes:  351.00000 361.00000 371.00000   0.00000   0.00000
N(5)   N                 0.38533   0.20298  -0.04227   3.09700   1.00000           0    0    0    8
Codes:  381.00000 391.00000 401.00000   0.00000   0.00000
N(6)   N                 0.35655   0.54262   0.01049   3.43200   1.00000           0    0    0    8
Codes:  411.00000 421.00000 431.00000   0.00000   0.00000
C(1)   C                 0.34605   0.43642   0.19790   2.89510   1.00000           0    0    0    8
Codes:  441.00000 451.00000 461.00000   0.00000   0.00000
C(2)   C                 0.38722   0.21280   0.15754   2.70030   1.00000           0    0    0    8
Codes:  471.00000 481.00000 491.00000   0.00000   0.00000
C(3)   C                 0.23515   0.33775   0.05249   2.55740   1.00000           0    0    0    8
```

```
Codes:  501.00000 511.00000 521.00000   0.00000   0.00000
H(1A)  H                  0.40289   0.52403   0.20773   5.13220   1.00000           0    0    0    8
Codes:    0.00000   0.00000   0.00000   0.00000   0.00000
H(1B)  H                  0.29071   0.42024   0.23991   4.84270   1.00000           0    0    0    8
Codes:    0.00000   0.00000   0.00000   0.00000   0.00000
H(2A)  H                  0.44331   0.13918   0.14950   4.60580   1.00000           0    0    0    8
Codes:    0.00000   0.00000   0.00000   0.00000   0.00000
H(2B)  H                  0.31742   0.19390   0.20730   4.97430   1.00000           0    0    0    8
Codes:    0.00000   0.00000   0.00000   0.00000   0.00000
H(3A)  H                  0.20936   0.35364  -0.02527   4.50050   1.00000           0    0    0    8
Codes:    0.00000   0.00000   0.00000   0.00000   0.00000
H(3B)  H                  0.17213   0.32091   0.10070   3.92150   1.00000           0    0    0    8
Codes:    0.00000   0.00000   0.00000   0.00000   0.00000

=> IT IS ASSUMED THAT THE FIRST GIVEN SITE IS FULLY OCCUPIED
OR THE FIRST AND SECOND ATOMS ARE IN THE SAME SITE WITH TOTAL FULL OCCUPATION
(If this is not the case, change the order of atoms to obtain correct values for the content of the unit cell)
The given occupation factors have been obtained mutiplying m/M by   1.0000
-> Atom: O   ,  Chemical element: O   Atomic Mass:    15.9994
-> Atom: O   ,  Chemical element: O   Atomic Mass:    15.9994
-> Atom: O   ,  Chemical element: O   Atomic Mass:    15.9994
-> Atom: O   ,  Chemical element: O   Atomic Mass:    15.9994
-> Atom: O   ,  Chemical element: O   Atomic Mass:    15.9994
-> Atom: O   ,  Chemical element: O   Atomic Mass:    15.9994
-> Atom: N   ,  Chemical element: N   Atomic Mass:    14.0067
-> Atom: N   ,  Chemical element: N   Atomic Mass:    14.0067
-> Atom: N   ,  Chemical element: N   Atomic Mass:    14.0067
-> Atom: N   ,  Chemical element: N   Atomic Mass:    14.0067
-> Atom: N   ,  Chemical element: N   Atomic Mass:    14.0067
-> Atom: N   ,  Chemical element: N   Atomic Mass:    14.0067
-> Atom: C   ,  Chemical element: C   Atomic Mass:    12.0110
-> Atom: C   ,  Chemical element: C   Atomic Mass:    12.0110
-> Atom: C   ,  Chemical element: C   Atomic Mass:    12.0110
-> Atom: H   ,  Chemical element: H   Atomic Mass:     1.0080
-> Atom: H   ,  Chemical element: H   Atomic Mass:     1.0080
-> Atom: H   ,  Chemical element: H   Atomic Mass:     1.0080
-> Atom: H   ,  Chemical element: H   Atomic Mass:     1.0080
-> Atom: H   ,  Chemical element: H   Atomic Mass:     1.0080
-> Atom: H   ,  Chemical element: H   Atomic Mass:     1.0080
=> The given value of ATZ is       1776.94 the program has calculated:        1776.94
The value of ATZ given in the input PCR file will be used for quantitative analysis
=> The chemical content of the unit cell is:
8.0000 O    +   8.0000 O    +   8.0000 O    +   8.0000 O    +   8.0000 O    +   8.0000 O    +   8.0000 N    +     ↙
    8.0000 N    +   8.0000 N    +   8.0000 N    +
8.0000 N    +   8.0000 N    +   8.0000 C    +   8.0000 C    +   8.0000 C    +   8.0000 H    +   8.0000 H    +     ↙
    8.0000 H    +   8.0000 H    +   8.0000 H    +
8.0000 H
=> The normalized site occupation numbers in % are:
100.0000 O(1)   :      100.0000 O(2)   :      100.0000 O(3)   :      100.0000 O(4)   :      100.0000 O(5)   :        ↙
    100.0000 O(6)   :      100.0000 N(1)   :      100.0000 N(2)   :      100.0000 N(3)   :      100.0000 N(4)   :
100.0000 N(5)   :      100.0000 N(6)   :      100.0000 C(1)   :      100.0000 C(2)   :      100.0000 C(3)   :        ↙
    100.0000 H(1A)  :      100.0000 H(1B)  :      100.0000 H(2A)  :      100.0000 H(2B)  :      100.0000 H(3A)  :
100.0000 H(3B)
=> The density (volumic mass) of the compound is:    1.818 g/cm3

=>-------> PROFILE PARAMETERS FOR PATTERN:  1

=> Overall scale factor:   0.366470E-02
=> ETA (p-Voigt) OR M (Pearson VII):   0.0000
=> Overall temperature factor:      0.00000
=> Halfwidth U,V,W:     -0.01481     0.00000     0.00000
=> X and Y parameters:       0.0000      0.0000
=> Direct cell parameters:   11.5606  10.6800  13.1449  90.0000  90.0000  90.0000
=> Preferred orientation parameters:   1.0000  0.0000
=> Asymmetry parameters     :      0.20251     0.04985     0.00000     0.00000
=> Strain parameters        :      0.00000     0.00000     0.00000
=> Size   parameters        :      0.01453     0.00000
=> Further shape parameters (S_L and D_L):   0.00000   0.00000
S_L is source width/detector distance
D_L is detector width/detector distance

==> CODEWORDS FOR PROFILE PARAMETERS of PATTERN#  1

=> Overall scale factor:   31.000
=> ETA (p-Voigt) OR M (Pearson VII):    0.000
=> Overall temperature factor:    0.000
=> Halfwidth U,V,W:   41.000   0.000   0.000
=> X and Y parameters:    0.000   0.000
=> Direct cell parameters:   51.000  61.000  71.000   0.000   0.000   0.000
=> Preferred orientation parameters:    0.000   0.000
=> Asymmetry parameters     :  531.000 541.000   0.000   0.000
=> Strain parameters        :    0.000   0.000   0.000
=> Size   parameters        :   11.000 551.000
=> The 18th model for size is used

=> Orthorhombic Anisotropic Broadening using Spherical Harmonics up
to 4-th order (Laue class: mmm, SPG:16-74, only lorentzian comp.)
Ylm's up to 4th order: Y00,Y20,Y22+,Y40,Y42+,Y44+
RJP - Ref: M. Jarvinen, J. Appl. C. (1993),p.527
=> Coefficients of Spherical Harmonics for anisotropic size
```

```
broadening for an orthorhombic lattice
Y00         Y20          Y22+        Y40          Y42+       Y44+
0.000000    0.000000    0.000000    0.000000    0.000000    0.000000
551.0000    561.0000    571.0000    581.0000    591.0000    601.0000

=> Cell constraints according to Laue symmetry: mmm

Metric information:
-------------------

=> Direct cell parameters:

a =      11.5606      b =      10.6800      c =      13.1449
alpha =       90.000   beta =       90.000  gamma =       90.000
Direct Cell Volume =    1622.9507

=> Reciprocal cell parameters:

a*=     0.086501      b*=     0.093633      c*=     0.076075
alpha*=       90.000   beta*=       90.000  gamma*=       90.000
Reciprocal Cell Volume =   0.00061616

=> Direct and Reciprocal Metric Tensors:

GD                                      GR
133.6470      0.0000      0.0000          0.007482    0.000000    0.000000
0.0000    114.0614      0.0000          0.000000    0.008767    0.000000
0.0000      0.0000    172.7877          0.000000    0.000000    0.005787

=>  Cartesian frame: x // a; y is in the ab-plane; z is x ^ y

Crystal_to_Orthonormal_Matrix             Orthonormal_to_Crystal Matrix
Cr_Orth_cel                               Orth_Cr_cel
11.5606      0.0000      0.0000          0.086501    0.000000    0.000000
0.0000     10.6800      0.0000          0.000000    0.093633    0.000000
0.0000      0.0000     13.1449          0.000000    0.000000    0.076075

Busing-Levy B-matrix: Hc=B.H            Inverse of the Busing-Levy B-matrix
BL_M                                      BL_Minv
0.086501    0.000000    0.000000           11.5606      0.0000      0.0000
0.000000    0.093633    0.000000            0.0000     10.6800      0.0000
0.000000    0.000000    0.076075            0.0000      0.0000     13.1449

=> Laue symmetry mmm   will be used to generate HKL for pattern#   1
=> Reflections generated between S(1/d)min:  0.1129 A-1 and S(1/d)max:  0.5976 A-1
=>                                  dmax:  8.8599 A   and      dmin:  1.6733 A
=> The number of reflections generated is:    183
=> The max. scatt. variable (gen.ref.) is:        54.8173
=> Scattering coefficients from internal table


=> X-ray scattering coeff. (A1, B1, A2,...C, f(0), Z, Dfp,Dfpp)

O       3.0485  13.2771   2.2868   5.7011   1.5463   0.3239   0.8670  32.9089   0.2508   7.9994   8.0000   0.0470  ↙
      0.0320
N      12.2126   0.0057   3.1322   9.8933   2.0125  28.9975   1.1663   0.5826 -11.5290   6.9946   7.0000   0.0290  ↙
      0.0180
C       2.3100  20.8439   1.0200  10.2075   1.5886   0.5687   0.8650  51.6512   0.2156   5.9992   6.0000   0.0170  ↙
      0.0090
H       0.4930  10.5109   0.3229  26.1257   0.1402   3.1424   0.0408  57.7997   0.0030   1.0000   1.0000   0.0000  ↙
      0.0000

---------------------------------------------------------------
SYMBOLIC NAMES AND INITIAL VALUES OF PARAMETERS TO BE VARIED:
---------------------------------------------------------------

->  Parameter number    1   -> Symbolic Name:      G-Size_ph1_pat1    0.14526000E-01
->  Parameter number    2   -> Symbolic Name:           Zero_pat1   -0.20156001
->  Parameter number    3   -> Symbolic Name:       Scale_ph1_pat1    0.36647001E-02
->  Parameter number    4   -> Symbolic Name:      U-Cagl_ph1_pat1   -0.14806000E-01
->  Parameter number    5   -> Symbolic Name:      Cell_A_ph1_pat1     11.560578
->  Parameter number    6   -> Symbolic Name:      Cell_B_ph1_pat1     10.679955
->  Parameter number    7   -> Symbolic Name:      Cell_C_ph1_pat1     13.144872
->  Parameter number    8   -> Symbolic Name:           X_O(1)_ph1    0.56985003
->  Parameter number    9   -> Symbolic Name:           Y_O(1)_ph1    0.44154000
->  Parameter number   10   -> Symbolic Name:           Z_O(1)_ph1    0.26708999
->  Parameter number   11   -> Symbolic Name:           X_O(2)_ph1    0.59912002
->  Parameter number   12   -> Symbolic Name:           Y_O(2)_ph1    0.23244999
->  Parameter number   13   -> Symbolic Name:           Z_O(2)_ph1    0.22393000
->  Parameter number   14   -> Symbolic Name:           X_O(3)_ph1    0.47738999
->  Parameter number   15   -> Symbolic Name:           Y_O(3)_ph1    0.13248999
->  Parameter number   16   -> Symbolic Name:           Z_O(3)_ph1   -0.16700000E-01
->  Parameter number   17   -> Symbolic Name:           X_O(4)_ph1    0.34915000
->  Parameter number   18   -> Symbolic Name:           Y_O(4)_ph1    0.25988999
->  Parameter number   19   -> Symbolic Name:           Z_O(4)_ph1   -0.10972000
->  Parameter number   20   -> Symbolic Name:           X_O(5)_ph1    0.30776000
->  Parameter number   21   -> Symbolic Name:           Y_O(5)_ph1    0.51770002
->  Parameter number   22   -> Symbolic Name:           Z_O(5)_ph1   -0.78900002E-01
->  Parameter number   23   -> Symbolic Name:           X_O(6)_ph1    0.42684001
->  Parameter number   24   -> Symbolic Name:           Y_O(6)_ph1    0.60012001
```

```
->  Parameter number   25   -> Symbolic Name:          Z_O(6)_ph1    0.53580001E-01
->  Parameter number   26   -> Symbolic Name:          X_N(1)_ph1    0.44586000
->  Parameter number   27   -> Symbolic Name:          Y_N(1)_ph1    0.33585000
->  Parameter number   28   -> Symbolic Name:          Z_N(1)_ph1    0.17310999
->  Parameter number   29   -> Symbolic Name:          X_N(2)_ph1    0.32971999
->  Parameter number   30   -> Symbolic Name:          Y_N(2)_ph1    0.23289999
->  Parameter number   31   -> Symbolic Name:          Z_N(2)_ph1    0.54719999E-01
->  Parameter number   32   -> Symbolic Name:          X_N(3)_ph1    0.30485001
->  Parameter number   33   -> Symbolic Name:          Y_N(3)_ph1    0.45556000
->  Parameter number   34   -> Symbolic Name:          Z_N(3)_ph1    0.82680002E-01
->  Parameter number   35   -> Symbolic Name:          X_N(4)_ph1    0.53974003
->  Parameter number   36   -> Symbolic Name:          Y_N(4)_ph1    0.33263999
->  Parameter number   37   -> Symbolic Name:          Z_N(4)_ph1    0.23717000
->  Parameter number   38   -> Symbolic Name:          X_N(5)_ph1    0.38532999
->  Parameter number   39   -> Symbolic Name:          Y_N(5)_ph1    0.20298000
->  Parameter number   40   -> Symbolic Name:          Z_N(5)_ph1   -0.42270001E-01
->  Parameter number   41   -> Symbolic Name:          X_N(6)_ph1    0.35655001
->  Parameter number   42   -> Symbolic Name:          Y_N(6)_ph1    0.54262000
->  Parameter number   43   -> Symbolic Name:          Z_N(6)_ph1    0.10490000E-01
->  Parameter number   44   -> Symbolic Name:          X_C(1)_ph1    0.34604999
->  Parameter number   45   -> Symbolic Name:          Y_C(1)_ph1    0.43641999
->  Parameter number   46   -> Symbolic Name:          Z_C(1)_ph1    0.19790000
->  Parameter number   47   -> Symbolic Name:          X_C(2)_ph1    0.38722000
->  Parameter number   48   -> Symbolic Name:          Y_C(2)_ph1    0.21280000
->  Parameter number   49   -> Symbolic Name:          Z_C(2)_ph1    0.15753999
->  Parameter number   50   -> Symbolic Name:          X_C(3)_ph1    0.23514999
->  Parameter number   51   -> Symbolic Name:          Y_C(3)_ph1    0.33774999
->  Parameter number   52   -> Symbolic Name:          Z_C(3)_ph1    0.52490000E-01
->  Parameter number   53   -> Symbolic Name:       Asym1_ph1_pat1    0.20251000
->  Parameter number   54   -> Symbolic Name:       Asym2_ph1_pat1    0.49849998E-01
->  Parameter number   55   -> Symbolic Name:      L-Size_ph1_pat1     0.0000000
->  Parameter number   56   -> Symbolic Name:       Size2_ph1_pat1     0.0000000
->  Parameter number   57   -> Symbolic Name:       Size3_ph1_pat1     0.0000000
->  Parameter number   58   -> Symbolic Name:       Size4_ph1_pat1     0.0000000
->  Parameter number   59   -> Symbolic Name:       Size5_ph1_pat1     0.0000000
->  Parameter number   60   -> Symbolic Name:       Size6_ph1_pat1     0.0000000

=> Zero counts at step no.      1 at 2theta/TOF/E(KeV):       10.0000  Intensity fixed to 1.0 and variance to 1E6
=> Zero counts at step no.      3 at 2theta/TOF/E(KeV):       10.0074  Intensity fixed to 1.0 and variance to 1E6
=> Zero counts at step no.      4 at 2theta/TOF/E(KeV):       10.0111  Intensity fixed to 1.0 and variance to 1E6
=> Zero counts at step no.      5 at 2theta/TOF/E(KeV):       10.0148  Intensity fixed to 1.0 and variance to 1E6
=> Zero counts at step no.      8 at 2theta/TOF/E(KeV):       10.0259  Intensity fixed to 1.0 and variance to 1E6
=> Zero counts at step no.     10 at 2theta/TOF/E(KeV):       10.0333  Intensity fixed to 1.0 and variance to 1E6
=> Zero counts at step no.     11 at 2theta/TOF/E(KeV):       10.0370  Intensity fixed to 1.0 and variance to 1E6
=> Zero counts at step no.     12 at 2theta/TOF/E(KeV):       10.0407  Intensity fixed to 1.0 and variance to 1E6
=> Zero counts at step no.     14 at 2theta/TOF/E(KeV):       10.0481  Intensity fixed to 1.0 and variance to 1E6
=> Zero counts at step no.     16 at 2theta/TOF/E(KeV):       10.0555  Intensity fixed to 1.0 and variance to 1E6
=> Zero counts at step no.     21 at 2theta/TOF/E(KeV):       10.0740  Intensity fixed to 1.0 and variance to 1E6
=> Zero counts at step no.     23 at 2theta/TOF/E(KeV):       10.0814  Intensity fixed to 1.0 and variance to 1E6
=> Zero counts at step no.     24 at 2theta/TOF/E(KeV):       10.0851  Intensity fixed to 1.0 and variance to 1E6
=> Zero counts at step no.     28 at 2theta/TOF/E(KeV):       10.0999  Intensity fixed to 1.0 and variance to 1E6
=> Zero counts at step no.     31 at 2theta/TOF/E(KeV):       10.1110  Intensity fixed to 1.0 and variance to 1E6
=> Zero counts at step no.     36 at 2theta/TOF/E(KeV):       10.1295  Intensity fixed to 1.0 and variance to 1E6
=> Zero counts at step no.     38 at 2theta/TOF/E(KeV):       10.1369  Intensity fixed to 1.0 and variance to 1E6
=> Zero counts at step no.     41 at 2theta/TOF/E(KeV):       10.1480  Intensity fixed to 1.0 and variance to 1E6
=> Zero counts at step no.     42 at 2theta/TOF/E(KeV):       10.1517  Intensity fixed to 1.0 and variance to 1E6
=> Zero counts at step no.     47 at 2theta/TOF/E(KeV):       10.1702  Intensity fixed to 1.0 and variance to 1E6
=> Zero counts at step no.     50 at 2theta/TOF/E(KeV):       10.1813  Intensity fixed to 1.0 and variance to 1E6
=> Zero counts at step no.     60 at 2theta/TOF/E(KeV):       10.2183  Intensity fixed to 1.0 and variance to 1E6
=> Zero counts at step no.     61 at 2theta/TOF/E(KeV):       10.2220  Intensity fixed to 1.0 and variance to 1E6
=> Zero counts at step no.     64 at 2theta/TOF/E(KeV):       10.2331  Intensity fixed to 1.0 and variance to 1E6
=> Zero counts at step no.     77 at 2theta/TOF/E(KeV):       10.2812  Intensity fixed to 1.0 and variance to 1E6
=> Zero counts at step no.     78 at 2theta/TOF/E(KeV):       10.2849  Intensity fixed to 1.0 and variance to 1E6
=> Zero counts at step no.     84 at 2theta/TOF/E(KeV):       10.3071  Intensity fixed to 1.0 and variance to 1E6
=> Zero counts at step no.     92 at 2theta/TOF/E(KeV):       10.3367  Intensity fixed to 1.0 and variance to 1E6
=> Zero counts at step no.     93 at 2theta/TOF/E(KeV):       10.3404  Intensity fixed to 1.0 and variance to 1E6
=> Zero counts at step no.     94 at 2theta/TOF/E(KeV):       10.3441  Intensity fixed to 1.0 and variance to 1E6
=> Zero counts at step no.     97 at 2theta/TOF/E(KeV):       10.3552  Intensity fixed to 1.0 and variance to 1E6
=> Zero counts at step no.    101 at 2theta/TOF/E(KeV):       10.3700  Intensity fixed to 1.0 and variance to 1E6
=> Zero counts at step no.    104 at 2theta/TOF/E(KeV):       10.3811  Intensity fixed to 1.0 and variance to 1E6
=> Zero counts at step no.    105 at 2theta/TOF/E(KeV):       10.3848  Intensity fixed to 1.0 and variance to 1E6
=> Zero counts at step no.    107 at 2theta/TOF/E(KeV):       10.3922  Intensity fixed to 1.0 and variance to 1E6
=> Zero counts at step no.    116 at 2theta/TOF/E(KeV):       10.4255  Intensity fixed to 1.0 and variance to 1E6
=> Zero counts at step no.    118 at 2theta/TOF/E(KeV):       10.4329  Intensity fixed to 1.0 and variance to 1E6
=> Zero counts at step no.    119 at 2theta/TOF/E(KeV):       10.4366  Intensity fixed to 1.0 and variance to 1E6
=> Zero counts at step no.    122 at 2theta/TOF/E(KeV):       10.4477  Intensity fixed to 1.0 and variance to 1E6
=> Zero counts at step no.    126 at 2theta/TOF/E(KeV):       10.4625  Intensity fixed to 1.0 and variance to 1E6
=> Zero counts at step no.    130 at 2theta/TOF/E(KeV):       10.4773  Intensity fixed to 1.0 and variance to 1E6
=> Zero counts at step no.    132 at 2theta/TOF/E(KeV):       10.4847  Intensity fixed to 1.0 and variance to 1E6
=> Zero counts at step no.    144 at 2theta/TOF/E(KeV):       10.5291  Intensity fixed to 1.0 and variance to 1E6
=> Zero counts at step no.    148 at 2theta/TOF/E(KeV):       10.5439  Intensity fixed to 1.0 and variance to 1E6
=> Zero counts at step no.    155 at 2theta/TOF/E(KeV):       10.5698  Intensity fixed to 1.0 and variance to 1E6
=> Zero counts at step no.    168 at 2theta/TOF/E(KeV):       10.6179  Intensity fixed to 1.0 and variance to 1E6
=> Zero counts at step no.    176 at 2theta/TOF/E(KeV):       10.6475  Intensity fixed to 1.0 and variance to 1E6
=> Zero counts at step no.    180 at 2theta/TOF/E(KeV):       10.6623  Intensity fixed to 1.0 and variance to 1E6
=> Zero counts at step no.    182 at 2theta/TOF/E(KeV):       10.6697  Intensity fixed to 1.0 and variance to 1E6
=> Zero counts at step no.    185 at 2theta/TOF/E(KeV):       10.6808  Intensity fixed to 1.0 and variance to 1E6
=> Zero counts at step no.    198 at 2theta/TOF/E(KeV):       10.7289  Intensity fixed to 1.0 and variance to 1E6
=> Zero counts at step no.    200 at 2theta/TOF/E(KeV):       10.7363  Intensity fixed to 1.0 and variance to 1E6
=> Zero counts at step no.    204 at 2theta/TOF/E(KeV):       10.7511  Intensity fixed to 1.0 and variance to 1E6
```

```
=> Zero counts at step no.    206 at 2theta/TOF/E(KeV):       10.7585  Intensity fixed to 1.0 and variance to 1E6
=> Zero counts at step no.    208 at 2theta/TOF/E(KeV):       10.7659  Intensity fixed to 1.0 and variance to 1E6
=> Zero counts at step no.    209 at 2theta/TOF/E(KeV):       10.7696  Intensity fixed to 1.0 and variance to 1E6
=> Zero counts at step no.    212 at 2theta/TOF/E(KeV):       10.7807  Intensity fixed to 1.0 and variance to 1E6
=> Zero counts at step no.    213 at 2theta/TOF/E(KeV):       10.7844  Intensity fixed to 1.0 and variance to 1E6
=> Zero counts at step no.    218 at 2theta/TOF/E(KeV):       10.8029  Intensity fixed to 1.0 and variance to 1E6
=> Zero counts at step no.    220 at 2theta/TOF/E(KeV):       10.8103  Intensity fixed to 1.0 and variance to 1E6
=> Zero counts at step no.    225 at 2theta/TOF/E(KeV):       10.8288  Intensity fixed to 1.0 and variance to 1E6
=> Zero counts at step no.    227 at 2theta/TOF/E(KeV):       10.8362  Intensity fixed to 1.0 and variance to 1E6
=> Zero counts at step no.    231 at 2theta/TOF/E(KeV):       10.8510  Intensity fixed to 1.0 and variance to 1E6
=> Zero counts at step no.    232 at 2theta/TOF/E(KeV):       10.8547  Intensity fixed to 1.0 and variance to 1E6
=> Zero counts at step no.    233 at 2theta/TOF/E(KeV):       10.8584  Intensity fixed to 1.0 and variance to 1E6
=> Zero counts at step no.    236 at 2theta/TOF/E(KeV):       10.8695  Intensity fixed to 1.0 and variance to 1E6
=> Zero counts at step no.    237 at 2theta/TOF/E(KeV):       10.8732  Intensity fixed to 1.0 and variance to 1E6
=> Zero counts at step no.    242 at 2theta/TOF/E(KeV):       10.8917  Intensity fixed to 1.0 and variance to 1E6
=> Zero counts at step no.    247 at 2theta/TOF/E(KeV):       10.9102  Intensity fixed to 1.0 and variance to 1E6
=> Zero counts at step no.    250 at 2theta/TOF/E(KeV):       10.9213  Intensity fixed to 1.0 and variance to 1E6
=> Zero counts at step no.    254 at 2theta/TOF/E(KeV):       10.9361  Intensity fixed to 1.0 and variance to 1E6
=> Zero counts at step no.    255 at 2theta/TOF/E(KeV):       10.9398  Intensity fixed to 1.0 and variance to 1E6
=> Zero counts at step no.    262 at 2theta/TOF/E(KeV):       10.9657  Intensity fixed to 1.0 and variance to 1E6
=> Zero counts at step no.    263 at 2theta/TOF/E(KeV):       10.9694  Intensity fixed to 1.0 and variance to 1E6
=> Zero counts at step no.    269 at 2theta/TOF/E(KeV):       10.9916  Intensity fixed to 1.0 and variance to 1E6
=> Zero counts at step no.    271 at 2theta/TOF/E(KeV):       10.9990  Intensity fixed to 1.0 and variance to 1E6
=> Zero counts at step no.    272 at 2theta/TOF/E(KeV):       11.0027  Intensity fixed to 1.0 and variance to 1E6
=> Zero counts at step no.    278 at 2theta/TOF/E(KeV):       11.0249  Intensity fixed to 1.0 and variance to 1E6
=> Zero counts at step no.    282 at 2theta/TOF/E(KeV):       11.0397  Intensity fixed to 1.0 and variance to 1E6
=> Zero counts at step no.    288 at 2theta/TOF/E(KeV):       11.0619  Intensity fixed to 1.0 and variance to 1E6
=> Zero counts at step no.    289 at 2theta/TOF/E(KeV):       11.0656  Intensity fixed to 1.0 and variance to 1E6
=> Zero counts at step no.    290 at 2theta/TOF/E(KeV):       11.0693  Intensity fixed to 1.0 and variance to 1E6
=> Zero counts at step no.    293 at 2theta/TOF/E(KeV):       11.0804  Intensity fixed to 1.0 and variance to 1E6
=> Zero counts at step no.    295 at 2theta/TOF/E(KeV):       11.0878  Intensity fixed to 1.0 and variance to 1E6
=> Zero counts at step no.    296 at 2theta/TOF/E(KeV):       11.0915  Intensity fixed to 1.0 and variance to 1E6
=> Zero counts at step no.    298 at 2theta/TOF/E(KeV):       11.0989  Intensity fixed to 1.0 and variance to 1E6
=> Zero counts at step no.    301 at 2theta/TOF/E(KeV):       11.1100  Intensity fixed to 1.0 and variance to 1E6
=> Zero counts at step no.    302 at 2theta/TOF/E(KeV):       11.1137  Intensity fixed to 1.0 and variance to 1E6
=> Zero counts at step no.    311 at 2theta/TOF/E(KeV):       11.1470  Intensity fixed to 1.0 and variance to 1E6
=> Zero counts at step no.    319 at 2theta/TOF/E(KeV):       11.1766  Intensity fixed to 1.0 and variance to 1E6
=> Zero counts at step no.    321 at 2theta/TOF/E(KeV):       11.1840  Intensity fixed to 1.0 and variance to 1E6
=> Zero counts at step no.    325 at 2theta/TOF/E(KeV):       11.1988  Intensity fixed to 1.0 and variance to 1E6
=> Zero counts at step no.    328 at 2theta/TOF/E(KeV):       11.2099  Intensity fixed to 1.0 and variance to 1E6
=> Zero counts at step no.    336 at 2theta/TOF/E(KeV):       11.2395  Intensity fixed to 1.0 and variance to 1E6
=> Zero counts at step no.    338 at 2theta/TOF/E(KeV):       11.2469  Intensity fixed to 1.0 and variance to 1E6
=> Zero counts at step no.    339 at 2theta/TOF/E(KeV):       11.2506  Intensity fixed to 1.0 and variance to 1E6
=> Zero counts at step no.    343 at 2theta/TOF/E(KeV):       11.2654  Intensity fixed to 1.0 and variance to 1E6
=> Zero counts at step no.    344 at 2theta/TOF/E(KeV):       11.2691  Intensity fixed to 1.0 and variance to 1E6
=> Zero counts at step no.    347 at 2theta/TOF/E(KeV):       11.2802  Intensity fixed to 1.0 and variance to 1E6
=> Zero counts at step no.    348 at 2theta/TOF/E(KeV):       11.2839  Intensity fixed to 1.0 and variance to 1E6
=> Zero counts at step no.    355 at 2theta/TOF/E(KeV):       11.3098  Intensity fixed to 1.0 and variance to 1E6
=> Zero counts at step no.    362 at 2theta/TOF/E(KeV):       11.3357  Intensity fixed to 1.0 and variance to 1E6
=> Zero counts at step no.    365 at 2theta/TOF/E(KeV):       11.3468  Intensity fixed to 1.0 and variance to 1E6
=> Zero counts at step no.    372 at 2theta/TOF/E(KeV):       11.3727  Intensity fixed to 1.0 and variance to 1E6
=> Zero counts at step no.    375 at 2theta/TOF/E(KeV):       11.3838  Intensity fixed to 1.0 and variance to 1E6
=> Zero counts at step no.    385 at 2theta/TOF/E(KeV):       11.4208  Intensity fixed to 1.0 and variance to 1E6
=> Zero counts at step no.    394 at 2theta/TOF/E(KeV):       11.4541  Intensity fixed to 1.0 and variance to 1E6
=> Zero counts at step no.    395 at 2theta/TOF/E(KeV):       11.4578  Intensity fixed to 1.0 and variance to 1E6
=> Zero counts at step no.    400 at 2theta/TOF/E(KeV):       11.4763  Intensity fixed to 1.0 and variance to 1E6
=> Zero counts at step no.    403 at 2theta/TOF/E(KeV):       11.4874  Intensity fixed to 1.0 and variance to 1E6
=> Zero counts at step no.    406 at 2theta/TOF/E(KeV):       11.4985  Intensity fixed to 1.0 and variance to 1E6
=> Zero counts at step no.    412 at 2theta/TOF/E(KeV):       11.5207  Intensity fixed to 1.0 and variance to 1E6
=> Zero counts at step no.    413 at 2theta/TOF/E(KeV):       11.5244  Intensity fixed to 1.0 and variance to 1E6
=> Zero counts at step no.    414 at 2theta/TOF/E(KeV):       11.5281  Intensity fixed to 1.0 and variance to 1E6
=> Zero counts at step no.    417 at 2theta/TOF/E(KeV):       11.5392  Intensity fixed to 1.0 and variance to 1E6
=> Zero counts at step no.    424 at 2theta/TOF/E(KeV):       11.5651  Intensity fixed to 1.0 and variance to 1E6
=> Zero counts at step no.    428 at 2theta/TOF/E(KeV):       11.5799  Intensity fixed to 1.0 and variance to 1E6
=> Zero counts at step no.    457 at 2theta/TOF/E(KeV):       11.6872  Intensity fixed to 1.0 and variance to 1E6
=> Zero counts at step no.    474 at 2theta/TOF/E(KeV):       11.7501  Intensity fixed to 1.0 and variance to 1E6
=> Zero counts at step no.    492 at 2theta/TOF/E(KeV):       11.8167  Intensity fixed to 1.0 and variance to 1E6
=> Zero counts at step no.    493 at 2theta/TOF/E(KeV):       11.8204  Intensity fixed to 1.0 and variance to 1E6
=> Zero counts at step no.    496 at 2theta/TOF/E(KeV):       11.8315  Intensity fixed to 1.0 and variance to 1E6
=> Zero counts at step no.    497 at 2theta/TOF/E(KeV):       11.8352  Intensity fixed to 1.0 and variance to 1E6
=> Zero counts at step no.    499 at 2theta/TOF/E(KeV):       11.8426  Intensity fixed to 1.0 and variance to 1E6
=> Zero counts at step no.    543 at 2theta/TOF/E(KeV):       12.0054  Intensity fixed to 1.0 and variance to 1E6
=> Zero counts at step no.    544 at 2theta/TOF/E(KeV):       12.0091  Intensity fixed to 1.0 and variance to 1E6
=> Zero counts at step no.    552 at 2theta/TOF/E(KeV):       12.0387  Intensity fixed to 1.0 and variance to 1E6
=> Zero counts at step no.    553 at 2theta/TOF/E(KeV):       12.0424  Intensity fixed to 1.0 and variance to 1E6
=> Zero counts at step no.    555 at 2theta/TOF/E(KeV):       12.0498  Intensity fixed to 1.0 and variance to 1E6
=> Zero counts at step no.    559 at 2theta/TOF/E(KeV):       12.0646  Intensity fixed to 1.0 and variance to 1E6
=> Zero counts at step no.    568 at 2theta/TOF/E(KeV):       12.0979  Intensity fixed to 1.0 and variance to 1E6
=> Zero counts at step no.    570 at 2theta/TOF/E(KeV):       12.1053  Intensity fixed to 1.0 and variance to 1E6
=> Zero counts at step no.    576 at 2theta/TOF/E(KeV):       12.1275  Intensity fixed to 1.0 and variance to 1E6
=> Zero counts at step no.    579 at 2theta/TOF/E(KeV):       12.1386  Intensity fixed to 1.0 and variance to 1E6
=> Zero counts at step no.    580 at 2theta/TOF/E(KeV):       12.1423  Intensity fixed to 1.0 and variance to 1E6
=> Zero counts at step no.    582 at 2theta/TOF/E(KeV):       12.1497  Intensity fixed to 1.0 and variance to 1E6
=> Zero counts at step no.    586 at 2theta/TOF/E(KeV):       12.1645  Intensity fixed to 1.0 and variance to 1E6
=> Zero counts at step no.    588 at 2theta/TOF/E(KeV):       12.1719  Intensity fixed to 1.0 and variance to 1E6
=> Zero counts at step no.    591 at 2theta/TOF/E(KeV):       12.1830  Intensity fixed to 1.0 and variance to 1E6
=> Zero counts at step no.    592 at 2theta/TOF/E(KeV):       12.1867  Intensity fixed to 1.0 and variance to 1E6
=> Zero counts at step no.    594 at 2theta/TOF/E(KeV):       12.1941  Intensity fixed to 1.0 and variance to 1E6
=> Zero counts at step no.    597 at 2theta/TOF/E(KeV):       12.2052  Intensity fixed to 1.0 and variance to 1E6
=> Zero counts at step no.    599 at 2theta/TOF/E(KeV):       12.2126  Intensity fixed to 1.0 and variance to 1E6
```

```
=> Zero counts at step no.    601 at 2theta/TOF/E(KeV):      12.2200  Intensity fixed to 1.0 and variance to 1E6
=> Zero counts at step no.    606 at 2theta/TOF/E(KeV):      12.2385  Intensity fixed to 1.0 and variance to 1E6
=> Zero counts at step no.    607 at 2theta/TOF/E(KeV):      12.2422  Intensity fixed to 1.0 and variance to 1E6
=> Zero counts at step no.    608 at 2theta/TOF/E(KeV):      12.2459  Intensity fixed to 1.0 and variance to 1E6
=> Zero counts at step no.    610 at 2theta/TOF/E(KeV):      12.2533  Intensity fixed to 1.0 and variance to 1E6
=> Zero counts at step no.    614 at 2theta/TOF/E(KeV):      12.2681  Intensity fixed to 1.0 and variance to 1E6
=> Zero counts at step no.    618 at 2theta/TOF/E(KeV):      12.2829  Intensity fixed to 1.0 and variance to 1E6
=> Zero counts at step no.    619 at 2theta/TOF/E(KeV):      12.2866  Intensity fixed to 1.0 and variance to 1E6
=> Zero counts at step no.    623 at 2theta/TOF/E(KeV):      12.3014  Intensity fixed to 1.0 and variance to 1E6
=> Zero counts at step no.    624 at 2theta/TOF/E(KeV):      12.3051  Intensity fixed to 1.0 and variance to 1E6
=> Zero counts at step no.    627 at 2theta/TOF/E(KeV):      12.3162  Intensity fixed to 1.0 and variance to 1E6
=> Zero counts at step no.    633 at 2theta/TOF/E(KeV):      12.3384  Intensity fixed to 1.0 and variance to 1E6
=> Zero counts at step no.    636 at 2theta/TOF/E(KeV):      12.3495  Intensity fixed to 1.0 and variance to 1E6
=> Zero counts at step no.    642 at 2theta/TOF/E(KeV):      12.3717  Intensity fixed to 1.0 and variance to 1E6
=> Zero counts at step no.    643 at 2theta/TOF/E(KeV):      12.3754  Intensity fixed to 1.0 and variance to 1E6
=> Zero counts at step no.    644 at 2theta/TOF/E(KeV):      12.3791  Intensity fixed to 1.0 and variance to 1E6
=> Zero counts at step no.    645 at 2theta/TOF/E(KeV):      12.3828  Intensity fixed to 1.0 and variance to 1E6
=> Zero counts at step no.    646 at 2theta/TOF/E(KeV):      12.3865  Intensity fixed to 1.0 and variance to 1E6
=> Zero counts at step no.    648 at 2theta/TOF/E(KeV):      12.3939  Intensity fixed to 1.0 and variance to 1E6
=> Zero counts at step no.    650 at 2theta/TOF/E(KeV):      12.4013  Intensity fixed to 1.0 and variance to 1E6
=> Zero counts at step no.    652 at 2theta/TOF/E(KeV):      12.4087  Intensity fixed to 1.0 and variance to 1E6
=> Zero counts at step no.    656 at 2theta/TOF/E(KeV):      12.4235  Intensity fixed to 1.0 and variance to 1E6
=> Zero counts at step no.    662 at 2theta/TOF/E(KeV):      12.4457  Intensity fixed to 1.0 and variance to 1E6
=> Zero counts at step no.    663 at 2theta/TOF/E(KeV):      12.4494  Intensity fixed to 1.0 and variance to 1E6
=> Zero counts at step no.    932 at 2theta/TOF/E(KeV):      13.4447  Intensity fixed to 1.0 and variance to 1E6
=> Zero counts at step no.    934 at 2theta/TOF/E(KeV):      13.4521  Intensity fixed to 1.0 and variance to 1E6
=> Zero counts at step no.    935 at 2theta/TOF/E(KeV):      13.4558  Intensity fixed to 1.0 and variance to 1E6
=> Zero counts at step no.    944 at 2theta/TOF/E(KeV):      13.4891  Intensity fixed to 1.0 and variance to 1E6
=> Zero counts at step no.    945 at 2theta/TOF/E(KeV):      13.4928  Intensity fixed to 1.0 and variance to 1E6
=> Zero counts at step no.    947 at 2theta/TOF/E(KeV):      13.5002  Intensity fixed to 1.0 and variance to 1E6
=> Zero counts at step no.    949 at 2theta/TOF/E(KeV):      13.5076  Intensity fixed to 1.0 and variance to 1E6
=> Zero counts at step no.    951 at 2theta/TOF/E(KeV):      13.5150  Intensity fixed to 1.0 and variance to 1E6
=> Zero counts at step no.    952 at 2theta/TOF/E(KeV):      13.5187  Intensity fixed to 1.0 and variance to 1E6
=> Zero counts at step no.    953 at 2theta/TOF/E(KeV):      13.5224  Intensity fixed to 1.0 and variance to 1E6
=> Zero counts at step no.    957 at 2theta/TOF/E(KeV):      13.5372  Intensity fixed to 1.0 and variance to 1E6
=> Zero counts at step no.    959 at 2theta/TOF/E(KeV):      13.5446  Intensity fixed to 1.0 and variance to 1E6
=> Zero counts at step no.    961 at 2theta/TOF/E(KeV):      13.5520  Intensity fixed to 1.0 and variance to 1E6
=> Zero counts at step no.    962 at 2theta/TOF/E(KeV):      13.5557  Intensity fixed to 1.0 and variance to 1E6
=> Zero counts at step no.    965 at 2theta/TOF/E(KeV):      13.5668  Intensity fixed to 1.0 and variance to 1E6
=> Zero counts at step no.    968 at 2theta/TOF/E(KeV):      13.5779  Intensity fixed to 1.0 and variance to 1E6
=> Zero counts at step no.    969 at 2theta/TOF/E(KeV):      13.5816  Intensity fixed to 1.0 and variance to 1E6
=> Zero counts at step no.    971 at 2theta/TOF/E(KeV):      13.5890  Intensity fixed to 1.0 and variance to 1E6
=> Zero counts at step no.    972 at 2theta/TOF/E(KeV):      13.5927  Intensity fixed to 1.0 and variance to 1E6
=> Zero counts at step no.    977 at 2theta/TOF/E(KeV):      13.6112  Intensity fixed to 1.0 and variance to 1E6
=> Zero counts at step no.    978 at 2theta/TOF/E(KeV):      13.6149  Intensity fixed to 1.0 and variance to 1E6
=> Zero counts at step no.    980 at 2theta/TOF/E(KeV):      13.6223  Intensity fixed to 1.0 and variance to 1E6
=> Zero counts at step no.    981 at 2theta/TOF/E(KeV):      13.6260  Intensity fixed to 1.0 and variance to 1E6
=> Zero counts at step no.    984 at 2theta/TOF/E(KeV):      13.6371  Intensity fixed to 1.0 and variance to 1E6
=> Zero counts at step no.    988 at 2theta/TOF/E(KeV):      13.6519  Intensity fixed to 1.0 and variance to 1E6
=> Zero counts at step no.    989 at 2theta/TOF/E(KeV):      13.6556  Intensity fixed to 1.0 and variance to 1E6
=> Zero counts at step no.    992 at 2theta/TOF/E(KeV):      13.6667  Intensity fixed to 1.0 and variance to 1E6
=> Zero counts at step no.    995 at 2theta/TOF/E(KeV):      13.6778  Intensity fixed to 1.0 and variance to 1E6
=> Zero counts at step no.    997 at 2theta/TOF/E(KeV):      13.6852  Intensity fixed to 1.0 and variance to 1E6
=> Zero counts at step no.   1000 at 2theta/TOF/E(KeV):      13.6963  Intensity fixed to 1.0 and variance to 1E6
=> Zero counts at step no.   1003 at 2theta/TOF/E(KeV):      13.7074  Intensity fixed to 1.0 and variance to 1E6
=> Zero counts at step no.   1004 at 2theta/TOF/E(KeV):      13.7111  Intensity fixed to 1.0 and variance to 1E6
=> Zero counts at step no.   1006 at 2theta/TOF/E(KeV):      13.7185  Intensity fixed to 1.0 and variance to 1E6
=> Zero counts at step no.   1009 at 2theta/TOF/E(KeV):      13.7296  Intensity fixed to 1.0 and variance to 1E6
=> Zero counts at step no.   1010 at 2theta/TOF/E(KeV):      13.7333  Intensity fixed to 1.0 and variance to 1E6
=> Zero counts at step no.   1011 at 2theta/TOF/E(KeV):      13.7370  Intensity fixed to 1.0 and variance to 1E6
=> Zero counts at step no.   1015 at 2theta/TOF/E(KeV):      13.7518  Intensity fixed to 1.0 and variance to 1E6
=> Zero counts at step no.   1017 at 2theta/TOF/E(KeV):      13.7592  Intensity fixed to 1.0 and variance to 1E6
=> Zero counts at step no.   1018 at 2theta/TOF/E(KeV):      13.7629  Intensity fixed to 1.0 and variance to 1E6
=> Zero counts at step no.   1022 at 2theta/TOF/E(KeV):      13.7777  Intensity fixed to 1.0 and variance to 1E6
=> Zero counts at step no.   1025 at 2theta/TOF/E(KeV):      13.7888  Intensity fixed to 1.0 and variance to 1E6
=> Zero counts at step no.   1027 at 2theta/TOF/E(KeV):      13.7962  Intensity fixed to 1.0 and variance to 1E6
=> Zero counts at step no.   1034 at 2theta/TOF/E(KeV):      13.8221  Intensity fixed to 1.0 and variance to 1E6
=> Zero counts at step no.   1035 at 2theta/TOF/E(KeV):      13.8258  Intensity fixed to 1.0 and variance to 1E6
=> Zero counts at step no.   1036 at 2theta/TOF/E(KeV):      13.8295  Intensity fixed to 1.0 and variance to 1E6
=> Zero counts at step no.   1038 at 2theta/TOF/E(KeV):      13.8369  Intensity fixed to 1.0 and variance to 1E6
=> Zero counts at step no.   1040 at 2theta/TOF/E(KeV):      13.8443  Intensity fixed to 1.0 and variance to 1E6
=> Zero counts at step no.   1043 at 2theta/TOF/E(KeV):      13.8554  Intensity fixed to 1.0 and variance to 1E6
=> Zero counts at step no.   1052 at 2theta/TOF/E(KeV):      13.8887  Intensity fixed to 1.0 and variance to 1E6
=> Zero counts at step no.   1053 at 2theta/TOF/E(KeV):      13.8924  Intensity fixed to 1.0 and variance to 1E6
=> Zero counts at step no.   1059 at 2theta/TOF/E(KeV):      13.9146  Intensity fixed to 1.0 and variance to 1E6
=> Zero counts at step no.   1063 at 2theta/TOF/E(KeV):      13.9294  Intensity fixed to 1.0 and variance to 1E6
=> Zero counts at step no.   1066 at 2theta/TOF/E(KeV):      13.9405  Intensity fixed to 1.0 and variance to 1E6
=> Zero counts at step no.   1067 at 2theta/TOF/E(KeV):      13.9442  Intensity fixed to 1.0 and variance to 1E6
=> Zero counts at step no.   1070 at 2theta/TOF/E(KeV):      13.9553  Intensity fixed to 1.0 and variance to 1E6
=> Zero counts at step no.   1071 at 2theta/TOF/E(KeV):      13.9590  Intensity fixed to 1.0 and variance to 1E6
=> Zero counts at step no.   1072 at 2theta/TOF/E(KeV):      13.9627  Intensity fixed to 1.0 and variance to 1E6
=> Zero counts at step no.   1075 at 2theta/TOF/E(KeV):      13.9738  Intensity fixed to 1.0 and variance to 1E6
=> Zero counts at step no.   1080 at 2theta/TOF/E(KeV):      13.9923  Intensity fixed to 1.0 and variance to 1E6
=> Zero counts at step no.   1081 at 2theta/TOF/E(KeV):      13.9960  Intensity fixed to 1.0 and variance to 1E6
=> Zero counts at step no.   1082 at 2theta/TOF/E(KeV):      13.9997  Intensity fixed to 1.0 and variance to 1E6
=> Zero counts at step no.   1089 at 2theta/TOF/E(KeV):      14.0256  Intensity fixed to 1.0 and variance to 1E6
=> Zero counts at step no.   1090 at 2theta/TOF/E(KeV):      14.0293  Intensity fixed to 1.0 and variance to 1E6
=> Zero counts at step no.   1091 at 2theta/TOF/E(KeV):      14.0330  Intensity fixed to 1.0 and variance to 1E6
=> Zero counts at step no.   1092 at 2theta/TOF/E(KeV):      14.0367  Intensity fixed to 1.0 and variance to 1E6
=> Zero counts at step no.   1093 at 2theta/TOF/E(KeV):      14.0404  Intensity fixed to 1.0 and variance to 1E6
```

```
=> Zero counts at step no.   1096 at 2theta/TOF/E(KeV):       14.0515  Intensity fixed to 1.0 and variance to 1E6
=> Zero counts at step no.   1098 at 2theta/TOF/E(KeV):       14.0589  Intensity fixed to 1.0 and variance to 1E6
=> Zero counts at step no.   1104 at 2theta/TOF/E(KeV):       14.0811  Intensity fixed to 1.0 and variance to 1E6
=> Zero counts at step no.   1108 at 2theta/TOF/E(KeV):       14.0959  Intensity fixed to 1.0 and variance to 1E6
=> Zero counts at step no.   1109 at 2theta/TOF/E(KeV):       14.0996  Intensity fixed to 1.0 and variance to 1E6
=> Zero counts at step no.   1111 at 2theta/TOF/E(KeV):       14.1070  Intensity fixed to 1.0 and variance to 1E6
=> Zero counts at step no.   1116 at 2theta/TOF/E(KeV):       14.1255  Intensity fixed to 1.0 and variance to 1E6
=> Zero counts at step no.   1117 at 2theta/TOF/E(KeV):       14.1292  Intensity fixed to 1.0 and variance to 1E6
=> Zero counts at step no.   1120 at 2theta/TOF/E(KeV):       14.1403  Intensity fixed to 1.0 and variance to 1E6
=> Zero counts at step no.   1122 at 2theta/TOF/E(KeV):       14.1477  Intensity fixed to 1.0 and variance to 1E6
=> Zero counts at step no.   1123 at 2theta/TOF/E(KeV):       14.1514  Intensity fixed to 1.0 and variance to 1E6
=> Zero counts at step no.   1124 at 2theta/TOF/E(KeV):       14.1551  Intensity fixed to 1.0 and variance to 1E6
=> Zero counts at step no.   1126 at 2theta/TOF/E(KeV):       14.1625  Intensity fixed to 1.0 and variance to 1E6
=> Zero counts at step no.   1127 at 2theta/TOF/E(KeV):       14.1662  Intensity fixed to 1.0 and variance to 1E6
=> Zero counts at step no.   1130 at 2theta/TOF/E(KeV):       14.1773  Intensity fixed to 1.0 and variance to 1E6
=> Zero counts at step no.   1132 at 2theta/TOF/E(KeV):       14.1847  Intensity fixed to 1.0 and variance to 1E6
=> Zero counts at step no.   1134 at 2theta/TOF/E(KeV):       14.1921  Intensity fixed to 1.0 and variance to 1E6
=> Zero counts at step no.   1135 at 2theta/TOF/E(KeV):       14.1958  Intensity fixed to 1.0 and variance to 1E6
=> Zero counts at step no.   1137 at 2theta/TOF/E(KeV):       14.2032  Intensity fixed to 1.0 and variance to 1E6
=> Zero counts at step no.   1138 at 2theta/TOF/E(KeV):       14.2069  Intensity fixed to 1.0 and variance to 1E6
=> Zero counts at step no.   1145 at 2theta/TOF/E(KeV):       14.2328  Intensity fixed to 1.0 and variance to 1E6
=> Zero counts at step no.   1146 at 2theta/TOF/E(KeV):       14.2365  Intensity fixed to 1.0 and variance to 1E6
=> Zero counts at step no.   1147 at 2theta/TOF/E(KeV):       14.2402  Intensity fixed to 1.0 and variance to 1E6
=> Zero counts at step no.   1153 at 2theta/TOF/E(KeV):       14.2624  Intensity fixed to 1.0 and variance to 1E6
=> Zero counts at step no.   1164 at 2theta/TOF/E(KeV):       14.3031  Intensity fixed to 1.0 and variance to 1E6
=> Zero counts at step no.   1166 at 2theta/TOF/E(KeV):       14.3105  Intensity fixed to 1.0 and variance to 1E6
=> Zero counts at step no.   1167 at 2theta/TOF/E(KeV):       14.3142  Intensity fixed to 1.0 and variance to 1E6
=> Zero counts at step no.   1173 at 2theta/TOF/E(KeV):       14.3364  Intensity fixed to 1.0 and variance to 1E6
=> Zero counts at step no.   1174 at 2theta/TOF/E(KeV):       14.3401  Intensity fixed to 1.0 and variance to 1E6
=> Zero counts at step no.   1183 at 2theta/TOF/E(KeV):       14.3734  Intensity fixed to 1.0 and variance to 1E6
=> Zero counts at step no.   1186 at 2theta/TOF/E(KeV):       14.3845  Intensity fixed to 1.0 and variance to 1E6
=> Zero counts at step no.   1187 at 2theta/TOF/E(KeV):       14.3882  Intensity fixed to 1.0 and variance to 1E6
=> Zero counts at step no.   1191 at 2theta/TOF/E(KeV):       14.4030  Intensity fixed to 1.0 and variance to 1E6
=> Zero counts at step no.   1192 at 2theta/TOF/E(KeV):       14.4067  Intensity fixed to 1.0 and variance to 1E6
=> Zero counts at step no.   1193 at 2theta/TOF/E(KeV):       14.4104  Intensity fixed to 1.0 and variance to 1E6
=> Zero counts at step no.   1195 at 2theta/TOF/E(KeV):       14.4178  Intensity fixed to 1.0 and variance to 1E6
=> Zero counts at step no.   1201 at 2theta/TOF/E(KeV):       14.4400  Intensity fixed to 1.0 and variance to 1E6
=> Zero counts at step no.   1202 at 2theta/TOF/E(KeV):       14.4437  Intensity fixed to 1.0 and variance to 1E6
=> Zero counts at step no.   1204 at 2theta/TOF/E(KeV):       14.4511  Intensity fixed to 1.0 and variance to 1E6
=> Zero counts at step no.   1210 at 2theta/TOF/E(KeV):       14.4733  Intensity fixed to 1.0 and variance to 1E6
=> Zero counts at step no.   1213 at 2theta/TOF/E(KeV):       14.4844  Intensity fixed to 1.0 and variance to 1E6
=> Zero counts at step no.   1219 at 2theta/TOF/E(KeV):       14.5066  Intensity fixed to 1.0 and variance to 1E6
=> Zero counts at step no.   1220 at 2theta/TOF/E(KeV):       14.5103  Intensity fixed to 1.0 and variance to 1E6
=> Zero counts at step no.   1221 at 2theta/TOF/E(KeV):       14.5140  Intensity fixed to 1.0 and variance to 1E6
=> Zero counts at step no.   1222 at 2theta/TOF/E(KeV):       14.5177  Intensity fixed to 1.0 and variance to 1E6
=> Zero counts at step no.   1224 at 2theta/TOF/E(KeV):       14.5251  Intensity fixed to 1.0 and variance to 1E6
=> Zero counts at step no.   1228 at 2theta/TOF/E(KeV):       14.5399  Intensity fixed to 1.0 and variance to 1E6
=> Zero counts at step no.   1231 at 2theta/TOF/E(KeV):       14.5510  Intensity fixed to 1.0 and variance to 1E6
=> Zero counts at step no.   1235 at 2theta/TOF/E(KeV):       14.5658  Intensity fixed to 1.0 and variance to 1E6
=> Zero counts at step no.   1236 at 2theta/TOF/E(KeV):       14.5695  Intensity fixed to 1.0 and variance to 1E6
=> Zero counts at step no.   1237 at 2theta/TOF/E(KeV):       14.5732  Intensity fixed to 1.0 and variance to 1E6
=> Zero counts at step no.   1239 at 2theta/TOF/E(KeV):       14.5806  Intensity fixed to 1.0 and variance to 1E6
=> Zero counts at step no.   1241 at 2theta/TOF/E(KeV):       14.5880  Intensity fixed to 1.0 and variance to 1E6
=> Zero counts at step no.   1243 at 2theta/TOF/E(KeV):       14.5954  Intensity fixed to 1.0 and variance to 1E6
=> Zero counts at step no.   1245 at 2theta/TOF/E(KeV):       14.6028  Intensity fixed to 1.0 and variance to 1E6
=> Zero counts at step no.   1248 at 2theta/TOF/E(KeV):       14.6139  Intensity fixed to 1.0 and variance to 1E6
=> Zero counts at step no.   1251 at 2theta/TOF/E(KeV):       14.6250  Intensity fixed to 1.0 and variance to 1E6
=> Zero counts at step no.   1259 at 2theta/TOF/E(KeV):       14.6546  Intensity fixed to 1.0 and variance to 1E6
=> Zero counts at step no.   1264 at 2theta/TOF/E(KeV):       14.6731  Intensity fixed to 1.0 and variance to 1E6
=> Zero counts at step no.   1266 at 2theta/TOF/E(KeV):       14.6805  Intensity fixed to 1.0 and variance to 1E6
=> Zero counts at step no.   1267 at 2theta/TOF/E(KeV):       14.6842  Intensity fixed to 1.0 and variance to 1E6
=> Zero counts at step no.   1271 at 2theta/TOF/E(KeV):       14.6990  Intensity fixed to 1.0 and variance to 1E6
=> Zero counts at step no.   1275 at 2theta/TOF/E(KeV):       14.7138  Intensity fixed to 1.0 and variance to 1E6
=> Zero counts at step no.   1276 at 2theta/TOF/E(KeV):       14.7175  Intensity fixed to 1.0 and variance to 1E6
=> Zero counts at step no.   1277 at 2theta/TOF/E(KeV):       14.7212  Intensity fixed to 1.0 and variance to 1E6
=> Zero counts at step no.   1278 at 2theta/TOF/E(KeV):       14.7249  Intensity fixed to 1.0 and variance to 1E6
=> Zero counts at step no.   1281 at 2theta/TOF/E(KeV):       14.7360  Intensity fixed to 1.0 and variance to 1E6
=> Zero counts at step no.   1282 at 2theta/TOF/E(KeV):       14.7397  Intensity fixed to 1.0 and variance to 1E6
=> Zero counts at step no.   1284 at 2theta/TOF/E(KeV):       14.7471  Intensity fixed to 1.0 and variance to 1E6
=> Zero counts at step no.   1285 at 2theta/TOF/E(KeV):       14.7508  Intensity fixed to 1.0 and variance to 1E6
=> Zero counts at step no.   1286 at 2theta/TOF/E(KeV):       14.7545  Intensity fixed to 1.0 and variance to 1E6
=> Zero counts at step no.   1287 at 2theta/TOF/E(KeV):       14.7582  Intensity fixed to 1.0 and variance to 1E6
=> Zero counts at step no.   1293 at 2theta/TOF/E(KeV):       14.7804  Intensity fixed to 1.0 and variance to 1E6
=> Zero counts at step no.   1298 at 2theta/TOF/E(KeV):       14.7989  Intensity fixed to 1.0 and variance to 1E6
=> Zero counts at step no.   1300 at 2theta/TOF/E(KeV):       14.8063  Intensity fixed to 1.0 and variance to 1E6
=> Zero counts at step no.   1304 at 2theta/TOF/E(KeV):       14.8211  Intensity fixed to 1.0 and variance to 1E6
=> Zero counts at step no.   1305 at 2theta/TOF/E(KeV):       14.8248  Intensity fixed to 1.0 and variance to 1E6
=> Zero counts at step no.   1306 at 2theta/TOF/E(KeV):       14.8285  Intensity fixed to 1.0 and variance to 1E6
=> Zero counts at step no.   1308 at 2theta/TOF/E(KeV):       14.8359  Intensity fixed to 1.0 and variance to 1E6
=> Zero counts at step no.   1309 at 2theta/TOF/E(KeV):       14.8396  Intensity fixed to 1.0 and variance to 1E6
=> Zero counts at step no.   1312 at 2theta/TOF/E(KeV):       14.8507  Intensity fixed to 1.0 and variance to 1E6
=> Zero counts at step no.   1313 at 2theta/TOF/E(KeV):       14.8544  Intensity fixed to 1.0 and variance to 1E6
=> Zero counts at step no.   1318 at 2theta/TOF/E(KeV):       14.8729  Intensity fixed to 1.0 and variance to 1E6
=> Zero counts at step no.   1319 at 2theta/TOF/E(KeV):       14.8766  Intensity fixed to 1.0 and variance to 1E6
=> Zero counts at step no.   1320 at 2theta/TOF/E(KeV):       14.8803  Intensity fixed to 1.0 and variance to 1E6
=> Zero counts at step no.   1321 at 2theta/TOF/E(KeV):       14.8840  Intensity fixed to 1.0 and variance to 1E6
=> Zero counts at step no.   1323 at 2theta/TOF/E(KeV):       14.8914  Intensity fixed to 1.0 and variance to 1E6
=> Zero counts at step no.   1324 at 2theta/TOF/E(KeV):       14.8951  Intensity fixed to 1.0 and variance to 1E6
=> Zero counts at step no.   1325 at 2theta/TOF/E(KeV):       14.8988  Intensity fixed to 1.0 and variance to 1E6
=> Zero counts at step no.   1326 at 2theta/TOF/E(KeV):       14.9025  Intensity fixed to 1.0 and variance to 1E6
```

```
=> Zero counts at step no.   1327 at 2theta/TOF/E(KeV):      14.9062  Intensity fixed to 1.0 and variance to 1E6
=> Zero counts at step no.   1332 at 2theta/TOF/E(KeV):      14.9247  Intensity fixed to 1.0 and variance to 1E6
=> Zero counts at step no.   1333 at 2theta/TOF/E(KeV):      14.9284  Intensity fixed to 1.0 and variance to 1E6
=> Zero counts at step no.   1335 at 2theta/TOF/E(KeV):      14.9358  Intensity fixed to 1.0 and variance to 1E6
=> Zero counts at step no.   1492 at 2theta/TOF/E(KeV):      15.5167  Intensity fixed to 1.0 and variance to 1E6
=> Zero counts at step no.   1505 at 2theta/TOF/E(KeV):      15.5648  Intensity fixed to 1.0 and variance to 1E6
=> Zero counts at step no.   1507 at 2theta/TOF/E(KeV):      15.5722  Intensity fixed to 1.0 and variance to 1E6
=> Zero counts at step no.   1508 at 2theta/TOF/E(KeV):      15.5759  Intensity fixed to 1.0 and variance to 1E6
=> Zero counts at step no.   1510 at 2theta/TOF/E(KeV):      15.5833  Intensity fixed to 1.0 and variance to 1E6
=> Zero counts at step no.   1516 at 2theta/TOF/E(KeV):      15.6055  Intensity fixed to 1.0 and variance to 1E6
=> Zero counts at step no.   1517 at 2theta/TOF/E(KeV):      15.6092  Intensity fixed to 1.0 and variance to 1E6
=> Zero counts at step no.   1518 at 2theta/TOF/E(KeV):      15.6129  Intensity fixed to 1.0 and variance to 1E6
=> Zero counts at step no.   1519 at 2theta/TOF/E(KeV):      15.6166  Intensity fixed to 1.0 and variance to 1E6
=> Zero counts at step no.   1520 at 2theta/TOF/E(KeV):      15.6203  Intensity fixed to 1.0 and variance to 1E6
=> Zero counts at step no.   1523 at 2theta/TOF/E(KeV):      15.6314  Intensity fixed to 1.0 and variance to 1E6
=> Zero counts at step no.   1525 at 2theta/TOF/E(KeV):      15.6388  Intensity fixed to 1.0 and variance to 1E6
=> Zero counts at step no.   1526 at 2theta/TOF/E(KeV):      15.6425  Intensity fixed to 1.0 and variance to 1E6
=> Zero counts at step no.   1529 at 2theta/TOF/E(KeV):      15.6536  Intensity fixed to 1.0 and variance to 1E6
=> Zero counts at step no.   1530 at 2theta/TOF/E(KeV):      15.6573  Intensity fixed to 1.0 and variance to 1E6
=> Zero counts at step no.   1537 at 2theta/TOF/E(KeV):      15.6832  Intensity fixed to 1.0 and variance to 1E6
=> Zero counts at step no.   1541 at 2theta/TOF/E(KeV):      15.6980  Intensity fixed to 1.0 and variance to 1E6
=> Zero counts at step no.   1544 at 2theta/TOF/E(KeV):      15.7091  Intensity fixed to 1.0 and variance to 1E6
=> Zero counts at step no.   1545 at 2theta/TOF/E(KeV):      15.7128  Intensity fixed to 1.0 and variance to 1E6
=> Zero counts at step no.   1547 at 2theta/TOF/E(KeV):      15.7202  Intensity fixed to 1.0 and variance to 1E6
=> Zero counts at step no.   1550 at 2theta/TOF/E(KeV):      15.7313  Intensity fixed to 1.0 and variance to 1E6
=> Zero counts at step no.   1552 at 2theta/TOF/E(KeV):      15.7387  Intensity fixed to 1.0 and variance to 1E6
=> Zero counts at step no.   1554 at 2theta/TOF/E(KeV):      15.7461  Intensity fixed to 1.0 and variance to 1E6
=> Zero counts at step no.   1556 at 2theta/TOF/E(KeV):      15.7535  Intensity fixed to 1.0 and variance to 1E6
=> Zero counts at step no.   1559 at 2theta/TOF/E(KeV):      15.7646  Intensity fixed to 1.0 and variance to 1E6
=> Zero counts at step no.   1564 at 2theta/TOF/E(KeV):      15.7831  Intensity fixed to 1.0 and variance to 1E6
=> Zero counts at step no.   1565 at 2theta/TOF/E(KeV):      15.7868  Intensity fixed to 1.0 and variance to 1E6
=> Zero counts at step no.   1574 at 2theta/TOF/E(KeV):      15.8201  Intensity fixed to 1.0 and variance to 1E6
=> Zero counts at step no.   1586 at 2theta/TOF/E(KeV):      15.8645  Intensity fixed to 1.0 and variance to 1E6
=> Zero counts at step no.   1589 at 2theta/TOF/E(KeV):      15.8756  Intensity fixed to 1.0 and variance to 1E6
=> Zero counts at step no.   1631 at 2theta/TOF/E(KeV):      16.0310  Intensity fixed to 1.0 and variance to 1E6
=> Zero counts at step no.   1777 at 2theta/TOF/E(KeV):      16.5712  Intensity fixed to 1.0 and variance to 1E6
=> Zero counts at step no.   1798 at 2theta/TOF/E(KeV):      16.6489  Intensity fixed to 1.0 and variance to 1E6
=> Zero counts at step no.   1805 at 2theta/TOF/E(KeV):      16.6748  Intensity fixed to 1.0 and variance to 1E6
=> Zero counts at step no.   1807 at 2theta/TOF/E(KeV):      16.6822  Intensity fixed to 1.0 and variance to 1E6
=> Zero counts at step no.   1813 at 2theta/TOF/E(KeV):      16.7044  Intensity fixed to 1.0 and variance to 1E6
=> Zero counts at step no.   1814 at 2theta/TOF/E(KeV):      16.7081  Intensity fixed to 1.0 and variance to 1E6
=> Zero counts at step no.   1816 at 2theta/TOF/E(KeV):      16.7155  Intensity fixed to 1.0 and variance to 1E6
=> Zero counts at step no.   1817 at 2theta/TOF/E(KeV):      16.7192  Intensity fixed to 1.0 and variance to 1E6
=> Zero counts at step no.   1823 at 2theta/TOF/E(KeV):      16.7414  Intensity fixed to 1.0 and variance to 1E6
=> Zero counts at step no.   1825 at 2theta/TOF/E(KeV):      16.7488  Intensity fixed to 1.0 and variance to 1E6
=> Zero counts at step no.   1828 at 2theta/TOF/E(KeV):      16.7599  Intensity fixed to 1.0 and variance to 1E6
=> Zero counts at step no.   1829 at 2theta/TOF/E(KeV):      16.7636  Intensity fixed to 1.0 and variance to 1E6
=> Zero counts at step no.   1830 at 2theta/TOF/E(KeV):      16.7673  Intensity fixed to 1.0 and variance to 1E6
=> Zero counts at step no.   1831 at 2theta/TOF/E(KeV):      16.7710  Intensity fixed to 1.0 and variance to 1E6
=> Zero counts at step no.   1832 at 2theta/TOF/E(KeV):      16.7747  Intensity fixed to 1.0 and variance to 1E6
=> Zero counts at step no.   1834 at 2theta/TOF/E(KeV):      16.7821  Intensity fixed to 1.0 and variance to 1E6
=> Zero counts at step no.   1836 at 2theta/TOF/E(KeV):      16.7895  Intensity fixed to 1.0 and variance to 1E6
=> Zero counts at step no.   1837 at 2theta/TOF/E(KeV):      16.7932  Intensity fixed to 1.0 and variance to 1E6
=> Zero counts at step no.   1840 at 2theta/TOF/E(KeV):      16.8043  Intensity fixed to 1.0 and variance to 1E6
=> Zero counts at step no.   1841 at 2theta/TOF/E(KeV):      16.8080  Intensity fixed to 1.0 and variance to 1E6
=> Zero counts at step no.   1843 at 2theta/TOF/E(KeV):      16.8154  Intensity fixed to 1.0 and variance to 1E6
=> Zero counts at step no.   1846 at 2theta/TOF/E(KeV):      16.8265  Intensity fixed to 1.0 and variance to 1E6
=> Zero counts at step no.   1848 at 2theta/TOF/E(KeV):      16.8339  Intensity fixed to 1.0 and variance to 1E6
=> Zero counts at step no.   1849 at 2theta/TOF/E(KeV):      16.8376  Intensity fixed to 1.0 and variance to 1E6
=> Zero counts at step no.   1850 at 2theta/TOF/E(KeV):      16.8413  Intensity fixed to 1.0 and variance to 1E6
=> Zero counts at step no.   1852 at 2theta/TOF/E(KeV):      16.8487  Intensity fixed to 1.0 and variance to 1E6
=> Zero counts at step no.   1853 at 2theta/TOF/E(KeV):      16.8524  Intensity fixed to 1.0 and variance to 1E6
=> Zero counts at step no.   1855 at 2theta/TOF/E(KeV):      16.8598  Intensity fixed to 1.0 and variance to 1E6
=> Zero counts at step no.   1858 at 2theta/TOF/E(KeV):      16.8709  Intensity fixed to 1.0 and variance to 1E6
=> Zero counts at step no.   1860 at 2theta/TOF/E(KeV):      16.8783  Intensity fixed to 1.0 and variance to 1E6
=> Zero counts at step no.   1861 at 2theta/TOF/E(KeV):      16.8820  Intensity fixed to 1.0 and variance to 1E6
=> Zero counts at step no.   1863 at 2theta/TOF/E(KeV):      16.8894  Intensity fixed to 1.0 and variance to 1E6
=> Zero counts at step no.   1864 at 2theta/TOF/E(KeV):      16.8931  Intensity fixed to 1.0 and variance to 1E6
=> Zero counts at step no.   1865 at 2theta/TOF/E(KeV):      16.8968  Intensity fixed to 1.0 and variance to 1E6
=> Zero counts at step no.   1868 at 2theta/TOF/E(KeV):      16.9079  Intensity fixed to 1.0 and variance to 1E6
=> Zero counts at step no.   1870 at 2theta/TOF/E(KeV):      16.9153  Intensity fixed to 1.0 and variance to 1E6
=> Zero counts at step no.   1873 at 2theta/TOF/E(KeV):      16.9264  Intensity fixed to 1.0 and variance to 1E6
=> Zero counts at step no.   1881 at 2theta/TOF/E(KeV):      16.9560  Intensity fixed to 1.0 and variance to 1E6
=> Zero counts at step no.   2138 at 2theta/TOF/E(KeV):      17.9069  Intensity fixed to 1.0 and variance to 1E6
=> Zero counts at step no.   2139 at 2theta/TOF/E(KeV):      17.9106  Intensity fixed to 1.0 and variance to 1E6
=> Zero counts at step no.   2143 at 2theta/TOF/E(KeV):      17.9254  Intensity fixed to 1.0 and variance to 1E6
=> Zero counts at step no.   2145 at 2theta/TOF/E(KeV):      17.9328  Intensity fixed to 1.0 and variance to 1E6
=> Zero counts at step no.   2146 at 2theta/TOF/E(KeV):      17.9365  Intensity fixed to 1.0 and variance to 1E6
=> Zero counts at step no.   2147 at 2theta/TOF/E(KeV):      17.9402  Intensity fixed to 1.0 and variance to 1E6
=> Zero counts at step no.   2148 at 2theta/TOF/E(KeV):      17.9439  Intensity fixed to 1.0 and variance to 1E6
=> Zero counts at step no.   2151 at 2theta/TOF/E(KeV):      17.9550  Intensity fixed to 1.0 and variance to 1E6
=> Zero counts at step no.   2157 at 2theta/TOF/E(KeV):      17.9772  Intensity fixed to 1.0 and variance to 1E6
=> Zero counts at step no.   2158 at 2theta/TOF/E(KeV):      17.9809  Intensity fixed to 1.0 and variance to 1E6
=> Zero counts at step no.   2159 at 2theta/TOF/E(KeV):      17.9846  Intensity fixed to 1.0 and variance to 1E6
=> Zero counts at step no.   2160 at 2theta/TOF/E(KeV):      17.9883  Intensity fixed to 1.0 and variance to 1E6
=> Zero counts at step no.   2161 at 2theta/TOF/E(KeV):      17.9920  Intensity fixed to 1.0 and variance to 1E6
=> Zero counts at step no.   2162 at 2theta/TOF/E(KeV):      17.9957  Intensity fixed to 1.0 and variance to 1E6
=> Zero counts at step no.   2163 at 2theta/TOF/E(KeV):      17.9994  Intensity fixed to 1.0 and variance to 1E6
=> Zero counts at step no.   2165 at 2theta/TOF/E(KeV):      18.0068  Intensity fixed to 1.0 and variance to 1E6
=> Zero counts at step no.   2167 at 2theta/TOF/E(KeV):      18.0142  Intensity fixed to 1.0 and variance to 1E6
```

```
=> Zero counts at step no.   2168 at 2theta/TOF/E(KeV):       18.0179  Intensity fixed to 1.0 and variance to 1E6
=> Zero counts at step no.   2169 at 2theta/TOF/E(KeV):       18.0216  Intensity fixed to 1.0 and variance to 1E6
=> Zero counts at step no.   2171 at 2theta/TOF/E(KeV):       18.0290  Intensity fixed to 1.0 and variance to 1E6
=> Zero counts at step no.   2172 at 2theta/TOF/E(KeV):       18.0327  Intensity fixed to 1.0 and variance to 1E6
=> Zero counts at step no.   2173 at 2theta/TOF/E(KeV):       18.0364  Intensity fixed to 1.0 and variance to 1E6
=> Zero counts at step no.   2174 at 2theta/TOF/E(KeV):       18.0401  Intensity fixed to 1.0 and variance to 1E6
=> Zero counts at step no.   2175 at 2theta/TOF/E(KeV):       18.0438  Intensity fixed to 1.0 and variance to 1E6
=> Zero counts at step no.   2176 at 2theta/TOF/E(KeV):       18.0475  Intensity fixed to 1.0 and variance to 1E6
=> Zero counts at step no.   2177 at 2theta/TOF/E(KeV):       18.0512  Intensity fixed to 1.0 and variance to 1E6
=> Zero counts at step no.   2178 at 2theta/TOF/E(KeV):       18.0549  Intensity fixed to 1.0 and variance to 1E6
=> Zero counts at step no.   2180 at 2theta/TOF/E(KeV):       18.0623  Intensity fixed to 1.0 and variance to 1E6
=> Zero counts at step no.   2181 at 2theta/TOF/E(KeV):       18.0660  Intensity fixed to 1.0 and variance to 1E6
=> Zero counts at step no.   2182 at 2theta/TOF/E(KeV):       18.0697  Intensity fixed to 1.0 and variance to 1E6
=> Zero counts at step no.   2183 at 2theta/TOF/E(KeV):       18.0734  Intensity fixed to 1.0 and variance to 1E6
=> Zero counts at step no.   2184 at 2theta/TOF/E(KeV):       18.0771  Intensity fixed to 1.0 and variance to 1E6
=> Zero counts at step no.   2185 at 2theta/TOF/E(KeV):       18.0808  Intensity fixed to 1.0 and variance to 1E6
=> Zero counts at step no.   2186 at 2theta/TOF/E(KeV):       18.0845  Intensity fixed to 1.0 and variance to 1E6
=> Zero counts at step no.   2187 at 2theta/TOF/E(KeV):       18.0882  Intensity fixed to 1.0 and variance to 1E6
=> Zero counts at step no.   2188 at 2theta/TOF/E(KeV):       18.0919  Intensity fixed to 1.0 and variance to 1E6
=> Zero counts at step no.   2189 at 2theta/TOF/E(KeV):       18.0956  Intensity fixed to 1.0 and variance to 1E6
=> Zero counts at step no.   2190 at 2theta/TOF/E(KeV):       18.0993  Intensity fixed to 1.0 and variance to 1E6
=> Zero counts at step no.   2191 at 2theta/TOF/E(KeV):       18.1030  Intensity fixed to 1.0 and variance to 1E6
=> Zero counts at step no.   2192 at 2theta/TOF/E(KeV):       18.1067  Intensity fixed to 1.0 and variance to 1E6
=> Zero counts at step no.   2194 at 2theta/TOF/E(KeV):       18.1141  Intensity fixed to 1.0 and variance to 1E6
=> Zero counts at step no.   2195 at 2theta/TOF/E(KeV):       18.1178  Intensity fixed to 1.0 and variance to 1E6
=> Zero counts at step no.   2196 at 2theta/TOF/E(KeV):       18.1215  Intensity fixed to 1.0 and variance to 1E6
=> Zero counts at step no.   2197 at 2theta/TOF/E(KeV):       18.1252  Intensity fixed to 1.0 and variance to 1E6
=> Zero counts at step no.   2198 at 2theta/TOF/E(KeV):       18.1289  Intensity fixed to 1.0 and variance to 1E6
=> Zero counts at step no.   2199 at 2theta/TOF/E(KeV):       18.1326  Intensity fixed to 1.0 and variance to 1E6
=> Zero counts at step no.   2201 at 2theta/TOF/E(KeV):       18.1400  Intensity fixed to 1.0 and variance to 1E6
=> Zero counts at step no.   2202 at 2theta/TOF/E(KeV):       18.1437  Intensity fixed to 1.0 and variance to 1E6
=> Zero counts at step no.   2203 at 2theta/TOF/E(KeV):       18.1474  Intensity fixed to 1.0 and variance to 1E6
=> Zero counts at step no.   2204 at 2theta/TOF/E(KeV):       18.1511  Intensity fixed to 1.0 and variance to 1E6
=> Zero counts at step no.   2205 at 2theta/TOF/E(KeV):       18.1548  Intensity fixed to 1.0 and variance to 1E6
=> Zero counts at step no.   2206 at 2theta/TOF/E(KeV):       18.1585  Intensity fixed to 1.0 and variance to 1E6
=> Zero counts at step no.   2207 at 2theta/TOF/E(KeV):       18.1622  Intensity fixed to 1.0 and variance to 1E6
=> Zero counts at step no.   2208 at 2theta/TOF/E(KeV):       18.1659  Intensity fixed to 1.0 and variance to 1E6
=> Zero counts at step no.   2209 at 2theta/TOF/E(KeV):       18.1696  Intensity fixed to 1.0 and variance to 1E6
=> Zero counts at step no.   2210 at 2theta/TOF/E(KeV):       18.1733  Intensity fixed to 1.0 and variance to 1E6
=> Zero counts at step no.   2212 at 2theta/TOF/E(KeV):       18.1807  Intensity fixed to 1.0 and variance to 1E6
=> Zero counts at step no.   2213 at 2theta/TOF/E(KeV):       18.1844  Intensity fixed to 1.0 and variance to 1E6
=> Zero counts at step no.   2214 at 2theta/TOF/E(KeV):       18.1881  Intensity fixed to 1.0 and variance to 1E6
=> Zero counts at step no.   2215 at 2theta/TOF/E(KeV):       18.1918  Intensity fixed to 1.0 and variance to 1E6
=> Zero counts at step no.   2216 at 2theta/TOF/E(KeV):       18.1955  Intensity fixed to 1.0 and variance to 1E6
=> Zero counts at step no.   2217 at 2theta/TOF/E(KeV):       18.1992  Intensity fixed to 1.0 and variance to 1E6
=> Zero counts at step no.   2219 at 2theta/TOF/E(KeV):       18.2066  Intensity fixed to 1.0 and variance to 1E6
=> Zero counts at step no.   2222 at 2theta/TOF/E(KeV):       18.2177  Intensity fixed to 1.0 and variance to 1E6
=> Zero counts at step no.   2223 at 2theta/TOF/E(KeV):       18.2214  Intensity fixed to 1.0 and variance to 1E6
=> Zero counts at step no.   2224 at 2theta/TOF/E(KeV):       18.2251  Intensity fixed to 1.0 and variance to 1E6
=> Zero counts at step no.   2225 at 2theta/TOF/E(KeV):       18.2288  Intensity fixed to 1.0 and variance to 1E6
=> Zero counts at step no.   2226 at 2theta/TOF/E(KeV):       18.2325  Intensity fixed to 1.0 and variance to 1E6
=> Zero counts at step no.   2227 at 2theta/TOF/E(KeV):       18.2362  Intensity fixed to 1.0 and variance to 1E6
=> Zero counts at step no.   2228 at 2theta/TOF/E(KeV):       18.2399  Intensity fixed to 1.0 and variance to 1E6
=> Zero counts at step no.   2229 at 2theta/TOF/E(KeV):       18.2436  Intensity fixed to 1.0 and variance to 1E6
=> Zero counts at step no.   2230 at 2theta/TOF/E(KeV):       18.2473  Intensity fixed to 1.0 and variance to 1E6
=> Zero counts at step no.   2231 at 2theta/TOF/E(KeV):       18.2510  Intensity fixed to 1.0 and variance to 1E6
=> Zero counts at step no.   2232 at 2theta/TOF/E(KeV):       18.2547  Intensity fixed to 1.0 and variance to 1E6
=> Zero counts at step no.   2234 at 2theta/TOF/E(KeV):       18.2621  Intensity fixed to 1.0 and variance to 1E6
=> Zero counts at step no.   2235 at 2theta/TOF/E(KeV):       18.2658  Intensity fixed to 1.0 and variance to 1E6
=> Zero counts at step no.   2236 at 2theta/TOF/E(KeV):       18.2695  Intensity fixed to 1.0 and variance to 1E6
=> Zero counts at step no.   2237 at 2theta/TOF/E(KeV):       18.2732  Intensity fixed to 1.0 and variance to 1E6
=> Zero counts at step no.   2238 at 2theta/TOF/E(KeV):       18.2769  Intensity fixed to 1.0 and variance to 1E6
=> Zero counts at step no.   2239 at 2theta/TOF/E(KeV):       18.2806  Intensity fixed to 1.0 and variance to 1E6
=> Zero counts at step no.   2240 at 2theta/TOF/E(KeV):       18.2843  Intensity fixed to 1.0 and variance to 1E6
=> Zero counts at step no.   2241 at 2theta/TOF/E(KeV):       18.2880  Intensity fixed to 1.0 and variance to 1E6
=> Zero counts at step no.   2242 at 2theta/TOF/E(KeV):       18.2917  Intensity fixed to 1.0 and variance to 1E6
=> Zero counts at step no.   2243 at 2theta/TOF/E(KeV):       18.2954  Intensity fixed to 1.0 and variance to 1E6
=> Zero counts at step no.   2244 at 2theta/TOF/E(KeV):       18.2991  Intensity fixed to 1.0 and variance to 1E6
=> Zero counts at step no.   2245 at 2theta/TOF/E(KeV):       18.3028  Intensity fixed to 1.0 and variance to 1E6
=> Zero counts at step no.   2246 at 2theta/TOF/E(KeV):       18.3065  Intensity fixed to 1.0 and variance to 1E6
=> Zero counts at step no.   2247 at 2theta/TOF/E(KeV):       18.3102  Intensity fixed to 1.0 and variance to 1E6
=> Zero counts at step no.   2248 at 2theta/TOF/E(KeV):       18.3139  Intensity fixed to 1.0 and variance to 1E6
=> Zero counts at step no.   2249 at 2theta/TOF/E(KeV):       18.3176  Intensity fixed to 1.0 and variance to 1E6
=> Zero counts at step no.   2252 at 2theta/TOF/E(KeV):       18.3287  Intensity fixed to 1.0 and variance to 1E6
=> Zero counts at step no.   2253 at 2theta/TOF/E(KeV):       18.3324  Intensity fixed to 1.0 and variance to 1E6
=> Zero counts at step no.   2254 at 2theta/TOF/E(KeV):       18.3361  Intensity fixed to 1.0 and variance to 1E6
=> Zero counts at step no.   2255 at 2theta/TOF/E(KeV):       18.3398  Intensity fixed to 1.0 and variance to 1E6
=> Zero counts at step no.   2256 at 2theta/TOF/E(KeV):       18.3435  Intensity fixed to 1.0 and variance to 1E6
=> Zero counts at step no.   2257 at 2theta/TOF/E(KeV):       18.3472  Intensity fixed to 1.0 and variance to 1E6
=> Zero counts at step no.   2258 at 2theta/TOF/E(KeV):       18.3509  Intensity fixed to 1.0 and variance to 1E6
=> Zero counts at step no.   2259 at 2theta/TOF/E(KeV):       18.3546  Intensity fixed to 1.0 and variance to 1E6
=> Zero counts at step no.   2260 at 2theta/TOF/E(KeV):       18.3583  Intensity fixed to 1.0 and variance to 1E6
=> Zero counts at step no.   2261 at 2theta/TOF/E(KeV):       18.3620  Intensity fixed to 1.0 and variance to 1E6
=> Zero counts at step no.   2262 at 2theta/TOF/E(KeV):       18.3657  Intensity fixed to 1.0 and variance to 1E6
=> Zero counts at step no.   2263 at 2theta/TOF/E(KeV):       18.3694  Intensity fixed to 1.0 and variance to 1E6
=> Zero counts at step no.   2264 at 2theta/TOF/E(KeV):       18.3731  Intensity fixed to 1.0 and variance to 1E6
=> Zero counts at step no.   2265 at 2theta/TOF/E(KeV):       18.3768  Intensity fixed to 1.0 and variance to 1E6
=> Zero counts at step no.   2267 at 2theta/TOF/E(KeV):       18.3842  Intensity fixed to 1.0 and variance to 1E6
=> Zero counts at step no.   2269 at 2theta/TOF/E(KeV):       18.3916  Intensity fixed to 1.0 and variance to 1E6
=> Zero counts at step no.   2270 at 2theta/TOF/E(KeV):       18.3953  Intensity fixed to 1.0 and variance to 1E6
```

```
=> Zero counts at step no.   2273 at 2theta/TOF/E(KeV):      18.4064  Intensity fixed to 1.0 and variance to 1E6
=> Zero counts at step no.   2320 at 2theta/TOF/E(KeV):      18.5803  Intensity fixed to 1.0 and variance to 1E6
=> Zero counts at step no.   2324 at 2theta/TOF/E(KeV):      18.5951  Intensity fixed to 1.0 and variance to 1E6
=> Zero counts at step no.   2325 at 2theta/TOF/E(KeV):      18.5988  Intensity fixed to 1.0 and variance to 1E6
=> Zero counts at step no.   2326 at 2theta/TOF/E(KeV):      18.6025  Intensity fixed to 1.0 and variance to 1E6
=> Zero counts at step no.   2329 at 2theta/TOF/E(KeV):      18.6136  Intensity fixed to 1.0 and variance to 1E6
=> Zero counts at step no.   2330 at 2theta/TOF/E(KeV):      18.6173  Intensity fixed to 1.0 and variance to 1E6
=> Zero counts at step no.   2332 at 2theta/TOF/E(KeV):      18.6247  Intensity fixed to 1.0 and variance to 1E6
=> Zero counts at step no.   2334 at 2theta/TOF/E(KeV):      18.6321  Intensity fixed to 1.0 and variance to 1E6
=> Zero counts at step no.   2336 at 2theta/TOF/E(KeV):      18.6395  Intensity fixed to 1.0 and variance to 1E6
=> Zero counts at step no.   2337 at 2theta/TOF/E(KeV):      18.6432  Intensity fixed to 1.0 and variance to 1E6
=> Zero counts at step no.   2338 at 2theta/TOF/E(KeV):      18.6469  Intensity fixed to 1.0 and variance to 1E6
=> Zero counts at step no.   2339 at 2theta/TOF/E(KeV):      18.6506  Intensity fixed to 1.0 and variance to 1E6
=> Zero counts at step no.   2341 at 2theta/TOF/E(KeV):      18.6580  Intensity fixed to 1.0 and variance to 1E6
=> Zero counts at step no.   2342 at 2theta/TOF/E(KeV):      18.6617  Intensity fixed to 1.0 and variance to 1E6
=> Zero counts at step no.   2343 at 2theta/TOF/E(KeV):      18.6654  Intensity fixed to 1.0 and variance to 1E6
=> Zero counts at step no.   2344 at 2theta/TOF/E(KeV):      18.6691  Intensity fixed to 1.0 and variance to 1E6
=> Zero counts at step no.   2345 at 2theta/TOF/E(KeV):      18.6728  Intensity fixed to 1.0 and variance to 1E6
=> Zero counts at step no.   2346 at 2theta/TOF/E(KeV):      18.6765  Intensity fixed to 1.0 and variance to 1E6
=> Zero counts at step no.   2347 at 2theta/TOF/E(KeV):      18.6802  Intensity fixed to 1.0 and variance to 1E6
=> Zero counts at step no.   2348 at 2theta/TOF/E(KeV):      18.6839  Intensity fixed to 1.0 and variance to 1E6
=> Zero counts at step no.   2350 at 2theta/TOF/E(KeV):      18.6913  Intensity fixed to 1.0 and variance to 1E6
=> Zero counts at step no.   2352 at 2theta/TOF/E(KeV):      18.6987  Intensity fixed to 1.0 and variance to 1E6
=> Zero counts at step no.   2353 at 2theta/TOF/E(KeV):      18.7024  Intensity fixed to 1.0 and variance to 1E6
=> Zero counts at step no.   2354 at 2theta/TOF/E(KeV):      18.7061  Intensity fixed to 1.0 and variance to 1E6
=> Zero counts at step no.   2355 at 2theta/TOF/E(KeV):      18.7098  Intensity fixed to 1.0 and variance to 1E6
=> Zero counts at step no.   2356 at 2theta/TOF/E(KeV):      18.7135  Intensity fixed to 1.0 and variance to 1E6
=> Zero counts at step no.   2357 at 2theta/TOF/E(KeV):      18.7172  Intensity fixed to 1.0 and variance to 1E6
=> Zero counts at step no.   2359 at 2theta/TOF/E(KeV):      18.7246  Intensity fixed to 1.0 and variance to 1E6
=> Zero counts at step no.   2363 at 2theta/TOF/E(KeV):      18.7394  Intensity fixed to 1.0 and variance to 1E6
=> Zero counts at step no.   2364 at 2theta/TOF/E(KeV):      18.7431  Intensity fixed to 1.0 and variance to 1E6
=> Zero counts at step no.   2365 at 2theta/TOF/E(KeV):      18.7468  Intensity fixed to 1.0 and variance to 1E6
=> Zero counts at step no.   2366 at 2theta/TOF/E(KeV):      18.7505  Intensity fixed to 1.0 and variance to 1E6
=> Zero counts at step no.   2368 at 2theta/TOF/E(KeV):      18.7579  Intensity fixed to 1.0 and variance to 1E6
=> Zero counts at step no.   2369 at 2theta/TOF/E(KeV):      18.7616  Intensity fixed to 1.0 and variance to 1E6
=> Zero counts at step no.   2371 at 2theta/TOF/E(KeV):      18.7690  Intensity fixed to 1.0 and variance to 1E6
=> Zero counts at step no.   2372 at 2theta/TOF/E(KeV):      18.7727  Intensity fixed to 1.0 and variance to 1E6
=> Zero counts at step no.   2373 at 2theta/TOF/E(KeV):      18.7764  Intensity fixed to 1.0 and variance to 1E6
=> Zero counts at step no.   2374 at 2theta/TOF/E(KeV):      18.7801  Intensity fixed to 1.0 and variance to 1E6
=> Zero counts at step no.   2375 at 2theta/TOF/E(KeV):      18.7838  Intensity fixed to 1.0 and variance to 1E6
=> Zero counts at step no.   2378 at 2theta/TOF/E(KeV):      18.7949  Intensity fixed to 1.0 and variance to 1E6
=> Zero counts at step no.   2379 at 2theta/TOF/E(KeV):      18.7986  Intensity fixed to 1.0 and variance to 1E6
=> Zero counts at step no.   2380 at 2theta/TOF/E(KeV):      18.8023  Intensity fixed to 1.0 and variance to 1E6
=> Zero counts at step no.   2381 at 2theta/TOF/E(KeV):      18.8060  Intensity fixed to 1.0 and variance to 1E6
=> Zero counts at step no.   2382 at 2theta/TOF/E(KeV):      18.8097  Intensity fixed to 1.0 and variance to 1E6
=> Zero counts at step no.   2383 at 2theta/TOF/E(KeV):      18.8134  Intensity fixed to 1.0 and variance to 1E6
=> Zero counts at step no.   2384 at 2theta/TOF/E(KeV):      18.8171  Intensity fixed to 1.0 and variance to 1E6
=> Zero counts at step no.   2385 at 2theta/TOF/E(KeV):      18.8208  Intensity fixed to 1.0 and variance to 1E6
=> Zero counts at step no.   2386 at 2theta/TOF/E(KeV):      18.8245  Intensity fixed to 1.0 and variance to 1E6
=> Zero counts at step no.   2387 at 2theta/TOF/E(KeV):      18.8282  Intensity fixed to 1.0 and variance to 1E6
=> Zero counts at step no.   2389 at 2theta/TOF/E(KeV):      18.8356  Intensity fixed to 1.0 and variance to 1E6
=> Zero counts at step no.   2390 at 2theta/TOF/E(KeV):      18.8393  Intensity fixed to 1.0 and variance to 1E6
=> Zero counts at step no.   2392 at 2theta/TOF/E(KeV):      18.8467  Intensity fixed to 1.0 and variance to 1E6
=> Zero counts at step no.   2393 at 2theta/TOF/E(KeV):      18.8504  Intensity fixed to 1.0 and variance to 1E6
=> Zero counts at step no.   2394 at 2theta/TOF/E(KeV):      18.8541  Intensity fixed to 1.0 and variance to 1E6
=> Zero counts at step no.   2395 at 2theta/TOF/E(KeV):      18.8578  Intensity fixed to 1.0 and variance to 1E6
=> Zero counts at step no.   2396 at 2theta/TOF/E(KeV):      18.8615  Intensity fixed to 1.0 and variance to 1E6
=> Zero counts at step no.   2397 at 2theta/TOF/E(KeV):      18.8652  Intensity fixed to 1.0 and variance to 1E6
=> Zero counts at step no.   2398 at 2theta/TOF/E(KeV):      18.8689  Intensity fixed to 1.0 and variance to 1E6
=> Zero counts at step no.   2399 at 2theta/TOF/E(KeV):      18.8726  Intensity fixed to 1.0 and variance to 1E6
=> Zero counts at step no.   2400 at 2theta/TOF/E(KeV):      18.8763  Intensity fixed to 1.0 and variance to 1E6
=> Zero counts at step no.   2401 at 2theta/TOF/E(KeV):      18.8800  Intensity fixed to 1.0 and variance to 1E6
=> Zero counts at step no.   2402 at 2theta/TOF/E(KeV):      18.8837  Intensity fixed to 1.0 and variance to 1E6
=> Zero counts at step no.   2404 at 2theta/TOF/E(KeV):      18.8911  Intensity fixed to 1.0 and variance to 1E6
=> Zero counts at step no.   2406 at 2theta/TOF/E(KeV):      18.8985  Intensity fixed to 1.0 and variance to 1E6
=> Zero counts at step no.   2408 at 2theta/TOF/E(KeV):      18.9059  Intensity fixed to 1.0 and variance to 1E6
=> Zero counts at step no.   2409 at 2theta/TOF/E(KeV):      18.9096  Intensity fixed to 1.0 and variance to 1E6
=> Zero counts at step no.   2410 at 2theta/TOF/E(KeV):      18.9133  Intensity fixed to 1.0 and variance to 1E6
=> Zero counts at step no.   2411 at 2theta/TOF/E(KeV):      18.9170  Intensity fixed to 1.0 and variance to 1E6
=> Zero counts at step no.   2413 at 2theta/TOF/E(KeV):      18.9244  Intensity fixed to 1.0 and variance to 1E6
=> Zero counts at step no.   2414 at 2theta/TOF/E(KeV):      18.9281  Intensity fixed to 1.0 and variance to 1E6
=> Zero counts at step no.   2415 at 2theta/TOF/E(KeV):      18.9318  Intensity fixed to 1.0 and variance to 1E6
=> Zero counts at step no.   2416 at 2theta/TOF/E(KeV):      18.9355  Intensity fixed to 1.0 and variance to 1E6
=> Zero counts at step no.   2417 at 2theta/TOF/E(KeV):      18.9392  Intensity fixed to 1.0 and variance to 1E6
=> Zero counts at step no.   2418 at 2theta/TOF/E(KeV):      18.9429  Intensity fixed to 1.0 and variance to 1E6
=> Zero counts at step no.   2419 at 2theta/TOF/E(KeV):      18.9466  Intensity fixed to 1.0 and variance to 1E6
=> Zero counts at step no.   2420 at 2theta/TOF/E(KeV):      18.9503  Intensity fixed to 1.0 and variance to 1E6
=> Zero counts at step no.   2421 at 2theta/TOF/E(KeV):      18.9540  Intensity fixed to 1.0 and variance to 1E6
=> Zero counts at step no.   2422 at 2theta/TOF/E(KeV):      18.9577  Intensity fixed to 1.0 and variance to 1E6
=> Zero counts at step no.   2423 at 2theta/TOF/E(KeV):      18.9614  Intensity fixed to 1.0 and variance to 1E6
=> Zero counts at step no.   2424 at 2theta/TOF/E(KeV):      18.9651  Intensity fixed to 1.0 and variance to 1E6
=> Zero counts at step no.   2425 at 2theta/TOF/E(KeV):      18.9688  Intensity fixed to 1.0 and variance to 1E6
=> Zero counts at step no.   2427 at 2theta/TOF/E(KeV):      18.9762  Intensity fixed to 1.0 and variance to 1E6
=> Zero counts at step no.   2428 at 2theta/TOF/E(KeV):      18.9799  Intensity fixed to 1.0 and variance to 1E6
=> Zero counts at step no.   2429 at 2theta/TOF/E(KeV):      18.9836  Intensity fixed to 1.0 and variance to 1E6
=> Zero counts at step no.   2430 at 2theta/TOF/E(KeV):      18.9873  Intensity fixed to 1.0 and variance to 1E6
=> Zero counts at step no.   2431 at 2theta/TOF/E(KeV):      18.9910  Intensity fixed to 1.0 and variance to 1E6
=> Zero counts at step no.   2434 at 2theta/TOF/E(KeV):      19.0021  Intensity fixed to 1.0 and variance to 1E6
=> Zero counts at step no.   2435 at 2theta/TOF/E(KeV):      19.0058  Intensity fixed to 1.0 and variance to 1E6
=> Zero counts at step no.   2437 at 2theta/TOF/E(KeV):      19.0132  Intensity fixed to 1.0 and variance to 1E6
```

```
=> Zero counts at step no.   2440 at 2theta/TOF/E(KeV):       19.0243  Intensity fixed to 1.0 and variance to 1E6
=> Zero counts at step no.   2441 at 2theta/TOF/E(KeV):       19.0280  Intensity fixed to 1.0 and variance to 1E6
=> Zero counts at step no.   2442 at 2theta/TOF/E(KeV):       19.0317  Intensity fixed to 1.0 and variance to 1E6
=> Zero counts at step no.   2444 at 2theta/TOF/E(KeV):       19.0391  Intensity fixed to 1.0 and variance to 1E6
=> Zero counts at step no.   2445 at 2theta/TOF/E(KeV):       19.0428  Intensity fixed to 1.0 and variance to 1E6
=> Zero counts at step no.   2446 at 2theta/TOF/E(KeV):       19.0465  Intensity fixed to 1.0 and variance to 1E6
=> Zero counts at step no.   2447 at 2theta/TOF/E(KeV):       19.0502  Intensity fixed to 1.0 and variance to 1E6
=> Zero counts at step no.   2448 at 2theta/TOF/E(KeV):       19.0539  Intensity fixed to 1.0 and variance to 1E6
=> Zero counts at step no.   2449 at 2theta/TOF/E(KeV):       19.0576  Intensity fixed to 1.0 and variance to 1E6
=> Zero counts at step no.   2450 at 2theta/TOF/E(KeV):       19.0613  Intensity fixed to 1.0 and variance to 1E6
=> Zero counts at step no.   2451 at 2theta/TOF/E(KeV):       19.0650  Intensity fixed to 1.0 and variance to 1E6
=> Zero counts at step no.   2453 at 2theta/TOF/E(KeV):       19.0724  Intensity fixed to 1.0 and variance to 1E6
=> Zero counts at step no.   2454 at 2theta/TOF/E(KeV):       19.0761  Intensity fixed to 1.0 and variance to 1E6
=> Zero counts at step no.   2455 at 2theta/TOF/E(KeV):       19.0798  Intensity fixed to 1.0 and variance to 1E6
=> Zero counts at step no.   2456 at 2theta/TOF/E(KeV):       19.0835  Intensity fixed to 1.0 and variance to 1E6
=> Zero counts at step no.   2457 at 2theta/TOF/E(KeV):       19.0872  Intensity fixed to 1.0 and variance to 1E6
=> Zero counts at step no.   2458 at 2theta/TOF/E(KeV):       19.0909  Intensity fixed to 1.0 and variance to 1E6
=> Zero counts at step no.   2459 at 2theta/TOF/E(KeV):       19.0946  Intensity fixed to 1.0 and variance to 1E6
=> Zero counts at step no.   2461 at 2theta/TOF/E(KeV):       19.1020  Intensity fixed to 1.0 and variance to 1E6
=> Zero counts at step no.   2462 at 2theta/TOF/E(KeV):       19.1057  Intensity fixed to 1.0 and variance to 1E6
=> Zero counts at step no.   2463 at 2theta/TOF/E(KeV):       19.1094  Intensity fixed to 1.0 and variance to 1E6
=> Zero counts at step no.   2464 at 2theta/TOF/E(KeV):       19.1131  Intensity fixed to 1.0 and variance to 1E6
=> Zero counts at step no.   2465 at 2theta/TOF/E(KeV):       19.1168  Intensity fixed to 1.0 and variance to 1E6
=> Zero counts at step no.   2467 at 2theta/TOF/E(KeV):       19.1242  Intensity fixed to 1.0 and variance to 1E6
=> Zero counts at step no.   2468 at 2theta/TOF/E(KeV):       19.1279  Intensity fixed to 1.0 and variance to 1E6
=> Zero counts at step no.   2469 at 2theta/TOF/E(KeV):       19.1316  Intensity fixed to 1.0 and variance to 1E6
=> Zero counts at step no.   2470 at 2theta/TOF/E(KeV):       19.1353  Intensity fixed to 1.0 and variance to 1E6
=> Zero counts at step no.   2471 at 2theta/TOF/E(KeV):       19.1390  Intensity fixed to 1.0 and variance to 1E6
=> Zero counts at step no.   2472 at 2theta/TOF/E(KeV):       19.1427  Intensity fixed to 1.0 and variance to 1E6
=> Zero counts at step no.   2473 at 2theta/TOF/E(KeV):       19.1464  Intensity fixed to 1.0 and variance to 1E6
=> Zero counts at step no.   2476 at 2theta/TOF/E(KeV):       19.1575  Intensity fixed to 1.0 and variance to 1E6
=> Zero counts at step no.   2482 at 2theta/TOF/E(KeV):       19.1797  Intensity fixed to 1.0 and variance to 1E6
=> Zero counts at step no.   2483 at 2theta/TOF/E(KeV):       19.1834  Intensity fixed to 1.0 and variance to 1E6
=> Zero counts at step no.   2485 at 2theta/TOF/E(KeV):       19.1908  Intensity fixed to 1.0 and variance to 1E6
=> Zero counts at step no.   2487 at 2theta/TOF/E(KeV):       19.1982  Intensity fixed to 1.0 and variance to 1E6
=> Zero counts at step no.   2488 at 2theta/TOF/E(KeV):       19.2019  Intensity fixed to 1.0 and variance to 1E6
=> Zero counts at step no.   2489 at 2theta/TOF/E(KeV):       19.2056  Intensity fixed to 1.0 and variance to 1E6
=> Zero counts at step no.   2491 at 2theta/TOF/E(KeV):       19.2130  Intensity fixed to 1.0 and variance to 1E6
=> Zero counts at step no.   2493 at 2theta/TOF/E(KeV):       19.2204  Intensity fixed to 1.0 and variance to 1E6
=> Zero counts at step no.   2494 at 2theta/TOF/E(KeV):       19.2241  Intensity fixed to 1.0 and variance to 1E6
=> Zero counts at step no.   2536 at 2theta/TOF/E(KeV):       19.3795  Intensity fixed to 1.0 and variance to 1E6
=> Zero counts at step no.   2538 at 2theta/TOF/E(KeV):       19.3869  Intensity fixed to 1.0 and variance to 1E6
=> Zero counts at step no.   2539 at 2theta/TOF/E(KeV):       19.3906  Intensity fixed to 1.0 and variance to 1E6
=> Zero counts at step no.   2542 at 2theta/TOF/E(KeV):       19.4017  Intensity fixed to 1.0 and variance to 1E6
=> Zero counts at step no.   2544 at 2theta/TOF/E(KeV):       19.4091  Intensity fixed to 1.0 and variance to 1E6
=> Zero counts at step no.   2548 at 2theta/TOF/E(KeV):       19.4239  Intensity fixed to 1.0 and variance to 1E6
=> Zero counts at step no.   2549 at 2theta/TOF/E(KeV):       19.4276  Intensity fixed to 1.0 and variance to 1E6
=> Zero counts at step no.   2551 at 2theta/TOF/E(KeV):       19.4350  Intensity fixed to 1.0 and variance to 1E6
=> Zero counts at step no.   2552 at 2theta/TOF/E(KeV):       19.4387  Intensity fixed to 1.0 and variance to 1E6
=> Zero counts at step no.   2553 at 2theta/TOF/E(KeV):       19.4424  Intensity fixed to 1.0 and variance to 1E6
=> Zero counts at step no.   2554 at 2theta/TOF/E(KeV):       19.4461  Intensity fixed to 1.0 and variance to 1E6
=> Zero counts at step no.   2555 at 2theta/TOF/E(KeV):       19.4498  Intensity fixed to 1.0 and variance to 1E6
=> Zero counts at step no.   2557 at 2theta/TOF/E(KeV):       19.4572  Intensity fixed to 1.0 and variance to 1E6
=> Zero counts at step no.   2559 at 2theta/TOF/E(KeV):       19.4646  Intensity fixed to 1.0 and variance to 1E6
=> Zero counts at step no.   2560 at 2theta/TOF/E(KeV):       19.4683  Intensity fixed to 1.0 and variance to 1E6
=> Zero counts at step no.   2561 at 2theta/TOF/E(KeV):       19.4720  Intensity fixed to 1.0 and variance to 1E6
=> Zero counts at step no.   2562 at 2theta/TOF/E(KeV):       19.4757  Intensity fixed to 1.0 and variance to 1E6
=> Zero counts at step no.   2563 at 2theta/TOF/E(KeV):       19.4794  Intensity fixed to 1.0 and variance to 1E6
=> Zero counts at step no.   2565 at 2theta/TOF/E(KeV):       19.4868  Intensity fixed to 1.0 and variance to 1E6
=> Zero counts at step no.   2566 at 2theta/TOF/E(KeV):       19.4905  Intensity fixed to 1.0 and variance to 1E6
=> Zero counts at step no.   2567 at 2theta/TOF/E(KeV):       19.4942  Intensity fixed to 1.0 and variance to 1E6
=> Zero counts at step no.   2568 at 2theta/TOF/E(KeV):       19.4979  Intensity fixed to 1.0 and variance to 1E6
=> Zero counts at step no.   2569 at 2theta/TOF/E(KeV):       19.5016  Intensity fixed to 1.0 and variance to 1E6
=> Zero counts at step no.   2570 at 2theta/TOF/E(KeV):       19.5053  Intensity fixed to 1.0 and variance to 1E6
=> Zero counts at step no.   2571 at 2theta/TOF/E(KeV):       19.5090  Intensity fixed to 1.0 and variance to 1E6
=> Zero counts at step no.   2572 at 2theta/TOF/E(KeV):       19.5127  Intensity fixed to 1.0 and variance to 1E6
=> Zero counts at step no.   2574 at 2theta/TOF/E(KeV):       19.5201  Intensity fixed to 1.0 and variance to 1E6
=> Zero counts at step no.   2575 at 2theta/TOF/E(KeV):       19.5238  Intensity fixed to 1.0 and variance to 1E6
=> Zero counts at step no.   2577 at 2theta/TOF/E(KeV):       19.5312  Intensity fixed to 1.0 and variance to 1E6
=> Zero counts at step no.   2578 at 2theta/TOF/E(KeV):       19.5349  Intensity fixed to 1.0 and variance to 1E6
=> Zero counts at step no.   2579 at 2theta/TOF/E(KeV):       19.5386  Intensity fixed to 1.0 and variance to 1E6
=> Zero counts at step no.   2582 at 2theta/TOF/E(KeV):       19.5497  Intensity fixed to 1.0 and variance to 1E6
=> Zero counts at step no.   2583 at 2theta/TOF/E(KeV):       19.5534  Intensity fixed to 1.0 and variance to 1E6
=> Zero counts at step no.   2584 at 2theta/TOF/E(KeV):       19.5571  Intensity fixed to 1.0 and variance to 1E6
=> Zero counts at step no.   2585 at 2theta/TOF/E(KeV):       19.5608  Intensity fixed to 1.0 and variance to 1E6
=> Zero counts at step no.   2586 at 2theta/TOF/E(KeV):       19.5645  Intensity fixed to 1.0 and variance to 1E6
=> Zero counts at step no.   2587 at 2theta/TOF/E(KeV):       19.5682  Intensity fixed to 1.0 and variance to 1E6
=> Zero counts at step no.   2588 at 2theta/TOF/E(KeV):       19.5719  Intensity fixed to 1.0 and variance to 1E6
=> Zero counts at step no.   2589 at 2theta/TOF/E(KeV):       19.5756  Intensity fixed to 1.0 and variance to 1E6
=> Zero counts at step no.   2591 at 2theta/TOF/E(KeV):       19.5830  Intensity fixed to 1.0 and variance to 1E6
=> Zero counts at step no.   2594 at 2theta/TOF/E(KeV):       19.5941  Intensity fixed to 1.0 and variance to 1E6
=> Zero counts at step no.   2595 at 2theta/TOF/E(KeV):       19.5978  Intensity fixed to 1.0 and variance to 1E6
=> Zero counts at step no.   2597 at 2theta/TOF/E(KeV):       19.6052  Intensity fixed to 1.0 and variance to 1E6
=> Zero counts at step no.   2598 at 2theta/TOF/E(KeV):       19.6089  Intensity fixed to 1.0 and variance to 1E6
=> Zero counts at step no.   2600 at 2theta/TOF/E(KeV):       19.6163  Intensity fixed to 1.0 and variance to 1E6
=> Zero counts at step no.   2601 at 2theta/TOF/E(KeV):       19.6200  Intensity fixed to 1.0 and variance to 1E6
=> Zero counts at step no.   2602 at 2theta/TOF/E(KeV):       19.6237  Intensity fixed to 1.0 and variance to 1E6
=> Zero counts at step no.   2603 at 2theta/TOF/E(KeV):       19.6274  Intensity fixed to 1.0 and variance to 1E6
=> Zero counts at step no.   2604 at 2theta/TOF/E(KeV):       19.6311  Intensity fixed to 1.0 and variance to 1E6
=> Zero counts at step no.   2606 at 2theta/TOF/E(KeV):       19.6385  Intensity fixed to 1.0 and variance to 1E6
```

```
=> Zero counts at step no.   2607 at 2theta/TOF/E(KeV):      19.6422  Intensity fixed to 1.0 and variance to 1E6
=> Zero counts at step no.   2611 at 2theta/TOF/E(KeV):      19.6570  Intensity fixed to 1.0 and variance to 1E6
=> Zero counts at step no.   2613 at 2theta/TOF/E(KeV):      19.6644  Intensity fixed to 1.0 and variance to 1E6
=> Zero counts at step no.   2617 at 2theta/TOF/E(KeV):      19.6792  Intensity fixed to 1.0 and variance to 1E6
=> Zero counts at step no.   2620 at 2theta/TOF/E(KeV):      19.6903  Intensity fixed to 1.0 and variance to 1E6
=> Zero counts at step no.   2621 at 2theta/TOF/E(KeV):      19.6940  Intensity fixed to 1.0 and variance to 1E6
=> Zero counts at step no.   2622 at 2theta/TOF/E(KeV):      19.6977  Intensity fixed to 1.0 and variance to 1E6
=> Zero counts at step no.   2623 at 2theta/TOF/E(KeV):      19.7014  Intensity fixed to 1.0 and variance to 1E6
=> Zero counts at step no.   2624 at 2theta/TOF/E(KeV):      19.7051  Intensity fixed to 1.0 and variance to 1E6
=> Zero counts at step no.   2625 at 2theta/TOF/E(KeV):      19.7088  Intensity fixed to 1.0 and variance to 1E6
=> Zero counts at step no.   2627 at 2theta/TOF/E(KeV):      19.7162  Intensity fixed to 1.0 and variance to 1E6
=> Zero counts at step no.   2628 at 2theta/TOF/E(KeV):      19.7199  Intensity fixed to 1.0 and variance to 1E6
=> Zero counts at step no.   2629 at 2theta/TOF/E(KeV):      19.7236  Intensity fixed to 1.0 and variance to 1E6
=> Zero counts at step no.   2630 at 2theta/TOF/E(KeV):      19.7273  Intensity fixed to 1.0 and variance to 1E6
=> Zero counts at step no.   2631 at 2theta/TOF/E(KeV):      19.7310  Intensity fixed to 1.0 and variance to 1E6
=> Zero counts at step no.   2632 at 2theta/TOF/E(KeV):      19.7347  Intensity fixed to 1.0 and variance to 1E6
=> Zero counts at step no.   2635 at 2theta/TOF/E(KeV):      19.7458  Intensity fixed to 1.0 and variance to 1E6
=> Zero counts at step no.   2637 at 2theta/TOF/E(KeV):      19.7532  Intensity fixed to 1.0 and variance to 1E6
=> Zero counts at step no.   2640 at 2theta/TOF/E(KeV):      19.7643  Intensity fixed to 1.0 and variance to 1E6
=> Zero counts at step no.   2641 at 2theta/TOF/E(KeV):      19.7680  Intensity fixed to 1.0 and variance to 1E6
=> Zero counts at step no.   2643 at 2theta/TOF/E(KeV):      19.7754  Intensity fixed to 1.0 and variance to 1E6
=> Zero counts at step no.   2645 at 2theta/TOF/E(KeV):      19.7828  Intensity fixed to 1.0 and variance to 1E6
=> Zero counts at step no.   2646 at 2theta/TOF/E(KeV):      19.7865  Intensity fixed to 1.0 and variance to 1E6
=> Zero counts at step no.   2649 at 2theta/TOF/E(KeV):      19.7976  Intensity fixed to 1.0 and variance to 1E6
=> Zero counts at step no.   2650 at 2theta/TOF/E(KeV):      19.8013  Intensity fixed to 1.0 and variance to 1E6
=> Zero counts at step no.   2651 at 2theta/TOF/E(KeV):      19.8050  Intensity fixed to 1.0 and variance to 1E6
=> Zero counts at step no.   2652 at 2theta/TOF/E(KeV):      19.8087  Intensity fixed to 1.0 and variance to 1E6
=> Zero counts at step no.   2653 at 2theta/TOF/E(KeV):      19.8124  Intensity fixed to 1.0 and variance to 1E6
=> Zero counts at step no.   2656 at 2theta/TOF/E(KeV):      19.8235  Intensity fixed to 1.0 and variance to 1E6
=> Zero counts at step no.   2658 at 2theta/TOF/E(KeV):      19.8309  Intensity fixed to 1.0 and variance to 1E6
=> Zero counts at step no.   2662 at 2theta/TOF/E(KeV):      19.8457  Intensity fixed to 1.0 and variance to 1E6
=> Zero counts at step no.   2667 at 2theta/TOF/E(KeV):      19.8642  Intensity fixed to 1.0 and variance to 1E6
=> Zero counts at step no.   2668 at 2theta/TOF/E(KeV):      19.8679  Intensity fixed to 1.0 and variance to 1E6
=> Zero counts at step no.   2670 at 2theta/TOF/E(KeV):      19.8753  Intensity fixed to 1.0 and variance to 1E6
=> Zero counts at step no.   2672 at 2theta/TOF/E(KeV):      19.8827  Intensity fixed to 1.0 and variance to 1E6
=> Zero counts at step no.   2673 at 2theta/TOF/E(KeV):      19.8864  Intensity fixed to 1.0 and variance to 1E6
=> Zero counts at step no.   2678 at 2theta/TOF/E(KeV):      19.9049  Intensity fixed to 1.0 and variance to 1E6
=> Zero counts at step no.   2679 at 2theta/TOF/E(KeV):      19.9086  Intensity fixed to 1.0 and variance to 1E6
=> Zero counts at step no.   2680 at 2theta/TOF/E(KeV):      19.9123  Intensity fixed to 1.0 and variance to 1E6
=> Zero counts at step no.   2681 at 2theta/TOF/E(KeV):      19.9160  Intensity fixed to 1.0 and variance to 1E6
=> Zero counts at step no.   2682 at 2theta/TOF/E(KeV):      19.9197  Intensity fixed to 1.0 and variance to 1E6
=> Zero counts at step no.   2835 at 2theta/TOF/E(KeV):      20.4858  Intensity fixed to 1.0 and variance to 1E6
=> Zero counts at step no.   2837 at 2theta/TOF/E(KeV):      20.4932  Intensity fixed to 1.0 and variance to 1E6
=> Zero counts at step no.   2839 at 2theta/TOF/E(KeV):      20.5006  Intensity fixed to 1.0 and variance to 1E6
=> Zero counts at step no.   2840 at 2theta/TOF/E(KeV):      20.5043  Intensity fixed to 1.0 and variance to 1E6
=> Zero counts at step no.   2846 at 2theta/TOF/E(KeV):      20.5265  Intensity fixed to 1.0 and variance to 1E6
=> Zero counts at step no.   2849 at 2theta/TOF/E(KeV):      20.5376  Intensity fixed to 1.0 and variance to 1E6
=> Zero counts at step no.   2852 at 2theta/TOF/E(KeV):      20.5487  Intensity fixed to 1.0 and variance to 1E6
=> Zero counts at step no.   2854 at 2theta/TOF/E(KeV):      20.5561  Intensity fixed to 1.0 and variance to 1E6
=> Zero counts at step no.   2855 at 2theta/TOF/E(KeV):      20.5598  Intensity fixed to 1.0 and variance to 1E6
=> Zero counts at step no.   2856 at 2theta/TOF/E(KeV):      20.5635  Intensity fixed to 1.0 and variance to 1E6
=> Zero counts at step no.   2858 at 2theta/TOF/E(KeV):      20.5709  Intensity fixed to 1.0 and variance to 1E6
=> Zero counts at step no.   2859 at 2theta/TOF/E(KeV):      20.5746  Intensity fixed to 1.0 and variance to 1E6
=> Zero counts at step no.   2861 at 2theta/TOF/E(KeV):      20.5820  Intensity fixed to 1.0 and variance to 1E6
=> Zero counts at step no.   2862 at 2theta/TOF/E(KeV):      20.5857  Intensity fixed to 1.0 and variance to 1E6
=> Zero counts at step no.   2864 at 2theta/TOF/E(KeV):      20.5931  Intensity fixed to 1.0 and variance to 1E6
=> Zero counts at step no.   2865 at 2theta/TOF/E(KeV):      20.5968  Intensity fixed to 1.0 and variance to 1E6
=> Zero counts at step no.   2867 at 2theta/TOF/E(KeV):      20.6042  Intensity fixed to 1.0 and variance to 1E6
=> Zero counts at step no.   2868 at 2theta/TOF/E(KeV):      20.6079  Intensity fixed to 1.0 and variance to 1E6
=> Zero counts at step no.   2870 at 2theta/TOF/E(KeV):      20.6153  Intensity fixed to 1.0 and variance to 1E6
=> Zero counts at step no.   2872 at 2theta/TOF/E(KeV):      20.6227  Intensity fixed to 1.0 and variance to 1E6
=> Zero counts at step no.   2873 at 2theta/TOF/E(KeV):      20.6264  Intensity fixed to 1.0 and variance to 1E6
=> Zero counts at step no.   2874 at 2theta/TOF/E(KeV):      20.6301  Intensity fixed to 1.0 and variance to 1E6
=> Zero counts at step no.   2876 at 2theta/TOF/E(KeV):      20.6375  Intensity fixed to 1.0 and variance to 1E6
=> Zero counts at step no.   2877 at 2theta/TOF/E(KeV):      20.6412  Intensity fixed to 1.0 and variance to 1E6
=> Zero counts at step no.   2879 at 2theta/TOF/E(KeV):      20.6486  Intensity fixed to 1.0 and variance to 1E6
=> Zero counts at step no.   2882 at 2theta/TOF/E(KeV):      20.6597  Intensity fixed to 1.0 and variance to 1E6
=> Zero counts at step no.   2883 at 2theta/TOF/E(KeV):      20.6634  Intensity fixed to 1.0 and variance to 1E6
=> Zero counts at step no.   2884 at 2theta/TOF/E(KeV):      20.6671  Intensity fixed to 1.0 and variance to 1E6
=> Zero counts at step no.   2886 at 2theta/TOF/E(KeV):      20.6745  Intensity fixed to 1.0 and variance to 1E6
=> Zero counts at step no.   2887 at 2theta/TOF/E(KeV):      20.6782  Intensity fixed to 1.0 and variance to 1E6
=> Zero counts at step no.   2888 at 2theta/TOF/E(KeV):      20.6819  Intensity fixed to 1.0 and variance to 1E6
=> Zero counts at step no.   2896 at 2theta/TOF/E(KeV):      20.7115  Intensity fixed to 1.0 and variance to 1E6
=> Zero counts at step no.   2897 at 2theta/TOF/E(KeV):      20.7152  Intensity fixed to 1.0 and variance to 1E6
=> Zero counts at step no.   2901 at 2theta/TOF/E(KeV):      20.7300  Intensity fixed to 1.0 and variance to 1E6
=> Zero counts at step no.   2902 at 2theta/TOF/E(KeV):      20.7337  Intensity fixed to 1.0 and variance to 1E6
=> Zero counts at step no.   2903 at 2theta/TOF/E(KeV):      20.7374  Intensity fixed to 1.0 and variance to 1E6
=> Zero counts at step no.   2904 at 2theta/TOF/E(KeV):      20.7411  Intensity fixed to 1.0 and variance to 1E6
=> Zero counts at step no.   2909 at 2theta/TOF/E(KeV):      20.7596  Intensity fixed to 1.0 and variance to 1E6
=> Zero counts at step no.   2911 at 2theta/TOF/E(KeV):      20.7670  Intensity fixed to 1.0 and variance to 1E6
=> Zero counts at step no.   2912 at 2theta/TOF/E(KeV):      20.7707  Intensity fixed to 1.0 and variance to 1E6
=> Zero counts at step no.   2914 at 2theta/TOF/E(KeV):      20.7781  Intensity fixed to 1.0 and variance to 1E6
=> Zero counts at step no.   2915 at 2theta/TOF/E(KeV):      20.7818  Intensity fixed to 1.0 and variance to 1E6
=> Zero counts at step no.   2918 at 2theta/TOF/E(KeV):      20.7929  Intensity fixed to 1.0 and variance to 1E6
=> Zero counts at step no.   2919 at 2theta/TOF/E(KeV):      20.7966  Intensity fixed to 1.0 and variance to 1E6
=> Zero counts at step no.   2924 at 2theta/TOF/E(KeV):      20.8151  Intensity fixed to 1.0 and variance to 1E6
=> Zero counts at step no.   2927 at 2theta/TOF/E(KeV):      20.8262  Intensity fixed to 1.0 and variance to 1E6
=> Zero counts at step no.   2929 at 2theta/TOF/E(KeV):      20.8336  Intensity fixed to 1.0 and variance to 1E6
=> Zero counts at step no.   2930 at 2theta/TOF/E(KeV):      20.8373  Intensity fixed to 1.0 and variance to 1E6
=> Zero counts at step no.   2931 at 2theta/TOF/E(KeV):      20.8410  Intensity fixed to 1.0 and variance to 1E6
```

```
=> Zero counts at step no.   2934 at 2theta/TOF/E(KeV):       20.8521  Intensity fixed to 1.0 and variance to 1E6
=> Zero counts at step no.   2936 at 2theta/TOF/E(KeV):       20.8595  Intensity fixed to 1.0 and variance to 1E6
=> Zero counts at step no.   2938 at 2theta/TOF/E(KeV):       20.8669  Intensity fixed to 1.0 and variance to 1E6
=> Zero counts at step no.   2939 at 2theta/TOF/E(KeV):       20.8706  Intensity fixed to 1.0 and variance to 1E6
=> Zero counts at step no.   2947 at 2theta/TOF/E(KeV):       20.9002  Intensity fixed to 1.0 and variance to 1E6
=> Zero counts at step no.   2951 at 2theta/TOF/E(KeV):       20.9150  Intensity fixed to 1.0 and variance to 1E6
=> Zero counts at step no.   2954 at 2theta/TOF/E(KeV):       20.9261  Intensity fixed to 1.0 and variance to 1E6
=> Zero counts at step no.   2956 at 2theta/TOF/E(KeV):       20.9335  Intensity fixed to 1.0 and variance to 1E6
=> Zero counts at step no.   2957 at 2theta/TOF/E(KeV):       20.9372  Intensity fixed to 1.0 and variance to 1E6
=> Zero counts at step no.   2960 at 2theta/TOF/E(KeV):       20.9483  Intensity fixed to 1.0 and variance to 1E6
=> Zero counts at step no.   2962 at 2theta/TOF/E(KeV):       20.9557  Intensity fixed to 1.0 and variance to 1E6
=> Zero counts at step no.   2963 at 2theta/TOF/E(KeV):       20.9594  Intensity fixed to 1.0 and variance to 1E6
=> Zero counts at step no.   2964 at 2theta/TOF/E(KeV):       20.9631  Intensity fixed to 1.0 and variance to 1E6
=> Zero counts at step no.   2965 at 2theta/TOF/E(KeV):       20.9668  Intensity fixed to 1.0 and variance to 1E6
=> Zero counts at step no.   2966 at 2theta/TOF/E(KeV):       20.9705  Intensity fixed to 1.0 and variance to 1E6
=> Zero counts at step no.   2971 at 2theta/TOF/E(KeV):       20.9890  Intensity fixed to 1.0 and variance to 1E6
=> Zero counts at step no.   2974 at 2theta/TOF/E(KeV):       21.0001  Intensity fixed to 1.0 and variance to 1E6
=> Zero counts at step no.   2975 at 2theta/TOF/E(KeV):       21.0038  Intensity fixed to 1.0 and variance to 1E6
=> Zero counts at step no.   3070 at 2theta/TOF/E(KeV):       21.3553  Intensity fixed to 1.0 and variance to 1E6
=> Zero counts at step no.   3079 at 2theta/TOF/E(KeV):       21.3886  Intensity fixed to 1.0 and variance to 1E6
=> Zero counts at step no.   3081 at 2theta/TOF/E(KeV):       21.3960  Intensity fixed to 1.0 and variance to 1E6
=> Zero counts at step no.   3086 at 2theta/TOF/E(KeV):       21.4145  Intensity fixed to 1.0 and variance to 1E6
=> Zero counts at step no.   3089 at 2theta/TOF/E(KeV):       21.4256  Intensity fixed to 1.0 and variance to 1E6
=> Zero counts at step no.   3091 at 2theta/TOF/E(KeV):       21.4330  Intensity fixed to 1.0 and variance to 1E6
=> Zero counts at step no.   3092 at 2theta/TOF/E(KeV):       21.4367  Intensity fixed to 1.0 and variance to 1E6
=> Zero counts at step no.   3094 at 2theta/TOF/E(KeV):       21.4441  Intensity fixed to 1.0 and variance to 1E6
=> Zero counts at step no.   3097 at 2theta/TOF/E(KeV):       21.4552  Intensity fixed to 1.0 and variance to 1E6
=> Zero counts at step no.   3099 at 2theta/TOF/E(KeV):       21.4626  Intensity fixed to 1.0 and variance to 1E6
=> Zero counts at step no.   3100 at 2theta/TOF/E(KeV):       21.4663  Intensity fixed to 1.0 and variance to 1E6
=> Zero counts at step no.   3101 at 2theta/TOF/E(KeV):       21.4700  Intensity fixed to 1.0 and variance to 1E6
=> Zero counts at step no.   3102 at 2theta/TOF/E(KeV):       21.4737  Intensity fixed to 1.0 and variance to 1E6
=> Zero counts at step no.   3105 at 2theta/TOF/E(KeV):       21.4848  Intensity fixed to 1.0 and variance to 1E6
=> Zero counts at step no.   3106 at 2theta/TOF/E(KeV):       21.4885  Intensity fixed to 1.0 and variance to 1E6
=> Zero counts at step no.   3108 at 2theta/TOF/E(KeV):       21.4959  Intensity fixed to 1.0 and variance to 1E6
=> Zero counts at step no.   3109 at 2theta/TOF/E(KeV):       21.4996  Intensity fixed to 1.0 and variance to 1E6
=> Zero counts at step no.   3113 at 2theta/TOF/E(KeV):       21.5144  Intensity fixed to 1.0 and variance to 1E6
=> Zero counts at step no.   3115 at 2theta/TOF/E(KeV):       21.5218  Intensity fixed to 1.0 and variance to 1E6
=> Zero counts at step no.   3121 at 2theta/TOF/E(KeV):       21.5440  Intensity fixed to 1.0 and variance to 1E6
=> Zero counts at step no.   3124 at 2theta/TOF/E(KeV):       21.5551  Intensity fixed to 1.0 and variance to 1E6
=> Zero counts at step no.   3273 at 2theta/TOF/E(KeV):       22.1064  Intensity fixed to 1.0 and variance to 1E6
=> Zero counts at step no.   3276 at 2theta/TOF/E(KeV):       22.1175  Intensity fixed to 1.0 and variance to 1E6
=> Zero counts at step no.   3282 at 2theta/TOF/E(KeV):       22.1397  Intensity fixed to 1.0 and variance to 1E6
=> Zero counts at step no.   3285 at 2theta/TOF/E(KeV):       22.1508  Intensity fixed to 1.0 and variance to 1E6
=> Zero counts at step no.   3287 at 2theta/TOF/E(KeV):       22.1582  Intensity fixed to 1.0 and variance to 1E6
=> Zero counts at step no.   3288 at 2theta/TOF/E(KeV):       22.1619  Intensity fixed to 1.0 and variance to 1E6
=> Zero counts at step no.   3289 at 2theta/TOF/E(KeV):       22.1656  Intensity fixed to 1.0 and variance to 1E6
=> Zero counts at step no.   3293 at 2theta/TOF/E(KeV):       22.1804  Intensity fixed to 1.0 and variance to 1E6
=> Zero counts at step no.   3294 at 2theta/TOF/E(KeV):       22.1841  Intensity fixed to 1.0 and variance to 1E6
=> Zero counts at step no.   3295 at 2theta/TOF/E(KeV):       22.1878  Intensity fixed to 1.0 and variance to 1E6
=> Zero counts at step no.   3303 at 2theta/TOF/E(KeV):       22.2174  Intensity fixed to 1.0 and variance to 1E6
=> Zero counts at step no.   3305 at 2theta/TOF/E(KeV):       22.2248  Intensity fixed to 1.0 and variance to 1E6
=> Zero counts at step no.   3310 at 2theta/TOF/E(KeV):       22.2433  Intensity fixed to 1.0 and variance to 1E6
=> Zero counts at step no.   3311 at 2theta/TOF/E(KeV):       22.2470  Intensity fixed to 1.0 and variance to 1E6
=> Zero counts at step no.   3312 at 2theta/TOF/E(KeV):       22.2507  Intensity fixed to 1.0 and variance to 1E6
=> Zero counts at step no.   3431 at 2theta/TOF/E(KeV):       22.6910  Intensity fixed to 1.0 and variance to 1E6
=> Zero counts at step no.   3432 at 2theta/TOF/E(KeV):       22.6947  Intensity fixed to 1.0 and variance to 1E6
=> Zero counts at step no.   3434 at 2theta/TOF/E(KeV):       22.7021  Intensity fixed to 1.0 and variance to 1E6
=> Zero counts at step no.   3438 at 2theta/TOF/E(KeV):       22.7169  Intensity fixed to 1.0 and variance to 1E6
=> Zero counts at step no.   3440 at 2theta/TOF/E(KeV):       22.7243  Intensity fixed to 1.0 and variance to 1E6
=> Zero counts at step no.   3441 at 2theta/TOF/E(KeV):       22.7280  Intensity fixed to 1.0 and variance to 1E6
=> Zero counts at step no.   3444 at 2theta/TOF/E(KeV):       22.7391  Intensity fixed to 1.0 and variance to 1E6
=> Zero counts at step no.   3447 at 2theta/TOF/E(KeV):       22.7502  Intensity fixed to 1.0 and variance to 1E6
=> Zero counts at step no.   3449 at 2theta/TOF/E(KeV):       22.7576  Intensity fixed to 1.0 and variance to 1E6
=> Zero counts at step no.   3450 at 2theta/TOF/E(KeV):       22.7613  Intensity fixed to 1.0 and variance to 1E6
=> Zero counts at step no.   3452 at 2theta/TOF/E(KeV):       22.7687  Intensity fixed to 1.0 and variance to 1E6
=> Zero counts at step no.   3453 at 2theta/TOF/E(KeV):       22.7724  Intensity fixed to 1.0 and variance to 1E6
=> Zero counts at step no.   3459 at 2theta/TOF/E(KeV):       22.7946  Intensity fixed to 1.0 and variance to 1E6
=> Zero counts at step no.   3460 at 2theta/TOF/E(KeV):       22.7983  Intensity fixed to 1.0 and variance to 1E6
=> Zero counts at step no.   3461 at 2theta/TOF/E(KeV):       22.8020  Intensity fixed to 1.0 and variance to 1E6
=> Zero counts at step no.   3462 at 2theta/TOF/E(KeV):       22.8057  Intensity fixed to 1.0 and variance to 1E6
=> Zero counts at step no.   3463 at 2theta/TOF/E(KeV):       22.8094  Intensity fixed to 1.0 and variance to 1E6
=> Zero counts at step no.   3464 at 2theta/TOF/E(KeV):       22.8131  Intensity fixed to 1.0 and variance to 1E6
=> Zero counts at step no.   3467 at 2theta/TOF/E(KeV):       22.8242  Intensity fixed to 1.0 and variance to 1E6
=> Zero counts at step no.   3468 at 2theta/TOF/E(KeV):       22.8279  Intensity fixed to 1.0 and variance to 1E6
=> Zero counts at step no.   3469 at 2theta/TOF/E(KeV):       22.8316  Intensity fixed to 1.0 and variance to 1E6
=> Zero counts at step no.   3470 at 2theta/TOF/E(KeV):       22.8353  Intensity fixed to 1.0 and variance to 1E6
=> Zero counts at step no.   3471 at 2theta/TOF/E(KeV):       22.8390  Intensity fixed to 1.0 and variance to 1E6
=> Zero counts at step no.   3472 at 2theta/TOF/E(KeV):       22.8427  Intensity fixed to 1.0 and variance to 1E6
=> Zero counts at step no.   3474 at 2theta/TOF/E(KeV):       22.8501  Intensity fixed to 1.0 and variance to 1E6
=> Zero counts at step no.   3477 at 2theta/TOF/E(KeV):       22.8612  Intensity fixed to 1.0 and variance to 1E6
=> Zero counts at step no.   3480 at 2theta/TOF/E(KeV):       22.8723  Intensity fixed to 1.0 and variance to 1E6
=> Zero counts at step no.   3481 at 2theta/TOF/E(KeV):       22.8760  Intensity fixed to 1.0 and variance to 1E6
=> Zero counts at step no.   3483 at 2theta/TOF/E(KeV):       22.8834  Intensity fixed to 1.0 and variance to 1E6
=> Zero counts at step no.   3485 at 2theta/TOF/E(KeV):       22.8908  Intensity fixed to 1.0 and variance to 1E6
=> Zero counts at step no.   3486 at 2theta/TOF/E(KeV):       22.8945  Intensity fixed to 1.0 and variance to 1E6
=> Zero counts at step no.   3555 at 2theta/TOF/E(KeV):       23.1498  Intensity fixed to 1.0 and variance to 1E6
=> Zero counts at step no.   3561 at 2theta/TOF/E(KeV):       23.1720  Intensity fixed to 1.0 and variance to 1E6
=> Zero counts at step no.   3563 at 2theta/TOF/E(KeV):       23.1794  Intensity fixed to 1.0 and variance to 1E6
=> Zero counts at step no.   3564 at 2theta/TOF/E(KeV):       23.1831  Intensity fixed to 1.0 and variance to 1E6
=> Zero counts at step no.   3566 at 2theta/TOF/E(KeV):       23.1905  Intensity fixed to 1.0 and variance to 1E6
```

```
=> Zero counts at step no.   3567 at 2theta/TOF/E(KeV):      23.1942  Intensity fixed to 1.0 and variance to 1E6
=> Zero counts at step no.   3569 at 2theta/TOF/E(KeV):      23.2016  Intensity fixed to 1.0 and variance to 1E6
=> Zero counts at step no.   3572 at 2theta/TOF/E(KeV):      23.2127  Intensity fixed to 1.0 and variance to 1E6
=> Zero counts at step no.   3575 at 2theta/TOF/E(KeV):      23.2238  Intensity fixed to 1.0 and variance to 1E6
=> Zero counts at step no.   3682 at 2theta/TOF/E(KeV):      23.6197  Intensity fixed to 1.0 and variance to 1E6
=> Zero counts at step no.   3687 at 2theta/TOF/E(KeV):      23.6382  Intensity fixed to 1.0 and variance to 1E6
=> Zero counts at step no.   3693 at 2theta/TOF/E(KeV):      23.6604  Intensity fixed to 1.0 and variance to 1E6
=> Zero counts at step no.   3694 at 2theta/TOF/E(KeV):      23.6641  Intensity fixed to 1.0 and variance to 1E6
=> Zero counts at step no.   3695 at 2theta/TOF/E(KeV):      23.6678  Intensity fixed to 1.0 and variance to 1E6
=> Zero counts at step no.   3703 at 2theta/TOF/E(KeV):      23.6974  Intensity fixed to 1.0 and variance to 1E6
=> Zero counts at step no.   3705 at 2theta/TOF/E(KeV):      23.7048  Intensity fixed to 1.0 and variance to 1E6
=> Zero counts at step no.   3706 at 2theta/TOF/E(KeV):      23.7085  Intensity fixed to 1.0 and variance to 1E6
=> Zero counts at step no.   3707 at 2theta/TOF/E(KeV):      23.7122  Intensity fixed to 1.0 and variance to 1E6
=> Zero counts at step no.   3710 at 2theta/TOF/E(KeV):      23.7233  Intensity fixed to 1.0 and variance to 1E6
=> Zero counts at step no.   3712 at 2theta/TOF/E(KeV):      23.7307  Intensity fixed to 1.0 and variance to 1E6
=> Zero counts at step no.   3718 at 2theta/TOF/E(KeV):      23.7529  Intensity fixed to 1.0 and variance to 1E6
=> Zero counts at step no.   3719 at 2theta/TOF/E(KeV):      23.7566  Intensity fixed to 1.0 and variance to 1E6
=> Zero counts at step no.   3722 at 2theta/TOF/E(KeV):      23.7677  Intensity fixed to 1.0 and variance to 1E6
=> Zero counts at step no.   3727 at 2theta/TOF/E(KeV):      23.7862  Intensity fixed to 1.0 and variance to 1E6
=> Zero counts at step no.   3734 at 2theta/TOF/E(KeV):      23.8121  Intensity fixed to 1.0 and variance to 1E6
=> Zero counts at step no.   3735 at 2theta/TOF/E(KeV):      23.8158  Intensity fixed to 1.0 and variance to 1E6
=> Zero counts at step no.   3744 at 2theta/TOF/E(KeV):      23.8491  Intensity fixed to 1.0 and variance to 1E6
=> Zero counts at step no.   3745 at 2theta/TOF/E(KeV):      23.8528  Intensity fixed to 1.0 and variance to 1E6
=> Zero counts at step no.   3746 at 2theta/TOF/E(KeV):      23.8565  Intensity fixed to 1.0 and variance to 1E6
=> Zero counts at step no.   3751 at 2theta/TOF/E(KeV):      23.8750  Intensity fixed to 1.0 and variance to 1E6
=> Zero counts at step no.   3766 at 2theta/TOF/E(KeV):      23.9305  Intensity fixed to 1.0 and variance to 1E6
=> Zero counts at step no.   3768 at 2theta/TOF/E(KeV):      23.9379  Intensity fixed to 1.0 and variance to 1E6
=> Zero counts at step no.   3775 at 2theta/TOF/E(KeV):      23.9638  Intensity fixed to 1.0 and variance to 1E6
=> Zero counts at step no.   3778 at 2theta/TOF/E(KeV):      23.9749  Intensity fixed to 1.0 and variance to 1E6
=> Zero counts at step no.   3781 at 2theta/TOF/E(KeV):      23.9860  Intensity fixed to 1.0 and variance to 1E6
=> Zero counts at step no.   3785 at 2theta/TOF/E(KeV):      24.0008  Intensity fixed to 1.0 and variance to 1E6
=> Zero counts at step no.   3786 at 2theta/TOF/E(KeV):      24.0045  Intensity fixed to 1.0 and variance to 1E6
=> Zero counts at step no.   3787 at 2theta/TOF/E(KeV):      24.0082  Intensity fixed to 1.0 and variance to 1E6
=> Zero counts at step no.   3790 at 2theta/TOF/E(KeV):      24.0193  Intensity fixed to 1.0 and variance to 1E6
=> Zero counts at step no.   3793 at 2theta/TOF/E(KeV):      24.0304  Intensity fixed to 1.0 and variance to 1E6
=> Zero counts at step no.   3795 at 2theta/TOF/E(KeV):      24.0378  Intensity fixed to 1.0 and variance to 1E6
=> Zero counts at step no.   3803 at 2theta/TOF/E(KeV):      24.0674  Intensity fixed to 1.0 and variance to 1E6
=> Zero counts at step no.   3807 at 2theta/TOF/E(KeV):      24.0822  Intensity fixed to 1.0 and variance to 1E6
=> Zero counts at step no.   3808 at 2theta/TOF/E(KeV):      24.0859  Intensity fixed to 1.0 and variance to 1E6
=> Zero counts at step no.   3817 at 2theta/TOF/E(KeV):      24.1192  Intensity fixed to 1.0 and variance to 1E6
=> Zero counts at step no.   3838 at 2theta/TOF/E(KeV):      24.1969  Intensity fixed to 1.0 and variance to 1E6
=> Zero counts at step no.   3844 at 2theta/TOF/E(KeV):      24.2191  Intensity fixed to 1.0 and variance to 1E6
=> Zero counts at step no.   3845 at 2theta/TOF/E(KeV):      24.2228  Intensity fixed to 1.0 and variance to 1E6
=> Zero counts at step no.   4772 at 2theta/TOF/E(KeV):      27.6527  Intensity fixed to 1.0 and variance to 1E6
=> Zero counts at step no.   4778 at 2theta/TOF/E(KeV):      27.6749  Intensity fixed to 1.0 and variance to 1E6
=> Zero counts at step no.   4799 at 2theta/TOF/E(KeV):      27.7526  Intensity fixed to 1.0 and variance to 1E6
=> Zero counts at step no.   4806 at 2theta/TOF/E(KeV):      27.7785  Intensity fixed to 1.0 and variance to 1E6
=> Zero counts at step no.   4816 at 2theta/TOF/E(KeV):      27.8155  Intensity fixed to 1.0 and variance to 1E6
=> Zero counts at step no.   4818 at 2theta/TOF/E(KeV):      27.8229  Intensity fixed to 1.0 and variance to 1E6
=> Zero counts at step no.   4819 at 2theta/TOF/E(KeV):      27.8266  Intensity fixed to 1.0 and variance to 1E6
=> Zero counts at step no.   4823 at 2theta/TOF/E(KeV):      27.8414  Intensity fixed to 1.0 and variance to 1E6
=> Zero counts at step no.   4830 at 2theta/TOF/E(KeV):      27.8673  Intensity fixed to 1.0 and variance to 1E6
=> Zero counts at step no.   4839 at 2theta/TOF/E(KeV):      27.9006  Intensity fixed to 1.0 and variance to 1E6
=> Zero counts at step no.   4856 at 2theta/TOF/E(KeV):      27.9635  Intensity fixed to 1.0 and variance to 1E6
=> Zero counts at step no.   4857 at 2theta/TOF/E(KeV):      27.9672  Intensity fixed to 1.0 and variance to 1E6
=> Zero counts at step no.   4862 at 2theta/TOF/E(KeV):      27.9857  Intensity fixed to 1.0 and variance to 1E6
=> Zero counts at step no.   4865 at 2theta/TOF/E(KeV):      27.9968  Intensity fixed to 1.0 and variance to 1E6
=> Zero counts at step no.   4866 at 2theta/TOF/E(KeV):      28.0005  Intensity fixed to 1.0 and variance to 1E6
=> Zero counts at step no.   4872 at 2theta/TOF/E(KeV):      28.0227  Intensity fixed to 1.0 and variance to 1E6
=> Zero counts at step no.   4874 at 2theta/TOF/E(KeV):      28.0301  Intensity fixed to 1.0 and variance to 1E6
=> Zero counts at step no.   4876 at 2theta/TOF/E(KeV):      28.0375  Intensity fixed to 1.0 and variance to 1E6
=> Zero counts at step no.   4879 at 2theta/TOF/E(KeV):      28.0486  Intensity fixed to 1.0 and variance to 1E6
=> Zero counts at step no.   4884 at 2theta/TOF/E(KeV):      28.0671  Intensity fixed to 1.0 and variance to 1E6
=> Zero counts at step no.   4885 at 2theta/TOF/E(KeV):      28.0708  Intensity fixed to 1.0 and variance to 1E6
=> Zero counts at step no.   4890 at 2theta/TOF/E(KeV):      28.0893  Intensity fixed to 1.0 and variance to 1E6
=> Zero counts at step no.   4891 at 2theta/TOF/E(KeV):      28.0930  Intensity fixed to 1.0 and variance to 1E6
=> Zero counts at step no.   4893 at 2theta/TOF/E(KeV):      28.1004  Intensity fixed to 1.0 and variance to 1E6
=> Zero counts at step no.   4894 at 2theta/TOF/E(KeV):      28.1041  Intensity fixed to 1.0 and variance to 1E6
=> Zero counts at step no.   4900 at 2theta/TOF/E(KeV):      28.1263  Intensity fixed to 1.0 and variance to 1E6
=> Zero counts at step no.   4901 at 2theta/TOF/E(KeV):      28.1300  Intensity fixed to 1.0 and variance to 1E6
=> Zero counts at step no.   4907 at 2theta/TOF/E(KeV):      28.1522  Intensity fixed to 1.0 and variance to 1E6
=> Zero counts at step no.   4913 at 2theta/TOF/E(KeV):      28.1744  Intensity fixed to 1.0 and variance to 1E6
=> Zero counts at step no.   4916 at 2theta/TOF/E(KeV):      28.1855  Intensity fixed to 1.0 and variance to 1E6
=> Zero counts at step no.   5336 at 2theta/TOF/E(KeV):      29.7395  Intensity fixed to 1.0 and variance to 1E6
=> Zero counts at step no.   5355 at 2theta/TOF/E(KeV):      29.8098  Intensity fixed to 1.0 and variance to 1E6
=> Zero counts at step no.   5357 at 2theta/TOF/E(KeV):      29.8172  Intensity fixed to 1.0 and variance to 1E6
=> Zero counts at step no.   5359 at 2theta/TOF/E(KeV):      29.8246  Intensity fixed to 1.0 and variance to 1E6
=> Zero counts at step no.   5362 at 2theta/TOF/E(KeV):      29.8357  Intensity fixed to 1.0 and variance to 1E6
=> Zero counts at step no.   5373 at 2theta/TOF/E(KeV):      29.8764  Intensity fixed to 1.0 and variance to 1E6
=> Zero counts at step no.   5374 at 2theta/TOF/E(KeV):      29.8801  Intensity fixed to 1.0 and variance to 1E6
=> Zero counts at step no.   5375 at 2theta/TOF/E(KeV):      29.8838  Intensity fixed to 1.0 and variance to 1E6
=> Zero counts at step no.   5385 at 2theta/TOF/E(KeV):      29.9208  Intensity fixed to 1.0 and variance to 1E6
=> Zero counts at step no.   5386 at 2theta/TOF/E(KeV):      29.9245  Intensity fixed to 1.0 and variance to 1E6
=> Zero counts at step no.   5389 at 2theta/TOF/E(KeV):      29.9356  Intensity fixed to 1.0 and variance to 1E6
=> Zero counts at step no.   5391 at 2theta/TOF/E(KeV):      29.9430  Intensity fixed to 1.0 and variance to 1E6
=> Zero counts at step no.   5392 at 2theta/TOF/E(KeV):      29.9467  Intensity fixed to 1.0 and variance to 1E6
=> Zero counts at step no.   5393 at 2theta/TOF/E(KeV):      29.9504  Intensity fixed to 1.0 and variance to 1E6
=> Zero counts at step no.   5394 at 2theta/TOF/E(KeV):      29.9541  Intensity fixed to 1.0 and variance to 1E6
=> Zero counts at step no.   5398 at 2theta/TOF/E(KeV):      29.9689  Intensity fixed to 1.0 and variance to 1E6
=> Zero counts at step no.   5400 at 2theta/TOF/E(KeV):      29.9763  Intensity fixed to 1.0 and variance to 1E6
```

```
=> Zero counts at step no.   5402 at 2theta/TOF/E(KeV):       29.9837  Intensity fixed to 1.0 and variance to 1E6
=> Zero counts at step no.   5403 at 2theta/TOF/E(KeV):       29.9874  Intensity fixed to 1.0 and variance to 1E6
=> Zero counts at step no.   5405 at 2theta/TOF/E(KeV):       29.9948  Intensity fixed to 1.0 and variance to 1E6
=> Zero counts at step no.   5408 at 2theta/TOF/E(KeV):       30.0059  Intensity fixed to 1.0 and variance to 1E6
=> Zero counts at step no.   5409 at 2theta/TOF/E(KeV):       30.0096  Intensity fixed to 1.0 and variance to 1E6
=> Zero counts at step no.   5410 at 2theta/TOF/E(KeV):       30.0133  Intensity fixed to 1.0 and variance to 1E6
=> Zero counts at step no.   5422 at 2theta/TOF/E(KeV):       30.0577  Intensity fixed to 1.0 and variance to 1E6
=> Zero counts at step no.   6360 at 2theta/TOF/E(KeV):       33.5283  Intensity fixed to 1.0 and variance to 1E6
=> Zero counts at step no.   6362 at 2theta/TOF/E(KeV):       33.5357  Intensity fixed to 1.0 and variance to 1E6
=> Zero counts at step no.   6364 at 2theta/TOF/E(KeV):       33.5431  Intensity fixed to 1.0 and variance to 1E6
=> Zero counts at step no.   6426 at 2theta/TOF/E(KeV):       33.7725  Intensity fixed to 1.0 and variance to 1E6
=> Zero counts at step no.   6436 at 2theta/TOF/E(KeV):       33.8095  Intensity fixed to 1.0 and variance to 1E6
=> Zero counts at step no.   6438 at 2theta/TOF/E(KeV):       33.8169  Intensity fixed to 1.0 and variance to 1E6
=> Zero counts at step no.   6442 at 2theta/TOF/E(KeV):       33.8317  Intensity fixed to 1.0 and variance to 1E6
=> Zero counts at step no.   6443 at 2theta/TOF/E(KeV):       33.8354  Intensity fixed to 1.0 and variance to 1E6
=> Zero counts at step no.   6445 at 2theta/TOF/E(KeV):       33.8428  Intensity fixed to 1.0 and variance to 1E6
=> Zero counts at step no.   6446 at 2theta/TOF/E(KeV):       33.8465  Intensity fixed to 1.0 and variance to 1E6
=> Zero counts at step no.   6447 at 2theta/TOF/E(KeV):       33.8502  Intensity fixed to 1.0 and variance to 1E6
=> Zero counts at step no.   6550 at 2theta/TOF/E(KeV):       34.2313  Intensity fixed to 1.0 and variance to 1E6
=> Zero counts at step no.   6554 at 2theta/TOF/E(KeV):       34.2461  Intensity fixed to 1.0 and variance to 1E6
=> Zero counts at step no.   6556 at 2theta/TOF/E(KeV):       34.2535  Intensity fixed to 1.0 and variance to 1E6
=> Zero counts at step no.   6558 at 2theta/TOF/E(KeV):       34.2609  Intensity fixed to 1.0 and variance to 1E6
=> Zero counts at step no.   6560 at 2theta/TOF/E(KeV):       34.2683  Intensity fixed to 1.0 and variance to 1E6
=> Zero counts at step no.   6561 at 2theta/TOF/E(KeV):       34.2720  Intensity fixed to 1.0 and variance to 1E6
=> Zero counts at step no.   6562 at 2theta/TOF/E(KeV):       34.2757  Intensity fixed to 1.0 and variance to 1E6
=> Zero counts at step no.   6565 at 2theta/TOF/E(KeV):       34.2868  Intensity fixed to 1.0 and variance to 1E6
=> Zero counts at step no.   6566 at 2theta/TOF/E(KeV):       34.2905  Intensity fixed to 1.0 and variance to 1E6
=> Zero counts at step no.   6571 at 2theta/TOF/E(KeV):       34.3090  Intensity fixed to 1.0 and variance to 1E6
=> Zero counts at step no.   6573 at 2theta/TOF/E(KeV):       34.3164  Intensity fixed to 1.0 and variance to 1E6
=> Zero counts at step no.   6575 at 2theta/TOF/E(KeV):       34.3238  Intensity fixed to 1.0 and variance to 1E6
=> Zero counts at step no.   6577 at 2theta/TOF/E(KeV):       34.3312  Intensity fixed to 1.0 and variance to 1E6
=> Zero counts at step no.   6582 at 2theta/TOF/E(KeV):       34.3497  Intensity fixed to 1.0 and variance to 1E6
=> Zero counts at step no.   6585 at 2theta/TOF/E(KeV):       34.3608  Intensity fixed to 1.0 and variance to 1E6
=> Zero counts at step no.   6587 at 2theta/TOF/E(KeV):       34.3682  Intensity fixed to 1.0 and variance to 1E6
=> Zero counts at step no.   6589 at 2theta/TOF/E(KeV):       34.3756  Intensity fixed to 1.0 and variance to 1E6
=> Zero counts at step no.   6594 at 2theta/TOF/E(KeV):       34.3941  Intensity fixed to 1.0 and variance to 1E6
=> Zero counts at step no.   6604 at 2theta/TOF/E(KeV):       34.4311  Intensity fixed to 1.0 and variance to 1E6
=> Zero counts at step no.   6607 at 2theta/TOF/E(KeV):       34.4422  Intensity fixed to 1.0 and variance to 1E6
=> Zero counts at step no.   6867 at 2theta/TOF/E(KeV):       35.4042  Intensity fixed to 1.0 and variance to 1E6
=> Zero counts at step no.   6885 at 2theta/TOF/E(KeV):       35.4708  Intensity fixed to 1.0 and variance to 1E6
=> Zero counts at step no.   7019 at 2theta/TOF/E(KeV):       35.9666  Intensity fixed to 1.0 and variance to 1E6
=> Zero counts at step no.   7034 at 2theta/TOF/E(KeV):       36.0221  Intensity fixed to 1.0 and variance to 1E6
=> Zero counts at step no.   7036 at 2theta/TOF/E(KeV):       36.0295  Intensity fixed to 1.0 and variance to 1E6
=> Zero counts at step no.   7040 at 2theta/TOF/E(KeV):       36.0443  Intensity fixed to 1.0 and variance to 1E6
=> Zero counts at step no.   7045 at 2theta/TOF/E(KeV):       36.0628  Intensity fixed to 1.0 and variance to 1E6
=> Zero counts at step no.   7046 at 2theta/TOF/E(KeV):       36.0665  Intensity fixed to 1.0 and variance to 1E6
=> Zero counts at step no.   7047 at 2theta/TOF/E(KeV):       36.0702  Intensity fixed to 1.0 and variance to 1E6
=> Zero counts at step no.   7050 at 2theta/TOF/E(KeV):       36.0813  Intensity fixed to 1.0 and variance to 1E6
=> Zero counts at step no.   7051 at 2theta/TOF/E(KeV):       36.0850  Intensity fixed to 1.0 and variance to 1E6
=> Zero counts at step no.   7055 at 2theta/TOF/E(KeV):       36.0998  Intensity fixed to 1.0 and variance to 1E6
=> Zero counts at step no.   7056 at 2theta/TOF/E(KeV):       36.1035  Intensity fixed to 1.0 and variance to 1E6
=> Zero counts at step no.   7057 at 2theta/TOF/E(KeV):       36.1072  Intensity fixed to 1.0 and variance to 1E6
=> Zero counts at step no.   7059 at 2theta/TOF/E(KeV):       36.1146  Intensity fixed to 1.0 and variance to 1E6
=> Zero counts at step no.   7060 at 2theta/TOF/E(KeV):       36.1183  Intensity fixed to 1.0 and variance to 1E6
=> Zero counts at step no.   7068 at 2theta/TOF/E(KeV):       36.1479  Intensity fixed to 1.0 and variance to 1E6
=> Zero counts at step no.   7069 at 2theta/TOF/E(KeV):       36.1516  Intensity fixed to 1.0 and variance to 1E6
=> Zero counts at step no.   7072 at 2theta/TOF/E(KeV):       36.1627  Intensity fixed to 1.0 and variance to 1E6
=> Zero counts at step no.   7075 at 2theta/TOF/E(KeV):       36.1738  Intensity fixed to 1.0 and variance to 1E6
=> Zero counts at step no.   7079 at 2theta/TOF/E(KeV):       36.1886  Intensity fixed to 1.0 and variance to 1E6
=> Zero counts at step no.   7080 at 2theta/TOF/E(KeV):       36.1923  Intensity fixed to 1.0 and variance to 1E6
=> Zero counts at step no.   7082 at 2theta/TOF/E(KeV):       36.1997  Intensity fixed to 1.0 and variance to 1E6
=> Zero counts at step no.   7089 at 2theta/TOF/E(KeV):       36.2256  Intensity fixed to 1.0 and variance to 1E6
=> Zero counts at step no.   7096 at 2theta/TOF/E(KeV):       36.2515  Intensity fixed to 1.0 and variance to 1E6
=> Zero counts at step no.   7098 at 2theta/TOF/E(KeV):       36.2589  Intensity fixed to 1.0 and variance to 1E6
=> Zero counts at step no.   7101 at 2theta/TOF/E(KeV):       36.2700  Intensity fixed to 1.0 and variance to 1E6
=> Zero counts at step no.   7102 at 2theta/TOF/E(KeV):       36.2737  Intensity fixed to 1.0 and variance to 1E6
=> Zero counts at step no.   7103 at 2theta/TOF/E(KeV):       36.2774  Intensity fixed to 1.0 and variance to 1E6
=> Zero counts at step no.   7105 at 2theta/TOF/E(KeV):       36.2848  Intensity fixed to 1.0 and variance to 1E6
=> Zero counts at step no.   7117 at 2theta/TOF/E(KeV):       36.3292  Intensity fixed to 1.0 and variance to 1E6
=> Zero counts at step no.   7123 at 2theta/TOF/E(KeV):       36.3514  Intensity fixed to 1.0 and variance to 1E6
=> Zero counts at step no.   7126 at 2theta/TOF/E(KeV):       36.3625  Intensity fixed to 1.0 and variance to 1E6
=> Zero counts at step no.   7129 at 2theta/TOF/E(KeV):       36.3736  Intensity fixed to 1.0 and variance to 1E6
=> Zero counts at step no.   7134 at 2theta/TOF/E(KeV):       36.3921  Intensity fixed to 1.0 and variance to 1E6
=> Zero counts at step no.   7365 at 2theta/TOF/E(KeV):       37.2468  Intensity fixed to 1.0 and variance to 1E6
=> Zero counts at step no.   7698 at 2theta/TOF/E(KeV):       38.4789  Intensity fixed to 1.0 and variance to 1E6
=> Zero counts at step no.   7710 at 2theta/TOF/E(KeV):       38.5233  Intensity fixed to 1.0 and variance to 1E6
=> Zero counts at step no.   7715 at 2theta/TOF/E(KeV):       38.5418  Intensity fixed to 1.0 and variance to 1E6
=> Zero counts at step no.   7716 at 2theta/TOF/E(KeV):       38.5455  Intensity fixed to 1.0 and variance to 1E6
=> Zero counts at step no.   7717 at 2theta/TOF/E(KeV):       38.5492  Intensity fixed to 1.0 and variance to 1E6
=> Zero counts at step no.   7743 at 2theta/TOF/E(KeV):       38.6454  Intensity fixed to 1.0 and variance to 1E6
=> Zero counts at step no.   7807 at 2theta/TOF/E(KeV):       38.8822  Intensity fixed to 1.0 and variance to 1E6
=> Zero counts at step no.   7840 at 2theta/TOF/E(KeV):       39.0043  Intensity fixed to 1.0 and variance to 1E6
=> Zero counts at step no.  10685 at 2theta/TOF/E(KeV):       49.5308  Intensity fixed to 1.0 and variance to 1E6

=> Optimizations for routine tasks applied:
=> Calculation mode for patter#:   1  CM_PSEUDO_VOIGT

=> Lorentzian FWHM < 0 at 2theta:   17.921 for phase no.    1 -> Fixing to HL=1.0e-10
=> Lorentzian FWHM < 0 at 2theta:   17.966 for phase no.    1 -> Fixing to HL=1.0e-10
=> Lorentzian FWHM < 0 at 2theta:   17.921 for phase no.    1 -> Fixing to HL=1.0e-10
```

```
=> Lorentzian FWHM < 0 at 2theta:   17.966 for phase no.    1 -> Fixing to HL=1.0e-10
=> Lorentzian FWHM < 0 at 2theta:   17.921 for phase no.    1 -> Fixing to HL=1.0e-10
=> Lorentzian FWHM < 0 at 2theta:   17.965 for phase no.    1 -> Fixing to HL=1.0e-10
=> Lorentzian FWHM < 0 at 2theta:   17.920 for phase no.    1 -> Fixing to HL=1.0e-10
=> Lorentzian FWHM < 0 at 2theta:   17.965 for phase no.    1 -> Fixing to HL=1.0e-10
=> Lorentzian FWHM < 0 at 2theta:   17.920 for phase no.    1 -> Fixing to HL=1.0e-10
=> Lorentzian FWHM < 0 at 2theta:   17.965 for phase no.    1 -> Fixing to HL=1.0e-10
=> Lorentzian FWHM < 0 at 2theta:   17.920 for phase no.    1 -> Fixing to HL=1.0e-10
=> Lorentzian FWHM < 0 at 2theta:   17.965 for phase no.    1 -> Fixing to HL=1.0e-10
=> Lorentzian FWHM < 0 at 2theta:   17.920 for phase no.    1 -> Fixing to HL=1.0e-10
=> Lorentzian FWHM < 0 at 2theta:   17.965 for phase no.    1 -> Fixing to HL=1.0e-10
=> Lorentzian FWHM < 0 at 2theta:   17.920 for phase no.    1 -> Fixing to HL=1.0e-10
=> Lorentzian FWHM < 0 at 2theta:   17.965 for phase no.    1 -> Fixing to HL=1.0e-10
=> Lorentzian FWHM < 0 at 2theta:   17.920 for phase no.    1 -> Fixing to HL=1.0e-10
=> Lorentzian FWHM < 0 at 2theta:   17.965 for phase no.    1 -> Fixing to HL=1.0e-10
=> Lorentzian FWHM < 0 at 2theta:   17.920 for phase no.    1 -> Fixing to HL=1.0e-10
=> Lorentzian FWHM < 0 at 2theta:   17.965 for phase no.    1 -> Fixing to HL=1.0e-10
=> Lorentzian FWHM < 0 at 2theta:   17.920 for phase no.    1 -> Fixing to HL=1.0e-10
=> Lorentzian FWHM < 0 at 2theta:   17.965 for phase no.    1 -> Fixing to HL=1.0e-10
=> Lorentzian FWHM < 0 at 2theta:   17.920 for phase no.    1 -> Fixing to HL=1.0e-10
=> Lorentzian FWHM < 0 at 2theta:   17.965 for phase no.    1 -> Fixing to HL=1.0e-10
=> Lorentzian FWHM < 0 at 2theta:   17.920 for phase no.    1 -> Fixing to HL=1.0e-10
=> Lorentzian FWHM < 0 at 2theta:   17.965 for phase no.    1 -> Fixing to HL=1.0e-10
=> Lorentzian FWHM < 0 at 2theta:   17.920 for phase no.    1 -> Fixing to HL=1.0e-10
=> Lorentzian FWHM < 0 at 2theta:   17.965 for phase no.    1 -> Fixing to HL=1.0e-10
=> Lorentzian FWHM < 0 at 2theta:   17.920 for phase no.    1 -> Fixing to HL=1.0e-10
=> Lorentzian FWHM < 0 at 2theta:   17.965 for phase no.    1 -> Fixing to HL=1.0e-10
=> Lorentzian FWHM < 0 at 2theta:   17.920 for phase no.    1 -> Fixing to HL=1.0e-10
=> Lorentzian FWHM < 0 at 2theta:   17.965 for phase no.    1 -> Fixing to HL=1.0e-10
=> Lorentzian FWHM < 0 at 2theta:   17.920 for phase no.    1 -> Fixing to HL=1.0e-10
=> Lorentzian FWHM < 0 at 2theta:   17.965 for phase no.    1 -> Fixing to HL=1.0e-10
=> Lorentzian FWHM < 0 at 2theta:   17.920 for phase no.    1 -> Fixing to HL=1.0e-10
=> Lorentzian FWHM < 0 at 2theta:   17.965 for phase no.    1 -> Fixing to HL=1.0e-10
=> Lorentzian FWHM < 0 at 2theta:   17.920 for phase no.    1 -> Fixing to HL=1.0e-10
=> Lorentzian FWHM < 0 at 2theta:   17.964 for phase no.    1 -> Fixing to HL=1.0e-10
=> Lorentzian FWHM < 0 at 2theta:   17.920 for phase no.    1 -> Fixing to HL=1.0e-10
=> Lorentzian FWHM < 0 at 2theta:   17.965 for phase no.    1 -> Fixing to HL=1.0e-10
=> Lorentzian FWHM < 0 at 2theta:   17.920 for phase no.    1 -> Fixing to HL=1.0e-10
=> Lorentzian FWHM < 0 at 2theta:   17.964 for phase no.    1 -> Fixing to HL=1.0e-10
=> Lorentzian FWHM < 0 at 2theta:   17.920 for phase no.    1 -> Fixing to HL=1.0e-10
=> Lorentzian FWHM < 0 at 2theta:   17.965 for phase no.    1 -> Fixing to HL=1.0e-10
=> Lorentzian FWHM < 0 at 2theta:   17.920 for phase no.    1 -> Fixing to HL=1.0e-10
=> Lorentzian FWHM < 0 at 2theta:   17.965 for phase no.    1 -> Fixing to HL=1.0e-10
=> Lorentzian FWHM < 0 at 2theta:   17.920 for phase no.    1 -> Fixing to HL=1.0e-10
=> Lorentzian FWHM < 0 at 2theta:   17.965 for phase no.    1 -> Fixing to HL=1.0e-10
=> Lorentzian FWHM < 0 at 2theta:   17.920 for phase no.    1 -> Fixing to HL=1.0e-10
=> Lorentzian FWHM < 0 at 2theta:   17.965 for phase no.    1 -> Fixing to HL=1.0e-10
=> Lorentzian FWHM < 0 at 2theta:   17.920 for phase no.    1 -> Fixing to HL=1.0e-10
=> Lorentzian FWHM < 0 at 2theta:   17.965 for phase no.    1 -> Fixing to HL=1.0e-10
=> Lorentzian FWHM < 0 at 2theta:   17.920 for phase no.    1 -> Fixing to HL=1.0e-10
=> Lorentzian FWHM < 0 at 2theta:   17.965 for phase no.    1 -> Fixing to HL=1.0e-10
=> Lorentzian FWHM < 0 at 2theta:   17.920 for phase no.    1 -> Fixing to HL=1.0e-10
=> Lorentzian FWHM < 0 at 2theta:   17.965 for phase no.    1 -> Fixing to HL=1.0e-10
=> Lorentzian FWHM < 0 at 2theta:   17.920 for phase no.    1 -> Fixing to HL=1.0e-10
=> Lorentzian FWHM < 0 at 2theta:   17.965 for phase no.    1 -> Fixing to HL=1.0e-10
=> Lorentzian FWHM < 0 at 2theta:   17.920 for phase no.    1 -> Fixing to HL=1.0e-10
=> Lorentzian FWHM < 0 at 2theta:   17.965 for phase no.    1 -> Fixing to HL=1.0e-10
=> Lorentzian FWHM < 0 at 2theta:   17.920 for phase no.    1 -> Fixing to HL=1.0e-10
=> Lorentzian FWHM < 0 at 2theta:   17.965 for phase no.    1 -> Fixing to HL=1.0e-10
=> Lorentzian FWHM < 0 at 2theta:   17.920 for phase no.    1 -> Fixing to HL=1.0e-10
=> Lorentzian FWHM < 0 at 2theta:   17.965 for phase no.    1 -> Fixing to HL=1.0e-10
=> Lorentzian FWHM < 0 at 2theta:   17.920 for phase no.    1 -> Fixing to HL=1.0e-10
=> Lorentzian FWHM < 0 at 2theta:   17.965 for phase no.    1 -> Fixing to HL=1.0e-10


Standard deviations have to be multiplied by:15.9393
(correlated residuals) See references:
-J.F.Berar & P.Lelann, J. Appl. Cryst. 24, 1-5 (1991)
-J.F.Berar, Acc. in Pow. Diff. II,NIST Sp.Pub. 846, 63(1992)

++++++++++++++++++++++++++++++++++++++++++++++++++++++++++++++++++++++++++++++++++++++++++++++++++++++++++++++++++++++++++++++++++++++++++++++ ↙


=> CYCLE No.:   50
-------------------------------------------------------------------------------
=> Phase  1 Name:   rdx
-------------------------------------------------------------------------------
=> New parameters, shifts, and standard deviations

Atom        x       dx      sx       y       dy      sy       z       dz      sz       B       dB      sB      occ.  ↙
        docc.   socc.

O(1)     0.57031-0.00006 0.00051  0.44054-0.00055 0.00058  0.26807 0.00048 0.00054  3.70830 0.00000 0.00000    ↙
    1.00000 0.00000 0.00000
O(2)     0.59822-0.00031 0.00059  0.23070 0.00064 0.00058  0.22522 0.00040 0.00052  4.41110 0.00000 0.00000    ↙
    1.00000 0.00000 0.00000
O(3)     0.47699 0.00009 0.00058  0.13120 0.00018 0.00053 -0.01647 0.00023 0.00051  4.98480 0.00000 0.00000    ↙
    1.00000 0.00000 0.00000
```

```
O(4)     0.34889-0.00020 0.00060  0.25899 0.00047 0.00067 -0.11069 0.00089 0.00058  4.76640 0.00000 0.00000    ↙
     1.00000 0.00000 0.00000
O(5)     0.30778-0.00041 0.00055  0.51705 0.00000 0.00064 -0.07906 0.00024 0.00050  5.32170 0.00000 0.00000    ↙
     1.00000 0.00000 0.00000
O(6)     0.42722 0.00009 0.00051  0.60061 0.00022 0.00075  0.05273 0.00019 0.00053  5.10850 0.00000 0.00000    ↙
     1.00000 0.00000 0.00000
N(1)     0.44409-0.00072 0.00076  0.33100 0.00024 0.00099  0.17287-0.00033 0.00062  2.73980 0.00000 0.00000    ↙
     1.00000 0.00000 0.00000
N(2)     0.32742 0.00057 0.00094  0.23491 0.00001 0.00089  0.05328 0.00024 0.00072  2.40240 0.00000 0.00000    ↙
     1.00000 0.00000 0.00000
N(3)     0.30725 0.00026 0.00086  0.45634 0.00035 0.00082  0.08289 0.00044 0.00067  2.59240 0.00000 0.00000    ↙
     1.00000 0.00000 0.00000
N(4)     0.53933-0.00008 0.00068  0.33542 0.00005 0.00070  0.23515-0.00027 0.00068  2.76530 0.00000 0.00000    ↙
     1.00000 0.00000 0.00000
N(5)     0.38598-0.00021 0.00079  0.20331-0.00051 0.00092 -0.04141-0.00031 0.00080  3.09700 0.00000 0.00000    ↙
     1.00000 0.00000 0.00000
N(6)     0.35495 0.00025 0.00069  0.54361-0.00009 0.00092  0.00991-0.00094 0.00079  3.43200 0.00000 0.00000    ↙
     1.00000 0.00000 0.00000
C(1)     0.34679-0.00010 0.00085  0.43854 0.00078 0.00093  0.19868 0.00007 0.00074  2.89510 0.00000 0.00000    ↙
     1.00000 0.00000 0.00000
C(2)     0.38559-0.00019 0.00087  0.21305-0.00041 0.00094  0.15540 0.00145 0.00097  2.70030 0.00000 0.00000    ↙
     1.00000 0.00000 0.00000
C(3)     0.23576 0.00017 0.00071  0.34062-0.00031 0.00131  0.05232-0.00037 0.00063  2.55740 0.00000 0.00000    ↙
     1.00000 0.00000 0.00000
H(1A)    0.40289 0.00000 0.00000  0.52403 0.00000 0.00000  0.20773 0.00000 0.00000  5.13220 0.00000 0.00000    ↙
     1.00000 0.00000 0.00000
H(1B)    0.29071 0.00000 0.00000  0.42024 0.00000 0.00000  0.23991 0.00000 0.00000  4.84270 0.00000 0.00000    ↙
     1.00000 0.00000 0.00000
H(2A)    0.44331 0.00000 0.00000  0.13918 0.00000 0.00000  0.14950 0.00000 0.00000  4.60580 0.00000 0.00000    ↙
     1.00000 0.00000 0.00000
H(2B)    0.31742 0.00000 0.00000  0.19390 0.00000 0.00000  0.20730 0.00000 0.00000  4.97430 0.00000 0.00000    ↙
     1.00000 0.00000 0.00000
H(3A)    0.20936 0.00000 0.00000  0.35364 0.00000 0.00000 -0.02527 0.00000 0.00000  4.50050 0.00000 0.00000    ↙
     1.00000 0.00000 0.00000
H(3B)    0.17213 0.00000 0.00000  0.32091 0.00000 0.00000  0.10070 0.00000 0.00000  3.92150 0.00000 0.00000    ↙
     1.00000 0.00000 0.00000

==> PROFILE PARAMETERS FOR PATTERN#  1

=> Overall scale factor:      0.003677659    -0.000000780     0.000011493
=> Eta(p-Voigt) or m(Pearson VII):   0.000000  0.000000  0.000000
=> Overall tem. factor:   0.000000  0.000000  0.000000
=> Halfwidth parameters:
0.014150  0.000261  0.003446
0.000000  0.000000  0.000000
0.000000  0.000000  0.000000
=> Cell parameters:
11.557671   0.000021   0.000273
10.676690   0.000017   0.000281
13.141932   0.000026   0.000305
90.000000   0.000000   0.000000
90.000000   0.000000   0.000000
90.000000   0.000000   0.000000
=> Preferred orientation:
1.000000  0.000000  0.000000
0.000000  0.000000  0.000000
=> Asymmetry parameters:
0.165592 -0.000072  0.008782
0.053462 -0.000027  0.001781
0.000000  0.000000  0.000000
0.000000  0.000000  0.000000
=> X and Y parameters:
0.000000  0.000000  0.000000
0.000000  0.000000  0.000000
=> Strain parameters:
0.000000  0.000000  0.000000
0.000000  0.000000  0.000000
0.000000  0.000000  0.000000
=> Size   parameters (G,L):
0.012007 -0.000010  0.000086
-0.025048  0.000745  0.004665
=> Further shape parameters (S_L and D_L):
0.000000  0.000000  0.000000
0.000000  0.000000  0.000000

=> Spherical Harmonics coeff.(size):

-0.025048      0.000745      0.004665       0.019418     -0.001630      0.013391       0.197667      0.002007       ↙
     0.010955
0.210143      0.000007      0.013803      -0.039622     -0.001868      0.013335       0.019753      0.000117       ↙
     0.011426
0.000000      0.000000      0.000000       0.000000      0.000000      0.000000       0.000000      0.000000       ↙
     0.000000

==> GLOBAL PARAMETERS FOR PATTERN#  1


=> Zero-point:    -0.2154    0.0001    0.0022
=> Background Polynomial Parameters ==>
0.11847E+06  0.0000      0.0000
```

```
0.72376E+06  0.0000      0.0000
-47087.      0.0000      0.0000
-0.18536E+07  0.0000      0.0000
-0.14029E+07  0.0000      0.0000
-35943.      0.0000      0.0000

=> Cos( theta)-shift parameter :   0.0000  0.0000  0.0000
=> Sin(2theta)-shift parameter :   0.0000  0.0000  0.0000

==> RELIABILITY FACTORS WITH ALL NON-EXCLUDED POINTS FOR PATTERN:  1

=> R-Factors:   14.1      23.3     Chi2:  263.     DW-Stat.:  0.3668   Patt#:  1
=> Expected :            1.44                              1.9515
=> Deviance : 0.530E+07     Dev*:   0.000
=> GoF-index:  16.         Sqrt(Residual/N)
=> N-P+C: 10751

=>    SumYdif       SumYobs      SumYcal      SumwYobsSQ     Residual    Condition
0.7320E+07    0.5204E+08    0.4932E+08    0.5204E+08    0.2830E+07    0.9401E+11


=> Conventional Rietveld Rp,Rwp,Re and Chi2:   14.1      23.3      1.44      263.3
=> (Values obtained using Ynet, but true sigma(y))
=>  SumYnet, Sum(w Ynet**2):     0.5204E+08    0.5204E+08

=> N-sigma of the GoF: ********

==> RELIABILITY FACTORS FOR POINTS WITH BRAGG CONTRIBUTIONS FOR PATTERN:  1

=> R-Factors:   14.1      23.3     Chi2:  264.     DW-Stat.:  0.3676   Patt#:
=> Expected :            1.43                              1.9515
=> Deviance : 0.530E+07     Dev*:         NaN
=> GoF-index:  16.         Sqrt(Residual/N)
=> N-P+C: 10703

=>    SumYdif       SumYobs      SumYcal      SumwYobsSQ     Residual    Condition
0.7314E+07    0.5204E+08    0.4932E+08    0.5203E+08    0.2825E+07    0.9401E+11


=> Conventional Rietveld Rp,Rwp,Re and Chi2:   14.1      23.3      1.43      263.9
=> (Values obtained using Ynet, but true sigma(y))
=>  SumYnet, Sum(w Ynet**2):     0.5204E+08    0.5203E+08

=> N-sigma of the GoF:    19232.480

=> Global user-weigthed Chi2 (Bragg contrib.):   264.

-------------------------------------------------------------------------------------------------------------------
Pattern#  1 Phase No:   1 Phase name:   rdx
-------------------------------------------------------------------------------------------------------------------

No.  Code     H   K   L  Mult     Hw         2theta      Icalc       Iobs      Sigma      HwG     HwL        ETA   ↙
          d-hkl        CORR

1   1      1   1   1     8  0.125905      13.135     7400.6     7435.7     37.146  0.125352  0.001030  0.011141    ↙
     6.734526    599.986450
2   1      0   0   2     2  0.135719      13.464     3914.7     4242.5    359.647  0.125367  0.019245  0.184427    ↙
     6.570953    142.453094
3   1      2   0   0     2  0.138997      15.320      432.2      496.0     73.923  0.125491  0.024955  0.230516    ↙
     5.778825    109.673416
4   1      1   0   2     4  0.130631      15.499     3895.5     3969.7     77.041  0.125506  0.009575  0.097605    ↙
     5.712286    214.182709
5   1      0   2   0     2  0.125689      16.593     2391.2     2407.5     16.614  0.125610  0.000147  0.001592    ↙
     5.338336     93.177208
6   1      2   1   0     4  0.135834      17.435     6610.1     6821.9    220.092  0.125705  0.018840  0.180585    ↙
     5.082146    168.343307
7   1      1   1   2     8  0.128285      17.594      890.0      967.3     84.113  0.125724  0.004778  0.050219    ↙
     5.036711    330.477875
8   1      0   2   1     4  0.125765      17.920     9551.0     9544.6      8.160  0.125765  0.000000  0.000001    ↙
     4.945864    159.142273
9   1      2   1   1     8  0.133015      18.705       87.1       108.7     29.086  0.125870  0.013337  0.132278    ↙
     4.740059    291.393860
10   1      1   2   1     8  0.127286      19.506       72.3       65.2     11.936  0.125990  0.002413  0.025729    ↙
     4.547022    267.251007
11   1      2   0   2     4  0.131441      20.449     6928.3     7170.5    251.909  0.126144  0.009894  0.100171    ↙
     4.339426    121.185120
12   1      0   2   2     4  0.126957      21.428      478.9      532.6     59.672  0.126322  0.001181  0.012670    ↙
     4.143332    109.990654
13   1      2   1   2     8  0.131203      22.093     5415.9     5618.9    210.642  0.126453  0.008875  0.090252    ↙
     4.020066    206.420044
14   1      2   2   0     4  0.133632      22.657     1099.0      976.5    108.777  0.126570  0.013184  0.130233    ↙
     3.921263     97.934937
15   1      1   2   2     8  0.128155      22.781      185.1      182.9      2.276  0.126596  0.002904  0.030711    ↙
     3.900279    193.656250
16   1      1   1   3     8  0.133704      23.239      135.2      158.2     27.456  0.126696  0.013083  0.129202    ↙
     3.824453    185.759048
17   1      2   2   1     8  0.132625      23.658      894.3     1020.2    143.528  0.126791  0.010897  0.109076    ↙
     3.757561    178.948746
18   1      3   1   1     8  0.139661      25.476     7116.8     7401.6    295.258  0.127241  0.023010  0.212609    ↙
     3.493464    153.183014
```

19	1	0	2	3	4	0.131814	26.295	477.2	468.6	8.507	0.127464	0.008127	0.082439
	3.386409		71.641670										
20	1	2	2	2	8	0.132086	26.448	155.3	169.9	16.049	0.127506	0.008555	0.086508
	3.367263		141.548569										
21	1	3	0	2	4	0.137329	26.803	238.4	281.9	51.333	0.127608	0.018097	0.171977
	3.323452		68.801903										
22	1	2	1	3	8	0.133806	26.847	919.2	1051.8	151.421	0.127620	0.011554	0.114468
	3.318106		137.125809										
23	1	1	3	1	8	0.131024	27.057	3627.0	3717.6	92.802	0.127682	0.006239	0.063979
	3.292796		134.894226										
24	1	0	0	4	2	0.142545	27.118	2486.4	2612.2	131.679	0.127700	0.027363	0.245424
	3.285477		33.511250										
25	1	1	2	3	8	0.132196	27.422	1171.2	1287.3	127.507	0.127790	0.008230	0.083217
	3.249784		131.103256										
26	1	3	1	2	8	0.137330	28.097	23.2	22.8	4.775	0.127997	0.017384	0.165495
	3.173267		124.503151										
27	1	1	0	4	4	0.140893	28.215	0.1	0.1	0.046	0.128034	0.023806	0.217723
	3.160269		61.695866										
28	1	3	2	1	8	0.139158	29.362	4563.9	4918.6	381.135	0.128409	0.019979	0.186618
	3.039301		113.341644										
29	1	2	3	0	4	0.135282	29.451	3494.9	3560.3	66.512	0.128439	0.012778	0.124866
	3.030329		56.308575										
30	1	1	1	4	8	0.139500	29.451	6978.2	7140.8	165.994	0.128439	0.020550	0.191234
	3.030306		112.600906										
31	1	1	3	2	8	0.131619	29.548	161.6	159.0	2.566	0.128472	0.005875	0.060035
	3.020613		111.827347										
32	1	2	3	1	8	0.135019	30.242	3.7	2.0	1.291	0.128713	0.011779	0.115616
	2.952845		106.401863										
33	1	2	2	3	8	0.134357	30.572	2758.7	2709.9	47.994	0.128831	0.010324	0.102197
	2.921708		103.943840										
34	1	4	0	0	2	0.147857	30.923	1299.6	1311.4	11.983	0.128958	0.034495	0.294131
	2.889412		25.357378										
35	1	2	0	4	4	0.139196	31.292	2039.8	1894.2	134.858	0.129095	0.018797	0.176039
	2.856143		49.432896										
36	1	3	2	2	8	0.138136	31.688	522.2	458.6	55.691	0.129245	0.016572	0.157202
	2.821367		96.230141										
37	1	0	2	4	4	0.137891	31.959	117.9	99.8	15.267	0.129349	0.015927	0.151586
	2.798023		47.235935										
38	1	3	1	3	8	0.137773	32.027	431.8	412.0	18.845	0.129375	0.015661	0.149279
	2.792263		94.040718										
39	1	4	1	0	4	0.147340	32.064	1102.2	1112.0	9.881	0.129390	0.032849	0.282068
	2.789081		46.902782										
40	1	2	1	4	8	0.138870	32.422	3338.3	3440.9	105.543	0.129530	0.017398	0.163870
	2.759124		91.578934										
41	1	2	3	2	8	0.135195	32.511	3523.3	3602.1	80.514	0.129566	0.010517	0.103425
	2.751801		91.048225										
42	1	4	1	1	8	0.146314	32.798	425.0	376.3	42.985	0.129681	0.030543	0.265378
	2.728315		89.322853										
43	1	1	2	4	8	0.137946	32.908	305.6	299.0	6.479	0.129726	0.015334	0.146104
	2.719465		88.677109										
44	1	1	3	3	8	0.134355	33.323	1831.2	1906.9	78.738	0.129896	0.008330	0.082886
	2.686560		86.305656										
45	1	0	4	0	2	0.135222	33.546	480.4	496.1	16.214	0.129989	0.009777	0.096312
	2.669168		21.267042										
46	1	4	0	2	4	0.144470	33.862	60.0	46.5	10.628	0.130122	0.026491	0.235129
	2.644990		41.670956										
47	1	0	4	1	4	0.135324	34.252	507.9	372.5	99.203	0.130290	0.009406	0.092680
	2.615762		40.650150										
48	1	4	1	2	8	0.144594	34.918	433.3	440.3	7.320	0.130582	0.025893	0.229955
	2.567380		77.947098										
49	1	3	3	1	8	0.140847	34.967	2357.7	2417.3	61.202	0.130604	0.019059	0.176388
	2.563941		77.716850										
50	1	1	4	1	8	0.136465	35.146	12.1	12.7	0.641	0.130685	0.010799	0.105165
	2.551238		76.854652										
51	1	3	2	3	8	0.139057	35.257	2207.0	2394.2	202.655	0.130734	0.015524	0.146704
	2.543478		76.320084										
52	1	4	2	0	4	0.146900	35.292	432.8	477.0	48.558	0.130750	0.029701	0.257600
	2.541073		38.079384										
53	1	2	2	4	8	0.139058	35.621	11.9	8.5	2.600	0.130900	0.015219	0.143933
	2.518355		74.625305										
54	1	3	0	4	4	0.140942	35.893	441.0	525.6	100.615	0.131026	0.018461	0.170986
	2.499869		36.694248										
55	1	4	2	1	8	0.146327	35.967	311.8	328.8	17.971	0.131061	0.028134	0.245796
	2.494863		73.060226										
56	1	2	3	3	8	0.137190	36.008	13.1	12.4	0.665	0.131080	0.011414	0.110410
	2.492157		72.881706										
57	1	1	1	5	8	0.145736	36.008	64.0	60.7	3.126	0.131080	0.027048	0.237803
	2.492144		72.874344										
58	1	0	4	2	4	0.136142	36.297	12.7	5.9	6.289	0.131217	0.009202	0.090185
	2.472932		35.807941										
59	1	3	1	4	8	0.141211	36.898	49.9	73.2	34.195	0.131505	0.018076	0.167275
	2.434039		69.069946										
60	1	3	3	2	8	0.140774	36.977	726.8	849.2	142.751	0.131544	0.017201	0.159991
	2.429007		68.750153										

No.	Code	H	K	L	Mult	Hw	2theta	Icalc	Iobs	Sigma	HwG	HwL	ETA
	d-hkl		CORR										
61	1	2	4	0	4	0.139729	37.070	1512.4	1524.9	12.934	0.131589	0.015187	0.142978
	2.423174		34.188881										

62	1	1	4	2	8	0.137220	37.149	488.4	455.9	30.297	0.131628	0.010448	0.101293
	2.418198		68.057114										
63	1	2	4	1	8	0.139793	37.718	417.5	375.2	37.881	0.131911	0.014708	0.138575
	2.383004		65.814056										
64	1	4	2	2	8	0.145468	37.932	2.0	3.1	1.691	0.132019	0.024890	0.220317
	2.370030		64.990669										
65	1	1	3	4	8	0.139193	38.048	2.2	2.9	0.929	0.132078	0.013285	0.126126
	2.363066		64.553917										
66	1	0	2	5	4	0.144664	38.132	403.0	419.6	17.278	0.132121	0.023255	0.207719
	2.358058		32.118649										
67	1	4	1	3	8	0.144386	38.222	1692.6	1640.2	50.692	0.132167	0.022666	0.203114
	2.352699		63.903545										
68	1	2	1	5	8	0.145221	38.530	25.4	31.0	6.909	0.132326	0.023891	0.212316
	2.334634		62.779404										
69	1	1	2	5	8	0.144670	38.949	8.8	20.8	28.151	0.132546	0.022495	0.201292
	2.310460		61.293552										
70	1	0	4	3	4	0.138517	39.502	139.8	138.8	1.122	0.132842	0.010603	0.101815
	2.279377		29.705997										
71	1	2	4	2	8	0.140414	39.608	691.6	672.3	18.744	0.132899	0.014028	0.131817
	2.273511		59.059425										
72	1	3	2	4	8	0.142474	39.783	234.7	278.8	52.341	0.132994	0.017661	0.162214
	2.263932		58.479618										
73	1	3	3	3	8	0.142116	40.136	92.2	145.1	82.930	0.133189	0.016644	0.153619
	2.244842		57.344933										
74	1	4	3	0	4	0.148204	40.167	9.4	14.2	7.327	0.133206	0.027673	0.239153
	2.243188		28.623936										
75	1	1	4	3	8	0.139476	40.296	266.8	410.4	220.572	0.133278	0.011579	0.110176
	2.236301		56.841805										
76	1	2	3	4	8	0.141342	40.462	15.3	26.6	19.638	0.133370	0.014877	0.138621
	2.227513		56.321148										
77	1	5	1	1	8	0.153845	40.480	59.6	105.4	80.546	0.133381	0.037264	0.304463
	2.226528		56.262371										
78	1	4	3	1	8	0.148020	40.773	253.2	366.1	162.566	0.133546	0.026738	0.231839
	2.211207		55.367920										
79	1	4	2	3	8	0.145868	41.028	78.9	143.1	116.093	0.133691	0.022595	0.200563
	2.198041		54.600323										
80	1	0	0	6	2	0.153747	41.180	270.2	346.2	96.974	0.133778	0.036414	0.298241
	2.190318		13.519185										
81	1	2	2	5	8	0.145394	41.318	6.5	7.4	0.990	0.133858	0.021430	0.191331
	2.183288		53.747250										
82	1	5	0	2	4	0.152570	41.373	205.2	250.3	54.811	0.133890	0.034177	0.283304
	2.180544		26.795231										
83	1	4	0	4	4	0.146163	41.589	6.6	20.0	40.716	0.134016	0.022543	0.199743
	2.169713		26.484529										
84	1	3	4	1	8	0.145067	41.702	9.7	36.5	100.091	0.134083	0.020426	0.183187
	2.164080		52.653618										
85	1	1	0	6	4	0.153262	41.947	410.9	483.1	84.542	0.134227	0.034800	0.286870
	2.152014		25.980547										
86	1	5	1	2	8	0.152841	42.267	2.2	10.5	40.534	0.134418	0.033734	0.279447
	2.136442		51.086533										
87	1	3	1	5	8	0.146840	42.450	14.8	27.2	22.546	0.134528	0.022844	0.201384
	2.127660		50.592857										
88	1	4	1	4	8	0.146667	42.480	218.1	352.4	216.317	0.134546	0.022498	0.198718
	2.126251		50.514965										
89	1	4	3	2	8	0.147955	42.550	276.5	416.9	211.109	0.134588	0.024753	0.215702
	2.122895		50.330738										
90	1	2	4	3	8	0.142391	42.603	119.1	182.5	96.935	0.134621	0.014503	0.134305
	2.120392		50.192627										
91	1	1	1	6	8	0.152810	42.832	8.6	56.8	317.859	0.134760	0.033085	0.274517
	2.109587		49.586857										
92	1	5	2	1	8	0.154445	43.164	0.6	12.6	246.240	0.134965	0.035583	0.290752
	2.094108		48.737232										
93	1	3	4	2	8	0.145589	43.448	61.2	262.6	862.094	0.135141	0.019444	0.174196
	2.081088		48.027515										
94	1	1	3	5	8	0.145658	43.477	1.5	5.6	14.663	0.135159	0.019537	0.174911
	2.079766		47.952202										
95	1	1	5	1	8	0.143733	43.615	78.4	151.3	140.411	0.135247	0.015831	0.144812
	2.073497		47.616844										
96	1	0	4	4	4	0.142793	43.655	233.7	408.4	304.666	0.135272	0.014041	0.129816
	2.071666		23.757120										
97	1	2	0	6	4	0.152734	44.183	234.0	461.2	445.975	0.135607	0.031470	0.262177
	2.048136		23.120661										
98	1	3	3	4	8	0.145497	44.240	28.9	48.7	33.306	0.135644	0.018353	0.164943
	2.045635		46.110989										
99	1	1	4	4	8	0.143619	44.388	50.9	114.7	143.656	0.135739	0.014707	0.135001
	2.039166		45.767258										
100	1	0	2	6	4	0.152281	44.683	44.9	139.9	295.294	0.135931	0.030099	0.252217
	2.026382		22.542385										
101	1	5	2	2	8	0.153976	44.864	116.7	201.2	145.092	0.136050	0.032881	0.271036
	2.018636		44.678234										
102	1	2	1	6	8	0.152668	45.033	381.8	504.5	161.474	0.136161	0.030379	0.253806
	2.011459		44.298351										
103	1	3	2	5	8	0.148038	45.038	16.5	21.3	6.253	0.136164	0.022053	0.193276
	2.011223		44.287319										
104	1	4	2	4	8	0.148401	45.066	284.6	367.8	107.263	0.136183	0.022680	0.198019
	2.010033		44.225571										
105	1	5	1	3	8	0.152766	45.117	180.2	237.5	75.063	0.136217	0.030455	0.254243
	2.007895		44.113476										
106	1	2	5	0	4	0.146533	45.234	3.6	5.5	2.959	0.136295	0.019062	0.169870
	2.002968		21.930689										

```
107   1      1   5   2     8  0.144726      45.301        4.0         8.0       7.976  0.136340  0.015646  0.142244  ↙
     2.000154      43.714397
108   1      4   3   3     8  0.148983      45.385       48.2       133.9     237.399  0.136396  0.023351  0.202813  ↙
     1.996637      43.527786
109   1      1   2   6     8  0.152351      45.402       15.6        45.2      85.406  0.136407  0.029381  0.246491  ↙
     1.995937      43.488667
110   1      2   3   5     8  0.147379      45.653      110.4       290.6     472.772  0.136575  0.020099  0.177704  ↙
     1.985559      42.952629
111   1      2   5   1     8  0.146777      45.786       26.0        74.3     137.757  0.136666  0.018829  0.167624  ↙
     1.980102      42.675720
112   1      3   4   3     8  0.147295      46.239        2.5         3.3       0.968  0.136975  0.019213  0.170313  ↙
     1.961735      41.732731
113   1      4   4   0     4  0.151994      46.267     1084.3      1397.4     402.098  0.136994  0.027700  0.233777  ↙
     1.960631      20.838533
114   1      2   4   4     8  0.146202      46.530        7.1        19.9      35.734  0.137177  0.016829  0.151086  ↙
     1.950139      41.143612
115   1      4   4   1     8  0.152075      46.809      423.6       524.9     125.033  0.137371  0.027174  0.229487  ↙
     1.939170      40.591351
116   1      6   0   0     2  0.162899      47.141        3.2        13.1      40.673  0.137605  0.045561  0.347164  ↙
     1.926275       9.985799
117   1      5   3   1     8  0.156524      47.363      324.0       462.4     196.551  0.137763  0.034363  0.278069  ↙
     1.917771      39.521759
118   1      2   5   2     8  0.147731      47.411       87.0       110.0      29.080  0.137798  0.018504  0.163835  ↙
     1.915934      39.433163
119   1      4   1   5     8  0.151386      47.493        4.7         6.7       2.766  0.137856  0.025063  0.213579  ↙
     1.912836      39.274673
120   1      2   2   6     8  0.153063      47.509        1.8         2.7       1.322  0.137868  0.028056  0.235041  ↙
     1.912226      39.244450

No.  Code      H   K   L  Mult      Hw          2theta       Icalc       Iobs       Sigma       HwG      HwL        ETA   ↙
           d-hkl          CORR

121   1      5   2   3     8  0.154413      47.590       13.1        26.9      28.187  0.137926  0.030357  0.250960  ↙
     1.909163      39.094662
122   1      3   0   6     4  0.153864      47.724       28.3        87.7     183.311  0.138023  0.029210  0.242893  ↙
     1.904096      19.421478
123   1      6   1   0     4  0.163132      47.950       72.1       175.1     248.695  0.138186  0.044986  0.342748  ↙
     1.895669      19.215900
124   1      1   5   3     8  0.146969      48.008       14.8        35.8      50.545  0.138229  0.016303  0.145807  ↙
     1.893506      38.329342
125   1      5   0   4     4  0.154006      48.089       29.1        81.0     144.198  0.138288  0.028994  0.241001  ↙
     1.890512      19.089468
126   1      4   4   2     8  0.152597      48.408       49.8        88.8      69.344  0.138523  0.026048  0.219824  ↙
     1.878781      37.612156
127   1      6   1   1     8  0.162876      48.478       68.6       104.1      53.305  0.138574  0.043908  0.335755  ↙
     1.876250      37.487667
128   1      3   1   6     8  0.154167      48.525      253.2       358.7     148.539  0.138609  0.028710  0.238558  ↙
     1.874519      37.402283
129   1      0   4   5     4  0.148898      48.573       16.2        22.8       9.296  0.138645  0.019095  0.167568  ↙
     1.872800      18.661100
130   1      5   1   4     8  0.154620      48.885      487.1       674.0     257.052  0.138878  0.029039  0.240460  ↙
     1.861554      36.780247
131   1      5   3   2     8  0.156642      48.949      185.4       249.5      85.774  0.138925  0.032542  0.264187  ↙
     1.859300      36.674236
132   1      3   3   5     8  0.150943      49.112        0.4         0.4       0.059  0.139048  0.022101  0.190128  ↙
     1.853503      36.396729
133   1      4   3   4     8  0.151822      49.138        8.6         9.3       0.712  0.139068  0.023665  0.201750  ↙
     1.852572      36.352833
134   1      3   5   1     8  0.151793      49.238       37.1        36.7       0.448  0.139144  0.023474  0.200252  ↙
     1.849062      36.189026
135   1      1   4   5     8  0.149623      49.248        0.8         0.8       0.013  0.139151  0.019497  0.170146  ↙
     1.848687      36.168797
136   1      6   0   2     4  0.162073      49.254      317.4       315.1       2.426  0.139156  0.041565  0.320818  ↙
     1.848485      18.078987
137   1      1   3   6     8  0.153527      49.453      489.8       438.0      45.944  0.139307  0.026315  0.220682  ↙
     1.841518      35.827904
138   1      4   2   5     8  0.153203      49.875       91.5        89.2       2.564  0.139632  0.025146  0.211847  ↙
     1.826896      35.140564
139   1      1   1   7     8  0.161109      49.907       72.2        71.7       0.776  0.139656  0.039063  0.304740  ↙
     1.825828      35.089111
140   1      3   4   4     8  0.150733      49.943        0.0         0.0       0.000  0.139684  0.020556  0.177695  ↙
     1.824592      35.034904
141   1      2   5   3     8  0.149882      50.031      211.6       217.3       5.734  0.139753  0.018869  0.164628  ↙
     1.821587      34.896233
142   1      6   1   2     8  0.162498      50.037        0.3         0.3       0.006  0.139757  0.041274  0.318004  ↙
     1.821389      34.884033

-------------------------------------------------------
BRAGG R-Factors and weight fractions for Pattern #  1
-------------------------------------------------------

=> Phase:  1       rdx
=> Bragg R-factor:   6.97       Vol: 1621.684( 0.069)  Fract(%):  100.00( 0.44)
=> Rf-factor=  9.79             ATZ:        1776.939   Brindley:  1.0000

---------------------------------------------------------------------
SYMBOLIC NAMES AND FINAL VALUES AND SIGMA OF REFINED PARAMETERS:
---------------------------------------------------------------------

->  Parameter number    1 :      G-Size_ph1_pat1    0.12007418E-01( +/-    0.85642365E-04 )
```

```
->  Parameter number    2 :            Zero_pat1   -0.21540712    ( +/-    0.21793407E-02 )
->  Parameter number    3 :       Scale_ph1_pat1    0.36776587E-02( +/-    0.11493407E-04 )
->  Parameter number    4 :     U-Cagl_ph1_pat1    0.14149698E-01( +/-    0.34455676E-02 )
->  Parameter number    5 :     Cell_A_ph1_pat1     11.557671    ( +/-    0.27274666E-03 )
->  Parameter number    6 :     Cell_B_ph1_pat1     10.676690    ( +/-    0.28143937E-03 )
->  Parameter number    7 :     Cell_C_ph1_pat1     13.141932    ( +/-    0.30492945E-03 )
->  Parameter number    8 :          X_O(1)_ph1    0.57030642    ( +/-    0.50944550E-03 )
->  Parameter number    9 :          Y_O(1)_ph1    0.44054043    ( +/-    0.58024272E-03 )
->  Parameter number   10 :          Z_O(1)_ph1    0.26806968    ( +/-    0.53565676E-03 )
->  Parameter number   11 :          X_O(2)_ph1    0.59821874    ( +/-    0.59325760E-03 )
->  Parameter number   12 :          Y_O(2)_ph1    0.23070036    ( +/-    0.58002409E-03 )
->  Parameter number   13 :          Z_O(2)_ph1    0.22521888    ( +/-    0.52235578E-03 )
->  Parameter number   14 :          X_O(3)_ph1    0.47699246    ( +/-    0.58257120E-03 )
->  Parameter number   15 :          Y_O(3)_ph1    0.13119514    ( +/-    0.53428166E-03 )
->  Parameter number   16 :          Z_O(3)_ph1   -0.16466578E-01( +/-    0.51274599E-03 )
->  Parameter number   17 :          X_O(4)_ph1    0.34888738    ( +/-    0.59821649E-03 )
->  Parameter number   18 :          Y_O(4)_ph1    0.25898808    ( +/-    0.66673080E-03 )
->  Parameter number   19 :          Z_O(4)_ph1   -0.11068642    ( +/-    0.58052666E-03 )
->  Parameter number   20 :          X_O(5)_ph1    0.30777898    ( +/-    0.54655079E-03 )
->  Parameter number   21 :          Y_O(5)_ph1    0.51705146    ( +/-    0.63611532E-03 )
->  Parameter number   22 :          Z_O(5)_ph1   -0.79056025E-01( +/-    0.50401402E-03 )
->  Parameter number   23 :          X_O(6)_ph1    0.42721874    ( +/-    0.51176769E-03 )
->  Parameter number   24 :          Y_O(6)_ph1    0.60060859    ( +/-    0.74724230E-03 )
->  Parameter number   25 :          Z_O(6)_ph1    0.52727856E-01( +/-    0.53174264E-03 )
->  Parameter number   26 :          X_N(1)_ph1    0.44408569    ( +/-    0.76306117E-03 )
->  Parameter number   27 :          Y_N(1)_ph1    0.33099678    ( +/-    0.98512415E-03 )
->  Parameter number   28 :          Z_N(1)_ph1    0.17287177    ( +/-    0.62338362E-03 )
->  Parameter number   29 :          X_N(2)_ph1    0.32741672    ( +/-    0.94491179E-03 )
->  Parameter number   30 :          Y_N(2)_ph1    0.23490509    ( +/-    0.88645355E-03 )
->  Parameter number   31 :          Z_N(2)_ph1    0.53277619E-01( +/-    0.72490342E-03 )
->  Parameter number   32 :          X_N(3)_ph1    0.30725399    ( +/-    0.85900084E-03 )
->  Parameter number   33 :          Y_N(3)_ph1    0.45634460    ( +/-    0.81957324E-03 )
->  Parameter number   34 :          Z_N(3)_ph1    0.82887992E-01( +/-    0.67181664E-03 )
->  Parameter number   35 :          X_N(4)_ph1    0.53932601    ( +/-    0.68082550E-03 )
->  Parameter number   36 :          Y_N(4)_ph1    0.33542445    ( +/-    0.69672387E-03 )
->  Parameter number   37 :          Z_N(4)_ph1    0.23514608    ( +/-    0.67948614E-03 )
->  Parameter number   38 :          X_N(5)_ph1    0.38598049    ( +/-    0.79134514E-03 )
->  Parameter number   39 :          Y_N(5)_ph1    0.20331475    ( +/-    0.91921864E-03 )
->  Parameter number   40 :          Z_N(5)_ph1   -0.41405533E-01( +/-    0.79785188E-03 )
->  Parameter number   41 :          X_N(6)_ph1    0.35495391    ( +/-    0.68654644E-03 )
->  Parameter number   42 :          Y_N(6)_ph1    0.54360700    ( +/-    0.92109625E-03 )
->  Parameter number   43 :          Z_N(6)_ph1    0.99107744E-02( +/-    0.78920758E-03 )
->  Parameter number   44 :          X_C(1)_ph1    0.34678712    ( +/-    0.84853295E-03 )
->  Parameter number   45 :          Y_C(1)_ph1    0.43853557    ( +/-    0.93395612E-03 )
->  Parameter number   46 :          Z_C(1)_ph1    0.19867958    ( +/-    0.73884765E-03 )
->  Parameter number   47 :          X_C(2)_ph1    0.38558781    ( +/-    0.87032176E-03 )
->  Parameter number   48 :          Y_C(2)_ph1    0.21305369    ( +/-    0.93864364E-03 )
->  Parameter number   49 :          Z_C(2)_ph1    0.15540366    ( +/-    0.96520188E-03 )
->  Parameter number   50 :          X_C(3)_ph1    0.23576419    ( +/-    0.71329746E-03 )
->  Parameter number   51 :          Y_C(3)_ph1    0.34061772    ( +/-    0.13099160E-02 )
->  Parameter number   52 :          Z_C(3)_ph1    0.52318119E-01( +/-    0.63173153E-03 )
->  Parameter number   53 :       Asym1_ph1_pat1    0.16559245    ( +/-    0.87822555E-02 )
->  Parameter number   54 :       Asym2_ph1_pat1    0.53462289E-01( +/-    0.17806906E-02 )
->  Parameter number   55 :      L-Size_ph1_pat1   -0.25047939E-01( +/-    0.46645673E-02 )
->  Parameter number   56 :       Size2_ph1_pat1    0.19417906E-01( +/-    0.13390562E-01 )
->  Parameter number   57 :       Size3_ph1_pat1    0.19766724    ( +/-    0.10954754E-01 )
->  Parameter number   58 :       Size4_ph1_pat1    0.21014285    ( +/-    0.13802625E-01 )
->  Parameter number   59 :       Size5_ph1_pat1   -0.39622393E-01( +/-    0.13335176E-01 )
->  Parameter number   60 :       Size6_ph1_pat1    0.19753376E-01( +/-    0.11426117E-01 )

------------------------------------------------------------------
=> Number of bytes for floating point variables: 4
=> Dimensions of dynamic allocated arrays in this run of FullProf:
------------------------------------------------------------------

=> Total approximate array memory (dynamic + static): 107719993 bytes

MaxPOINT=    60000 Max.num. of points(+int. Inten.)/diffraction pattern
MaxREFLT=    20000 Max.num. of reflections/diffraction pattern
MaxPARAM=      300 Max.num. of refinable parameters
MaxOVERL=     2096 Max.num. of overlapping reflections

-----------------------------------------------------------
=> Number of bytes for floating point arrays: 4
=> Dimensions of fixed arrays in this release of FullProf:
-----------------------------------------------------------

NPATT   =       80 Max.num. of powder diffraction patterns
NATS    =      830 Max.num. of atoms (all kind) in asymmetric unit
MPAR    =     1800 Max.num. of non atomic parameters/phase
IEXCL   =       30 Max.num. of excluded regions
IBACP   =      277 Max.num. of background points for interpolation
NPHT    =       16 Max.num. of phases
NMAGM   =        8 Max.num. of rotation-matrices sets for magnetic structure
NBASIS  =       12 Max.num. of basis functions associated to a single atom
NIREPS  =        9 Max.num. of irreducible representations to be combined
N_EQ    =      384 Max.num. of user-supplied symmetry operators/propagation vectors
NGL     =      300 Max.num. of global parameters/diffraction pattern
N_LINC  =       30 Max.num. of global linear restraints
NAT_P   =       64 Max.num. of atomic parameters per atom
```

```
NCONST  =      500 Max.num. of slack constraints per phase
N_SPE   =       16 Max.num. of different chemical species
N_FORM  =       60 Max.num. of scattering factor values in a table
NPR     =      150 Max.num. of points defining a numerical profile
INPR    =       25 Max.num. of different numerical peak shapes
NPRC    =      150 Max.num. of terms in the table for correcting intensities
NSOL    =       10 Max.num. of solutions to be stored in Montecarlo searchs


CPU Time:    96.906 seconds
1.615 minutes

=> Run finished at:     Date: 15/06/2015  Time: 11:02:11.361
```

A.3 Sample of n-RDX processed pure at 3 wt% in acetone

```
*******************************************************
** PROGRAM FullProf.2k (Version 5.50 - Dec2014-ILL JRC) **
*******************************************************
M U L T I -- P A T T E R N
Rietveld, Profile Matching & Integrated Intensity
Refinement of X-ray and/or Neutron Data


Date: 18/02/2015  Time: 13:16:26.953

=> PCR file code: 3b
=> DAT file code: 3b.dat               -> Relative contribution: 1.0000

==> CONDITIONS OF THIS RUN FOR PATTERN No.:  1

=> Global Refinement of X-ray powder diffraction data
=> Global Refinement of X-ray powder diffraction data
Flat plate with PSD
=> Title:RDX

=> Number of phases:    1
=> Number of excluded regions:    0
=> Number of scattering factors supplied:    0
=> March-Dollase model for preferred orientation
=> Conventional weights: w=1.0/Variance(yobs)
=> Asymmetry correction as in J.Appl.Cryst. 26,128(1993)
=> Background linearly interpolated between the    6 points given
=> The    5th default profile function was selected
=> Pseudo-Voigt function (ETA variable)
X-parameter correspond to: ETA=ETA0+X*2theta
pV(x)= ETA*L(x)+(1-ETA)*G(x)

==> INPUT/OUTPUT OPTIONS:

=> Generate file *.PRF for plot
=> Output Integrated Intensities
=> Generate new input file *.PCR

=> Data supplied in free format for pattern:  1
=> Plot pattern at each cycle
=> Wavelengths:  1.54056 1.54439
=> Alpha2/Alpha1 ratio:   0.5000
=> Cos(Monochromator angle)=   1.0000
=> Asymmetry correction for angles lower than   90.000 degrees
=> Absorption correction (AC), muR-eff =   0.0000  0.0000
=> Base of peaks: 2.0*HW*   20.00

=> Number of cycles:   50
=> Relaxation factors ==>    for coordinates:  1.00
=> for anisotropic temperature factors:  1.00
=> for halfwidth/strain/size parameters:  1.00
=> for lattice constants and propagation vectors:  1.00
=> EPS-value for convergence:    0.0
=> Background ==>
Position   Intensity
15.00       16.91        0.00
20.00      -27.69        0.00
25.00       30.87        0.00
30.00       13.02        0.00
35.00       -2.55        0.00
38.00       37.25        0.00


=> Instrumental Resolution read from file: xray-res.irf
=> Title of data: Approximate resolution function of a conventional X-ray diffractometer CuKalpha1,2

=> The resolution function is IRESOL:   1 for profile function #   5
Input resolution parameters:

U-inst     V-inst     W-inst     X-inst     Y-inst     Z-inst
0.00136   -0.00500    0.00391    0.06389    0.00008    0.00000
0.00136   -0.00500    0.00391    0.06389    0.00008    0.00000
```

```
=> Number of Least-Squares parameters varied:     5

=>--------------------------->
=>-------->  PATTERN number:  1
=>--------------------------->
=> Global parameters and codes ==>
=> Zero-point:    -0.0410    0.0000
=> Displacement peak-shift parameter and code:    -0.10    0.00
=> Transparency peak-shift parameter and code:     0.26    0.00

=> Reading Intensity data  =>>

==> Angular range, step and number of points:
2Thmin:      12.113000  2Thmax:      38.910702  Step:       0.024900  No. of points:   1077
------------------------------------------------------------------------------
=> Phase  No. 1
rdx
------------------------------------------------------------------------------
=>--------> Pattern#  1
=> Crystal Structure Refinement
=> The    7th profile function was selected for phase no.  1
=> Preferred orientation vector:   0.0000  0.0000  1.0000

=>--------> Data for PHASE: 1
=> Number of atoms:   21
=> Number of distance  constraints:    0
=> Number of angle     constraints:    0

=> Symmetry information on space group: P b c a
-> The multiplicity of the general position is:   8
-> The space group is Centric (-1 at origin)
-> Lattice type  P: { 000 }
-> Reduced set of symmetry operators:

No.  IT   Symmetry symbol    Rotation part     Associated Translation
1: ( 1)   1            -->     ( x, y, z) + {  0.0000  0.0000  0.0000}
2: ( 4)   2 ( x, 0, 0) -->     ( x,-y,-z) + {  0.5000  0.5000  0.0000}
3: ( 3)   2 ( 0, y, 0) -->     (-x, y,-z) + {  0.0000  0.5000  0.5000}
4: ( 2)   2 ( 0, 0, z) -->     (-x,-y, z) + {  0.5000  0.0000  0.5000}


Information on Space Group:
---------------------------

=>  Number of Space group:  61
=> Hermann-Mauguin Symbol: P b c a
=>            Hall Symbol: -P 2ac 2ab
=>   Table Setting Choice:
=>           Setting Type: IT (Generated from Hermann-Mauguin symbol)
=>         Crystal System: Orthorhombic
=>             Laue Class: mmm
=>            Point Group: mmm
=>        Bravais Lattice: P
=>         Lattice Symbol: oP
=> Reduced Number of S.O.:   4
=>   General multiplicity:   8
=>         Centrosymmetry: Centric (-1 at origin)
=> Generators (exc. -1&L):   2
=>        Asymmetric unit:  0.000 <= x <=  0.500
0.000 <= y <=  0.500
0.000 <= z <=  0.500

=> List of S.O. without inversion and lattice centring translations
=> SYMM(  1): x,y,z                              => SYMM(  2): x+1/2,-y+1/2,-z
=> SYMM(  3): -x,y+1/2,-z+1/2                    => SYMM(  4): -x+1/2,-y,z+1/2


=> Initial parameters ==>
Atom    Ntyp                  X         Y         Z         B         occ.         in  fin  Spc  Mult
B11       B22       B33       B12       B13       B23
O(1)   O                  0.56846   0.43427   0.26465   3.70830   1.00000          0    0    0    8
Codes:    0.00000   0.00000   0.00000   0.00000   0.00000
O(2)   O                  0.59453   0.24040   0.23053   4.41110   1.00000          0    0    0    8
Codes:    0.00000   0.00000   0.00000   0.00000   0.00000
O(3)   O                  0.47340   0.13880  -0.02250   4.98480   1.00000          0    0    0    8
Codes:    0.00000   0.00000   0.00000   0.00000   0.00000
O(4)   O                  0.35580   0.24950  -0.11238   4.76640   1.00000          0    0    0    8
Codes:    0.00000   0.00000   0.00000   0.00000   0.00000
O(5)   O                  0.31810   0.53030  -0.06806   5.32170   1.00000          0    0    0    8
Codes:    0.00000   0.00000   0.00000   0.00000   0.00000
O(6)   O                  0.42860   0.60110   0.04920   5.10850   1.00000          0    0    0    8
Codes:    0.00000   0.00000   0.00000   0.00000   0.00000
N(1)   N                  0.43638   0.33385   0.17584   2.73980   1.00000          0    0    0    8
Codes:    0.00000   0.00000   0.00000   0.00000   0.00000
N(2)   N                  0.32231   0.23197   0.05389   2.40240   1.00000          0    0    0    8
Codes:    0.00000   0.00000   0.00000   0.00000   0.00000
N(3)   N                  0.29900   0.45348   0.08838   2.59240   1.00000          0    0    0    8
Codes:    0.00000   0.00000   0.00000   0.00000   0.00000
N(4)   N                  0.53777   0.33516   0.22628   2.76530   1.00000          0    0    0    8
```

```
Codes:    0.00000   0.00000   0.00000   0.00000   0.00000
N(5)   N                0.38834   0.20759  -0.03308   3.09700   1.00000          0    0    0    8
Codes:    0.00000   0.00000   0.00000   0.00000   0.00000
N(6)   N                0.35299   0.52971   0.01650   3.43200   1.00000          0    0    0    8
Codes:    0.00000   0.00000   0.00000   0.00000   0.00000
C(1)   C                0.35799   0.43950   0.18450   2.89510   1.00000          0    0    0    8
Codes:    0.00000   0.00000   0.00000   0.00000   0.00000
C(2)   C                0.38140   0.21557   0.14950   2.70030   1.00000          0    0    0    8
Codes:    0.00000   0.00000   0.00000   0.00000   0.00000
C(3)   C                0.24458   0.33936   0.05038   2.55740   1.00000          0    0    0    8
Codes:    0.00000   0.00000   0.00000   0.00000   0.00000
H(1A)  H                0.40289   0.52403   0.20773   5.13220   1.00000          0    0    0    8
Codes:    0.00000   0.00000   0.00000   0.00000   0.00000
H(1B)  H                0.29071   0.42024   0.23991   4.84270   1.00000          0    0    0    8
Codes:    0.00000   0.00000   0.00000   0.00000   0.00000
H(2A)  H                0.44331   0.13918   0.14950   4.60580   1.00000          0    0    0    8
Codes:    0.00000   0.00000   0.00000   0.00000   0.00000
H(2B)  H                0.31742   0.19390   0.20730   4.97430   1.00000          0    0    0    8
Codes:    0.00000   0.00000   0.00000   0.00000   0.00000
H(3A)  H                0.20936   0.35364  -0.02527   4.50050   1.00000          0    0    0    8
Codes:    0.00000   0.00000   0.00000   0.00000   0.00000
H(3B)  H                0.17213   0.32091   0.10070   3.92150   1.00000          0    0    0    8
Codes:    0.00000   0.00000   0.00000   0.00000   0.00000

=> IT IS ASSUMED THAT THE FIRST GIVEN SITE IS FULLY OCCUPIED
OR THE FIRST AND SECOND ATOMS ARE IN THE SAME SITE WITH TOTAL FULL OCCUPATION
(If this is not the case, change the order of atoms to obtain correct values for the content of the unit cell)
The given occupation factors have been obtained mutiplying m/M by   1.0000
-> Atom: O    ,  Chemical element: O   Atomic Mass:    15.9994
-> Atom: O    ,  Chemical element: O   Atomic Mass:    15.9994
-> Atom: O    ,  Chemical element: O   Atomic Mass:    15.9994
-> Atom: O    ,  Chemical element: O   Atomic Mass:    15.9994
-> Atom: O    ,  Chemical element: O   Atomic Mass:    15.9994
-> Atom: O    ,  Chemical element: O   Atomic Mass:    15.9994
-> Atom: N    ,  Chemical element: N   Atomic Mass:    14.0067
-> Atom: N    ,  Chemical element: N   Atomic Mass:    14.0067
-> Atom: N    ,  Chemical element: N   Atomic Mass:    14.0067
-> Atom: N    ,  Chemical element: N   Atomic Mass:    14.0067
-> Atom: N    ,  Chemical element: N   Atomic Mass:    14.0067
-> Atom: N    ,  Chemical element: N   Atomic Mass:    14.0067
-> Atom: C    ,  Chemical element: C   Atomic Mass:    12.0110
-> Atom: C    ,  Chemical element: C   Atomic Mass:    12.0110
-> Atom: C    ,  Chemical element: C   Atomic Mass:    12.0110
-> Atom: H    ,  Chemical element: H   Atomic Mass:     1.0080
-> Atom: H    ,  Chemical element: H   Atomic Mass:     1.0080
-> Atom: H    ,  Chemical element: H   Atomic Mass:     1.0080
-> Atom: H    ,  Chemical element: H   Atomic Mass:     1.0080
-> Atom: H    ,  Chemical element: H   Atomic Mass:     1.0080
-> Atom: H    ,  Chemical element: H   Atomic Mass:     1.0080
=> The given value of ATZ is       1776.94 the program has calculated:        1776.94
The value of ATZ given in the input PCR file will be used for quantitative analysis
=> The chemical content of the unit cell is:
8.0000 O    +   8.0000 O    +   8.0000 O    +   8.0000 O    +   8.0000 O    +   8.0000 O    +   8.0000 N    +   ↙
     8.0000 N    +   8.0000 N    +   8.0000 N    +
8.0000 N    +   8.0000 N    +   8.0000 C    +   8.0000 C    +   8.0000 C    +   8.0000 H    +   8.0000 H    +   ↙
     8.0000 H    +   8.0000 H    +   8.0000 H    +
8.0000 H
=> The normalized site occupation numbers in % are:
100.0000 O(1)   :      100.0000 O(2)   :      100.0000 O(3)   :      100.0000 O(4)   :      100.0000 O(5)   :      ↙
     100.0000 O(6)   :      100.0000 N(1)   :      100.0000 N(2)   :      100.0000 N(3)   :      100.0000 N(4)   :
100.0000 N(5)   :      100.0000 N(6)   :      100.0000 C(1)   :      100.0000 C(2)   :      100.0000 C(3)   :      ↙
     100.0000 H(1A)  :      100.0000 H(1B)  :      100.0000 H(2A)  :      100.0000 H(2B)  :      100.0000 H(3A)  :
100.0000 H(3B)
=> The density (volumic mass) of the compound is:    1.785 g/cm3

=>-------> PROFILE PARAMETERS FOR PATTERN:  1

=> Overall scale factor:   0.666440E-03
=> ETA (p-Voigt) OR M (Pearson VII):   0.0000
=> Overall temperature factor:      0.00000
=> Halfwidth U,V,W:     -0.00587     0.00000     0.00000
=> X and Y parameters:       0.0000      0.0000
=> Direct cell parameters:   11.6304  10.7431  13.2279  90.0000  90.0000  90.0000
=> Preferred orientation parameters:   1.0000  0.0000
=> Asymmetry parameters     :     -0.21721     0.00510     0.00000     0.00000
=> Strain parameters        :      0.00000     0.00000     0.00000
=> Size   parameters        :      0.00000     0.00000
=> Further shape parameters (S_L and D_L):   0.00000   0.00000
S_L is source width/detector distance
D_L is detector width/detector distance

==> CODEWORDS FOR PROFILE PARAMETERS of PATTERN#  1

=> Overall scale factor:   11.000
=> ETA (p-Voigt) OR M (Pearson VII):    0.000
=> Overall temperature factor:    0.000
=> Halfwidth U,V,W:   21.000   0.000   0.000
=> X and Y parameters:    0.000   0.000
=> Direct cell parameters:    0.000   0.000   0.000   0.000   0.000   0.000
=> Preferred orientation parameters:    0.000   0.000
```

```
=> Asymmetry parameters     :   41.000  51.000   0.000   0.000
=> Strain parameters        :    0.000   0.000   0.000
=> Size   parameters        :   31.000   0.000

=> Cell constraints according to Laue symmetry: mmm

Metric information:
-------------------

=> Direct cell parameters:

a =      11.6304      b =      10.7431      c =      13.2279
alpha =       90.000   beta =       90.000  gamma =       90.000
Direct Cell Volume =    1652.7814

=> Reciprocal cell parameters:

a*=     0.085981      b*=     0.093083      c*=     0.075598
alpha*=       90.000   beta*=       90.000  gamma*=       90.000
Reciprocal Cell Volume =   0.00060504

=> Direct and Reciprocal Metric Tensors:

GD                                      GR
135.2666      0.0000      0.0000          0.007393    0.000000    0.000000
0.0000    115.4133      0.0000          0.000000    0.008665    0.000000
0.0000      0.0000    174.9783          0.000000    0.000000    0.005715

=>  Cartesian frame: x // a; y is in the ab-plane; z is x ^ y

Crystal_to_Orthonormal_Matrix             Orthonormal_to_Crystal Matrix
Cr_Orth_cel                               Orth_Cr_cel
11.6304      0.0000      0.0000          0.085981    0.000000    0.000000
0.0000     10.7431      0.0000          0.000000    0.093083    0.000000
0.0000      0.0000     13.2279          0.000000    0.000000    0.075598

Busing-Levy B-matrix: Hc=B.H            Inverse of the Busing-Levy B-matrix
BL_M                                      BL_Minv
0.085981    0.000000    0.000000            11.6304      0.0000      0.0000
0.000000    0.093083    0.000000             0.0000     10.7431      0.0000
0.000000    0.000000    0.075598             0.0000      0.0000     13.2279

=> Laue symmetry mmm   will be used to generate HKL for pattern#   1
=> Reflections generated between S(1/d)min:  0.1366 A-1 and S(1/d)max:  0.4324 A-1
=>                                  dmax:  7.3188 A   and      dmin:  2.3127 A
=> The number of reflections generated is:     69
=> The max. scatt. variable (gen.ref.) is:        38.9107
=> Scattering coefficients from internal table


=> X-ray scattering coeff. (A1, B1, A2,...C, f(0), Z, Dfp,Dfpp)

O       3.0485  13.2771   2.2868   5.7011   1.5463   0.3239   0.8670  32.9089   0.2508   7.9994   8.0000   0.0470  ↙
      0.0320
N      12.2126   0.0057   3.1322   9.8933   2.0125  28.9975   1.1663   0.5826 -11.5290   6.9946   7.0000   0.0290  ↙
      0.0180
C       2.3100  20.8439   1.0200  10.2075   1.5886   0.5687   0.8650  51.6512   0.2156   5.9992   6.0000   0.0170  ↙
      0.0090
H       0.4930  10.5109   0.3229  26.1257   0.1402   3.1424   0.0408  57.7997   0.0030   1.0000   1.0000   0.0000  ↙
      0.0000

---------------------------------------------------------------
SYMBOLIC NAMES AND INITIAL VALUES OF PARAMETERS TO BE VARIED:
---------------------------------------------------------------

->  Parameter number    1   -> Symbolic Name:       Scale_ph1_pat1    0.66644000E-03
->  Parameter number    2   -> Symbolic Name:      U-Cagl_ph1_pat1   -0.58700000E-02
->  Parameter number    3   -> Symbolic Name:      G-Size_ph1_pat1     0.0000000
->  Parameter number    4   -> Symbolic Name:       Asym1_ph1_pat1   -0.21720999
->  Parameter number    5   -> Symbolic Name:       Asym2_ph1_pat1    0.51000002E-02

=> Zero counts at step no.      3 at 2theta/TOF/E(KeV):        12.1628  Intensity fixed to 1.0 and variance to 1E6
=> Zero counts at step no.      4 at 2theta/TOF/E(KeV):        12.1877  Intensity fixed to 1.0 and variance to 1E6
=> Zero counts at step no.      5 at 2theta/TOF/E(KeV):        12.2126  Intensity fixed to 1.0 and variance to 1E6
=> Zero counts at step no.      6 at 2theta/TOF/E(KeV):        12.2375  Intensity fixed to 1.0 and variance to 1E6
=> Zero counts at step no.      9 at 2theta/TOF/E(KeV):        12.3122  Intensity fixed to 1.0 and variance to 1E6
=> Zero counts at step no.     10 at 2theta/TOF/E(KeV):        12.3371  Intensity fixed to 1.0 and variance to 1E6
=> Zero counts at step no.     11 at 2theta/TOF/E(KeV):        12.3620  Intensity fixed to 1.0 and variance to 1E6
=> Zero counts at step no.     14 at 2theta/TOF/E(KeV):        12.4367  Intensity fixed to 1.0 and variance to 1E6
=> Zero counts at step no.     15 at 2theta/TOF/E(KeV):        12.4616  Intensity fixed to 1.0 and variance to 1E6
=> Zero counts at step no.     22 at 2theta/TOF/E(KeV):        12.6359  Intensity fixed to 1.0 and variance to 1E6
=> Zero counts at step no.     61 at 2theta/TOF/E(KeV):        13.6070  Intensity fixed to 1.0 and variance to 1E6
=> Zero counts at step no.     62 at 2theta/TOF/E(KeV):        13.6319  Intensity fixed to 1.0 and variance to 1E6
=> Zero counts at step no.     69 at 2theta/TOF/E(KeV):        13.8062  Intensity fixed to 1.0 and variance to 1E6
=> Zero counts at step no.     77 at 2theta/TOF/E(KeV):        14.0054  Intensity fixed to 1.0 and variance to 1E6
=> Zero counts at step no.     79 at 2theta/TOF/E(KeV):        14.0552  Intensity fixed to 1.0 and variance to 1E6
=> Zero counts at step no.     81 at 2theta/TOF/E(KeV):        14.1050  Intensity fixed to 1.0 and variance to 1E6
=> Zero counts at step no.     86 at 2theta/TOF/E(KeV):        14.2295  Intensity fixed to 1.0 and variance to 1E6
=> Zero counts at step no.     87 at 2theta/TOF/E(KeV):        14.2544  Intensity fixed to 1.0 and variance to 1E6
=> Zero counts at step no.     93 at 2theta/TOF/E(KeV):        14.4038  Intensity fixed to 1.0 and variance to 1E6
```

```
=> Zero counts at step no.     98 at 2theta/TOF/E(KeV):       14.5283  Intensity fixed to 1.0 and variance to 1E6
=> Zero counts at step no.    102 at 2theta/TOF/E(KeV):       14.6279  Intensity fixed to 1.0 and variance to 1E6
=> Zero counts at step no.    106 at 2theta/TOF/E(KeV):       14.7275  Intensity fixed to 1.0 and variance to 1E6
=> Zero counts at step no.    107 at 2theta/TOF/E(KeV):       14.7524  Intensity fixed to 1.0 and variance to 1E6
=> Zero counts at step no.    108 at 2theta/TOF/E(KeV):       14.7773  Intensity fixed to 1.0 and variance to 1E6
=> Zero counts at step no.    110 at 2theta/TOF/E(KeV):       14.8271  Intensity fixed to 1.0 and variance to 1E6
=> Zero counts at step no.    114 at 2theta/TOF/E(KeV):       14.9267  Intensity fixed to 1.0 and variance to 1E6
=> Zero counts at step no.    116 at 2theta/TOF/E(KeV):       14.9765  Intensity fixed to 1.0 and variance to 1E6
=> Zero counts at step no.    117 at 2theta/TOF/E(KeV):       15.0014  Intensity fixed to 1.0 and variance to 1E6
=> Zero counts at step no.    141 at 2theta/TOF/E(KeV):       15.5990  Intensity fixed to 1.0 and variance to 1E6
=> Zero counts at step no.    142 at 2theta/TOF/E(KeV):       15.6239  Intensity fixed to 1.0 and variance to 1E6
=> Zero counts at step no.    144 at 2theta/TOF/E(KeV):       15.6737  Intensity fixed to 1.0 and variance to 1E6
=> Zero counts at step no.    145 at 2theta/TOF/E(KeV):       15.6986  Intensity fixed to 1.0 and variance to 1E6
=> Zero counts at step no.    146 at 2theta/TOF/E(KeV):       15.7235  Intensity fixed to 1.0 and variance to 1E6
=> Zero counts at step no.    148 at 2theta/TOF/E(KeV):       15.7733  Intensity fixed to 1.0 and variance to 1E6
=> Zero counts at step no.    152 at 2theta/TOF/E(KeV):       15.8729  Intensity fixed to 1.0 and variance to 1E6
=> Zero counts at step no.    163 at 2theta/TOF/E(KeV):       16.1468  Intensity fixed to 1.0 and variance to 1E6
=> Zero counts at step no.    187 at 2theta/TOF/E(KeV):       16.7444  Intensity fixed to 1.0 and variance to 1E6
=> Zero counts at step no.    188 at 2theta/TOF/E(KeV):       16.7693  Intensity fixed to 1.0 and variance to 1E6
=> Zero counts at step no.    189 at 2theta/TOF/E(KeV):       16.7942  Intensity fixed to 1.0 and variance to 1E6
=> Zero counts at step no.    191 at 2theta/TOF/E(KeV):       16.8440  Intensity fixed to 1.0 and variance to 1E6
=> Zero counts at step no.    192 at 2theta/TOF/E(KeV):       16.8689  Intensity fixed to 1.0 and variance to 1E6
=> Zero counts at step no.    196 at 2theta/TOF/E(KeV):       16.9685  Intensity fixed to 1.0 and variance to 1E6
=> Zero counts at step no.    197 at 2theta/TOF/E(KeV):       16.9934  Intensity fixed to 1.0 and variance to 1E6
=> Zero counts at step no.    199 at 2theta/TOF/E(KeV):       17.0432  Intensity fixed to 1.0 and variance to 1E6
=> Zero counts at step no.    237 at 2theta/TOF/E(KeV):       17.9894  Intensity fixed to 1.0 and variance to 1E6
=> Zero counts at step no.    240 at 2theta/TOF/E(KeV):       18.0641  Intensity fixed to 1.0 and variance to 1E6
=> Zero counts at step no.    241 at 2theta/TOF/E(KeV):       18.0890  Intensity fixed to 1.0 and variance to 1E6
=> Zero counts at step no.    243 at 2theta/TOF/E(KeV):       18.1388  Intensity fixed to 1.0 and variance to 1E6
=> Zero counts at step no.    244 at 2theta/TOF/E(KeV):       18.1637  Intensity fixed to 1.0 and variance to 1E6
=> Zero counts at step no.    245 at 2theta/TOF/E(KeV):       18.1886  Intensity fixed to 1.0 and variance to 1E6
=> Zero counts at step no.    246 at 2theta/TOF/E(KeV):       18.2135  Intensity fixed to 1.0 and variance to 1E6
=> Zero counts at step no.    247 at 2theta/TOF/E(KeV):       18.2384  Intensity fixed to 1.0 and variance to 1E6
=> Zero counts at step no.    248 at 2theta/TOF/E(KeV):       18.2633  Intensity fixed to 1.0 and variance to 1E6
=> Zero counts at step no.    249 at 2theta/TOF/E(KeV):       18.2882  Intensity fixed to 1.0 and variance to 1E6
=> Zero counts at step no.    250 at 2theta/TOF/E(KeV):       18.3131  Intensity fixed to 1.0 and variance to 1E6
=> Zero counts at step no.    251 at 2theta/TOF/E(KeV):       18.3380  Intensity fixed to 1.0 and variance to 1E6
=> Zero counts at step no.    253 at 2theta/TOF/E(KeV):       18.3878  Intensity fixed to 1.0 and variance to 1E6
=> Zero counts at step no.    254 at 2theta/TOF/E(KeV):       18.4127  Intensity fixed to 1.0 and variance to 1E6
=> Zero counts at step no.    255 at 2theta/TOF/E(KeV):       18.4376  Intensity fixed to 1.0 and variance to 1E6
=> Zero counts at step no.    256 at 2theta/TOF/E(KeV):       18.4625  Intensity fixed to 1.0 and variance to 1E6
=> Zero counts at step no.    261 at 2theta/TOF/E(KeV):       18.5870  Intensity fixed to 1.0 and variance to 1E6
=> Zero counts at step no.    264 at 2theta/TOF/E(KeV):       18.6617  Intensity fixed to 1.0 and variance to 1E6
=> Zero counts at step no.    265 at 2theta/TOF/E(KeV):       18.6866  Intensity fixed to 1.0 and variance to 1E6
=> Zero counts at step no.    266 at 2theta/TOF/E(KeV):       18.7115  Intensity fixed to 1.0 and variance to 1E6
=> Zero counts at step no.    267 at 2theta/TOF/E(KeV):       18.7364  Intensity fixed to 1.0 and variance to 1E6
=> Zero counts at step no.    268 at 2theta/TOF/E(KeV):       18.7613  Intensity fixed to 1.0 and variance to 1E6
=> Zero counts at step no.    269 at 2theta/TOF/E(KeV):       18.7862  Intensity fixed to 1.0 and variance to 1E6
=> Zero counts at step no.    270 at 2theta/TOF/E(KeV):       18.8111  Intensity fixed to 1.0 and variance to 1E6
=> Zero counts at step no.    271 at 2theta/TOF/E(KeV):       18.8360  Intensity fixed to 1.0 and variance to 1E6
=> Zero counts at step no.    272 at 2theta/TOF/E(KeV):       18.8609  Intensity fixed to 1.0 and variance to 1E6
=> Zero counts at step no.    273 at 2theta/TOF/E(KeV):       18.8858  Intensity fixed to 1.0 and variance to 1E6
=> Zero counts at step no.    274 at 2theta/TOF/E(KeV):       18.9107  Intensity fixed to 1.0 and variance to 1E6
=> Zero counts at step no.    275 at 2theta/TOF/E(KeV):       18.9356  Intensity fixed to 1.0 and variance to 1E6
=> Zero counts at step no.    276 at 2theta/TOF/E(KeV):       18.9605  Intensity fixed to 1.0 and variance to 1E6
=> Zero counts at step no.    277 at 2theta/TOF/E(KeV):       18.9854  Intensity fixed to 1.0 and variance to 1E6
=> Zero counts at step no.    278 at 2theta/TOF/E(KeV):       19.0103  Intensity fixed to 1.0 and variance to 1E6
=> Zero counts at step no.    279 at 2theta/TOF/E(KeV):       19.0352  Intensity fixed to 1.0 and variance to 1E6
=> Zero counts at step no.    280 at 2theta/TOF/E(KeV):       19.0601  Intensity fixed to 1.0 and variance to 1E6
=> Zero counts at step no.    281 at 2theta/TOF/E(KeV):       19.0850  Intensity fixed to 1.0 and variance to 1E6
=> Zero counts at step no.    283 at 2theta/TOF/E(KeV):       19.1348  Intensity fixed to 1.0 and variance to 1E6
=> Zero counts at step no.    284 at 2theta/TOF/E(KeV):       19.1597  Intensity fixed to 1.0 and variance to 1E6
=> Zero counts at step no.    285 at 2theta/TOF/E(KeV):       19.1846  Intensity fixed to 1.0 and variance to 1E6
=> Zero counts at step no.    286 at 2theta/TOF/E(KeV):       19.2095  Intensity fixed to 1.0 and variance to 1E6
=> Zero counts at step no.    287 at 2theta/TOF/E(KeV):       19.2344  Intensity fixed to 1.0 and variance to 1E6
=> Zero counts at step no.    288 at 2theta/TOF/E(KeV):       19.2593  Intensity fixed to 1.0 and variance to 1E6
=> Zero counts at step no.    295 at 2theta/TOF/E(KeV):       19.4336  Intensity fixed to 1.0 and variance to 1E6
=> Zero counts at step no.    296 at 2theta/TOF/E(KeV):       19.4585  Intensity fixed to 1.0 and variance to 1E6
=> Zero counts at step no.    297 at 2theta/TOF/E(KeV):       19.4834  Intensity fixed to 1.0 and variance to 1E6
=> Zero counts at step no.    298 at 2theta/TOF/E(KeV):       19.5083  Intensity fixed to 1.0 and variance to 1E6
=> Zero counts at step no.    299 at 2theta/TOF/E(KeV):       19.5332  Intensity fixed to 1.0 and variance to 1E6
=> Zero counts at step no.    300 at 2theta/TOF/E(KeV):       19.5581  Intensity fixed to 1.0 and variance to 1E6
=> Zero counts at step no.    301 at 2theta/TOF/E(KeV):       19.5830  Intensity fixed to 1.0 and variance to 1E6
=> Zero counts at step no.    302 at 2theta/TOF/E(KeV):       19.6079  Intensity fixed to 1.0 and variance to 1E6
=> Zero counts at step no.    303 at 2theta/TOF/E(KeV):       19.6328  Intensity fixed to 1.0 and variance to 1E6
=> Zero counts at step no.    304 at 2theta/TOF/E(KeV):       19.6577  Intensity fixed to 1.0 and variance to 1E6
=> Zero counts at step no.    305 at 2theta/TOF/E(KeV):       19.6826  Intensity fixed to 1.0 and variance to 1E6
=> Zero counts at step no.    306 at 2theta/TOF/E(KeV):       19.7075  Intensity fixed to 1.0 and variance to 1E6
=> Zero counts at step no.    308 at 2theta/TOF/E(KeV):       19.7573  Intensity fixed to 1.0 and variance to 1E6
=> Zero counts at step no.    310 at 2theta/TOF/E(KeV):       19.8071  Intensity fixed to 1.0 and variance to 1E6
=> Zero counts at step no.    311 at 2theta/TOF/E(KeV):       19.8320  Intensity fixed to 1.0 and variance to 1E6
=> Zero counts at step no.    312 at 2theta/TOF/E(KeV):       19.8569  Intensity fixed to 1.0 and variance to 1E6
=> Zero counts at step no.    313 at 2theta/TOF/E(KeV):       19.8818  Intensity fixed to 1.0 and variance to 1E6
=> Zero counts at step no.    314 at 2theta/TOF/E(KeV):       19.9067  Intensity fixed to 1.0 and variance to 1E6
=> Zero counts at step no.    316 at 2theta/TOF/E(KeV):       19.9565  Intensity fixed to 1.0 and variance to 1E6
=> Zero counts at step no.    317 at 2theta/TOF/E(KeV):       19.9814  Intensity fixed to 1.0 and variance to 1E6
=> Zero counts at step no.    319 at 2theta/TOF/E(KeV):       20.0312  Intensity fixed to 1.0 and variance to 1E6
=> Zero counts at step no.    340 at 2theta/TOF/E(KeV):       20.5541  Intensity fixed to 1.0 and variance to 1E6
=> Zero counts at step no.    342 at 2theta/TOF/E(KeV):       20.6039  Intensity fixed to 1.0 and variance to 1E6
=> Zero counts at step no.    343 at 2theta/TOF/E(KeV):       20.6288  Intensity fixed to 1.0 and variance to 1E6
```

```
=> Zero counts at step no.    344 at 2theta/TOF/E(KeV):      20.6537  Intensity fixed to 1.0 and variance to 1E6
=> Zero counts at step no.    346 at 2theta/TOF/E(KeV):      20.7035  Intensity fixed to 1.0 and variance to 1E6
=> Zero counts at step no.    348 at 2theta/TOF/E(KeV):      20.7533  Intensity fixed to 1.0 and variance to 1E6
=> Zero counts at step no.    349 at 2theta/TOF/E(KeV):      20.7782  Intensity fixed to 1.0 and variance to 1E6
=> Zero counts at step no.    350 at 2theta/TOF/E(KeV):      20.8031  Intensity fixed to 1.0 and variance to 1E6
=> Zero counts at step no.    352 at 2theta/TOF/E(KeV):      20.8529  Intensity fixed to 1.0 and variance to 1E6
=> Zero counts at step no.    353 at 2theta/TOF/E(KeV):      20.8778  Intensity fixed to 1.0 and variance to 1E6
=> Zero counts at step no.    354 at 2theta/TOF/E(KeV):      20.9027  Intensity fixed to 1.0 and variance to 1E6
=> Zero counts at step no.    356 at 2theta/TOF/E(KeV):      20.9525  Intensity fixed to 1.0 and variance to 1E6
=> Zero counts at step no.    357 at 2theta/TOF/E(KeV):      20.9774  Intensity fixed to 1.0 and variance to 1E6
=> Zero counts at step no.    358 at 2theta/TOF/E(KeV):      21.0023  Intensity fixed to 1.0 and variance to 1E6
=> Zero counts at step no.    360 at 2theta/TOF/E(KeV):      21.0521  Intensity fixed to 1.0 and variance to 1E6
=> Zero counts at step no.    361 at 2theta/TOF/E(KeV):      21.0770  Intensity fixed to 1.0 and variance to 1E6
=> Zero counts at step no.    362 at 2theta/TOF/E(KeV):      21.1019  Intensity fixed to 1.0 and variance to 1E6
=> Zero counts at step no.    375 at 2theta/TOF/E(KeV):      21.4256  Intensity fixed to 1.0 and variance to 1E6
=> Zero counts at step no.    376 at 2theta/TOF/E(KeV):      21.4505  Intensity fixed to 1.0 and variance to 1E6
=> Zero counts at step no.    379 at 2theta/TOF/E(KeV):      21.5252  Intensity fixed to 1.0 and variance to 1E6
=> Zero counts at step no.    380 at 2theta/TOF/E(KeV):      21.5501  Intensity fixed to 1.0 and variance to 1E6
=> Zero counts at step no.    381 at 2theta/TOF/E(KeV):      21.5750  Intensity fixed to 1.0 and variance to 1E6
=> Zero counts at step no.    382 at 2theta/TOF/E(KeV):      21.5999  Intensity fixed to 1.0 and variance to 1E6
=> Zero counts at step no.    406 at 2theta/TOF/E(KeV):      22.1975  Intensity fixed to 1.0 and variance to 1E6
=> Zero counts at step no.    407 at 2theta/TOF/E(KeV):      22.2224  Intensity fixed to 1.0 and variance to 1E6
=> Zero counts at step no.    408 at 2theta/TOF/E(KeV):      22.2473  Intensity fixed to 1.0 and variance to 1E6
=> Zero counts at step no.    410 at 2theta/TOF/E(KeV):      22.2971  Intensity fixed to 1.0 and variance to 1E6
=> Zero counts at step no.    411 at 2theta/TOF/E(KeV):      22.3220  Intensity fixed to 1.0 and variance to 1E6
=> Zero counts at step no.    428 at 2theta/TOF/E(KeV):      22.7453  Intensity fixed to 1.0 and variance to 1E6
=> Zero counts at step no.    430 at 2theta/TOF/E(KeV):      22.7951  Intensity fixed to 1.0 and variance to 1E6
=> Zero counts at step no.    431 at 2theta/TOF/E(KeV):      22.8200  Intensity fixed to 1.0 and variance to 1E6
=> Zero counts at step no.    433 at 2theta/TOF/E(KeV):      22.8698  Intensity fixed to 1.0 and variance to 1E6
=> Zero counts at step no.    446 at 2theta/TOF/E(KeV):      23.1935  Intensity fixed to 1.0 and variance to 1E6
=> Zero counts at step no.    447 at 2theta/TOF/E(KeV):      23.2184  Intensity fixed to 1.0 and variance to 1E6
=> Zero counts at step no.    448 at 2theta/TOF/E(KeV):      23.2433  Intensity fixed to 1.0 and variance to 1E6
=> Zero counts at step no.    450 at 2theta/TOF/E(KeV):      23.2931  Intensity fixed to 1.0 and variance to 1E6
=> Zero counts at step no.    471 at 2theta/TOF/E(KeV):      23.8160  Intensity fixed to 1.0 and variance to 1E6
=> Zero counts at step no.    473 at 2theta/TOF/E(KeV):      23.8658  Intensity fixed to 1.0 and variance to 1E6
=> Zero counts at step no.    476 at 2theta/TOF/E(KeV):      23.9405  Intensity fixed to 1.0 and variance to 1E6
=> Zero counts at step no.    478 at 2theta/TOF/E(KeV):      23.9903  Intensity fixed to 1.0 and variance to 1E6
=> Zero counts at step no.    479 at 2theta/TOF/E(KeV):      24.0152  Intensity fixed to 1.0 and variance to 1E6
=> Zero counts at step no.    480 at 2theta/TOF/E(KeV):      24.0401  Intensity fixed to 1.0 and variance to 1E6
=> Zero counts at step no.    482 at 2theta/TOF/E(KeV):      24.0899  Intensity fixed to 1.0 and variance to 1E6
=> Zero counts at step no.    484 at 2theta/TOF/E(KeV):      24.1397  Intensity fixed to 1.0 and variance to 1E6
=> Zero counts at step no.    488 at 2theta/TOF/E(KeV):      24.2393  Intensity fixed to 1.0 and variance to 1E6
=> Zero counts at step no.    491 at 2theta/TOF/E(KeV):      24.3140  Intensity fixed to 1.0 and variance to 1E6
=> Zero counts at step no.    492 at 2theta/TOF/E(KeV):      24.3389  Intensity fixed to 1.0 and variance to 1E6
=> Zero counts at step no.    511 at 2theta/TOF/E(KeV):      24.8120  Intensity fixed to 1.0 and variance to 1E6
=> Zero counts at step no.    549 at 2theta/TOF/E(KeV):      25.7582  Intensity fixed to 1.0 and variance to 1E6
=> Zero counts at step no.    620 at 2theta/TOF/E(KeV):      27.5261  Intensity fixed to 1.0 and variance to 1E6
=> Zero counts at step no.    624 at 2theta/TOF/E(KeV):      27.6257  Intensity fixed to 1.0 and variance to 1E6
=> Zero counts at step no.    628 at 2theta/TOF/E(KeV):      27.7253  Intensity fixed to 1.0 and variance to 1E6
=> Zero counts at step no.    630 at 2theta/TOF/E(KeV):      27.7751  Intensity fixed to 1.0 and variance to 1E6
=> Zero counts at step no.    632 at 2theta/TOF/E(KeV):      27.8249  Intensity fixed to 1.0 and variance to 1E6
=> Zero counts at step no.    638 at 2theta/TOF/E(KeV):      27.9743  Intensity fixed to 1.0 and variance to 1E6
=> Zero counts at step no.    639 at 2theta/TOF/E(KeV):      27.9992  Intensity fixed to 1.0 and variance to 1E6
=> Zero counts at step no.    640 at 2theta/TOF/E(KeV):      28.0241  Intensity fixed to 1.0 and variance to 1E6
=> Zero counts at step no.    644 at 2theta/TOF/E(KeV):      28.1237  Intensity fixed to 1.0 and variance to 1E6
=> Zero counts at step no.    647 at 2theta/TOF/E(KeV):      28.1984  Intensity fixed to 1.0 and variance to 1E6
=> Zero counts at step no.    659 at 2theta/TOF/E(KeV):      28.4972  Intensity fixed to 1.0 and variance to 1E6
=> Zero counts at step no.    669 at 2theta/TOF/E(KeV):      28.7462  Intensity fixed to 1.0 and variance to 1E6
=> Zero counts at step no.    709 at 2theta/TOF/E(KeV):      29.7422  Intensity fixed to 1.0 and variance to 1E6
=> Zero counts at step no.    712 at 2theta/TOF/E(KeV):      29.8169  Intensity fixed to 1.0 and variance to 1E6
=> Zero counts at step no.    716 at 2theta/TOF/E(KeV):      29.9165  Intensity fixed to 1.0 and variance to 1E6
=> Zero counts at step no.    720 at 2theta/TOF/E(KeV):      30.0161  Intensity fixed to 1.0 and variance to 1E6
=> Zero counts at step no.    721 at 2theta/TOF/E(KeV):      30.0410  Intensity fixed to 1.0 and variance to 1E6
=> Zero counts at step no.    722 at 2theta/TOF/E(KeV):      30.0659  Intensity fixed to 1.0 and variance to 1E6
=> Zero counts at step no.    723 at 2theta/TOF/E(KeV):      30.0908  Intensity fixed to 1.0 and variance to 1E6
=> Zero counts at step no.    862 at 2theta/TOF/E(KeV):      33.5519  Intensity fixed to 1.0 and variance to 1E6
=> Zero counts at step no.    863 at 2theta/TOF/E(KeV):      33.5768  Intensity fixed to 1.0 and variance to 1E6
=> Zero counts at step no.    864 at 2theta/TOF/E(KeV):      33.6017  Intensity fixed to 1.0 and variance to 1E6
=> Zero counts at step no.    871 at 2theta/TOF/E(KeV):      33.7760  Intensity fixed to 1.0 and variance to 1E6
=> Zero counts at step no.    872 at 2theta/TOF/E(KeV):      33.8009  Intensity fixed to 1.0 and variance to 1E6
=> Zero counts at step no.    875 at 2theta/TOF/E(KeV):      33.8756  Intensity fixed to 1.0 and variance to 1E6
=> Zero counts at step no.    877 at 2theta/TOF/E(KeV):      33.9254  Intensity fixed to 1.0 and variance to 1E6
=> Zero counts at step no.    895 at 2theta/TOF/E(KeV):      34.3736  Intensity fixed to 1.0 and variance to 1E6
=> Zero counts at step no.    896 at 2theta/TOF/E(KeV):      34.3985  Intensity fixed to 1.0 and variance to 1E6
=> Zero counts at step no.    899 at 2theta/TOF/E(KeV):      34.4732  Intensity fixed to 1.0 and variance to 1E6
=> Zero counts at step no.    939 at 2theta/TOF/E(KeV):      35.4692  Intensity fixed to 1.0 and variance to 1E6
=> Zero counts at step no.    961 at 2theta/TOF/E(KeV):      36.0170  Intensity fixed to 1.0 and variance to 1E6
=> Zero counts at step no.    964 at 2theta/TOF/E(KeV):      36.0917  Intensity fixed to 1.0 and variance to 1E6
=> Zero counts at step no.    967 at 2theta/TOF/E(KeV):      36.1664  Intensity fixed to 1.0 and variance to 1E6
=> Zero counts at step no.    968 at 2theta/TOF/E(KeV):      36.1913  Intensity fixed to 1.0 and variance to 1E6
=> Zero counts at step no.    971 at 2theta/TOF/E(KeV):      36.2660  Intensity fixed to 1.0 and variance to 1E6
=> Zero counts at step no.    972 at 2theta/TOF/E(KeV):      36.2909  Intensity fixed to 1.0 and variance to 1E6
=> Zero counts at step no.    973 at 2theta/TOF/E(KeV):      36.3158  Intensity fixed to 1.0 and variance to 1E6
=> Zero counts at step no.    976 at 2theta/TOF/E(KeV):      36.3905  Intensity fixed to 1.0 and variance to 1E6
=> Zero counts at step no.   1008 at 2theta/TOF/E(KeV):      37.1873  Intensity fixed to 1.0 and variance to 1E6
=> Zero counts at step no.   1012 at 2theta/TOF/E(KeV):      37.2869  Intensity fixed to 1.0 and variance to 1E6
=> Zero counts at step no.   1054 at 2theta/TOF/E(KeV):      38.3327  Intensity fixed to 1.0 and variance to 1E6
=> Zero counts at step no.   1069 at 2theta/TOF/E(KeV):      38.7062  Intensity fixed to 1.0 and variance to 1E6
=> Zero counts at step no.   1070 at 2theta/TOF/E(KeV):      38.7311  Intensity fixed to 1.0 and variance to 1E6
=> Zero counts at step no.   1072 at 2theta/TOF/E(KeV):      38.7809  Intensity fixed to 1.0 and variance to 1E6
```

```
=> Optimizations for routine tasks applied:
=> Calculation mode for patter#:   1  CM_PSEUDO_VOIGT


Standard deviations have to be multiplied by: 3.5344
(correlated residuals) See references:
-J.F.Berar & P.Lelann, J. Appl. Cryst. 24, 1-5 (1991)
-J.F.Berar, Acc. in Pow. Diff. II,NIST Sp.Pub. 846, 63(1992)

++++++++++++++++++++++++++++++++++++++++++++++++++++++++++++++++++++++++++++++++++++++++++++++++++++++++++++++++++++++++++++++++++++++ ↙


=> CYCLE No.:   18
=>  Convergence reached at this CYCLE !!!!
=>  Parameter shifts set to zero
-------------------------------------------------------------------------------
=> Phase  1 Name:   rdx
-------------------------------------------------------------------------------
=> New parameters, shifts, and standard deviations

Atom         x       dx      sx       y       dy      sy       z       dz      sz       B       dB      sB      occ.  ↙
        docc.   socc.

O(1)      0.56846 0.00000 0.00000  0.43427 0.00000 0.00000  0.26465 0.00000 0.00000  3.70830 0.00000 0.00000    ↙
     1.00000 0.00000 0.00000
O(2)      0.59453 0.00000 0.00000  0.24040 0.00000 0.00000  0.23053 0.00000 0.00000  4.41110 0.00000 0.00000    ↙
     1.00000 0.00000 0.00000
O(3)      0.47340 0.00000 0.00000  0.13880 0.00000 0.00000 -0.02250 0.00000 0.00000  4.98480 0.00000 0.00000    ↙
     1.00000 0.00000 0.00000
O(4)      0.35580 0.00000 0.00000  0.24950 0.00000 0.00000 -0.11238 0.00000 0.00000  4.76640 0.00000 0.00000    ↙
     1.00000 0.00000 0.00000
O(5)      0.31810 0.00000 0.00000  0.53030 0.00000 0.00000 -0.06806 0.00000 0.00000  5.32170 0.00000 0.00000    ↙
     1.00000 0.00000 0.00000
O(6)      0.42860 0.00000 0.00000  0.60110 0.00000 0.00000  0.04920 0.00000 0.00000  5.10850 0.00000 0.00000    ↙
     1.00000 0.00000 0.00000
N(1)      0.43638 0.00000 0.00000  0.33385 0.00000 0.00000  0.17584 0.00000 0.00000  2.73980 0.00000 0.00000    ↙
     1.00000 0.00000 0.00000
N(2)      0.32231 0.00000 0.00000  0.23197 0.00000 0.00000  0.05389 0.00000 0.00000  2.40240 0.00000 0.00000    ↙
     1.00000 0.00000 0.00000
N(3)      0.29900 0.00000 0.00000  0.45348 0.00000 0.00000  0.08838 0.00000 0.00000  2.59240 0.00000 0.00000    ↙
     1.00000 0.00000 0.00000
N(4)      0.53777 0.00000 0.00000  0.33516 0.00000 0.00000  0.22628 0.00000 0.00000  2.76530 0.00000 0.00000    ↙
     1.00000 0.00000 0.00000
N(5)      0.38834 0.00000 0.00000  0.20759 0.00000 0.00000 -0.03308 0.00000 0.00000  3.09700 0.00000 0.00000    ↙
     1.00000 0.00000 0.00000
N(6)      0.35299 0.00000 0.00000  0.52971 0.00000 0.00000  0.01650 0.00000 0.00000  3.43200 0.00000 0.00000    ↙
     1.00000 0.00000 0.00000
C(1)      0.35799 0.00000 0.00000  0.43950 0.00000 0.00000  0.18450 0.00000 0.00000  2.89510 0.00000 0.00000    ↙
     1.00000 0.00000 0.00000
C(2)      0.38140 0.00000 0.00000  0.21557 0.00000 0.00000  0.14950 0.00000 0.00000  2.70030 0.00000 0.00000    ↙
     1.00000 0.00000 0.00000
C(3)      0.24458 0.00000 0.00000  0.33936 0.00000 0.00000  0.05038 0.00000 0.00000  2.55740 0.00000 0.00000    ↙
     1.00000 0.00000 0.00000
H(1A)     0.40289 0.00000 0.00000  0.52403 0.00000 0.00000  0.20773 0.00000 0.00000  5.13220 0.00000 0.00000    ↙
     1.00000 0.00000 0.00000
H(1B)     0.29071 0.00000 0.00000  0.42024 0.00000 0.00000  0.23991 0.00000 0.00000  4.84270 0.00000 0.00000    ↙
     1.00000 0.00000 0.00000
H(2A)     0.44331 0.00000 0.00000  0.13918 0.00000 0.00000  0.14950 0.00000 0.00000  4.60580 0.00000 0.00000    ↙
     1.00000 0.00000 0.00000
H(2B)     0.31742 0.00000 0.00000  0.19390 0.00000 0.00000  0.20730 0.00000 0.00000  4.97430 0.00000 0.00000    ↙
     1.00000 0.00000 0.00000
H(3A)     0.20936 0.00000 0.00000  0.35364 0.00000 0.00000 -0.02527 0.00000 0.00000  4.50050 0.00000 0.00000    ↙
     1.00000 0.00000 0.00000
H(3B)     0.17213 0.00000 0.00000  0.32091 0.00000 0.00000  0.10070 0.00000 0.00000  3.92150 0.00000 0.00000    ↙
     1.00000 0.00000 0.00000

==> PROFILE PARAMETERS FOR PATTERN#  1

=> Overall scale factor:      0.000451821     0.000000000     0.000003839
=> Eta(p-Voigt) or m(Pearson VII):   0.000000  0.000000  0.000000
=> Overall tem. factor:   0.000000  0.000000  0.000000
=> Halfwidth parameters:
-0.004847  0.000000  0.013262
0.000000  0.000000  0.000000
0.000000  0.000000  0.000000
=> Cell parameters:
11.630419   0.000000   0.000000
10.743058   0.000000   0.000000
13.227938   0.000000   0.000000
90.000000   0.000000   0.000000
90.000000   0.000000   0.000000
90.000000   0.000000   0.000000
=> Preferred orientation:
1.000000  0.000000  0.000000
0.000000  0.000000  0.000000
=> Asymmetry parameters:
0.032918  0.000000  0.006054
0.042103  0.000000  0.003202
```

```
0.000000  0.000000  0.000000
0.000000  0.000000  0.000000
=> X and Y parameters:
0.000000  0.000000  0.000000
0.000000  0.000000  0.000000
=> Strain parameters:
0.000000  0.000000  0.000000
0.000000  0.000000  0.000000
0.000000  0.000000  0.000000
=> Size   parameters (G,L):
0.010384  0.000000  0.000253
0.000000  0.000000  0.000000
=> Further shape parameters (S_L and D_L):
0.000000  0.000000  0.000000
0.000000  0.000000  0.000000

==> GLOBAL PARAMETERS FOR PATTERN#  1


=> Zero-point:    -0.0410    0.0000    0.0000

=> Cos( theta)-shift parameter :  -0.1020  0.0000  0.0000
=> Sin(2theta)-shift parameter :   0.2630  0.0000  0.0000

==> RELIABILITY FACTORS WITH ALL NON-EXCLUDED POINTS FOR PATTERN:  1

=> R-Factors:   20.1      26.6     Chi2:  68.3     DW-Stat.:  0.7185   Patt#:  1
=> Expected :            3.22                                1.8193
=> Deviance : 0.870E+05     Dev*:   81.04
=> GoF-index:  8.2         Sqrt(Residual/N)
=> N-P+C:  1072

=>    SumYdif       SumYobs      SumYcal      SumwYobsSQ     Residual    Condition
0.2080E+06    0.1034E+07    0.9677E+06    0.1034E+07    0.7325E+05    0.1251E+08


=> Conventional Rietveld Rp,Rwp,Re and Chi2:   20.3      26.8      3.24      68.33
=> (Values obtained using Ynet, but true sigma(y))
=>  SumYnet, Sum(w Ynet**2):     0.1024E+07    0.1020E+07

=> N-sigma of the GoF: 1558.821

==> RELIABILITY FACTORS FOR POINTS WITH BRAGG CONTRIBUTIONS FOR PATTERN:  1

=> R-Factors:   20.1      26.6     Chi2:  68.3     DW-Stat.:  0.7185   Patt#:
=> Expected :            3.22                                1.8193
=> Deviance : 0.870E+05     Dev*:   81.04
=> GoF-index:  8.2         Sqrt(Residual/N)
=> N-P+C:  1072

=>    SumYdif       SumYobs      SumYcal      SumwYobsSQ     Residual    Condition
0.2080E+06    0.1034E+07    0.9677E+06    0.1034E+07    0.7325E+05    0.1251E+08


=> Conventional Rietveld Rp,Rwp,Re and Chi2:   20.3      26.8      3.24      68.33
=> (Values obtained using Ynet, but true sigma(y))
=>  SumYnet, Sum(w Ynet**2):     0.1024E+07    0.1020E+07

=> N-sigma of the GoF:     1558.821

=> Global user-weigthed Chi2 (Bragg contrib.):   68.3

-------------------------------------------------------------------------------------------------------------
Pattern#  1 Phase No:   1 Phase name:   rdx
-------------------------------------------------------------------------------------------------------------

No.  Code      H   K   L  Mult     Hw         2theta      Icalc       Iobs      Sigma      HwG     HwL       ETA   ↙
          d-hkl         CORR

1   1      1   1   1     8  0.121476      13.052     1251.5      994.7    209.519  0.117519  0.007393  0.081390    ↙
     6.777159     607.424438
2   1      0   0   2     2  0.121533      13.376      615.4      524.7     81.556  0.117477  0.007575  0.083321    ↙
     6.613969     144.491653
3   1      2   0   0     2  0.121864      15.223       83.3       51.4     26.997  0.117249  0.008622  0.094298    ↙
     5.815209     111.037720
4   1      1   0   2     4  0.121897      15.399      794.1      560.8    173.189  0.117228  0.008722  0.095336    ↙
     5.749331     216.941605
5   1      0   2   0     2  0.122102      16.489      378.8      358.2     27.066  0.117101  0.009342  0.101767    ↙
     5.371529      94.315758
6   1      2   1   0     4  0.122263      17.326      976.1      922.9     64.119  0.117007  0.009818  0.106679    ↙
     5.114053     170.442551
7   1      1   1   2     8  0.122294      17.481      128.0      136.4      9.973  0.116990  0.009907  0.107586    ↙
     5.069075     334.714142
8   1      0   2   1     4  0.122358      17.807     1572.9     1430.3    156.574  0.116955  0.010093  0.109498    ↙
     4.976847     161.115646
9   1      2   1   1     8  0.122514      18.586       23.0       13.8     34.306  0.116872  0.010539  0.114047    ↙
     4.769984     295.069672
10   1      1   2   1     8  0.122677      19.384       22.5       18.6     46.407  0.116789  0.010996  0.118687    ↙
     4.575528     270.592194
11   1      2   0   2     4  0.122872      20.318      980.1     1062.1    132.544  0.116696  0.011533  0.124103    ↙
```

	4.367220	122.753159											
12	1 0	2 2 4	0.123082	21.291	68.1	86.2	33.725	0.116603	0.012094	0.129725	↙		
	4.169635	111.398773											
13	1 2	1 2 8	0.123227	21.952	775.6	843.0	85.375	0.116543	0.012476	0.133524	↙		
	4.045709	209.094452											
14	1 2	2 0 4	0.123352	22.515	144.3	135.0	23.581	0.116493	0.012802	0.136755	↙		
	3.945786	99.174377											
15	1 1	2 2 8	0.123379	22.635	39.2	34.2	6.470	0.116482	0.012872	0.137447	↙		
	3.925016	196.149139											
16	1 1	1 3 8	0.123482	23.087	27.2	20.6	9.583	0.116443	0.013134	0.140032	↙		
	3.849222	188.221832											
17	1 2	2 1 8	0.123579	23.509	148.2	155.7	46.760	0.116408	0.013379	0.142440	↙		
	3.781150	181.234940											
18	1 3	1 1 8	0.124006	25.314	902.6	1096.9	241.947	0.116265	0.014433	0.152701	↙		
	3.515492	155.173340											
19	1 0	2 3 4	0.124205	26.125	37.3	64.9	47.910	0.116206	0.014909	0.157288	↙		
	3.408129	72.593018											
20	1 2	2 2 8	0.124243	26.278	9.1	16.6	13.432	0.116195	0.014999	0.158154	↙		
	3.388580	143.401276											
21	1 3	0 2 4	0.124331	26.630	6.6	9.1	3.570	0.116170	0.015206	0.160138	↙		
	3.344589	69.711670											
22	1 2	1 3 8	0.124341	26.672	146.0	189.7	56.634	0.116167	0.015231	0.160373	↙		
	3.339449	138.961929											
23	1 1	3 1 8	0.124395	26.886	522.6	614.0	107.796	0.116153	0.015357	0.161577	↙		
	3.313359	136.631302											
24	1 0	0 4 2	0.124408	26.939	325.3	373.2	55.441	0.116149	0.015388	0.161874	↙		
	3.306984	34.016178											
25	1 1	2 3 8	0.124486	27.244	146.1	200.2	74.655	0.116129	0.015568	0.163591	↙		
	3.270598	132.851700											
26	1 3	1 2 8	0.124659	27.916	3.2	0.3	16.861	0.116086	0.015966	0.167359	↙		
	3.193409	126.155663											
27	1 1	0 4 4	0.124688	28.028	0.1	0.2	1.590	0.116079	0.016032	0.167986	↙		
	3.180897	62.542797											
28	1 3	2 1 8	0.124991	29.175	586.2	784.3	264.693	0.116011	0.016713	0.174392	↙		
	3.058400	114.835915											
29	1 1	1 4 8	0.125013	29.257	889.3	1121.2	292.295	0.116006	0.016762	0.174849	↙		
	3.050011	114.149055											
30	1 2	3 0 4	0.125015	29.265	451.7	568.8	147.410	0.116006	0.016767	0.174891	↙		
	3.049236	57.042862											
31	1 1	3 2 8	0.125041	29.359	3.1	4.2	1.385	0.116000	0.016823	0.175419	↙		
	3.039620	113.300980											
32	1 2	3 1 8	0.125229	30.050	0.6	0.2	4.321	0.115963	0.017235	0.179258	↙		
	2.971314	107.799812											
33	1 2	2 3 8	0.125318	30.374	402.2	432.9	37.902	0.115947	0.017429	0.181055	↙		
	2.940360	105.349037											
34	1 4	0 0 2	0.125415	30.724	184.3	205.1	23.261	0.115929	0.017639	0.182997	↙		
	2.907605	25.696112											
35	1 2	0 4 4	0.125517	31.085	253.8	305.4	61.928	0.115912	0.017856	0.184993	↙		
	2.874666	50.117661											
36	1 3	2 2 8	0.125629	31.483	56.1	69.9	17.217	0.115893	0.018095	0.187192	↙		
	2.839199	97.524094											
37	1 0	2 4 4	0.125705	31.749	6.4	7.4	1.141	0.115882	0.018255	0.188655	↙		
	2.816087	47.887966											
38	1 3	1 3 8	0.125725	31.818	61.1	76.2	18.666	0.115879	0.018297	0.189037	↙		
	2.810112	95.326462											
39	1 4	1 0 4	0.125737	31.859	134.1	171.3	47.391	0.115877	0.018321	0.189260	↙		
	2.806627	47.532345											
40	1 2	1 4 8	0.125838	32.208	431.3	549.7	150.424	0.115862	0.018532	0.191184	↙		
	2.776968	92.850838											
41	1 2	3 2 8	0.125865	32.302	465.1	587.6	154.278	0.115858	0.018589	0.191699	↙		
	2.769119	92.268997											
42	1 4	1 1 8	0.125948	32.587	48.8	55.6	7.746	0.115847	0.018762	0.193268	↙		
	2.745508	90.529259											
43	1 1	2 4 8	0.125979	32.691	36.1	43.5	8.932	0.115843	0.018825	0.193840	↙		
	2.736998	89.905861											
44	1 1	3 3 8	0.126102	33.107	290.6	312.4	24.459	0.115827	0.019077	0.196118	↙		
	2.703608	87.479691											
45	1 0	4 0 2	0.126169	33.333	63.6	77.5	17.300	0.115819	0.019214	0.197357	↙		
	2.685765	21.548969											
46	1 4	0 2 4	0.126262	33.643	6.6	5.4	19.513	0.115808	0.019403	0.199051	↙		
	2.661751	42.241043											
47	1 0	4 1 4	0.126380	34.034	45.1	56.9	27.961	0.115795	0.019641	0.201187	↙		
	2.632060	41.192669											
48	1 4	1 2 8	0.126582	34.692	66.2	78.5	15.767	0.115775	0.020043	0.204774	↙		
	2.583631	79.018021											
49	1 3	3 1 8	0.126597	34.742	306.6	360.7	66.180	0.115774	0.020074	0.205047	↙		
	2.580004	78.768509											
50	1 1	4 1 8	0.126653	34.922	0.0	0.0	0.002	0.115769	0.020184	0.206025	↙		
	2.567142	77.886520											
51	1 3	2 3 8	0.126686	35.027	280.9	388.9	149.247	0.115766	0.020248	0.206597	↙		
	2.559662	77.375694											
52	1 4	2 0 4	0.126698	35.064	41.3	57.5	22.622	0.115765	0.020271	0.206800	↙		
	2.557027	38.598064											
53	1 2	2 4 8	0.126798	35.386	0.0	0.0	0.038	0.115757	0.020468	0.208545	↙		
	2.534537	75.671524											
54	1 3	0 4 4	0.126884	35.655	86.7	101.1	20.860	0.115750	0.020634	0.210009	↙		
	2.515971	37.211742											
55	1 4	2 1 8	0.126909	35.735	20.1	23.9	5.495	0.115748	0.020683	0.210440	↙		
	2.510551	74.061028											
56	1 1	1 5 8	0.126919	35.767	0.1	0.2	0.035	0.115748	0.020703	0.210613	↙		

```
     2.508384      73.916328
57   1      2   3   3     8  0.126921      35.773        5.5        6.3      1.378  0.115747  0.020707  0.210647    ↙
     2.507954      73.887573
58   1      0   4   2     4  0.127014      36.064        0.1        0.0      2.150  0.115741  0.020886  0.212219    ↙
     2.488423      36.294819
59   1      3   1   4     8  0.127204      36.654       30.6       34.8      7.231  0.115730  0.021251  0.215410    ↙
     2.449688      70.047195
60   1      3   3   2     8  0.127232      36.738      106.4      126.2     26.614  0.115728  0.021303  0.215862    ↙
     2.444295      69.696564

No.  Code      H   K   L  Mult      Hw         2theta      Icalc       Iobs      Sigma       HwG      HwL       ETA   ↙
          d-hkl         CORR

61   1      2   4   0     4  0.127262      36.832      170.5      217.3     61.355  0.115726  0.021361  0.216369    ↙
     2.438274      34.653053
62   1      1   4   2     8  0.127287      36.909       31.8       41.5     13.047  0.115725  0.021409  0.216785    ↙
     2.433349      68.987450
63   1      2   4   1     8  0.127474      37.475       52.9       58.0      9.209  0.115717  0.021760  0.219834    ↙
     2.397879      66.712807
64   1      4   2   2     8  0.127544      37.685        4.4        5.6      1.553  0.115714  0.021891  0.220963    ↙
     2.384992      65.895241
65   1      1   3   4     8  0.127582      37.797        0.1        0.1      0.058  0.115713  0.021961  0.221566    ↙
     2.378168      65.464195
66   1      0   2   5     4  0.127608      37.877       47.4       63.8     22.004  0.115712  0.022011  0.221994    ↙
     2.373343      32.580132
67   1      4   1   3     8  0.127640      37.971      166.0      225.5     80.815  0.115711  0.022069  0.222500    ↙
     2.367672      64.803848
68   1      2   1   5     8  0.127741      38.272        1.3        1.6      8.054  0.115708  0.022257  0.224110    ↙
     2.349785      63.685627
69   1      1   2   5     8  0.127883      38.689        1.1        0.0     25.305  0.115705  0.022518  0.226343    ↙
     2.325420      62.177151

-------------------------------------------------------
BRAGG R-Factors and weight fractions for Pattern #  1
-------------------------------------------------------

=> Phase:  1       rdx
=> Bragg R-factor:   17.2       Vol: 1652.781( 0.000)  Fract(%):  100.00( 1.20)
=> Rf-factor=  9.62             ATZ:        1776.939   Brindley:  1.0000

-------------------------------------------------------------------
SYMBOLIC NAMES AND FINAL VALUES AND SIGMA OF REFINED PARAMETERS:
-------------------------------------------------------------------

->  Parameter number    1 :       Scale_ph1_pat1    0.45182102E-03( +/-    0.38391618E-05 )
->  Parameter number    2 :      U-Cagl_ph1_pat1   -0.48470786E-02( +/-    0.13262363E-01 )
->  Parameter number    3 :      G-Size_ph1_pat1    0.10384443E-01( +/-    0.25276333E-03 )
->  Parameter number    4 :       Asym1_ph1_pat1    0.32917723E-01( +/-    0.60544414E-02 )
->  Parameter number    5 :       Asym2_ph1_pat1    0.42102702E-01( +/-    0.32015643E-02 )

-------------------------------------------------------------------
=> Number of bytes for floating point variables: 4
=> Dimensions of dynamic allocated arrays in this run of FullProf:
-------------------------------------------------------------------

=> Total approximate array memory (dynamic + static): 107719993 bytes

MaxPOINT=    60000 Max.num. of points(+int. Inten.)/diffraction pattern
MaxREFLT=    20000 Max.num. of reflections/diffraction pattern
MaxPARAM=      300 Max.num. of refinable parameters
MaxOVERL=     2096 Max.num. of overlapping reflections

-----------------------------------------------------------
=> Number of bytes for floating point arrays: 4
=> Dimensions of fixed arrays in this release of FullProf:
-----------------------------------------------------------

NPATT   =       80 Max.num. of powder diffraction patterns
NATS    =      830 Max.num. of atoms (all kind) in asymmetric unit
MPAR    =     1800 Max.num. of non atomic parameters/phase
IEXCL   =       30 Max.num. of excluded regions
IBACP   =      277 Max.num. of background points for interpolation
NPHT    =       16 Max.num. of phases
NMAGM   =        8 Max.num. of rotation-matrices sets for magnetic structure
NBASIS  =       12 Max.num. of basis functions associated to a single atom
NIREPS  =        9 Max.num. of irreducible representations to be combined
N_EQ    =      384 Max.num. of user-supplied symmetry operators/propagation vectors
NGL     =      300 Max.num. of global parameters/diffraction pattern
N_LINC  =       30 Max.num. of global linear restraints
NAT_P   =       64 Max.num. of atomic parameters per atom
NCONST  =      500 Max.num. of slack constraints per phase
N_SPE   =       16 Max.num. of different chemical species
N_FORM  =       60 Max.num. of scattering factor values in a table
NPR     =      150 Max.num. of points defining a numerical profile
INPR    =       25 Max.num. of different numerical peak shapes
NPRC    =      150 Max.num. of terms in the table for correcting intensities
NSOL    =       10 Max.num. of solutions to be stored in Montecarlo searchs


CPU Time:     6.645 seconds
```

```
0.111 minutes

=> Run finished at:     Date: 18/02/2015  Time: 13:16:33.614
```

A.4 Sample of n-RDX processed with 0.1 wt% of PEG

```
*******************************************************
** PROGRAM FullProf.2k (Version 5.60 - Jan2015-ILL JRC) **
*******************************************************
M U L T I -- P A T T E R N
Rietveld, Profile Matching & Integrated Intensity
Refinement of X-ray and/or Neutron Data


Date: 06/07/2015  Time: 15:52:37.093

=> PCR file code: rpg4std2e
=> DAT file code: rpg4std2e.dat        -> Relative contribution: 1.0000

==> CONDITIONS OF THIS RUN FOR PATTERN No.:  1

=> Global Refinement of X-ray powder diffraction data
=> Global Refinement of X-ray powder diffraction data
Flat plate with PSD
=> Title:RDX

=> Number of phases:    1
=> Number of excluded regions:    1
=> Number of scattering factors supplied:    0
=> March-Dollase model for preferred orientation
=> Conventional weights: w=1.0/Variance(yobs)
=> Asymmetry correction as in J.Appl.Cryst. 26,128(1993)
=> Background refined by polynomial function
=> The    7th default profile function was selected
=> T-C-H Pseudo-Voigt function
This function is convoluted with asymmetry due to axial
divergence as formulated by:
van Laar and Yelon, J. Appl. Cryst. 17, 47(1984).
and using the method of:
Finger, Cox and Jephcoat, J. Appl. Cryst. 27, 892 (1994).
Fortran 90 module adapted from function PROFVAL (in F77) :
L.W. Finger, J. Appl. Cryst. 31, 111 (1998).


==> INPUT/OUTPUT OPTIONS:

=> Generate file *.PRF for plot
=> Output Integrated Intensities
=> Generate new input file *.PCR

=> Data supplied in free format for pattern:  1
=> Plot pattern at each cycle
=> Wavelengths:  1.54056 1.54439
=> Alpha2/Alpha1 ratio:   0.5000
=> Cos(Monochromator angle)=   1.0000
=> Asymmetry correction for angles lower than   90.000 degrees
=> Absorption correction (AC), muR-eff =   0.0000  0.0000
=> Base of peaks: 2.0*HW*   20.00

=> Number of cycles:   50
=> Relaxation factors ==>    for coordinates:  1.00
=> for anisotropic temperature factors:  1.00
=> for halfwidth/strain/size parameters:  1.00
=> for lattice constants and propagation vectors:  1.00
=> EPS-value for convergence:    0.0

=> Excluded regions for Pattern#  1
From     to
39.0000     50.0000

=> Instrumental Resolution read from file: xray-res.irf
=> Title of data: Approximate resolution function of a conventional X-ray diffractometer CuKalpha1,2

=> The resolution function is IRESOL:   1 for profile function #   7
Input resolution parameters:

U-inst     V-inst     W-inst     X-inst     Y-inst     Z-inst
0.00136   -0.00500    0.00391    0.06389    0.00008    0.00000
0.00136   -0.00500    0.00391    0.06389    0.00008    0.00000

=> Number of Least-Squares parameters varied:    58

=>--------------------------->
=>-------->  PATTERN number:  1
=>--------------------------->
=> Global parameters and codes ==>
=> Zero-point:    -0.3162  541.0000
```

```
=> Background parameters and codes ==>
=> Origin of polynomial at 2theta/TOF/E(KeV):   40.000
0.0000      0.0000      0.0000      0.0000      0.0000      0.0000
0.00        0.00        0.00        0.00        0.00        0.00
=> Displacement peak-shift parameter and code:     0.00    0.00
=> Transparency peak-shift parameter and code:     0.00    0.00

=> Reading Intensity data  =>>

==> Angular range, step and number of points:
2Thmin:      12.000000  2Thmax:      39.002102  Step:       0.007400  No. of points:   3650
------------------------------------------------------------------------------
=> Phase  No. 1
rdx
------------------------------------------------------------------------------
=>-------> Pattern#  1
=> Crystal Structure Refinement
=> Preferred orientation vector:   0.0000  0.0000  1.0000

=>-------> Data for PHASE: 1
=> Number of atoms:   21
=> Number of distance  constraints:    0
=> Number of angle     constraints:    0

=> Symmetry information on space group: P b c a
-> The multiplicity of the general position is:   8
-> The space group is Centric (-1 at origin)
-> Lattice type  P: { 000 }
-> Reduced set of symmetry operators:

No.  IT   Symmetry symbol    Rotation part     Associated Translation
1: ( 1)   1            -->     ( x, y, z) + {  0.0000  0.0000  0.0000}
2: ( 4)   2 ( x, 0, 0) -->     ( x,-y,-z) + {  0.5000  0.5000  0.0000}
3: ( 3)   2 ( 0, y, 0) -->     (-x, y,-z) + {  0.0000  0.5000  0.5000}
4: ( 2)   2 ( 0, 0, z) -->     (-x,-y, z) + {  0.5000  0.0000  0.5000}


Information on Space Group:
---------------------------

=>   Number of Space group:  61
=>  Hermann-Mauguin Symbol: P b c a
=>             Hall Symbol: -P 2ac 2ab
=>            Setting Type: IT (Generated from Hermann-Mauguin symbol)
=>          Crystal System: Orthorhombic
=>              Laue Class: mmm
=>              Point Group: mmm
=>         Bravais Lattice: P
=>          Lattice Symbol: oP
=>  Reduced Number of S.O.:   4
=>    General multiplicity:   8
=>          Centrosymmetry: Centric (-1 at origin)
=>  Generators (exc. -1&L):   2
=>         Asymmetric unit:  0.000 <= x <=  0.500
0.000 <= y <=  0.500
0.000 <= z <=  0.500

=> List of S.O. without inversion and lattice centring translations
=> SYMM(  1): x,y,z                              => SYMM(  2): x+1/2,-y+1/2,-z
=> SYMM(  3): -x,y+1/2,-z+1/2                    => SYMM(  4): -x+1/2,-y,z+1/2


=> Initial parameters ==>
Atom    Ntyp                  X         Y         Z         B         occ.         in  fin  Spc  Mult
B11       B22       B33       B12       B13       B23
O(1)    O                  0.57608   0.43936   0.27021   3.70830   1.00000           0    0    0    8
Codes:   71.00000  81.00000  91.00000   0.00000   0.00000
O(2)    O                  0.59405   0.22852   0.22899   4.41110   1.00000           0    0    0    8
Codes:  101.00000 111.00000 121.00000   0.00000   0.00000
O(3)    O                  0.47165   0.13110  -0.01874   4.98480   1.00000           0    0    0    8
Codes:  131.00000 141.00000 151.00000   0.00000   0.00000
O(4)    O                  0.34305   0.25796  -0.11691   4.76640   1.00000           0    0    0    8
Codes:  161.00000 171.00000 181.00000   0.00000   0.00000
O(5)    O                  0.31082   0.51151  -0.07935   5.32170   1.00000           0    0    0    8
Codes:  191.00000 201.00000 211.00000   0.00000   0.00000
O(6)    O                  0.42897   0.59176   0.05201   5.10850   1.00000           0    0    0    8
Codes:  221.00000 231.00000 241.00000   0.00000   0.00000
N(1)    N                  0.44550   0.33187   0.17883   2.73980   1.00000           0    0    0    8
Codes:  251.00000 261.00000 271.00000   0.00000   0.00000
N(2)    N                  0.33005   0.24334   0.05173   2.40240   1.00000           0    0    0    8
Codes:  281.00000 291.00000 301.00000   0.00000   0.00000
N(3)    N                  0.30372   0.45297   0.07981   2.59240   1.00000           0    0    0    8
Codes:  311.00000 321.00000 331.00000   0.00000   0.00000
N(4)    N                  0.53997   0.33764   0.23203   2.76530   1.00000           0    0    0    8
Codes:  341.00000 351.00000 361.00000   0.00000   0.00000
N(5)    N                  0.38995   0.20392  -0.04081   3.09700   1.00000           0    0    0    8
Codes:  371.00000 381.00000 391.00000   0.00000   0.00000
N(6)    N                  0.35080   0.55348   0.01182   3.43200   1.00000           0    0    0    8
Codes:  401.00000 411.00000 421.00000   0.00000   0.00000
C(1)    C                  0.34908   0.43663   0.19413   2.89510   1.00000           0    0    0    8
```

```
Codes:  431.00000 441.00000 451.00000   0.00000   0.00000
C(2)   C                  0.38479   0.21557   0.14692   2.70030   1.00000           0    0    0    8
Codes:  461.00000 471.00000 481.00000   0.00000   0.00000
C(3)   C                  0.23190   0.33513   0.04874   2.55740   1.00000           0    0    0    8
Codes:  491.00000 501.00000 511.00000   0.00000   0.00000
H(1A)  H                  0.40289   0.52403   0.20773   5.13220   1.00000           0    0    0    8
Codes:    0.00000   0.00000   0.00000   0.00000   0.00000
H(1B)  H                  0.29071   0.42024   0.23991   4.84270   1.00000           0    0    0    8
Codes:    0.00000   0.00000   0.00000   0.00000   0.00000
H(2A)  H                  0.44331   0.13918   0.14950   4.60580   1.00000           0    0    0    8
Codes:    0.00000   0.00000   0.00000   0.00000   0.00000
H(2B)  H                  0.31742   0.19390   0.20730   4.97430   1.00000           0    0    0    8
Codes:    0.00000   0.00000   0.00000   0.00000   0.00000
H(3A)  H                  0.20936   0.35364  -0.02527   4.50050   1.00000           0    0    0    8
Codes:    0.00000   0.00000   0.00000   0.00000   0.00000
H(3B)  H                  0.17213   0.32091   0.10070   3.92150   1.00000           0    0    0    8
Codes:    0.00000   0.00000   0.00000   0.00000   0.00000

=> IT IS ASSUMED THAT THE FIRST GIVEN SITE IS FULLY OCCUPIED
OR THE FIRST AND SECOND ATOMS ARE IN THE SAME SITE WITH TOTAL FULL OCCUPATION
(If this is not the case, change the order of atoms to obtain correct values for the content of the unit cell)
The given occupation factors have been obtained mutiplying m/M by   1.0000
-> Atom: O   ,  Chemical element: O   Atomic Mass:    15.9994
-> Atom: O   ,  Chemical element: O   Atomic Mass:    15.9994
-> Atom: O   ,  Chemical element: O   Atomic Mass:    15.9994
-> Atom: O   ,  Chemical element: O   Atomic Mass:    15.9994
-> Atom: O   ,  Chemical element: O   Atomic Mass:    15.9994
-> Atom: O   ,  Chemical element: O   Atomic Mass:    15.9994
-> Atom: N   ,  Chemical element: N   Atomic Mass:    14.0067
-> Atom: N   ,  Chemical element: N   Atomic Mass:    14.0067
-> Atom: N   ,  Chemical element: N   Atomic Mass:    14.0067
-> Atom: N   ,  Chemical element: N   Atomic Mass:    14.0067
-> Atom: N   ,  Chemical element: N   Atomic Mass:    14.0067
-> Atom: N   ,  Chemical element: N   Atomic Mass:    14.0067
-> Atom: C   ,  Chemical element: C   Atomic Mass:    12.0110
-> Atom: C   ,  Chemical element: C   Atomic Mass:    12.0110
-> Atom: C   ,  Chemical element: C   Atomic Mass:    12.0110
-> Atom: H   ,  Chemical element: H   Atomic Mass:     1.0080
-> Atom: H   ,  Chemical element: H   Atomic Mass:     1.0080
-> Atom: H   ,  Chemical element: H   Atomic Mass:     1.0080
-> Atom: H   ,  Chemical element: H   Atomic Mass:     1.0080
-> Atom: H   ,  Chemical element: H   Atomic Mass:     1.0080
-> Atom: H   ,  Chemical element: H   Atomic Mass:     1.0080
=> The given value of ATZ is       1776.94 the program has calculated:        1776.94
The value of ATZ given in the input PCR file will be used for quantitative analysis
=> The chemical content of the unit cell is:
8.0000 O    +   8.0000 O    +   8.0000 O    +   8.0000 O    +   8.0000 O    +   8.0000 O    +   8.0000 N    +     ↙
    8.0000 N    +   8.0000 N    +   8.0000 N    +
8.0000 N    +   8.0000 N    +   8.0000 C    +   8.0000 C    +   8.0000 C    +   8.0000 H    +   8.0000 H    +     ↙
    8.0000 H    +   8.0000 H    +   8.0000 H    +
8.0000 H
=> The normalized site occupation numbers in % are:
100.0000 O(1)   :      100.0000 O(2)   :      100.0000 O(3)   :      100.0000 O(4)   :      100.0000 O(5)   :        ↙
    100.0000 O(6)   :      100.0000 N(1)   :      100.0000 N(2)   :      100.0000 N(3)   :      100.0000 N(4)   :
100.0000 N(5)   :      100.0000 N(6)   :      100.0000 C(1)   :      100.0000 C(2)   :      100.0000 C(3)   :        ↙
    100.0000 H(1A)  :      100.0000 H(1B)  :      100.0000 H(2A)  :      100.0000 H(2B)  :      100.0000 H(3A)  :
100.0000 H(3B)
=> The density (volumic mass) of the compound is:    1.826 g/cm3

=>-------> PROFILE PARAMETERS FOR PATTERN:  1

=> Overall scale factor:   0.766210E-03
=> ETA (p-Voigt) OR M (Pearson VII):   0.0000
=> Overall temperature factor:      0.00000
=> Halfwidth U,V,W:     -0.02544     0.00000     0.00000
=> X and Y parameters:       0.0000      0.0000
=> Direct cell parameters:   11.5436  10.6639  13.1261  90.0000  90.0000  90.0000
=> Preferred orientation parameters:   1.0000  0.0000
=> Asymmetry parameters     :      0.03402     0.04914     0.00000     0.00000
=> Strain parameters        :      0.00000     0.00000     0.00000
=> Size   parameters        :      0.01022    -0.01068
=> Further shape parameters (S_L and D_L):   0.00000   0.00000
S_L is source width/detector distance
D_L is detector width/detector distance

==> CODEWORDS FOR PROFILE PARAMETERS of PATTERN#  1

=> Overall scale factor:  521.000
=> ETA (p-Voigt) OR M (Pearson VII):    0.000
=> Overall temperature factor:    0.000
=> Halfwidth U,V,W:  551.000   0.000   0.000
=> X and Y parameters:    0.000   0.000
=> Direct cell parameters:  531.000 561.000 571.000   0.000   0.000   0.000
=> Preferred orientation parameters:    0.000   0.000
=> Asymmetry parameters     :    0.000   0.000   0.000   0.000
=> Strain parameters        :    0.000   0.000   0.000
=> Size   parameters        :  581.000  11.000
=> The 18th model for size is used

=> Orthorhombic Anisotropic Broadening using Spherical Harmonics up
```

```
to 4-th order (Laue class: mmm, SPG:16-74, only lorentzian comp.)
Ylm's up to 4th order: Y00,Y20,Y22+,Y40,Y42+,Y44+
RJP - Ref: M. Jarvinen, J. Appl. C. (1993),p.527
=> Coefficients of Spherical Harmonics for anisotropic size
broadening for an orthorhombic lattice
Y00         Y20          Y22+        Y40          Y42+       Y44+
-0.010678   -0.011090    0.072902    0.116701   -0.093789    0.019010
11.0000     21.0000     31.0000     41.0000     51.0000     61.0000

=> Cell constraints according to Laue symmetry: mmm

Metric information:
-------------------

=> Direct cell parameters:

a =      11.5436      b =      10.6639      c =      13.1261
alpha =       90.000   beta =       90.000  gamma =       90.000
Direct Cell Volume =    1615.8197

=> Reciprocal cell parameters:

a*=     0.086628      b*=     0.093774      c*=     0.076184
alpha*=       90.000   beta*=       90.000  gamma*=       90.000
Reciprocal Cell Volume =   0.00061888

=> Direct and Reciprocal Metric Tensors:

GD                                      GR
133.2541      0.0000      0.0000          0.007504    0.000000    0.000000
0.0000    113.7185      0.0000          0.000000    0.008794    0.000000
0.0000      0.0000    172.2956          0.000000    0.000000    0.005804

=>  Cartesian frame: x // a; y is in the ab-plane; z is x ^ y

Crystal_to_Orthonormal_Matrix             Orthonormal_to_Crystal Matrix
Cr_Orth_cel                               Orth_Cr_cel
11.5436      0.0000      0.0000          0.086628    0.000000    0.000000
0.0000     10.6639      0.0000          0.000000    0.093774    0.000000
0.0000      0.0000     13.1261          0.000000    0.000000    0.076184

Busing-Levy B-matrix: Hc=B.H            Inverse of the Busing-Levy B-matrix
BL_M                                      BL_Minv
0.086628    0.000000    0.000000           11.5436      0.0000      0.0000
0.000000    0.093774    0.000000            0.0000     10.6639      0.0000
0.000000    0.000000    0.076184            0.0000      0.0000     13.1261

=> Laue symmetry mmm   will be used to generate HKL for pattern#   1
=> Reflections generated between S(1/d)min:  0.1354 A-1 and S(1/d)max:  0.4753 A-1
=>                                  dmax:  7.3874 A   and      dmin:  2.1038 A
=> The number of reflections generated is:     91
=> The max. scatt. variable (gen.ref.) is:        42.9553
=> Scattering coefficients from internal table


=> X-ray scattering coeff. (A1, B1, A2,...C, f(0), Z, Dfp,Dfpp)

O       3.0485  13.2771   2.2868   5.7011   1.5463   0.3239   0.8670  32.9089   0.2508   7.9994   8.0000   0.0470  ↙
      0.0320
N      12.2126   0.0057   3.1322   9.8933   2.0125  28.9975   1.1663   0.5826 -11.5290   6.9946   7.0000   0.0290  ↙
      0.0180
C       2.3100  20.8439   1.0200  10.2075   1.5886   0.5687   0.8650  51.6512   0.2156   5.9992   6.0000   0.0170  ↙
      0.0090
H       0.4930  10.5109   0.3229  26.1257   0.1402   3.1424   0.0408  57.7997   0.0030   1.0000   1.0000   0.0000  ↙
      0.0000

---------------------------------------------------------------
SYMBOLIC NAMES AND INITIAL VALUES OF PARAMETERS TO BE VARIED:
---------------------------------------------------------------

->  Parameter number    1   -> Symbolic Name:      L-Size_ph1_pat1   -0.10678000E-01
->  Parameter number    2   -> Symbolic Name:       Size2_ph1_pat1   -0.11090000E-01
->  Parameter number    3   -> Symbolic Name:       Size3_ph1_pat1    0.72902001E-01
->  Parameter number    4   -> Symbolic Name:       Size4_ph1_pat1    0.11670100
->  Parameter number    5   -> Symbolic Name:       Size5_ph1_pat1   -0.93788996E-01
->  Parameter number    6   -> Symbolic Name:       Size6_ph1_pat1    0.19010000E-01
->  Parameter number    7   -> Symbolic Name:           X_O(1)_ph1    0.57608002
->  Parameter number    8   -> Symbolic Name:           Y_O(1)_ph1    0.43935999
->  Parameter number    9   -> Symbolic Name:           Z_O(1)_ph1    0.27021000
->  Parameter number   10   -> Symbolic Name:           X_O(2)_ph1    0.59404999
->  Parameter number   11   -> Symbolic Name:           Y_O(2)_ph1    0.22852001
->  Parameter number   12   -> Symbolic Name:           Z_O(2)_ph1    0.22899000
->  Parameter number   13   -> Symbolic Name:           X_O(3)_ph1    0.47165000
->  Parameter number   14   -> Symbolic Name:           Y_O(3)_ph1    0.13110000
->  Parameter number   15   -> Symbolic Name:           Z_O(3)_ph1   -0.18740000E-01
->  Parameter number   16   -> Symbolic Name:           X_O(4)_ph1    0.34305000
->  Parameter number   17   -> Symbolic Name:           Y_O(4)_ph1    0.25795999
->  Parameter number   18   -> Symbolic Name:           Z_O(4)_ph1   -0.11691000
->  Parameter number   19   -> Symbolic Name:           X_O(5)_ph1    0.31082001
->  Parameter number   20   -> Symbolic Name:           Y_O(5)_ph1    0.51151001
```

```
->  Parameter number   21   -> Symbolic Name:           Z_O(5)_ph1   -0.79350002E-01
->  Parameter number   22   -> Symbolic Name:           X_O(6)_ph1    0.42897001
->  Parameter number   23   -> Symbolic Name:           Y_O(6)_ph1    0.59175998
->  Parameter number   24   -> Symbolic Name:           Z_O(6)_ph1    0.52010000E-01
->  Parameter number   25   -> Symbolic Name:           X_N(1)_ph1    0.44549999
->  Parameter number   26   -> Symbolic Name:           Y_N(1)_ph1    0.33186999
->  Parameter number   27   -> Symbolic Name:           Z_N(1)_ph1    0.17883000
->  Parameter number   28   -> Symbolic Name:           X_N(2)_ph1    0.33004999
->  Parameter number   29   -> Symbolic Name:           Y_N(2)_ph1    0.24334000
->  Parameter number   30   -> Symbolic Name:           Z_N(2)_ph1    0.51729999E-01
->  Parameter number   31   -> Symbolic Name:           X_N(3)_ph1    0.30372000
->  Parameter number   32   -> Symbolic Name:           Y_N(3)_ph1    0.45297000
->  Parameter number   33   -> Symbolic Name:           Z_N(3)_ph1    0.79810001E-01
->  Parameter number   34   -> Symbolic Name:           X_N(4)_ph1    0.53996998
->  Parameter number   35   -> Symbolic Name:           Y_N(4)_ph1    0.33763999
->  Parameter number   36   -> Symbolic Name:           Z_N(4)_ph1    0.23203000
->  Parameter number   37   -> Symbolic Name:           X_N(5)_ph1    0.38995001
->  Parameter number   38   -> Symbolic Name:           Y_N(5)_ph1    0.20392001
->  Parameter number   39   -> Symbolic Name:           Z_N(5)_ph1   -0.40810000E-01
->  Parameter number   40   -> Symbolic Name:           X_N(6)_ph1    0.35080001
->  Parameter number   41   -> Symbolic Name:           Y_N(6)_ph1    0.55348003
->  Parameter number   42   -> Symbolic Name:           Z_N(6)_ph1    0.11820000E-01
->  Parameter number   43   -> Symbolic Name:           X_C(1)_ph1    0.34908000
->  Parameter number   44   -> Symbolic Name:           Y_C(1)_ph1    0.43663001
->  Parameter number   45   -> Symbolic Name:           Z_C(1)_ph1    0.19413000
->  Parameter number   46   -> Symbolic Name:           X_C(2)_ph1    0.38479000
->  Parameter number   47   -> Symbolic Name:           Y_C(2)_ph1    0.21557000
->  Parameter number   48   -> Symbolic Name:           Z_C(2)_ph1    0.14692000
->  Parameter number   49   -> Symbolic Name:           X_C(3)_ph1    0.23190001
->  Parameter number   50   -> Symbolic Name:           Y_C(3)_ph1    0.33513001
->  Parameter number   51   -> Symbolic Name:           Z_C(3)_ph1    0.48740000E-01
->  Parameter number   52   -> Symbolic Name:       Scale_ph1_pat1    0.76621003E-03
->  Parameter number   53   -> Symbolic Name:      Cell_A_ph1_pat1     11.543573
->  Parameter number   54   -> Symbolic Name:            Zero_pat1   -0.31615999
->  Parameter number   55   -> Symbolic Name:      U-Cagl_ph1_pat1   -0.25444999E-01
->  Parameter number   56   -> Symbolic Name:      Cell_B_ph1_pat1     10.663886
->  Parameter number   57   -> Symbolic Name:      Cell_C_ph1_pat1     13.126143
->  Parameter number   58   -> Symbolic Name:      G-Size_ph1_pat1    0.10217000E-01

=> Zero counts at step no.      1 at 2theta/TOF/E(KeV):       12.0000  Intensity fixed to 1.0 and variance to 1E6
=> Zero counts at step no.      3 at 2theta/TOF/E(KeV):       12.0148  Intensity fixed to 1.0 and variance to 1E6
=> Zero counts at step no.      4 at 2theta/TOF/E(KeV):       12.0222  Intensity fixed to 1.0 and variance to 1E6
=> Zero counts at step no.      9 at 2theta/TOF/E(KeV):       12.0592  Intensity fixed to 1.0 and variance to 1E6
=> Zero counts at step no.     10 at 2theta/TOF/E(KeV):       12.0666  Intensity fixed to 1.0 and variance to 1E6
=> Zero counts at step no.     15 at 2theta/TOF/E(KeV):       12.1036  Intensity fixed to 1.0 and variance to 1E6
=> Zero counts at step no.     20 at 2theta/TOF/E(KeV):       12.1406  Intensity fixed to 1.0 and variance to 1E6
=> Zero counts at step no.     25 at 2theta/TOF/E(KeV):       12.1776  Intensity fixed to 1.0 and variance to 1E6
=> Zero counts at step no.     29 at 2theta/TOF/E(KeV):       12.2072  Intensity fixed to 1.0 and variance to 1E6
=> Zero counts at step no.     32 at 2theta/TOF/E(KeV):       12.2294  Intensity fixed to 1.0 and variance to 1E6
=> Zero counts at step no.     36 at 2theta/TOF/E(KeV):       12.2590  Intensity fixed to 1.0 and variance to 1E6
=> Zero counts at step no.     39 at 2theta/TOF/E(KeV):       12.2812  Intensity fixed to 1.0 and variance to 1E6
=> Zero counts at step no.     41 at 2theta/TOF/E(KeV):       12.2960  Intensity fixed to 1.0 and variance to 1E6
=> Zero counts at step no.     48 at 2theta/TOF/E(KeV):       12.3478  Intensity fixed to 1.0 and variance to 1E6
=> Zero counts at step no.     49 at 2theta/TOF/E(KeV):       12.3552  Intensity fixed to 1.0 and variance to 1E6
=> Zero counts at step no.     52 at 2theta/TOF/E(KeV):       12.3774  Intensity fixed to 1.0 and variance to 1E6
=> Zero counts at step no.     53 at 2theta/TOF/E(KeV):       12.3848  Intensity fixed to 1.0 and variance to 1E6
=> Zero counts at step no.     54 at 2theta/TOF/E(KeV):       12.3922  Intensity fixed to 1.0 and variance to 1E6
=> Zero counts at step no.     60 at 2theta/TOF/E(KeV):       12.4366  Intensity fixed to 1.0 and variance to 1E6
=> Zero counts at step no.     67 at 2theta/TOF/E(KeV):       12.4884  Intensity fixed to 1.0 and variance to 1E6
=> Zero counts at step no.     79 at 2theta/TOF/E(KeV):       12.5772  Intensity fixed to 1.0 and variance to 1E6
=> Zero counts at step no.     81 at 2theta/TOF/E(KeV):       12.5920  Intensity fixed to 1.0 and variance to 1E6
=> Zero counts at step no.    182 at 2theta/TOF/E(KeV):       13.3394  Intensity fixed to 1.0 and variance to 1E6
=> Zero counts at step no.    192 at 2theta/TOF/E(KeV):       13.4134  Intensity fixed to 1.0 and variance to 1E6
=> Zero counts at step no.    193 at 2theta/TOF/E(KeV):       13.4208  Intensity fixed to 1.0 and variance to 1E6
=> Zero counts at step no.    194 at 2theta/TOF/E(KeV):       13.4282  Intensity fixed to 1.0 and variance to 1E6
=> Zero counts at step no.    199 at 2theta/TOF/E(KeV):       13.4652  Intensity fixed to 1.0 and variance to 1E6
=> Zero counts at step no.    203 at 2theta/TOF/E(KeV):       13.4948  Intensity fixed to 1.0 and variance to 1E6
=> Zero counts at step no.    205 at 2theta/TOF/E(KeV):       13.5096  Intensity fixed to 1.0 and variance to 1E6
=> Zero counts at step no.    208 at 2theta/TOF/E(KeV):       13.5318  Intensity fixed to 1.0 and variance to 1E6
=> Zero counts at step no.    210 at 2theta/TOF/E(KeV):       13.5466  Intensity fixed to 1.0 and variance to 1E6
=> Zero counts at step no.    211 at 2theta/TOF/E(KeV):       13.5540  Intensity fixed to 1.0 and variance to 1E6
=> Zero counts at step no.    214 at 2theta/TOF/E(KeV):       13.5762  Intensity fixed to 1.0 and variance to 1E6
=> Zero counts at step no.    215 at 2theta/TOF/E(KeV):       13.5836  Intensity fixed to 1.0 and variance to 1E6
=> Zero counts at step no.    217 at 2theta/TOF/E(KeV):       13.5984  Intensity fixed to 1.0 and variance to 1E6
=> Zero counts at step no.    219 at 2theta/TOF/E(KeV):       13.6132  Intensity fixed to 1.0 and variance to 1E6
=> Zero counts at step no.    221 at 2theta/TOF/E(KeV):       13.6280  Intensity fixed to 1.0 and variance to 1E6
=> Zero counts at step no.    224 at 2theta/TOF/E(KeV):       13.6502  Intensity fixed to 1.0 and variance to 1E6
=> Zero counts at step no.    226 at 2theta/TOF/E(KeV):       13.6650  Intensity fixed to 1.0 and variance to 1E6
=> Zero counts at step no.    230 at 2theta/TOF/E(KeV):       13.6946  Intensity fixed to 1.0 and variance to 1E6
=> Zero counts at step no.    233 at 2theta/TOF/E(KeV):       13.7168  Intensity fixed to 1.0 and variance to 1E6
=> Zero counts at step no.    235 at 2theta/TOF/E(KeV):       13.7316  Intensity fixed to 1.0 and variance to 1E6
=> Zero counts at step no.    237 at 2theta/TOF/E(KeV):       13.7464  Intensity fixed to 1.0 and variance to 1E6
=> Zero counts at step no.    239 at 2theta/TOF/E(KeV):       13.7612  Intensity fixed to 1.0 and variance to 1E6
=> Zero counts at step no.    241 at 2theta/TOF/E(KeV):       13.7760  Intensity fixed to 1.0 and variance to 1E6
=> Zero counts at step no.    246 at 2theta/TOF/E(KeV):       13.8130  Intensity fixed to 1.0 and variance to 1E6
=> Zero counts at step no.    247 at 2theta/TOF/E(KeV):       13.8204  Intensity fixed to 1.0 and variance to 1E6
=> Zero counts at step no.    248 at 2theta/TOF/E(KeV):       13.8278  Intensity fixed to 1.0 and variance to 1E6
=> Zero counts at step no.    250 at 2theta/TOF/E(KeV):       13.8426  Intensity fixed to 1.0 and variance to 1E6
=> Zero counts at step no.    254 at 2theta/TOF/E(KeV):       13.8722  Intensity fixed to 1.0 and variance to 1E6
=> Zero counts at step no.    263 at 2theta/TOF/E(KeV):       13.9388  Intensity fixed to 1.0 and variance to 1E6
```

```
=> Zero counts at step no.    265 at 2theta/TOF/E(KeV):      13.9536  Intensity fixed to 1.0 and variance to 1E6
=> Zero counts at step no.    272 at 2theta/TOF/E(KeV):      14.0054  Intensity fixed to 1.0 and variance to 1E6
=> Zero counts at step no.    276 at 2theta/TOF/E(KeV):      14.0350  Intensity fixed to 1.0 and variance to 1E6
=> Zero counts at step no.    280 at 2theta/TOF/E(KeV):      14.0646  Intensity fixed to 1.0 and variance to 1E6
=> Zero counts at step no.    282 at 2theta/TOF/E(KeV):      14.0794  Intensity fixed to 1.0 and variance to 1E6
=> Zero counts at step no.    285 at 2theta/TOF/E(KeV):      14.1016  Intensity fixed to 1.0 and variance to 1E6
=> Zero counts at step no.    287 at 2theta/TOF/E(KeV):      14.1164  Intensity fixed to 1.0 and variance to 1E6
=> Zero counts at step no.    295 at 2theta/TOF/E(KeV):      14.1756  Intensity fixed to 1.0 and variance to 1E6
=> Zero counts at step no.    301 at 2theta/TOF/E(KeV):      14.2200  Intensity fixed to 1.0 and variance to 1E6
=> Zero counts at step no.    303 at 2theta/TOF/E(KeV):      14.2348  Intensity fixed to 1.0 and variance to 1E6
=> Zero counts at step no.    304 at 2theta/TOF/E(KeV):      14.2422  Intensity fixed to 1.0 and variance to 1E6
=> Zero counts at step no.    311 at 2theta/TOF/E(KeV):      14.2940  Intensity fixed to 1.0 and variance to 1E6
=> Zero counts at step no.    315 at 2theta/TOF/E(KeV):      14.3236  Intensity fixed to 1.0 and variance to 1E6
=> Zero counts at step no.    316 at 2theta/TOF/E(KeV):      14.3310  Intensity fixed to 1.0 and variance to 1E6
=> Zero counts at step no.    317 at 2theta/TOF/E(KeV):      14.3384  Intensity fixed to 1.0 and variance to 1E6
=> Zero counts at step no.    320 at 2theta/TOF/E(KeV):      14.3606  Intensity fixed to 1.0 and variance to 1E6
=> Zero counts at step no.    321 at 2theta/TOF/E(KeV):      14.3680  Intensity fixed to 1.0 and variance to 1E6
=> Zero counts at step no.    322 at 2theta/TOF/E(KeV):      14.3754  Intensity fixed to 1.0 and variance to 1E6
=> Zero counts at step no.    324 at 2theta/TOF/E(KeV):      14.3902  Intensity fixed to 1.0 and variance to 1E6
=> Zero counts at step no.    339 at 2theta/TOF/E(KeV):      14.5012  Intensity fixed to 1.0 and variance to 1E6
=> Zero counts at step no.    342 at 2theta/TOF/E(KeV):      14.5234  Intensity fixed to 1.0 and variance to 1E6
=> Zero counts at step no.    348 at 2theta/TOF/E(KeV):      14.5678  Intensity fixed to 1.0 and variance to 1E6
=> Zero counts at step no.    353 at 2theta/TOF/E(KeV):      14.6048  Intensity fixed to 1.0 and variance to 1E6
=> Zero counts at step no.    354 at 2theta/TOF/E(KeV):      14.6122  Intensity fixed to 1.0 and variance to 1E6
=> Zero counts at step no.    355 at 2theta/TOF/E(KeV):      14.6196  Intensity fixed to 1.0 and variance to 1E6
=> Zero counts at step no.    357 at 2theta/TOF/E(KeV):      14.6344  Intensity fixed to 1.0 and variance to 1E6
=> Zero counts at step no.    361 at 2theta/TOF/E(KeV):      14.6640  Intensity fixed to 1.0 and variance to 1E6
=> Zero counts at step no.    362 at 2theta/TOF/E(KeV):      14.6714  Intensity fixed to 1.0 and variance to 1E6
=> Zero counts at step no.    363 at 2theta/TOF/E(KeV):      14.6788  Intensity fixed to 1.0 and variance to 1E6
=> Zero counts at step no.    366 at 2theta/TOF/E(KeV):      14.7010  Intensity fixed to 1.0 and variance to 1E6
=> Zero counts at step no.    369 at 2theta/TOF/E(KeV):      14.7232  Intensity fixed to 1.0 and variance to 1E6
=> Zero counts at step no.    372 at 2theta/TOF/E(KeV):      14.7454  Intensity fixed to 1.0 and variance to 1E6
=> Zero counts at step no.    373 at 2theta/TOF/E(KeV):      14.7528  Intensity fixed to 1.0 and variance to 1E6
=> Zero counts at step no.    375 at 2theta/TOF/E(KeV):      14.7676  Intensity fixed to 1.0 and variance to 1E6
=> Zero counts at step no.    376 at 2theta/TOF/E(KeV):      14.7750  Intensity fixed to 1.0 and variance to 1E6
=> Zero counts at step no.    378 at 2theta/TOF/E(KeV):      14.7898  Intensity fixed to 1.0 and variance to 1E6
=> Zero counts at step no.    381 at 2theta/TOF/E(KeV):      14.8120  Intensity fixed to 1.0 and variance to 1E6
=> Zero counts at step no.    383 at 2theta/TOF/E(KeV):      14.8268  Intensity fixed to 1.0 and variance to 1E6
=> Zero counts at step no.    384 at 2theta/TOF/E(KeV):      14.8342  Intensity fixed to 1.0 and variance to 1E6
=> Zero counts at step no.    386 at 2theta/TOF/E(KeV):      14.8490  Intensity fixed to 1.0 and variance to 1E6
=> Zero counts at step no.    387 at 2theta/TOF/E(KeV):      14.8564  Intensity fixed to 1.0 and variance to 1E6
=> Zero counts at step no.    388 at 2theta/TOF/E(KeV):      14.8638  Intensity fixed to 1.0 and variance to 1E6
=> Zero counts at step no.    390 at 2theta/TOF/E(KeV):      14.8786  Intensity fixed to 1.0 and variance to 1E6
=> Zero counts at step no.    391 at 2theta/TOF/E(KeV):      14.8860  Intensity fixed to 1.0 and variance to 1E6
=> Zero counts at step no.    395 at 2theta/TOF/E(KeV):      14.9156  Intensity fixed to 1.0 and variance to 1E6
=> Zero counts at step no.    396 at 2theta/TOF/E(KeV):      14.9230  Intensity fixed to 1.0 and variance to 1E6
=> Zero counts at step no.    397 at 2theta/TOF/E(KeV):      14.9304  Intensity fixed to 1.0 and variance to 1E6
=> Zero counts at step no.    460 at 2theta/TOF/E(KeV):      15.3966  Intensity fixed to 1.0 and variance to 1E6
=> Zero counts at step no.    461 at 2theta/TOF/E(KeV):      15.4040  Intensity fixed to 1.0 and variance to 1E6
=> Zero counts at step no.    462 at 2theta/TOF/E(KeV):      15.4114  Intensity fixed to 1.0 and variance to 1E6
=> Zero counts at step no.    463 at 2theta/TOF/E(KeV):      15.4188  Intensity fixed to 1.0 and variance to 1E6
=> Zero counts at step no.    465 at 2theta/TOF/E(KeV):      15.4336  Intensity fixed to 1.0 and variance to 1E6
=> Zero counts at step no.    466 at 2theta/TOF/E(KeV):      15.4410  Intensity fixed to 1.0 and variance to 1E6
=> Zero counts at step no.    467 at 2theta/TOF/E(KeV):      15.4484  Intensity fixed to 1.0 and variance to 1E6
=> Zero counts at step no.    468 at 2theta/TOF/E(KeV):      15.4558  Intensity fixed to 1.0 and variance to 1E6
=> Zero counts at step no.    469 at 2theta/TOF/E(KeV):      15.4632  Intensity fixed to 1.0 and variance to 1E6
=> Zero counts at step no.    470 at 2theta/TOF/E(KeV):      15.4706  Intensity fixed to 1.0 and variance to 1E6
=> Zero counts at step no.    471 at 2theta/TOF/E(KeV):      15.4780  Intensity fixed to 1.0 and variance to 1E6
=> Zero counts at step no.    472 at 2theta/TOF/E(KeV):      15.4854  Intensity fixed to 1.0 and variance to 1E6
=> Zero counts at step no.    475 at 2theta/TOF/E(KeV):      15.5076  Intensity fixed to 1.0 and variance to 1E6
=> Zero counts at step no.    477 at 2theta/TOF/E(KeV):      15.5224  Intensity fixed to 1.0 and variance to 1E6
=> Zero counts at step no.    478 at 2theta/TOF/E(KeV):      15.5298  Intensity fixed to 1.0 and variance to 1E6
=> Zero counts at step no.    480 at 2theta/TOF/E(KeV):      15.5446  Intensity fixed to 1.0 and variance to 1E6
=> Zero counts at step no.    481 at 2theta/TOF/E(KeV):      15.5520  Intensity fixed to 1.0 and variance to 1E6
=> Zero counts at step no.    483 at 2theta/TOF/E(KeV):      15.5668  Intensity fixed to 1.0 and variance to 1E6
=> Zero counts at step no.    484 at 2theta/TOF/E(KeV):      15.5742  Intensity fixed to 1.0 and variance to 1E6
=> Zero counts at step no.    487 at 2theta/TOF/E(KeV):      15.5964  Intensity fixed to 1.0 and variance to 1E6
=> Zero counts at step no.    489 at 2theta/TOF/E(KeV):      15.6112  Intensity fixed to 1.0 and variance to 1E6
=> Zero counts at step no.    490 at 2theta/TOF/E(KeV):      15.6186  Intensity fixed to 1.0 and variance to 1E6
=> Zero counts at step no.    491 at 2theta/TOF/E(KeV):      15.6260  Intensity fixed to 1.0 and variance to 1E6
=> Zero counts at step no.    493 at 2theta/TOF/E(KeV):      15.6408  Intensity fixed to 1.0 and variance to 1E6
=> Zero counts at step no.    495 at 2theta/TOF/E(KeV):      15.6556  Intensity fixed to 1.0 and variance to 1E6
=> Zero counts at step no.    496 at 2theta/TOF/E(KeV):      15.6630  Intensity fixed to 1.0 and variance to 1E6
=> Zero counts at step no.    497 at 2theta/TOF/E(KeV):      15.6704  Intensity fixed to 1.0 and variance to 1E6
=> Zero counts at step no.    498 at 2theta/TOF/E(KeV):      15.6778  Intensity fixed to 1.0 and variance to 1E6
=> Zero counts at step no.    499 at 2theta/TOF/E(KeV):      15.6852  Intensity fixed to 1.0 and variance to 1E6
=> Zero counts at step no.    500 at 2theta/TOF/E(KeV):      15.6926  Intensity fixed to 1.0 and variance to 1E6
=> Zero counts at step no.    502 at 2theta/TOF/E(KeV):      15.7074  Intensity fixed to 1.0 and variance to 1E6
=> Zero counts at step no.    511 at 2theta/TOF/E(KeV):      15.7740  Intensity fixed to 1.0 and variance to 1E6
=> Zero counts at step no.    512 at 2theta/TOF/E(KeV):      15.7814  Intensity fixed to 1.0 and variance to 1E6
=> Zero counts at step no.    514 at 2theta/TOF/E(KeV):      15.7962  Intensity fixed to 1.0 and variance to 1E6
=> Zero counts at step no.    516 at 2theta/TOF/E(KeV):      15.8110  Intensity fixed to 1.0 and variance to 1E6
=> Zero counts at step no.    520 at 2theta/TOF/E(KeV):      15.8406  Intensity fixed to 1.0 and variance to 1E6
=> Zero counts at step no.    523 at 2theta/TOF/E(KeV):      15.8628  Intensity fixed to 1.0 and variance to 1E6
=> Zero counts at step no.    532 at 2theta/TOF/E(KeV):      15.9294  Intensity fixed to 1.0 and variance to 1E6
=> Zero counts at step no.    535 at 2theta/TOF/E(KeV):      15.9516  Intensity fixed to 1.0 and variance to 1E6
=> Zero counts at step no.    538 at 2theta/TOF/E(KeV):      15.9738  Intensity fixed to 1.0 and variance to 1E6
=> Zero counts at step no.    547 at 2theta/TOF/E(KeV):      16.0404  Intensity fixed to 1.0 and variance to 1E6
=> Zero counts at step no.    605 at 2theta/TOF/E(KeV):      16.4696  Intensity fixed to 1.0 and variance to 1E6
=> Zero counts at step no.    614 at 2theta/TOF/E(KeV):      16.5362  Intensity fixed to 1.0 and variance to 1E6
```

```
=> Zero counts at step no.    626 at 2theta/TOF/E(KeV):       16.6250  Intensity fixed to 1.0 and variance to 1E6
=> Zero counts at step no.    644 at 2theta/TOF/E(KeV):       16.7582  Intensity fixed to 1.0 and variance to 1E6
=> Zero counts at step no.    646 at 2theta/TOF/E(KeV):       16.7730  Intensity fixed to 1.0 and variance to 1E6
=> Zero counts at step no.    648 at 2theta/TOF/E(KeV):       16.7878  Intensity fixed to 1.0 and variance to 1E6
=> Zero counts at step no.    657 at 2theta/TOF/E(KeV):       16.8544  Intensity fixed to 1.0 and variance to 1E6
=> Zero counts at step no.    658 at 2theta/TOF/E(KeV):       16.8618  Intensity fixed to 1.0 and variance to 1E6
=> Zero counts at step no.    659 at 2theta/TOF/E(KeV):       16.8692  Intensity fixed to 1.0 and variance to 1E6
=> Zero counts at step no.    660 at 2theta/TOF/E(KeV):       16.8766  Intensity fixed to 1.0 and variance to 1E6
=> Zero counts at step no.    664 at 2theta/TOF/E(KeV):       16.9062  Intensity fixed to 1.0 and variance to 1E6
=> Zero counts at step no.    791 at 2theta/TOF/E(KeV):       17.8460  Intensity fixed to 1.0 and variance to 1E6
=> Zero counts at step no.    792 at 2theta/TOF/E(KeV):       17.8534  Intensity fixed to 1.0 and variance to 1E6
=> Zero counts at step no.    793 at 2theta/TOF/E(KeV):       17.8608  Intensity fixed to 1.0 and variance to 1E6
=> Zero counts at step no.    796 at 2theta/TOF/E(KeV):       17.8830  Intensity fixed to 1.0 and variance to 1E6
=> Zero counts at step no.    797 at 2theta/TOF/E(KeV):       17.8904  Intensity fixed to 1.0 and variance to 1E6
=> Zero counts at step no.    798 at 2theta/TOF/E(KeV):       17.8978  Intensity fixed to 1.0 and variance to 1E6
=> Zero counts at step no.    799 at 2theta/TOF/E(KeV):       17.9052  Intensity fixed to 1.0 and variance to 1E6
=> Zero counts at step no.    801 at 2theta/TOF/E(KeV):       17.9200  Intensity fixed to 1.0 and variance to 1E6
=> Zero counts at step no.    802 at 2theta/TOF/E(KeV):       17.9274  Intensity fixed to 1.0 and variance to 1E6
=> Zero counts at step no.    805 at 2theta/TOF/E(KeV):       17.9496  Intensity fixed to 1.0 and variance to 1E6
=> Zero counts at step no.    806 at 2theta/TOF/E(KeV):       17.9570  Intensity fixed to 1.0 and variance to 1E6
=> Zero counts at step no.    807 at 2theta/TOF/E(KeV):       17.9644  Intensity fixed to 1.0 and variance to 1E6
=> Zero counts at step no.    810 at 2theta/TOF/E(KeV):       17.9866  Intensity fixed to 1.0 and variance to 1E6
=> Zero counts at step no.    811 at 2theta/TOF/E(KeV):       17.9940  Intensity fixed to 1.0 and variance to 1E6
=> Zero counts at step no.    812 at 2theta/TOF/E(KeV):       18.0014  Intensity fixed to 1.0 and variance to 1E6
=> Zero counts at step no.    813 at 2theta/TOF/E(KeV):       18.0088  Intensity fixed to 1.0 and variance to 1E6
=> Zero counts at step no.    814 at 2theta/TOF/E(KeV):       18.0162  Intensity fixed to 1.0 and variance to 1E6
=> Zero counts at step no.    815 at 2theta/TOF/E(KeV):       18.0236  Intensity fixed to 1.0 and variance to 1E6
=> Zero counts at step no.    816 at 2theta/TOF/E(KeV):       18.0310  Intensity fixed to 1.0 and variance to 1E6
=> Zero counts at step no.    817 at 2theta/TOF/E(KeV):       18.0384  Intensity fixed to 1.0 and variance to 1E6
=> Zero counts at step no.    818 at 2theta/TOF/E(KeV):       18.0458  Intensity fixed to 1.0 and variance to 1E6
=> Zero counts at step no.    819 at 2theta/TOF/E(KeV):       18.0532  Intensity fixed to 1.0 and variance to 1E6
=> Zero counts at step no.    820 at 2theta/TOF/E(KeV):       18.0606  Intensity fixed to 1.0 and variance to 1E6
=> Zero counts at step no.    822 at 2theta/TOF/E(KeV):       18.0754  Intensity fixed to 1.0 and variance to 1E6
=> Zero counts at step no.    824 at 2theta/TOF/E(KeV):       18.0902  Intensity fixed to 1.0 and variance to 1E6
=> Zero counts at step no.    826 at 2theta/TOF/E(KeV):       18.1050  Intensity fixed to 1.0 and variance to 1E6
=> Zero counts at step no.    827 at 2theta/TOF/E(KeV):       18.1124  Intensity fixed to 1.0 and variance to 1E6
=> Zero counts at step no.    828 at 2theta/TOF/E(KeV):       18.1198  Intensity fixed to 1.0 and variance to 1E6
=> Zero counts at step no.    829 at 2theta/TOF/E(KeV):       18.1272  Intensity fixed to 1.0 and variance to 1E6
=> Zero counts at step no.    830 at 2theta/TOF/E(KeV):       18.1346  Intensity fixed to 1.0 and variance to 1E6
=> Zero counts at step no.    831 at 2theta/TOF/E(KeV):       18.1420  Intensity fixed to 1.0 and variance to 1E6
=> Zero counts at step no.    832 at 2theta/TOF/E(KeV):       18.1494  Intensity fixed to 1.0 and variance to 1E6
=> Zero counts at step no.    838 at 2theta/TOF/E(KeV):       18.1938  Intensity fixed to 1.0 and variance to 1E6
=> Zero counts at step no.    839 at 2theta/TOF/E(KeV):       18.2012  Intensity fixed to 1.0 and variance to 1E6
=> Zero counts at step no.    841 at 2theta/TOF/E(KeV):       18.2160  Intensity fixed to 1.0 and variance to 1E6
=> Zero counts at step no.    842 at 2theta/TOF/E(KeV):       18.2234  Intensity fixed to 1.0 and variance to 1E6
=> Zero counts at step no.    843 at 2theta/TOF/E(KeV):       18.2308  Intensity fixed to 1.0 and variance to 1E6
=> Zero counts at step no.    844 at 2theta/TOF/E(KeV):       18.2382  Intensity fixed to 1.0 and variance to 1E6
=> Zero counts at step no.    845 at 2theta/TOF/E(KeV):       18.2456  Intensity fixed to 1.0 and variance to 1E6
=> Zero counts at step no.    848 at 2theta/TOF/E(KeV):       18.2678  Intensity fixed to 1.0 and variance to 1E6
=> Zero counts at step no.    849 at 2theta/TOF/E(KeV):       18.2752  Intensity fixed to 1.0 and variance to 1E6
=> Zero counts at step no.    851 at 2theta/TOF/E(KeV):       18.2900  Intensity fixed to 1.0 and variance to 1E6
=> Zero counts at step no.    853 at 2theta/TOF/E(KeV):       18.3048  Intensity fixed to 1.0 and variance to 1E6
=> Zero counts at step no.    854 at 2theta/TOF/E(KeV):       18.3122  Intensity fixed to 1.0 and variance to 1E6
=> Zero counts at step no.    855 at 2theta/TOF/E(KeV):       18.3196  Intensity fixed to 1.0 and variance to 1E6
=> Zero counts at step no.    856 at 2theta/TOF/E(KeV):       18.3270  Intensity fixed to 1.0 and variance to 1E6
=> Zero counts at step no.    857 at 2theta/TOF/E(KeV):       18.3344  Intensity fixed to 1.0 and variance to 1E6
=> Zero counts at step no.    859 at 2theta/TOF/E(KeV):       18.3492  Intensity fixed to 1.0 and variance to 1E6
=> Zero counts at step no.    861 at 2theta/TOF/E(KeV):       18.3640  Intensity fixed to 1.0 and variance to 1E6
=> Zero counts at step no.    880 at 2theta/TOF/E(KeV):       18.5046  Intensity fixed to 1.0 and variance to 1E6
=> Zero counts at step no.    884 at 2theta/TOF/E(KeV):       18.5342  Intensity fixed to 1.0 and variance to 1E6
=> Zero counts at step no.    888 at 2theta/TOF/E(KeV):       18.5638  Intensity fixed to 1.0 and variance to 1E6
=> Zero counts at step no.    889 at 2theta/TOF/E(KeV):       18.5712  Intensity fixed to 1.0 and variance to 1E6
=> Zero counts at step no.    890 at 2theta/TOF/E(KeV):       18.5786  Intensity fixed to 1.0 and variance to 1E6
=> Zero counts at step no.    891 at 2theta/TOF/E(KeV):       18.5860  Intensity fixed to 1.0 and variance to 1E6
=> Zero counts at step no.    892 at 2theta/TOF/E(KeV):       18.5934  Intensity fixed to 1.0 and variance to 1E6
=> Zero counts at step no.    894 at 2theta/TOF/E(KeV):       18.6082  Intensity fixed to 1.0 and variance to 1E6
=> Zero counts at step no.    895 at 2theta/TOF/E(KeV):       18.6156  Intensity fixed to 1.0 and variance to 1E6
=> Zero counts at step no.    896 at 2theta/TOF/E(KeV):       18.6230  Intensity fixed to 1.0 and variance to 1E6
=> Zero counts at step no.    897 at 2theta/TOF/E(KeV):       18.6304  Intensity fixed to 1.0 and variance to 1E6
=> Zero counts at step no.    898 at 2theta/TOF/E(KeV):       18.6378  Intensity fixed to 1.0 and variance to 1E6
=> Zero counts at step no.    899 at 2theta/TOF/E(KeV):       18.6452  Intensity fixed to 1.0 and variance to 1E6
=> Zero counts at step no.    900 at 2theta/TOF/E(KeV):       18.6526  Intensity fixed to 1.0 and variance to 1E6
=> Zero counts at step no.    902 at 2theta/TOF/E(KeV):       18.6674  Intensity fixed to 1.0 and variance to 1E6
=> Zero counts at step no.    903 at 2theta/TOF/E(KeV):       18.6748  Intensity fixed to 1.0 and variance to 1E6
=> Zero counts at step no.    904 at 2theta/TOF/E(KeV):       18.6822  Intensity fixed to 1.0 and variance to 1E6
=> Zero counts at step no.    907 at 2theta/TOF/E(KeV):       18.7044  Intensity fixed to 1.0 and variance to 1E6
=> Zero counts at step no.    910 at 2theta/TOF/E(KeV):       18.7266  Intensity fixed to 1.0 and variance to 1E6
=> Zero counts at step no.    911 at 2theta/TOF/E(KeV):       18.7340  Intensity fixed to 1.0 and variance to 1E6
=> Zero counts at step no.    912 at 2theta/TOF/E(KeV):       18.7414  Intensity fixed to 1.0 and variance to 1E6
=> Zero counts at step no.    917 at 2theta/TOF/E(KeV):       18.7784  Intensity fixed to 1.0 and variance to 1E6
=> Zero counts at step no.    918 at 2theta/TOF/E(KeV):       18.7858  Intensity fixed to 1.0 and variance to 1E6
=> Zero counts at step no.    921 at 2theta/TOF/E(KeV):       18.8080  Intensity fixed to 1.0 and variance to 1E6
=> Zero counts at step no.    922 at 2theta/TOF/E(KeV):       18.8154  Intensity fixed to 1.0 and variance to 1E6
=> Zero counts at step no.    923 at 2theta/TOF/E(KeV):       18.8228  Intensity fixed to 1.0 and variance to 1E6
=> Zero counts at step no.    926 at 2theta/TOF/E(KeV):       18.8450  Intensity fixed to 1.0 and variance to 1E6
=> Zero counts at step no.    928 at 2theta/TOF/E(KeV):       18.8598  Intensity fixed to 1.0 and variance to 1E6
=> Zero counts at step no.    929 at 2theta/TOF/E(KeV):       18.8672  Intensity fixed to 1.0 and variance to 1E6
=> Zero counts at step no.    930 at 2theta/TOF/E(KeV):       18.8746  Intensity fixed to 1.0 and variance to 1E6
=> Zero counts at step no.    934 at 2theta/TOF/E(KeV):       18.9042  Intensity fixed to 1.0 and variance to 1E6
=> Zero counts at step no.    935 at 2theta/TOF/E(KeV):       18.9116  Intensity fixed to 1.0 and variance to 1E6
```

```
=> Zero counts at step no.    936 at 2theta/TOF/E(KeV):      18.9190  Intensity fixed to 1.0 and variance to 1E6
=> Zero counts at step no.    941 at 2theta/TOF/E(KeV):      18.9560  Intensity fixed to 1.0 and variance to 1E6
=> Zero counts at step no.    945 at 2theta/TOF/E(KeV):      18.9856  Intensity fixed to 1.0 and variance to 1E6
=> Zero counts at step no.    946 at 2theta/TOF/E(KeV):      18.9930  Intensity fixed to 1.0 and variance to 1E6
=> Zero counts at step no.    947 at 2theta/TOF/E(KeV):      19.0004  Intensity fixed to 1.0 and variance to 1E6
=> Zero counts at step no.    948 at 2theta/TOF/E(KeV):      19.0078  Intensity fixed to 1.0 and variance to 1E6
=> Zero counts at step no.    950 at 2theta/TOF/E(KeV):      19.0226  Intensity fixed to 1.0 and variance to 1E6
=> Zero counts at step no.    952 at 2theta/TOF/E(KeV):      19.0374  Intensity fixed to 1.0 and variance to 1E6
=> Zero counts at step no.    953 at 2theta/TOF/E(KeV):      19.0448  Intensity fixed to 1.0 and variance to 1E6
=> Zero counts at step no.    954 at 2theta/TOF/E(KeV):      19.0522  Intensity fixed to 1.0 and variance to 1E6
=> Zero counts at step no.    956 at 2theta/TOF/E(KeV):      19.0670  Intensity fixed to 1.0 and variance to 1E6
=> Zero counts at step no.    957 at 2theta/TOF/E(KeV):      19.0744  Intensity fixed to 1.0 and variance to 1E6
=> Zero counts at step no.    959 at 2theta/TOF/E(KeV):      19.0892  Intensity fixed to 1.0 and variance to 1E6
=> Zero counts at step no.    960 at 2theta/TOF/E(KeV):      19.0966  Intensity fixed to 1.0 and variance to 1E6
=> Zero counts at step no.    963 at 2theta/TOF/E(KeV):      19.1188  Intensity fixed to 1.0 and variance to 1E6
=> Zero counts at step no.    964 at 2theta/TOF/E(KeV):      19.1262  Intensity fixed to 1.0 and variance to 1E6
=> Zero counts at step no.    965 at 2theta/TOF/E(KeV):      19.1336  Intensity fixed to 1.0 and variance to 1E6
=> Zero counts at step no.    966 at 2theta/TOF/E(KeV):      19.1410  Intensity fixed to 1.0 and variance to 1E6
=> Zero counts at step no.    968 at 2theta/TOF/E(KeV):      19.1558  Intensity fixed to 1.0 and variance to 1E6
=> Zero counts at step no.    969 at 2theta/TOF/E(KeV):      19.1632  Intensity fixed to 1.0 and variance to 1E6
=> Zero counts at step no.    971 at 2theta/TOF/E(KeV):      19.1780  Intensity fixed to 1.0 and variance to 1E6
=> Zero counts at step no.    977 at 2theta/TOF/E(KeV):      19.2224  Intensity fixed to 1.0 and variance to 1E6
=> Zero counts at step no.    986 at 2theta/TOF/E(KeV):      19.2890  Intensity fixed to 1.0 and variance to 1E6
=> Zero counts at step no.    994 at 2theta/TOF/E(KeV):      19.3482  Intensity fixed to 1.0 and variance to 1E6
=> Zero counts at step no.    996 at 2theta/TOF/E(KeV):      19.3630  Intensity fixed to 1.0 and variance to 1E6
=> Zero counts at step no.    997 at 2theta/TOF/E(KeV):      19.3704  Intensity fixed to 1.0 and variance to 1E6
=> Zero counts at step no.    998 at 2theta/TOF/E(KeV):      19.3778  Intensity fixed to 1.0 and variance to 1E6
=> Zero counts at step no.   1000 at 2theta/TOF/E(KeV):      19.3926  Intensity fixed to 1.0 and variance to 1E6
=> Zero counts at step no.   1001 at 2theta/TOF/E(KeV):      19.4000  Intensity fixed to 1.0 and variance to 1E6
=> Zero counts at step no.   1002 at 2theta/TOF/E(KeV):      19.4074  Intensity fixed to 1.0 and variance to 1E6
=> Zero counts at step no.   1003 at 2theta/TOF/E(KeV):      19.4148  Intensity fixed to 1.0 and variance to 1E6
=> Zero counts at step no.   1004 at 2theta/TOF/E(KeV):      19.4222  Intensity fixed to 1.0 and variance to 1E6
=> Zero counts at step no.   1006 at 2theta/TOF/E(KeV):      19.4370  Intensity fixed to 1.0 and variance to 1E6
=> Zero counts at step no.   1008 at 2theta/TOF/E(KeV):      19.4518  Intensity fixed to 1.0 and variance to 1E6
=> Zero counts at step no.   1009 at 2theta/TOF/E(KeV):      19.4592  Intensity fixed to 1.0 and variance to 1E6
=> Zero counts at step no.   1011 at 2theta/TOF/E(KeV):      19.4740  Intensity fixed to 1.0 and variance to 1E6
=> Zero counts at step no.   1013 at 2theta/TOF/E(KeV):      19.4888  Intensity fixed to 1.0 and variance to 1E6
=> Zero counts at step no.   1017 at 2theta/TOF/E(KeV):      19.5184  Intensity fixed to 1.0 and variance to 1E6
=> Zero counts at step no.   1018 at 2theta/TOF/E(KeV):      19.5258  Intensity fixed to 1.0 and variance to 1E6
=> Zero counts at step no.   1024 at 2theta/TOF/E(KeV):      19.5702  Intensity fixed to 1.0 and variance to 1E6
=> Zero counts at step no.   1027 at 2theta/TOF/E(KeV):      19.5924  Intensity fixed to 1.0 and variance to 1E6
=> Zero counts at step no.   1028 at 2theta/TOF/E(KeV):      19.5998  Intensity fixed to 1.0 and variance to 1E6
=> Zero counts at step no.   1029 at 2theta/TOF/E(KeV):      19.6072  Intensity fixed to 1.0 and variance to 1E6
=> Zero counts at step no.   1030 at 2theta/TOF/E(KeV):      19.6146  Intensity fixed to 1.0 and variance to 1E6
=> Zero counts at step no.   1031 at 2theta/TOF/E(KeV):      19.6220  Intensity fixed to 1.0 and variance to 1E6
=> Zero counts at step no.   1032 at 2theta/TOF/E(KeV):      19.6294  Intensity fixed to 1.0 and variance to 1E6
=> Zero counts at step no.   1034 at 2theta/TOF/E(KeV):      19.6442  Intensity fixed to 1.0 and variance to 1E6
=> Zero counts at step no.   1035 at 2theta/TOF/E(KeV):      19.6516  Intensity fixed to 1.0 and variance to 1E6
=> Zero counts at step no.   1036 at 2theta/TOF/E(KeV):      19.6590  Intensity fixed to 1.0 and variance to 1E6
=> Zero counts at step no.   1038 at 2theta/TOF/E(KeV):      19.6738  Intensity fixed to 1.0 and variance to 1E6
=> Zero counts at step no.   1039 at 2theta/TOF/E(KeV):      19.6812  Intensity fixed to 1.0 and variance to 1E6
=> Zero counts at step no.   1040 at 2theta/TOF/E(KeV):      19.6886  Intensity fixed to 1.0 and variance to 1E6
=> Zero counts at step no.   1042 at 2theta/TOF/E(KeV):      19.7034  Intensity fixed to 1.0 and variance to 1E6
=> Zero counts at step no.   1043 at 2theta/TOF/E(KeV):      19.7108  Intensity fixed to 1.0 and variance to 1E6
=> Zero counts at step no.   1045 at 2theta/TOF/E(KeV):      19.7256  Intensity fixed to 1.0 and variance to 1E6
=> Zero counts at step no.   1046 at 2theta/TOF/E(KeV):      19.7330  Intensity fixed to 1.0 and variance to 1E6
=> Zero counts at step no.   1048 at 2theta/TOF/E(KeV):      19.7478  Intensity fixed to 1.0 and variance to 1E6
=> Zero counts at step no.   1050 at 2theta/TOF/E(KeV):      19.7626  Intensity fixed to 1.0 and variance to 1E6
=> Zero counts at step no.   1052 at 2theta/TOF/E(KeV):      19.7774  Intensity fixed to 1.0 and variance to 1E6
=> Zero counts at step no.   1053 at 2theta/TOF/E(KeV):      19.7848  Intensity fixed to 1.0 and variance to 1E6
=> Zero counts at step no.   1054 at 2theta/TOF/E(KeV):      19.7922  Intensity fixed to 1.0 and variance to 1E6
=> Zero counts at step no.   1055 at 2theta/TOF/E(KeV):      19.7996  Intensity fixed to 1.0 and variance to 1E6
=> Zero counts at step no.   1056 at 2theta/TOF/E(KeV):      19.8070  Intensity fixed to 1.0 and variance to 1E6
=> Zero counts at step no.   1058 at 2theta/TOF/E(KeV):      19.8218  Intensity fixed to 1.0 and variance to 1E6
=> Zero counts at step no.   1062 at 2theta/TOF/E(KeV):      19.8514  Intensity fixed to 1.0 and variance to 1E6
=> Zero counts at step no.   1063 at 2theta/TOF/E(KeV):      19.8588  Intensity fixed to 1.0 and variance to 1E6
=> Zero counts at step no.   1068 at 2theta/TOF/E(KeV):      19.8958  Intensity fixed to 1.0 and variance to 1E6
=> Zero counts at step no.   1071 at 2theta/TOF/E(KeV):      19.9180  Intensity fixed to 1.0 and variance to 1E6
=> Zero counts at step no.   1072 at 2theta/TOF/E(KeV):      19.9254  Intensity fixed to 1.0 and variance to 1E6
=> Zero counts at step no.   1076 at 2theta/TOF/E(KeV):      19.9550  Intensity fixed to 1.0 and variance to 1E6
=> Zero counts at step no.   1134 at 2theta/TOF/E(KeV):      20.3842  Intensity fixed to 1.0 and variance to 1E6
=> Zero counts at step no.   1135 at 2theta/TOF/E(KeV):      20.3916  Intensity fixed to 1.0 and variance to 1E6
=> Zero counts at step no.   1142 at 2theta/TOF/E(KeV):      20.4434  Intensity fixed to 1.0 and variance to 1E6
=> Zero counts at step no.   1143 at 2theta/TOF/E(KeV):      20.4508  Intensity fixed to 1.0 and variance to 1E6
=> Zero counts at step no.   1144 at 2theta/TOF/E(KeV):      20.4582  Intensity fixed to 1.0 and variance to 1E6
=> Zero counts at step no.   1146 at 2theta/TOF/E(KeV):      20.4730  Intensity fixed to 1.0 and variance to 1E6
=> Zero counts at step no.   1147 at 2theta/TOF/E(KeV):      20.4804  Intensity fixed to 1.0 and variance to 1E6
=> Zero counts at step no.   1149 at 2theta/TOF/E(KeV):      20.4952  Intensity fixed to 1.0 and variance to 1E6
=> Zero counts at step no.   1150 at 2theta/TOF/E(KeV):      20.5026  Intensity fixed to 1.0 and variance to 1E6
=> Zero counts at step no.   1152 at 2theta/TOF/E(KeV):      20.5174  Intensity fixed to 1.0 and variance to 1E6
=> Zero counts at step no.   1153 at 2theta/TOF/E(KeV):      20.5248  Intensity fixed to 1.0 and variance to 1E6
=> Zero counts at step no.   1157 at 2theta/TOF/E(KeV):      20.5544  Intensity fixed to 1.0 and variance to 1E6
=> Zero counts at step no.   1158 at 2theta/TOF/E(KeV):      20.5618  Intensity fixed to 1.0 and variance to 1E6
=> Zero counts at step no.   1159 at 2theta/TOF/E(KeV):      20.5692  Intensity fixed to 1.0 and variance to 1E6
=> Zero counts at step no.   1161 at 2theta/TOF/E(KeV):      20.5840  Intensity fixed to 1.0 and variance to 1E6
=> Zero counts at step no.   1164 at 2theta/TOF/E(KeV):      20.6062  Intensity fixed to 1.0 and variance to 1E6
=> Zero counts at step no.   1171 at 2theta/TOF/E(KeV):      20.6580  Intensity fixed to 1.0 and variance to 1E6
=> Zero counts at step no.   1172 at 2theta/TOF/E(KeV):      20.6654  Intensity fixed to 1.0 and variance to 1E6
=> Zero counts at step no.   1174 at 2theta/TOF/E(KeV):      20.6802  Intensity fixed to 1.0 and variance to 1E6
=> Zero counts at step no.   1175 at 2theta/TOF/E(KeV):      20.6876  Intensity fixed to 1.0 and variance to 1E6
```

```
=> Zero counts at step no.   1176 at 2theta/TOF/E(KeV):       20.6950  Intensity fixed to 1.0 and variance to 1E6
=> Zero counts at step no.   1178 at 2theta/TOF/E(KeV):       20.7098  Intensity fixed to 1.0 and variance to 1E6
=> Zero counts at step no.   1179 at 2theta/TOF/E(KeV):       20.7172  Intensity fixed to 1.0 and variance to 1E6
=> Zero counts at step no.   1181 at 2theta/TOF/E(KeV):       20.7320  Intensity fixed to 1.0 and variance to 1E6
=> Zero counts at step no.   1182 at 2theta/TOF/E(KeV):       20.7394  Intensity fixed to 1.0 and variance to 1E6
=> Zero counts at step no.   1185 at 2theta/TOF/E(KeV):       20.7616  Intensity fixed to 1.0 and variance to 1E6
=> Zero counts at step no.   1187 at 2theta/TOF/E(KeV):       20.7764  Intensity fixed to 1.0 and variance to 1E6
=> Zero counts at step no.   1189 at 2theta/TOF/E(KeV):       20.7912  Intensity fixed to 1.0 and variance to 1E6
=> Zero counts at step no.   1190 at 2theta/TOF/E(KeV):       20.7986  Intensity fixed to 1.0 and variance to 1E6
=> Zero counts at step no.   1193 at 2theta/TOF/E(KeV):       20.8208  Intensity fixed to 1.0 and variance to 1E6
=> Zero counts at step no.   1195 at 2theta/TOF/E(KeV):       20.8356  Intensity fixed to 1.0 and variance to 1E6
=> Zero counts at step no.   1197 at 2theta/TOF/E(KeV):       20.8504  Intensity fixed to 1.0 and variance to 1E6
=> Zero counts at step no.   1202 at 2theta/TOF/E(KeV):       20.8874  Intensity fixed to 1.0 and variance to 1E6
=> Zero counts at step no.   1203 at 2theta/TOF/E(KeV):       20.8948  Intensity fixed to 1.0 and variance to 1E6
=> Zero counts at step no.   1206 at 2theta/TOF/E(KeV):       20.9170  Intensity fixed to 1.0 and variance to 1E6
=> Zero counts at step no.   1208 at 2theta/TOF/E(KeV):       20.9318  Intensity fixed to 1.0 and variance to 1E6
=> Zero counts at step no.   1211 at 2theta/TOF/E(KeV):       20.9540  Intensity fixed to 1.0 and variance to 1E6
=> Zero counts at step no.   1213 at 2theta/TOF/E(KeV):       20.9688  Intensity fixed to 1.0 and variance to 1E6
=> Zero counts at step no.   1215 at 2theta/TOF/E(KeV):       20.9836  Intensity fixed to 1.0 and variance to 1E6
=> Zero counts at step no.   1221 at 2theta/TOF/E(KeV):       21.0280  Intensity fixed to 1.0 and variance to 1E6
=> Zero counts at step no.   1224 at 2theta/TOF/E(KeV):       21.0502  Intensity fixed to 1.0 and variance to 1E6
=> Zero counts at step no.   1255 at 2theta/TOF/E(KeV):       21.2796  Intensity fixed to 1.0 and variance to 1E6
=> Zero counts at step no.   1256 at 2theta/TOF/E(KeV):       21.2870  Intensity fixed to 1.0 and variance to 1E6
=> Zero counts at step no.   1257 at 2theta/TOF/E(KeV):       21.2944  Intensity fixed to 1.0 and variance to 1E6
=> Zero counts at step no.   1258 at 2theta/TOF/E(KeV):       21.3018  Intensity fixed to 1.0 and variance to 1E6
=> Zero counts at step no.   1259 at 2theta/TOF/E(KeV):       21.3092  Intensity fixed to 1.0 and variance to 1E6
=> Zero counts at step no.   1262 at 2theta/TOF/E(KeV):       21.3314  Intensity fixed to 1.0 and variance to 1E6
=> Zero counts at step no.   1264 at 2theta/TOF/E(KeV):       21.3462  Intensity fixed to 1.0 and variance to 1E6
=> Zero counts at step no.   1267 at 2theta/TOF/E(KeV):       21.3684  Intensity fixed to 1.0 and variance to 1E6
=> Zero counts at step no.   1269 at 2theta/TOF/E(KeV):       21.3832  Intensity fixed to 1.0 and variance to 1E6
=> Zero counts at step no.   1271 at 2theta/TOF/E(KeV):       21.3980  Intensity fixed to 1.0 and variance to 1E6
=> Zero counts at step no.   1272 at 2theta/TOF/E(KeV):       21.4054  Intensity fixed to 1.0 and variance to 1E6
=> Zero counts at step no.   1274 at 2theta/TOF/E(KeV):       21.4202  Intensity fixed to 1.0 and variance to 1E6
=> Zero counts at step no.   1278 at 2theta/TOF/E(KeV):       21.4498  Intensity fixed to 1.0 and variance to 1E6
=> Zero counts at step no.   1282 at 2theta/TOF/E(KeV):       21.4794  Intensity fixed to 1.0 and variance to 1E6
=> Zero counts at step no.   1283 at 2theta/TOF/E(KeV):       21.4868  Intensity fixed to 1.0 and variance to 1E6
=> Zero counts at step no.   1284 at 2theta/TOF/E(KeV):       21.4942  Intensity fixed to 1.0 and variance to 1E6
=> Zero counts at step no.   1286 at 2theta/TOF/E(KeV):       21.5090  Intensity fixed to 1.0 and variance to 1E6
=> Zero counts at step no.   1287 at 2theta/TOF/E(KeV):       21.5164  Intensity fixed to 1.0 and variance to 1E6
=> Zero counts at step no.   1288 at 2theta/TOF/E(KeV):       21.5238  Intensity fixed to 1.0 and variance to 1E6
=> Zero counts at step no.   1289 at 2theta/TOF/E(KeV):       21.5312  Intensity fixed to 1.0 and variance to 1E6
=> Zero counts at step no.   1294 at 2theta/TOF/E(KeV):       21.5682  Intensity fixed to 1.0 and variance to 1E6
=> Zero counts at step no.   1297 at 2theta/TOF/E(KeV):       21.5904  Intensity fixed to 1.0 and variance to 1E6
=> Zero counts at step no.   1298 at 2theta/TOF/E(KeV):       21.5978  Intensity fixed to 1.0 and variance to 1E6
=> Zero counts at step no.   1363 at 2theta/TOF/E(KeV):       22.0788  Intensity fixed to 1.0 and variance to 1E6
=> Zero counts at step no.   1364 at 2theta/TOF/E(KeV):       22.0862  Intensity fixed to 1.0 and variance to 1E6
=> Zero counts at step no.   1365 at 2theta/TOF/E(KeV):       22.0936  Intensity fixed to 1.0 and variance to 1E6
=> Zero counts at step no.   1366 at 2theta/TOF/E(KeV):       22.1010  Intensity fixed to 1.0 and variance to 1E6
=> Zero counts at step no.   1368 at 2theta/TOF/E(KeV):       22.1158  Intensity fixed to 1.0 and variance to 1E6
=> Zero counts at step no.   1369 at 2theta/TOF/E(KeV):       22.1232  Intensity fixed to 1.0 and variance to 1E6
=> Zero counts at step no.   1377 at 2theta/TOF/E(KeV):       22.1824  Intensity fixed to 1.0 and variance to 1E6
=> Zero counts at step no.   1378 at 2theta/TOF/E(KeV):       22.1898  Intensity fixed to 1.0 and variance to 1E6
=> Zero counts at step no.   1383 at 2theta/TOF/E(KeV):       22.2268  Intensity fixed to 1.0 and variance to 1E6
=> Zero counts at step no.   1435 at 2theta/TOF/E(KeV):       22.6116  Intensity fixed to 1.0 and variance to 1E6
=> Zero counts at step no.   1437 at 2theta/TOF/E(KeV):       22.6264  Intensity fixed to 1.0 and variance to 1E6
=> Zero counts at step no.   1439 at 2theta/TOF/E(KeV):       22.6412  Intensity fixed to 1.0 and variance to 1E6
=> Zero counts at step no.   1441 at 2theta/TOF/E(KeV):       22.6560  Intensity fixed to 1.0 and variance to 1E6
=> Zero counts at step no.   1444 at 2theta/TOF/E(KeV):       22.6782  Intensity fixed to 1.0 and variance to 1E6
=> Zero counts at step no.   1447 at 2theta/TOF/E(KeV):       22.7004  Intensity fixed to 1.0 and variance to 1E6
=> Zero counts at step no.   1449 at 2theta/TOF/E(KeV):       22.7152  Intensity fixed to 1.0 and variance to 1E6
=> Zero counts at step no.   1451 at 2theta/TOF/E(KeV):       22.7300  Intensity fixed to 1.0 and variance to 1E6
=> Zero counts at step no.   1452 at 2theta/TOF/E(KeV):       22.7374  Intensity fixed to 1.0 and variance to 1E6
=> Zero counts at step no.   1454 at 2theta/TOF/E(KeV):       22.7522  Intensity fixed to 1.0 and variance to 1E6
=> Zero counts at step no.   1456 at 2theta/TOF/E(KeV):       22.7670  Intensity fixed to 1.0 and variance to 1E6
=> Zero counts at step no.   1457 at 2theta/TOF/E(KeV):       22.7744  Intensity fixed to 1.0 and variance to 1E6
=> Zero counts at step no.   1463 at 2theta/TOF/E(KeV):       22.8188  Intensity fixed to 1.0 and variance to 1E6
=> Zero counts at step no.   1465 at 2theta/TOF/E(KeV):       22.8336  Intensity fixed to 1.0 and variance to 1E6
=> Zero counts at step no.   1467 at 2theta/TOF/E(KeV):       22.8484  Intensity fixed to 1.0 and variance to 1E6
=> Zero counts at step no.   1498 at 2theta/TOF/E(KeV):       23.0778  Intensity fixed to 1.0 and variance to 1E6
=> Zero counts at step no.   1499 at 2theta/TOF/E(KeV):       23.0852  Intensity fixed to 1.0 and variance to 1E6
=> Zero counts at step no.   1500 at 2theta/TOF/E(KeV):       23.0926  Intensity fixed to 1.0 and variance to 1E6
=> Zero counts at step no.   1502 at 2theta/TOF/E(KeV):       23.1074  Intensity fixed to 1.0 and variance to 1E6
=> Zero counts at step no.   1503 at 2theta/TOF/E(KeV):       23.1148  Intensity fixed to 1.0 and variance to 1E6
=> Zero counts at step no.   1504 at 2theta/TOF/E(KeV):       23.1222  Intensity fixed to 1.0 and variance to 1E6
=> Zero counts at step no.   1505 at 2theta/TOF/E(KeV):       23.1296  Intensity fixed to 1.0 and variance to 1E6
=> Zero counts at step no.   1507 at 2theta/TOF/E(KeV):       23.1444  Intensity fixed to 1.0 and variance to 1E6
=> Zero counts at step no.   1510 at 2theta/TOF/E(KeV):       23.1666  Intensity fixed to 1.0 and variance to 1E6
=> Zero counts at step no.   1511 at 2theta/TOF/E(KeV):       23.1740  Intensity fixed to 1.0 and variance to 1E6
=> Zero counts at step no.   1518 at 2theta/TOF/E(KeV):       23.2258  Intensity fixed to 1.0 and variance to 1E6
=> Zero counts at step no.   1519 at 2theta/TOF/E(KeV):       23.2332  Intensity fixed to 1.0 and variance to 1E6
=> Zero counts at step no.   1522 at 2theta/TOF/E(KeV):       23.2554  Intensity fixed to 1.0 and variance to 1E6
=> Zero counts at step no.   1564 at 2theta/TOF/E(KeV):       23.5662  Intensity fixed to 1.0 and variance to 1E6
=> Zero counts at step no.   1565 at 2theta/TOF/E(KeV):       23.5736  Intensity fixed to 1.0 and variance to 1E6
=> Zero counts at step no.   1567 at 2theta/TOF/E(KeV):       23.5884  Intensity fixed to 1.0 and variance to 1E6
=> Zero counts at step no.   1569 at 2theta/TOF/E(KeV):       23.6032  Intensity fixed to 1.0 and variance to 1E6
=> Zero counts at step no.   1571 at 2theta/TOF/E(KeV):       23.6180  Intensity fixed to 1.0 and variance to 1E6
=> Zero counts at step no.   1572 at 2theta/TOF/E(KeV):       23.6254  Intensity fixed to 1.0 and variance to 1E6
=> Zero counts at step no.   1577 at 2theta/TOF/E(KeV):       23.6624  Intensity fixed to 1.0 and variance to 1E6
=> Zero counts at step no.   1579 at 2theta/TOF/E(KeV):       23.6772  Intensity fixed to 1.0 and variance to 1E6
=> Zero counts at step no.   1581 at 2theta/TOF/E(KeV):       23.6920  Intensity fixed to 1.0 and variance to 1E6
```

```
=> Zero counts at step no.   1583 at 2theta/TOF/E(KeV):      23.7068  Intensity fixed to 1.0 and variance to 1E6
=> Zero counts at step no.   1584 at 2theta/TOF/E(KeV):      23.7142  Intensity fixed to 1.0 and variance to 1E6
=> Zero counts at step no.   1590 at 2theta/TOF/E(KeV):      23.7586  Intensity fixed to 1.0 and variance to 1E6
=> Zero counts at step no.   1593 at 2theta/TOF/E(KeV):      23.7808  Intensity fixed to 1.0 and variance to 1E6
=> Zero counts at step no.   1599 at 2theta/TOF/E(KeV):      23.8252  Intensity fixed to 1.0 and variance to 1E6
=> Zero counts at step no.   1602 at 2theta/TOF/E(KeV):      23.8474  Intensity fixed to 1.0 and variance to 1E6
=> Zero counts at step no.   1604 at 2theta/TOF/E(KeV):      23.8622  Intensity fixed to 1.0 and variance to 1E6
=> Zero counts at step no.   1606 at 2theta/TOF/E(KeV):      23.8770  Intensity fixed to 1.0 and variance to 1E6
=> Zero counts at step no.   1609 at 2theta/TOF/E(KeV):      23.8992  Intensity fixed to 1.0 and variance to 1E6
=> Zero counts at step no.   1610 at 2theta/TOF/E(KeV):      23.9066  Intensity fixed to 1.0 and variance to 1E6
=> Zero counts at step no.   1613 at 2theta/TOF/E(KeV):      23.9288  Intensity fixed to 1.0 and variance to 1E6
=> Zero counts at step no.   1620 at 2theta/TOF/E(KeV):      23.9806  Intensity fixed to 1.0 and variance to 1E6
=> Zero counts at step no.   1624 at 2theta/TOF/E(KeV):      24.0102  Intensity fixed to 1.0 and variance to 1E6
=> Zero counts at step no.   1626 at 2theta/TOF/E(KeV):      24.0250  Intensity fixed to 1.0 and variance to 1E6
=> Zero counts at step no.   1632 at 2theta/TOF/E(KeV):      24.0694  Intensity fixed to 1.0 and variance to 1E6
=> Zero counts at step no.   1633 at 2theta/TOF/E(KeV):      24.0768  Intensity fixed to 1.0 and variance to 1E6
=> Zero counts at step no.   1634 at 2theta/TOF/E(KeV):      24.0842  Intensity fixed to 1.0 and variance to 1E6
=> Zero counts at step no.   1650 at 2theta/TOF/E(KeV):      24.2026  Intensity fixed to 1.0 and variance to 1E6
=> Zero counts at step no.   1660 at 2theta/TOF/E(KeV):      24.2766  Intensity fixed to 1.0 and variance to 1E6
=> Zero counts at step no.   1664 at 2theta/TOF/E(KeV):      24.3062  Intensity fixed to 1.0 and variance to 1E6
=> Zero counts at step no.   1665 at 2theta/TOF/E(KeV):      24.3136  Intensity fixed to 1.0 and variance to 1E6
=> Zero counts at step no.   1684 at 2theta/TOF/E(KeV):      24.4542  Intensity fixed to 1.0 and variance to 1E6
=> Zero counts at step no.   1691 at 2theta/TOF/E(KeV):      24.5060  Intensity fixed to 1.0 and variance to 1E6
=> Zero counts at step no.   1708 at 2theta/TOF/E(KeV):      24.6318  Intensity fixed to 1.0 and variance to 1E6
=> Zero counts at step no.   2098 at 2theta/TOF/E(KeV):      27.5178  Intensity fixed to 1.0 and variance to 1E6
=> Zero counts at step no.   2104 at 2theta/TOF/E(KeV):      27.5622  Intensity fixed to 1.0 and variance to 1E6
=> Zero counts at step no.   2112 at 2theta/TOF/E(KeV):      27.6214  Intensity fixed to 1.0 and variance to 1E6
=> Zero counts at step no.   2115 at 2theta/TOF/E(KeV):      27.6436  Intensity fixed to 1.0 and variance to 1E6
=> Zero counts at step no.   2118 at 2theta/TOF/E(KeV):      27.6658  Intensity fixed to 1.0 and variance to 1E6
=> Zero counts at step no.   2145 at 2theta/TOF/E(KeV):      27.8656  Intensity fixed to 1.0 and variance to 1E6
=> Zero counts at step no.   2147 at 2theta/TOF/E(KeV):      27.8804  Intensity fixed to 1.0 and variance to 1E6
=> Zero counts at step no.   2149 at 2theta/TOF/E(KeV):      27.8952  Intensity fixed to 1.0 and variance to 1E6
=> Zero counts at step no.   2153 at 2theta/TOF/E(KeV):      27.9248  Intensity fixed to 1.0 and variance to 1E6
=> Zero counts at step no.   2155 at 2theta/TOF/E(KeV):      27.9396  Intensity fixed to 1.0 and variance to 1E6
=> Zero counts at step no.   2157 at 2theta/TOF/E(KeV):      27.9544  Intensity fixed to 1.0 and variance to 1E6
=> Zero counts at step no.   2161 at 2theta/TOF/E(KeV):      27.9840  Intensity fixed to 1.0 and variance to 1E6
=> Zero counts at step no.   2177 at 2theta/TOF/E(KeV):      28.1024  Intensity fixed to 1.0 and variance to 1E6
=> Zero counts at step no.   2182 at 2theta/TOF/E(KeV):      28.1394  Intensity fixed to 1.0 and variance to 1E6
=> Zero counts at step no.   2184 at 2theta/TOF/E(KeV):      28.1542  Intensity fixed to 1.0 and variance to 1E6
=> Zero counts at step no.   2205 at 2theta/TOF/E(KeV):      28.3096  Intensity fixed to 1.0 and variance to 1E6
=> Zero counts at step no.   2221 at 2theta/TOF/E(KeV):      28.4280  Intensity fixed to 1.0 and variance to 1E6
=> Zero counts at step no.   2235 at 2theta/TOF/E(KeV):      28.5316  Intensity fixed to 1.0 and variance to 1E6
=> Zero counts at step no.   2247 at 2theta/TOF/E(KeV):      28.6204  Intensity fixed to 1.0 and variance to 1E6
=> Zero counts at step no.   2248 at 2theta/TOF/E(KeV):      28.6278  Intensity fixed to 1.0 and variance to 1E6
=> Zero counts at step no.   2251 at 2theta/TOF/E(KeV):      28.6500  Intensity fixed to 1.0 and variance to 1E6
=> Zero counts at step no.   2252 at 2theta/TOF/E(KeV):      28.6574  Intensity fixed to 1.0 and variance to 1E6
=> Zero counts at step no.   2386 at 2theta/TOF/E(KeV):      29.6490  Intensity fixed to 1.0 and variance to 1E6
=> Zero counts at step no.   2393 at 2theta/TOF/E(KeV):      29.7008  Intensity fixed to 1.0 and variance to 1E6
=> Zero counts at step no.   2399 at 2theta/TOF/E(KeV):      29.7452  Intensity fixed to 1.0 and variance to 1E6
=> Zero counts at step no.   2404 at 2theta/TOF/E(KeV):      29.7822  Intensity fixed to 1.0 and variance to 1E6
=> Zero counts at step no.   2407 at 2theta/TOF/E(KeV):      29.8044  Intensity fixed to 1.0 and variance to 1E6
=> Zero counts at step no.   2408 at 2theta/TOF/E(KeV):      29.8118  Intensity fixed to 1.0 and variance to 1E6
=> Zero counts at step no.   2409 at 2theta/TOF/E(KeV):      29.8192  Intensity fixed to 1.0 and variance to 1E6
=> Zero counts at step no.   2411 at 2theta/TOF/E(KeV):      29.8340  Intensity fixed to 1.0 and variance to 1E6
=> Zero counts at step no.   2421 at 2theta/TOF/E(KeV):      29.9080  Intensity fixed to 1.0 and variance to 1E6
=> Zero counts at step no.   2423 at 2theta/TOF/E(KeV):      29.9228  Intensity fixed to 1.0 and variance to 1E6
=> Zero counts at step no.   2424 at 2theta/TOF/E(KeV):      29.9302  Intensity fixed to 1.0 and variance to 1E6
=> Zero counts at step no.   2425 at 2theta/TOF/E(KeV):      29.9376  Intensity fixed to 1.0 and variance to 1E6
=> Zero counts at step no.   2426 at 2theta/TOF/E(KeV):      29.9450  Intensity fixed to 1.0 and variance to 1E6
=> Zero counts at step no.   2427 at 2theta/TOF/E(KeV):      29.9524  Intensity fixed to 1.0 and variance to 1E6
=> Zero counts at step no.   2431 at 2theta/TOF/E(KeV):      29.9820  Intensity fixed to 1.0 and variance to 1E6
=> Zero counts at step no.   2435 at 2theta/TOF/E(KeV):      30.0116  Intensity fixed to 1.0 and variance to 1E6
=> Zero counts at step no.   2437 at 2theta/TOF/E(KeV):      30.0264  Intensity fixed to 1.0 and variance to 1E6
=> Zero counts at step no.   2438 at 2theta/TOF/E(KeV):      30.0338  Intensity fixed to 1.0 and variance to 1E6
=> Zero counts at step no.   2901 at 2theta/TOF/E(KeV):      33.4600  Intensity fixed to 1.0 and variance to 1E6
=> Zero counts at step no.   2902 at 2theta/TOF/E(KeV):      33.4674  Intensity fixed to 1.0 and variance to 1E6
=> Zero counts at step no.   2906 at 2theta/TOF/E(KeV):      33.4970  Intensity fixed to 1.0 and variance to 1E6
=> Zero counts at step no.   2907 at 2theta/TOF/E(KeV):      33.5044  Intensity fixed to 1.0 and variance to 1E6
=> Zero counts at step no.   2909 at 2theta/TOF/E(KeV):      33.5192  Intensity fixed to 1.0 and variance to 1E6
=> Zero counts at step no.   2915 at 2theta/TOF/E(KeV):      33.5636  Intensity fixed to 1.0 and variance to 1E6
=> Zero counts at step no.   2932 at 2theta/TOF/E(KeV):      33.6894  Intensity fixed to 1.0 and variance to 1E6
=> Zero counts at step no.   2937 at 2theta/TOF/E(KeV):      33.7264  Intensity fixed to 1.0 and variance to 1E6
=> Zero counts at step no.   2939 at 2theta/TOF/E(KeV):      33.7412  Intensity fixed to 1.0 and variance to 1E6
=> Zero counts at step no.   2941 at 2theta/TOF/E(KeV):      33.7560  Intensity fixed to 1.0 and variance to 1E6
=> Zero counts at step no.   2944 at 2theta/TOF/E(KeV):      33.7782  Intensity fixed to 1.0 and variance to 1E6
=> Zero counts at step no.   2950 at 2theta/TOF/E(KeV):      33.8226  Intensity fixed to 1.0 and variance to 1E6
=> Zero counts at step no.   2996 at 2theta/TOF/E(KeV):      34.1630  Intensity fixed to 1.0 and variance to 1E6
=> Zero counts at step no.   2997 at 2theta/TOF/E(KeV):      34.1704  Intensity fixed to 1.0 and variance to 1E6
=> Zero counts at step no.   2999 at 2theta/TOF/E(KeV):      34.1852  Intensity fixed to 1.0 and variance to 1E6
=> Zero counts at step no.   3001 at 2theta/TOF/E(KeV):      34.2000  Intensity fixed to 1.0 and variance to 1E6
=> Zero counts at step no.   3003 at 2theta/TOF/E(KeV):      34.2148  Intensity fixed to 1.0 and variance to 1E6
=> Zero counts at step no.   3004 at 2theta/TOF/E(KeV):      34.2222  Intensity fixed to 1.0 and variance to 1E6
=> Zero counts at step no.   3005 at 2theta/TOF/E(KeV):      34.2296  Intensity fixed to 1.0 and variance to 1E6
=> Zero counts at step no.   3007 at 2theta/TOF/E(KeV):      34.2444  Intensity fixed to 1.0 and variance to 1E6
=> Zero counts at step no.   3009 at 2theta/TOF/E(KeV):      34.2592  Intensity fixed to 1.0 and variance to 1E6
=> Zero counts at step no.   3012 at 2theta/TOF/E(KeV):      34.2814  Intensity fixed to 1.0 and variance to 1E6
=> Zero counts at step no.   3013 at 2theta/TOF/E(KeV):      34.2888  Intensity fixed to 1.0 and variance to 1E6
=> Zero counts at step no.   3014 at 2theta/TOF/E(KeV):      34.2962  Intensity fixed to 1.0 and variance to 1E6
=> Zero counts at step no.   3015 at 2theta/TOF/E(KeV):      34.3036  Intensity fixed to 1.0 and variance to 1E6
=> Zero counts at step no.   3016 at 2theta/TOF/E(KeV):      34.3110  Intensity fixed to 1.0 and variance to 1E6
```

```
=> Zero counts at step no.   3017 at 2theta/TOF/E(KeV):        34.3184  Intensity fixed to 1.0 and variance to 1E6
=> Zero counts at step no.   3022 at 2theta/TOF/E(KeV):        34.3554  Intensity fixed to 1.0 and variance to 1E6
=> Zero counts at step no.   3026 at 2theta/TOF/E(KeV):        34.3850  Intensity fixed to 1.0 and variance to 1E6
=> Zero counts at step no.   3147 at 2theta/TOF/E(KeV):        35.2804  Intensity fixed to 1.0 and variance to 1E6
=> Zero counts at step no.   3154 at 2theta/TOF/E(KeV):        35.3322  Intensity fixed to 1.0 and variance to 1E6
=> Zero counts at step no.   3158 at 2theta/TOF/E(KeV):        35.3618  Intensity fixed to 1.0 and variance to 1E6
=> Zero counts at step no.   3166 at 2theta/TOF/E(KeV):        35.4210  Intensity fixed to 1.0 and variance to 1E6
=> Zero counts at step no.   3170 at 2theta/TOF/E(KeV):        35.4506  Intensity fixed to 1.0 and variance to 1E6
=> Zero counts at step no.   3230 at 2theta/TOF/E(KeV):        35.8946  Intensity fixed to 1.0 and variance to 1E6
=> Zero counts at step no.   3233 at 2theta/TOF/E(KeV):        35.9168  Intensity fixed to 1.0 and variance to 1E6
=> Zero counts at step no.   3237 at 2theta/TOF/E(KeV):        35.9464  Intensity fixed to 1.0 and variance to 1E6
=> Zero counts at step no.   3238 at 2theta/TOF/E(KeV):        35.9538  Intensity fixed to 1.0 and variance to 1E6
=> Zero counts at step no.   3244 at 2theta/TOF/E(KeV):        35.9982  Intensity fixed to 1.0 and variance to 1E6
=> Zero counts at step no.   3246 at 2theta/TOF/E(KeV):        36.0130  Intensity fixed to 1.0 and variance to 1E6
=> Zero counts at step no.   3247 at 2theta/TOF/E(KeV):        36.0204  Intensity fixed to 1.0 and variance to 1E6
=> Zero counts at step no.   3252 at 2theta/TOF/E(KeV):        36.0574  Intensity fixed to 1.0 and variance to 1E6
=> Zero counts at step no.   3254 at 2theta/TOF/E(KeV):        36.0722  Intensity fixed to 1.0 and variance to 1E6
=> Zero counts at step no.   3258 at 2theta/TOF/E(KeV):        36.1018  Intensity fixed to 1.0 and variance to 1E6
=> Zero counts at step no.   3261 at 2theta/TOF/E(KeV):        36.1240  Intensity fixed to 1.0 and variance to 1E6
=> Zero counts at step no.   3262 at 2theta/TOF/E(KeV):        36.1314  Intensity fixed to 1.0 and variance to 1E6
=> Zero counts at step no.   3263 at 2theta/TOF/E(KeV):        36.1388  Intensity fixed to 1.0 and variance to 1E6
=> Zero counts at step no.   3272 at 2theta/TOF/E(KeV):        36.2054  Intensity fixed to 1.0 and variance to 1E6
=> Zero counts at step no.   3275 at 2theta/TOF/E(KeV):        36.2276  Intensity fixed to 1.0 and variance to 1E6
=> Zero counts at step no.   3277 at 2theta/TOF/E(KeV):        36.2424  Intensity fixed to 1.0 and variance to 1E6
=> Zero counts at step no.   3279 at 2theta/TOF/E(KeV):        36.2572  Intensity fixed to 1.0 and variance to 1E6
=> Zero counts at step no.   3287 at 2theta/TOF/E(KeV):        36.3164  Intensity fixed to 1.0 and variance to 1E6
=> Zero counts at step no.   3301 at 2theta/TOF/E(KeV):        36.4200  Intensity fixed to 1.0 and variance to 1E6
=> Zero counts at step no.   3399 at 2theta/TOF/E(KeV):        37.1452  Intensity fixed to 1.0 and variance to 1E6
=> Zero counts at step no.   3410 at 2theta/TOF/E(KeV):        37.2266  Intensity fixed to 1.0 and variance to 1E6
=> Zero counts at step no.   3411 at 2theta/TOF/E(KeV):        37.2340  Intensity fixed to 1.0 and variance to 1E6
=> Zero counts at step no.   3414 at 2theta/TOF/E(KeV):        37.2562  Intensity fixed to 1.0 and variance to 1E6
=> Zero counts at step no.   3416 at 2theta/TOF/E(KeV):        37.2710  Intensity fixed to 1.0 and variance to 1E6
=> Zero counts at step no.   3554 at 2theta/TOF/E(KeV):        38.2922  Intensity fixed to 1.0 and variance to 1E6
=> Zero counts at step no.   3571 at 2theta/TOF/E(KeV):        38.4180  Intensity fixed to 1.0 and variance to 1E6
=> Zero counts at step no.   3572 at 2theta/TOF/E(KeV):        38.4254  Intensity fixed to 1.0 and variance to 1E6
=> Zero counts at step no.   3574 at 2theta/TOF/E(KeV):        38.4402  Intensity fixed to 1.0 and variance to 1E6
=> Zero counts at step no.   3589 at 2theta/TOF/E(KeV):        38.5512  Intensity fixed to 1.0 and variance to 1E6
=> Zero counts at step no.   3591 at 2theta/TOF/E(KeV):        38.5660  Intensity fixed to 1.0 and variance to 1E6
=> Zero counts at step no.   3594 at 2theta/TOF/E(KeV):        38.5882  Intensity fixed to 1.0 and variance to 1E6
=> Zero counts at step no.   3596 at 2theta/TOF/E(KeV):        38.6030  Intensity fixed to 1.0 and variance to 1E6
=> Zero counts at step no.   3597 at 2theta/TOF/E(KeV):        38.6104  Intensity fixed to 1.0 and variance to 1E6
=> Zero counts at step no.   3599 at 2theta/TOF/E(KeV):        38.6252  Intensity fixed to 1.0 and variance to 1E6
=> Zero counts at step no.   3601 at 2theta/TOF/E(KeV):        38.6400  Intensity fixed to 1.0 and variance to 1E6
=> Zero counts at step no.   3610 at 2theta/TOF/E(KeV):        38.7066  Intensity fixed to 1.0 and variance to 1E6
=> Zero counts at step no.   3614 at 2theta/TOF/E(KeV):        38.7362  Intensity fixed to 1.0 and variance to 1E6
=> Zero counts at step no.   3619 at 2theta/TOF/E(KeV):        38.7732  Intensity fixed to 1.0 and variance to 1E6
=> Zero counts at step no.   3622 at 2theta/TOF/E(KeV):        38.7954  Intensity fixed to 1.0 and variance to 1E6
=> Zero counts at step no.   3632 at 2theta/TOF/E(KeV):        38.8694  Intensity fixed to 1.0 and variance to 1E6
=> Zero counts at step no.   3635 at 2theta/TOF/E(KeV):        38.8916  Intensity fixed to 1.0 and variance to 1E6
=> Zero counts at step no.   3637 at 2theta/TOF/E(KeV):        38.9064  Intensity fixed to 1.0 and variance to 1E6
=> Zero counts at step no.   3640 at 2theta/TOF/E(KeV):        38.9286  Intensity fixed to 1.0 and variance to 1E6

=> Optimizations for routine tasks applied:
=> Calculation mode for patter#:   1  CM_PSEUDO_VOIGT


Standard deviations have to be multiplied by: 2.8680
(correlated residuals) See references:
-J.F.Berar & P.Lelann, J. Appl. Cryst. 24, 1-5 (1991)
-J.F.Berar, Acc. in Pow. Diff. II,NIST Sp.Pub. 846, 63(1992)

++++++++++++++++++++++++++++++++++++++++++++++++++++++++++++++++++++++++++++++++++++++++++++++++++++++++++++++++++++++++++++++++++++++ ↙


=> CYCLE No.:   50
-------------------------------------------------------------------------------
=> Phase  1 Name:   rdx
-------------------------------------------------------------------------------
=> New parameters, shifts, and standard deviations

Atom        x       dx      sx       y       dy      sy       z       dz      sz       B       dB      sB      occ.  ↙
        docc.   socc.

O(1)      0.57541 0.00006 0.00111  0.43966 0.00018 0.00121  0.27100 0.00021 0.00116  3.70830 0.00000 0.00000    ↙
     1.00000 0.00000 0.00000
O(2)      0.59412-0.00010 0.00109  0.22895 0.00026 0.00125  0.22888-0.00002 0.00110  4.41110 0.00000 0.00000    ↙
     1.00000 0.00000 0.00000
O(3)      0.47339 0.00003 0.00127  0.13057-0.00006 0.00093 -0.01945-0.00008 0.00102  4.98480 0.00000 0.00000    ↙
     1.00000 0.00000 0.00000
O(4)      0.34382-0.00038 0.00141  0.25728 0.00003 0.00127 -0.11679 0.00034 0.00152  4.76640 0.00000 0.00000    ↙
     1.00000 0.00000 0.00000
O(5)      0.31071 0.00015 0.00095  0.51082 0.00000 0.00123 -0.07997 0.00003 0.00109  5.32170 0.00000 0.00000    ↙
     1.00000 0.00000 0.00000
O(6)      0.42943 0.00027 0.00131  0.59145-0.00018 0.00188  0.05247-0.00002 0.00097  5.10850 0.00000 0.00000    ↙
     1.00000 0.00000 0.00000
N(1)      0.44482-0.00035 0.00172  0.33537 0.00167 0.00432  0.17979 0.00063 0.00178  2.73980 0.00000 0.00000    ↙
     1.00000 0.00000 0.00000
N(2)      0.33223 0.00110 0.00326  0.24145-0.00093 0.00346  0.05161 0.00085 0.00237  2.40240 0.00000 0.00000    ↙
     1.00000 0.00000 0.00000
```

```
N(3)     0.30317-0.00024 0.00212  0.45272-0.00105 0.00286  0.07823-0.00117 0.00295  2.59240 0.00000 0.00000    ↙
     1.00000 0.00000 0.00000
N(4)     0.54016 0.00004 0.00120  0.33696-0.00050 0.00200  0.23162-0.00032 0.00145  2.76530 0.00000 0.00000    ↙
     1.00000 0.00000 0.00000
N(5)     0.38838 0.00000 0.00167  0.20531 0.00023 0.00223 -0.03977-0.00035 0.00168  3.09700 0.00000 0.00000    ↙
     1.00000 0.00000 0.00000
N(6)     0.35084-0.00040 0.00174  0.55483 0.00053 0.00274  0.01185 0.00034 0.00170  3.43200 0.00000 0.00000    ↙
     1.00000 0.00000 0.00000
C(1)     0.34746-0.00103 0.00277  0.43892 0.00117 0.00301  0.19352-0.00048 0.00175  2.89510 0.00000 0.00000    ↙
     1.00000 0.00000 0.00000
C(2)     0.38532 0.00068 0.00240  0.21724 0.00058 0.00218  0.14879 0.00076 0.00247  2.70030 0.00000 0.00000    ↙
     1.00000 0.00000 0.00000
C(3)     0.23213-0.00011 0.00129  0.33451-0.00112 0.00396  0.04931 0.00009 0.00116  2.55740 0.00000 0.00000    ↙
     1.00000 0.00000 0.00000
H(1A)    0.40289 0.00000 0.00000  0.52403 0.00000 0.00000  0.20773 0.00000 0.00000  5.13220 0.00000 0.00000    ↙
     1.00000 0.00000 0.00000
H(1B)    0.29071 0.00000 0.00000  0.42024 0.00000 0.00000  0.23991 0.00000 0.00000  4.84270 0.00000 0.00000    ↙
     1.00000 0.00000 0.00000
H(2A)    0.44331 0.00000 0.00000  0.13918 0.00000 0.00000  0.14950 0.00000 0.00000  4.60580 0.00000 0.00000    ↙
     1.00000 0.00000 0.00000
H(2B)    0.31742 0.00000 0.00000  0.19390 0.00000 0.00000  0.20730 0.00000 0.00000  4.97430 0.00000 0.00000    ↙
     1.00000 0.00000 0.00000
H(3A)    0.20936 0.00000 0.00000  0.35364 0.00000 0.00000 -0.02527 0.00000 0.00000  4.50050 0.00000 0.00000    ↙
     1.00000 0.00000 0.00000
H(3B)    0.17213 0.00000 0.00000  0.32091 0.00000 0.00000  0.10070 0.00000 0.00000  3.92150 0.00000 0.00000    ↙
     1.00000 0.00000 0.00000

==> PROFILE PARAMETERS FOR PATTERN#  1

=> Overall scale factor:      0.000769464     0.000000243     0.000004678
=> Eta(p-Voigt) or m(Pearson VII):   0.000000  0.000000  0.000000
=> Overall tem. factor:     0.000000    0.000000    0.000000
=> Halfwidth parameters:
-0.014575    0.000012    0.004497
0.000000    0.000000    0.000000
0.000000    0.000000    0.000000
=> Cell parameters:
11.545714   -0.000002    0.000240
10.665313    0.000007    0.000249
13.129634    0.000005    0.000308
90.000000    0.000000    0.000000
90.000000    0.000000    0.000000
90.000000    0.000000    0.000000
=> Preferred orientation:
1.000000    0.000000    0.000000
0.000000    0.000000    0.000000
=> Asymmetry parameters:
0.034020    0.000000    0.000000
0.049140    0.000000    0.000000
0.000000    0.000000    0.000000
0.000000    0.000000    0.000000
=> X and Y parameters:
0.000000    0.000000    0.000000
0.000000    0.000000    0.000000
=> Strain parameters:
0.000000    0.000000    0.000000
0.000000    0.000000    0.000000
0.000000    0.000000    0.000000
=> Size   parameters (G,L):
0.009228    0.000000    0.000107
0.003242   -0.000001    0.007229
=> Further shape parameters (S_L and D_L):
0.000000  0.000000  0.000000
0.000000  0.000000  0.000000

=> Spherical Harmonics coeff.(size):

0.003242     -0.000001      0.007229      -0.004081      0.000619      0.018743      0.077268     -0.000633       ↙
     0.014164
0.118944     -0.000412      0.019819      -0.100242      0.000038      0.018840      0.021744     -0.000283       ↙
     0.015851
0.000000      0.000000      0.000000       0.000000      0.000000      0.000000      0.000000      0.000000       ↙
     0.000000

==> GLOBAL PARAMETERS FOR PATTERN#  1


=> Zero-point:    -0.3110    0.0000    0.0008
=> Background Polynomial Parameters ==>
0.0000      0.0000      0.0000
0.0000      0.0000      0.0000
0.0000      0.0000      0.0000
0.0000      0.0000      0.0000
0.0000      0.0000      0.0000
0.0000      0.0000      0.0000

=> Cos( theta)-shift parameter :   0.0000  0.0000  0.0000
=> Sin(2theta)-shift parameter :   0.0000  0.0000  0.0000

==> RELIABILITY FACTORS WITH ALL NON-EXCLUDED POINTS FOR PATTERN:  1
```

```
=> R-Factors:   10.4      19.9     Chi2:  54.7     DW-Stat.:  1.0389   Patt#:  1
=> Expected :            2.69                                1.9295
=> Deviance : 0.399E+06     Dev*:   110.6
=> GoF-index:  7.3         Sqrt(Residual/N)
=> N-P+C:  3591

=>    SumYdif       SumYobs      SumYcal      SumwYobsSQ     Residual    Condition
0.5173E+06    0.4951E+07    0.4772E+07    0.4950E+07    0.1964E+06    0.1010E+12


=> Conventional Rietveld Rp,Rwp,Re and Chi2:   10.4      19.9      2.69      54.70
=> (Values obtained using Ynet, but true sigma(y))
=>  SumYnet, Sum(w Ynet**2):     0.4951E+07    0.4950E+07

=> N-sigma of the GoF: 2275.477

==> RELIABILITY FACTORS FOR POINTS WITH BRAGG CONTRIBUTIONS FOR PATTERN:  1

=> R-Factors:   10.4      19.9     Chi2:  54.7     DW-Stat.:  1.0389   Patt#:
=> Expected :            2.69                                1.9295
=> Deviance : 0.399E+06     Dev*:   110.6
=> GoF-index:  7.3         Sqrt(Residual/N)
=> N-P+C:  3591

=>    SumYdif       SumYobs      SumYcal      SumwYobsSQ     Residual    Condition
0.5173E+06    0.4951E+07    0.4772E+07    0.4950E+07    0.1964E+06    0.1010E+12


=> Conventional Rietveld Rp,Rwp,Re and Chi2:   10.4      19.9      2.69      54.70
=> (Values obtained using Ynet, but true sigma(y))
=>  SumYnet, Sum(w Ynet**2):     0.4951E+07    0.4950E+07

=> N-sigma of the GoF:     2275.477

=> Global user-weigthed Chi2 (Bragg contrib.):   54.7

-------------------------------------------------------------------------------------------------------------
Pattern#  1 Phase No:   1 Phase name:   rdx
-------------------------------------------------------------------------------------------------------------

No.  Code      H   K   L  Mult     Hw         2theta      Icalc       Iobs      Sigma      HwG     HwL       ETA   ↙
          d-hkl         CORR

1   1      1   1   1     8  0.114452      13.149     1589.6     1602.9     21.583  0.111843  0.004870  0.057273    ↙
     6.727660     598.186646
2   1      0   0   2     2  0.119441      13.477      824.1      867.7     51.675  0.111766  0.014306  0.156956    ↙
     6.564814     142.231522
3   1      2   0   0     2  0.123020      15.336       83.2       89.4     18.485  0.111321  0.021631  0.226040    ↙
     5.772858     109.342499
4   1      1   0   2     4  0.114272      15.514      798.1      806.3     20.784  0.111278  0.005590  0.065698    ↙
     5.706813     213.551315
5   1      0   2   0     2  0.113511      16.610      494.6      543.5     54.025  0.111009  0.004669  0.055388    ↙
     5.332653      92.888382
6   1      2   1   0     4  0.119996      17.454     1405.2     1455.1     55.354  0.110799  0.017099  0.185281    ↙
     5.076861     167.828903
7   1      1   1   2     8  0.115043      17.611      162.0      179.2     19.069  0.110759  0.008003  0.092754    ↙
     5.031765     329.485962
8   1      0   2   1     4  0.114453      17.939     2073.1     2054.6     31.008  0.110677  0.007053  0.082398    ↙
     4.940690     158.650269
9   1      2   1   1     8  0.117198      18.724       12.8       23.0     21.357  0.110476  0.012541  0.140843    ↙
     4.735196     290.503296
10   1      1   2   1     8  0.114644      19.527        4.5       14.6     34.928  0.110269  0.008173  0.094998    ↙
     4.542274     266.421509
11   1      2   0   2     4  0.113556      20.470     1507.5     1482.5     44.012  0.110022  0.006601  0.077816    ↙
     4.335131     120.817383
12   1      0   2   2     4  0.116199      21.450      105.7      112.1     14.984  0.109761  0.012015  0.136269    ↙
     4.139135     109.650375
13   1      2   1   2     8  0.114268      22.116     1162.9     1165.7     21.433  0.109582  0.008755  0.101909    ↙
     4.016045     205.785873
14   1      2   2   0     4  0.116848      22.681      200.5      215.5     18.496  0.109427  0.013833  0.155209    ↙
     3.917146      97.626900
15   1      1   2   2     8  0.115385      22.804       41.2       45.3      4.926  0.109394  0.011185  0.128038    ↙
     3.896320     193.053589
16   1      1   1   3     8  0.116703      23.261       31.0       36.9     11.121  0.109267  0.013861  0.155696    ↙
     3.820774     185.192505
17   1      2   2   1     8  0.116079      23.683      210.4      220.4     20.453  0.109151  0.012923  0.146323    ↙
     3.753652     178.385330
18   1      3   1   1     8  0.119871      25.503     1454.2     1625.5    191.625  0.108635  0.020784  0.223082    ↙
     3.489869     152.700531
19   1      0   2   3     4  0.117643      26.322      102.7      126.9     29.776  0.108398  0.017178  0.189639    ↙
     3.383067      71.417328
20   1      2   2   2     8  0.115046      26.475       49.4       50.2      0.898  0.108353  0.012487  0.142785    ↙
     3.363830     141.100296
21   1      3   0   2     4  0.116247      26.830       68.0       75.7      8.631  0.108249  0.014896  0.167437    ↙
     3.320104      68.585548
22   1      2   1   3     8  0.114080      26.874      193.6      207.1     14.468  0.108236  0.010911  0.126383    ↙
     3.314857     136.697861
23   1      1   3   1     8  0.114507      27.086      766.4      803.5     38.882  0.108174  0.011820  0.136049    ↙
     3.289326     134.458557
```

24	1	0	0	4	2	0.120255	27.144	548.0	569.4	22.361	0.108156	0.022329	0.237905
	3.282407		33.453438										
25	1	1	2	3	8	0.116490	27.450	256.7	286.5	33.311	0.108065	0.015678	0.175474
	3.246566		130.690033										
26	1	3	1	2	8	0.116262	28.126	10.2	13.5	6.874	0.107863	0.015629	0.175285
	3.170054		124.107910										
27	1	1	0	4	4	0.118133	28.242	0.5	0.8	1.225	0.107828	0.019102	0.208881
	3.157293		61.504566										
28	1	3	2	1	8	0.118126	29.394	1024.5	1096.0	76.588	0.107477	0.019722	0.215285
	3.036147		112.975456										
29	1	2	3	0	4	0.115499	29.483	791.1	809.4	19.011	0.107450	0.014987	0.169462
	3.027129		56.124577										
30	1	1	1	4	8	0.117972	29.480	1326.3	1362.5	37.895	0.107450	0.019493	0.213191
	3.027423		112.247955										
31	1	1	3	2	8	0.115156	29.579	45.9	46.5	0.684	0.107420	0.014412	0.163700
	3.017487		111.464195										
32	1	2	3	1	8	0.115350	30.275	4.3	2.9	6.251	0.107204	0.015165	0.171595
	2.949745		106.053535										
33	1	2	2	3	8	0.114925	30.604	535.8	575.9	43.369	0.107100	0.014574	0.165781
	2.918791		103.610107										
34	1	4	0	0	2	0.124103	30.955	278.4	278.4	1.736	0.106989	0.031092	0.314029
	2.886429		25.275221										
35	1	2	0	4	4	0.114772	31.323	426.0	393.2	30.233	0.106872	0.014711	0.167492
	2.853406		49.276196										
36	1	3	2	2	8	0.116152	31.721	90.3	96.5	6.710	0.106745	0.017468	0.195022
	2.818480		95.916832										
37	1	0	2	4	4	0.118624	31.991	11.4	11.6	0.167	0.106657	0.022083	0.238480
	2.795308		47.084553										
38	1	3	1	3	8	0.114124	32.060	90.9	96.2	5.667	0.106635	0.013954	0.160098
	2.789485		93.737595										
39	1	4	1	0	4	0.123057	32.098	222.8	239.1	17.497	0.106623	0.029918	0.305505
	2.786195		46.749615										
40	1	2	1	4	8	0.115034	32.454	707.6	732.6	25.955	0.106507	0.015861	0.179568
	2.756460		91.285904										
41	1	2	3	2	8	0.115153	32.545	721.3	740.2	19.466	0.106478	0.016132	0.182308
	2.748954		90.748207										
42	1	4	1	1	8	0.121574	32.833	64.3	64.2	0.500	0.106384	0.027761	0.288373
	2.725504		89.030365										
43	1	1	2	4	8	0.117505	32.941	83.5	77.7	5.419	0.106348	0.020631	0.225732
	2.716817		88.391113										
44	1	1	3	3	8	0.116005	33.358	402.1	413.4	11.926	0.106211	0.018170	0.202680
	2.683836		86.021950										
45	1	0	4	0	2	0.113904	33.583	97.6	103.0	5.828	0.106136	0.014467	0.166031
	2.666327		21.195532										
46	1	4	0	2	4	0.118643	33.898	14.5	12.9	8.073	0.106031	0.023227	0.249980
	2.642302		41.534412										
47	1	0	4	1	4	0.114155	34.290	82.8	78.9	5.977	0.105899	0.015362	0.175457
	2.612991		40.513195										
48	1	4	1	2	8	0.118379	34.955	144.1	149.8	7.138	0.105673	0.023389	0.252129
	2.564763		77.689751										
49	1	3	3	1	8	0.116709	35.004	415.4	444.2	31.704	0.105657	0.020438	0.225181
	2.561261		77.456558										
50	1	1	4	1	8	0.114304	35.185	6.9	7.5	0.669	0.105595	0.016191	0.184239
	2.548538		76.594688										
51	1	3	2	3	8	0.114733	35.294	509.0	524.0	16.274	0.105557	0.017044	0.192759
	2.540918		76.068130										
52	1	4	2	0	4	0.120829	35.330	82.4	85.7	3.705	0.105545	0.027912	0.291470
	2.538431		37.952309										
53	1	2	2	4	8	0.115457	35.657	0.0	0.0	0.017	0.105432	0.018584	0.207979
	2.515882		74.380379										
54	1	3	0	4	4	0.113298	35.929	104.1	128.6	30.518	0.105338	0.014820	0.170763
	2.497430		36.574226										
55	1	4	2	1	8	0.119876	36.006	45.7	51.8	7.310	0.105311	0.026658	0.281403
	2.492279		72.815781										
56	1	2	3	3	8	0.115227	36.046	1.6	1.7	0.154	0.105297	0.018412	0.206543
	2.489624		72.638481										
57	1	1	1	5	8	0.118795	36.043	8.7	9.4	0.962	0.105298	0.024786	0.265254
	2.489787		72.637939										
58	1	0	4	2	4	0.114798	36.337	0.7	0.9	3.032	0.105196	0.017818	0.200946
	2.470345		35.686577										
59	1	3	1	4	8	0.113612	36.936	31.1	40.9	12.825	0.104984	0.016042	0.183679
	2.431653		68.842255										
60	1	3	3	2	8	0.115805	37.017	141.3	165.2	28.082	0.104956	0.020070	0.222994
	2.426496		68.518265										

No.	Code	H	K	L	Mult	Hw	2theta	Icalc	Iobs	Sigma	HwG	HwL	ETA
	d-hkl				CORR								
61	1	2	4	0	4	0.114804	37.110	322.5	331.5	10.798	0.104923	0.018322	0.206312
	2.420608		34.072071										
62	1	1	4	2	8	0.114771	37.189	94.1	88.8	5.271	0.104895	0.018314	0.206276
	2.415669		67.825462										
63	1	2	4	1	8	0.114806	37.759	76.8	89.1	14.661	0.104690	0.018745	0.210802
	2.380490		65.588745										
64	1	4	2	2	8	0.117713	37.973	1.8	3.6	3.562	0.104613	0.024079	0.260416
	2.367598		64.771576										
65	1	1	3	4	8	0.116825	38.088	4.0	5.8	2.527	0.104571	0.022580	0.246999
	2.360713		64.337578										
66	1	0	2	5	4	0.119243	38.170	86.5	99.7	15.297	0.104541	0.026889	0.285045
	2.355795		32.012554										

```
67   1      4   1   3     8  0.115489      38.262       323.4       335.6      13.735  0.104508  0.020305  0.226021    ↙
     2.350333      63.689579
68   1      2   1   5     8  0.116062      38.568         7.4         9.7       5.100  0.104396  0.021530  0.237695    ↙
     2.332401      62.572159
69   1      1   2   5     8  0.118256      38.988         1.9         5.1      10.965  0.104242  0.025683  0.275304    ↙
     2.308236      61.089981

-----------------------------------------------------
BRAGG R-Factors and weight fractions for Pattern #  1
-----------------------------------------------------

=> Phase:  1       rdx
=> Bragg R-factor:   4.39       Vol: 1616.766( 0.063)  Fract(%):  100.00( 0.86)
=> Rf-factor=  3.29             ATZ:        1776.939   Brindley:  1.0000

---------------------------------------------------------------
SYMBOLIC NAMES AND FINAL VALUES AND SIGMA OF REFINED PARAMETERS:
---------------------------------------------------------------

->  Parameter number    1 :      L-Size_ph1_pat1    0.32420373E-02( +/-    0.72292127E-02 )
->  Parameter number    2 :       Size2_ph1_pat1   -0.40812818E-02( +/-    0.18743467E-01 )
->  Parameter number    3 :       Size3_ph1_pat1    0.77267610E-01( +/-    0.14163993E-01 )
->  Parameter number    4 :       Size4_ph1_pat1    0.11894368    ( +/-    0.19819405E-01 )
->  Parameter number    5 :       Size5_ph1_pat1   -0.10024197    ( +/-    0.18839633E-01 )
->  Parameter number    6 :       Size6_ph1_pat1    0.21744350E-01( +/-    0.15851058E-01 )
->  Parameter number    7 :           X_O(1)_ph1    0.57541239    ( +/-    0.11092700E-02 )
->  Parameter number    8 :           Y_O(1)_ph1    0.43966007    ( +/-    0.12116111E-02 )
->  Parameter number    9 :           Z_O(1)_ph1    0.27099708    ( +/-    0.11624396E-02 )
->  Parameter number   10 :           X_O(2)_ph1    0.59412211    ( +/-    0.10898095E-02 )
->  Parameter number   11 :           Y_O(2)_ph1    0.22895293    ( +/-    0.12537022E-02 )
->  Parameter number   12 :           Z_O(2)_ph1    0.22888340    ( +/-    0.11001484E-02 )
->  Parameter number   13 :           X_O(3)_ph1    0.47338510    ( +/-    0.12744585E-02 )
->  Parameter number   14 :           Y_O(3)_ph1    0.13057353    ( +/-    0.92790980E-03 )
->  Parameter number   15 :           Z_O(3)_ph1   -0.19450795E-01( +/-    0.10155203E-02 )
->  Parameter number   16 :           X_O(4)_ph1    0.34381583    ( +/-    0.14120982E-02 )
->  Parameter number   17 :           Y_O(4)_ph1    0.25728008    ( +/-    0.12697025E-02 )
->  Parameter number   18 :           Z_O(4)_ph1   -0.11679447    ( +/-    0.15248761E-02 )
->  Parameter number   19 :           X_O(5)_ph1    0.31070611    ( +/-    0.94801566E-03 )
->  Parameter number   20 :           Y_O(5)_ph1    0.51081645    ( +/-    0.12307854E-02 )
->  Parameter number   21 :           Z_O(5)_ph1   -0.79970337E-01( +/-    0.10943528E-02 )
->  Parameter number   22 :           X_O(6)_ph1    0.42943338    ( +/-    0.13071131E-02 )
->  Parameter number   23 :           Y_O(6)_ph1    0.59145427    ( +/-    0.18751499E-02 )
->  Parameter number   24 :           Z_O(6)_ph1    0.52474596E-01( +/-    0.96871122E-03 )
->  Parameter number   25 :           X_N(1)_ph1    0.44482139    ( +/-    0.17220172E-02 )
->  Parameter number   26 :           Y_N(1)_ph1    0.33536911    ( +/-    0.43182792E-02 )
->  Parameter number   27 :           Z_N(1)_ph1    0.17979442    ( +/-    0.17772377E-02 )
->  Parameter number   28 :           X_N(2)_ph1    0.33223259    ( +/-    0.32609324E-02 )
->  Parameter number   29 :           Y_N(2)_ph1    0.24144928    ( +/-    0.34579535E-02 )
->  Parameter number   30 :           Z_N(2)_ph1    0.51606905E-01( +/-    0.23675738E-02 )
->  Parameter number   31 :           X_N(3)_ph1    0.30316588    ( +/-    0.21229470E-02 )
->  Parameter number   32 :           Y_N(3)_ph1    0.45272210    ( +/-    0.28552911E-02 )
->  Parameter number   33 :           Z_N(3)_ph1    0.78225881E-01( +/-    0.29536241E-02 )
->  Parameter number   34 :           X_N(4)_ph1    0.54015791    ( +/-    0.11990828E-02 )
->  Parameter number   35 :           Y_N(4)_ph1    0.33695599    ( +/-    0.19951391E-02 )
->  Parameter number   36 :           Z_N(4)_ph1    0.23162104    ( +/-    0.14471047E-02 )
->  Parameter number   37 :           X_N(5)_ph1    0.38837519    ( +/-    0.16739216E-02 )
->  Parameter number   38 :           Y_N(5)_ph1    0.20530595    ( +/-    0.22275527E-02 )
->  Parameter number   39 :           Z_N(5)_ph1   -0.39772190E-01( +/-    0.16845398E-02 )
->  Parameter number   40 :           X_N(6)_ph1    0.35083801    ( +/-    0.17355493E-02 )
->  Parameter number   41 :           Y_N(6)_ph1    0.55482548    ( +/-    0.27362476E-02 )
->  Parameter number   42 :           Z_N(6)_ph1    0.11853519E-01( +/-    0.16991830E-02 )
->  Parameter number   43 :           X_C(1)_ph1    0.34745705    ( +/-    0.27718858E-02 )
->  Parameter number   44 :           Y_C(1)_ph1    0.43892241    ( +/-    0.30111372E-02 )
->  Parameter number   45 :           Z_C(1)_ph1    0.19351751    ( +/-    0.17470347E-02 )
->  Parameter number   46 :           X_C(2)_ph1    0.38531837    ( +/-    0.24003256E-02 )
->  Parameter number   47 :           Y_C(2)_ph1    0.21723603    ( +/-    0.21812750E-02 )
->  Parameter number   48 :           Z_C(2)_ph1    0.14879125    ( +/-    0.24698584E-02 )
->  Parameter number   49 :           X_C(3)_ph1    0.23212539    ( +/-    0.12938807E-02 )
->  Parameter number   50 :           Y_C(3)_ph1    0.33450860    ( +/-    0.39550792E-02 )
->  Parameter number   51 :           Z_C(3)_ph1    0.49307033E-01( +/-    0.11598649E-02 )
->  Parameter number   52 :       Scale_ph1_pat1    0.76946447E-03( +/-    0.46780219E-05 )
->  Parameter number   53 :      Cell_A_ph1_pat1     11.545714    ( +/-    0.23961758E-03 )
->  Parameter number   54 :            Zero_pat1   -0.31102592    ( +/-    0.82943856E-03 )
->  Parameter number   55 :      U-Cagl_ph1_pat1   -0.14575286E-01( +/-    0.44974512E-02 )
->  Parameter number   56 :      Cell_B_ph1_pat1     10.665313    ( +/-    0.24886982E-03 )
->  Parameter number   57 :      Cell_C_ph1_pat1     13.129634    ( +/-    0.30849580E-03 )
->  Parameter number   58 :      G-Size_ph1_pat1    0.92282938E-02( +/-    0.10682658E-03 )

---------------------------------------------------------------
=> Number of bytes for floating point variables: 4
=> Dimensions of dynamic allocated arrays in this run of FullProf:
---------------------------------------------------------------

=> Total approximate array memory (dynamic + static): 107719993 bytes

MaxPOINT=    60000 Max.num. of points(+int. Inten.)/diffraction pattern
MaxREFLT=    20000 Max.num. of reflections/diffraction pattern
MaxPARAM=      300 Max.num. of refinable parameters
MaxOVERL=     2096 Max.num. of overlapping reflections
```

```
-----------------------------------------------------------
=> Number of bytes for floating point arrays: 4
=> Dimensions of fixed arrays in this release of FullProf:
-----------------------------------------------------------

NPATT   =       80 Max.num. of powder diffraction patterns
NATS    =      830 Max.num. of atoms (all kind) in asymmetric unit
MPAR    =     1800 Max.num. of non atomic parameters/phase
IEXCL   =       30 Max.num. of excluded regions
IBACP   =      277 Max.num. of background points for interpolation
NPHT    =       16 Max.num. of phases
NMAGM   =        8 Max.num. of rotation-matrices sets for magnetic structure
NBASIS  =       12 Max.num. of basis functions associated to a single atom
NIREPS  =        9 Max.num. of irreducible representations to be combined
N_EQ    =      384 Max.num. of user-supplied symmetry operators/propagation vectors
NGL     =      300 Max.num. of global parameters/diffraction pattern
N_LINC  =       30 Max.num. of global linear restraints
NAT_P   =       64 Max.num. of atomic parameters per atom
NCONST  =      500 Max.num. of slack constraints per phase
N_SPE   =       16 Max.num. of different chemical species
N_FORM  =       60 Max.num. of scattering factor values in a table
NPR     =      150 Max.num. of points defining a numerical profile
INPR    =       25 Max.num. of different numerical peak shapes
NPRC    =      150 Max.num. of terms in the table for correcting intensities
NSOL    =       10 Max.num. of solutions to be stored in Montecarlo searchs


CPU Time:    26.688 seconds
0.445 minutes

=> Run finished at:     Date: 06/07/2015  Time: 15:53:03.785
```

A.5 Sample of n-RDX processed with 10 wt% of PVP

```
*********************************************************
** PROGRAM FullProf.2k (Version 5.60 - Jan2015-ILL JRC) **
*********************************************************
M U L T I -- P A T T E R N
Rietveld, Profile Matching & Integrated Intensity
Refinement of X-ray and/or Neutron Data


Date: 15/06/2015  Time: 14:26:29.403

=> PCR file code: rpvp102a
=> DAT file code: rpvp102a.dat         -> Relative contribution: 1.0000

==> CONDITIONS OF THIS RUN FOR PATTERN No.:  1

=> Global Refinement of X-ray powder diffraction data
=> Global Refinement of X-ray powder diffraction data
Flat plate with PSD
=> Title:RDX

=> Number of phases:    1
=> Number of excluded regions:    1
=> Number of scattering factors supplied:    0
=> March-Dollase model for preferred orientation
=> Conventional weights: w=1.0/Variance(yobs)
=> Asymmetry correction as in J.Appl.Cryst. 26,128(1993)
=> Background refined by polynomial function
=> The    5th default profile function was selected
=> Pseudo-Voigt function (ETA variable)
X-parameter correspond to: ETA=ETA0+X*2theta
pV(x)= ETA*L(x)+(1-ETA)*G(x)

==> INPUT/OUTPUT OPTIONS:

=> Generate file *.PRF for plot
=> Output Integrated Intensities
=> Generate new input file *.PCR

=> Data supplied in free format for pattern:  1
=> Plot pattern at each cycle
=> Wavelengths:  1.54056 1.54439
=> Alpha2/Alpha1 ratio:   0.5000
=> Cos(Monochromator angle)=   1.0000
=> Asymmetry correction for angles lower than   90.000 degrees
=> Absorption correction (AC), muR-eff =   0.0000  0.0000
=> Base of peaks: 2.0*HW*   20.00

=> Number of cycles:   10
=> Relaxation factors ==>    for coordinates:  1.00
=> for anisotropic temperature factors:  1.00
=> for halfwidth/strain/size parameters:  1.00
=> for lattice constants and propagation vectors:  1.00
```

```
=> EPS-value for convergence:    0.0

=> Excluded regions for Pattern#  1
From     to
39.0000     50.0000

=> Instrumental Resolution read from file: xray-res.irf
=> Title of data: Approximate resolution function of a conventional X-ray diffractometer CuKalpha1,2

=> The resolution function is IRESOL:   1 for profile function #   5
Input resolution parameters:

U-inst     V-inst     W-inst     X-inst     Y-inst     Z-inst
0.00136   -0.00500    0.00391    0.06389    0.00008    0.00000
0.00136   -0.00500    0.00391    0.06389    0.00008    0.00000

=> Number of Least-Squares parameters varied:    10

=>---------------------------->
=>-------->  PATTERN number:  1
=>---------------------------->
=> Global parameters and codes ==>
=> Zero-point:    -0.2646    0.0000
=> Background parameters and codes ==>
=> Origin of polynomial at 2theta/TOF/E(KeV):   40.000
499.36      17910.      54941.      47295.      0.0000      0.0000
101.00       91.00       81.00       71.00       0.00        0.00
=> Displacement peak-shift parameter and code:     0.00    0.00
=> Transparency peak-shift parameter and code:     0.00    0.00

=> Reading Intensity data  =>>

==> Angular range, step and number of points:
2Thmin:      12.000000  2Thmax:      43.012600  Step:       0.012900  No. of points:   2405
--------------------------------------------------------------------------------
=> Phase  No. 1
rdx
--------------------------------------------------------------------------------
=>--------> Pattern#  1
=> Crystal Structure Refinement
=> The    7th profile function was selected for phase no.  1
=> Preferred orientation vector:   0.0000  0.0000  1.0000

=>--------> Data for PHASE: 1
=> Number of atoms:   21
=> Number of distance  constraints:    0
=> Number of angle     constraints:    0

=> Symmetry information on space group: P b c a
-> The multiplicity of the general position is:   8
-> The space group is Centric (-1 at origin)
-> Lattice type  P: { 000 }
-> Reduced set of symmetry operators:

No.  IT   Symmetry symbol    Rotation part     Associated Translation
1: ( 1)   1            -->     ( x, y, z) + {  0.0000  0.0000  0.0000}
2: ( 4)   2 ( x, 0, 0) -->     ( x,-y,-z) + {  0.5000  0.5000  0.0000}
3: ( 3)   2 ( 0, y, 0) -->     (-x, y,-z) + {  0.0000  0.5000  0.5000}
4: ( 2)   2 ( 0, 0, z) -->     (-x,-y, z) + {  0.5000  0.0000  0.5000}


Information on Space Group:
---------------------------

=>  Number of Space group:  61
=> Hermann-Mauguin Symbol: P b c a
=>            Hall Symbol: -P 2ac 2ab
=>   Table Setting Choice:
=>           Setting Type: IT (Generated from Hermann-Mauguin symbol)
=>         Crystal System: Orthorhombic
=>             Laue Class: mmm
=>            Point Group: mmm
=>        Bravais Lattice: P
=>         Lattice Symbol: oP
=> Reduced Number of S.O.:   4
=>   General multiplicity:   8
=>         Centrosymmetry: Centric (-1 at origin)
=> Generators (exc. -1&L):   2
=>        Asymmetric unit:  0.000 <= x <=  0.500
0.000 <= y <=  0.500
0.000 <= z <=  0.500

=> List of S.O. without inversion and lattice centring translations
=> SYMM(  1): x,y,z                              => SYMM(  2): x+1/2,-y+1/2,-z
=> SYMM(  3): -x,y+1/2,-z+1/2                    => SYMM(  4): -x+1/2,-y,z+1/2


=> Initial parameters ==>
Atom    Ntyp                X         Y         Z         B         occ.         in  fin  Spc  Mult
B11       B22       B33       B12       B13       B23
```

```
O(1)   O                  0.56112   0.44709   0.27123   3.70830   1.00000          0    0    0    8
Codes:    0.00000   0.00000   0.00000   0.00000   0.00000
O(2)   O                  0.58940   0.23581   0.22281   4.41110   1.00000          0    0    0    8
Codes:    0.00000   0.00000   0.00000   0.00000   0.00000
O(3)   O                  0.46916   0.14686  -0.03710   4.98480   1.00000          0    0    0    8
Codes:    0.00000   0.00000   0.00000   0.00000   0.00000
O(4)   O                  0.34711   0.25153  -0.11162   4.76640   1.00000          0    0    0    8
Codes:    0.00000   0.00000   0.00000   0.00000   0.00000
O(5)   O                  0.32210   0.52051  -0.08441   5.32170   1.00000          0    0    0    8
Codes:    0.00000   0.00000   0.00000   0.00000   0.00000
O(6)   O                  0.43381   0.59954   0.04827   5.10850   1.00000          0    0    0    8
Codes:    0.00000   0.00000   0.00000   0.00000   0.00000
N(1)   N                  0.44160   0.33969   0.18271   2.73980   1.00000          0    0    0    8
Codes:    0.00000   0.00000   0.00000   0.00000   0.00000
N(2)   N                  0.33383   0.24622   0.06392   2.40240   1.00000          0    0    0    8
Codes:    0.00000   0.00000   0.00000   0.00000   0.00000
N(3)   N                  0.30468   0.46123   0.06171   2.59240   1.00000          0    0    0    8
Codes:    0.00000   0.00000   0.00000   0.00000   0.00000
N(4)   N                  0.54554   0.33062   0.23341   2.76530   1.00000          0    0    0    8
Codes:    0.00000   0.00000   0.00000   0.00000   0.00000
N(5)   N                  0.38005   0.19333  -0.02755   3.09700   1.00000          0    0    0    8
Codes:    0.00000   0.00000   0.00000   0.00000   0.00000
N(6)   N                  0.35044   0.55394   0.00906   3.43200   1.00000          0    0    0    8
Codes:    0.00000   0.00000   0.00000   0.00000   0.00000
C(1)   C                  0.33877   0.43604   0.17023   2.89510   1.00000          0    0    0    8
Codes:    0.00000   0.00000   0.00000   0.00000   0.00000
C(2)   C                  0.38264   0.20846   0.14721   2.70030   1.00000          0    0    0    8
Codes:    0.00000   0.00000   0.00000   0.00000   0.00000
C(3)   C                  0.23896   0.33552   0.05796   2.55740   1.00000          0    0    0    8
Codes:    0.00000   0.00000   0.00000   0.00000   0.00000
H(1A)  H                  0.40289   0.52403   0.20773   5.13220   1.00000          0    0    0    8
Codes:    0.00000   0.00000   0.00000   0.00000   0.00000
H(1B)  H                  0.29071   0.42024   0.23991   4.84270   1.00000          0    0    0    8
Codes:    0.00000   0.00000   0.00000   0.00000   0.00000
H(2A)  H                  0.44331   0.13918   0.14950   4.60580   1.00000          0    0    0    8
Codes:    0.00000   0.00000   0.00000   0.00000   0.00000
H(2B)  H                  0.31742   0.19390   0.20730   4.97430   1.00000          0    0    0    8
Codes:    0.00000   0.00000   0.00000   0.00000   0.00000
H(3A)  H                  0.20936   0.35364  -0.02527   4.50050   1.00000          0    0    0    8
Codes:    0.00000   0.00000   0.00000   0.00000   0.00000
H(3B)  H                  0.17213   0.32091   0.10070   3.92150   1.00000          0    0    0    8
Codes:    0.00000   0.00000   0.00000   0.00000   0.00000

=> IT IS ASSUMED THAT THE FIRST GIVEN SITE IS FULLY OCCUPIED
OR THE FIRST AND SECOND ATOMS ARE IN THE SAME SITE WITH TOTAL FULL OCCUPATION
(If this is not the case, change the order of atoms to obtain correct values for the content of the unit cell)
The given occupation factors have been obtained mutiplying m/M by   1.0000
-> Atom: O    ,  Chemical element: O   Atomic Mass:    15.9994
-> Atom: O    ,  Chemical element: O   Atomic Mass:    15.9994
-> Atom: O    ,  Chemical element: O   Atomic Mass:    15.9994
-> Atom: O    ,  Chemical element: O   Atomic Mass:    15.9994
-> Atom: O    ,  Chemical element: O   Atomic Mass:    15.9994
-> Atom: O    ,  Chemical element: O   Atomic Mass:    15.9994
-> Atom: N    ,  Chemical element: N   Atomic Mass:    14.0067
-> Atom: N    ,  Chemical element: N   Atomic Mass:    14.0067
-> Atom: N    ,  Chemical element: N   Atomic Mass:    14.0067
-> Atom: N    ,  Chemical element: N   Atomic Mass:    14.0067
-> Atom: N    ,  Chemical element: N   Atomic Mass:    14.0067
-> Atom: N    ,  Chemical element: N   Atomic Mass:    14.0067
-> Atom: C    ,  Chemical element: C   Atomic Mass:    12.0110
-> Atom: C    ,  Chemical element: C   Atomic Mass:    12.0110
-> Atom: C    ,  Chemical element: C   Atomic Mass:    12.0110
-> Atom: H    ,  Chemical element: H   Atomic Mass:     1.0080
-> Atom: H    ,  Chemical element: H   Atomic Mass:     1.0080
-> Atom: H    ,  Chemical element: H   Atomic Mass:     1.0080
-> Atom: H    ,  Chemical element: H   Atomic Mass:     1.0080
-> Atom: H    ,  Chemical element: H   Atomic Mass:     1.0080
-> Atom: H    ,  Chemical element: H   Atomic Mass:     1.0080
=> The given value of ATZ is       1776.94 the program has calculated:        1776.94
The value of ATZ given in the input PCR file will be used for quantitative analysis
=> The chemical content of the unit cell is:
8.0000 O    +   8.0000 O    +   8.0000 O    +   8.0000 O    +   8.0000 O    +   8.0000 O    +   8.0000 N    +     ↙
    8.0000 N    +   8.0000 N    +   8.0000 N    +
8.0000 N    +   8.0000 N    +   8.0000 C    +   8.0000 C    +   8.0000 C    +   8.0000 H    +   8.0000 H    +     ↙
    8.0000 H    +   8.0000 H    +   8.0000 H    +
8.0000 H
=> The normalized site occupation numbers in % are:
100.0000 O(1)   :      100.0000 O(2)   :      100.0000 O(3)   :      100.0000 O(4)   :      100.0000 O(5)   :        ↙
    100.0000 O(6)   :      100.0000 N(1)   :      100.0000 N(2)   :      100.0000 N(3)   :      100.0000 N(4)   :
100.0000 N(5)   :      100.0000 N(6)   :      100.0000 C(1)   :      100.0000 C(2)   :      100.0000 C(3)   :        ↙
    100.0000 H(1A)  :      100.0000 H(1B)  :      100.0000 H(2A)  :      100.0000 H(2B)  :      100.0000 H(3A)  :
100.0000 H(3B)
=> The density (volumic mass) of the compound is:    1.806 g/cm3

=>-------> PROFILE PARAMETERS FOR PATTERN:  1

=> Overall scale factor:   0.380410E-03
=> ETA (p-Voigt) OR M (Pearson VII):   0.0000
=> Overall temperature factor:      0.00000
=> Halfwidth U,V,W:      0.03415     0.00000     0.00000
```

```
=> X and Y parameters:       0.0000      0.0000
=> Direct cell parameters:   11.5898  10.7002  13.1733  90.0000  90.0000  90.0000
=> Preferred orientation parameters:   1.0000  0.0000
=> Asymmetry parameters     :      0.08378     0.04153     0.00000     0.00000
=> Strain parameters        :      0.00000     0.00000     0.00000
=> Size   parameters        :      0.01062     0.00000
=> Further shape parameters (S_L and D_L):   0.00000   0.00000
S_L is source width/detector distance
D_L is detector width/detector distance

==> CODEWORDS FOR PROFILE PARAMETERS of PATTERN#  1

=> Overall scale factor:    0.000
=> ETA (p-Voigt) OR M (Pearson VII):    0.000
=> Overall temperature factor:    0.000
=> Halfwidth U,V,W:    0.000   0.000   0.000
=> X and Y parameters:    0.000   0.000
=> Direct cell parameters:    0.000   0.000   0.000   0.000   0.000   0.000
=> Preferred orientation parameters:    0.000   0.000
=> Asymmetry parameters     :    0.000   0.000   0.000   0.000
=> Strain parameters        :    0.000   0.000   0.000
=> Size   parameters        :    0.000  11.000
=> The 18th model for size is used

=> Orthorhombic Anisotropic Broadening using Spherical Harmonics up
to 4-th order (Laue class: mmm, SPG:16-74, only lorentzian comp.)
Ylm's up to 4th order: Y00,Y20,Y22+,Y40,Y42+,Y44+
RJP - Ref: M. Jarvinen, J. Appl. C. (1993),p.527
=> Coefficients of Spherical Harmonics for anisotropic size
broadening for an orthorhombic lattice
Y00         Y20          Y22+        Y40          Y42+       Y44+
0.000000    0.000000    0.000000    0.000000    0.000000    0.000000
11.0000     21.0000     31.0000     41.0000     51.0000     61.0000

=> Cell constraints according to Laue symmetry: mmm

Metric information:
-------------------

=> Direct cell parameters:

a =      11.5898      b =      10.7002      c =      13.1733
alpha =       90.000   beta =       90.000  gamma =       90.000
Direct Cell Volume =    1633.6707

=> Reciprocal cell parameters:

a*=     0.086283      b*=     0.093456      c*=     0.075911
alpha*=       90.000   beta*=       90.000  gamma*=       90.000
Reciprocal Cell Volume =   0.00061212

=> Direct and Reciprocal Metric Tensors:

GD                                      GR
134.3239      0.0000      0.0000          0.007445    0.000000    0.000000
0.0000    114.4947      0.0000          0.000000    0.008734    0.000000
0.0000      0.0000    173.5363          0.000000    0.000000    0.005762

=>  Cartesian frame: x // a; y is in the ab-plane; z is x ^ y

Crystal_to_Orthonormal_Matrix             Orthonormal_to_Crystal Matrix
Cr_Orth_cel                               Orth_Cr_cel
11.5898      0.0000      0.0000          0.086283    0.000000    0.000000
0.0000     10.7002      0.0000          0.000000    0.093456    0.000000
0.0000      0.0000     13.1733          0.000000    0.000000    0.075911

Busing-Levy B-matrix: Hc=B.H            Inverse of the Busing-Levy B-matrix
BL_M                                      BL_Minv
0.086283    0.000000    0.000000          11.5898      0.0000      0.0000
0.000000    0.093456    0.000000            0.0000     10.7002      0.0000
0.000000    0.000000    0.075911            0.0000      0.0000     13.1733

=> Laue symmetry mmm   will be used to generate HKL for pattern#   1
=> Reflections generated between S(1/d)min:  0.1354 A-1 and S(1/d)max:  0.5222 A-1
=>                                  dmax:  7.3874 A   and      dmin:  1.9150 A
=> The number of reflections generated is:    120
=> The max. scatt. variable (gen.ref.) is:        47.4372
=> Scattering coefficients from internal table


=> X-ray scattering coeff. (A1, B1, A2,...C, f(0), Z, Dfp,Dfpp)

O       3.0485  13.2771   2.2868   5.7011   1.5463   0.3239   0.8670  32.9089   0.2508   7.9994   8.0000   0.0470  ↙
      0.0320
N      12.2126   0.0057   3.1322   9.8933   2.0125  28.9975   1.1663   0.5826 -11.5290   6.9946   7.0000   0.0290  ↙
      0.0180
C       2.3100  20.8439   1.0200  10.2075   1.5886   0.5687   0.8650  51.6512   0.2156   5.9992   6.0000   0.0170  ↙
      0.0090
H       0.4930  10.5109   0.3229  26.1257   0.1402   3.1424   0.0408  57.7997   0.0030   1.0000   1.0000   0.0000  ↙
      0.0000
```

```
------------------------------------------------------------
SYMBOLIC NAMES AND INITIAL VALUES OF PARAMETERS TO BE VARIED:
------------------------------------------------------------

->  Parameter number    1   -> Symbolic Name:      L-Size_ph1_pat1     0.0000000
->  Parameter number    2   -> Symbolic Name:       Size2_ph1_pat1     0.0000000
->  Parameter number    3   -> Symbolic Name:       Size3_ph1_pat1     0.0000000
->  Parameter number    4   -> Symbolic Name:       Size4_ph1_pat1     0.0000000
->  Parameter number    5   -> Symbolic Name:       Size5_ph1_pat1     0.0000000
->  Parameter number    6   -> Symbolic Name:       Size6_ph1_pat1     0.0000000
->  Parameter number    7   -> Symbolic Name:           Bck_3_pat1     47294.730
->  Parameter number    8   -> Symbolic Name:           Bck_2_pat1     54940.645
->  Parameter number    9   -> Symbolic Name:           Bck_1_pat1     17910.160
->  Parameter number   10   -> Symbolic Name:           Bck_0_pat1     499.36499

=> Zero counts at step no.      1 at 2theta/TOF/E(KeV):        12.0000  Intensity fixed to 1.0 and variance to 1E6
=> Zero counts at step no.    110 at 2theta/TOF/E(KeV):        13.4061  Intensity fixed to 1.0 and variance to 1E6
=> Zero counts at step no.    112 at 2theta/TOF/E(KeV):        13.4319  Intensity fixed to 1.0 and variance to 1E6
=> Zero counts at step no.    113 at 2theta/TOF/E(KeV):        13.4448  Intensity fixed to 1.0 and variance to 1E6
=> Zero counts at step no.    118 at 2theta/TOF/E(KeV):        13.5093  Intensity fixed to 1.0 and variance to 1E6
=> Zero counts at step no.    121 at 2theta/TOF/E(KeV):        13.5480  Intensity fixed to 1.0 and variance to 1E6
=> Zero counts at step no.    123 at 2theta/TOF/E(KeV):        13.5738  Intensity fixed to 1.0 and variance to 1E6
=> Zero counts at step no.    128 at 2theta/TOF/E(KeV):        13.6383  Intensity fixed to 1.0 and variance to 1E6
=> Zero counts at step no.    129 at 2theta/TOF/E(KeV):        13.6512  Intensity fixed to 1.0 and variance to 1E6
=> Zero counts at step no.    136 at 2theta/TOF/E(KeV):        13.7415  Intensity fixed to 1.0 and variance to 1E6
=> Zero counts at step no.    140 at 2theta/TOF/E(KeV):        13.7931  Intensity fixed to 1.0 and variance to 1E6
=> Zero counts at step no.    145 at 2theta/TOF/E(KeV):        13.8576  Intensity fixed to 1.0 and variance to 1E6
=> Zero counts at step no.    146 at 2theta/TOF/E(KeV):        13.8705  Intensity fixed to 1.0 and variance to 1E6
=> Zero counts at step no.    147 at 2theta/TOF/E(KeV):        13.8834  Intensity fixed to 1.0 and variance to 1E6
=> Zero counts at step no.    155 at 2theta/TOF/E(KeV):        13.9866  Intensity fixed to 1.0 and variance to 1E6
=> Zero counts at step no.    157 at 2theta/TOF/E(KeV):        14.0124  Intensity fixed to 1.0 and variance to 1E6
=> Zero counts at step no.    158 at 2theta/TOF/E(KeV):        14.0253  Intensity fixed to 1.0 and variance to 1E6
=> Zero counts at step no.    160 at 2theta/TOF/E(KeV):        14.0511  Intensity fixed to 1.0 and variance to 1E6
=> Zero counts at step no.    165 at 2theta/TOF/E(KeV):        14.1156  Intensity fixed to 1.0 and variance to 1E6
=> Zero counts at step no.    166 at 2theta/TOF/E(KeV):        14.1285  Intensity fixed to 1.0 and variance to 1E6
=> Zero counts at step no.    167 at 2theta/TOF/E(KeV):        14.1414  Intensity fixed to 1.0 and variance to 1E6
=> Zero counts at step no.    168 at 2theta/TOF/E(KeV):        14.1543  Intensity fixed to 1.0 and variance to 1E6
=> Zero counts at step no.    179 at 2theta/TOF/E(KeV):        14.2962  Intensity fixed to 1.0 and variance to 1E6
=> Zero counts at step no.    203 at 2theta/TOF/E(KeV):        14.6058  Intensity fixed to 1.0 and variance to 1E6
=> Zero counts at step no.    204 at 2theta/TOF/E(KeV):        14.6187  Intensity fixed to 1.0 and variance to 1E6
=> Zero counts at step no.    206 at 2theta/TOF/E(KeV):        14.6445  Intensity fixed to 1.0 and variance to 1E6
=> Zero counts at step no.    216 at 2theta/TOF/E(KeV):        14.7735  Intensity fixed to 1.0 and variance to 1E6
=> Zero counts at step no.    217 at 2theta/TOF/E(KeV):        14.7864  Intensity fixed to 1.0 and variance to 1E6
=> Zero counts at step no.    219 at 2theta/TOF/E(KeV):        14.8122  Intensity fixed to 1.0 and variance to 1E6
=> Zero counts at step no.    222 at 2theta/TOF/E(KeV):        14.8509  Intensity fixed to 1.0 and variance to 1E6
=> Zero counts at step no.    266 at 2theta/TOF/E(KeV):        15.4185  Intensity fixed to 1.0 and variance to 1E6
=> Zero counts at step no.    267 at 2theta/TOF/E(KeV):        15.4314  Intensity fixed to 1.0 and variance to 1E6
=> Zero counts at step no.    268 at 2theta/TOF/E(KeV):        15.4443  Intensity fixed to 1.0 and variance to 1E6
=> Zero counts at step no.    272 at 2theta/TOF/E(KeV):        15.4959  Intensity fixed to 1.0 and variance to 1E6
=> Zero counts at step no.    273 at 2theta/TOF/E(KeV):        15.5088  Intensity fixed to 1.0 and variance to 1E6
=> Zero counts at step no.    275 at 2theta/TOF/E(KeV):        15.5346  Intensity fixed to 1.0 and variance to 1E6
=> Zero counts at step no.    277 at 2theta/TOF/E(KeV):        15.5604  Intensity fixed to 1.0 and variance to 1E6
=> Zero counts at step no.    279 at 2theta/TOF/E(KeV):        15.5862  Intensity fixed to 1.0 and variance to 1E6
=> Zero counts at step no.    280 at 2theta/TOF/E(KeV):        15.5991  Intensity fixed to 1.0 and variance to 1E6
=> Zero counts at step no.    284 at 2theta/TOF/E(KeV):        15.6507  Intensity fixed to 1.0 and variance to 1E6
=> Zero counts at step no.    286 at 2theta/TOF/E(KeV):        15.6765  Intensity fixed to 1.0 and variance to 1E6
=> Zero counts at step no.    288 at 2theta/TOF/E(KeV):        15.7023  Intensity fixed to 1.0 and variance to 1E6
=> Zero counts at step no.    289 at 2theta/TOF/E(KeV):        15.7152  Intensity fixed to 1.0 and variance to 1E6
=> Zero counts at step no.    290 at 2theta/TOF/E(KeV):        15.7281  Intensity fixed to 1.0 and variance to 1E6
=> Zero counts at step no.    292 at 2theta/TOF/E(KeV):        15.7539  Intensity fixed to 1.0 and variance to 1E6
=> Zero counts at step no.    294 at 2theta/TOF/E(KeV):        15.7797  Intensity fixed to 1.0 and variance to 1E6
=> Zero counts at step no.    295 at 2theta/TOF/E(KeV):        15.7926  Intensity fixed to 1.0 and variance to 1E6
=> Zero counts at step no.    301 at 2theta/TOF/E(KeV):        15.8700  Intensity fixed to 1.0 and variance to 1E6
=> Zero counts at step no.    302 at 2theta/TOF/E(KeV):        15.8829  Intensity fixed to 1.0 and variance to 1E6
=> Zero counts at step no.    303 at 2theta/TOF/E(KeV):        15.8958  Intensity fixed to 1.0 and variance to 1E6
=> Zero counts at step no.    307 at 2theta/TOF/E(KeV):        15.9474  Intensity fixed to 1.0 and variance to 1E6
=> Zero counts at step no.    308 at 2theta/TOF/E(KeV):        15.9603  Intensity fixed to 1.0 and variance to 1E6
=> Zero counts at step no.    309 at 2theta/TOF/E(KeV):        15.9732  Intensity fixed to 1.0 and variance to 1E6
=> Zero counts at step no.    310 at 2theta/TOF/E(KeV):        15.9861  Intensity fixed to 1.0 and variance to 1E6
=> Zero counts at step no.    312 at 2theta/TOF/E(KeV):        16.0119  Intensity fixed to 1.0 and variance to 1E6
=> Zero counts at step no.    314 at 2theta/TOF/E(KeV):        16.0377  Intensity fixed to 1.0 and variance to 1E6
=> Zero counts at step no.    320 at 2theta/TOF/E(KeV):        16.1151  Intensity fixed to 1.0 and variance to 1E6
=> Zero counts at step no.    344 at 2theta/TOF/E(KeV):        16.4247  Intensity fixed to 1.0 and variance to 1E6
=> Zero counts at step no.    354 at 2theta/TOF/E(KeV):        16.5537  Intensity fixed to 1.0 and variance to 1E6
=> Zero counts at step no.    355 at 2theta/TOF/E(KeV):        16.5666  Intensity fixed to 1.0 and variance to 1E6
=> Zero counts at step no.    356 at 2theta/TOF/E(KeV):        16.5795  Intensity fixed to 1.0 and variance to 1E6
=> Zero counts at step no.    357 at 2theta/TOF/E(KeV):        16.5924  Intensity fixed to 1.0 and variance to 1E6
=> Zero counts at step no.    358 at 2theta/TOF/E(KeV):        16.6053  Intensity fixed to 1.0 and variance to 1E6
=> Zero counts at step no.    359 at 2theta/TOF/E(KeV):        16.6182  Intensity fixed to 1.0 and variance to 1E6
=> Zero counts at step no.    362 at 2theta/TOF/E(KeV):        16.6569  Intensity fixed to 1.0 and variance to 1E6
=> Zero counts at step no.    363 at 2theta/TOF/E(KeV):        16.6698  Intensity fixed to 1.0 and variance to 1E6
=> Zero counts at step no.    364 at 2theta/TOF/E(KeV):        16.6827  Intensity fixed to 1.0 and variance to 1E6
=> Zero counts at step no.    365 at 2theta/TOF/E(KeV):        16.6956  Intensity fixed to 1.0 and variance to 1E6
=> Zero counts at step no.    369 at 2theta/TOF/E(KeV):        16.7472  Intensity fixed to 1.0 and variance to 1E6
=> Zero counts at step no.    370 at 2theta/TOF/E(KeV):        16.7601  Intensity fixed to 1.0 and variance to 1E6
=> Zero counts at step no.    371 at 2theta/TOF/E(KeV):        16.7730  Intensity fixed to 1.0 and variance to 1E6
=> Zero counts at step no.    373 at 2theta/TOF/E(KeV):        16.7988  Intensity fixed to 1.0 and variance to 1E6
=> Zero counts at step no.    374 at 2theta/TOF/E(KeV):        16.8117  Intensity fixed to 1.0 and variance to 1E6
=> Zero counts at step no.    375 at 2theta/TOF/E(KeV):        16.8246  Intensity fixed to 1.0 and variance to 1E6
```

```
=> Zero counts at step no.    378 at 2theta/TOF/E(KeV):       16.8633  Intensity fixed to 1.0 and variance to 1E6
=> Zero counts at step no.    379 at 2theta/TOF/E(KeV):       16.8762  Intensity fixed to 1.0 and variance to 1E6
=> Zero counts at step no.    380 at 2theta/TOF/E(KeV):       16.8891  Intensity fixed to 1.0 and variance to 1E6
=> Zero counts at step no.    453 at 2theta/TOF/E(KeV):       17.8308  Intensity fixed to 1.0 and variance to 1E6
=> Zero counts at step no.    455 at 2theta/TOF/E(KeV):       17.8566  Intensity fixed to 1.0 and variance to 1E6
=> Zero counts at step no.    456 at 2theta/TOF/E(KeV):       17.8695  Intensity fixed to 1.0 and variance to 1E6
=> Zero counts at step no.    460 at 2theta/TOF/E(KeV):       17.9211  Intensity fixed to 1.0 and variance to 1E6
=> Zero counts at step no.    463 at 2theta/TOF/E(KeV):       17.9598  Intensity fixed to 1.0 and variance to 1E6
=> Zero counts at step no.    464 at 2theta/TOF/E(KeV):       17.9727  Intensity fixed to 1.0 and variance to 1E6
=> Zero counts at step no.    465 at 2theta/TOF/E(KeV):       17.9856  Intensity fixed to 1.0 and variance to 1E6
=> Zero counts at step no.    466 at 2theta/TOF/E(KeV):       17.9985  Intensity fixed to 1.0 and variance to 1E6
=> Zero counts at step no.    467 at 2theta/TOF/E(KeV):       18.0114  Intensity fixed to 1.0 and variance to 1E6
=> Zero counts at step no.    470 at 2theta/TOF/E(KeV):       18.0501  Intensity fixed to 1.0 and variance to 1E6
=> Zero counts at step no.    471 at 2theta/TOF/E(KeV):       18.0630  Intensity fixed to 1.0 and variance to 1E6
=> Zero counts at step no.    476 at 2theta/TOF/E(KeV):       18.1275  Intensity fixed to 1.0 and variance to 1E6
=> Zero counts at step no.    480 at 2theta/TOF/E(KeV):       18.1791  Intensity fixed to 1.0 and variance to 1E6
=> Zero counts at step no.    482 at 2theta/TOF/E(KeV):       18.2049  Intensity fixed to 1.0 and variance to 1E6
=> Zero counts at step no.    484 at 2theta/TOF/E(KeV):       18.2307  Intensity fixed to 1.0 and variance to 1E6
=> Zero counts at step no.    485 at 2theta/TOF/E(KeV):       18.2436  Intensity fixed to 1.0 and variance to 1E6
=> Zero counts at step no.    487 at 2theta/TOF/E(KeV):       18.2694  Intensity fixed to 1.0 and variance to 1E6
=> Zero counts at step no.    488 at 2theta/TOF/E(KeV):       18.2823  Intensity fixed to 1.0 and variance to 1E6
=> Zero counts at step no.    509 at 2theta/TOF/E(KeV):       18.5532  Intensity fixed to 1.0 and variance to 1E6
=> Zero counts at step no.    513 at 2theta/TOF/E(KeV):       18.6048  Intensity fixed to 1.0 and variance to 1E6
=> Zero counts at step no.    517 at 2theta/TOF/E(KeV):       18.6564  Intensity fixed to 1.0 and variance to 1E6
=> Zero counts at step no.    520 at 2theta/TOF/E(KeV):       18.6951  Intensity fixed to 1.0 and variance to 1E6
=> Zero counts at step no.    526 at 2theta/TOF/E(KeV):       18.7725  Intensity fixed to 1.0 and variance to 1E6
=> Zero counts at step no.    533 at 2theta/TOF/E(KeV):       18.8628  Intensity fixed to 1.0 and variance to 1E6
=> Zero counts at step no.    534 at 2theta/TOF/E(KeV):       18.8757  Intensity fixed to 1.0 and variance to 1E6
=> Zero counts at step no.    547 at 2theta/TOF/E(KeV):       19.0434  Intensity fixed to 1.0 and variance to 1E6
=> Zero counts at step no.    609 at 2theta/TOF/E(KeV):       19.8432  Intensity fixed to 1.0 and variance to 1E6
=> Zero counts at step no.    662 at 2theta/TOF/E(KeV):       20.5269  Intensity fixed to 1.0 and variance to 1E6
=> Zero counts at step no.    663 at 2theta/TOF/E(KeV):       20.5398  Intensity fixed to 1.0 and variance to 1E6
=> Zero counts at step no.    665 at 2theta/TOF/E(KeV):       20.5656  Intensity fixed to 1.0 and variance to 1E6
=> Zero counts at step no.    668 at 2theta/TOF/E(KeV):       20.6043  Intensity fixed to 1.0 and variance to 1E6
=> Zero counts at step no.    669 at 2theta/TOF/E(KeV):       20.6172  Intensity fixed to 1.0 and variance to 1E6
=> Zero counts at step no.    670 at 2theta/TOF/E(KeV):       20.6301  Intensity fixed to 1.0 and variance to 1E6
=> Zero counts at step no.    674 at 2theta/TOF/E(KeV):       20.6817  Intensity fixed to 1.0 and variance to 1E6
=> Zero counts at step no.    675 at 2theta/TOF/E(KeV):       20.6946  Intensity fixed to 1.0 and variance to 1E6
=> Zero counts at step no.    679 at 2theta/TOF/E(KeV):       20.7462  Intensity fixed to 1.0 and variance to 1E6
=> Zero counts at step no.    680 at 2theta/TOF/E(KeV):       20.7591  Intensity fixed to 1.0 and variance to 1E6
=> Zero counts at step no.    681 at 2theta/TOF/E(KeV):       20.7720  Intensity fixed to 1.0 and variance to 1E6
=> Zero counts at step no.    683 at 2theta/TOF/E(KeV):       20.7978  Intensity fixed to 1.0 and variance to 1E6
=> Zero counts at step no.    684 at 2theta/TOF/E(KeV):       20.8107  Intensity fixed to 1.0 and variance to 1E6
=> Zero counts at step no.    686 at 2theta/TOF/E(KeV):       20.8365  Intensity fixed to 1.0 and variance to 1E6
=> Zero counts at step no.    688 at 2theta/TOF/E(KeV):       20.8623  Intensity fixed to 1.0 and variance to 1E6
=> Zero counts at step no.    694 at 2theta/TOF/E(KeV):       20.9397  Intensity fixed to 1.0 and variance to 1E6
=> Zero counts at step no.    695 at 2theta/TOF/E(KeV):       20.9526  Intensity fixed to 1.0 and variance to 1E6
=> Zero counts at step no.    698 at 2theta/TOF/E(KeV):       20.9913  Intensity fixed to 1.0 and variance to 1E6
=> Zero counts at step no.    717 at 2theta/TOF/E(KeV):       21.2364  Intensity fixed to 1.0 and variance to 1E6
=> Zero counts at step no.    718 at 2theta/TOF/E(KeV):       21.2493  Intensity fixed to 1.0 and variance to 1E6
=> Zero counts at step no.    719 at 2theta/TOF/E(KeV):       21.2622  Intensity fixed to 1.0 and variance to 1E6
=> Zero counts at step no.    720 at 2theta/TOF/E(KeV):       21.2751  Intensity fixed to 1.0 and variance to 1E6
=> Zero counts at step no.    721 at 2theta/TOF/E(KeV):       21.2880  Intensity fixed to 1.0 and variance to 1E6
=> Zero counts at step no.    722 at 2theta/TOF/E(KeV):       21.3009  Intensity fixed to 1.0 and variance to 1E6
=> Zero counts at step no.    727 at 2theta/TOF/E(KeV):       21.3654  Intensity fixed to 1.0 and variance to 1E6
=> Zero counts at step no.    730 at 2theta/TOF/E(KeV):       21.4041  Intensity fixed to 1.0 and variance to 1E6
=> Zero counts at step no.    732 at 2theta/TOF/E(KeV):       21.4299  Intensity fixed to 1.0 and variance to 1E6
=> Zero counts at step no.    735 at 2theta/TOF/E(KeV):       21.4686  Intensity fixed to 1.0 and variance to 1E6
=> Zero counts at step no.    736 at 2theta/TOF/E(KeV):       21.4815  Intensity fixed to 1.0 and variance to 1E6
=> Zero counts at step no.    737 at 2theta/TOF/E(KeV):       21.4944  Intensity fixed to 1.0 and variance to 1E6
=> Zero counts at step no.    739 at 2theta/TOF/E(KeV):       21.5202  Intensity fixed to 1.0 and variance to 1E6
=> Zero counts at step no.    742 at 2theta/TOF/E(KeV):       21.5589  Intensity fixed to 1.0 and variance to 1E6
=> Zero counts at step no.    780 at 2theta/TOF/E(KeV):       22.0491  Intensity fixed to 1.0 and variance to 1E6
=> Zero counts at step no.    782 at 2theta/TOF/E(KeV):       22.0749  Intensity fixed to 1.0 and variance to 1E6
=> Zero counts at step no.    785 at 2theta/TOF/E(KeV):       22.1136  Intensity fixed to 1.0 and variance to 1E6
=> Zero counts at step no.    787 at 2theta/TOF/E(KeV):       22.1394  Intensity fixed to 1.0 and variance to 1E6
=> Zero counts at step no.    788 at 2theta/TOF/E(KeV):       22.1523  Intensity fixed to 1.0 and variance to 1E6
=> Zero counts at step no.    791 at 2theta/TOF/E(KeV):       22.1910  Intensity fixed to 1.0 and variance to 1E6
=> Zero counts at step no.    821 at 2theta/TOF/E(KeV):       22.5780  Intensity fixed to 1.0 and variance to 1E6
=> Zero counts at step no.    822 at 2theta/TOF/E(KeV):       22.5909  Intensity fixed to 1.0 and variance to 1E6
=> Zero counts at step no.    828 at 2theta/TOF/E(KeV):       22.6683  Intensity fixed to 1.0 and variance to 1E6
=> Zero counts at step no.    829 at 2theta/TOF/E(KeV):       22.6812  Intensity fixed to 1.0 and variance to 1E6
=> Zero counts at step no.    830 at 2theta/TOF/E(KeV):       22.6941  Intensity fixed to 1.0 and variance to 1E6
=> Zero counts at step no.    831 at 2theta/TOF/E(KeV):       22.7070  Intensity fixed to 1.0 and variance to 1E6
=> Zero counts at step no.    835 at 2theta/TOF/E(KeV):       22.7586  Intensity fixed to 1.0 and variance to 1E6
=> Zero counts at step no.    838 at 2theta/TOF/E(KeV):       22.7973  Intensity fixed to 1.0 and variance to 1E6
=> Zero counts at step no.    839 at 2theta/TOF/E(KeV):       22.8102  Intensity fixed to 1.0 and variance to 1E6
=> Zero counts at step no.    843 at 2theta/TOF/E(KeV):       22.8618  Intensity fixed to 1.0 and variance to 1E6
=> Zero counts at step no.    845 at 2theta/TOF/E(KeV):       22.8876  Intensity fixed to 1.0 and variance to 1E6
=> Zero counts at step no.    853 at 2theta/TOF/E(KeV):       22.9908  Intensity fixed to 1.0 and variance to 1E6
=> Zero counts at step no.    857 at 2theta/TOF/E(KeV):       23.0424  Intensity fixed to 1.0 and variance to 1E6
=> Zero counts at step no.    858 at 2theta/TOF/E(KeV):       23.0553  Intensity fixed to 1.0 and variance to 1E6
=> Zero counts at step no.    859 at 2theta/TOF/E(KeV):       23.0682  Intensity fixed to 1.0 and variance to 1E6
=> Zero counts at step no.    862 at 2theta/TOF/E(KeV):       23.1069  Intensity fixed to 1.0 and variance to 1E6
=> Zero counts at step no.    864 at 2theta/TOF/E(KeV):       23.1327  Intensity fixed to 1.0 and variance to 1E6
=> Zero counts at step no.    870 at 2theta/TOF/E(KeV):       23.2101  Intensity fixed to 1.0 and variance to 1E6
=> Zero counts at step no.    894 at 2theta/TOF/E(KeV):       23.5197  Intensity fixed to 1.0 and variance to 1E6
=> Zero counts at step no.    896 at 2theta/TOF/E(KeV):       23.5455  Intensity fixed to 1.0 and variance to 1E6
=> Zero counts at step no.    902 at 2theta/TOF/E(KeV):       23.6229  Intensity fixed to 1.0 and variance to 1E6
=> Zero counts at step no.    905 at 2theta/TOF/E(KeV):       23.6616  Intensity fixed to 1.0 and variance to 1E6
```

```
=> Zero counts at step no.    906 at 2theta/TOF/E(KeV):      23.6745  Intensity fixed to 1.0 and variance to 1E6
=> Zero counts at step no.    909 at 2theta/TOF/E(KeV):      23.7132  Intensity fixed to 1.0 and variance to 1E6
=> Zero counts at step no.    913 at 2theta/TOF/E(KeV):      23.7648  Intensity fixed to 1.0 and variance to 1E6
=> Zero counts at step no.    918 at 2theta/TOF/E(KeV):      23.8293  Intensity fixed to 1.0 and variance to 1E6
=> Zero counts at step no.    920 at 2theta/TOF/E(KeV):      23.8551  Intensity fixed to 1.0 and variance to 1E6
=> Zero counts at step no.    922 at 2theta/TOF/E(KeV):      23.8809  Intensity fixed to 1.0 and variance to 1E6
=> Zero counts at step no.    926 at 2theta/TOF/E(KeV):      23.9325  Intensity fixed to 1.0 and variance to 1E6
=> Zero counts at step no.    928 at 2theta/TOF/E(KeV):      23.9583  Intensity fixed to 1.0 and variance to 1E6
=> Zero counts at step no.    930 at 2theta/TOF/E(KeV):      23.9841  Intensity fixed to 1.0 and variance to 1E6
=> Zero counts at step no.    931 at 2theta/TOF/E(KeV):      23.9970  Intensity fixed to 1.0 and variance to 1E6
=> Zero counts at step no.    932 at 2theta/TOF/E(KeV):      24.0099  Intensity fixed to 1.0 and variance to 1E6
=> Zero counts at step no.    934 at 2theta/TOF/E(KeV):      24.0357  Intensity fixed to 1.0 and variance to 1E6
=> Zero counts at step no.    938 at 2theta/TOF/E(KeV):      24.0873  Intensity fixed to 1.0 and variance to 1E6
=> Zero counts at step no.    940 at 2theta/TOF/E(KeV):      24.1131  Intensity fixed to 1.0 and variance to 1E6
=> Zero counts at step no.    949 at 2theta/TOF/E(KeV):      24.2292  Intensity fixed to 1.0 and variance to 1E6
=> Zero counts at step no.    955 at 2theta/TOF/E(KeV):      24.3066  Intensity fixed to 1.0 and variance to 1E6
=> Zero counts at step no.    989 at 2theta/TOF/E(KeV):      24.7452  Intensity fixed to 1.0 and variance to 1E6
=> Zero counts at step no.   1047 at 2theta/TOF/E(KeV):      25.4934  Intensity fixed to 1.0 and variance to 1E6
=> Zero counts at step no.   1051 at 2theta/TOF/E(KeV):      25.5450  Intensity fixed to 1.0 and variance to 1E6
=> Zero counts at step no.   1052 at 2theta/TOF/E(KeV):      25.5579  Intensity fixed to 1.0 and variance to 1E6
=> Zero counts at step no.   1053 at 2theta/TOF/E(KeV):      25.5708  Intensity fixed to 1.0 and variance to 1E6
=> Zero counts at step no.   1054 at 2theta/TOF/E(KeV):      25.5837  Intensity fixed to 1.0 and variance to 1E6
=> Zero counts at step no.   1055 at 2theta/TOF/E(KeV):      25.5966  Intensity fixed to 1.0 and variance to 1E6
=> Zero counts at step no.   1057 at 2theta/TOF/E(KeV):      25.6224  Intensity fixed to 1.0 and variance to 1E6
=> Zero counts at step no.   1058 at 2theta/TOF/E(KeV):      25.6353  Intensity fixed to 1.0 and variance to 1E6
=> Zero counts at step no.   1061 at 2theta/TOF/E(KeV):      25.6740  Intensity fixed to 1.0 and variance to 1E6
=> Zero counts at step no.   1063 at 2theta/TOF/E(KeV):      25.6998  Intensity fixed to 1.0 and variance to 1E6
=> Zero counts at step no.   1064 at 2theta/TOF/E(KeV):      25.7127  Intensity fixed to 1.0 and variance to 1E6
=> Zero counts at step no.   1065 at 2theta/TOF/E(KeV):      25.7256  Intensity fixed to 1.0 and variance to 1E6
=> Zero counts at step no.   1068 at 2theta/TOF/E(KeV):      25.7643  Intensity fixed to 1.0 and variance to 1E6
=> Zero counts at step no.   1069 at 2theta/TOF/E(KeV):      25.7772  Intensity fixed to 1.0 and variance to 1E6
=> Zero counts at step no.   1070 at 2theta/TOF/E(KeV):      25.7901  Intensity fixed to 1.0 and variance to 1E6
=> Zero counts at step no.   1072 at 2theta/TOF/E(KeV):      25.8159  Intensity fixed to 1.0 and variance to 1E6
=> Zero counts at step no.   1077 at 2theta/TOF/E(KeV):      25.8804  Intensity fixed to 1.0 and variance to 1E6
=> Zero counts at step no.   1096 at 2theta/TOF/E(KeV):      26.1255  Intensity fixed to 1.0 and variance to 1E6
=> Zero counts at step no.   1102 at 2theta/TOF/E(KeV):      26.2029  Intensity fixed to 1.0 and variance to 1E6
=> Zero counts at step no.   1104 at 2theta/TOF/E(KeV):      26.2287  Intensity fixed to 1.0 and variance to 1E6
=> Zero counts at step no.   1105 at 2theta/TOF/E(KeV):      26.2416  Intensity fixed to 1.0 and variance to 1E6
=> Zero counts at step no.   1108 at 2theta/TOF/E(KeV):      26.2803  Intensity fixed to 1.0 and variance to 1E6
=> Zero counts at step no.   1109 at 2theta/TOF/E(KeV):      26.2932  Intensity fixed to 1.0 and variance to 1E6
=> Zero counts at step no.   1111 at 2theta/TOF/E(KeV):      26.3190  Intensity fixed to 1.0 and variance to 1E6
=> Zero counts at step no.   1112 at 2theta/TOF/E(KeV):      26.3319  Intensity fixed to 1.0 and variance to 1E6
=> Zero counts at step no.   1192 at 2theta/TOF/E(KeV):      27.3639  Intensity fixed to 1.0 and variance to 1E6
=> Zero counts at step no.   1194 at 2theta/TOF/E(KeV):      27.3897  Intensity fixed to 1.0 and variance to 1E6
=> Zero counts at step no.   1212 at 2theta/TOF/E(KeV):      27.6219  Intensity fixed to 1.0 and variance to 1E6
=> Zero counts at step no.   1218 at 2theta/TOF/E(KeV):      27.6993  Intensity fixed to 1.0 and variance to 1E6
=> Zero counts at step no.   1221 at 2theta/TOF/E(KeV):      27.7380  Intensity fixed to 1.0 and variance to 1E6
=> Zero counts at step no.   1226 at 2theta/TOF/E(KeV):      27.8025  Intensity fixed to 1.0 and variance to 1E6
=> Zero counts at step no.   1228 at 2theta/TOF/E(KeV):      27.8283  Intensity fixed to 1.0 and variance to 1E6
=> Zero counts at step no.   1229 at 2theta/TOF/E(KeV):      27.8412  Intensity fixed to 1.0 and variance to 1E6
=> Zero counts at step no.   1240 at 2theta/TOF/E(KeV):      27.9831  Intensity fixed to 1.0 and variance to 1E6
=> Zero counts at step no.   1241 at 2theta/TOF/E(KeV):      27.9960  Intensity fixed to 1.0 and variance to 1E6
=> Zero counts at step no.   1242 at 2theta/TOF/E(KeV):      28.0089  Intensity fixed to 1.0 and variance to 1E6
=> Zero counts at step no.   1248 at 2theta/TOF/E(KeV):      28.0863  Intensity fixed to 1.0 and variance to 1E6
=> Zero counts at step no.   1252 at 2theta/TOF/E(KeV):      28.1379  Intensity fixed to 1.0 and variance to 1E6
=> Zero counts at step no.   1255 at 2theta/TOF/E(KeV):      28.1766  Intensity fixed to 1.0 and variance to 1E6
=> Zero counts at step no.   1262 at 2theta/TOF/E(KeV):      28.2669  Intensity fixed to 1.0 and variance to 1E6
=> Zero counts at step no.   1267 at 2theta/TOF/E(KeV):      28.3314  Intensity fixed to 1.0 and variance to 1E6
=> Zero counts at step no.   1275 at 2theta/TOF/E(KeV):      28.4346  Intensity fixed to 1.0 and variance to 1E6
=> Zero counts at step no.   1278 at 2theta/TOF/E(KeV):      28.4733  Intensity fixed to 1.0 and variance to 1E6
=> Zero counts at step no.   1290 at 2theta/TOF/E(KeV):      28.6281  Intensity fixed to 1.0 and variance to 1E6
=> Zero counts at step no.   1355 at 2theta/TOF/E(KeV):      29.4666  Intensity fixed to 1.0 and variance to 1E6
=> Zero counts at step no.   1362 at 2theta/TOF/E(KeV):      29.5569  Intensity fixed to 1.0 and variance to 1E6
=> Zero counts at step no.   1364 at 2theta/TOF/E(KeV):      29.5827  Intensity fixed to 1.0 and variance to 1E6
=> Zero counts at step no.   1365 at 2theta/TOF/E(KeV):      29.5956  Intensity fixed to 1.0 and variance to 1E6
=> Zero counts at step no.   1366 at 2theta/TOF/E(KeV):      29.6085  Intensity fixed to 1.0 and variance to 1E6
=> Zero counts at step no.   1369 at 2theta/TOF/E(KeV):      29.6472  Intensity fixed to 1.0 and variance to 1E6
=> Zero counts at step no.   1371 at 2theta/TOF/E(KeV):      29.6730  Intensity fixed to 1.0 and variance to 1E6
=> Zero counts at step no.   1373 at 2theta/TOF/E(KeV):      29.6988  Intensity fixed to 1.0 and variance to 1E6
=> Zero counts at step no.   1374 at 2theta/TOF/E(KeV):      29.7117  Intensity fixed to 1.0 and variance to 1E6
=> Zero counts at step no.   1377 at 2theta/TOF/E(KeV):      29.7504  Intensity fixed to 1.0 and variance to 1E6
=> Zero counts at step no.   1378 at 2theta/TOF/E(KeV):      29.7633  Intensity fixed to 1.0 and variance to 1E6
=> Zero counts at step no.   1380 at 2theta/TOF/E(KeV):      29.7891  Intensity fixed to 1.0 and variance to 1E6
=> Zero counts at step no.   1384 at 2theta/TOF/E(KeV):      29.8407  Intensity fixed to 1.0 and variance to 1E6
=> Zero counts at step no.   1386 at 2theta/TOF/E(KeV):      29.8665  Intensity fixed to 1.0 and variance to 1E6
=> Zero counts at step no.   1387 at 2theta/TOF/E(KeV):      29.8794  Intensity fixed to 1.0 and variance to 1E6
=> Zero counts at step no.   1454 at 2theta/TOF/E(KeV):      30.7437  Intensity fixed to 1.0 and variance to 1E6
=> Zero counts at step no.   1455 at 2theta/TOF/E(KeV):      30.7566  Intensity fixed to 1.0 and variance to 1E6
=> Zero counts at step no.   1484 at 2theta/TOF/E(KeV):      31.1307  Intensity fixed to 1.0 and variance to 1E6
=> Zero counts at step no.   1487 at 2theta/TOF/E(KeV):      31.1694  Intensity fixed to 1.0 and variance to 1E6
=> Zero counts at step no.   1490 at 2theta/TOF/E(KeV):      31.2081  Intensity fixed to 1.0 and variance to 1E6
=> Zero counts at step no.   1493 at 2theta/TOF/E(KeV):      31.2468  Intensity fixed to 1.0 and variance to 1E6
=> Zero counts at step no.   1657 at 2theta/TOF/E(KeV):      33.3624  Intensity fixed to 1.0 and variance to 1E6
=> Zero counts at step no.   1658 at 2theta/TOF/E(KeV):      33.3753  Intensity fixed to 1.0 and variance to 1E6
=> Zero counts at step no.   1664 at 2theta/TOF/E(KeV):      33.4527  Intensity fixed to 1.0 and variance to 1E6
=> Zero counts at step no.   1665 at 2theta/TOF/E(KeV):      33.4656  Intensity fixed to 1.0 and variance to 1E6
=> Zero counts at step no.   1667 at 2theta/TOF/E(KeV):      33.4914  Intensity fixed to 1.0 and variance to 1E6
=> Zero counts at step no.   1671 at 2theta/TOF/E(KeV):      33.5430  Intensity fixed to 1.0 and variance to 1E6
=> Zero counts at step no.   1674 at 2theta/TOF/E(KeV):      33.5817  Intensity fixed to 1.0 and variance to 1E6
=> Zero counts at step no.   1675 at 2theta/TOF/E(KeV):      33.5946  Intensity fixed to 1.0 and variance to 1E6
```

```
=> Zero counts at step no.   1679 at 2theta/TOF/E(KeV):        33.6462  Intensity fixed to 1.0 and variance to 1E6
=> Zero counts at step no.   1682 at 2theta/TOF/E(KeV):        33.6849  Intensity fixed to 1.0 and variance to 1E6
=> Zero counts at step no.   1683 at 2theta/TOF/E(KeV):        33.6978  Intensity fixed to 1.0 and variance to 1E6
=> Zero counts at step no.   1687 at 2theta/TOF/E(KeV):        33.7494  Intensity fixed to 1.0 and variance to 1E6
=> Zero counts at step no.   1688 at 2theta/TOF/E(KeV):        33.7623  Intensity fixed to 1.0 and variance to 1E6
=> Zero counts at step no.   1715 at 2theta/TOF/E(KeV):        34.1106  Intensity fixed to 1.0 and variance to 1E6
=> Zero counts at step no.   1723 at 2theta/TOF/E(KeV):        34.2138  Intensity fixed to 1.0 and variance to 1E6
=> Zero counts at step no.   1725 at 2theta/TOF/E(KeV):        34.2396  Intensity fixed to 1.0 and variance to 1E6
=> Zero counts at step no.   1727 at 2theta/TOF/E(KeV):        34.2654  Intensity fixed to 1.0 and variance to 1E6
=> Zero counts at step no.   1806 at 2theta/TOF/E(KeV):        35.2845  Intensity fixed to 1.0 and variance to 1E6
=> Zero counts at step no.   1809 at 2theta/TOF/E(KeV):        35.3232  Intensity fixed to 1.0 and variance to 1E6
=> Zero counts at step no.   1855 at 2theta/TOF/E(KeV):        35.9166  Intensity fixed to 1.0 and variance to 1E6
=> Zero counts at step no.   1857 at 2theta/TOF/E(KeV):        35.9424  Intensity fixed to 1.0 and variance to 1E6
=> Zero counts at step no.   1858 at 2theta/TOF/E(KeV):        35.9553  Intensity fixed to 1.0 and variance to 1E6
=> Zero counts at step no.   1859 at 2theta/TOF/E(KeV):        35.9682  Intensity fixed to 1.0 and variance to 1E6
=> Zero counts at step no.   1861 at 2theta/TOF/E(KeV):        35.9940  Intensity fixed to 1.0 and variance to 1E6
=> Zero counts at step no.   1865 at 2theta/TOF/E(KeV):        36.0456  Intensity fixed to 1.0 and variance to 1E6
=> Zero counts at step no.   1866 at 2theta/TOF/E(KeV):        36.0585  Intensity fixed to 1.0 and variance to 1E6
=> Zero counts at step no.   1867 at 2theta/TOF/E(KeV):        36.0714  Intensity fixed to 1.0 and variance to 1E6
=> Zero counts at step no.   1868 at 2theta/TOF/E(KeV):        36.0843  Intensity fixed to 1.0 and variance to 1E6
=> Zero counts at step no.   1880 at 2theta/TOF/E(KeV):        36.2391  Intensity fixed to 1.0 and variance to 1E6
=> Zero counts at step no.   1883 at 2theta/TOF/E(KeV):        36.2778  Intensity fixed to 1.0 and variance to 1E6
=> Zero counts at step no.   1942 at 2theta/TOF/E(KeV):        37.0389  Intensity fixed to 1.0 and variance to 1E6
=> Zero counts at step no.   1948 at 2theta/TOF/E(KeV):        37.1163  Intensity fixed to 1.0 and variance to 1E6
=> Zero counts at step no.   2025 at 2theta/TOF/E(KeV):        38.1096  Intensity fixed to 1.0 and variance to 1E6
=> Zero counts at step no.   2031 at 2theta/TOF/E(KeV):        38.1870  Intensity fixed to 1.0 and variance to 1E6
=> Zero counts at step no.   2055 at 2theta/TOF/E(KeV):        38.4966  Intensity fixed to 1.0 and variance to 1E6
=> Zero counts at step no.   2060 at 2theta/TOF/E(KeV):        38.5611  Intensity fixed to 1.0 and variance to 1E6
=> Zero counts at step no.   2061 at 2theta/TOF/E(KeV):        38.5740  Intensity fixed to 1.0 and variance to 1E6
=> Zero counts at step no.   2067 at 2theta/TOF/E(KeV):        38.6514  Intensity fixed to 1.0 and variance to 1E6
=> Zero counts at step no.   2069 at 2theta/TOF/E(KeV):        38.6772  Intensity fixed to 1.0 and variance to 1E6
=> Zero counts at step no.   2071 at 2theta/TOF/E(KeV):        38.7030  Intensity fixed to 1.0 and variance to 1E6
=> Zero counts at step no.   2072 at 2theta/TOF/E(KeV):        38.7159  Intensity fixed to 1.0 and variance to 1E6
=> Zero counts at step no.   2086 at 2theta/TOF/E(KeV):        38.8965  Intensity fixed to 1.0 and variance to 1E6
=> Zero counts at step no.   2093 at 2theta/TOF/E(KeV):        38.9868  Intensity fixed to 1.0 and variance to 1E6
=> Zero counts at step no.   2141 at 2theta/TOF/E(KeV):        39.6060  Intensity fixed to 1.0 and variance to 1E6
=> Zero counts at step no.   2312 at 2theta/TOF/E(KeV):        41.8119  Intensity fixed to 1.0 and variance to 1E6
=> Zero counts at step no.   2313 at 2theta/TOF/E(KeV):        41.8248  Intensity fixed to 1.0 and variance to 1E6
=> Zero counts at step no.   2317 at 2theta/TOF/E(KeV):        41.8764  Intensity fixed to 1.0 and variance to 1E6
=> Zero counts at step no.   2363 at 2theta/TOF/E(KeV):        42.4698  Intensity fixed to 1.0 and variance to 1E6
=> Zero counts at step no.   2374 at 2theta/TOF/E(KeV):        42.6117  Intensity fixed to 1.0 and variance to 1E6
=> Zero counts at step no.   2377 at 2theta/TOF/E(KeV):        42.6504  Intensity fixed to 1.0 and variance to 1E6
=> Zero counts at step no.   2378 at 2theta/TOF/E(KeV):        42.6633  Intensity fixed to 1.0 and variance to 1E6
=> Zero counts at step no.   2380 at 2theta/TOF/E(KeV):        42.6891  Intensity fixed to 1.0 and variance to 1E6
=> Zero counts at step no.   2382 at 2theta/TOF/E(KeV):        42.7149  Intensity fixed to 1.0 and variance to 1E6
=> Zero counts at step no.   2383 at 2theta/TOF/E(KeV):        42.7278  Intensity fixed to 1.0 and variance to 1E6
=> Zero counts at step no.   2386 at 2theta/TOF/E(KeV):        42.7665  Intensity fixed to 1.0 and variance to 1E6
=> Zero counts at step no.   2394 at 2theta/TOF/E(KeV):        42.8697  Intensity fixed to 1.0 and variance to 1E6
=> Zero counts at step no.   2395 at 2theta/TOF/E(KeV):        42.8826  Intensity fixed to 1.0 and variance to 1E6
=> Zero counts at step no.   2398 at 2theta/TOF/E(KeV):        42.9213  Intensity fixed to 1.0 and variance to 1E6
=> Zero counts at step no.   2399 at 2theta/TOF/E(KeV):        42.9342  Intensity fixed to 1.0 and variance to 1E6
=> Zero counts at step no.   2400 at 2theta/TOF/E(KeV):        42.9471  Intensity fixed to 1.0 and variance to 1E6
=> Zero counts at step no.   2403 at 2theta/TOF/E(KeV):        42.9858  Intensity fixed to 1.0 and variance to 1E6
=> Zero counts at step no.   2404 at 2theta/TOF/E(KeV):        42.9987  Intensity fixed to 1.0 and variance to 1E6

=> Optimizations for routine tasks applied:
=> Calculation mode for patter#:   1  CM_PSEUDO_VOIGT


Standard deviations have to be multiplied by: 2.6583
(correlated residuals) See references:
-J.F.Berar & P.Lelann, J. Appl. Cryst. 24, 1-5 (1991)
-J.F.Berar, Acc. in Pow. Diff. II,NIST Sp.Pub. 846, 63(1992)

++++++++++++++++++++++++++++++++++++++++++++++++++++++++++++++++++++++++++++++++++++++++++++++++++++++++++++++++++++++++++++++++++++++ ↙


=> CYCLE No.:   10
-------------------------------------------------------------------------------
=> Phase  1 Name:   rdx
-------------------------------------------------------------------------------
=> New parameters, shifts, and standard deviations

Atom        x       dx      sx       y       dy      sy       z       dz      sz       B       dB      sB      occ.  ↙
        docc.   socc.

O(1)     0.56112 0.00000 0.00000  0.44709 0.00000 0.00000  0.27123 0.00000 0.00000  3.70830 0.00000 0.00000    ↙
    1.00000 0.00000 0.00000
O(2)     0.58940 0.00000 0.00000  0.23581 0.00000 0.00000  0.22281 0.00000 0.00000  4.41110 0.00000 0.00000    ↙
    1.00000 0.00000 0.00000
O(3)     0.46916 0.00000 0.00000  0.14686 0.00000 0.00000 -0.03710 0.00000 0.00000  4.98480 0.00000 0.00000    ↙
    1.00000 0.00000 0.00000
O(4)     0.34711 0.00000 0.00000  0.25153 0.00000 0.00000 -0.11162 0.00000 0.00000  4.76640 0.00000 0.00000    ↙
    1.00000 0.00000 0.00000
O(5)     0.32210 0.00000 0.00000  0.52051 0.00000 0.00000 -0.08441 0.00000 0.00000  5.32170 0.00000 0.00000    ↙
    1.00000 0.00000 0.00000
O(6)     0.43381 0.00000 0.00000  0.59954 0.00000 0.00000  0.04827 0.00000 0.00000  5.10850 0.00000 0.00000    ↙
    1.00000 0.00000 0.00000
N(1)     0.44160 0.00000 0.00000  0.33969 0.00000 0.00000  0.18271 0.00000 0.00000  2.73980 0.00000 0.00000    ↙
```

```
     1.00000 0.00000 0.00000
N(2)      0.33383 0.00000 0.00000  0.24622 0.00000 0.00000  0.06392 0.00000 0.00000  2.40240 0.00000 0.00000    ↙
     1.00000 0.00000 0.00000
N(3)      0.30468 0.00000 0.00000  0.46123 0.00000 0.00000  0.06171 0.00000 0.00000  2.59240 0.00000 0.00000    ↙
     1.00000 0.00000 0.00000
N(4)      0.54554 0.00000 0.00000  0.33062 0.00000 0.00000  0.23341 0.00000 0.00000  2.76530 0.00000 0.00000    ↙
     1.00000 0.00000 0.00000
N(5)      0.38005 0.00000 0.00000  0.19333 0.00000 0.00000 -0.02755 0.00000 0.00000  3.09700 0.00000 0.00000    ↙
     1.00000 0.00000 0.00000
N(6)      0.35044 0.00000 0.00000  0.55394 0.00000 0.00000  0.00906 0.00000 0.00000  3.43200 0.00000 0.00000    ↙
     1.00000 0.00000 0.00000
C(1)      0.33877 0.00000 0.00000  0.43604 0.00000 0.00000  0.17023 0.00000 0.00000  2.89510 0.00000 0.00000    ↙
     1.00000 0.00000 0.00000
C(2)      0.38264 0.00000 0.00000  0.20846 0.00000 0.00000  0.14721 0.00000 0.00000  2.70030 0.00000 0.00000    ↙
     1.00000 0.00000 0.00000
C(3)      0.23896 0.00000 0.00000  0.33552 0.00000 0.00000  0.05796 0.00000 0.00000  2.55740 0.00000 0.00000    ↙
     1.00000 0.00000 0.00000
H(1A)     0.40289 0.00000 0.00000  0.52403 0.00000 0.00000  0.20773 0.00000 0.00000  5.13220 0.00000 0.00000    ↙
     1.00000 0.00000 0.00000
H(1B)     0.29071 0.00000 0.00000  0.42024 0.00000 0.00000  0.23991 0.00000 0.00000  4.84270 0.00000 0.00000    ↙
     1.00000 0.00000 0.00000
H(2A)     0.44331 0.00000 0.00000  0.13918 0.00000 0.00000  0.14950 0.00000 0.00000  4.60580 0.00000 0.00000    ↙
     1.00000 0.00000 0.00000
H(2B)     0.31742 0.00000 0.00000  0.19390 0.00000 0.00000  0.20730 0.00000 0.00000  4.97430 0.00000 0.00000    ↙
     1.00000 0.00000 0.00000
H(3A)     0.20936 0.00000 0.00000  0.35364 0.00000 0.00000 -0.02527 0.00000 0.00000  4.50050 0.00000 0.00000    ↙
     1.00000 0.00000 0.00000
H(3B)     0.17213 0.00000 0.00000  0.32091 0.00000 0.00000  0.10070 0.00000 0.00000  3.92150 0.00000 0.00000    ↙
     1.00000 0.00000 0.00000

==> PROFILE PARAMETERS FOR PATTERN#  1

=> Overall scale factor:      0.000380410     0.000000000     0.000000000
=> Eta(p-Voigt) or m(Pearson VII):   0.000000  0.000000  0.000000
=> Overall tem. factor:   0.000000  0.000000  0.000000
=> Halfwidth parameters:
0.034153  0.000000  0.000000
0.000000  0.000000  0.000000
0.000000  0.000000  0.000000
=> Cell parameters:
11.589819   0.000000   0.000000
10.700219   0.000000   0.000000
13.173317   0.000000   0.000000
90.000000   0.000000   0.000000
90.000000   0.000000   0.000000
90.000000   0.000000   0.000000
=> Preferred orientation:
1.000000  0.000000  0.000000
0.000000  0.000000  0.000000
=> Asymmetry parameters:
0.083780  0.000000  0.000000
0.041530  0.000000  0.000000
0.000000  0.000000  0.000000
0.000000  0.000000  0.000000
=> X and Y parameters:
0.000000  0.000000  0.000000
0.000000  0.000000  0.000000
=> Strain parameters:
0.000000  0.000000  0.000000
0.000000  0.000000  0.000000
0.000000  0.000000  0.000000
=> Size   parameters (G,L):
0.010621  0.000000  0.000000
0.047821 -0.000006  0.014780
=> Further shape parameters (S_L and D_L):
0.000000  0.000000  0.000000
0.000000  0.000000  0.000000

=> Spherical Harmonics coeff.(size):

0.047821     -0.000006      0.014780       0.072264     -0.000017      0.040111       0.124992      0.000011       ↙
     0.029142
0.079216      0.000001      0.041181       0.006204      0.000018      0.040141       0.011800      0.000014       ↙
     0.033870
0.000000      0.000000      0.000000       0.000000      0.000000      0.000000       0.000000      0.000000       ↙
     0.000000

==> GLOBAL PARAMETERS FOR PATTERN#  1


=> Zero-point:    -0.2646    0.0000    0.0000
=> Background Polynomial Parameters ==>
564.83      6.2519      5.4257
20303.      236.60      74.327
64170.      915.43      244.22
55266.      790.96      223.17
0.0000      0.0000      0.0000
0.0000      0.0000      0.0000

=> Cos( theta)-shift parameter :   0.0000  0.0000  0.0000
```

```
=> Sin(2theta)-shift parameter :   0.0000  0.0000  0.0000

==> RELIABILITY FACTORS WITH ALL NON-EXCLUDED POINTS FOR PATTERN:  1

=> R-Factors:   13.4      25.7     Chi2:  50.6     DW-Stat.:  1.0048   Patt#:  1
=> Expected :            3.62                                1.8736
=> Deviance : 0.267E+06     Dev*:   127.5
=> GoF-index:  7.1         Sqrt(Residual/N)
=> N-P+C:  2083

=>    SumYdif       SumYobs      SumYcal      SumwYobsSQ     Residual    Condition
0.2129E+06    0.1592E+07    0.1483E+07    0.1592E+07    0.1055E+06    0.1514E+10


=> Conventional Rietveld Rp,Rwp,Re and Chi2:   13.4      25.7      3.62      50.64
=> (Values obtained using Ynet, but true sigma(y))
=>  SumYnet, Sum(w Ynet**2):     0.1591E+07    0.1591E+07

=> N-sigma of the GoF: 1602.135

==> RELIABILITY FACTORS FOR POINTS WITH BRAGG CONTRIBUTIONS FOR PATTERN:  1

=> R-Factors:   13.4      25.7     Chi2:  50.6     DW-Stat.:  1.0048   Patt#:
=> Expected :            3.62                                1.8736
=> Deviance : 0.267E+06     Dev*:   127.5
=> GoF-index:  7.1         Sqrt(Residual/N)
=> N-P+C:  2083

=>    SumYdif       SumYobs      SumYcal      SumwYobsSQ     Residual    Condition
0.2129E+06    0.1592E+07    0.1483E+07    0.1592E+07    0.1055E+06    0.1514E+10


=> Conventional Rietveld Rp,Rwp,Re and Chi2:   13.4      25.7      3.62      50.64
=> (Values obtained using Ynet, but true sigma(y))
=>  SumYnet, Sum(w Ynet**2):     0.1591E+07    0.1591E+07

=> N-sigma of the GoF:     1602.135

=> Global user-weigthed Chi2 (Bragg contrib.):   50.6

-------------------------------------------------------------------------------------------------------------
Pattern#  1 Phase No:   1 Phase name:   rdx
-------------------------------------------------------------------------------------------------------------

No.  Code     H   K   L  Mult     Hw         2theta      Icalc       Iobs      Sigma      HwG     HwL       ETA   ↙
          d-hkl         CORR

1   1      1   1   1     8  0.124715      13.103     1013.3     1116.2    113.426  0.120686  0.007526  0.080717    ↙
    6.751026     602.658569
2   1      0   0   2     2  0.130916      13.432      528.4      610.7     97.893  0.120755  0.018885  0.187455    ↙
    6.586658     143.276764
3   1      2   0   0     2  0.131142      15.277       63.2       78.4     21.222  0.121203  0.018481  0.183336    ↙
    5.794909     110.243629
4   1      1   0   2     4  0.130005      15.461      474.9      548.8     90.345  0.121253  0.016303  0.164017    ↙
    5.726488     215.175110
5   1      0   2   0     2  0.124560      16.556      297.7      301.5     15.913  0.121573  0.005575  0.060197    ↙
    5.350110      93.542114
6   1      2   1   0     4  0.130248      17.389      772.8      827.6     66.775  0.121841  0.015670  0.157633    ↙
    5.095625     169.175110
7   1      1   1   2     8  0.128551      17.551       93.6      107.6     16.133  0.121895  0.012427  0.127698    ↙
    5.048918     331.966187
8   1      0   2   1     4  0.125093      17.879     1148.7     1154.9     23.940  0.122008  0.005758  0.061881    ↙
    4.956901     159.781006
9   1      2   1   1     8  0.130353      18.655        0.1        2.5     45.038  0.122288  0.015038  0.151414    ↙
    4.752470     292.823120
10   1      1   2   1     8  0.127024      19.461       27.0       43.0     26.403  0.122597  0.008270  0.086942    ↙
    4.557557     268.381683
11   1      2   0   2     4  0.132416      20.395      892.2     1023.0    152.315  0.122981  0.017563  0.173044    ↙
    4.350759     121.787003
12   1      0   2   2     4  0.128230      21.379       55.8       56.5     13.314  0.123413  0.008998  0.093548    ↙
    4.152773     110.454323
13   1      2   1   2     8  0.132372      22.036      630.1      672.0     53.995  0.123719  0.016124  0.159519    ↙
    4.030334     207.423492
14   1      2   2   0     4  0.131499      22.601      109.2      120.0     18.338  0.123991  0.014008  0.140237    ↙
    3.930954      98.388397
15   1      1   2   2     8  0.129797      22.727        6.4        8.7      3.667  0.124054  0.010729  0.109720    ↙
    3.909391     194.502167
16   1      1   1   3     8  0.134321      23.182        0.0        0.0      0.200  0.124282  0.018670  0.180947    ↙
    3.833667     186.614227
17   1      2   2   1     8  0.131987      23.599      108.4      132.1     37.049  0.124498  0.013976  0.139429    ↙
    3.766823     179.780441
18   1      3   1   1     8  0.137002      25.406      750.9      876.6    150.280  0.125491  0.021358  0.201780    ↙
    3.502875     153.983307
19   1      0   2   3     4  0.133939      26.234        8.0       17.3     21.185  0.125979  0.014849  0.145729    ↙
    3.394251      71.958969
20   1      2   2   2     8  0.134201      26.382        2.7        5.2      7.080  0.126068  0.015167  0.148447    ↙
    3.375513     142.214142
21   1      3   0   2     4  0.138195      26.730        6.8        6.7      1.940  0.126281  0.022090  0.206614    ↙
    3.332368      69.163780
22   1      2   1   3     8  0.136993      26.778      111.3      117.4     12.184  0.126311  0.019851  0.188259    ↙
```

					3.326408	137.794662							
23	1	1	3	1	8	0.132845	26.995	457.7	472.9	16.783	0.126446	0.011951	0.119107
					3.300250	135.467346							
24	1	0	0	4	2	0.141115	27.053	191.9	208.8	19.037	0.126482	0.026975	0.244466
					3.293329	33.713680							
25	1	1	2	3	8	0.135113	27.356	134.4	150.8	18.695	0.126674	0.015733	0.152769
					3.257430	131.697845							
26	1	3	1	2	8	0.138645	28.021	8.8	13.1	16.666	0.127104	0.021416	0.200031
					3.181646	125.149506							
27	1	1	0	4	4	0.141402	28.145	2.0	3.3	3.772	0.127186	0.026236	0.237736
					3.167915	61.989910							
28	1	3	2	1	8	0.138869	29.285	575.4	632.3	63.210	0.127960	0.020272	0.189584
					3.047127	113.913353							
29	1	1	1	4	8	0.141197	29.379	771.0	805.9	39.929	0.128025	0.024370	0.222125
					3.037585	113.135292							
30	1	2	3	0	4	0.136439	29.380	334.3	344.9	11.925	0.128026	0.015688	0.150931
					3.037493	56.563869							
31	1	1	3	2	8	0.135174	29.479	22.6	22.8	0.376	0.128095	0.013215	0.129094
					3.027512	112.316452							
32	1	2	3	1	8	0.137066	30.169	4.4	3.1	8.149	0.128587	0.015811	0.151400
					2.959830	106.887421							
33	1	2	2	3	8	0.138745	30.496	273.1	285.7	14.020	0.128825	0.018463	0.173595
					2.928823	104.442360							
34	1	4	0	0	2	0.144166	30.835	137.2	137.0	2.405	0.129075	0.027810	0.246550
					2.897455	25.498945							
35	1	2	0	4	4	0.143264	31.212	224.0	201.1	21.370	0.129358	0.025696	0.230302
					2.863244	49.679192							
36	1	3	2	2	8	0.140837	31.605	36.8	43.8	12.932	0.129657	0.020769	0.191425
					2.828560	96.717529							
37	1	0	2	4	4	0.141255	31.883	8.4	8.6	0.233	0.129871	0.021142	0.194140
					2.804568	47.455128							
38	1	3	1	3	8	0.142476	31.942	21.3	22.1	0.820	0.129917	0.023274	0.210893
					2.799478	94.528854							
39	1	4	1	0	4	0.144695	31.974	142.9	148.4	5.901	0.129942	0.027214	0.240776
					2.796734	47.161793							
40	1	2	1	4	8	0.143561	32.340	351.9	374.5	24.130	0.130229	0.024669	0.221208
					2.765931	92.033249							
41	1	2	3	2	8	0.139293	32.432	391.0	394.3	3.992	0.130302	0.016758	0.157632
					2.758319	91.471329							
42	1	4	1	1	8	0.145160	32.707	37.6	34.5	2.848	0.130521	0.027014	0.238403
					2.735760	89.815369							
43	1	1	2	4	8	0.142235	32.828	37.8	36.6	1.231	0.130619	0.021566	0.196537
					2.725893	89.095551							
44	1	1	3	3	8	0.139743	33.244	190.2	197.3	8.386	0.130956	0.016381	0.153752
					2.692755	86.697815							
45	1	0	4	0	2	0.139380	33.470	49.0	47.6	3.041	0.131142	0.015367	0.144955
					2.675055	21.357391							
46	1	4	0	2	4	0.146193	33.768	1.7	3.8	10.207	0.131389	0.027316	0.239302
					2.652184	41.901897							
47	1	0	4	1	4	0.140057	34.174	24.3	35.7	19.269	0.131730	0.015532	0.145770
					2.621550	40.824486							
48	1	4	1	2	8	0.146900	34.822	65.2	64.1	3.921	0.132285	0.026982	0.235499
					2.574286	78.375824							
49	1	3	3	1	8	0.143646	34.878	251.1	244.1	10.615	0.132334	0.021019	0.190013
					2.570270	78.100563							
50	1	1	4	1	8	0.141362	35.065	0.4	0.4	0.021	0.132497	0.016527	0.153363
					2.556954	77.191193							
51	1	3	2	3	8	0.144832	35.166	249.3	266.6	18.907	0.132585	0.022718	0.202963
					2.549886	76.710526							
52	1	4	2	0	4	0.146890	35.195	41.6	44.5	3.206	0.132611	0.026383	0.230602
					2.547813	38.284893							
53	1	2	2	4	8	0.145383	35.532	4.5	5.5	6.507	0.132909	0.023132	0.205721
					2.524459	74.992844							
54	1	3	0	4	4	0.147866	35.798	58.0	64.7	8.116	0.133147	0.027174	0.235616
					2.506258	36.887241							
55	1	4	2	1	8	0.147470	35.869	31.1	30.4	1.700	0.133211	0.026351	0.229494
					2.501457	73.454659							
56	1	1	1	5	8	0.149388	35.919	0.4	0.4	0.054	0.133255	0.029692	0.253531
					2.498121	73.232788							
57	1	2	3	3	8	0.143590	35.920	7.8	6.8	0.979	0.133256	0.019232	0.174668
					2.498070	73.229378							
58	1	0	4	2	4	0.142334	36.214	3.1	3.2	15.198	0.133522	0.016430	0.151500
					2.478451	35.965515							
59	1	3	1	4	8	0.148526	36.801	29.3	33.5	5.660	0.134063	0.026722	0.230968
					2.440215	69.431854							
60	1	3	3	2	8	0.145810	36.883	85.3	89.3	5.900	0.134139	0.021679	0.192915
					2.434983	69.093094							

No.	Code	H	K	L	Mult	Hw	2theta	Icalc	Iobs	Sigma	HwG	HwL	ETA
					d-hkl	CORR							
61	1	2	4	0	4	0.144533	36.981	127.0	138.5	13.228	0.134230	0.019177	0.173104
					2.428764	34.345711							
62	1	1	4	2	8	0.143640	37.062	36.3	41.7	6.220	0.134306	0.017396	0.158639
					2.423652	68.362068							
63	1	2	4	1	8	0.145235	37.628	31.0	42.5	15.911	0.134841	0.019346	0.173758
					2.388508	66.117844							
64	1	4	2	2	8	0.149444	37.829	2.8	3.8	1.219	0.135034	0.026633	0.228919
					2.376235	65.342354							
65	1	1	3	4	8	0.146469	37.957	0.7	0.7	0.102	0.135157	0.021028	0.186606

```
     2.368560      64.859573
66   1      0   2   5     4  0.149967      38.039       57.6       58.0      1.712  0.135236  0.027209  0.232800    ↙
     2.363609      32.274525
67   1      4   1   3     8  0.150496      38.118      148.1      151.8      6.447  0.135312  0.028018  0.238495    ↙
     2.358914      64.255211
68   1      2   1   5     8  0.151800      38.432        3.0        5.6      7.937  0.135619  0.029797  0.250596    ↙
     2.340343      63.099045
69   1      1   2   5     8  0.150892      38.853        2.1        4.9     15.308  0.136034  0.027441  0.233313    ↙
     2.315939      61.594719

------------------------------------------------------
BRAGG R-Factors and weight fractions for Pattern #  1
------------------------------------------------------

=> Phase:  1       rdx
=> Bragg R-factor:   7.51       Vol: 1633.671( 0.000)  Fract(%):  100.00( 0.00)
=> Rf-factor=  4.81             ATZ:        1776.939   Brindley:  1.0000

---------------------------------------------------------------------
SYMBOLIC NAMES AND FINAL VALUES AND SIGMA OF REFINED PARAMETERS:
---------------------------------------------------------------------

->  Parameter number    1 :      L-Size_ph1_pat1    0.47820579E-01( +/-    0.14780403E-01 )
->  Parameter number    2 :       Size2_ph1_pat1    0.72263569E-01( +/-    0.40111270E-01 )
->  Parameter number    3 :       Size3_ph1_pat1    0.12499154    ( +/-    0.29142125E-01 )
->  Parameter number    4 :       Size4_ph1_pat1    0.79216398E-01( +/-    0.41180771E-01 )
->  Parameter number    5 :       Size5_ph1_pat1    0.62037650E-02( +/-    0.40140565E-01 )
->  Parameter number    6 :       Size6_ph1_pat1    0.11800204E-01( +/-    0.33870187E-01 )
->  Parameter number    7 :           Bck_3_pat1     55265.500    ( +/-     223.17101     )
->  Parameter number    8 :           Bck_2_pat1     64169.578    ( +/-     244.21664     )
->  Parameter number    9 :           Bck_1_pat1     20303.109    ( +/-     74.326691     )
->  Parameter number   10 :           Bck_0_pat1     564.83319    ( +/-     5.4257102     )

---------------------------------------------------------------------
=> Number of bytes for floating point variables: 4
=> Dimensions of dynamic allocated arrays in this run of FullProf:
---------------------------------------------------------------------

=> Total approximate array memory (dynamic + static): 107719993 bytes

MaxPOINT=    60000 Max.num. of points(+int. Inten.)/diffraction pattern
MaxREFLT=    20000 Max.num. of reflections/diffraction pattern
MaxPARAM=      300 Max.num. of refinable parameters
MaxOVERL=     2096 Max.num. of overlapping reflections

-----------------------------------------------------------
=> Number of bytes for floating point arrays: 4
=> Dimensions of fixed arrays in this release of FullProf:
-----------------------------------------------------------

NPATT   =       80 Max.num. of powder diffraction patterns
NATS    =      830 Max.num. of atoms (all kind) in asymmetric unit
MPAR    =     1800 Max.num. of non atomic parameters/phase
IEXCL   =       30 Max.num. of excluded regions
IBACP   =      277 Max.num. of background points for interpolation
NPHT    =       16 Max.num. of phases
NMAGM   =        8 Max.num. of rotation-matrices sets for magnetic structure
NBASIS  =       12 Max.num. of basis functions associated to a single atom
NIREPS  =        9 Max.num. of irreducible representations to be combined
N_EQ    =      384 Max.num. of user-supplied symmetry operators/propagation vectors
NGL     =      300 Max.num. of global parameters/diffraction pattern
N_LINC  =       30 Max.num. of global linear restraints
NAT_P   =       64 Max.num. of atomic parameters per atom
NCONST  =      500 Max.num. of slack constraints per phase
N_SPE   =       16 Max.num. of different chemical species
N_FORM  =       60 Max.num. of scattering factor values in a table
NPR     =      150 Max.num. of points defining a numerical profile
INPR    =       25 Max.num. of different numerical peak shapes
NPRC    =      150 Max.num. of terms in the table for correcting intensities
NSOL    =       10 Max.num. of solutions to be stored in Montecarlo searchs


CPU Time:     6.805 seconds
0.113 minutes

=> Run finished at:     Date: 15/06/2015  Time: 14:26:36.221
```

A.6 Sample of n-RDX with 1 wt% of PVP through a 80 micron nozzle

```
*******************************************************
** PROGRAM FullProf.2k (Version 5.50 - Dec2014-ILL JRC) **
*******************************************************
M U L T I -- P A T T E R N
Rietveld, Profile Matching & Integrated Intensity
Refinement of X-ray and/or Neutron Data
```

```
Date: 20/02/2015  Time: 16:02:20.266

=> PCR file code: rpvp1_80_2a_woB_stillKa2_fullprof
=> DAT file code: rpvp1_80_2a_woB_stil -> Relative contribution: 1.0000

==> CONDITIONS OF THIS RUN FOR PATTERN No.:  1

=> Global Refinement of X-ray powder diffraction data
=> Global Refinement of X-ray powder diffraction data
Flat plate with PSD
=> Title:RDX

=> Number of phases:    1
=> Number of excluded regions:    0
=> Number of scattering factors supplied:    0
=> March-Dollase model for preferred orientation
=> Conventional weights: w=1.0/Variance(yobs)
=> Asymmetry correction as in J.Appl.Cryst. 26,128(1993)
=> Background linearly interpolated between the    2 points given
=> The    5th default profile function was selected
=> Pseudo-Voigt function (ETA variable)
X-parameter correspond to: ETA=ETA0+X*2theta
pV(x)= ETA*L(x)+(1-ETA)*G(x)

==> INPUT/OUTPUT OPTIONS:

=> Generate file *.PRF for plot
=> Output Integrated Intensities
=> Generate new input file *.PCR

=> Data supplied in free format for pattern:  1
=> Plot pattern at each cycle
=> Wavelengths:  1.54056 1.54439
=> Alpha2/Alpha1 ratio:   0.5000
=> Cos(Monochromator angle)=   1.0000
=> Asymmetry correction for angles lower than   90.000 degrees
=> Absorption correction (AC), muR-eff =   0.0000  0.0000
=> Base of peaks: 2.0*HW*   20.00

=> Number of cycles:   50
=> Relaxation factors ==>    for coordinates:  1.00
=> for anisotropic temperature factors:  1.00
=> for halfwidth/strain/size parameters:  1.00
=> for lattice constants and propagation vectors:  1.00
=> EPS-value for convergence:    0.0
=> Instrumental Resolution read from file: xray-res.irf
=> Title of data: Approximate resolution function of a conventional X-ray diffractometer CuKalpha1,2

=> The resolution function is IRESOL:   1 for profile function #   5
Input resolution parameters:

U-inst     V-inst     W-inst     X-inst     Y-inst     Z-inst
0.00136   -0.00500    0.00391    0.06389    0.00008    0.00000
0.00136   -0.00500    0.00391    0.06389    0.00008    0.00000

=> Number of Least-Squares parameters varied:     6

=>---------------------------->
=>-------->  PATTERN number:  1
=>---------------------------->
=> Global parameters and codes ==>
=> Zero-point:    -0.0558    0.0000
=> Displacement peak-shift parameter and code:    -0.12   11.00
=> Transparency peak-shift parameter and code:     0.25   31.00

=> Reading Intensity data  =>>

==> Angular range, step and number of points:
2Thmin:      12.000000  2Thmax:      38.784801  Step:       0.012900  No. of points:   2077
------------------------------------------------------------------------------
=> Phase  No. 1
rdx
------------------------------------------------------------------------------
=>--------> Pattern#  1
=> Crystal Structure Refinement
=> The    7th profile function was selected for phase no.  1
=> Preferred orientation vector:   0.0000  0.0000  1.0000

=>--------> Data for PHASE: 1
=> Number of atoms:   21
=> Number of distance  constraints:    0
=> Number of angle     constraints:    0

=> Symmetry information on space group: P b c a
-> The multiplicity of the general position is:   8
-> The space group is Centric (-1 at origin)
-> Lattice type  P: { 000 }
-> Reduced set of symmetry operators:
```

```
No.  IT   Symmetry symbol    Rotation part     Associated Translation
1: ( 1)   1            -->     ( x, y, z) + {  0.0000  0.0000  0.0000}
2: ( 4)   2 ( x, 0, 0) -->     ( x,-y,-z) + {  0.5000  0.5000  0.0000}
3: ( 3)   2 ( 0, y, 0) -->     (-x, y,-z) + {  0.0000  0.5000  0.5000}
4: ( 2)   2 ( 0, 0, z) -->     (-x,-y, z) + {  0.5000  0.0000  0.5000}


Information on Space Group:
---------------------------

=>  Number of Space group:  61
=> Hermann-Mauguin Symbol: P b c a
=>            Hall Symbol: -P 2ac 2ab
=>   Table Setting Choice:
=>           Setting Type: IT (Generated from Hermann-Mauguin symbol)
=>         Crystal System: Orthorhombic
=>             Laue Class: mmm
=>            Point Group: mmm
=>        Bravais Lattice: P
=>         Lattice Symbol: oP
=> Reduced Number of S.O.:   4
=>   General multiplicity:   8
=>         Centrosymmetry: Centric (-1 at origin)
=> Generators (exc. -1&L):   2
=>        Asymmetric unit:  0.000 <= x <=  0.500
0.000 <= y <=  0.500
0.000 <= z <=  0.500

=> List of S.O. without inversion and lattice centring translations
=> SYMM(  1): x,y,z                           => SYMM(  2): x+1/2,-y+1/2,-z
=> SYMM(  3): -x,y+1/2,-z+1/2                 => SYMM(  4): -x+1/2,-y,z+1/2


=> Initial parameters ==>
Atom    Ntyp                  X         Y         Z         B         occ.          in  fin  Spc  Mult
B11       B22       B33       B12       B13       B23
O(1)   O                  0.56846   0.43427   0.26465   3.70830   1.00000           0    0    0    8
Codes:    0.00000   0.00000   0.00000   0.00000   0.00000
O(2)   O                  0.59453   0.24040   0.23053   4.41110   1.00000           0    0    0    8
Codes:    0.00000   0.00000   0.00000   0.00000   0.00000
O(3)   O                  0.47340   0.13880  -0.02250   4.98480   1.00000           0    0    0    8
Codes:    0.00000   0.00000   0.00000   0.00000   0.00000
O(4)   O                  0.35580   0.24950  -0.11238   4.76640   1.00000           0    0    0    8
Codes:    0.00000   0.00000   0.00000   0.00000   0.00000
O(5)   O                  0.31810   0.53030  -0.06806   5.32170   1.00000           0    0    0    8
Codes:    0.00000   0.00000   0.00000   0.00000   0.00000
O(6)   O                  0.42860   0.60110   0.04920   5.10850   1.00000           0    0    0    8
Codes:    0.00000   0.00000   0.00000   0.00000   0.00000
N(1)   N                  0.43638   0.33385   0.17584   2.73980   1.00000           0    0    0    8
Codes:    0.00000   0.00000   0.00000   0.00000   0.00000
N(2)   N                  0.32231   0.23197   0.05389   2.40240   1.00000           0    0    0    8
Codes:    0.00000   0.00000   0.00000   0.00000   0.00000
N(3)   N                  0.29900   0.45348   0.08838   2.59240   1.00000           0    0    0    8
Codes:    0.00000   0.00000   0.00000   0.00000   0.00000
N(4)   N                  0.53777   0.33516   0.22628   2.76530   1.00000           0    0    0    8
Codes:    0.00000   0.00000   0.00000   0.00000   0.00000
N(5)   N                  0.38834   0.20759  -0.03308   3.09700   1.00000           0    0    0    8
Codes:    0.00000   0.00000   0.00000   0.00000   0.00000
N(6)   N                  0.35299   0.52971   0.01650   3.43200   1.00000           0    0    0    8
Codes:    0.00000   0.00000   0.00000   0.00000   0.00000
C(1)   C                  0.35799   0.43950   0.18450   2.89510   1.00000           0    0    0    8
Codes:    0.00000   0.00000   0.00000   0.00000   0.00000
C(2)   C                  0.38140   0.21557   0.14950   2.70030   1.00000           0    0    0    8
Codes:    0.00000   0.00000   0.00000   0.00000   0.00000
C(3)   C                  0.24458   0.33936   0.05038   2.55740   1.00000           0    0    0    8
Codes:    0.00000   0.00000   0.00000   0.00000   0.00000
H(1A)  H                  0.40289   0.52403   0.20773   5.13220   1.00000           0    0    0    8
Codes:    0.00000   0.00000   0.00000   0.00000   0.00000
H(1B)  H                  0.29071   0.42024   0.23991   4.84270   1.00000           0    0    0    8
Codes:    0.00000   0.00000   0.00000   0.00000   0.00000
H(2A)  H                  0.44331   0.13918   0.14950   4.60580   1.00000           0    0    0    8
Codes:    0.00000   0.00000   0.00000   0.00000   0.00000
H(2B)  H                  0.31742   0.19390   0.20730   4.97430   1.00000           0    0    0    8
Codes:    0.00000   0.00000   0.00000   0.00000   0.00000
H(3A)  H                  0.20936   0.35364  -0.02527   4.50050   1.00000           0    0    0    8
Codes:    0.00000   0.00000   0.00000   0.00000   0.00000
H(3B)  H                  0.17213   0.32091   0.10070   3.92150   1.00000           0    0    0    8
Codes:    0.00000   0.00000   0.00000   0.00000   0.00000

=> IT IS ASSUMED THAT THE FIRST GIVEN SITE IS FULLY OCCUPIED
OR THE FIRST AND SECOND ATOMS ARE IN THE SAME SITE WITH TOTAL FULL OCCUPATION
(If this is not the case, change the order of atoms to obtain correct values for the content of the unit cell)
The given occupation factors have been obtained mutiplying m/M by   1.0000
-> Atom: O    ,  Chemical element: O   Atomic Mass:    15.9994
-> Atom: O    ,  Chemical element: O   Atomic Mass:    15.9994
-> Atom: O    ,  Chemical element: O   Atomic Mass:    15.9994
-> Atom: O    ,  Chemical element: O   Atomic Mass:    15.9994
-> Atom: O    ,  Chemical element: O   Atomic Mass:    15.9994
-> Atom: O    ,  Chemical element: O   Atomic Mass:    15.9994
```

```
-> Atom: N    ,  Chemical element: N   Atomic Mass:    14.0067
-> Atom: N    ,  Chemical element: N   Atomic Mass:    14.0067
-> Atom: N    ,  Chemical element: N   Atomic Mass:    14.0067
-> Atom: N    ,  Chemical element: N   Atomic Mass:    14.0067
-> Atom: N    ,  Chemical element: N   Atomic Mass:    14.0067
-> Atom: N    ,  Chemical element: N   Atomic Mass:    14.0067
-> Atom: C    ,  Chemical element: C   Atomic Mass:    12.0110
-> Atom: C    ,  Chemical element: C   Atomic Mass:    12.0110
-> Atom: C    ,  Chemical element: C   Atomic Mass:    12.0110
-> Atom: H    ,  Chemical element: H   Atomic Mass:     1.0080
-> Atom: H    ,  Chemical element: H   Atomic Mass:     1.0080
-> Atom: H    ,  Chemical element: H   Atomic Mass:     1.0080
-> Atom: H    ,  Chemical element: H   Atomic Mass:     1.0080
-> Atom: H    ,  Chemical element: H   Atomic Mass:     1.0080
-> Atom: H    ,  Chemical element: H   Atomic Mass:     1.0080
=> The given value of ATZ is       1776.94 the program has calculated:        1776.94
The value of ATZ given in the input PCR file will be used for quantitative analysis
=> The chemical content of the unit cell is:
8.0000 O    +   8.0000 O    +   8.0000 O    +   8.0000 O    +   8.0000 O    +   8.0000 O    +   8.0000 N    +     ↙
    8.0000 N    +   8.0000 N    +   8.0000 N    +
8.0000 N    +   8.0000 N    +   8.0000 C    +   8.0000 C    +   8.0000 C    +   8.0000 H    +   8.0000 H    +     ↙
    8.0000 H    +   8.0000 H    +   8.0000 H    +
8.0000 H
=> The normalized site occupation numbers in % are:
100.0000 O(1)   :      100.0000 O(2)   :      100.0000 O(3)   :      100.0000 O(4)   :      100.0000 O(5)   :        ↙
    100.0000 O(6)   :      100.0000 N(1)   :      100.0000 N(2)   :      100.0000 N(3)   :      100.0000 N(4)   :
100.0000 N(5)   :      100.0000 N(6)   :      100.0000 C(1)   :      100.0000 C(2)   :      100.0000 C(3)   :        ↙
    100.0000 H(1A)  :      100.0000 H(1B)  :      100.0000 H(2A)  :      100.0000 H(2B)  :      100.0000 H(3A)  :
100.0000 H(3B)
=> The density (volumic mass) of the compound is:    1.785 g/cm3

=>-------> PROFILE PARAMETERS FOR PATTERN:  1

=> Overall scale factor:   0.484280E-03
=> ETA (p-Voigt) OR M (Pearson VII):   0.0000
=> Overall temperature factor:      0.00000
=> Halfwidth U,V,W:     -0.00329     0.00000     0.00000
=> X and Y parameters:       0.0000      0.0000
=> Direct cell parameters:   11.6304  10.7431  13.2279  90.0000  90.0000  90.0000
=> Preferred orientation parameters:   1.0000  0.0000
=> Asymmetry parameters     :      0.05091     0.04932     0.00000     0.00000
=> Strain parameters        :      0.00000     0.00000     0.00000
=> Size   parameters        :      0.00901     0.05242
=> Further shape parameters (S_L and D_L):   0.00000   0.00000
S_L is source width/detector distance
D_L is detector width/detector distance

==> CODEWORDS FOR PROFILE PARAMETERS of PATTERN#  1

=> Overall scale factor:    0.000
=> ETA (p-Voigt) OR M (Pearson VII):    0.000
=> Overall temperature factor:    0.000
=> Halfwidth U,V,W:   21.000   0.000   0.000
=> X and Y parameters:    0.000   0.000
=> Direct cell parameters:    0.000   0.000   0.000   0.000   0.000   0.000
=> Preferred orientation parameters:    0.000   0.000
=> Asymmetry parameters     :   41.000  61.000   0.000   0.000
=> Strain parameters        :    0.000   0.000   0.000
=> Size   parameters        :   51.000   0.000
=> The 18th model for size is used

=> Orthorhombic Anisotropic Broadening using Spherical Harmonics up
to 4-th order (Laue class: mmm, SPG:16-74, only lorentzian comp.)
Ylm's up to 4th order: Y00,Y20,Y22+,Y40,Y42+,Y44+
RJP - Ref: M. Jarvinen, J. Appl. C. (1993),p.527
=> Coefficients of Spherical Harmonics for anisotropic size
broadening for an orthorhombic lattice
Y00         Y20         Y22+        Y40         Y42+        Y44+
0.052419    0.087274    0.142427    0.127726   -0.069125   -0.017749
0.0000      0.0000      0.0000      0.0000      0.0000      0.0000

=> Cell constraints according to Laue symmetry: mmm

Metric information:
-------------------

=> Direct cell parameters:

a =      11.6304      b =      10.7431      c =      13.2279
alpha =       90.000   beta =       90.000  gamma =       90.000
Direct Cell Volume =    1652.7814

=> Reciprocal cell parameters:

a*=     0.085981      b*=     0.093083      c*=     0.075598
alpha*=       90.000   beta*=       90.000  gamma*=       90.000
Reciprocal Cell Volume =   0.00060504

=> Direct and Reciprocal Metric Tensors:
```

```
GD                                      GR
135.2666      0.0000      0.0000          0.007393    0.000000    0.000000
0.0000    115.4133      0.0000          0.000000    0.008665    0.000000
0.0000      0.0000    174.9783          0.000000    0.000000    0.005715

=>  Cartesian frame: x // a; y is in the ab-plane; z is x ^ y

Crystal_to_Orthonormal_Matrix             Orthonormal_to_Crystal Matrix
Cr_Orth_cel                               Orth_Cr_cel
11.6304      0.0000      0.0000          0.085981    0.000000    0.000000
0.0000     10.7431      0.0000          0.000000    0.093083    0.000000
0.0000      0.0000     13.2279          0.000000    0.000000    0.075598

Busing-Levy B-matrix: Hc=B.H            Inverse of the Busing-Levy B-matrix
BL_M                                      BL_Minv
0.085981    0.000000    0.000000           11.6304      0.0000      0.0000
0.000000    0.093083    0.000000            0.0000     10.7431      0.0000
0.000000    0.000000    0.075598            0.0000      0.0000     13.2279

=> Laue symmetry mmm   will be used to generate HKL for pattern#   1
=> Reflections generated between S(1/d)min:  0.1354 A-1 and S(1/d)max:  0.4718 A-1
=>                                  dmax:  7.3874 A   and      dmin:  2.1197 A
=> The number of reflections generated is:     91
=> The max. scatt. variable (gen.ref.) is:        42.6163
=> Scattering coefficients from internal table


=> X-ray scattering coeff. (A1, B1, A2,...C, f(0), Z, Dfp,Dfpp)

O       3.0485  13.2771   2.2868   5.7011   1.5463   0.3239   0.8670  32.9089   0.2508   7.9994   8.0000   0.0470  ↙
      0.0320
N      12.2126   0.0057   3.1322   9.8933   2.0125  28.9975   1.1663   0.5826 -11.5290   6.9946   7.0000   0.0290  ↙
      0.0180
C       2.3100  20.8439   1.0200  10.2075   1.5886   0.5687   0.8650  51.6512   0.2156   5.9992   6.0000   0.0170  ↙
      0.0090
H       0.4930  10.5109   0.3229  26.1257   0.1402   3.1424   0.0408  57.7997   0.0030   1.0000   1.0000   0.0000  ↙
      0.0000

---------------------------------------------------------------
SYMBOLIC NAMES AND INITIAL VALUES OF PARAMETERS TO BE VARIED:
---------------------------------------------------------------

->  Parameter number    1   -> Symbolic Name:           SyCos_pat1   -0.12224000
->  Parameter number    2   -> Symbolic Name:      U-Cagl_ph1_pat1   -0.32860001E-02
->  Parameter number    3   -> Symbolic Name:           SySin_pat1    0.24594000
->  Parameter number    4   -> Symbolic Name:       Asym1_ph1_pat1    0.50910000E-01
->  Parameter number    5   -> Symbolic Name:      G-Size_ph1_pat1    0.90079997E-02
->  Parameter number    6   -> Symbolic Name:       Asym2_ph1_pat1    0.49320001E-01

=> Zero counts at step no.      1 at 2theta/TOF/E(KeV):        12.0000  Intensity fixed to 1.0 and variance to 1E6
=> Zero counts at step no.      2 at 2theta/TOF/E(KeV):        12.0129  Intensity fixed to 1.0 and variance to 1E6
=> Zero counts at step no.      5 at 2theta/TOF/E(KeV):        12.0516  Intensity fixed to 1.0 and variance to 1E6
=> Zero counts at step no.      8 at 2theta/TOF/E(KeV):        12.0903  Intensity fixed to 1.0 and variance to 1E6
=> Zero counts at step no.     12 at 2theta/TOF/E(KeV):        12.1419  Intensity fixed to 1.0 and variance to 1E6
=> Zero counts at step no.     13 at 2theta/TOF/E(KeV):        12.1548  Intensity fixed to 1.0 and variance to 1E6
=> Zero counts at step no.     14 at 2theta/TOF/E(KeV):        12.1677  Intensity fixed to 1.0 and variance to 1E6
=> Zero counts at step no.     15 at 2theta/TOF/E(KeV):        12.1806  Intensity fixed to 1.0 and variance to 1E6
=> Zero counts at step no.     16 at 2theta/TOF/E(KeV):        12.1935  Intensity fixed to 1.0 and variance to 1E6
=> Zero counts at step no.     19 at 2theta/TOF/E(KeV):        12.2322  Intensity fixed to 1.0 and variance to 1E6
=> Zero counts at step no.     22 at 2theta/TOF/E(KeV):        12.2709  Intensity fixed to 1.0 and variance to 1E6
=> Zero counts at step no.     28 at 2theta/TOF/E(KeV):        12.3483  Intensity fixed to 1.0 and variance to 1E6
=> Zero counts at step no.     35 at 2theta/TOF/E(KeV):        12.4386  Intensity fixed to 1.0 and variance to 1E6
=> Zero counts at step no.     36 at 2theta/TOF/E(KeV):        12.4515  Intensity fixed to 1.0 and variance to 1E6
=> Zero counts at step no.     37 at 2theta/TOF/E(KeV):        12.4644  Intensity fixed to 1.0 and variance to 1E6
=> Zero counts at step no.     38 at 2theta/TOF/E(KeV):        12.4773  Intensity fixed to 1.0 and variance to 1E6
=> Zero counts at step no.     41 at 2theta/TOF/E(KeV):        12.5160  Intensity fixed to 1.0 and variance to 1E6
=> Zero counts at step no.    119 at 2theta/TOF/E(KeV):        13.5222  Intensity fixed to 1.0 and variance to 1E6
=> Zero counts at step no.    125 at 2theta/TOF/E(KeV):        13.5996  Intensity fixed to 1.0 and variance to 1E6
=> Zero counts at step no.    126 at 2theta/TOF/E(KeV):        13.6125  Intensity fixed to 1.0 and variance to 1E6
=> Zero counts at step no.    127 at 2theta/TOF/E(KeV):        13.6254  Intensity fixed to 1.0 and variance to 1E6
=> Zero counts at step no.    133 at 2theta/TOF/E(KeV):        13.7028  Intensity fixed to 1.0 and variance to 1E6
=> Zero counts at step no.    137 at 2theta/TOF/E(KeV):        13.7544  Intensity fixed to 1.0 and variance to 1E6
=> Zero counts at step no.    139 at 2theta/TOF/E(KeV):        13.7802  Intensity fixed to 1.0 and variance to 1E6
=> Zero counts at step no.    144 at 2theta/TOF/E(KeV):        13.8447  Intensity fixed to 1.0 and variance to 1E6
=> Zero counts at step no.    147 at 2theta/TOF/E(KeV):        13.8834  Intensity fixed to 1.0 and variance to 1E6
=> Zero counts at step no.    150 at 2theta/TOF/E(KeV):        13.9221  Intensity fixed to 1.0 and variance to 1E6
=> Zero counts at step no.    157 at 2theta/TOF/E(KeV):        14.0124  Intensity fixed to 1.0 and variance to 1E6
=> Zero counts at step no.    159 at 2theta/TOF/E(KeV):        14.0382  Intensity fixed to 1.0 and variance to 1E6
=> Zero counts at step no.    161 at 2theta/TOF/E(KeV):        14.0640  Intensity fixed to 1.0 and variance to 1E6
=> Zero counts at step no.    162 at 2theta/TOF/E(KeV):        14.0769  Intensity fixed to 1.0 and variance to 1E6
=> Zero counts at step no.    164 at 2theta/TOF/E(KeV):        14.1027  Intensity fixed to 1.0 and variance to 1E6
=> Zero counts at step no.    169 at 2theta/TOF/E(KeV):        14.1672  Intensity fixed to 1.0 and variance to 1E6
=> Zero counts at step no.    170 at 2theta/TOF/E(KeV):        14.1801  Intensity fixed to 1.0 and variance to 1E6
=> Zero counts at step no.    174 at 2theta/TOF/E(KeV):        14.2317  Intensity fixed to 1.0 and variance to 1E6
=> Zero counts at step no.    177 at 2theta/TOF/E(KeV):        14.2704  Intensity fixed to 1.0 and variance to 1E6
=> Zero counts at step no.    179 at 2theta/TOF/E(KeV):        14.2962  Intensity fixed to 1.0 and variance to 1E6
=> Zero counts at step no.    182 at 2theta/TOF/E(KeV):        14.3349  Intensity fixed to 1.0 and variance to 1E6
=> Zero counts at step no.    187 at 2theta/TOF/E(KeV):        14.3994  Intensity fixed to 1.0 and variance to 1E6
=> Zero counts at step no.    189 at 2theta/TOF/E(KeV):        14.4252  Intensity fixed to 1.0 and variance to 1E6
=> Zero counts at step no.    194 at 2theta/TOF/E(KeV):        14.4897  Intensity fixed to 1.0 and variance to 1E6
```

```
=> Zero counts at step no.    195 at 2theta/TOF/E(KeV):      14.5026  Intensity fixed to 1.0 and variance to 1E6
=> Zero counts at step no.    198 at 2theta/TOF/E(KeV):      14.5413  Intensity fixed to 1.0 and variance to 1E6
=> Zero counts at step no.    199 at 2theta/TOF/E(KeV):      14.5542  Intensity fixed to 1.0 and variance to 1E6
=> Zero counts at step no.    200 at 2theta/TOF/E(KeV):      14.5671  Intensity fixed to 1.0 and variance to 1E6
=> Zero counts at step no.    207 at 2theta/TOF/E(KeV):      14.6574  Intensity fixed to 1.0 and variance to 1E6
=> Zero counts at step no.    208 at 2theta/TOF/E(KeV):      14.6703  Intensity fixed to 1.0 and variance to 1E6
=> Zero counts at step no.    210 at 2theta/TOF/E(KeV):      14.6961  Intensity fixed to 1.0 and variance to 1E6
=> Zero counts at step no.    211 at 2theta/TOF/E(KeV):      14.7090  Intensity fixed to 1.0 and variance to 1E6
=> Zero counts at step no.    213 at 2theta/TOF/E(KeV):      14.7348  Intensity fixed to 1.0 and variance to 1E6
=> Zero counts at step no.    216 at 2theta/TOF/E(KeV):      14.7735  Intensity fixed to 1.0 and variance to 1E6
=> Zero counts at step no.    217 at 2theta/TOF/E(KeV):      14.7864  Intensity fixed to 1.0 and variance to 1E6
=> Zero counts at step no.    218 at 2theta/TOF/E(KeV):      14.7993  Intensity fixed to 1.0 and variance to 1E6
=> Zero counts at step no.    224 at 2theta/TOF/E(KeV):      14.8767  Intensity fixed to 1.0 and variance to 1E6
=> Zero counts at step no.    225 at 2theta/TOF/E(KeV):      14.8896  Intensity fixed to 1.0 and variance to 1E6
=> Zero counts at step no.    226 at 2theta/TOF/E(KeV):      14.9025  Intensity fixed to 1.0 and variance to 1E6
=> Zero counts at step no.    228 at 2theta/TOF/E(KeV):      14.9283  Intensity fixed to 1.0 and variance to 1E6
=> Zero counts at step no.    229 at 2theta/TOF/E(KeV):      14.9412  Intensity fixed to 1.0 and variance to 1E6
=> Zero counts at step no.    232 at 2theta/TOF/E(KeV):      14.9799  Intensity fixed to 1.0 and variance to 1E6
=> Zero counts at step no.    234 at 2theta/TOF/E(KeV):      15.0057  Intensity fixed to 1.0 and variance to 1E6
=> Zero counts at step no.    235 at 2theta/TOF/E(KeV):      15.0186  Intensity fixed to 1.0 and variance to 1E6
=> Zero counts at step no.    237 at 2theta/TOF/E(KeV):      15.0444  Intensity fixed to 1.0 and variance to 1E6
=> Zero counts at step no.    274 at 2theta/TOF/E(KeV):      15.5217  Intensity fixed to 1.0 and variance to 1E6
=> Zero counts at step no.    277 at 2theta/TOF/E(KeV):      15.5604  Intensity fixed to 1.0 and variance to 1E6
=> Zero counts at step no.    280 at 2theta/TOF/E(KeV):      15.5991  Intensity fixed to 1.0 and variance to 1E6
=> Zero counts at step no.    282 at 2theta/TOF/E(KeV):      15.6249  Intensity fixed to 1.0 and variance to 1E6
=> Zero counts at step no.    285 at 2theta/TOF/E(KeV):      15.6636  Intensity fixed to 1.0 and variance to 1E6
=> Zero counts at step no.    286 at 2theta/TOF/E(KeV):      15.6765  Intensity fixed to 1.0 and variance to 1E6
=> Zero counts at step no.    287 at 2theta/TOF/E(KeV):      15.6894  Intensity fixed to 1.0 and variance to 1E6
=> Zero counts at step no.    288 at 2theta/TOF/E(KeV):      15.7023  Intensity fixed to 1.0 and variance to 1E6
=> Zero counts at step no.    289 at 2theta/TOF/E(KeV):      15.7152  Intensity fixed to 1.0 and variance to 1E6
=> Zero counts at step no.    291 at 2theta/TOF/E(KeV):      15.7410  Intensity fixed to 1.0 and variance to 1E6
=> Zero counts at step no.    292 at 2theta/TOF/E(KeV):      15.7539  Intensity fixed to 1.0 and variance to 1E6
=> Zero counts at step no.    293 at 2theta/TOF/E(KeV):      15.7668  Intensity fixed to 1.0 and variance to 1E6
=> Zero counts at step no.    294 at 2theta/TOF/E(KeV):      15.7797  Intensity fixed to 1.0 and variance to 1E6
=> Zero counts at step no.    296 at 2theta/TOF/E(KeV):      15.8055  Intensity fixed to 1.0 and variance to 1E6
=> Zero counts at step no.    298 at 2theta/TOF/E(KeV):      15.8313  Intensity fixed to 1.0 and variance to 1E6
=> Zero counts at step no.    301 at 2theta/TOF/E(KeV):      15.8700  Intensity fixed to 1.0 and variance to 1E6
=> Zero counts at step no.    302 at 2theta/TOF/E(KeV):      15.8829  Intensity fixed to 1.0 and variance to 1E6
=> Zero counts at step no.    303 at 2theta/TOF/E(KeV):      15.8958  Intensity fixed to 1.0 and variance to 1E6
=> Zero counts at step no.    306 at 2theta/TOF/E(KeV):      15.9345  Intensity fixed to 1.0 and variance to 1E6
=> Zero counts at step no.    307 at 2theta/TOF/E(KeV):      15.9474  Intensity fixed to 1.0 and variance to 1E6
=> Zero counts at step no.    311 at 2theta/TOF/E(KeV):      15.9990  Intensity fixed to 1.0 and variance to 1E6
=> Zero counts at step no.    318 at 2theta/TOF/E(KeV):      16.0893  Intensity fixed to 1.0 and variance to 1E6
=> Zero counts at step no.    322 at 2theta/TOF/E(KeV):      16.1409  Intensity fixed to 1.0 and variance to 1E6
=> Zero counts at step no.    323 at 2theta/TOF/E(KeV):      16.1538  Intensity fixed to 1.0 and variance to 1E6
=> Zero counts at step no.    325 at 2theta/TOF/E(KeV):      16.1796  Intensity fixed to 1.0 and variance to 1E6
=> Zero counts at step no.    326 at 2theta/TOF/E(KeV):      16.1925  Intensity fixed to 1.0 and variance to 1E6
=> Zero counts at step no.    355 at 2theta/TOF/E(KeV):      16.5666  Intensity fixed to 1.0 and variance to 1E6
=> Zero counts at step no.    357 at 2theta/TOF/E(KeV):      16.5924  Intensity fixed to 1.0 and variance to 1E6
=> Zero counts at step no.    358 at 2theta/TOF/E(KeV):      16.6053  Intensity fixed to 1.0 and variance to 1E6
=> Zero counts at step no.    362 at 2theta/TOF/E(KeV):      16.6569  Intensity fixed to 1.0 and variance to 1E6
=> Zero counts at step no.    365 at 2theta/TOF/E(KeV):      16.6956  Intensity fixed to 1.0 and variance to 1E6
=> Zero counts at step no.    368 at 2theta/TOF/E(KeV):      16.7343  Intensity fixed to 1.0 and variance to 1E6
=> Zero counts at step no.    369 at 2theta/TOF/E(KeV):      16.7472  Intensity fixed to 1.0 and variance to 1E6
=> Zero counts at step no.    372 at 2theta/TOF/E(KeV):      16.7859  Intensity fixed to 1.0 and variance to 1E6
=> Zero counts at step no.    373 at 2theta/TOF/E(KeV):      16.7988  Intensity fixed to 1.0 and variance to 1E6
=> Zero counts at step no.    375 at 2theta/TOF/E(KeV):      16.8246  Intensity fixed to 1.0 and variance to 1E6
=> Zero counts at step no.    376 at 2theta/TOF/E(KeV):      16.8375  Intensity fixed to 1.0 and variance to 1E6
=> Zero counts at step no.    377 at 2theta/TOF/E(KeV):      16.8504  Intensity fixed to 1.0 and variance to 1E6
=> Zero counts at step no.    378 at 2theta/TOF/E(KeV):      16.8633  Intensity fixed to 1.0 and variance to 1E6
=> Zero counts at step no.    379 at 2theta/TOF/E(KeV):      16.8762  Intensity fixed to 1.0 and variance to 1E6
=> Zero counts at step no.    380 at 2theta/TOF/E(KeV):      16.8891  Intensity fixed to 1.0 and variance to 1E6
=> Zero counts at step no.    383 at 2theta/TOF/E(KeV):      16.9278  Intensity fixed to 1.0 and variance to 1E6
=> Zero counts at step no.    385 at 2theta/TOF/E(KeV):      16.9536  Intensity fixed to 1.0 and variance to 1E6
=> Zero counts at step no.    386 at 2theta/TOF/E(KeV):      16.9665  Intensity fixed to 1.0 and variance to 1E6
=> Zero counts at step no.    387 at 2theta/TOF/E(KeV):      16.9794  Intensity fixed to 1.0 and variance to 1E6
=> Zero counts at step no.    461 at 2theta/TOF/E(KeV):      17.9340  Intensity fixed to 1.0 and variance to 1E6
=> Zero counts at step no.    466 at 2theta/TOF/E(KeV):      17.9985  Intensity fixed to 1.0 and variance to 1E6
=> Zero counts at step no.    467 at 2theta/TOF/E(KeV):      18.0114  Intensity fixed to 1.0 and variance to 1E6
=> Zero counts at step no.    468 at 2theta/TOF/E(KeV):      18.0243  Intensity fixed to 1.0 and variance to 1E6
=> Zero counts at step no.    472 at 2theta/TOF/E(KeV):      18.0759  Intensity fixed to 1.0 and variance to 1E6
=> Zero counts at step no.    474 at 2theta/TOF/E(KeV):      18.1017  Intensity fixed to 1.0 and variance to 1E6
=> Zero counts at step no.    475 at 2theta/TOF/E(KeV):      18.1146  Intensity fixed to 1.0 and variance to 1E6
=> Zero counts at step no.    476 at 2theta/TOF/E(KeV):      18.1275  Intensity fixed to 1.0 and variance to 1E6
=> Zero counts at step no.    477 at 2theta/TOF/E(KeV):      18.1404  Intensity fixed to 1.0 and variance to 1E6
=> Zero counts at step no.    478 at 2theta/TOF/E(KeV):      18.1533  Intensity fixed to 1.0 and variance to 1E6
=> Zero counts at step no.    483 at 2theta/TOF/E(KeV):      18.2178  Intensity fixed to 1.0 and variance to 1E6
=> Zero counts at step no.    484 at 2theta/TOF/E(KeV):      18.2307  Intensity fixed to 1.0 and variance to 1E6
=> Zero counts at step no.    489 at 2theta/TOF/E(KeV):      18.2952  Intensity fixed to 1.0 and variance to 1E6
=> Zero counts at step no.    492 at 2theta/TOF/E(KeV):      18.3339  Intensity fixed to 1.0 and variance to 1E6
=> Zero counts at step no.    493 at 2theta/TOF/E(KeV):      18.3468  Intensity fixed to 1.0 and variance to 1E6
=> Zero counts at step no.    495 at 2theta/TOF/E(KeV):      18.3726  Intensity fixed to 1.0 and variance to 1E6
=> Zero counts at step no.    498 at 2theta/TOF/E(KeV):      18.4113  Intensity fixed to 1.0 and variance to 1E6
=> Zero counts at step no.    519 at 2theta/TOF/E(KeV):      18.6822  Intensity fixed to 1.0 and variance to 1E6
=> Zero counts at step no.    521 at 2theta/TOF/E(KeV):      18.7080  Intensity fixed to 1.0 and variance to 1E6
=> Zero counts at step no.    522 at 2theta/TOF/E(KeV):      18.7209  Intensity fixed to 1.0 and variance to 1E6
=> Zero counts at step no.    538 at 2theta/TOF/E(KeV):      18.9273  Intensity fixed to 1.0 and variance to 1E6
=> Zero counts at step no.    545 at 2theta/TOF/E(KeV):      19.0176  Intensity fixed to 1.0 and variance to 1E6
=> Zero counts at step no.    564 at 2theta/TOF/E(KeV):      19.2627  Intensity fixed to 1.0 and variance to 1E6
=> Zero counts at step no.    668 at 2theta/TOF/E(KeV):      20.6043  Intensity fixed to 1.0 and variance to 1E6
```

```
=> Zero counts at step no.    671 at 2theta/TOF/E(KeV):       20.6430  Intensity fixed to 1.0 and variance to 1E6
=> Zero counts at step no.    674 at 2theta/TOF/E(KeV):       20.6817  Intensity fixed to 1.0 and variance to 1E6
=> Zero counts at step no.    678 at 2theta/TOF/E(KeV):       20.7333  Intensity fixed to 1.0 and variance to 1E6
=> Zero counts at step no.    679 at 2theta/TOF/E(KeV):       20.7462  Intensity fixed to 1.0 and variance to 1E6
=> Zero counts at step no.    682 at 2theta/TOF/E(KeV):       20.7849  Intensity fixed to 1.0 and variance to 1E6
=> Zero counts at step no.    684 at 2theta/TOF/E(KeV):       20.8107  Intensity fixed to 1.0 and variance to 1E6
=> Zero counts at step no.    687 at 2theta/TOF/E(KeV):       20.8494  Intensity fixed to 1.0 and variance to 1E6
=> Zero counts at step no.    688 at 2theta/TOF/E(KeV):       20.8623  Intensity fixed to 1.0 and variance to 1E6
=> Zero counts at step no.    690 at 2theta/TOF/E(KeV):       20.8881  Intensity fixed to 1.0 and variance to 1E6
=> Zero counts at step no.    694 at 2theta/TOF/E(KeV):       20.9397  Intensity fixed to 1.0 and variance to 1E6
=> Zero counts at step no.    697 at 2theta/TOF/E(KeV):       20.9784  Intensity fixed to 1.0 and variance to 1E6
=> Zero counts at step no.    698 at 2theta/TOF/E(KeV):       20.9913  Intensity fixed to 1.0 and variance to 1E6
=> Zero counts at step no.    701 at 2theta/TOF/E(KeV):       21.0300  Intensity fixed to 1.0 and variance to 1E6
=> Zero counts at step no.    705 at 2theta/TOF/E(KeV):       21.0816  Intensity fixed to 1.0 and variance to 1E6
=> Zero counts at step no.    728 at 2theta/TOF/E(KeV):       21.3783  Intensity fixed to 1.0 and variance to 1E6
=> Zero counts at step no.    732 at 2theta/TOF/E(KeV):       21.4299  Intensity fixed to 1.0 and variance to 1E6
=> Zero counts at step no.    734 at 2theta/TOF/E(KeV):       21.4557  Intensity fixed to 1.0 and variance to 1E6
=> Zero counts at step no.    736 at 2theta/TOF/E(KeV):       21.4815  Intensity fixed to 1.0 and variance to 1E6
=> Zero counts at step no.    737 at 2theta/TOF/E(KeV):       21.4944  Intensity fixed to 1.0 and variance to 1E6
=> Zero counts at step no.    738 at 2theta/TOF/E(KeV):       21.5073  Intensity fixed to 1.0 and variance to 1E6
=> Zero counts at step no.    739 at 2theta/TOF/E(KeV):       21.5202  Intensity fixed to 1.0 and variance to 1E6
=> Zero counts at step no.    740 at 2theta/TOF/E(KeV):       21.5331  Intensity fixed to 1.0 and variance to 1E6
=> Zero counts at step no.    741 at 2theta/TOF/E(KeV):       21.5460  Intensity fixed to 1.0 and variance to 1E6
=> Zero counts at step no.    742 at 2theta/TOF/E(KeV):       21.5589  Intensity fixed to 1.0 and variance to 1E6
=> Zero counts at step no.    743 at 2theta/TOF/E(KeV):       21.5718  Intensity fixed to 1.0 and variance to 1E6
=> Zero counts at step no.    744 at 2theta/TOF/E(KeV):       21.5847  Intensity fixed to 1.0 and variance to 1E6
=> Zero counts at step no.    748 at 2theta/TOF/E(KeV):       21.6363  Intensity fixed to 1.0 and variance to 1E6
=> Zero counts at step no.    786 at 2theta/TOF/E(KeV):       22.1265  Intensity fixed to 1.0 and variance to 1E6
=> Zero counts at step no.    787 at 2theta/TOF/E(KeV):       22.1394  Intensity fixed to 1.0 and variance to 1E6
=> Zero counts at step no.    791 at 2theta/TOF/E(KeV):       22.1910  Intensity fixed to 1.0 and variance to 1E6
=> Zero counts at step no.    793 at 2theta/TOF/E(KeV):       22.2168  Intensity fixed to 1.0 and variance to 1E6
=> Zero counts at step no.    794 at 2theta/TOF/E(KeV):       22.2297  Intensity fixed to 1.0 and variance to 1E6
=> Zero counts at step no.    795 at 2theta/TOF/E(KeV):       22.2426  Intensity fixed to 1.0 and variance to 1E6
=> Zero counts at step no.    796 at 2theta/TOF/E(KeV):       22.2555  Intensity fixed to 1.0 and variance to 1E6
=> Zero counts at step no.    798 at 2theta/TOF/E(KeV):       22.2813  Intensity fixed to 1.0 and variance to 1E6
=> Zero counts at step no.    836 at 2theta/TOF/E(KeV):       22.7715  Intensity fixed to 1.0 and variance to 1E6
=> Zero counts at step no.    839 at 2theta/TOF/E(KeV):       22.8102  Intensity fixed to 1.0 and variance to 1E6
=> Zero counts at step no.    841 at 2theta/TOF/E(KeV):       22.8360  Intensity fixed to 1.0 and variance to 1E6
=> Zero counts at step no.    842 at 2theta/TOF/E(KeV):       22.8489  Intensity fixed to 1.0 and variance to 1E6
=> Zero counts at step no.    843 at 2theta/TOF/E(KeV):       22.8618  Intensity fixed to 1.0 and variance to 1E6
=> Zero counts at step no.    847 at 2theta/TOF/E(KeV):       22.9134  Intensity fixed to 1.0 and variance to 1E6
=> Zero counts at step no.    867 at 2theta/TOF/E(KeV):       23.1714  Intensity fixed to 1.0 and variance to 1E6
=> Zero counts at step no.    868 at 2theta/TOF/E(KeV):       23.1843  Intensity fixed to 1.0 and variance to 1E6
=> Zero counts at step no.    873 at 2theta/TOF/E(KeV):       23.2488  Intensity fixed to 1.0 and variance to 1E6
=> Zero counts at step no.    904 at 2theta/TOF/E(KeV):       23.6487  Intensity fixed to 1.0 and variance to 1E6
=> Zero counts at step no.    905 at 2theta/TOF/E(KeV):       23.6616  Intensity fixed to 1.0 and variance to 1E6
=> Zero counts at step no.    906 at 2theta/TOF/E(KeV):       23.6745  Intensity fixed to 1.0 and variance to 1E6
=> Zero counts at step no.    907 at 2theta/TOF/E(KeV):       23.6874  Intensity fixed to 1.0 and variance to 1E6
=> Zero counts at step no.    909 at 2theta/TOF/E(KeV):       23.7132  Intensity fixed to 1.0 and variance to 1E6
=> Zero counts at step no.    914 at 2theta/TOF/E(KeV):       23.7777  Intensity fixed to 1.0 and variance to 1E6
=> Zero counts at step no.    920 at 2theta/TOF/E(KeV):       23.8551  Intensity fixed to 1.0 and variance to 1E6
=> Zero counts at step no.    921 at 2theta/TOF/E(KeV):       23.8680  Intensity fixed to 1.0 and variance to 1E6
=> Zero counts at step no.    922 at 2theta/TOF/E(KeV):       23.8809  Intensity fixed to 1.0 and variance to 1E6
=> Zero counts at step no.    931 at 2theta/TOF/E(KeV):       23.9970  Intensity fixed to 1.0 and variance to 1E6
=> Zero counts at step no.    933 at 2theta/TOF/E(KeV):       24.0228  Intensity fixed to 1.0 and variance to 1E6
=> Zero counts at step no.    934 at 2theta/TOF/E(KeV):       24.0357  Intensity fixed to 1.0 and variance to 1E6
=> Zero counts at step no.    936 at 2theta/TOF/E(KeV):       24.0615  Intensity fixed to 1.0 and variance to 1E6
=> Zero counts at step no.    938 at 2theta/TOF/E(KeV):       24.0873  Intensity fixed to 1.0 and variance to 1E6
=> Zero counts at step no.    940 at 2theta/TOF/E(KeV):       24.1131  Intensity fixed to 1.0 and variance to 1E6
=> Zero counts at step no.    941 at 2theta/TOF/E(KeV):       24.1260  Intensity fixed to 1.0 and variance to 1E6
=> Zero counts at step no.    947 at 2theta/TOF/E(KeV):       24.2034  Intensity fixed to 1.0 and variance to 1E6
=> Zero counts at step no.    950 at 2theta/TOF/E(KeV):       24.2421  Intensity fixed to 1.0 and variance to 1E6
=> Zero counts at step no.    955 at 2theta/TOF/E(KeV):       24.3066  Intensity fixed to 1.0 and variance to 1E6
=> Zero counts at step no.   1219 at 2theta/TOF/E(KeV):       27.7122  Intensity fixed to 1.0 and variance to 1E6
=> Zero counts at step no.   1221 at 2theta/TOF/E(KeV):       27.7380  Intensity fixed to 1.0 and variance to 1E6
=> Zero counts at step no.   1225 at 2theta/TOF/E(KeV):       27.7896  Intensity fixed to 1.0 and variance to 1E6
=> Zero counts at step no.   1232 at 2theta/TOF/E(KeV):       27.8799  Intensity fixed to 1.0 and variance to 1E6
=> Zero counts at step no.   1235 at 2theta/TOF/E(KeV):       27.9186  Intensity fixed to 1.0 and variance to 1E6
=> Zero counts at step no.   1240 at 2theta/TOF/E(KeV):       27.9831  Intensity fixed to 1.0 and variance to 1E6
=> Zero counts at step no.   1243 at 2theta/TOF/E(KeV):       28.0218  Intensity fixed to 1.0 and variance to 1E6
=> Zero counts at step no.   1249 at 2theta/TOF/E(KeV):       28.0992  Intensity fixed to 1.0 and variance to 1E6
=> Zero counts at step no.   1251 at 2theta/TOF/E(KeV):       28.1250  Intensity fixed to 1.0 and variance to 1E6
=> Zero counts at step no.   1262 at 2theta/TOF/E(KeV):       28.2669  Intensity fixed to 1.0 and variance to 1E6
=> Zero counts at step no.   1263 at 2theta/TOF/E(KeV):       28.2798  Intensity fixed to 1.0 and variance to 1E6
=> Zero counts at step no.   1266 at 2theta/TOF/E(KeV):       28.3185  Intensity fixed to 1.0 and variance to 1E6
=> Zero counts at step no.   1269 at 2theta/TOF/E(KeV):       28.3572  Intensity fixed to 1.0 and variance to 1E6
=> Zero counts at step no.   1279 at 2theta/TOF/E(KeV):       28.4862  Intensity fixed to 1.0 and variance to 1E6
=> Zero counts at step no.   1369 at 2theta/TOF/E(KeV):       29.6472  Intensity fixed to 1.0 and variance to 1E6
=> Zero counts at step no.   1374 at 2theta/TOF/E(KeV):       29.7117  Intensity fixed to 1.0 and variance to 1E6
=> Zero counts at step no.   1380 at 2theta/TOF/E(KeV):       29.7891  Intensity fixed to 1.0 and variance to 1E6
=> Zero counts at step no.   1381 at 2theta/TOF/E(KeV):       29.8020  Intensity fixed to 1.0 and variance to 1E6
=> Zero counts at step no.   1387 at 2theta/TOF/E(KeV):       29.8794  Intensity fixed to 1.0 and variance to 1E6
=> Zero counts at step no.   1388 at 2theta/TOF/E(KeV):       29.8923  Intensity fixed to 1.0 and variance to 1E6
=> Zero counts at step no.   1390 at 2theta/TOF/E(KeV):       29.9181  Intensity fixed to 1.0 and variance to 1E6
=> Zero counts at step no.   1393 at 2theta/TOF/E(KeV):       29.9568  Intensity fixed to 1.0 and variance to 1E6
=> Zero counts at step no.   1396 at 2theta/TOF/E(KeV):       29.9955  Intensity fixed to 1.0 and variance to 1E6
=> Zero counts at step no.   1397 at 2theta/TOF/E(KeV):       30.0084  Intensity fixed to 1.0 and variance to 1E6
=> Zero counts at step no.   1400 at 2theta/TOF/E(KeV):       30.0471  Intensity fixed to 1.0 and variance to 1E6
=> Zero counts at step no.   1401 at 2theta/TOF/E(KeV):       30.0600  Intensity fixed to 1.0 and variance to 1E6
=> Zero counts at step no.   1496 at 2theta/TOF/E(KeV):       31.2855  Intensity fixed to 1.0 and variance to 1E6
```

```
=> Zero counts at step no.   1617 at 2theta/TOF/E(KeV):        32.8464  Intensity fixed to 1.0 and variance to 1E6
=> Zero counts at step no.   1621 at 2theta/TOF/E(KeV):        32.8980  Intensity fixed to 1.0 and variance to 1E6
=> Zero counts at step no.   1667 at 2theta/TOF/E(KeV):        33.4914  Intensity fixed to 1.0 and variance to 1E6
=> Zero counts at step no.   1669 at 2theta/TOF/E(KeV):        33.5172  Intensity fixed to 1.0 and variance to 1E6
=> Zero counts at step no.   1671 at 2theta/TOF/E(KeV):        33.5430  Intensity fixed to 1.0 and variance to 1E6
=> Zero counts at step no.   1682 at 2theta/TOF/E(KeV):        33.6849  Intensity fixed to 1.0 and variance to 1E6
=> Zero counts at step no.   1684 at 2theta/TOF/E(KeV):        33.7107  Intensity fixed to 1.0 and variance to 1E6
=> Zero counts at step no.   1687 at 2theta/TOF/E(KeV):        33.7494  Intensity fixed to 1.0 and variance to 1E6
=> Zero counts at step no.   1690 at 2theta/TOF/E(KeV):        33.7881  Intensity fixed to 1.0 and variance to 1E6
=> Zero counts at step no.   1691 at 2theta/TOF/E(KeV):        33.8010  Intensity fixed to 1.0 and variance to 1E6
=> Zero counts at step no.   1693 at 2theta/TOF/E(KeV):        33.8268  Intensity fixed to 1.0 and variance to 1E6
=> Zero counts at step no.   1696 at 2theta/TOF/E(KeV):        33.8655  Intensity fixed to 1.0 and variance to 1E6
=> Zero counts at step no.   1700 at 2theta/TOF/E(KeV):        33.9171  Intensity fixed to 1.0 and variance to 1E6
=> Zero counts at step no.   1724 at 2theta/TOF/E(KeV):        34.2267  Intensity fixed to 1.0 and variance to 1E6
=> Zero counts at step no.   1726 at 2theta/TOF/E(KeV):        34.2525  Intensity fixed to 1.0 and variance to 1E6
=> Zero counts at step no.   1727 at 2theta/TOF/E(KeV):        34.2654  Intensity fixed to 1.0 and variance to 1E6
=> Zero counts at step no.   1731 at 2theta/TOF/E(KeV):        34.3170  Intensity fixed to 1.0 and variance to 1E6
=> Zero counts at step no.   1732 at 2theta/TOF/E(KeV):        34.3299  Intensity fixed to 1.0 and variance to 1E6
=> Zero counts at step no.   1735 at 2theta/TOF/E(KeV):        34.3686  Intensity fixed to 1.0 and variance to 1E6
=> Zero counts at step no.   1738 at 2theta/TOF/E(KeV):        34.4073  Intensity fixed to 1.0 and variance to 1E6
=> Zero counts at step no.   1739 at 2theta/TOF/E(KeV):        34.4202  Intensity fixed to 1.0 and variance to 1E6
=> Zero counts at step no.   1816 at 2theta/TOF/E(KeV):        35.4135  Intensity fixed to 1.0 and variance to 1E6
=> Zero counts at step no.   1818 at 2theta/TOF/E(KeV):        35.4393  Intensity fixed to 1.0 and variance to 1E6
=> Zero counts at step no.   1819 at 2theta/TOF/E(KeV):        35.4522  Intensity fixed to 1.0 and variance to 1E6
=> Zero counts at step no.   1820 at 2theta/TOF/E(KeV):        35.4651  Intensity fixed to 1.0 and variance to 1E6
=> Zero counts at step no.   1856 at 2theta/TOF/E(KeV):        35.9295  Intensity fixed to 1.0 and variance to 1E6
=> Zero counts at step no.   1861 at 2theta/TOF/E(KeV):        35.9940  Intensity fixed to 1.0 and variance to 1E6
=> Zero counts at step no.   1862 at 2theta/TOF/E(KeV):        36.0069  Intensity fixed to 1.0 and variance to 1E6
=> Zero counts at step no.   1870 at 2theta/TOF/E(KeV):        36.1101  Intensity fixed to 1.0 and variance to 1E6
=> Zero counts at step no.   1873 at 2theta/TOF/E(KeV):        36.1488  Intensity fixed to 1.0 and variance to 1E6
=> Zero counts at step no.   1875 at 2theta/TOF/E(KeV):        36.1746  Intensity fixed to 1.0 and variance to 1E6
=> Zero counts at step no.   1878 at 2theta/TOF/E(KeV):        36.2133  Intensity fixed to 1.0 and variance to 1E6
=> Zero counts at step no.   1879 at 2theta/TOF/E(KeV):        36.2262  Intensity fixed to 1.0 and variance to 1E6
=> Zero counts at step no.   1881 at 2theta/TOF/E(KeV):        36.2520  Intensity fixed to 1.0 and variance to 1E6
=> Zero counts at step no.   1883 at 2theta/TOF/E(KeV):        36.2778  Intensity fixed to 1.0 and variance to 1E6
=> Zero counts at step no.   1884 at 2theta/TOF/E(KeV):        36.2907  Intensity fixed to 1.0 and variance to 1E6
=> Zero counts at step no.   1888 at 2theta/TOF/E(KeV):        36.3423  Intensity fixed to 1.0 and variance to 1E6
=> Zero counts at step no.   1947 at 2theta/TOF/E(KeV):        37.1034  Intensity fixed to 1.0 and variance to 1E6
=> Zero counts at step no.   1953 at 2theta/TOF/E(KeV):        37.1808  Intensity fixed to 1.0 and variance to 1E6
=> Zero counts at step no.   1959 at 2theta/TOF/E(KeV):        37.2582  Intensity fixed to 1.0 and variance to 1E6
=> Zero counts at step no.   1962 at 2theta/TOF/E(KeV):        37.2969  Intensity fixed to 1.0 and variance to 1E6
=> Zero counts at step no.   1963 at 2theta/TOF/E(KeV):        37.3098  Intensity fixed to 1.0 and variance to 1E6
=> Zero counts at step no.   1965 at 2theta/TOF/E(KeV):        37.3356  Intensity fixed to 1.0 and variance to 1E6
=> Zero counts at step no.   2041 at 2theta/TOF/E(KeV):        38.3160  Intensity fixed to 1.0 and variance to 1E6
=> Zero counts at step no.   2042 at 2theta/TOF/E(KeV):        38.3289  Intensity fixed to 1.0 and variance to 1E6
=> Zero counts at step no.   2043 at 2theta/TOF/E(KeV):        38.3418  Intensity fixed to 1.0 and variance to 1E6
=> Zero counts at step no.   2045 at 2theta/TOF/E(KeV):        38.3676  Intensity fixed to 1.0 and variance to 1E6
=> Zero counts at step no.   2047 at 2theta/TOF/E(KeV):        38.3934  Intensity fixed to 1.0 and variance to 1E6
=> Zero counts at step no.   2050 at 2theta/TOF/E(KeV):        38.4321  Intensity fixed to 1.0 and variance to 1E6
=> Zero counts at step no.   2057 at 2theta/TOF/E(KeV):        38.5224  Intensity fixed to 1.0 and variance to 1E6
=> Zero counts at step no.   2059 at 2theta/TOF/E(KeV):        38.5482  Intensity fixed to 1.0 and variance to 1E6
=> Zero counts at step no.   2062 at 2theta/TOF/E(KeV):        38.5869  Intensity fixed to 1.0 and variance to 1E6
=> Zero counts at step no.   2066 at 2theta/TOF/E(KeV):        38.6385  Intensity fixed to 1.0 and variance to 1E6
=> Zero counts at step no.   2068 at 2theta/TOF/E(KeV):        38.6643  Intensity fixed to 1.0 and variance to 1E6
=> Zero counts at step no.   2071 at 2theta/TOF/E(KeV):        38.7030  Intensity fixed to 1.0 and variance to 1E6
=> Zero counts at step no.   2074 at 2theta/TOF/E(KeV):        38.7417  Intensity fixed to 1.0 and variance to 1E6
=> Zero counts at step no.   2075 at 2theta/TOF/E(KeV):        38.7546  Intensity fixed to 1.0 and variance to 1E6
=> Zero counts at step no.   2076 at 2theta/TOF/E(KeV):        38.7675  Intensity fixed to 1.0 and variance to 1E6

=> Optimizations for routine tasks applied:
=> Calculation mode for patter#:   1  CM_PSEUDO_VOIGT


Standard deviations have to be multiplied by: 4.9699
(correlated residuals) See references:
-J.F.Berar & P.Lelann, J. Appl. Cryst. 24, 1-5 (1991)
-J.F.Berar, Acc. in Pow. Diff. II,NIST Sp.Pub. 846, 63(1992)

++++++++++++++++++++++++++++++++++++++++++++++++++++++++++++++++++++++++++++++++++++++++++++++++++++++++++++++++++++++++++++++++++++++ ↙


=> CYCLE No.:   17
=>  Convergence reached at this CYCLE !!!!
=>  Parameter shifts set to zero
-------------------------------------------------------------------------------
=> Phase  1 Name:   rdx
-------------------------------------------------------------------------------
=> New parameters, shifts, and standard deviations

Atom        x       dx      sx       y       dy      sy       z       dz      sz       B       dB      sB      occ.  ↙
        docc.   socc.

O(1)     0.56846 0.00000 0.00000  0.43427 0.00000 0.00000  0.26465 0.00000 0.00000  3.70830 0.00000 0.00000    ↙
     1.00000 0.00000 0.00000
O(2)     0.59453 0.00000 0.00000  0.24040 0.00000 0.00000  0.23053 0.00000 0.00000  4.41110 0.00000 0.00000    ↙
     1.00000 0.00000 0.00000
O(3)     0.47340 0.00000 0.00000  0.13880 0.00000 0.00000 -0.02250 0.00000 0.00000  4.98480 0.00000 0.00000    ↙
     1.00000 0.00000 0.00000
O(4)     0.35580 0.00000 0.00000  0.24950 0.00000 0.00000 -0.11238 0.00000 0.00000  4.76640 0.00000 0.00000    ↙
```

```
     1.00000 0.00000 0.00000
O(5)      0.31810 0.00000 0.00000  0.53030 0.00000 0.00000 -0.06806 0.00000 0.00000  5.32170 0.00000 0.00000    ↙
     1.00000 0.00000 0.00000
O(6)      0.42860 0.00000 0.00000  0.60110 0.00000 0.00000  0.04920 0.00000 0.00000  5.10850 0.00000 0.00000    ↙
     1.00000 0.00000 0.00000
N(1)      0.43638 0.00000 0.00000  0.33385 0.00000 0.00000  0.17584 0.00000 0.00000  2.73980 0.00000 0.00000    ↙
     1.00000 0.00000 0.00000
N(2)      0.32231 0.00000 0.00000  0.23197 0.00000 0.00000  0.05389 0.00000 0.00000  2.40240 0.00000 0.00000    ↙
     1.00000 0.00000 0.00000
N(3)      0.29900 0.00000 0.00000  0.45348 0.00000 0.00000  0.08838 0.00000 0.00000  2.59240 0.00000 0.00000    ↙
     1.00000 0.00000 0.00000
N(4)      0.53777 0.00000 0.00000  0.33516 0.00000 0.00000  0.22628 0.00000 0.00000  2.76530 0.00000 0.00000    ↙
     1.00000 0.00000 0.00000
N(5)      0.38834 0.00000 0.00000  0.20759 0.00000 0.00000 -0.03308 0.00000 0.00000  3.09700 0.00000 0.00000    ↙
     1.00000 0.00000 0.00000
N(6)      0.35299 0.00000 0.00000  0.52971 0.00000 0.00000  0.01650 0.00000 0.00000  3.43200 0.00000 0.00000    ↙
     1.00000 0.00000 0.00000
C(1)      0.35799 0.00000 0.00000  0.43950 0.00000 0.00000  0.18450 0.00000 0.00000  2.89510 0.00000 0.00000    ↙
     1.00000 0.00000 0.00000
C(2)      0.38140 0.00000 0.00000  0.21557 0.00000 0.00000  0.14950 0.00000 0.00000  2.70030 0.00000 0.00000    ↙
     1.00000 0.00000 0.00000
C(3)      0.24458 0.00000 0.00000  0.33936 0.00000 0.00000  0.05038 0.00000 0.00000  2.55740 0.00000 0.00000    ↙
     1.00000 0.00000 0.00000
H(1A)     0.40289 0.00000 0.00000  0.52403 0.00000 0.00000  0.20773 0.00000 0.00000  5.13220 0.00000 0.00000    ↙
     1.00000 0.00000 0.00000
H(1B)     0.29071 0.00000 0.00000  0.42024 0.00000 0.00000  0.23991 0.00000 0.00000  4.84270 0.00000 0.00000    ↙
     1.00000 0.00000 0.00000
H(2A)     0.44331 0.00000 0.00000  0.13918 0.00000 0.00000  0.14950 0.00000 0.00000  4.60580 0.00000 0.00000    ↙
     1.00000 0.00000 0.00000
H(2B)     0.31742 0.00000 0.00000  0.19390 0.00000 0.00000  0.20730 0.00000 0.00000  4.97430 0.00000 0.00000    ↙
     1.00000 0.00000 0.00000
H(3A)     0.20936 0.00000 0.00000  0.35364 0.00000 0.00000 -0.02527 0.00000 0.00000  4.50050 0.00000 0.00000    ↙
     1.00000 0.00000 0.00000
H(3B)     0.17213 0.00000 0.00000  0.32091 0.00000 0.00000  0.10070 0.00000 0.00000  3.92150 0.00000 0.00000    ↙
     1.00000 0.00000 0.00000

==> PROFILE PARAMETERS FOR PATTERN#  1

=> Overall scale factor:      0.000484280     0.000000000     0.000000000
=> Eta(p-Voigt) or m(Pearson VII):   0.000000  0.000000  0.000000
=> Overall tem. factor:   0.000000  0.000000  0.000000
=> Halfwidth parameters:
-0.021873  0.000000  0.008126
0.000000  0.000000  0.000000
0.000000  0.000000  0.000000
=> Cell parameters:
11.630419   0.000000   0.000000
10.743058   0.000000   0.000000
13.227938   0.000000   0.000000
90.000000   0.000000   0.000000
90.000000   0.000000   0.000000
90.000000   0.000000   0.000000
=> Preferred orientation:
1.000000  0.000000  0.000000
0.000000  0.000000  0.000000
=> Asymmetry parameters:
0.016548  0.000000  0.022682
0.042495  0.000000  0.004085
0.000000  0.000000  0.000000
0.000000  0.000000  0.000000
=> X and Y parameters:
0.000000  0.000000  0.000000
0.000000  0.000000  0.000000
=> Strain parameters:
0.000000  0.000000  0.000000
0.000000  0.000000  0.000000
0.000000  0.000000  0.000000
=> Size   parameters (G,L):
0.009841  0.000000  0.000166
0.052419  0.000000  0.000000
=> Further shape parameters (S_L and D_L):
0.000000  0.000000  0.000000
0.000000  0.000000  0.000000

=> Spherical Harmonics coeff.(size):

0.052419      0.000000      0.000000       0.087274      0.000000      0.000000       0.142427      0.000000       ↙
     0.000000
0.127726      0.000000      0.000000      -0.069125      0.000000      0.000000      -0.017749      0.000000       ↙
     0.000000
0.000000      0.000000      0.000000       0.000000      0.000000      0.000000       0.000000      0.000000       ↙
     0.000000

==> GLOBAL PARAMETERS FOR PATTERN#  1


=> Zero-point:    -0.0558    0.0000    0.0000

=> Cos( theta)-shift parameter :  -0.1317  0.0000  0.0059
=> Sin(2theta)-shift parameter :   0.2589  0.0000  0.0079
```

```
==> RELIABILITY FACTORS WITH ALL NON-EXCLUDED POINTS FOR PATTERN:  1

=> R-Factors:   16.8      25.9     Chi2:  68.7     DW-Stat.:  0.7701   Patt#:  1
=> Expected :            3.13                                1.8693
=> Deviance : 0.279E+06     Dev*:   134.1
=> GoF-index:  8.3         Sqrt(Residual/N)
=> N-P+C:  2071

=>    SumYdif       SumYobs      SumYcal      SumwYobsSQ     Residual    Condition
0.3554E+06    0.2119E+07    0.1985E+07    0.2119E+07    0.1423E+06    0.1073E+06


=> Conventional Rietveld Rp,Rwp,Re and Chi2:   16.8      25.9      3.13      68.71
=> (Values obtained using Ynet, but true sigma(y))
=>  SumYnet, Sum(w Ynet**2):     0.2119E+07    0.2119E+07

=> N-sigma of the GoF: 2178.849

==> RELIABILITY FACTORS FOR POINTS WITH BRAGG CONTRIBUTIONS FOR PATTERN:  1

=> R-Factors:   16.8      25.9     Chi2:  68.7     DW-Stat.:  0.7701   Patt#:
=> Expected :            3.13                                1.8693
=> Deviance : 0.279E+06     Dev*:   134.1
=> GoF-index:  8.3         Sqrt(Residual/N)
=> N-P+C:  2071

=>    SumYdif       SumYobs      SumYcal      SumwYobsSQ     Residual    Condition
0.3554E+06    0.2119E+07    0.1985E+07    0.2119E+07    0.1423E+06    0.1073E+06


=> Conventional Rietveld Rp,Rwp,Re and Chi2:   16.8      25.9      3.13      68.71
=> (Values obtained using Ynet, but true sigma(y))
=>  SumYnet, Sum(w Ynet**2):     0.2119E+07    0.2119E+07

=> N-sigma of the GoF:     2178.849

=> Global user-weigthed Chi2 (Bragg contrib.):   68.7

-------------------------------------------------------------------------------------------------------------
Pattern#  1 Phase No:   1 Phase name:   rdx
-------------------------------------------------------------------------------------------------------------

No.  Code     H   K   L  Mult     Hw         2theta      Icalc       Iobs      Sigma      HwG     HwL       ETA   ↙
          d-hkl        CORR

1   1      1   1   1     8  0.118374      13.052     1341.4     1219.3    113.321  0.114185  0.007826  0.088258    ↙
    6.777159    607.424438
2   1      0   0   2     2  0.126380      13.376      657.3      681.0     37.365  0.114091  0.022705  0.230664    ↙
    6.613969    144.491653
3   1      2   0   0     2  0.125409      15.223       89.1       60.5     27.340  0.113539  0.021952  0.225085    ↙
    5.815209    111.037720
4   1      1   0   2     4  0.120902      15.399      850.4      651.2    156.651  0.113485  0.013832  0.150205    ↙
    5.749331    216.941605
5   1      0   2   0     2  0.113365      16.489      406.7      343.2     53.789  0.113143  0.000412  0.004962    ↙
    5.371529     94.315758
6   1      2   1   0     4  0.123410      17.326     1044.6     1098.6     67.817  0.112873  0.019543  0.204799    ↙
    5.114053    170.442551
7   1      1   1   2     8  0.119619      17.481      137.1      143.0      6.578  0.112822  0.012683  0.139605    ↙
    5.069075    334.714142
8   1      0   2   1     4  0.114554      17.807     1687.8     1517.1    154.129  0.112715  0.003429  0.040470    ↙
    4.976847    161.115646
9   1      2   1   1     8  0.121062      18.586       24.6       43.4     36.296  0.112454  0.016023  0.172697    ↙
    4.769984    295.069672
10   1      1   2   1     8  0.116204      19.384       24.1       48.6     50.338  0.112181  0.007515  0.086376    ↙
    4.575528    270.592194
11   1      2   0   2     4  0.118758      20.318     1050.2     1304.2    315.392  0.111854  0.012881  0.142690    ↙
    4.367220    122.753159
12   1      0   2   2     4  0.117124      21.291       73.0       81.7     15.723  0.111503  0.010498  0.118683    ↙
    4.169635    111.398773
13   1      2   1   2     8  0.118763      21.952      831.1      909.0     90.704  0.111260  0.013988  0.154455    ↙
    4.045709    209.094452
14   1      2   2   0     4  0.119735      22.515      154.5      158.6     13.850  0.111049  0.016163  0.175980    ↙
    3.945786     99.174377
15   1      1   2   2     8  0.117218      22.635       42.0       42.1      1.812  0.111003  0.011603  0.130649    ↙
    3.925016    196.149139
16   1      1   1   3     8  0.121592      23.087       29.2       31.6     13.325  0.110831  0.019940  0.211672    ↙
    3.849222    188.221832
17   1      2   2   1     8  0.118923      23.509      158.8      180.2     30.275  0.110668  0.015372  0.168838    ↙
    3.781150    181.234940
18   1      3   1   1     8  0.122567      25.314      966.1     1261.9    385.418  0.109949  0.023265  0.242864    ↙
    3.515492    155.173340
19   1      0   2   3     4  0.119412      26.125       40.0       93.6    125.152  0.109615  0.018188  0.197387    ↙
    3.408129     72.593018
20   1      2   2   2     8  0.117845      26.278        9.8       27.3     48.974  0.109550  0.015441  0.171049    ↙
    3.388580    143.401276
21   1      3   0   2     4  0.119745      26.630        7.0       11.2      6.632  0.109402  0.019178  0.206992    ↙
    3.344589     69.711670
22   1      2   1   3     8  0.118751      26.672      156.4      217.4     84.493  0.109384  0.017402  0.190283    ↙
    3.339449    138.961929
```

No.	Code	H	K	L	Mult	Hw	2theta	Icalc	Iobs	Sigma	HwG	HwL	ETA	d-hkl	CORR
23	1	1	3	1	8	0.114347	26.886	560.6	613.0	57.368	0.109293	0.009439	0.109578	3.313359	136.631302
24	1	0	0	4	2	0.126217	26.939	347.8	402.2	62.654	0.109271	0.030840	0.306910	3.306984	34.016178
25	1	1	2	3	8	0.118708	27.244	156.5	221.0	90.833	0.109140	0.017770	0.194165	3.270598	132.851700
26	1	3	1	2	8	0.119594	27.916	3.4	7.2	12.216	0.108848	0.019902	0.214625	3.193409	126.155663
27	1	1	0	4	4	0.123939	28.028	0.1	0.3	0.678	0.108799	0.027703	0.282736	3.180897	62.542797
28	1	3	2	1	8	0.120652	29.175	627.7	767.4	170.350	0.108286	0.022805	0.241903	3.058400	114.835915
29	1	1	1	4	8	0.122676	29.257	951.7	1094.2	163.707	0.108249	0.026449	0.273448	3.050011	114.149055
30	1	2	3	0	4	0.116597	29.265	484.2	549.3	73.805	0.108246	0.015543	0.173882	3.049236	57.042862
31	1	1	3	2	8	0.114976	29.359	3.3	3.8	0.560	0.108202	0.012636	0.144515	3.039620	113.300980
32	1	2	3	1	8	0.116344	30.050	0.6	0.4	1.999	0.107884	0.015741	0.176364	2.971314	107.799812
33	1	2	2	3	8	0.117646	30.374	430.9	414.2	19.103	0.107733	0.018392	0.202318	2.940360	105.349037
34	1	4	0	0	2	0.124821	30.724	197.1	194.9	3.155	0.107568	0.031341	0.314667	2.907605	25.696112
35	1	2	0	4	4	0.119938	31.085	271.8	275.4	4.980	0.107396	0.023113	0.246316	2.874666	50.117661
36	1	3	2	2	8	0.118689	31.483	60.1	64.6	5.770	0.107204	0.021223	0.229644	2.839199	97.524094
37	1	0	2	4	4	0.120765	31.749	6.9	7.0	0.133	0.107075	0.025141	0.264706	2.816087	47.887966
38	1	3	1	3	8	0.117748	31.818	65.5	72.3	7.496	0.107041	0.019824	0.216993	2.810112	95.326462
39	1	4	1	0	4	0.124096	31.859	143.5	161.2	19.817	0.107022	0.031024	0.313420	2.806627	47.532345
40	1	2	1	4	8	0.119402	32.208	461.9	512.0	55.336	0.106850	0.023127	0.247495	2.776968	92.850838
41	1	2	3	2	8	0.115916	32.302	498.6	531.9	35.575	0.106803	0.016932	0.189705	2.769119	92.268997
42	1	4	1	1	8	0.122854	32.587	52.3	48.9	3.243	0.106662	0.029502	0.302057	2.745508	90.529259
43	1	1	2	4	8	0.119819	32.691	38.6	42.7	4.585	0.106610	0.024290	0.258237	2.736998	89.905861
44	1	1	3	3	8	0.115856	33.107	311.5	281.3	28.946	0.106401	0.017555	0.196420	2.703608	87.479691
45	1	0	4	0	2	0.111635	33.333	68.3	65.5	3.108	0.106286	0.009990	0.118499	2.685765	21.548969
46	1	4	0	2	4	0.120426	33.643	7.1	7.2	8.589	0.106127	0.026203	0.275777	2.661751	42.241043
47	1	0	4	1	4	0.111828	34.034	48.4	47.1	13.746	0.105925	0.011019	0.130079	2.632060	41.192669
48	1	4	1	2	8	0.120126	34.692	70.9	73.9	5.635	0.105580	0.026628	0.280566	2.583631	79.018021
49	1	3	3	1	8	0.117938	34.742	328.4	334.0	14.687	0.105554	0.022818	0.247235	2.580004	78.768509
50	1	1	4	1	8	0.112391	34.922	0.0	0.0	0.001	0.105458	0.012928	0.150981	2.567142	77.886520
51	1	3	2	3	8	0.117125	35.027	300.9	367.0	80.552	0.105402	0.021638	0.236780	2.559662	77.375694
52	1	4	2	0	4	0.122081	35.064	44.2	53.9	11.899	0.105382	0.030354	0.311852	2.557027	38.598064
53	1	2	2	4	8	0.117894	35.386	0.0	0.0	0.027	0.105209	0.023349	0.252687	2.534537	75.671524
54	1	3	0	4	4	0.117223	35.655	92.9	97.3	11.789	0.105063	0.022415	0.244538	2.515971	37.211742
55	1	4	2	1	8	0.121172	35.735	21.5	22.1	2.499	0.105020	0.029407	0.305007	2.510551	74.061028
56	1	1	1	5	8	0.122855	35.767	0.1	0.1	0.020	0.105003	0.032317	0.328338	2.508384	73.916328
57	1	2	3	3	8	0.115701	35.773	5.9	5.9	0.530	0.104999	0.019805	0.220407	2.507954	73.887573
58	1	0	4	2	4	0.112335	36.064	0.1	0.4	0.974	0.104840	0.013962	0.162629	2.488423	36.294819
59	1	3	1	4	8	0.117009	36.654	32.8	37.2	5.785	0.104513	0.023008	0.251009	2.449688	70.047195
60	1	3	3	2	8	0.116759	36.738	114.0	120.5	9.645	0.104466	0.022648	0.247833	2.444295	69.696564
61	1	2	4	0	4	0.113760	36.832	182.9	199.4	19.304	0.104413	0.017351	0.197645	2.438274	34.653053
62	1	1	4	2	8	0.112654	36.909	34.1	40.1	7.158	0.104370	0.015412	0.178234	2.433349	68.987450
63	1	2	4	1	8	0.113642	37.475	56.7	51.6	13.826	0.104048	0.017797	0.202657	2.397879	66.712807
64	1	4	2	2	8	0.119049	37.685	4.7	7.3	3.987	0.103928	0.027610	0.292529	2.384992	65.895241
65	1	1	3	4	8	0.116575	37.797	0.1	0.1	0.032	0.103863	0.023386	0.255728	2.378168	65.464195

```
66   1      0   2   5     4  0.121164      37.877       50.7       62.8     15.171  0.103817  0.031435  0.324228    ↙
     2.373343      32.580132
67   1      4   1   3     8  0.117489      37.971      177.6      217.2     49.240  0.103762  0.025174  0.271878    ↙
     2.367672      64.803848
68   1      2   1   5     8  0.119694      38.272        1.4        3.4      6.285  0.103587  0.029308  0.307508    ↙
     2.349785      63.685627
69   1      1   2   5     8  0.120194      38.689        1.2        3.3     13.353  0.103342  0.030582  0.318513    ↙
     2.325420      62.177151

------------------------------------------------------
BRAGG R-Factors and weight fractions for Pattern #  1
------------------------------------------------------

=> Phase:  1       rdx
=> Bragg R-factor:   13.0       Vol: 1652.781( 0.000)  Fract(%):  100.00( 0.00)
=> Rf-factor=  7.18             ATZ:        1776.939   Brindley:  1.0000

---------------------------------------------------------------------
SYMBOLIC NAMES AND FINAL VALUES AND SIGMA OF REFINED PARAMETERS:
---------------------------------------------------------------------

->  Parameter number    1 :           SyCos_pat1   -0.13173719    ( +/-    0.58904295E-02 )
->  Parameter number    2 :      U-Cagl_ph1_pat1   -0.21872528E-01( +/-    0.81257941E-02 )
->  Parameter number    3 :           SySin_pat1    0.25886813    ( +/-    0.79076700E-02 )
->  Parameter number    4 :       Asym1_ph1_pat1    0.16548268E-01( +/-    0.22681832E-01 )
->  Parameter number    5 :      G-Size_ph1_pat1    0.98405704E-02( +/-    0.16556507E-03 )
->  Parameter number    6 :       Asym2_ph1_pat1    0.42495131E-01( +/-    0.40853349E-02 )

---------------------------------------------------------------------
=> Number of bytes for floating point variables: 4
=> Dimensions of dynamic allocated arrays in this run of FullProf:
---------------------------------------------------------------------

=> Total approximate array memory (dynamic + static): 107719993 bytes

MaxPOINT=    60000 Max.num. of points(+int. Inten.)/diffraction pattern
MaxREFLT=    20000 Max.num. of reflections/diffraction pattern
MaxPARAM=      300 Max.num. of refinable parameters
MaxOVERL=     2096 Max.num. of overlapping reflections

-----------------------------------------------------------
=> Number of bytes for floating point arrays: 4
=> Dimensions of fixed arrays in this release of FullProf:
-----------------------------------------------------------

NPATT   =       80 Max.num. of powder diffraction patterns
NATS    =      830 Max.num. of atoms (all kind) in asymmetric unit
MPAR    =     1800 Max.num. of non atomic parameters/phase
IEXCL   =       30 Max.num. of excluded regions
IBACP   =      277 Max.num. of background points for interpolation
NPHT    =       16 Max.num. of phases
NMAGM   =        8 Max.num. of rotation-matrices sets for magnetic structure
NBASIS  =       12 Max.num. of basis functions associated to a single atom
NIREPS  =        9 Max.num. of irreducible representations to be combined
N_EQ    =      384 Max.num. of user-supplied symmetry operators/propagation vectors
NGL     =      300 Max.num. of global parameters/diffraction pattern
N_LINC  =       30 Max.num. of global linear restraints
NAT_P   =       64 Max.num. of atomic parameters per atom
NCONST  =      500 Max.num. of slack constraints per phase
N_SPE   =       16 Max.num. of different chemical species
N_FORM  =       60 Max.num. of scattering factor values in a table
NPR     =      150 Max.num. of points defining a numerical profile
INPR    =       25 Max.num. of different numerical peak shapes
NPRC    =      150 Max.num. of terms in the table for correcting intensities
NSOL    =       10 Max.num. of solutions to be stored in Montecarlo searchs


CPU Time:     7.385 seconds
0.123 minutes

=> Run finished at:     Date: 20/02/2015  Time: 16:02:27.667
```

Glossary

ADN Ammonium DiNitramide 46

AFM Atomic Force Microscopy 4, 40, 66, 67, 97, 99, 102–105, 107, 108, 110, 116, 117, 119, 120, 138, 139, 170, 173, 282, 283, 285

AN Ammonium Nitrate 32, 66

AP Ammonium Perchlorate 32, 64

API Active Pharmaceutical Ingredient 134

ASES Aerosol Solvent Extraction System 68, 69, 73

BAM Bundesanstalt für Materialprüfung 43–45, 281

BET Brunauer–Emmett–Teller theory 40, 52, 95, 96, 103, 285

CL-20 2,4,6,8,10,12-hexanitro-2,4,6,8,10,12-hexaazaisowurtzitane 32, 35–38, 46, 47, 49, 54, 55, 62, 65, 70, 71, 138–141, 281, 283

CL-20:HMX co-crystal from CL-20 and HMX 36, 38, 65, 71, 130, 137, 139–141, 174, 283

CNT Classical Nucleation Theory 125, 141

CTA 2,4,6-triazido-1,3,5-triazine or cyanuric triazide 64

CVD Chemical Vapor Deposition 72

DBTDL Dibutyltin dilaurate 64

DLS Dynamic Light Scaterring 53, 55, 62, 65, 73, 281, 285

DMA Differential Mobility Analysis 96

DME DiMethyl Ether 70

DMF DiMethylFormamide 33, 34, 63, 68

DMSO dimethylsulfoxide 33, 34, 149

DSC Differential Scanning Calorimetry 41

ESD Electrostatic Discharge 43–45, 47, 163, 281

ESEM Environmental Scanning Electron Microscopy 51, 55, 173, 281

FOX-7 1,1-diamino-2,2-dinitroethene 46, 62, 71

FPM Full Pattern Matching 50, 111

FTIR Fourier Transform Infrared Spectroscopy 42, 158, 162, 284

FWHM Full Width at Half Maximum 111, 113

GAP Glycidyl Azide Polymer 64

GAS Gas AntiSolvent 68

HMX octahydro-1,3,5,7-tetranitro-1,3,5,7-tetrazocine 32, 34, 36–38, 46–48, 55, 62, 63, 65, 66, 71, 138, 281

IM Insensitive Munitions 46

IR Infrared 81

LASER Light Amplification by Stimulated Emission of Radiation 66, 70, 72, 73, 75, 82, 96, 130

MD Molecular Dynamics 125

MSF Multi Stage Flash 75, 77

NC NitroCellulose 64, 68

NMP N-Methyl-2-pyrrolidone 33, 34

NMR Nuclear Magnetic Resonance 9, 42, 149, 150, 283

NRTL Non-Random Two-Liquid 128

NTO 5-nitro-1,2,4-triazol-3-one 68, 173

ONC Octanitrocubane 46

PDA Phase Doppler Analysis 5, 12, 96, 130–132, 141, 166, 169, 170, 175, 283

PEG PolyEthylene Glycol 5, 12, 107, 116, 118, 142, 147–149, 151–158, 160, 162–166, 174, 282, 284, 286

PGSS Particles from Gas-Saturated Solutions 69

PhSD Phase Solubility Diagram 134, 136, 137, 174

PID Proportional-Integral-Derivative 78, 139

PIV Particle Image Velocimetry 130

PSD Particle Size Distribution 22, 48, 53, 55, 65, 97, 98, 103, 106–108, 128, 129, 132, 133, 138, 153, 157, 160, 281, 283

PVAc Polyvinyl acetate 71

PVD Physical Vapor Deposition 66, 72, 73, 82

PVOH Polyvinyl alcohol 65

PVP PolyVinylPyrrolidone 5, 12, 52, 53, 70, 107–110, 116–119, 138, 142, 147–149, 151, 154, 157–165, 174, 281, 282, 284

RDX 1,3,5-trinitroperhydro-1,3,5-triazine 4, 11, 12, 31–34, 37, 45–48, 50, 51, 54–56, 61–73, 75, 81, 82, 95, 97–99, 103, 105, 108–110, 117–119, 126–129, 138, 147–150, 152–166, 173, 174, 281–286

RESS Rapid Expansion of Supercritical Solutions 47, 69, 70, 73, 82, 173

RESS-AS Rapid Expansion of Supercritical Solutions into an Aqueous Solution 70, 74

RfD reference dose 54

SAS Supercritical Anti-Solvent precipitation 68

SATP Standard Ambient Temperature and Pressure as a temperature of 298.15 K and an absolute pressure of 100 kPa (1 bar) 34, 35

SAXS Small-Angle X-ray Scattering 141, 166, 170

SCF SuperCritical Fluid 74, 75

SDBD Surface Dielectric Barrier Discharge 67

SEDS Solution Enhanced Dispersion by Supercritical fluids 68, 69, 73

SEM Scanning Electron Microscopy 39, 51, 62, 65, 70, 81, 96, 103, 106–110, 116–120, 128, 152–154, 159, 281, 282, 284, 285

SFE Spray Flash Evaporation 4, 46, 48, 72, 73, 75, 78–83, 98, 99, 105, 111, 112, 117, 120, 126–129, 132, 137–141, 147–149, 152–154, 156–159, 162, 163, 166, 173–175, 282–284

SHYMAN Sustainable Hydrothermal Manufacturing of Nanomaterials 72

SMPS Scanning Mobility Particle Sizer 70

SMRT-TEM single-molecule real-time transmission electron microscopy 125

STM Scanning Tunneling Microscopy 4, 173

TDI Toluene Dilsocyanate 64

TEM Transmission Electron Microscopy 120

TERS Tip Enhanced Raman Spectroscopy 164, 166

TIL Threshold Initiation Level 45

TNAZ 1,3,3-trinitroazetidine 46

TNT 2,4,6-trinitrotoluene 4, 11, 13, 64, 67, 69, 72

VLE Vapor-Liquid Equilibrium 127, 128, 283

XRD X-Ray Difraction 36, 39, 40, 49, 50, 64–66, 73, 99, 111, 120, 138, 140, 153, 155, 158, 161, 170, 281, 283–285

List of Figures

List of Tables

Florent PESSINA

Toward Particle Size Reduction by Spray Flash Evaporation

the case of organic energetic crystals and cocrystals

Résumé

La cristallisation en continu de nanoparticules énergétiques est un défi de longue date. Le Spray Flash Evaporation (SFE) est une technique majeure développée et brevetée en interne, pour la production en continu de matériaux énergétiques submicroniques ou nanométriques ; la technologie se base sur la surchauffe d'un solvant pulvérisé dans le vide et s'évaporant alors de manière flash.

Ce présent travail de recherche a pour but de comprendre et contrôler la cristallisation au sein du procédé SFE, ceci afin de réduire encore la taille de particules de cristaux énergétiques. Le RDX est choisi comme matériaux de référence ; le cocristal CL-20:HMX 2:1 a été également étudié pour aller au-delà des limitations de mesures *in-situ*. La sursaturation gouverne la cristallisation, et concernant le SFE, est une fonction du temps et de l'espace liée aux tailles et vitesses de gouttes. La sursaturation fut variée par un anti-solvant et par l'amélioration du SFE avec un système double buse. Finalement, un Interféromètre Phase Doppler fut utilisé pour résoudre cette question de la sursaturation.

Dans un second temps, PVP 40K et PEG 400 ont été utilisés afin de contrôler les deux étapes de la cristallisation, nommément la nucléation et la croissance. Les particules ont pu être ajustées d'une taille de 160 nm à 5 µm, avec des morphologies facettées ou sphériques. De plus, les échantillons de RDX ainsi cristallisés furent aussi moins sensibles, notamment de manière très marquée à la décharge électrostatique.

Mots clés : Spray Flash Evaporation, 1,3,5-trinitroperhydro-1,3,5-triazine, RDX, CL-20, HMX, cristallisation, nanoparticules, particules fines, explosif, cocristal

Résumé en anglais

The continuous formation of nanosized energetic material is a long-standing challenge. Spray Flash Evaporation (SFE) is a major technique, internally developed and patented, for continuously producing energetic materials at submicron or nano scale; it relies on the superheating of a solvent sprayed into vacuum and thus flashing.

This present research project aims to understand and control the crystallisation occurring in the SFE process, in order to reduce further the particle size of energetic crystals. RDX has been chosen as a reference material; the cocrystal CL-20:HMX 2:1 was studied overcome the limited *in situ* characterizations also. The supersaturation governs the crystallization and is a function of time and space in SFE, linked to the size distribution and velocity of droplets. Supersaturation was raised with an anti-solvent and by the enhancement of the SFE with a dual nozzle system. Later, a Phase Doppler Interferometer was used to elucidate the question of supersaturation.

Another route to control the crystallisation is the addition of chemical agent. PVP 40K and PEG 400 were successfully used to alter the two steps of the crystallisation, namely the nucleation and the growth. The particle was subsequently tuned from 160 nm spheres to 5 µm grains. Additionally, the synthesized RDX samples were less sensitive, especially toward electrostatic discharge.

Keywords: Spray Flash Evaporation, 1,3,5-trinitroperhydro-1,3,5-triazine, RDX, CL-20, HMX, crystallisation, nanoparticles, fine particles, nanoparticles, explosive, cocrystal